ACR Announcements

AMERICAN COLLEGE OF RHEUMATOLOGY
2200 Lake Boulevard NE, Atlanta, Georgia 30319-5312
www.rheumatology.org

ACR 2021 Pediatric Rheumatology Symposium

Join your pediatric colleagues from across the country in this year's Pediatric Rheumatology Symposium (PRSYM) being held virtually May 19–22. This unique symposium will provide you with the most up-to-date, practical clinical information and basic science knowledge on the diagnosis and management of pediatric patients with rheumatic diseases and immune disorders. Visit www.rheumatology.org/Learning-Center/Educational-Activities to learn more and register.

Nominations for ACR Awards of Distinction and Masters Due May 17

The ACR has many Awards of Distinction, including the Presidential Gold Medal. Members who wish to nominate a colleague or mentor for an Award of Distinction must complete the online form at www.rheumatology.org by May 17, 2021. The nomination process includes a letter of nomination, 2 additional letters of recommendation, and a copy of the nominee's curriculum vitae. Recognition as a Master of the American College of Rheumatology is one of the highest honors the ACR bestows. The designation of Master is conferred on ACR members age 65 or older who have made outstanding contributions to the field of rheumatology through scholarly achievements and/or service to their patients, students, and the profession. To nominate someone for a Master designation, members must complete the online nomination form at www.rheumatology.org and include a letter of nomination, 2 supporting letters from voting members of the ACR, and the nominee's curriculum vitae. Nominees for ACR Master must have reached the age of 65 before October 1, 2021.

ACR Invites Nominations for Volunteer Positions

The ACR encourages all members to participate in forming policy and conducting activities by assuming positions of leadership in the organization. Positions are available in all areas of the work of the American College of Rheumatology and the Rheumatology Research Foundation. Please visit www.rheumatology.org for information about nominating yourself or a colleague for a volunteer position with the College. The deadline for volunteer nominations is June 1, 2021. Letters of recommendation are not required but are preferred.

Arthritis & Rheumatology

An Official Journal of the American College of Rheumatology
www.arthritisrheum.org and wileyonlinelibrary.com

Cover design: Todd Machen

This journal is printed on acid-free paper.

Arthritis & Rheumatology

An Official Journal of the American College of Rheumatology
www.arthritisrheum.org and wileyonlinelibrary.com

VOLUME 73 • May 2021 • NO. 5

Systemic Sclerosis

Myositis

Pediatric Rheumatology

Letters

Clinical Images

Cover image: The figure on the cover (from Yuba et al, pages 769–778) shows immunofluorescence staining of popliteal lymph node from an arthritic BALB/c mouse after intravenous injection of DyLight 594–labeled serum albumin–fused interleukin-10 (SA–IL-10). Specimens were stained for anti-CD3 (green) and DAPI (blue). Location of SA–IL-10 appears in red.

In this Issue

Highlights from this issue of *A&R* | By Lara C. Pullen, PhD

Treatment of Patients with Suspected Nonradiographic Axial Spondyloarthritis

Until now, there have been only 2 published placebo-controlled trials that included patients with nonradiographic axial spondyloarthritis (SpA) with high disease activity without the requirement of elevated C-reactive protein (CRP) level and/or inflammatory lesions seen on sacroiliac (SI) joint magnetic resonance imaging (MRI). These 2 studies found a significantly higher rate of Assessment of SpondyloArthritis international Society 20 (ASAS20) response in groups treated with tumor necrosis factor inhibitors (TNFi) compared to placebo. In contrast, in this issue, Rusman et al (p. 806) report that 16 weeks of treatment with etanercept (ETN) was ineffective for patients with suspected SpA.

p. 806

The study included TNFi-naive patients with inflammatory back pain with ≥2 SpA features and high disease activity. The researchers did not require a positive finding on MRI of the SI joint and/or elevated CRP level for enrollment in the study, but approximately one-third of patients had positive SI joint MRI findings. The investigators randomized the 80 patients into ETN and placebo groups. Patients were treated for 16 weeks and followed up for an additional 8 weeks without study medication. The primary end point was the ASAS20 response at 16 weeks. Secondary end points at 16 and 24 weeks included the Ankylosing Spondylitis Disease Activity Score and changes in disease parameters, including the Bath Ankylosing Spondylitis Metrology Index (BASMI), CRP level, erythrocyte sedimentation rate (ESR), and Spondyloarthritis Research Consortium of Canada index scores.

Patient characteristics at baseline were comparable between the 2 groups and, at 16 weeks, the researchers saw no significant difference between them in the percentage of patients exhibiting ASAS20 response. While improvement in ESR was observed at 16 weeks in the ETN group compared to the placebo group, the difference did not reach statistical significance. Between 16 and 24 weeks, without study medication, the BASMI, CRP level, and ESR had worsened to a greater extent in the ETN group compared to the placebo group, and this difference was significant for the CRP level.

Obinutuzumab Effective in Murine Lupus Model

The chimeric type I anti-CD20 monoclonal antibody (mAb) rituximab (RTX) has failed to meet end points in 2 randomized clinical trials of patients with lupus. In this issue, Marinov et al (p. 826) report that the type II anti-CD20 antibody obinutuzumab (GA101) and RTX were both able to ameliorate early disease in a murine lupus model. GA101, however, was more effective than RTX for important parameters such as glomerulonephritis score. GA101 also proved beneficial in an advanced disease model, in which it prolonged survival.

p. 826

The investigators found that a single dose of GA101 was more effective than RTX in depleting B cells in MRL/lpr mice expressing human CD20 on B cells with established disease (hCD20 MRL/lpr mice). With continuous treatment, however, RTX was able to overcome resistance to B cell depletion in diseased MRL/lpr mice. Not only was GA101 more effective in treating hCD20 MRL/lpr mice with early disease, treated mice had reduced glomerulonephritis, lower anti-RNA autoantibody titers, and fewer activated CD4+ T cells compared to RTX-treated mice. The authors also detail their use of variants of GA101 to elucidate B cell depletion mechanisms in vivo in mice with lupus. They conclude that their data support clinical testing of GA101 in systemic lupus erythematosus and lupus nephritis.

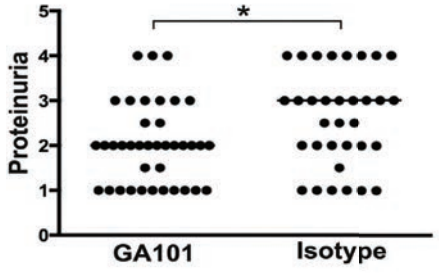

Figure 1. Effects of GA 101 treatment on clinical disease when initiated in mice with established autoimmunity. Thirteen-week-old MRL/lpr mice expressing human CD20 on B cells with established disease were treated with GA101 or isotype control for 6 weeks. Proteinuria in mice treated as indicated, evaluated by dipstick assay the day before mice were euthanized.

Meta-Analysis Suggests that JAK Inhibitors Do Not Increase Venous Thrombosis Risk

JAK inhibitor therapies are effective options for treating immune-mediated inflammatory diseases (IMIDs). However, their product labels include a warning for increased venous thromboembolism (VTE) risk, and this risk warning from licensing authorities has limited their use. p. 779 In this issue, Yates et al (p. 779) report the results of their meta-analysis of randomized controlled trial (RCT) data to ascertain the VTE risk of JAK inhibitors in IMID patients. They conclude that the pooled incidence rate ratios (IRRs) do not support the current warnings of VTE risk for JAK inhibitors but acknowledge that, even given the low event rates, they cannot rule out a true effect involving a small increase in risk.

The investigators performed systematic searches of Medline and Embase databases from inception to September 30, 2020. They included phase II and III double-blind RCTs of JAK inhibitors at licensed doses and excluded long-term extension studies, RCTs with no placebo arm, post hoc analyses, and pooled analyses. Three researchers independently extracted data on exposure to JAK inhibitors or placebo, as well as VTE events, and assessed study quality.

The team initially identified 619 studies but included results from 42 studies with 6,542 JAK inhibitor patient exposure years (PEYs) and 1,578 placebo PEYs. They identified 15 VTE events in the JAK inhibitor group and 4 events in the placebo group and calculated pooled IRRs of VTE, pulmonary embolism, and deep vein thrombosis in patients receiving JAK inhibitors as 0.68, 0.44, and 0.59, respectively. The authors conclude by suggesting that their findings be used in the continued development of clinical guidelines for the use of JAK inhibitors in IMIDs.

Journal Club

A monthly feature designed to facilitate discussion on research methods in rheumatology.

Nonsteroidal Antiinflammatory Drugs and Susceptibility to COVID-19

Chandan et al. *Arthritis Rheumatol.* 2021;88:731–739

Nonsteroidal antiinflammatory drugs (NSAIDs) are widely used for the management of pain in patients with chronic diseases such as osteoarthritis (OA), including older patients. However, concerns were raised during the early stages of the coronavirus disease 2019 (COVID-19) pandemic regarding the use of NSAIDs in the context of this infection. A 2020 study by Fang et al suggested that ibuprofen, one of the most commonly used NSAIDs, could up-regulate angiotensin-converting enzyme 2 expression, thereby increasing susceptibility to COVID-19 infection. Rapid reviews conducted on the association between the use of NSAIDs and the susceptibility and severity of COVID-19 were inconclusive, as data on the effects of NSAIDs on this new virus remained sparse.

A retrospective cohort study was conducted to investigate the association between the use of NSAIDs and subsequent development of COVID-19 in patients with OA, using data from a large primary care database. Propensity score–matched cohorts of patients who were prescribed an NSAID were compared with those prescribed either co-codamol (acetaminophen + codeine) or co-dydramol (acetaminophen + dihydrocodeine). Participants were defined as patients with a record of prescription lasting beyond the index date or those with prescriptions that lasted until the preceding 90 days of the index date and with evidence of further prescription during the pandemic period. The groups were mutually exclusive, and patients with a current prescription for both medications were excluded from the study. Patients were followed up from January 30, 2020 (index date) until the earliest of the following dates: date of outcome, date of death, date patient left practice, date practice ceased to contribute data, or study end date (July 31, 2020). The primary outcome measure was diagnosis of COVID-19, and the secondary outcome measure was the risk of all-cause mortality and was limited to confirmed COVID-19 cases in a sensitivity analysis.

Questions

1. **What is currently known about the effects of NSAIDs on the risk of COVID-19 across different risk groups?**
2. **Is there a better way of defining current treatment users for the purpose of this study?**
3. **What is the advantage of using active comparator drugs in the study rather than no drugs at all?**
4. **Are there other methods that could have been employed given that this was a new virus and confirmed cases were few and far between during the early stages of the pandemic?**

Clinical Connections

RNA Sequencing Reveals Interacting Key Determinants of Osteoarthritis Acting in Subchondral Bone and Articular Cartilage

Tuerlings et al, *Arthritis Rheumatol* 2021;88:789–799

CORRESPONDENCE
Ingrid Meulenbelt, PhD: i.meulenbelt@lumc.nl

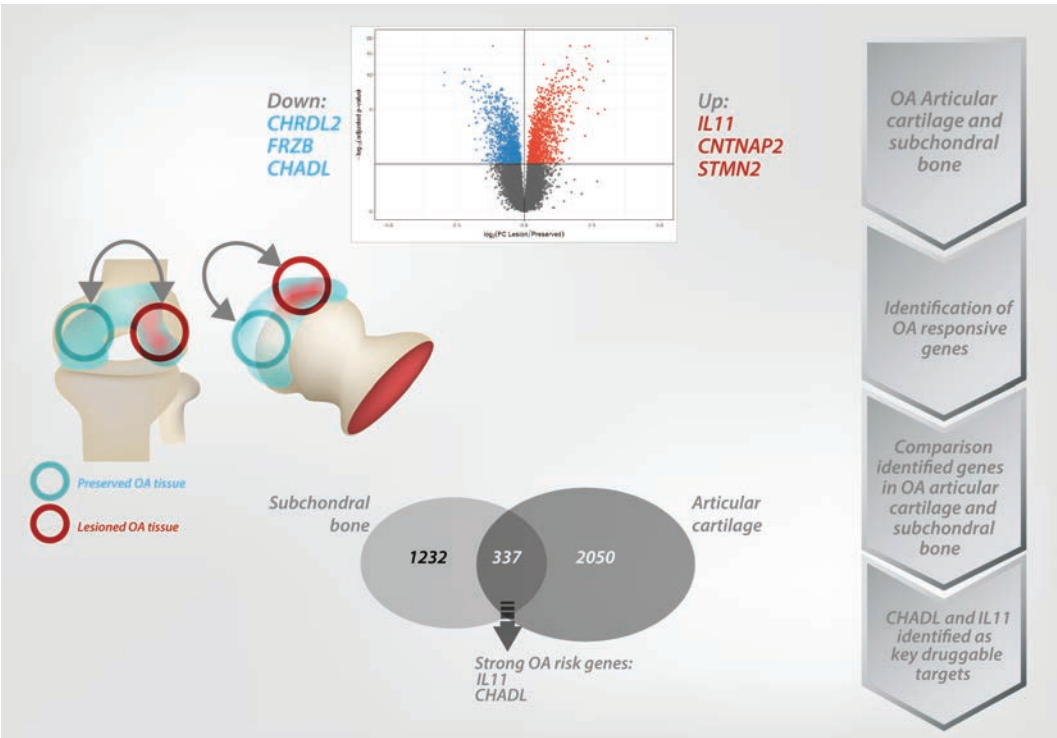

KEY POINTS

- Unlike cartilage, there is a distinct OA pathophysiology between subchondral bone of hips and knees based on the transcriptome.
- *IL11* and *CHADL* were among the overlapping differentially expressed genes between macroscopically preserved and lesioned OA bone and cartilage.
- *CHADL* was particularly differentially expressed in knee subchondral bone, suggesting that this gene may be a potential drug target for knee OA exclusively.

SUMMARY

The osteoarthritis (OA) disease process is characterized by unfavorable dynamic regulation of gene transcription in articular cartilage and subchondral bone in response to environmental perturbations. Nonetheless, studies exploring the transcriptome with OA pathophysiology have, thus far, focused solely on either articular cartilage or subchondral bone, leaving the dysregulation of interacting processes obscure. Tuerlings et al focused on expression profiling of OA subchondral bone in interaction with articular cartilage, using RNA sequencing data of overlapping bone and cartilage samples. Upon comparing the OA responsive genes in the subchondral bone to those in the cartilage, they found 337 overlapping genes. Among them, they identified *IL11* and *CHADL*, recently recognized as strong OA risk genes, as attractive targets for therapy development, effectively acting in the OA disease process in both tissues.

Suppression of Rheumatoid Arthritis by Enhanced Lymph Node Trafficking of Engineered Interleukin-10 in Murine Models

Yuba et al, *Arthritis Rheumatol* 2021;88:769–778

CORRESPONDENCE
Jun Ishihara, PhD: j.ishihara@imperial.ac.uk
Jeffrey A. Hubbell, PhD: jhubbell@uchicago.edu

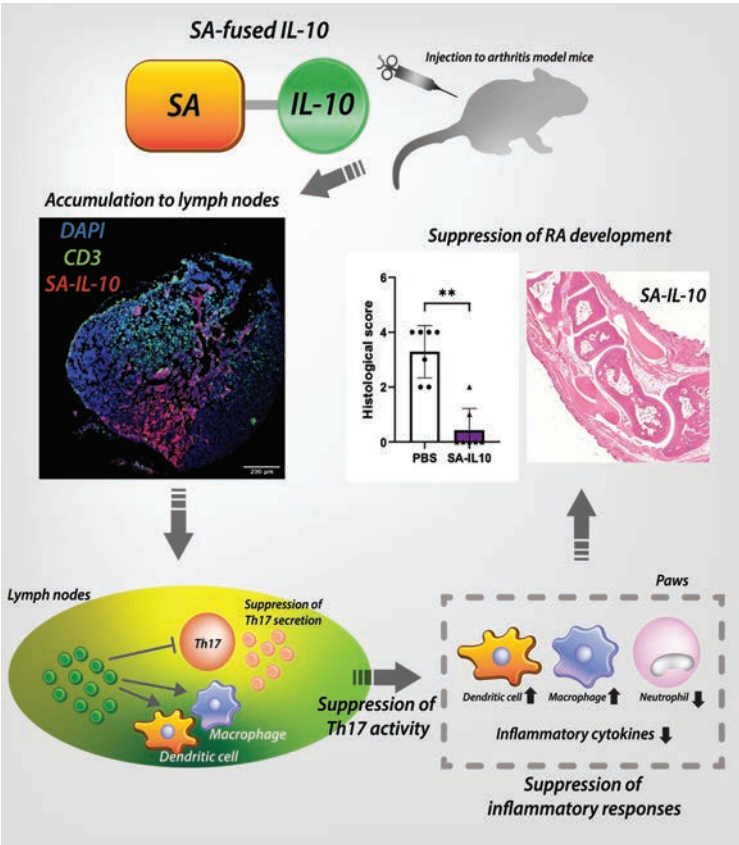

KEY POINTS

- SA fusion to IL-10 achieved increased persistence within the lymph nodes.
- SA–IL-10 suppressed the main inflammatory pathway of RA progression and exhibited marked therapeutic effects in both the CIA and CAIA models.
- SA–IL-10 induced high anti-inflammatory responses by any of the following administration routes: intravenous, subcutaneous, or footpad injections.

SUMMARY

Rheumatoid arthritis (RA) is a major autoimmune disease that causes synovitis and joint damage. Although clinical trials have been performed using interleukin-10 (IL-10), an antiinflammatory cytokine, as a potential treatment of RA, the therapeutic effects of IL-10 have been limited. This is potentially due to insufficient residence in lymphoid organs, where antigen recognition primarily occurs. Yuba et al engineered an IL-10–serum albumin (SA) fusion protein and evaluated its effects in murine models of RA. SA-fused IL-10 (SA–IL-10) was recombinantly expressed. Mice with collagen antibody–induced arthritis (CAIA) or collagen-induced arthritis (CIA) were injected intravenously with wild-type IL-10 or SA–IL-10, and the retention of SA–IL-10 in the lymph nodes (LNs), immune cell composition in the paws, and therapeutic effect of SA–IL-10 on mice with arthritis were assessed. SA fusion to IL-10 led to enhanced accumulation in the mouse LNs compared to unmodified IL-10. Intravenous SA–IL-10 treatment restored immune cell composition in the paws to a normal status, elevated the frequency of suppressive M2 macrophages, reduced IL-17A levels in the paw-draining LN, and protected joint morphology. Intravenous SA–IL-10 treatment showed similar efficacy as treatment with an anti–tumor necrosis factor antibody. SA–IL-10 was equally effective when administered intravenously, locally, or subcutaneously, which is a benefit for clinical translation of this molecule. Therefore, SA fusion to IL-10 is a simple but effective engineering strategy for RA therapy and has potential for clinical translation.

Arthritis & Rheumatology
Vol. 73, No. 5, May 2021, pp 721–724
DOI 10.1002/art.41638

American College of Rheumatology
Empowering Rheumatology Professionals

NOTES FROM THE FIELD

Reassessing the Cardiovascular Safety of Febuxostat: Implications of the Febuxostat Versus Allopurinol Streamlined Trial

Hyon K. Choi,[1] Tuhina Neogi,[2] Lisa K. Stamp,[3] Robert Terkeltaub,[4] and Nicola Dalbeth[5]

The US Food and Drug Administration (FDA)–mandated Cardiovascular Safety of Febuxostat and Allopurinol in Patients with Gout and Cardiovascular Morbidities (CARES) trial, published in 2018, demonstrated increased all-cause mortality and death from cardiovascular causes in participants randomized to receive febuxostat compared with allopurinol (1). The outcome of this trial and the subsequent FDA Drug Safety Communication and Boxed Warning (2) resulted in substantial reductions in febuxostat use in the US (3). The European Medicines Agency (EMA)–mandated Febuxostat versus Allopurinol Streamlined Trial (FAST), published in 2020, demonstrated no increased risk of composite cardiovascular events, cardiovascular disease (CVD) mortality, or all-cause mortality with febuxostat as compared with allopurinol (4). We will discuss implications of these new findings for gout management.

CARES trial findings

As described in our previous commentary (5), CARES was a multicenter, double-blind, noninferiority cardiovascular outcomes trial in 6,190 patients with gout and established CVD, with a median follow-up period of 32 months (Table 1) (1). Though CARES was a large clinical trial, there were important limitations including very high rates of study medication discontinuation (>50% of participants), large amounts of missing data (45% of participants did not complete all trial visits), and concerns about incomplete capture of cardiovascular and mortality events. Moreover, the majority of mortality events in the CARES trial (~85%) occurred when participants were not taking urate-lowering therapy (ULT). Hence, results of the EMA-mandated FAST study were widely anticipated.

The FAST study

The FAST study was a prospective, randomized, open-label, blinded–end point, noninferiority cardiovascular outcomes trial in 6,128 participants with gout and at least 1 additional cardiovascular risk factor, who were already receiving allopurinol (Table 1) (4). Following a run-in period in which allopurinol doses were optimized to achieve a serum urate level of <6 mg/dl, participants were randomized to either resume allopurinol at the optimized dose or begin treatment with febuxostat at 80 mg/day (increasing to 120 mg daily if required to achieve a serum urate level <6 mg/dl) after a washout period of 7–21 days. During the median follow-up period of ~43 months, the primary (on-treatment) analysis of major adverse cardiovascular events (MACE) (Table 1) revealed that febuxostat was noninferior to allopurinol, with an adjusted hazard ratio (HR) of 0.85 (95% confidence interval [95% CI] 0.70–1.03). In the febuxostat group, 3.8% of participants died (of any cause), compared with 5.7% of participants in the allopurinol group (HR 0.75 [95% CI 0.59–0.95]). Febuxostat (median dose 80 mg/day) led to lower serum urate levels than allopurinol (median dose 300 mg/day) throughout the study follow-up (mean 3.6 mg/dl versus 5.0 mg/dl). End points were assessed in a blinded manner by an independent clinical events classification committee.

FAST participant retention was excellent (94%). However, there was differential withdrawal of ULT during the first year (32.4% in the febuxostat group versus 16.5% in the allopurinol group),

[1]Hyon Choi, MD, DrPH: Massachusetts General Hospital, Boston; [2]Tuhina Neogi, MD, PhD: Boston University School of Medicine, Boston, Massachusetts; [3]Lisa K. Stamp, MBChB, PhD, FRACP: University of Otago, Christchurch, New Zealand; [4]Robert Terkeltaub, MD: VA San Diego Healthcare System and University of California San Diego; [5]Nicola Dalbeth, MBChB, MD, FRACP: University of Auckland, Auckland, New Zealand.

Dr. Choi has received consulting fees from Takeda and Selecta (less than $10,000 each) and research support from Horizon. Dr. Neogi has received consulting fees from Arthrosi (less than $10,000). Dr. Terkeltaub has received consulting fees from AstraZeneca, Horizon, Genentech, and Sobi (less than $10,000 each) and from Selecta (more than $10,000). Dr. Dalbeth has received consulting fees, speaking fees, and/or honoraria from AstraZeneca, Dyve, Selecta, Horizon, Arthrosi, Cello Health, AbbVie, and Janssen (less than $10,000 each). No other disclosures relevant to this article were reported.

Address correspondence to Hyon Choi, MD, DrPH, Massachusetts General Hospital, Division of Rheumatology, Allergy, and Immunology, 55 Fruit Street, Boston, MA 02114 (email: hchoi@mgh.harvard.edu); or to Nicola Dalbeth, MBChB, MD, FRACP, University of Auckland, Department of Medicine, Faculty of Medical and Health Sciences, 85 Park Road, Grafton, Auckland 1023, New Zealand (email: n.dalbeth@auckland.ac.nz).

Submitted for publication November 26, 2020; accepted in revised form December 31, 2020.

Table 1. Comparison of the CARES trial and the FAST study*

	CARES study (ref. 1)	FAST study (ref. 4)
Trial design	Prospective, randomized, multicenter noninferiority trial	Prospective, randomized, multicenter noninferiority trial
Blinding	Double-blind, blinded–end point adjudication	Open-label, blinded–end point adjudication
Setting	US, Mexico, and Canada	Scotland, England, Denmark, and Sweden
Start date	April 2010	December 2011
No. of participants randomized	6,190	6,128
Study population characteristics	Gout, history of major CVD, serum urate level ≥7.0 mg/dl (0.42 mmoles/liter) or ≥6.0 mg/dl (0.36 mmoles/liter), inadequately controlled gout	Gout, age ≥60 years, already receiving allopurinol, at least 1 additional cardiovascular risk factor
Relevant exclusions	MI or stroke within 60 days prior to screening, severe renal impairment	MI or stroke in the previous 6 months, congestive heart failure (NYHA class III or IV), severe renal impairment
% with established CVD	100	33.4
% with tophaceous gout	21.3	10.2
Run-in period	No	Yes, to optimize allopurinol dose to achieve serum urate levels <6 mg/dl (0.36 mmoles/liter) prior to randomization
Final daily febuxostat dose	Median dose 40 mg; 61.0% receiving 40 mg, 39.0% receiving 80 mg	Median dose 80 mg; 97.5% receiving 80 mg, 2.5% receiving 120 mg
Final daily allopurinol dose	Median dose 300 mg; 21.8% receiving 200 mg, 44.6% receiving 300 mg, 33.6% receiving ≥400 mg	Median dose 300 mg; 10.0% receiving 100 mg, 23.3% receiving 200 mg, 50.9% receiving 300 mg, 15.8% receiving ≥400 mg
Primary end point	Composite of death from cardiovascular cause, nonfatal MI, nonfatal stroke, or unstable angina with urgent revascularization	Composite of hospitalization for nonfatal MI or biomarker-positive acute coronary syndrome, nonfatal stroke, or death due to a cardiovascular event
Follow-up strategy for primary analysis	Study visits and telephone follow-up	Record linkage to centralized databases for hospitalizations, deaths, and cancer diagnoses, in addition to study visits and telephone follow-up
Primary analysis	Modified ITT noninferiority analysis with a noninferior limit of HR of 1.3	On-treatment noninferiority analysis with a noninferior limit of HR of 1.3
Median follow-up duration, days	Febuxostat 968; allopurinol 942	All 1,467
% lost to follow-up	45.0	5.8
% assigned drug discontinuation	Febuxostat 57.3; allopurinol 55.9	Febuxostat 32.4; allopurinol 16.5
% prescribed colchicine for gout flare prophylaxis (first 6 months)	Febuxostat 84.1; allopurinol 83.8	Febuxostat 71.4; allopurinol 52.6
Primary end point result	Primary ITT analysis: Febuxostat (10.8%) was noninferior to allopurinol (10.4%) (HR 1.03 [97% CI 0.87–1.23])	Primary on-treatment analysis: Febuxostat (5.6%) was noninferior to allopurinol (7.9%) (HR 0.85 [95% CI 0.70–1.03]) Secondary ITT analysis: Febuxostat (8.4%) was noninferior to allopurinol (9.3%) (HR 0.89 [95% CI 0.75–1.06])
All-cause deaths	Primary ITT analysis: There were more deaths with febuxostat (7.8%) than with allopurinol (6.4%) (HR 1.22 [95% CI 1.01–1.47])	Primary on-treatment analysis: Febuxostat (3.8%) was noninferior to allopurinol (5.7%) (HR 0.75 [95% CI 0.59–0.95]) Secondary ITT analysis: Febuxostat (7.2%) was noninferior to allopurinol (8.6%) (HR 0.84 [95% CI 0.71–1.01])
Death from cardiovascular causes	Primary ITT analysis: There were more deaths with febuxostat (4.3%) than with allopurinol (3.2%) (HR 1.34 [95% CI 1.03–1.73])	Primary on-treatment analysis: Febuxostat (2.0%) was noninferior to allopurinol (2.7%) (HR 0.91 [95% CI 0.66–1.27]) Secondary ITT analysis: Febuxostat (3.8%) was noninferior to allopurinol (4.0%) (HR 0.96 [95% CI 0.74–1.23])
Serum urate outcome	Similar proportion of participants had serum urate levels <6 mg/dl; more in the febuxostat group had serum urate levels <5 mg/dl	Mean follow-up serum urate level 3.6 mg/dl in the febuxostat group and 5.0 mg/dl in the allopurinol group
Gout flare outcome	Febuxostat 0.68 flares per patient-year; allopurinol 0.63 flares per patient-year	Febuxostat at least 1 flare (18 flares per 100 patient-years); allopurinol 20 flares per 100 patient-years

* CARES = Cardiovascular Safety of Febuxostat and Allopurinol in Patients with Gout and Cardiovascular Morbidities; FAST = Febuxostat versus Allopurinol Streamlined Trial; CVD = cardiovascular disease; MI = myocardial infarction; NYHA = New York Heart Association; ITT = intent-to-treat; HR = hazard ratio; 97% CI = 97% confidence interval.

and more participants in the febuxostat group (71.4%) received colchicine as gout flare prophylaxis compared with participants in the allopurinol group (52.6%). The fact that participants had previously been receiving allopurinol (for a median duration of 6 years) and had achieved the target urate level of <6 mg/dl by the time of randomization likely contributed to higher intolerance or discontinuation of febuxostat in this open-label study. Additional intent-to-treat (ITT) analyses, which kept the original trial assignment until the end of the follow-up period without differential loss, demonstrated results consistent with the primary findings (HR for MACE 0.89 [95% CI 0.75–1.06] and HR for all-cause death 0.84 [95% CI 0.71–1.01]), which supports the trial's internal validity. Similarly, unblinded switching to febuxostat, which was considered more potent than allopurinol, could have contributed to more prescriptions for colchicine gout flare prophylaxis in the febuxostat arm after the post-randomization washout period. Given the cardiovascular-protective effect of low-dose colchicine (6,7), these participants could have experienced the cardiovascular benefits, at least while exposed to colchicine. Nevertheless, subgroup analyses of participants not exposed to colchicine for gout flare prophylaxis showed consistent findings (HR 0.84 in on-treatment analysis and 0.82 in ITT analysis), suggesting that colchicine was probably not a significant factor.

Participants in the FAST study were recruited mainly in primary care settings, reflecting the clinical setting in which most gout is managed. As such, the study population (33% with CVD) is broadly applicable to the gout population at large. The FAST study excluded people who experienced myocardial infarction (MI) or stroke in the preceding 6 months or who had severe heart failure or chronic kidney disease, whereas in the CARES trial, patients who had experienced MI or stroke were excluded only if the event had occurred within 60 days prior to screening and a history of major CVD was required for enrollment in the CARES trial. The CARES trial also enrolled a higher proportion of participants with tophaceous gout (21% versus 10%), indicative of more severe disease. Considering the trial design, FAST findings should be most generalizable to febuxostat use after allopurinol use. However, if cardiovascular risk is not affected by (pre-trial) allopurinol use among people with gout (thus, not causing selection bias such as depletion of participants susceptible to cardiovascular conditions), generalizability of cardiovascular outcomes in the FAST study would also be analogous to that of a trial without universal pre-trial exposure to allopurinol (e.g., CARES).

To date, there is no high-level evidence for the mortality or cardiovascular impact of allopurinol, leaving unclear the inference of the generalizability of the FAST study in relation to trials without a lead-in exposure to allopurinol. Overall rates of serious adverse events (SAEs) were similar between groups, and there were fewer neoplasms, including malignant neoplasms, in the febuxostat group in the FAST study. Nevertheless, patients who had experienced AEs or other tolerability issues associated with the initiation of allopurinol would have been selected out before the FAST study, while febuxostat was an incident exposure, thus not benefiting from such a selection process.

Remaining uncertainties after the FAST trial

Below we discuss some remaining uncertainties after the FAST study, some of which are more readily addressable than others.

1. The absence of a placebo arm in the FAST study or CARES trial makes it unclear whether allopurinol or febuxostat has any impact on cardiovascular events compared with no use of ULT in people with gout. However, use of a placebo would be ethically challenging given the indications for ULT in these trial participants with gout (8).
2. While the results from the subgroup analysis among those not exposed to colchicine prophylaxis were consistent with the main findings, formal mediation analysis of post-randomization exposure to colchicine would be valuable in this at-risk gout population.
3. A formal time-varying analysis would have been helpful to assess potential reasons for ULT discontinuation beyond postulating simple reluctance and resistance to switching to a new drug (febuxostat) from an effective drug.
4. There was a lower risk of the primary cardiovascular end point for febuxostat (adjusted HR 0.66 [95% CI 0.51–0.86]) in the subgroup with baseline serum urate levels <5 mg/dl, but no such difference among those with baseline serum urate levels ≥5 mg/dl. Clarifying associations between serum urate levels and cardiovascular risk in the FAST study would be valuable.
5. Additional data on requirements for ULT, particularly after discontinuation of febuxostat, would be helpful, as findings of the ITT analysis could potentially be impacted if participants began treatment with the other urate-lowering agent (including reinitiating allopurinol after stopping febuxostat) during the trial follow-up.
6. The potential role of gout flares in cardiovascular risk remains unclear. Neither the CARES nor the FAST trial provided characterization of flare burden (severity, duration, frequency) that might mediate cardiovascular events.

Implications of the FAST findings together with CARES trial data

Notwithstanding some uncertainties associated with the FAST study, and the differences from the CARES trial (Table 1), the FAST findings suggest that the CARES trial could have been critically hampered by its high rate of loss to follow-up (45%), as shown by its post hoc ascertainment nullifying the mortality risk associated with febuxostat use (1). Despite the higher febuxostat doses in the FAST study (median 80 mg daily, versus 40 mg daily in CARES), febuxostat tended to have a lower mortality risk

than allopurinol in the FAST study, significantly lower in the on-treatment analysis (primary approach), by ~25%, as discussed above. It remains unclear whether further lowering serum urate levels with a higher febuxostat dose mediated this finding. While the FAST findings may not clarify all the concerns raised by the CARES trial for patients with gout and established CVD, it is also important to remember that >55% of CARES participants discontinued study medication and 45% were lost to follow-up. With discontinuation and rates of loss to follow-up this extreme, it is very difficult to ensure the internal validity of the findings, as noted in the conflicting findings from the fuller post hoc ascertainment (1). Furthermore, the CARES trial showed internal inconsistency between primary MACE and CVD mortality end points, whereas FAST findings were internally consistent. Finally, results of several recent large-scale pharmacoepidemiologic studies also support the findings of the FAST study but not the CARES trial (9–11).

If results from the FAST study had demonstrated any evidence of increased risk of mortality, it would have furthered the concerns raised by the CARES trial findings. However, FAST findings did not demonstrate any such signal, and there was actually a suggestion of survival benefit associated with febuxostat use in the FAST study, even with a mean doubling of the febuxostat exposure dose. While there are a number of differences between the CARES study and the FAST study, the most important one threatening internal validity is the rate of loss to follow-up in the CARES trial (45%, versus 6% in FAST). To this end, the FAST study is considered to have superior internal validity compared with the CARES study, regardless of generalizability (external validity). Naturally, generalizability matters as well; however, without internal validity, i.e., valid effect estimates, generalizability is meaningless. Thus, based on the current evidence, it is our view that the collective verdict on the cardiovascular safety of febuxostat should rely more on results from the FAST study than CARES results. To this end, we support the FAST authors' suggestion that regulatory agencies update their guidance on the cardiovascular risk associated with the use of febuxostat (4).

AUTHOR CONTRIBUTIONS

All authors drafted the article, revised it critically for important intellectual content, and approved the final version to be published.

REFERENCES

1. White WB, Saag KG, Becker MA, Borer JS, Gorelick PB, Whelton A, et al. Cardiovascular safety of febuxostat or allopurinol in patients with gout. N Engl J Med 2018;378:1200–10.
2. US Food and Drug Administration. FDA adds boxed warning for increased risk of death with gout medicine Uloric (febuxostat): FDA drug safety communication. February 2019. URL: https://www.fda.gov/drugs/drug-safety-and-availability/fda-adds-boxed-warning-increased-risk-death-gout-medicine-uloric-febuxostat.
3. Kim SC, Neogi T, Kim E, Lii J, Desai RJ. Trends in utilization of urate-lowering therapies following the US Food and Drug Administration's boxed warning on febuxostat. Arthritis Rheumatol 2021;73:542–3.
4. Mackenzie IS, Ford I, Nuki G, Hallas J, Hawkey CJ, Webster J, et al. Long-term cardiovascular safety of febuxostat compared with allopurinol in patients with gout (FAST): a multicentre, prospective, randomised, open-label, non-inferiority trial. Lancet 2020;396:1745–57.
5. Choi H, Neogi T, Stamp L, Dalbeth N, Terkeltaub R. Implications of the Cardiovascular Safety of Febuxostat and Allopurinol in Patients With Gout and Cardiovascular Morbidities trial and the associated Food and Drug Administration public safety alert. Arthritis Rheumatol 2018;70:1702–9.
6. Tardif JC, Kouz S, Waters DD, Bertrand OF, Diaz R, Maggioni AP, et al. Efficacy and safety of low-dose colchicine after myocardial infarction. N Engl J Med 2019;381:2497–505.
7. Nidorf SM, Fiolet AT, Mosterd A, Eikelboom JW, Schut A, Opstal TS, et al. Colchicine in patients with chronic coronary disease. N Engl J Med 2020;383:1838–47.
8. Shmerling RH. The ethics of recent gout trials [editorial]. Arthritis Rheumatol 2016;68:2057–60.
9. Zhang M, Solomon DH, Desai RJ, Kang EH, Liu J, Neogi T, et al. Assessment of cardiovascular risk in older patients with gout initiating febuxostat versus allopurinol: population-based cohort study. Circulation 2018;138:1116–26.
10. Chen CH, Chen CB, Chang CJ, Lin YJ, Wang CW, Chi CC, et al. Hypersensitivity and cardiovascular risks related to allopurinol and febuxostat therapy in Asians: a population-based cohort study and meta-analysis. Clin Pharmacol Ther 2019;106:391–401.
11. Kang EH, Choi HK, Shin A, Lee YJ, Lee EB, Song YW, et al. Comparative cardiovascular risk of allopurinol versus febuxostat in patients with gout: a nation-wide cohort study. Rheumatology (Oxford) 2019;58:2122–9.

Arthritis & Rheumatology
Vol. 73, No. 5, May 2021, pp 725–727
DOI 10.1002/art.41670

American College of Rheumatology
Empowering Rheumatology Professionals

EDITORIAL

Combining Data Sets as Well as Therapies Shows Improved Outcome in Connective Tissue Disease–Associated Pulmonary Hypertension

Christopher P. Denton and Julia Spierings

The article by Khanna et al in this issue of *Arthritis & Rheumatology* (1) is an important summary of more than two decades of progress in management of connective tissue disease (CTD)–associated pulmonary hypertension (PH) that provides a robust platform for further advances. It also clearly shows the positive impact of current practice, in which combination therapy is introduced early and emphasis is placed on proactive screening to make an early diagnosis of PH.

PH remains a major cause of death in some forms of CTD and is challenging to manage in the context of multisystem complications and potentially overlapping pathogenetic mechanisms. This is particularly true in patients with systemic sclerosis (SSc), in whom PH has been shown to be associated with high mortality in small observational cohorts (2) as well as larger, more comprehensive data sets. Fortunately, there has been substantial progress in managing some forms of PH, notably precapillary pulmonary arterial hypertension (PAH). This clinical progress has been built on a foundation of robust pivotal clinical trials and underscored by observational cohorts and registries that explore long-term outcomes with standard licensed therapies. Of these registries, some include all forms of PH (3,4), whereas others focus on PAH of specific disease associations (5).

The classification of PH was fundamentally changed in 1998 at the Second World Health Organization (WHO) meeting in Evian, Switzerland. In this WHO meeting, 5 subgroups of PH were proposed to reflect different pathogenic mechanisms. This template has been refined and updated at subsequent meetings that became designated the World Symposia in Pulmonary Hypertension, with the third meeting and subsequent meetings occurring at 5-year intervals. The most recent was the 6th World Symposium in Nice, France in 2018 (6) (Table 1). The latest classification retains the basic groups that differentiate primary vasculopathy from secondary causes of PH, with the associated diagnosis including CTD for group 1 PAH. Definition of these different forms of PH, and especially group 1 PAH, is central to therapeutic advances, because by linking forms of PH with likely shared pathogenesis, it has allowed trials to recruit mixed cohorts, including those with CTD-PAH, and has thus led to these groups being included within the licensed indication as regulatory approval was obtained based on robust phase III clinical trials.

Terminology matters in CTD-PAH, because the real progress has been made for patients with group 1 precapillary PAH. This needs to be distinguished from other frequent causes of PH in CTD, which include group 2 PH due to cardiac disease and associated with elevated postcapillary pressure, and group 3 PH due to hypoxia from lung fibrosis or muscle weakness. The latest classification of the World Symposium (from 2018) can be used to distinguish these groups (Table 1).

As in idiopathic and familial forms of PAH, improvements in group 1 PAH are underpinned by the use of pulmonary vasodilator drugs of 3 classes, which most recently became available in oral formulation. The first orally active drug was bosentan, an endothelin receptor antagonist (ERA), which was approved by the US Food and Drug Administration in November 2001. Pivotal trials showed benefit, with evidence of improvement in exercise distance measured using a 6-minute walk test. CTD-PAH patients showed a blunted but congruent response to bosentan in comparison to the overall study population, and this allowed the subgroup of CTD-PAH to be included within the regulatory approval (7). The same trial template was used for licensing studies of phosphodiesterase 5 (PDE5) inhibitors, which work as agonists of the nitric oxide pathway (8), and more recently for the

Dr. Spierings's work was supported by travel awards from the European Scleroderma Trials and Research group, the European League Against Rheumatism, and the Catharine van Tussenbroek Fund.

Christopher P. Denton, PhD, FRCP, Julia Spierings, MD, PhD: University College London and Royal Free Hospital, London, UK.

Dr. Denton has received consulting fees, speaking fees, and/or honoraria from GlaxoSmithKline, Mitsubishi Tanabe, Boehringer Ingelheim, Servier, Arxx Therapeutics, Bayer, Inventiva, Galápagos, Horizon, Roche, CSL Behring, Sanofi, and Novartis (less than $10,000 each). No other disclosures relevant to this article were reported.

Address correspondence to Christopher P. Denton, PhD, FRCP, University College London, Rowland Hill Street, London NW3 2PF, UK. Email: c.denton@ucl.ac.uk.

Submitted for publication November 24, 2020; accepted in revised form January 26, 2021.

Table 1. Classification of pulmonary hypertension*

Group 1: PAH
Idiopathic PAH
Heritable PAH
Drug- and toxin-induced PAH
PAH associated with
CTDs†
HIV
Portal hypertension
Congenital heart disease
Schistosomiasis
PAH with venous/capillary involvement†
Group 2: PH due to left-sided heart disease
PH due to heart failure with preserved LVEF†
PH due to heart failure with reduced LVEF†
Vascular heart disease
Congenital/acquired cardiovascular conditions leading to postcapillary PH
Group 3: PH due to lung disease
Obstructive lung disease
Restrictive lung disease†
Other lung disease with mixed restrictive/obstructive pattern
Hypoxia without lung disease
Developmental lung disorders
Group 4: PH due to pulmonary artery obstructions
Chronic thromboembolic PH†
Other pulmonary artery obstructions
Group 5: PH with unclear and/or multifactorial mechanisms
Hematologic disorders
Systemic and metabolic disorders
Complex congenital heart disease
Others

* Classification of pulmonary hypertension (PH) is based on the definitions from the 2018 6th World Symposium in Nice, France. PAH = pulmonary arterial hypertension; HIV = human immunodeficiency virus; LVEF = left ventricular ejection fraction; PVOD = pulmonary veno-occlusive disease.
† Mixed patterns of PH with more than one mechanism are frequent in connective tissue diseases (CTDs). See ref. 6 for a more detailed description of the current classification.

oral soluble guanylate cyclase stimulator riociguat, which works on the same pathway (9).

Prostacyclin agonists have been available for many years for parenteral use, and more recently administered by inhalation, but it was the oral prostacyclin receptor agonist selexipag that really offered the full potential to target all 3 pathways easily in PAH, and especially in CTD-PAH (10). This therapeutic advance was important because the efficacy of new therapies, including selexipag and macitentan, was recently approved on the basis of findings from much larger and more robust clinical trials in which mortality and morbidity were assessed in a composite outcome of "time to clinical worsening" between treatment arms (9,10). Moreover, because the therapeutic landscape changed, approved therapies became widely available, which enabled trials to permit appropriate background treatment and test the benefit of adding a new agent on top of 1 or even 2 approved drugs. Importantly, these event-driven studies have shown much more comparable relative benefit of treatment in the CTD-PAH subgroup, and also the SSc-PAH group. This is important because studies of different cohorts and other studies, including analyses of pooled individual patient data from some earlier PAH trials, have shown that outcomes, including survival, are especially poor in patients with SSc-PAH (11,12).

A third area of progress was the use of initial combination treatment, with results strongly suggesting that the combination of an ERA with a PDE5 inhibitor was better than either treatment alone. This was the pretext of the AMBITION trial (Ambrisentan plus Tadalafil in PAH), which demonstrated benefit from this combination treatment and confirmed an equivalent benefit in patients with CTD and patients with SSc-PAH (13). These trials have underpinned common clinical practice over the last decade, particularly in patients with SSc, in whom PAH moved from being untreatable, inevitably leading to early death (median survival of only 12 months from diagnosis [2]), to a highly treatable complication. Single-center studies have also produced results suggesting benefit from combination therapy (14), but Khanna et al (1) provide a compendium of evidence showing how much outcomes have improved, by pooling the data from high-quality, event-driven trials and large, well-collected clinical cohorts.

The meta-analyses by Khanna et al (1) are timely and important, because previous well-performed meta-analyses of the early pivotal trials had suggested the opposite, that CTD-PAH outcomes were not better, that high-cost drugs may not be justified, and that other approaches to treatment were needed. Notably, the present meta-analyses (1) again confirm that outcomes are worse in patients with CTD-PAH than in those with idiopathic or familial forms of PAH, and the impact of treatments should no longer be regarded as insignificant. This is a practice-changing observation, especially now that many of the drugs are available in generic formulations, and therefore the cost of modern PAH treatment has declined at the same time as its true value is convincingly demonstrated.

Although the apparent improvement in overall survival in CTD-PAH is encouraging, it is important to recognize that there are multiple confounding factors that could also lead to apparent gains. These include the increased emphasis on PH and PAH as a result of the availability of new therapies, which can increase vigilance and awareness and may lead to more diagnoses of milder cases or cases at an early stage. This may also lead to lead time bias. In addition, the establishment of screening methods and algorithms such as DETECT (the first evidence-based algorithm for the screening of PAH in SSc) and others could result in earlier detection and diagnosis of PAH and more identification of milder cases. Finally, better organization of care and coordinated management may improve outcome and survival, even when there is no major benefit from treatments. However, it seems unlikely that these factors would have a major impact, because regular screening has been a management cornerstone for CTD-PAH for many years, and therefore increased detection likely occurred before more treatment became available.

In conclusion, it is now clear there is strong evidence for the value of combination therapies in CTD-PAH. This includes

PAH-targeted drugs often used in combination, and the concurrent use of immunosuppression and PH-specific drugs in cases of CTD-PAH associated with systemic lupus erythematosus or mixed CTD (15). Not all treatment can be translated from idiopathic PAH to CTD-PAH, and the large registries also underscore this. A good example is oral anticoagulation therapy, which may improve overall survival in those with idiopathic PAH but could be associated with higher mortality in patients with CTD-PAH (3). Unfortunately, there is still no cure for CTD-PAH, and most patients will die from right-sided heart failure. Therefore, there is still much unmet need and work to be done. It is exciting that new drugs targeting different pathways or mechanisms are looking promising (including bardoxelone [ClinicalTrials.gov identifier NCT02036970] and sotatercept [ClinicalTrials.gov identifier NCT03496207]), and in the future these and other approaches may also be added to the armamentarium for the management of CTD-PAH.

AUTHOR CONTRIBUTIONS

Drs. Denton and Spierings drafted the article, revised it critically for important intellectual content, and approved the final version to be published.

REFERENCES

1. Khanna D, Zhao C, Saggar R, Mathai SC, Chung L, Coghlan JG, et al. Long-term outcomes in patients with connective tissue disease–associated pulmonary arterial hypertension in the modern treatment era: meta-analyses of randomized, controlled trials and observational registries. Arthritis Rheumatol 2021;73:837–47.
2. Koh ET, Lee P, Gladman DD, Abu-Shakra M. Pulmonary hypertension in systemic sclerosis: an analysis of 17 patients. Br J Rheumatol 1996;35:989–93.
3. Hoeper MM, Kramer T, Pan Z, Eichstaedt CA, Spiesshoefer J, Benjamin N, et al. Mortality in pulmonary arterial hypertension: prediction by the 2015 European pulmonary hypertension guidelines risk stratification model. Eur Respir J 2017;50:1700740.
4. Benza RL, Miller DP, Barst RJ, Badesch DB, Frost AE, McGoon MD. An evaluation of long-term survival from time of diagnosis in pulmonary arterial hypertension from the REVEAL Registry. Chest 2012;142:448–56.
5. Kolstad KD, Li S, Steen V, Chung L, on behalf of the PHAROS Investigators. Long-term outcomes in systemic sclerosis-associated pulmonary arterial hypertension from the Pulmonary Hypertension Assessment and Recognition of Outcomes in Scleroderma Registry (PHAROS). Chest 2018;154:862–71.
6. Simonneau G, Montani D, Celermajer DS, Denton CP, Gatzoulis MA, Krowka M, et al. Haemodynamic definitions and updated clinical classification of pulmonary hypertension. Eur Respir J 2019;53:1801913.
7. Denton CP, Humbert M, Rubin L, Black CM. Bosentan treatment for pulmonary arterial hypertension related to connective tissue disease: a subgroup analysis of the pivotal clinical trials and their open-label extensions. Ann Rheum Dis 2006;65:1336–40.
8. Galiè N, Ghofrani HA, Torbicki A, Barst RJ, Rubin LJ, Badesch D, et al, for the Sildenafil Use in Pulmonary Arterial Hypertension (SUPER) Study Group. Sildenafil citrate therapy for pulmonary arterial hypertension. N Engl J Med 2005;353:2148–57.
9. Humbert M, Coghlan JG, Ghofrani HA, Grimminger F, He JG, Riemekasten G, et al. Riociguat for the treatment of pulmonary arterial hypertension associated with connective tissue disease: results from PATENT-1 and PATENT-2. Ann Rheum Dis 2017;76:422–6.
10. Sitbon O, Channick R, Chin KM, Frey A, Gaine S, Galiè N, et al. Selexipag for the treatment of pulmonary arterial hypertension. N Engl J Med 2015;373:2522–33.
11. Pulido T, Adzerikho I, Channick RN, Delcroix M, Galiè N, Ghofrani HA, et al. Macitentan and morbidity and mortality in pulmonary arterial hypertension. N Engl J Med 2013;369:809–18.
12. Rhee RL, Gabler NB, Sangani S, Praestgaard A, Merkel PA, Kawut SM. Comparison of treatment response in idiopathic and connective tissue disease-associated pulmonary arterial hypertension. Am J Respir Crit Care Med 2015;192:1111–7.
13. Coghlan JG, Galiè N, Barberà JA, Frost AE, Ghofrani HA, Hoeper MM, et al. Initial combination therapy with ambrisentan and tadalafil in connective tissue disease-associated pulmonary arterial hypertension (CTD-PAH): subgroup analysis from the AMBITION trial. Ann Rheum Dis 2017;76:1219–27.
14. Williams MH, Das C, Handler CE, Akram MR, Davar J, Denton CP, et al. Systemic sclerosis associated pulmonary hypertension: improved survival in the current era. Heart 2006;92:926–32.
15. Sanchez O, Sitbon O, Jaïs X, Simonneau G, Humbert M. Immunosuppressive therapy in connective tissue diseases-associated pulmonary arterial hypertension. Chest 2006;130:182–9.

American College of Rheumatology
Empowering Rheumatology Professionals

Arthritis & Rheumatology
Vol. 73, No. 5, May 2021, pp 728–730
DOI 10.1002/art.41673

EDITORIAL

Could Compensatory Autoantibody Production Affect Rheumatoid Arthritis Etiopathogenesis?

Gregg J. Silverman

The article by Anaparti and coworkers published in this issue of *Arthritis & Rheumatology* (1) represents an important chapter in the study of rheumatoid arthritis (RA) in a unique cohort of First Nations patients and their at-risk first-degree relatives (FDRs). These members of the Cree and Chippewa tribes in rural Manitoba, Canada share racial/ethnic (and presumed genetic) features distinct from other RA cohorts. Anaparti et al show that during the preclinical phase, when patients were asymptomatic, these First Nations FDRs expressed serum RA disease–associated anti–citrullinated protein antibodies (ACPAs), anti–carbamylated protein antibodies, and rheumatoid factors (RFs). However, unique to this cohort, during the preclinical phase these First Nations FDRs also had high levels of antinuclear antibodies (ANAs), and more than half had ANAs detectable by indirect immunofluorescence assay of HEp-2 cells at a serum dilution of ≥1:160 (1). In this context, this type of parallel autoantibody response has been termed "latent autoimmunity"(2,3). Notably, the RA patients in this First Nations cohort have relatives that display much higher rates of both the preclinical autoantibody expressors and RA progressors than have been reported in White RA FDR populations (4). Yet there appears to be a paradox, since in the First Nations FDRs, serum ACPA levels generally increased as the onset of overt disease approached, even though in the same individual the serum ANA levels remained stable over time (1). The authors rightly wonder what these ANAs represented in these individuals, and whether these autoantibodies may also contribute to RA pathogenesis.

In general, we do not understand what triggers the onset of systemic autoimmunity during the preclinical phase of the disease. In these individuals, the ANA could be a reflection of a form of generalized immune dysregulation that is an integral step toward the development of overt RA, just as this has been reported to be part of the preclinical phase of systemic lupus erythematosus (SLE). Of relevance, it has been postulated that the RA-associated autoimmune responses may be initiated at mucosal surfaces, such as in the lungs where infectious and inflammatory immune encounters are not uncommon (5).

The earliest evidence of a preclinical systemic autoimmune state in RA was reported decades ago, with studies demonstrating that circulating RFs preceded the diagnosis of RA, often by many years (6–10). With the later discovery of ACPAs, it was perhaps inevitable that ACPAs would also be found to arise during this preclinical phase (11). However, those earlier reports described retrospective surveys that were inadequate to determine whether such periods of RF or ACPA expression were always followed by overt synovial disease. Equally important, we do not know whether there are also FDRs who develop circulating ACPA and/or RF responses that later disappear because their presumed breaches in immunologic tolerance are mended. These questions are in part the focus of several recent and ongoing prospective studies (12–14), including the study by Anaparti et al (1).

As clinicians, we focus on the evaluation and treatment of patients at the self-perpetuating phase of RA. For practical reasons, few people are studied for autoantibody expression in the absence of clinically evident disease, and it has therefore been difficult to gain an accurate and detailed understanding of the molecular and cellular events associated with the moment of transition from preclinical phase to overt joint disease and tissue injury. It has been postulated that this transition is the consequence of the flooding of diverse adaptive and innate immune cells into the synovium. These disorganized synovial infiltrates may then undergo a transformation into the invasive pannus, which causes bone, tendon, and cartilage damage. This transition phase is believed to be paralleled by increases in serum levels of inflammatory cytokines (e.g., interleukin-6), chemokines (15,16), and a broadening range of autoantibody types and specificities (17,18). This process could initially be triggered by local synovial deposition of immune complexes, composed of ACPAs and RFs, that locally activate the classical complement cascade.

Gregg J. Silverman, MD: New York University Grossman School of Medicine, New York.
No potential conflicts of interest relevant to this article were reported.
Address correspondence to Gregg J. Silverman, MD, New York University Grossman School of Medicine, 435 East 30th Street, New York, NY 10016. Email: Gregg.Silverman@nyulangone.org.
Submitted for publication January 4, 2021; accepted in revised form January 28, 2021.

It has been suggested that the triggering event, which is at the checkpoint for disease development, is intertwined with increases in gut permeability that are regulated by the release of zonulin by gut epithelial cells (19). With the resultant dissolution of the tight junctions between epithelial cells that maintain the gut barrier, intestinal luminal factors, such as bacterial endotoxins and lipoglycans, then gain entry to the systemic immune system, resulting in the activation of host sentinel immune cells that produce the inflammatory factors.

In their study, Anaparti and colleagues did a convincing job of proving that the antibodies, which were detected based on ANA properties, were not also reactive in the ACPA immunoassay (1). It may be relevant that in truth there are few antibody binding autospecificities among ANAs that have been shown to be directly pathogenic (e.g., anti–native DNA in renal disease and anti-Ro in the fetus). Indeed, as the authors mention, low levels of ANAs are not uncommon, even in healthy individuals. Yet the isotype and subclass of an antibody are major determinants of functional effector activity, as even among IgG antibodies not all subclasses trigger activating Fc receptors that can mediate tissue injury. Of high relevance, anti–native DNA antibodies of the IgM isotype are reported to correlate with protection against kidney involvement in lupus (20). Anaparti et al used only a limited set of assays, so much could have been overlooked. Therefore, many types of coexpressed autoantibodies would have been undetected, especially if their true antigenic targets were not even suspected. In fact, IgM and IgA antibodies were also not considered.

In one scenario, in these First Nations patients with new-onset RA, the detected ANAs and the truly disease-associated autoantibodies (i.e., ACPA and RF) may be produced by lymphocyte clones from distinct B cell subsets. In theory, during the transition to overt RA, the production of ANAs and other "natural antibodies" in these FDRs could be bystander effects, possibly due to damage-associated molecular pattern–mediated activation (e.g., Toll-like receptor) of innate-like B cells (such as B-1 cells and marginal zone B cells). Indeed, antibodies that utilize the V_H4–34 gene segment can have the properties of ANAs, or apoptotic cell binders, or even RFs. All of these types of autoantibodies may represent forms of protective antibodies, which, through recognition of neoepitopes on apoptotic cells (21), can function in vivo to enhance neat and clean clearance of debris of injured, apoptotic, and necrotic cells to reinforce homeostasis, and ameliorate inflammatory responses (22). Such induced autoantibody responses can block the development of experimental collagen-induced arthritis that shares key molecular and cellular pathologic features with clinical RA (23). Hence, the stable levels of ANAs could be the misidentified tip of an iceberg of diverse clonal sets of natural autoantibodies, which could be counterregulatory for RA progression. Therefore, in the First Nations FDRs described by Anaparti et al, this parallel set of autoantibodies could represent an attempt by the immune system to clear injured tissue and reestablish homeostasis.

Future studies are needed to consider whether these First Nations RA patients have shared genetic or epigenetic abnormalities that are at the source of this broad autoimmunity. To determine how unique these high-level ANAs in this First Nations FDR group are, other RA cohorts should also be investigated at this period of transition to more closely search for patterns similar to those of SLE-associated autoantibodies. In addition, investigations should widen the scope to survey for other potential types of autoantibody specificities that include different specificities of apoptotic cell binders. It is possible that in the newly developing synovial infiltrates there are ANA/antiapoptotic cell–producing protective B cells, which act to slow local pathogenesis and disease progression. To examine the other side of these questions, the clinically unaffected First Nations FDRs should be examined to determine if there are also FDRs who do not develop RA because of the production of protective and perhaps preventative autoantibodies.

AUTHOR CONTRIBUTIONS

Dr. Silverman drafted the article, revised it critically for important intellectual content, and approved the final version to be published.

REFERENCES

1. Anaparti V, Smolik I, Meng X, O'Neil L, Jantz MA, Fritzler MJ, et al. Expansion of alternative autoantibodies does not follow the evolution of anti–citrullinated protein antibodies in preclinical rheumatoid arthritis: an analysis in at-risk first-degree relatives. Arthritis Rheumatol 2021;73:740–9.
2. Molano-Gonzalez N, Rojas M, Monsalve DM, Pacheco Y, Acosta-Ampudia Y, Rodriguez Y, et al. Cluster analysis of autoimmune rheumatic diseases based on autoantibodies. New insights for polyautoimmunity. J Autoimmun 2019;98:24–32.
3. James JA, Chen H, Young KA, Bemis EA, Seifert J, Bourn RL, et al. Latent autoimmunity across disease-specific boundaries in at-risk first-degree relatives of SLE and RA patients. EBioMedicine 2019;42:76–85.
4. Peschken CA, Hitchon CA, Robinson DB, Smolik I, Barnabe CR, Prematilake S, et al. Rheumatoid arthritis in a North American native population: longitudinal followup and comparison with a white population. J Rheumatol 2010;37:1589–95.
5. Holers VM, Demoruelle MK, Kuhn KA, Buckner JH, Robinson WH, Okamoto Y, et al. Rheumatoid arthritis and the mucosal origins hypothesis: protection turns to destruction [review]. Nat Rev Rheumatol 2018;14:542–57.
6. Aho K, Heliovaara M, Maatela J, Tuomi T, Palosuo T. Rheumatoid factors antedating clinical rheumatoid arthritis. J Rheumatol 1991; 18:1282–4.
7. Silman AJ, Hennessy E, Ollier B. Incidence of rheumatoid arthritis in a genetically predisposed population. Br J Rheumatol 1992;31:365–8.
8. Kurki P, Aho K, Palosuo T, Heliövaara M. Immunopathology of rheumatoid arthritis: antikeratin antibodies precede the clinical disease. Arthritis Rheum 1992;35:914–7.
9. Del Puente A, Knowler WC, Pettitt DJ, Bennett PH. The incidence of rheumatoid arthritis is predicted by rheumatoid factor titer in a longitudinal population study. Arthritis Rheum 1988;31:1239–44.
10. Walker DJ, Pound JD, Griffiths ID, Powell RJ. Rheumatoid factor tests in the diagnosis and prediction of rheumatoid arthritis. Ann Rheum Dis 1986;45:684–90.

11. Rantapää-Dahlqvist S, de Jong BA, Berglin E, Hallmans G, Wadell G, Stenlund H, et al. Antibodies against cyclic citrullinated peptide and IgA rheumatoid factor predict the development of rheumatoid arthritis. Arthritis Rheum 2003;48:2741–9.
12. Gerlag DM, Safy M, Maijer KI, Tang MW, Tas SW, Starmans-Kool MJ, et al. Effects of B-cell directed therapy on the preclinical stage of rheumatoid arthritis: the PRAIRI study. Ann Rheum Dis 2019;78:179–85.
13. Kolfenbach JR, Deane KD, Derber LA, O'Donnell C, Weisman MH, Buckner JH, et al. A prospective approach to investigating the natural history of preclinical rheumatoid arthritis (RA) using first-degree relatives of probands with RA. Arthritis Rheum 2009;61:1735–42.
14. Al-Laith M, Jasenecova M, Abraham S, Bosworth A, Bruce IN, Buckley CD, et al. Arthritis prevention in the pre-clinical phase of RA with abatacept (the APIPPRA study): a multi-centre, randomised, double-blind, parallel-group, placebo-controlled clinical trial protocol. Trials 2019;20:429.
15. Lingampalli N, Sokolove J, Lahey LJ, Edison JD, Gilliland WR, Holers VM, et al. Combination of anti-citrullinated protein antibodies and rheumatoid factor is associated with increased systemic inflammatory mediators and more rapid progression from preclinical to clinical rheumatoid arthritis. Clin Immunol 2018;195:119–26.
16. Moura RA, Canhao H, Polido-Pereira J, Rodrigues AM, Navalho M, Mourao AF, et al. BAFF and TACI gene expression are increased in patients with untreated very early rheumatoid arthritis. J Rheumatol 2013;40:1293–302.
17. Sokolove J, Bromberg R, Deane KD, Lahey LJ, Derber LA, Chandra PE, et al. Autoantibody epitope spreading in the pre-clinical phase predicts progression to rheumatoid arthritis. PLoS One 2012; 7:e35296.
18. Nielen MM, van Schaardenburg D, Reesink HW, van de Stadt RJ, van der Horst-Bruinsma IE, de Koning MH, et al. Specific autoantibodies precede the symptoms of rheumatoid arthritis: a study of serial measurements in blood donors. Arthritis Rheum 2004;50:380–6.
19. Tajik N, Frech M, Schulz O, Schalter F, Lucas S, Azizov V, et al. Targeting zonulin and intestinal epithelial barrier function to prevent onset of arthritis. Nat Commun 2020;11:1995.
20. Gronwall C, Akhter E, Oh C, Burlingame RW, Petri M, Silverman GJ. IgM autoantibodies to distinct apoptosis-associated antigens correlate with protection from cardiovascular events and renal disease in patients with SLE. Clin Immunol 2012;142:390–8.
21. Jenks SA, Palmer EM, Marin EY, Hartson L, Chida AS, Richardson C, et al. 9G4+ autoantibodies are an important source of apoptotic cell reactivity associated with high levels of disease activity in systemic lupus erythematosus. Arthritis Rheum 2013;65:3165–75.
22. Chen Y, Park YB, Patel E, Silverman GJ. IgM antibodies to apoptosis-associated determinants recruit C1q and enhance dendritic cell phagocytosis of apoptotic cells. J Immunol 2009;182:6031–43.
23. Chen Y, Khanna S, Goodyear CS, Park YB, Raz E, Thiel S, et al. Regulation of dendritic cells and macrophages by an anti-apoptotic cell natural antibody that suppresses TLR responses and inhibits inflammatory arthritis. J Immunol 2009;183:1346–59.

Arthritis & Rheumatology
Vol. 73, No. 5, May 2021, pp 731–739
DOI 10.1002/art.41593

American College of Rheumatology
Empowering Rheumatology Professionals

Nonsteroidal Antiinflammatory Drugs and Susceptibility to COVID-19

Joht Singh Chandan,[1] Dawit Tefra Zemedikun,[2] Rasiah Thayakaran,[2] Nathan Byne,[3] Samir Dhalla,[3] Dionisio Acosta-Mena,[3] Krishna M. Gokhale,[2] Tom Thomas,[4] Christopher Sainsbury,[2] Anuradhaa Subramanian,[2] Jennifer Cooper,[2] Astha Anand,[2] Kelvin O. Okoth,[2] Jingya Wang,[2] Nicola J. Adderley,[2] Thomas Taverner,[2] Alastair K. Denniston,[5] Janet Lord,[6] G. Neil Thomas,[2] Christopher D. Buckley,[7] Karim Raza,[8] Neeraj Bhala,[9] Krishnarajah Nirantharakumar,[10] and Shamil Haroon[2]

Objective. To identify whether active use of nonsteroidal antiinflammatory drugs (NSAIDs) increases susceptibility to developing suspected or confirmed coronavirus disease 2019 (COVID-19) compared to the use of other common analgesics.

Methods. We performed a propensity score–matched cohort study with active comparators, using a large UK primary care data set. The cohort consisted of adult patients age ≥18 years with osteoarthritis (OA) who were followed up from January 30 to July 31, 2020. Patients prescribed an NSAID (excluding topical preparations) were compared to those prescribed either co-codamol (paracetamol and codeine) or co-dydramol (paracetamol and dihydrocodeine). A total of 13,202 patients prescribed NSAIDs were identified, compared to 12,457 patients prescribed the comparator drugs. The primary outcome measure was the documentation of suspected or confirmed COVID-19, and the secondary outcome measure was all-cause mortality.

Results. During follow-up, the incidence rates of suspected/confirmed COVID-19 were 15.4 and 19.9 per 1,000 person-years in the NSAID-exposed group and comparator group, respectively. Adjusted hazard ratios for suspected or confirmed COVID-19 among the unmatched and propensity score–matched OA cohorts, using data from clinical consultations in primary care settings, were 0.82 (95% confidence interval [95% CI] 0.62–1.10) and 0.79 (95% CI 0.57–1.11), respectively, and adjusted hazard ratios for the risk of all-cause mortality were 0.97 (95% CI 0.75–1.27) and 0.85 (95% CI 0.61–1.20), respectively. There was no effect modification by age or sex.

Conclusion. No increase in the risk of suspected or confirmed COVID-19 or mortality was observed among patients with OA in a primary care setting who were prescribed NSAIDs as compared to those who received comparator drugs. These results are reassuring and suggest that in the absence of acute illness, NSAIDs can be safely prescribed during the ongoing pandemic.

INTRODUCTION

The coronavirus disease 2019 (COVID-19) pandemic, caused by severe acute respiratory syndrome coronavirus 2 (SARS–CoV-2), was originally declared a public health emergency on January 30, 2020 (1). Since then, the disease has led to the deaths of >700,000 individuals globally (2). Nonsteroidal antiinflammatory drugs (NSAIDs) are widely used to help control pain in chronic diseases such as osteoarthritis (OA) and are often used in groups at high risk for COVID-19, including older populations. However,

The views expressed are those of the authors and not necessarily those of the MRC, Arthritis Research UK, or Health Data Research UK.

Supported in part by the MRC-ARUK Centre for Musculoskeletal Ageing Research. Drs. Lord, Buckley, and Raza's work was supported in part by the NIHR Birmingham Biomedical Research Centre. Dr. Nirantharakumar's work was supported by Health Data Research UK.

[1]Joht Singh Chandan, PhD: Institute of Applied Health Research, University of Birmingham, Birmingham, UK, and Warwick Medical School, University of Warwick, Coventry, UK; [2]Dawit Tefra Zemedikun, PhD, Rasiah Thayakaran, PhD, Krishna M. Gokhale, MSc, Christopher Sainsbury, MD, Anuradhaa Subramanian, MSc, Jennifer Cooper, MBBCh, Astha Anand, BMBCh, Kelvin O. Okoth, MPH, Jingya Wang, PhD, Nicola J. Adderley, PhD, Thomas Taverner, PhD, G. Neil Thomas, PhD, Shamil Haroon, PhD: Institute of Applied Health Research, University of Birmingham, Birmingham, UK; [3]Nathan Byne, Samir Dhalla, MRPharmS, Dionisio Acosta-Mena, PhD: Cegedim Rx, London, UK; [4]Tom Thomas, MBBS: Kennedy Institute of Rheumatology, University of Oxford, Oxford, UK; [5]Alastair K. Denniston, PhD: Institute of Inflammation and Ageing, University of Birmingham, and Queen Elizabeth Hospital Birmingham, University Hospitals Birmingham NHS Foundation Trust, Birmingham, UK; [6]Janet Lord, PhD: Institute of Inflammation and Ageing, and MRC Versus Arthritis Centre for Musculoskeletal Ageing Research, University of Birmingham, Birmingham, UK; [7]Christopher D. Buckley, DPhil: Kennedy Institute of Rheumatology, University of Oxford, Oxford, UK, and Institute of Inflammation and Ageing and MRC Versus Arthritis Centre for Musculoskeletal Ageing Research, University of Birmingham, Birmingham, UK; [8]Karim Raza, PhD: Institute of Inflammation and Ageing, MRC Versus

concerns have been raised regarding the use of NSAIDs in the treatment of SARS–CoV-2 infection, particularly after the French Health Minister suggested in March 2020 that NSAIDs might aggravate the infection. Pre-pandemic evidence has also suggested a potential association between the use of NSAIDs and prolonged or complicated courses of respiratory infection (3–7).

Furthermore, biologic data raise the possibility of increased risk for COVID-19. Entry of SARS–CoV-2 into host cells is dependent on its receptor, angiotensin-converting enzyme 2 (ACE2) (8), as well as priming of the S protein by transmembrane protease serine 2 (9). Single-cell RNA sequencing has demonstrated ACE2 messenger RNA expression across multiple epithelial cell types throughout the human body, most notably in the nasal epithelium (10). It has been speculated that ibuprofen, one of the most commonly used NSAIDs, could up-regulate ACE2 expression and thereby increase susceptibility to SARS–CoV-2 (11). A single study has previously demonstrated ACE2 up-regulation in the cardiac tissue in response to ibuprofen in a rat model of diabetes (12). It is unknown if these results would translate to the specific cell types of interest in humans and thereby promote susceptibility to SARS–CoV-2.

Despite these concerns, NSAIDs have remained an important therapeutic approach to the management of pain, including among older patients (13). However, data on the effects of NSAIDs on susceptibility to SARS–CoV-2 remain sparse, especially in older cohorts. Both the National Health Service in England and the World Health Organization have conducted rapid reviews to examine the association between the use of NSAIDs and susceptibility to and severity of COVID-19 (14,15). In both reviews it was concluded that there was no clear association between NSAIDs and these outcomes but they noted that the evidence was scarce. Several studies examined the impact of NSAIDs on the disease course in patients with COVID-19 (16,17), including those with acute respiratory distress syndrome (18). However, smaller-scale clinical studies to date have been unable to adequately investigate whether use of NSAIDs could confer susceptibility to infection due to SARS–CoV-2. Challenges in the design of studies attempting to address this concern include selection bias, as well as an inability to account for confounding by indication bias.

To address this question, we conducted a retrospective cohort study exploring the association between NSAID use and the subsequent development of COVID-19, using real-world data from primary care (6).

PATIENTS AND METHODS

Study design. This was a population-based retrospective propensity score–matched cohort study of patients with OA, comparing the risk of suspected or confirmed COVID-19 infection among patients prescribed an NSAID (excluding topical preparations) to those prescribed either co-codamol or co-dydramol as active comparators.

Data source. This cohort study used patient data derived from The Health Improvement Network (THIN) database. The steps involved in data extraction were facilitated by the Data Extraction for Epidemiological Research tool (19). THIN is a collection of routinely collected primary care data from UK general practices, which use Vision electronic medical records software (20). In 2020, THIN included data on ~2.1 million active patients from 357 practices. The database is representative of the UK population in terms of demographic structure and prevalence of key comorbidities (21).

THIN has been used on numerous occasions in pharmacoepidemiologic studies to examine health outcomes and mortality risk in patients with OA or to assess drug safety during the COVID-19 pandemic (22–27). Symptoms, examinations, and diagnoses in THIN are recorded using a hierarchical clinical coding system called Read codes (28). Prescriptions are recorded based on the Dictionary of Medicines and Devices and Anatomical Therapeutic Classification systems (29,30). In order to reduce the underrecording of events, general practices were included 12 months following their installment of electronic practice records or from the practice's acceptable mortality recording date (31).

Study population. Adults age ≥18 years with a diagnosis of OA who had been registered with an eligible general practice for at least 1 year on or before January 30, 2020 (index date) were included. Patients with OA were specifically selected because they commonly take NSAIDs and other analgesics for chronic pain management, and selecting a specific population group helps to limit confounding by indication bias from other chronic pain conditions that may have differential risks for COVID-19. Patients with a record of rheumatoid arthritis, systemic lupus erythematosus, juvenile arthritis, enteropathic arthritis, reactive arthritis, scleroderma, or ankylosing spondylitis were thus excluded. In addition, patients with a history of gastrointestinal bleeding,

Arthritis Centre for Musculoskeletal Ageing Research, and Sandwell and West Birmingham NHS Hospitals Trust, Birmingham, UK; [9]Neeraj Bhala, DPhil: Institute of Applied Health Research, University of Birmingham, and Queen Elizabeth Hospital Birmingham, University Hospitals Birmingham NHS Foundation Trust, Birmingham, UK; [10]Krishnarajah Nirantharakumar, MD: Institute of Applied Health Research, University of Birmingham, and Health Data Research UK Midlands, Birmingham, UK.

Drs. Chandan, Zemedikun, and Thayakaran contributed equally to this work. Drs. Raza, Bhala, Nirantharakumar, and Haroon contributed equally to this work.

No potential conflicts of interest relevant to this article were reported.

Address correspondence to Krishnarajah Nirantharakumar, MD, IOEM Building, University of Birmingham, Edgbaston, Birmingham, B15 2TT, UK (k.nirantharan@bham.ac.uk) or to Karim Raza, PhD, Institute of Inflammation and Ageing, College of Medical and Dental Sciences, University of Birmingham, Queen Elizabeth Hospital, Birmingham, B15 2WB, UK (k.raza@bham.ac.uk).

Submitted for publication September 13, 2020; accepted in revised form November 10, 2020.

peptic ulcers, or allergy or adverse reactions to NSAIDs were also excluded.

Definition of exposed group and comparator group. Current users of NSAIDs or comparator drugs (co-codamol/co-dydramol) were defined as patients with prescriptions that lasted beyond the index date or those with prescriptions that lasted until 90 days preceding the index date and with evidence of further prescription during the pandemic period. NSAIDs included those in chapter 10.1.1 in the British National Formulary, such as ibuprofen, naproxen, and diclofenac, but excluded aspirin 300 mg due to a difference in the biologic mechanism of action (32). The complete list of NSAIDs included in the study is shown in Supplementary Table 1 (available on the *Arthritis & Rheumatology* website at http://onlinelibrary.wiley.com/doi/10.1002/art.41593/abstract).

Patients with OA with a current prescription for an NSAID (exposed group) were compared to patients with a current prescription for co-codamol or co-dydramol (comparator group). The 2 groups were mutually exclusive; patients with a current prescription for both medications were excluded from the study. Co-codamol and co-dydramol are analgesics that are alternative treatment options for the management of pain in patients with OA and have not been implicated in increasing susceptibility to COVID-19. While there is some evidence that opiates have immunosuppressive properties and may increase the risk of community-acquired pneumonia, this is only clinically evident in patients who are receiving doses of opiates above the equivalent of 20 mg of morphine daily (33). This is greater than the dose of opiates that patients in our active comparator cohort would be exposed to from taking co-codamol or co-dydramol.

Matching. Using data from the index date, participants in the exposed group were propensity score matched to participants in the comparator group. Propensity scores for the use of NSAIDs were estimated using a logistic regression model including a set of covariates as described below. To ensure positivity (having adequate variation in the treatment of interest within confounder strata), propensity scores were truncated and only participants with propensity scores that fell within the common support region using a caliper width of 0.2 were eligible for matching. Participants in the exposed group were then matched 1:1 to patients taking comparator drugs, by propensity score using the nearest neighbor algorithm.

Follow-up period. Patients were followed up from January 30, 2020 (index date) until the earliest of the following dates: date of the outcome, date of death, date patient left practice/data set, date practice ceased contributing to the database, or study end date (July 31, 2020). The latest available covariate data recorded on or before the index date were used to calculate propensity scores and to adjust for covariates in the analysis.

Outcome measures. The primary outcome measure was a composite of confirmed or clinician-suspected diagnoses of COVID-19. The secondary outcome measure was the risk of all-cause mortality and was limited to confirmed COVID-19 cases in a sensitivity analysis. The outcome measures were defined using the relevant clinical Read codes listed in Supplementary Table 2 (available on the *Arthritis & Rheumatology* website at http://onlinelibrary.wiley.com/doi/10.1002/art.41593/abstract).

Covariates. The latest available covariate data recorded prior to the index date were obtained and used for propensity score matching and adjustment in the outcome model. The list of covariates included currently known risk factors for the development of COVID-19 (34). These included 1) sociodemographic characteristics (age and sex); 2) lifestyle and metabolic profile measures (smoking status, body mass index [BMI], systolic and diastolic blood pressure, and estimated glomerular filtration rate); and 3) presence of comorbid conditions such as type 2 diabetes mellitus, cardiovascular

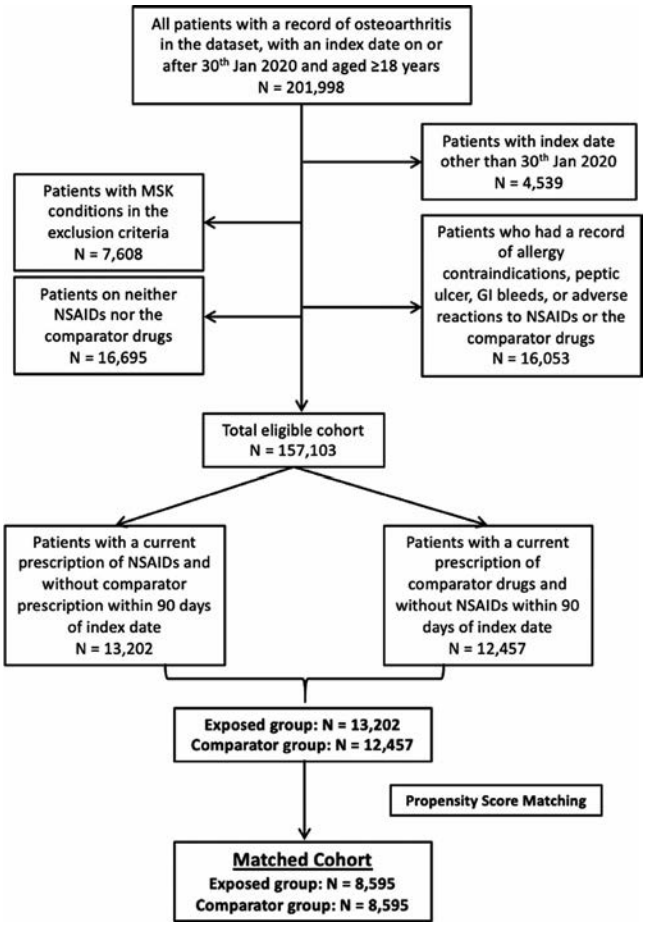

Figure 1. Flow chart showing disposition of the osteoarthritis patients in each group. MSK = musculoskeletal; NSAIDs = nonsteroidal anti-inflammatory drugs; GI = gastrointestinal.

disease (peripheral vascular disease, stroke, ischemic heart disease, and heart failure), atrial fibrillation, asthma, chronic obstructive pulmonary disease, cancer, liver disease (mild, moderate, and severe), psoriasis, neurologic disorders (Parkinson's disease, motor neuron disease, multiple sclerosis, myasthenia gravis, and epilepsy), dementia, vitamin D deficiency, solid organ transplant, and use of immunosuppressive drug therapies.

Smoking status was categorized as nonsmoker, ex-smoker, or current smoker. BMI was categorized as <25 kg/m^2 (normal/underweight), 25–30 kg/m^2 (overweight), >30–35 kg/m^2 (obese), or >35 kg/m^2 (severely obese). Physiologic and laboratory measures were categorized into appropriate clinically meaningful groups. All covariates listed above were included in the propensity score matching process and for adjustment in the analysis.

Table 1. Baseline characteristics of the study population*

	Unmatched cohort		Matched cohort	
	NSAID (n = 13,202)	Comparator (n = 12,457)	NSAID (n = 8,595)	Comparator (n = 8,595)
Male sex, no. (%)	4,992 (37.8)	4,156 (33.4)	2,990 (34.8)	2,938 (34.2)
Age, years	65.35 ± 10.7	71.71 ± 11.3	68.39 ± 10.4	68.08 ± 10.5
Age categories, no. (%)				
<40 years	123 (0.9)	69 (0.6)	48 (0.6)	66 (0.8)
40–49 years	727 (5.5)	308 (2.5)	283 (3.3)	297 (3.5)
50–59 years	3,097 (23.5)	1,420 (11.4)	1,372 (16.0)	1,380 (16.1)
60–69 years	4,539 (34.4)	3,177 (25.5)	2,825 (32.9)	2,810 (32.7)
70–79 years	3,484 (26.4)	4,219 (33.9)	2,867 (33.4)	2,859 (33.3)
≥80 years	1,232 (9.3)	3,264 (26.2)	1,200 (14.0)	1,183 (13.8)
Smoking status, no. (%)				
Nonsmoker	6,995 (53.0)	5,966 (47.9)	4,294 (50.0)	4,335 (50.4)
Ex-smoker	4,285 (32.5)	4,653 (37.4)	3,004 (35.0)	2,962 (34.5)
Smoker	1,824 (13.8)	1,798 (14.4)	1,259 (14.7)	1,271 (14.8)
Missing data	98 (0.7)	40 (0.3)	38 (0.4)	27 (0.3)
BMI, kg/m^2	31.03 ± 6.9	30.77 ± 7.0	30.86 ± 6.9	31.09 ± 7.1
BMI categories, no. (%)				
Normal/underweight (<25)	2,290 (17.4)	2,352 (18.9)	1,535 (17.9)	1,523 (17.7)
Overweight (25–30)	4,152 (31.5)	3,906 (31.4)	2,726 (31.7)	2,703 (31.5)
Obese (>30)	6,287 (47.6)	5,908 (47.4)	4,105 (47.8)	4,144 (48.2)
Missing data	473 (3.6)	291 (2.3)	229 (2.7)	225 (2.6)
Systolic BP, mm Hg	133.6 ± 14.5	133.8 ±14.9	133.9 ± 14.5	134.2 ± 14.5
Diastolic BP, mm Hg	78.43 ± 9.1	76.60 ± 9.5	77.62 ± 9.05	77.88 ± 9.19
eGFR, ml/minute	84.6 ± 18.74	79.9 ± 21.55	83.1 ± 19.4	84.4 ± 19.3
eGFR category, no. (%)				
>90 (stage 1)	4,478 (33.9)	3,601 (28.9)	2,797 (32.5)	2,875 (33.5)
60–90 (stage 2)	7,494 (56.8)	6,761 (54.3)	4,853 (56.5)	4,969 (57.8)
30–59 (stage 3)	833 (6.3)	1,830 (14.7)	764 (8.9)	598 (7.0)
<30 (stage 4)	13 (0.1)	92 (0.7)	13 (0.2)	2 (0.0)
Missing data	384 (2.9)	173 (1.4)	168 (2.0)	151 (1.8)
Baseline conditions, no. (%)				
AF	264 (2.0)	1,309 (10.5)	263 (3.1)	70 (0.8)
CVD	1,221 (9.3)	3,146 (25.3)	1,173 (13.7)	831 (9.7)
Diabetes	1,707 (12.9)	2,816 (22.6)	1,460 (17.0)	1,364 (15.9)
Dementia	114 (0.9)	358 (2.9)	110 (1.3)	63 (0.7)
Vitamin D deficiency	249 (1.9)	375 (3.0)	202 (2.4)	186 (2.2)
Cancer	1,188 (9.0)	1,509 (12.1)	921 (10.7)	895 (10.4)
Liver disease	297 (2.3)	392 (3.2)	242 (2.8)	243 (2.8)
Asthma	2,147 (16.3)	2,488 (20.0)	1,524 (17.7)	1,526 (17.8)
Psoriasis	740 (5.6)	1,506 (12.1)	694 (8.1)	610 (7.1)
COPD	740 (5.6)	1,506 (12.1)	694 (8.1)	610 (7.1)
Neurologic disorders†	144 (1.1)	170 (1.4)	107 (1.2)	112 (1.3)
Solid organ transplant	1 (0.0)	6 (0.1)	1 (0.0)	0 (0)
Immunologic therapies	80 (0.6)	91 (0.7)	60 (0.7)	59 (0.7)
NSAID use 1 year prior to index date	4,108 (31.12)	1,857 (14.91)	2,769 (32.22)	1,575 (18.32)

* Except where indicated otherwise, values are the mean ± SD. NSAID = nonsteroidal antiinflammatory drug; BMI = body mass index; BP = blood pressure; eGFR = estimated glomerular filtration rate; AF = atrial fibrillation; CVD = cardiovascular disease; COPD = chronic obstructive pulmonary disease.
† Neurologic disorders: Parkinson's disease, motor neuron disease, multiple sclerosis, myasthenia gravis, and epilepsy.

Table 2. Risk of developing COVID-19 or death in patients with osteoarthritis prescribed NSAIDs compared to those who received co-codamol or co-dydramol (comparator)*

	Unmatched patients				Propensity score–matched patients			
Outcome	NSAID-treated	Comparator	Unadjusted HR (95% CI)	Adjusted HR (95% CI)†	NSAID-treated	Comparator	Unadjusted HR (95% CI)	Adjusted HR (95% CI)†
Suspected/confirmed COVID-19								
n	13,202	12,457			8,595	8,595		
Outcome events, no. (%)	101 (0.77)	122 (0.98)			63 (0.73)	76 (0.88)		
Person-years	6,551	6,127			4,263	4,254		
Crude IR/1,000 person-years	15.4	19.9			14.8	17.9		
HR (95% CI)			0.77 (0.59–1.01)‡	0.82 (0.62–1.10)			0.83 (0.59–1.16)	0.79 (0.57–1.11)
Mortality								
n	13,202	12,457			8,595	8,595		
Outcome events, no. (%)	92 (0.70)	213 (1.71)			79 (0.92)	71 (0.83)		
Person-years	6,574	6,151			4,276	4,270		
Crude IR/1,000 person-years	14.0	34.6			18.5	16.6		
HR (95% CI)			0.40 (0.32–0.52)§	0.97 (0.75–1.27)			1.11 (0.81–1.53)	0.85 (0.61–1.20)

* COVID-19 = coronavirus disease 2019; NSAIDs = nonsteroidal antiinflammatory drugs; HR = hazard ratio; IR = incidence rate.
† Adjusted for age, sex, body mass index categories, smoking status, estimated glomerular filtration rate categories, systolic and diastolic blood pressure, type 2 diabetes mellitus, atrial fibrillation, cancer, vitamin D deficiency, cardiovascular disease (peripheral vascular disease, stroke, ischemic heart disease, and heart failure), dementia, liver disease (mild, moderate, and severe), asthma, chronic obstructive pulmonary disease, solid organ transplants, use of immunologic drug therapies, psoriasis, and other neurologic disorders (Parkinson's disease, motor neuron disease, multiple sclerosis, and myasthenia gravis).
‡ $P = 0.06$.
§ $P < 0.01$.

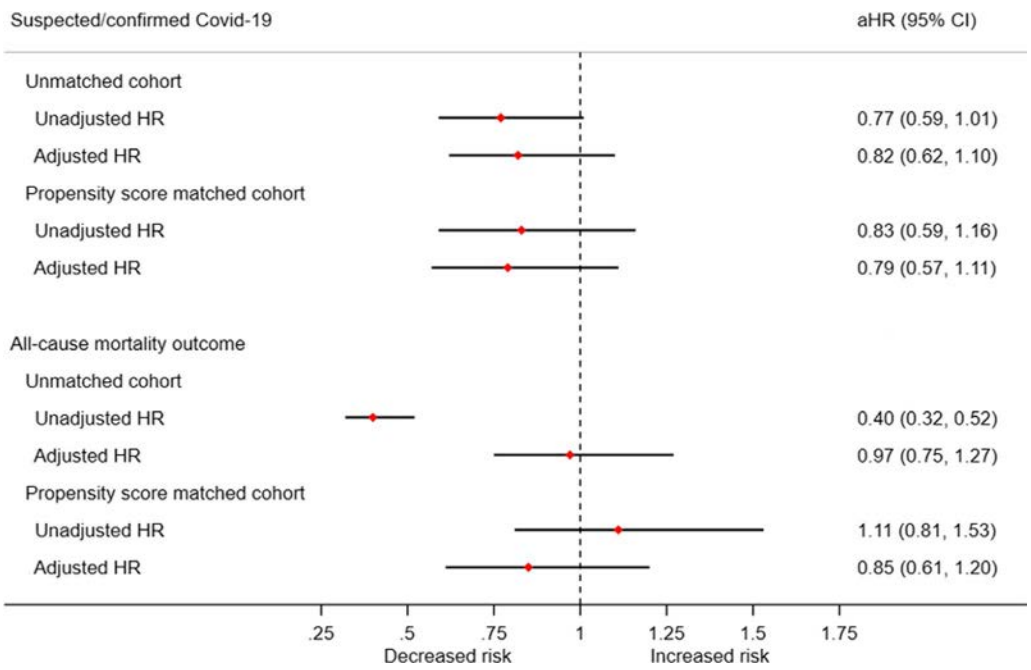

Figure 2. Adjusted hazard ratio (aHR) (with 95% confidence interval [95% CI]) for developing suspected/confirmed coronavirus disease 2019 (COVID-19) or mortality following medication use in both the exposed group and the comparator group. Color figure can be viewed in the online issue, which is available at http://onlinelibrary.wiley.com/doi/10.1002/art.41593/abstract.

Missing data. Missing values for smoking status and physiologic/laboratory measures were treated as a separate missing category for each variable. The absence of a record of any diagnosis was taken to indicate the absence of the condition.

Statistical analysis. Descriptive statistics were used to describe the exposed and comparator groups and were described for both groups before and after propensity score matching. Histograms of propensity scores in the exposed and the comparator groups were generated before and after matching, for a visual check of the global balance of propensity scores between the 2 groups.

Crude incidence rates per 1,000 person-years for the primary and secondary outcome measures were estimated for the exposed and comparator cohorts. A Cox proportional hazards regression model was used to determine crude incidence rates and adjusted hazard ratios (HRs) for NSAIDs compared to the comparator drugs for the outcome measure. Survival curves in the exposed and the comparator groups were generated for the unmatched and the propensity score–matched cohorts.

Subgroup analysis. Two subgroup analyses were conducted to assess for differential associations between COVID-19 and NSAID use by age (<65 years versus ≥65 years) and sex. Both older age and male sex have previously been identified as risk factors for COVID-19, and we investigated whether this extended to differential effects from NSAID exposure (34).

RESULTS

Study population. We identified 13,202 eligible patients with OA with a current prescription for an NSAID and 12,457 patients with a current prescription for comparator drugs (co-codamol or co-dydramol) (Figure 1).

Baseline characteristics. In the unmatched cohort (13,202 exposed patients compared to 12,457 comparator patients), the NSAID cohort was younger (mean age 65.4 versus 71.7 years) and had a greater proportion of men (37.8% versus 33.4%) compared to the comparator cohort (Table 1). Compared to the comparator cohort, the NSAID cohort had similar proportions of current smokers and a similar mean BMI. However, those taking NSAIDs had a lower prevalence of comorbidities compared to those taking the comparator drugs, including cardiovascular disease, diabetes, respiratory disease, and cancers.

Following 1:1 propensity score matching, 8,595 eligible patients prescribed NSAIDs were compared to 8,595 matched patients prescribed co-codamol or co-dydramol. After matching, the demographic and clinical characteristics of both cohorts were very similar (Table 1).

Primary and secondary outcome measures. In the unmatched cohort during the follow-up period, 101 individuals in the exposed group (current NSAID users only) and 122 in the comparator group (current co-codamol or co-dydramol users only)

were diagnosed as having suspected or confirmed COVID-19, corresponding to crude incidence rates (IRs) of 15.4 and 19.9 per 1,000 person-years, respectively (Table 2). After adjustment for potential confounders, no statistically significant difference in the risk of confirmed or suspected COVID-19 was observed in users of NSAIDs compared to users of the comparator drugs (adjusted HR 0.82 [95% CI 0.62–1.10]; Figure 2 and Supplementary Figure 1, available on the *Arthritis & Rheumatology* website at http://onlinelibrary.wiley.com/doi/10.1002/art.41593/abstract).

During the follow-up period, 92 patients in the exposed group died (IR 14.0 per 1,000 person-years), compared to 213 patients in the comparator group (IR 34.6 per 1,000 person-years). However, following adjustment for confounders, there was no significant difference in mortality between groups (adjusted HR 0.97 [95% CI 0.75–1.27]).

Following propensity score matching, 63 patients in the exposed group and 76 patients in the comparator group were diagnosed as having suspected or confirmed COVID-19, corresponding to crude IRs of 14.8 and 17.9 per 1,000 person-years, respectively. Similarly, no statistically significant difference in the risk of COVID-19 was observed between the 2 groups following adjustment (adjusted HR 0.79 [95% CI 0.57–1.11]). In addition, there was no significant difference in the mortality risk between the groups (adjusted HR 0.85 [95% CI 0.61–1.20]).

Sensitivity analysis. In a sensitivity analysis where outcomes were restricted to only those presenting as confirmed cases of COVID-19, the results remained similar to the main findings (Supplementary Table 3, available on the *Arthritis & Rheumatology* website at http://onlinelibrary.wiley.com/doi/10.1002/art.41593/abstract). When this exclusion criterion was applied to the cohort, there were no statistically significant differences in the risk of developing suspected/confirmed COVID-19 between the exposed and comparator groups in the adjusted unmatched cohort analysis (adjusted HR 0.71 [95% CI 0.35–1.43]) and propensity score–matched cohort analysis (adjusted HR 0.69 [95% CI 0.29–1.61]).

Subgroup analysis. There was no significant difference in the risk of suspected/confirmed COVID-19 between male patients who were prescribed NSAIDs compared to male patients who were prescribed the comparator drugs in either the unmatched cohort (adjusted HR 0.77 [95% CI 0.48–1.26]) or the propensity score–matched cohort (adjusted HR 0.72 [95% CI 0.40–1.28]) (Supplementary Table 4, available on the *Arthritis & Rheumatology* website at http://onlinelibrary.wiley.com/doi/10.1002/art.41593/abstract). The results were similar in female patients, both in the unmatched cohort (adjusted HR 0.86 [95% CI 0.60–1.23]) and in the propensity score–matched cohort (adjusted HR 0.83 [95% CI 0.55–1.26]).

No significant difference in the risk of all-cause mortality was observed between the exposed and comparator groups among men in either the unmatched cohort (adjusted HR 0.83 [95% CI 0.55–1.27]) or the propensity score–matched cohort (adjusted HR 0.78 [95% CI 0.47–1.32]). The same was also true among women in either the unmatched cohort (adjusted HR 1.11 [95% CI 0.78–1.57]) or the propensity score–matched cohort (adjusted HR 0.94 [95% CI 0.59–1.48]) (Supplementary Table 4).

No statistically significant differences in the primary outcome measure were found after stratification by age (patients age <65 and ≥65 years). Among patients age <65 years, there was no significant difference in the risk of developing suspected/confirmed COVID-19 between those prescribed NSAIDs compared to those prescribed the comparator drugs in either the unmatched cohort (adjusted HR 0.97 [95% CI 0.63–1.49]) or the propensity score–matched cohort (adjusted HR 0.93 [95% CI 0.57–1.51]) (Supplementary Table 5, http://onlinelibrary.wiley.com/doi/10.1002/art.41593/abstract). However, in those age ≥65 years, the adjusted HRs were lower, although not significantly so, when comparing the risk of developing suspected/confirmed COVID-19 between the NSAID-exposed and comparator groups in both the unmatched cohort (adjusted HR 0.73 [95% CI 0.49–1.09]) and the propensity score–matched cohort (adjusted HR 0.67 [95% CI 0.42–1.08]).

Similarly, among patients age <65 years, there were no differences in mortality risk between the NSAID-exposed and comparator groups in either the unmatched cohort (adjusted HR 1.32 [95% CI 0.56–1.11]) or the propensity score–matched cohort (adjusted HR 1.12 [95% CI 0.42–3.01]). There were also no differences in mortality risk between the groups in patients age ≥65 years, either in the unmatched cohort (adjusted HR 0.95 [95% CI 0.71–1.26]) or the propensity score–matched cohort (adjusted HR 0.82 [95% CI 0.57–1.19]).

DISCUSSION

To our knowledge, this is the first population-based cohort study accounting for confounding by indication bias as well as a wide range of other potential confounders to examine the effect of NSAIDs on subsequent development of suspected or confirmed COVID-19 or mortality. We found no significant association between NSAID use and confirmed or suspected COVID-19 or all-cause mortality, when compared to use of co-codamol or co-dydramol in a large primary care cohort of patients with OA. Additionally, there was no significant difference in the association between NSAID use and the risk of suspected or confirmed COVID-19 or mortality in men compared to women. Reassuringly, we also found no significant difference in the association between NSAID use and the risk of COVID-19 or mortality in older patients compared to younger patients, although older NSAID users had a reduction, though not statistically significant, in risk of COVID-19 compared to those prescribed comparator drugs. Overall, the data clearly show that the use of NSAIDs in this population was not associated with increased risk of infection or mortality.

SARS–CoV-2 enters host cells via the ACE2 receptor, and NSAIDs may increase expression of this enzyme. Therefore, concerns were raised at the outset of the pandemic about the use of NSAIDs and susceptibility to COVID-19. However, our findings do not support this conjecture. Indeed, there are parallels between our results and those from previous studies investigating the impact of ibuprofen on the severity of COVID-19 in South Korea (16) and Denmark (17). In those studies, NSAIDs conferred no additional risk of morbidity or mortality. Interestingly, Lund et al also attempted to examine the impact of age and sex on COVID-19 severity in patients taking NSAIDs compared to their matched controls. They identified no clear differences in outcomes across age or sex, although the study may not have been sufficiently powered to identify these as potential effect modifiers (17).

Our study supports these findings, demonstrating that there is no increased risk of susceptibility to COVID-19 across age or sex in patients taking NSAIDs. This is important because older patients are at a substantially higher risk of developing COVID-19 and have a poorer prognosis (34). These results are also reassuring given the high prevalence of NSAID use in this age group (35). Our findings will need to be confirmed in other cohorts, as we restricted our analysis to patients with preexisting OA to reduce the risk of confounding by indication and immortal time bias. Further research into the impact of NSAIDs on the expression of the ACE2 receptor and consequent susceptibility to SARS–CoV-2 in relevant human cell types is also urgently required.

Although not targeted at population-based use, the LIBERATE trial is currently exploring outcomes in patients given lipid ibuprofen versus standard care for acute hypoxemic respiratory failure due to COVID-19 (18). The findings of this trial will help confirm whether NSAIDs could be of benefit in the management of severe COVID-19.

Our study had several limitations. This was an observational, retrospective cohort study and is therefore prone to the effect of unmeasured confounding and confounding by indication bias. However, we used a propensity score–matched design to minimize the effect of a large number of potential confounders. We also attempted to limit confounding by indication bias by the inclusion of a carefully selected population group commonly prescribed the drugs of interest. The study also explored potential interactions by age and sex. The majority of studies on COVID-19 are based in secondary care settings, and this study is also one of the few that has explored susceptibility to COVID-19 in a primary care setting.

An important limitation of our study relates to data quality, as the use of electronic health records for epidemiologic research largely relies on the accuracy of documentation by health care professionals. While prescription data are adequately recorded in primary care, we could not account for NSAIDs purchased without a prescription nor could we verify medication compliance. However, we anticipate that a large proportion of patients taking NSAIDs for chronic pain associated with OA would receive this by prescription. Although we do not have details relating to patterns of NSAID prescription prior to study entry, we have been able to report the proportion of patients who had at least 1 recorded prescription for NSAIDs in the year preceding the index date (Table 1).

As the data were derived from a primary care setting, we did not have data on hospitalization, inpatient management, or cause-specific mortality. Additionally, we were unable to access data relating to socioeconomic status, an important risk factor associated with outcomes of COVID-19 (34). Our study was also limited by the number of outcome events, which were insufficient to explore effects of different types or doses of NSAIDs (36).

Our findings suggest that prescriptions of NSAIDs (excluding topical preparations) in primary care does not increase susceptibility to COVID-19 or all-cause mortality, including in older patients. These findings are reassuring given the high prevalence of NSAID use in at-risk groups. Further research is needed to investigate whether the use of NSAIDs is associated with adverse outcomes from COVID-19 in patients with confirmed SARS–CoV-2 infection and whether risks differ by NSAID type and dose.

AUTHOR CONTRIBUTIONS

All authors were involved in drafting the article or revising it critically for important intellectual content, and all authors approved the final version to be published. Dr. Chandan had full access to all of the data in the study and takes responsibility for the integrity of the data and the accuracy of the data analysis.

Study conception and design. Chandan, Zemedikun, Thayakaran, Gokhale, Thomas, Sainsbury, Subramanian, Cooper, Anand, Okoth, Wang, Adderley, Taverner, Denniston, Lord, Thomas, Buckley, Raza, Bhala, Nirantharakumar, Haroon.

Acquisition of data. Chandan, Zemedikun, Thayakaran, Byne, Dhalla, Acosta-Mena, Gokhale.

Analysis and interpretation of data. Chandan, Zemedikun, Thayakaran, Gokhale, Subramanian, Wang.

ADDITIONAL DISCLOSURES

Authors Byne, Dhalla, and Acosta-Mena are employees of Cegedim Rx.

REFERENCES

1. World Health Organization. Statement on the second meeting of the International Health Regulations (2005) Emergency Committee regarding the outbreak of novel coronavirus (2019-nCoV). January 2020. URL: https://www.who.int/news-room/detail/30-01-2020-statement-on-the-second-meeting-of-the-international-health-regulations-(2005)-emergency-committee-regarding-the-outbreak-of-novel-coronavirus-(2019-ncov).
2. John Hopkins University. COVID-19 Cashboard by the Center for Systems Science and Engineering (CSSE) at Johns Hopkins University (JHU). URL: https://coronavirus.jhu.edu/map.html.
3. Basille D, Thomsen RW, Madsen M, Duhaut P, Andrejak C, Jounieaux V, et al. Nonsteroidal antiinflammatory drug use and clinical outcomes of community-acquired pneumonia. Am J Respir Crit Care Med 2018;198:128–31.
4. Le Bourgeois M, Ferroni A, Leruez-Ville M, Varon E, Thumerelle C, Brémont F, et al. Nonsteroidal anti-inflammatory drug without antibiotics for acute viral infection increases the empyema risk in children: a matched case-control study. J Pediatr 2016;175:47–53.

5. Voiriot G, Philippot Q, Elabbadi A, Elbim C, Chalumeau M, Fartoukh M. Risks related to the use of non-steroidal anti-inflammatory drugs in community-acquired pneumonia in adult and pediatric patients [review]. J Clin Med 2019;8:786.
6. Day M. Covid-19: ibuprofen should not be used for managing symptoms, say doctors and scientists. BMJ 2020;368:m1086.
7. Little P. Non-steroidal anti-inflammatory drugs and COVID-19 [editorial]. BMJ 2020;368:m1185.
8. Zhou P, Lou YX, Wang XG, Hu B, Zhang L, Zhang W, et al. A pneumonia outbreak associated with a new coronavirus of probable bat origin. Nature 2020;579:270–3.
9. Hoffmann M, Kleine-Weber H, Schroeder S, Krüger N, Herrler T, Erichsen S, et al. SARS-CoV-2 cell entry depends on ACE2 and TMPRSS2 and is blocked by a clinically proven protease inhibitor. Cell 2020;181:271–80.
10. Sungnak W, Huang N, Bécavin C, Berg M, Queen R, Litvinukova M, et al. SARS-CoV-2 entry factors are highly expressed in nasal epithelial cells together with innate immune genes. Nat Med 2020;26:681–7.
11. Fang L, Karakiulakis G, Roth M. Are patients with hypertension and diabetes mellitus at increased risk for COVID-19 infection? [letter]. Lancet Respir Med 2020;8:e21.
12. Qiao W, Wang C, Chen B, Zhang F, Liu Y, Lu Q, et al. Ibuprofen attenuates cardiac fibrosis in streptozotocin-induced diabetic rats. Cardiology 2015;131:97–106.
13. COVIDSurg Collaborative. Elective surgery cancellations due to the COVID-19 pandemic: global predictive modelling to inform surgical recovery plans. Br J Surg 2020;107:1440–49.
14. NHS England. Acute use of non-steroidal anti-inflammatory drugs (NSAIDs) in people with or at risk of COVID-19. April 2020. URL: https://www.england.nhs.uk/coronavirus/publication/acute-use-of-non-steroidal-anti-inflammatory-drugs/.
15. World Health Organization. The use of non-steroidal anti-inflammatory drugs (NSAIDs) in patients with COVID-19. April 2020. URL: https://www.who.int/publications/i/item/the-use-of-non-steroidal-anti-inflammatory-drugs-(nsaids)-in-patients-with-covid-19.
16. Jeong HE, Lee H, Shin HJ, Choe YJ, Filion KB, Shin JY. Association between NSAIDs use and adverse clinical outcomes among adults hospitalised with COVID-19 in South Korea: a nationwide study. Clin Infect Dis 2020. E-pub ahead of print.
17. Lund LC, Kristensen KB, Reilev M, Christensen S, Thomsen RW, Christiansen CF, et al. Adverse outcomes and mortality in users of non-steroidal anti-inflammatory drugs tested positive for SARS-CoV-2: a Danish nationwide cohort study. PLoS Med 2020;17:e1003308.
18. King's College London, sponsor. LIBERATE Trial in COVID-19 (LIBERATE). ClinicalTrials.gov identifier: NCT04334629; 2020.
19. Gokhale KM, Chandan JS, Toulis K, Gkoutos G, Tino P, Nirantharakumar K. Data extraction for epidemiological research (DExtER): a novel tool for automated clinical epidemiology studies. Eur J Epidemiol 2020. E-pub ahead of print.
20. THIN: The Health Improvement Network. URL: https://www.the-health-improvement-network.com/en/.
21. Blak BT, Thompson M, Dattani H, Bourke A. Generalisability of The Health Improvement Network (THIN) database: demographics, chronic disease prevalence and mortality rates. Inform Prim Care 2011;19:251–5.
22. Zeng C, Dubreuil M, Larochelle MR, Lu N, Wei J, Choi HK, et al. Association of tramadol with all-cause mortality among patients with osteoarthritis. JAMA 2019;321:969–82.
23. Dubreuil M, Louie-Gao Q, Peloquin CE, Choi HK, Zhang Y, Neogi T. Risk of myocardial infarction with use of selected non-steroidal anti-inflammatory drugs in patients with spondyloarthritis and osteoarthritis. Ann Rheum Dis 2018;77:1137–42.
24. Wei J, Neogi T, Terkeltaub R, Fenves AZ, Zeng C, Misra D, et al. Thiazide diuretics and risk of knee replacement surgery among patients with knee osteoarthritis: a general population-based cohort study. Osteoarthritis Cartilage 2019;27:1454–61.
25. Wei J, Wood MJ, Dubreuil M, Tomasson G, LaRochelle MR, Zeng C, et al. Association of tramadol with risk of myocardial infarction among patients with osteoarthritis. Osteoarthritis Cartilage 2020;28:137–45.
26. Sainsbury C, Wang J, Gokhale K, Acosta-Mena D, Dhalla S, Byne N, et al. Sodium-glucose co-transporter-2 inhibitors and susceptibility to COVID-19: a population-based retrospective cohort study. Diabetes Obes Metab 2021;23:263–9.
27. Haroon S, Subramanian A, Cooper J, Anand A, Gokhale K, Byne N, et al. Renin-angiotensin system inhibitors and susceptibility to COVID-19 in patients with hypertension: a propensity score-matched cohort study in primary care. BMC Infect Dis 2021;21:262.
28. Booth N. What are the Read Codes? Health Libr Rev 1994;11:177–82.
29. World Health Organization. Anatomical Therapeutic Chemical (ATC) classification. URL: https://www.who.int/toolkits/atc-ddd-toolkit/atc-classification.
30. National Health Service Business Services Authority. Dictionary of medicines and devices (dm+d). URL: https://www.nhsbsa.nhs.uk/pharmacies-gp-practices-and-appliance-contractors/dictionary-medicines-and-devices-dmd.
31. Maguire A, Blak BT, Thompson M. The importance of defining periods of complete mortality reporting for research using automated data from primary care. Pharmacoepidemiol Drug Saf 2009;18:76–83.
32. OpenPrescribing. 10.1.1: Non-steroidal anti-inflammatory drugs. URL: https://openprescribing.net/bnf/100101/.
33. Edelman EJ, Gordon KS, Crothers K, Akgün K, Bryant KJ, Becker WC, et al. Association of prescribed opioids with increased risk of community-acquired pneumonia among patients with and without HIV. JAMA Intern Med 2019;179:297–304.
34. Williamson EJ, Walker AJ, Bhaskaran K, Bacon S, Bates C, Morton CE, et al. Factors associated with COVID-19 death using OpenSAFELY. Nature 2020;584:430–6.
35. Davis JS, Lee HY, Kim J, Advani SM, Peng HL, Banfield E, et al. Use of non-steroidal anti-inflammatory drugs in US adults: changes over time and by demographic. Open Hear 2017;4:e000550.
36. Baigent C, Bhala N, Emberson J, Merhi A, Abramson S, Arber N, et al. Vascular and upper gastrointestinal effects of non-steroidal anti-inflammatory drugs: meta-analyses of individual participant data from randomised trials. Lancet 2013;382:769–79.

American College of Rheumatology
Empowering Rheumatology Professionals

Arthritis & Rheumatology
Vol. 73, No. 5, May 2021, pp 740–749
DOI 10.1002/art.41675

Expansion of Alternative Autoantibodies Does Not Follow the Evolution of Anti–Citrullinated Protein Antibodies in Preclinical Rheumatoid Arthritis: An Analysis in At-Risk First-Degree Relatives

Vidyanand Anaparti,[1] Irene Smolik,[1] Xiaobo Meng,[1] Liam O'Neil,[1] Mackenzie A. Jantz,[2] Marvin J. Fritzler,[2] and Hani El-Gabalawy[1]

Objective. Co-occurrence of autoantibodies specific for ≥1 autoimmune disease is widely prevalent in rheumatoid arthritis (RA) patients. To understand the prevalence of polyautoimmunity in preclinical RA, we performed a comprehensive autoantibody assessment in a First Nations cohort of at-risk first-degree relatives (FDR) of RA patients, a subset of whom subsequently developed RA (progressors).

Methods. Venous blood was collected from all study participants (n = 50 RA patients and 64 FDR) at scheduled visits, and serum was stored at –20°C. High-sensitivity C-reactive protein level, anti–citrullinated protein antibody (ACPA) status, and autoantibody status were determined using commercially available enzyme-linked immunosorbent assay kits. Rheumatoid factor (RF) was detected by nephelometry. Antinuclear autoantibodies (ANA) were identified using Hep-2 indirect immunofluorescence assay (IFA) and classified according to international consensus nomenclature as various anti-cell (AC) patterns.

Results. Of our study cohort, 78.9% had positive ANA reactivity (≥1:80), which was either a homogenous, fine-speckled (AC-1 and AC-4) or mixed IFA pattern. Importantly, the AC-4 and mixed ANA patterns were also observed in progressors at the time of disease onset. While all of the RA patients showed a high prevalence of arthritis-associated autoantibodies, they also had a high prevalence of extractable nuclear antigen–positive autoantibodies to other autoantigens. In FDR, we did not observe any increase in serum autoreactivity to nonarthritis autoantigens, either cross-sectionally or in samples collected longitudinally from progressors prior to RA onset.

Conclusion. While alternative autoimmunity and ANA positivity are widely prevalent in First Nations populations, including asymptomatic, seronegative FDR, expansion of alternative autoimmunity does not occur in parallel with ACPA expansion in FDR and is restricted to patients with established RA.

INTRODUCTION

Rheumatoid arthritis (RA) is a chronic autoimmune inflammatory condition that leads to progressive joint damage, a decline in quality of life, increased mortality, and substantial economic costs to individuals and to society (1). Although the pathogenesis of RA is incompletely understood, a large body of literature suggests that specific autoantibodies, particularly anti–citrullinated protein autoantibodies (ACPAs) and rheumatoid factor (RF), play a central role in linking systemic autoimmunity to the destructive, progressive, joint-focused, chronic inflammatory response. As such, detection of ACPAs, RF, and other RA-associated autoantibodies, such as anti–carbamylated protein (anti-CarP) autoantibodies, is associated with disease progression and with erosive joint damage (2,3). Importantly, it is now well established in multiple populations worldwide that these RA-specific autoantibodies are serologically detectable months to years prior to the onset of inflammatory arthritis (4). This finding has led to speculation that

Dr. Anaparti is recipient of Postdoctoral Fellowships from Research Manitoba and the Arthritis Society of Canada (grant TPF-18-0219). Dr. El-Gabalawy's work was supported by the Canadian Institutes of Health Research (grant MOP77700).

[1]Vidyanand Anaparti, PhD, Irene Smolik, PhD, Xiaobo Meng, PhD, Liam O'Neil, MD, MHSc, Hani El-Gabalawy, MD, FRCPC: University of Manitoba, Winnipeg, Manitoba, Canada; [2]Mackenzie A. Jantz, BSc, Marvin J. Fritzler, PhD, MD: University of Calgary, Calgary, Alberta, Canada.

Dr. Fritzler has received consulting fees, speaking fees, and/or honoraria from Inova and Werfen (less than $10,000 each). No other disclosures relevant to this article were reported.

Address correspondence to Vidyanand Anaparti, PhD, University of Manitoba, Winnipeg, Manitoba R3E 3P4, Canada. Email: vidyanand.anaparti@umanitoba.ca.

Submitted for publication June 4, 2020; accepted in revised form January 28, 2021.

after a latency period characterized by nonpathogenic autoimmunity, there is a transition point in some individuals when these autoantibodies become pathogenic and might be predictive of the imminent onset of clinically defined RA.

Latent autoimmunity is described as a phenomenon where patients demonstrate an accumulation of alternative autoantibodies typically associated with another autoimmune condition, despite having disease-specific autoantibodies (5,6). Detection of alternative autoantibodies is well-documented in systemic lupus erythematosus (SLE), Sjögren's syndrome, autoimmune thyroid disease, and systemic sclerosis (5–7). In the case of RA, antinuclear antibodies (ANAs) are reported in ~13–50% of RA patients and were associated with poor treatment response in patients undergoing biologic disease-modifying antirheumatic drug (DMARD) therapy (7,8). While ACPAs, RF, and anti-CarP are detectable in preclinical RA, the detection of alternative autoantibodies during the preclinical period of RA has not been systematically studied (9). Moreover, it is not clear what role such nonspecific autoantibodies may play in facilitating and accelerating the progression toward the onset of inflammatory arthritis.

We have undertaken prospective studies of the preclinical phase of RA by following up the first-degree relatives (FDR) of indigenous (First Nations) peoples, a population known to have a disproportionately high prevalence of RA compared to nonindigenous populations (10). While the reasons for this high prevalence are multifactorial and incompletely understood, we and others have defined important genetic and environmental factors that contribute to the high prevalence rates observed (9,11,12). Indeed, in our prospective cohort, we showed that the likelihood that unaffected FDR who are positive for ACPAs and RF will develop inflammatory arthritis during 5 years of follow-up is 38%, with a mean transition time of 3.2 years for those going on to develop RA (9).

In this study, we evaluated our cohort of First Nations RA patients and their at-risk FDR for a broad spectrum of alternative autoantibodies. We studied preclinical longitudinal samples from individuals who ultimately developed RA and compared them to those who did not, and to RA patients with established disease. We hypothesized that alternative autoantibodies exist in the preclinical phase of RA and evolve with the onset of clinically imminent disease. Our findings indicate that despite an augmentation and broadening of the ACPA response as RA onset approaches, there is no suggestion of a parallel increase in the prevalence or levels of alternative autoantibodies.

PATIENTS AND METHODS

Study design. Study participants were recruited from urban and rural First Nations communities in Central Canada (13,14). The Biomedical Research Ethics Board of the University of Manitoba approved the overall design of the study and consent forms (Ethics: 2005:093; Protocol: HS14453). The conduct of the study was guided by Tri-Council Policy Statement: Ethical Conduct for Research Involving Humans – TCPS 2 (2018) Chapter 9: Research Involving the First Nations, Inuit and Métis Peoples of Canada, and the Principles of Community Based Participatory Research, a cornerstone of the Canadian Institutes of Health Research Guidelines for Health Research Involving Aboriginal People (http://www.cihr-irsc.gc.ca/e/29134.html). The study participants provided informed consent after the study was explained to them in detail.

Cross-sectional baseline serum samples were obtained for the following 3 groups: 1) cyclic citrullinated peptide (CCP)–positive RA patients, all of whom met the American College of Rheumatology/European League Against Rheumatism 2010 criteria (15) (n = 50) 2), CCP-positive FDR without any clinical evidence of joint or systemic inflammation whose serum had detectable anti-CCP titers (n = 50), and 3) unaffected CCP-negative FDR (n = 14) (Table 1). CCP-positive FDR were further categorized based on their anti-CCP titers as CCP low (20–60 units/ml; n = 20) or CCP high (>60 units/ml; n = 30) (Supplementary Table 1, available on the *Arthritis & Rheumatology* website at http://onlinelibrary.wiley.com/doi/10.1002/art.41675/abstract).

A subset of FDR who were followed up longitudinally until RA onset, hereafter referred to as "progressors," had serum samples from pre-RA time points (T-2 and T-1) available for analysis, as well as a sample from the study visit where they were found to have joint inflammation (referred as RA onset time [T0]). While T-2 and T-1 represent the preclinical stages of RA, T0 represents the RA onset time. This time point was defined as the first objective detection of the presence of ≥1 swollen joint, deemed by the study rheumatologist (HEG) to represent active synovitis (16). The mean ± SD time difference between T-1 and T0 was 3.68 ± 2.06 years, while the difference between T-2 and T0 was 5.16 ± 2.33 years, and the difference between T-2 and T-1 was 1.48 ± 1.01 years. For family-wise analysis, we used data from a subset of 3 families comprised of 3 RA patients and their 4 FDR.

Sample collection, storage, and immunoassays. Venous blood was collected into SST serum separation tubes (BD Vacutainer Systems) by a trained phlebotomist or study nurse, allowed to clot for 35 minutes, and then centrifuged to separate the serum. Aliquots of sera were stored at –20°C until used for serology assays. C-reactive protein (CRP) levels were measured using a human high-sensitivity CRP enzyme-linked immunosorbent assay (ELISA) kit (Biomatik) according to the manufacturer's instructions. ACPA was detected using either anti-CCP2 on a BioPlex 2200 System (Bio-Rad) or anti-CCP3 kits (Inova Diagnostics) with cutoff levels set according to the manufacturer's instructions. For analysis, CRP levels <3 mg/ml were considered within the normal range, while anti-CCP levels <20 units/ml were considered negative.

Serologic analysis for autoantibodies. Screening for ANAs and antigen specificities of autoantibodies was done at Mitogen Diagnostics (MitogenDx; www.mitogen.ca) (17). ANA test on HEp-2 substrates by indirect immunofluorescence assay (IFA) was processed and read on an automated indirect immunofluorescence

Table 1. Clinical features of the FDR and RA patients*

	FDR (n = 64)	RA patients (n = 50)	*P*†	Progressors (n = 14)
Age, years	41.74 ± 12.2	45.89 ± 12.3	–	35.7 ± 11.4
Sex, no. (%) female	47 (73.4)	44 (88)	0.055‡	9 (64.3)
hsCRP, mg/liter	6.23 ± 7.28	13.28 ± 16.4	0.0001§	9.7 ± 9.5
BMI, kg/m^2	32.74 ± 8.73	30.37 ± 7.53	0.151§	28.2 ± 7.7
DAS28	–	3.3 ± 1.19	–	–
RF titer, IU/ml	58.83 ± 240.8	472.6 ± 770.2	0.0001§	242.6 ± 218.2
ACPA, units/ml¶	63.52 ± 94.79	222.4 ± 107.6	0.0001§	436.7 ± 307.3
Type 2 diabetes mellitus, no. (%)	23 (36)	9 (20.9)	0.077‡	–
Smoking history, no. (%)			0.926‡	
Yes	44 (67.1)	32 (64)	–	13 (92.8)
No	14 (15.2)	7 (14)	–	1 (8.2)

* Except where indicated otherwise, values are the mean ± SD. FDR = first-degree relatives; RA = rheumatoid arthritis; hsCRP = high-sensitivity C-reactive protein; BMI = body mass index; DAS28 = Disease Activity Score in 28 joints; RF = rheumatoid factor; ACPA = anti–citrullinated protein antibody.
† *P* values less than 0.05 were considered significant.
‡ By Pearson's chi-square test.
§ By *t*-test for independent samples.
¶ Determined using CCP2 or CCP3.1 assay.

platform (Nova View; Inova Diagnostics) at a screening serum dilution of 1:80. Antibodies to an array of human and viral citrullinated peptides (histone 4 citrullinated peptide 1 [HCP1], HCP2, viral citrullinated peptide 1 [VCP1] and VCP2; Theradiag) were tested by addressable laser bead immunoassay (ALBIA) on a Luminex 200 luminometer (Luminex) using cutoffs suggested by the manufacturer. VCP1 and VCP2 are proteins encoded by the Epstein-Barr virus, while HCP1 and HCP2 are citrullinated peptides corresponding to histone 4. Studies suggest that the multiplexing of HCPs and VCPs increases the sensitivity of detecting both monospecific and cross-reactive ACPAs in RA sera (13,14). HCP1, HCP2, VCP1, and VCP2 peptides used in this assay are enzymatically citrullinated, synthetic peptides.

Antibodies to extractable nuclear antigens (ENAs; double-stranded DNA [dsDNA], ribosomal protein, and proliferating cell nuclear antigen [PCNA]), were tested by ALBIA on a commercially available kit (Connective 13; Theradiag). The CTD Panel (research use only; Inova Diagnostics) is an array based on particle-based multianalyte array technology and includes dense fine speckles 70, dsDNA, U1 RNP, Sm, SSA/Ro 60, TRIM21/Ro 52, SSB/La, Scl-70/topoisomerase I, Jo-1, CENP-B, and ribosomal P autoantigens (16). Anti-CarP was detected by an ELISA (Quanta Lite; Inova Diagnostics) that employed a native carbamylated protein. Anti-PAD4 was detected by an ALBIA (research use only; Inova Diagnostics). Cutoffs were established according to the manufacturers' instructions and were based on the values derived from controls and calibrators included with each kit and used on each assay run. For anti-PAD4, cutoff values were established using the 95th percentile in healthy individuals and set to 200 and 1,000 units for negativity and positivity, respectively.

ACPA reactivity to alternative autoantibodies. We selected 4 sera from our study cohort, 2 of which were strongly anti-CCP+/HEp-2+, and 2 of which were strongly CCP+/HEp-2–. Also, we used HEp-2+ serum from an SLE patient as a positive control and CCP–/HEp-2– normal human serum as a negative control. All of the sera were serially diluted (1:80–1:10,240) and preincubated overnight at room temperature on either Quanta Lite CCP3 IgG ELISA plates (Inova Diagnostics) or ELISA plates coated with ANAs. Adsorbed sera were then aspirated from the wells and retested on either Quanta Lite CCP3 IgG ELISA plates (Inova Diagnostics) or ANA-coated wells. As experimental controls, we used unadsorbed sera and sera adsorbed on plates precoated with 5 μg/ml bovine serum albumin.

Statistical analysis. GraphPad Prism version 8.0 and SPSS 25.0 for Windows (IBM) were used for data analysis and graphic representation of data. For analysis, data was log(x + 1) transformed. Continuous variables are presented as the mean ± SD. Data were analyzed using either *t*-test for independent samples, chi-square test, Mann-Whitney U test, two-way analysis of variance (ANOVA) (with Bonferroni correction) or repeated-measures ANOVA (with Geisser-Greenhouse correction) wherever required. *P* values less than 0.05 were considered significant.

RESULTS

Characteristics of the study population. The baseline characteristics of the FDR, RA patients, and progressors are shown in Table 1. In the FDR group, 73% of the subjects were women. The median age was 46.05 years. There was no difference between the FDR and RA patient groups in mean body mass index (BMI), smoking rate, or prevalence of type 2 diabetes mellitus (DM). All RA patients were receiving DMARDs (Supplementary Table 2, available on the *Arthritis & Rheumatology* website at http://onlinelibrary.wiley.com/doi/10.1002/art.41675/abstract). The progressor subset of the FDR (n = 14)

had a median age of 32.5 years at the time of disease onset, and a median BMI of 27.5 kg/m^2.

Arthritis-associated autoantibodies in RA patients and FDR. Figure 1 and Supplementary Figure 1, available on the *Arthritis & Rheumatology* website at http://onlinelibrary.wiley.com/doi/10.1002/art.41675/abstract, illustrate the serum concentrations of autoantibodies to arthritis-associated autoantigens in RA patients and FDR. Not unexpectedly, compared to FDR, RA patients had higher titers of all RA-associated autoantibodies, including HCP2, VCP2, RF, anti-CarP proteins, and PAD4. Furthermore, 100% of RA patients showed positive reactivity to ≥1 RA-related autoantigen, compared to 39% of FDR. Data on autoantibody prevalence rates and their concentrations are outlined in Supplementary Tables 3 and 4, available on the *Arthritis & Rheumatology* website at http://onlinelibrary.wiley.com/doi/10.1002/art.41675/abstract.

FDR were classified based on their anti-CCP levels as CCP negative, CCP low, or CCP high, as described in Patients and Methods (Supplementary Table 1, available on the *Arthritis & Rheumatology* website at http://onlinelibrary.wiley.com/doi/10.1002/art.41675/abstract). Based on this classification, FDR reactivity to the panel of other RA-associated autoantigens was observed in 21.4% (3 of 14) of the CCP-negative FDR, 30% (6 of 20) of the CCP-low FDR, and 73.3% (22 of 30) of the CCP-high FDR, based on predetermined cutoff levels for each of the assays (Supplementary Table 3, available on the *Arthritis & Rheumatology* website at http://onlinelibrary.wiley.com/doi/10.1002/art.41675/abstract). Not unexpectedly, CCP-high FDR demonstrated high-titer autoantibodies to the citrullinated antigens HCP1, VCP2, and PAD4 (Figure 1). Taken together, our findings demonstrate an expansion of the RA-associated autoantibody repertoire during this preclinical phase.

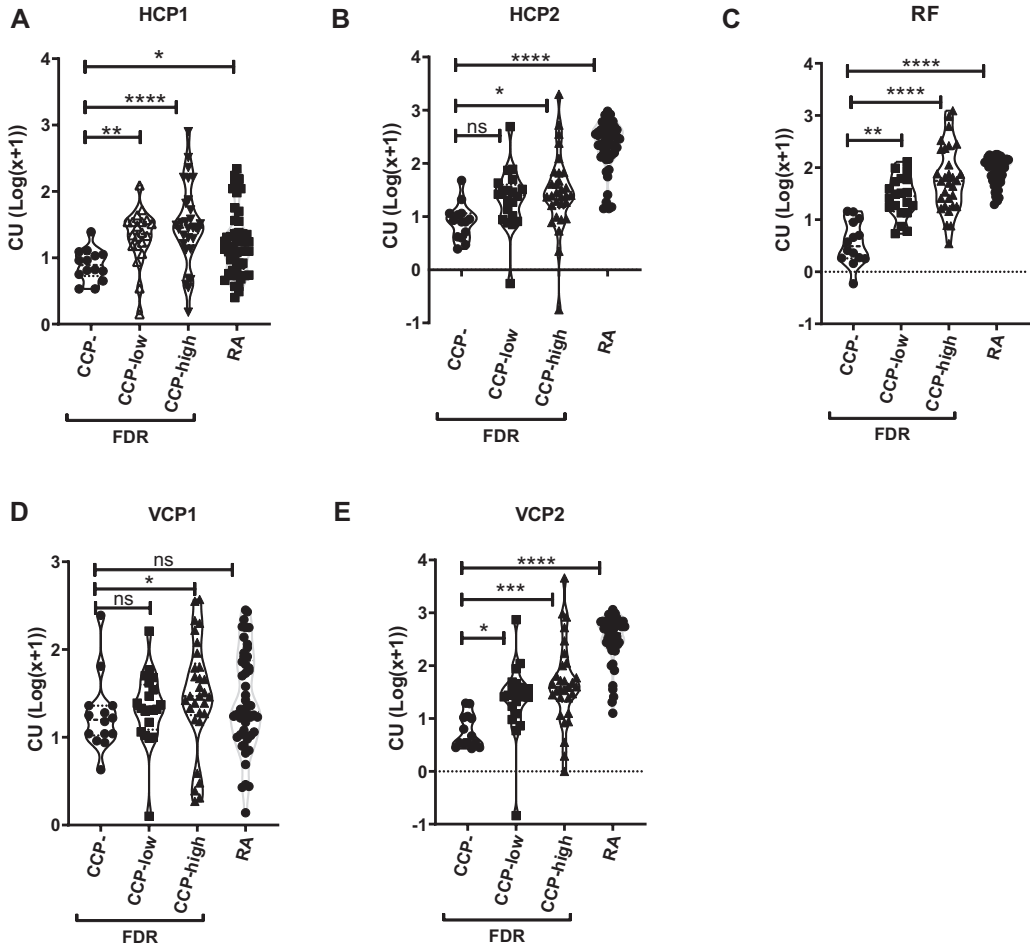

Figure 1. Violin plots showing the expression of the arthritis-specific autoantibodies histone 4 citrullinated peptide 1 (HCP1) (**A**), HCP2 (**B**), rheumatoid factor (RF) (**C**), viral citrullinated peptide (VCP1) (**D**), and VCP2 (**E**) in first-degree relatives (FDR) who were negative for cyclic citrullinated peptide (CCP–), FDR with low CCP titers, FDR with high CCP titers, and rheumatoid arthritis (RA) patients. Data are presented as concentration units (CU) after log (x + 1) transformation. Symbols represent individual subjects. * = $P < 0.05$; ** = $P = 0.01$; *** = $P = 0.001$; **** = $P < 0.0001$, by Kruskal-Wallis method with Dunn's post hoc test. NS = not significant.

Detection of alternative autoantibodies and their patterns in RA patients and FDR. ANAs were detected on HEp-2 substrates by a standard IFA and were classified as anti-cell (AC) patterns according to the International Consensus on Antinuclear Antibody Patterns (ICAP; www.anapatterns.org) (18). In total, 78.9% had positive ANA reactivity (≥1:80). Within the groups, 86% (43 of 50) of the RA patients and 57.8% (37 of 64) of the FDR were HEp-2 IFA positive at a titer of ≥1:160. The most frequent HEp-2 IFA patterns, classified based on the ICAP nomenclature, were the nuclear homogenous and/or fine-speckled patterns (AC-1 and AC-4), in both the FDR and the RA patients (Supplementary Tables 5 and 6, available on the *Arthritis & Rheumatology* website at http://onlinelibrary.wiley.com/doi/10.1002/art.41675/abstract). Compared to FDR, RA patients showed a more diverse repertoire of HEp-2 IFA patterns, including cytoplasmic staining (AC-17 and AC-20) and mitotic staining (AC-24 and AC-28), which were absent in FDR. HEp-2 IFA positivity was found in 50% of the CCP-negative FDR, 65% of the CCP-low FDR, and 57% of the CCP-high FDR, with nuclear fine-speckled pattern (AC-4 and AC-20) being the most frequent pattern, and the titers generally being low, in the 1:160 range.

When antigen specificity of alternative autoantibodies was determined using multiplexed immunoassay platforms, 47.4% (54 of 114) of all of the study participants showed positive reactivity to ≥1 autoantibody. Figure 2 illustrates the serum concentrations of autoantibodies to specific ENA autoantigens (DNA, ribosomal protein, PCNA, and CENP-B) that were significantly elevated in RA patients compared to FDR. Of the FDR, 7.14% (1 of 14) of those in the CCP-negative group, 45% (9 of 20) of those in the CCP-low group, and 53.3% (16 of 30) of those in the CCP-high group showed positive autoantibody reactivity for ≥1 nonarthritis autoantigen ($P = 0.0131$). However, no difference was observed in either the titers or prevalence of each individual autoantibody (Supplementary Tables 3 and 4, available on the *Arthritis & Rheumatology* website at http://onlinelibrary.wiley.com/doi/10.1002/art.41675/abstract). Analysis of data within the families of RA patients (n = 3) showed positive HEp-2 reactivity in 33.3% of the patients, while positive reactivity to alternative autoantibodies was observed in all of the RA patients. In contrast, only 1 of 4 FDR (25% prevalence rate) showed positive reactivity to SSA/Ro 60 (Supplementary Table 7, available on the *Arthritis & Rheumatology* website at http://onlinelibrary.wiley.com/doi/10.1002/art.41675/abstract).

Taken together, our findings demonstrate a high prevalence of ANA-associated autoantibodies in both the FDR and the RA patients, while an increase in the alternative autoantibody repertoire against specific ENA antigens was only detected in RA patients.

Distribution of autoantibody repertoire over time in FDR who developed RA. Baseline characteristics of the progressors who ultimately developed RA (n = 14) are listed in Table 1. We examined changes in RA-associated autoantibodies and alternative autoantibodies in longitudinal samples from this group. Two samples were from the preclinical time points (T-2 and T-1) and 1 sample was from the time of RA onset. Figure 3 illustrates the titers of RA-associated autoantibodies at these 3 time points in the progressors. There was a continuous increase in HCP1, HCP2, VCP1, VCP2, RF, and anti-CCP levels as individuals progressed toward disease onset (Figure 3 and Supplementary Figure 2, available on the

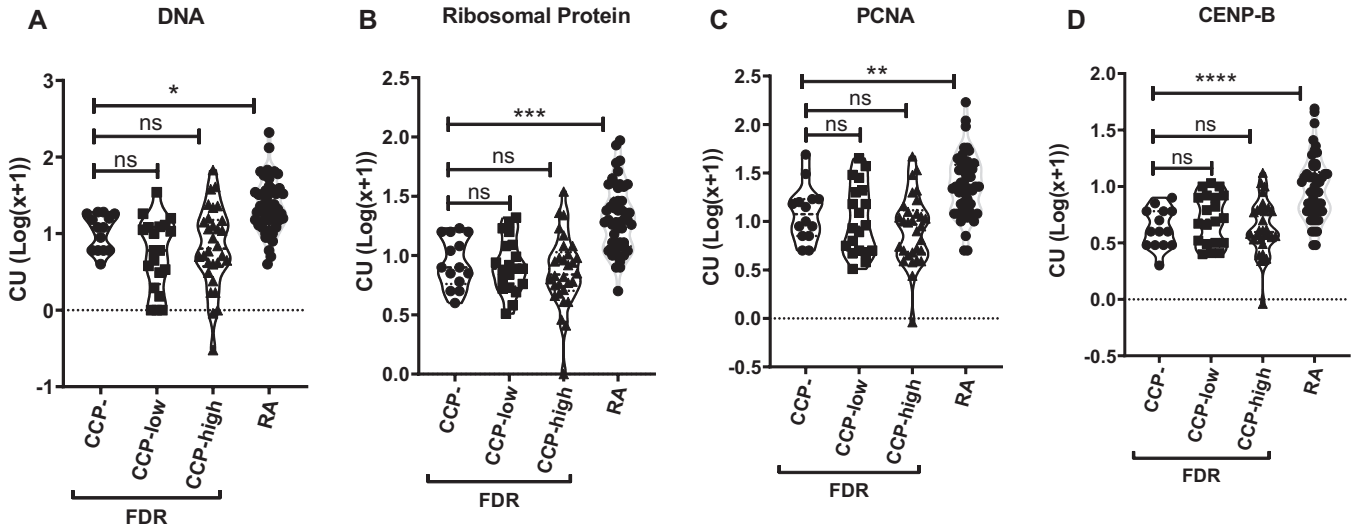

Figure 2. Violin plots showing the distribution of deoxyribonucleic acid (DNA) containing both double-stranded and single-stranded DNA, (**A**), ribosomal protein (**B**), proliferating cell nuclear antigen (PCNA) (**C**), and CENP-B (**D**) in FDR who were negative for CCP, FDR with low CCP titers, FDR with high CCP titers, and RA patients. Data are presented as concentration units after log (x + 1) transformation. Symbols represent individual subjects. * = $P < 0.05$; ** = $P = 0.01$; *** = $P = 0.001$; **** = $P < 0.0001$, by Kruskal-Wallis method with Dunn's post hoc test. See Figure 1 for other definitions.

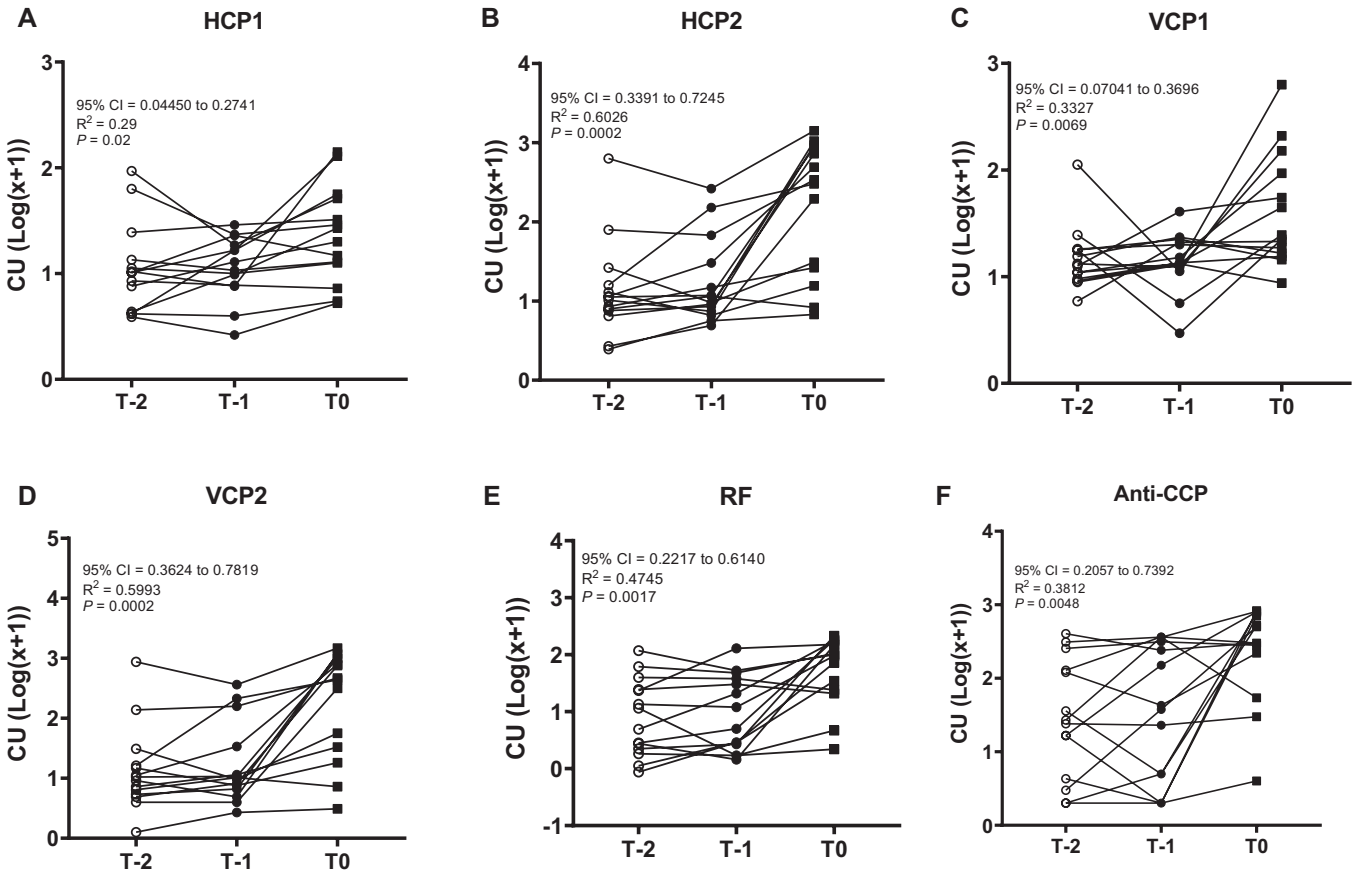

Figure 3. Longitudinal data on RA-specific autoantibodies in FDR who developed RA (progressors). Reactivity to the RA-specific autoantigens HCP1 (**A**), HCP2 (**B**), VCP1 (**C**), VCP2 (**D**), RF (**E**), and anti-CCP (**F**) was significantly elevated at the time of RA onset (T0) compared to the presymptomatic stages (T-2 and T-1). Data were analyzed using repeated-measures analysis of variance with Geisser-Greenhouse correction method and are presented as concentration units after log (x + 1) transformation. 95% CI = 95% confidence interval (see Figure 1 for other definitions).

Arthritis & Rheumatology website at http://onlinelibrary.wiley.com/doi/10.1002/art.41675/abstract). Based on the predetermined cutoff levels, 35.7% (5 of 14) and 28.5% (4 of 14) of the progressors were positive for ≥1 RA-associated autoantibody at T-2 and T-1, respectively, while 64.3% (9 of 14) were positive at RA onset ($P = 0.1298$) (Table 2). These findings are consistent with an expanded ACPA repertoire as RA onset approaches, as previously reported by us and others (9,19).

Table 3 summarizes the prevalence and distribution of ANA in progressors at these 3 time points. In total, 57.2% (8 of 14) were ANA positive at stage T-2, 64.2% (9 of 14) were ANA positive at stage T-1, and 85.8% (12 of 14) were ANA positive at stage T0, although the difference did not reach significance ($P = 0.23$). The most frequent HEp-2 IFA patterns observed in these individuals were AC-4 and AC-20, which are associated with nuclear and cytoplasmic fine-speckled patterns.

We assessed the overall prevalence of alternative autoantibodies, defined as the number of individuals who were positive for ≥1 non–RA-associated autoantibody (Table 2). This analysis showed a prevalence of 21.4% (3 of 14) at stage T0, 7% (1 of 14) at stage T-1, and 21.4% (3 of 14) at stage T-2 ($P = 0.5037$). Supplementary Table 8, available on the *Arthritis & Rheumatology* website at http://onlinelibrary.wiley.com/doi/10.1002/art.41675/abstract, lists fold change in the titers for specific non-RA autoantibodies over time. These data indicate that, in contrast to the RA-associated antibodies, there did not appear to be an increase in either the prevalence or titers of the non-RA autoantibodies as RA onset approached.

ANA reactivity is separate from ACPA reactivity. A previous study has suggested that monoclonal ACPAs are reactive with HEp-2 cell substrates and demonstrate positive staining (20). To further characterize the polyreactive alternative autoantibody responses, we screened for ANA and ACPA reactivity on a subset of optimally diluted and preabsorbed sera (Supplementary Figure 3, *Arthritis & Rheumatology* website at http://onlinelibrary.wiley.com/doi/10.1002/art.41675/abstract). CCP+ and CCP+/HEp-2+ sera preadsorbed on anti-CCP3 plates demonstrated reduced CCP3 activity when retested on CCP3-coated plates. In contrast, anti-CCP3 reactivity remained unaltered in ANA-adsorbed sera, indicating that ANA and ACPA reactivities are separate. Preadsorbed sera

Table 2. Prevalence of different autoantibodies at the indicated time points in FDR who progressed to RA (n = 14)*

	T-2	T-1	T0
Arthritis panel			
HCP1	2 (14.2)	0 (0)	3 (21.4)
HCP2	1 (7)	1 (7)	1 (7)
VCP1	0 (0)	1 (7)	3 (21.4)
VCP2	0 (0)	1 (7)	2 (14.2)
RF	1 (7)	1 (7)	5 (35.7)
CarP	1 (7)	0 (0)	2 (14.2)
PAD4	0 (0)	0 (0)	0 (0)
ENA panel			
DNA	1 (7)	0 (0)	1 (7)
Histone	1 (7)	1 (7)	1 (7)
Ribosomal protein	0 (0)	0 (0)	0 (0)
CENP-B	0 (0)	0 (0)	0 (0)
PCNA	1 (7)	0 (0)	1 (7)
CTD panel			
dsDNA	0 (0)	0 (0)	0 (0)
RNP	0 (0)	0 (0)	0 (0)
Sm	0 (0)	0 (0)	0 (0)
TRIM21/Ro 52	0 (0)	0 (0)	0 (0)
SSA/Ro 60	0 (0)	0 (0)	0 (0)
SSB/La	0 (0)	0 (0)	0 (0)
Scl-70	0 (0)	0 (0)	0 (0)
Jo-1	0 (0)	0 (0)	0 (0)
Centromere	0 (0)	0 (0)	0 (0)
DFS-70	0 (0)	0 (0)	0 (0)
Ribo-P	0 (0)	0 (0)	0 (0)
Ku	0 (0)	0 (0)	0 (0)
RNA Pol III	0 (0)	0 (0)	0 (0)
Rpp25	0 (0)	0 (0)	0 (0)
Rpp38	0 (0)	0 (0)	0 (0)
PM/Scl	0 (0)	0 (0)	0 (0)
BICD2	0 (0)	0 (0)	0 (0)

* T-2 and T-1 represent preclinical stages, and T0 represents the time of rheumatoid arthritis (RA) onset. Values are the number (%). FDR = first-degree relatives; HCP1 = histone 4 citrullinated peptide 1; VCP1 = viral citrullinated peptide; RF = rheumatoid factor; CarP = carbamylated protein; PAD4 = peptidylarginine deiminase 4; ENA = extractable nuclear antigen; PCNA = proliferating cell nuclear antigen; CTD = connective tissue disease; dsDNA = double-stranded DNA; DFS-70 = dense fine speckles 70; Ribo-P = ribosomal P C22 peptide; RNA Pol III = RNA polymerase III; BICD2 = bicaudal D2.

tested on ANA-coated plates demonstrated reduced HEp-2 reactivity in CCP+HEp-2+ and SLE sera, further supporting our findings.

DISCUSSION

It is now well established that RA autoimmunity directed toward posttranslationally modified autoantigens, particularly citrullinated autoantigens, develops over an extended timeframe during the preclinical period preceding the development of clinically detectable joint inflammation (4,9). It is hypothesized that this is a multistep process in which this autoimmune response is progressively matured and amplified until a critical threshold is reached and pathogenic autoimmunity is established. This notion is supported by increasing ACPA levels and epitope spreading to encompass an expanded spectrum of citrullinated autoantigens in the individuals who ultimately develop RA (21). It is also well known that patients with established RA not uncommonly exhibit autoantibodies that are not specific for this disorder, in particular those detected by HEp-2 IFA. It remains unclear whether these non–RA-specific autoantibodies develop during the preclinical phase and undergo an expansion parallel to that of ACPAs in individuals destined to develop RA.

To address this question, we undertook an extensive serologic evaluation of a prospective cohort of RA patients and their FDR, a number of whom ultimately developed RA. Our findings suggest that alternative autoantibodies are prevalent in RA patients, and in ACPA-positive and ACPA-negative FDR. Notably, there was a gradient of HEp-2 IFA positivity, with CCP-negative FDR having the lowest prevalence at ~50%, CCP-positive unaffected FDR having a prevalence of ~61%, and RA patients having a prevalence of ~86%. Importantly, we demonstrated that reactivity to a spectrum of autoantigens targeted by the alternative autoantibodies did not expand in parallel with ACPAs in the individuals who ultimately developed RA.

While latent autoimmunity is known to exist across different autoimmune diseases, the emergence and diversification of autoantibodies is still unclear (5,6,22). For instance, latent autoimmunity was observed in 34–56% of SLE patients, and was predominantly an RA-associated autoreactivity. In contrast, autoantibodies in patients with RA and Sjögren's syndrome were both systemic (SLE and antiphospholipid syndrome-associated) and organ-specific (anti–thyroid peroxidase [anti-TPO], anti–tissue transglutaminase, and type 1 DM–associated). Approximately 36.6% of patients with type 1 DM were anti-TPO positive (5,6). Based on our studies, it was not possible to determine whether latent autoimmunity patterns in RA are similar to other autoimmune

Table 3. ANA patterns at the indicated time points in FDR who progressed to RA (n = 14)*

ANA pattern†	T-2	T-1	T0
Negative	6 (42.8)	5 (35.7)	2 (14.3)
Nuclear			
AC-4	6 (42.8)	8 (57.1)	5 (35.7)
AC-6	1 (7.1)	0 (0)	0 (0)
AC-8	2 (14.2)	0 (0)	0 (0)
AC-9	1 (7.1)	0 (0)	0 (0)
Cytoplasmic			
AC-17	1 (7.1)	1 (7.1)	1 (7.1)
AC-20	3 (21.3)	3 (21.3)	3 (21.3)
Mitotic			
AC-24	1 (7.1)	0 (0)	0 (0)
AC-26	0 (0)	0 (0)	1 (7.1)
Mixed: homogeneous/ speckled	1 (7.1)	0 (0)	5 (35.7)

* T-2 and T-1 represent preclinical stages, and T0 represents the time of rheumatoid arthritis (RA) onset. Values are the number (%). FDR = first-degree relative.
† Anti-cell (AC) patterns were classified according to International Consensus on Antinuclear Autoantibody (ANA) Patterns consensus nomenclature (www.anapatterns.org).

conditions or not. However, we suggest that the autoantibodies to certain antigens such as RF and TPO are easily generated across different autoimmune conditions, thus indicating the presence of an underlying immune dysregulation that is common to these diseases. In our study, we observed an autoantibody prevalence of 50% in RA patients (25 of 50), which was primarily directed toward DNA (18%), PCNA (14%), SSA/Ro 60 (16%), and SSB/La (12%). Additional studies using multiplexed autoantibody arrays across different autoimmune conditions are required to better understand the phenomenon of latent autoimmunity patterns.

In the present study, we demonstrated a high background prevalence of alternative autoantibodies in FDR, which is consistent with observations in other healthy populations. ANAs and related autoantibodies are frequently detectable in healthy populations without apparent autoimmune conditions, with a prevalence rate ranging from ~14% to 50% depending on ethnic origin and other demographic and technical factors (23–25). Autoantibodies in otherwise healthy individuals may represent "natural autoantibodies," which are described as evolutionarily conserved innate molecules that appear in the cord blood at birth (26,27). In adults, natural autoantibodies are produced by autoreactive B cell clones that constitute 15–20% of circulating B cells. Furthermore, natural autoantibodies are typically low-affinity IgG or IgM antibodies, show reactivity to a range of self-antigens such as dsDNA, phospholipids, histones, and apoptotic cell membrane antigens, demonstrate anti–HEp-2 reactivity, are stable over time, and regulate innate inflammatory processes (27–31). It is likely that the survival of natural autoantibodies occurs through effective central and peripheral B cell checkpoint inhibition, which is defined very early in B cell development (32,33). Autoreactive B cell hyperactivation is also inhibited by low-level tonic B cell receptor signaling and anergy induction through retention of surface IgD and overexpression of BAFF (34–36).

Other mechanisms that govern self-reactive antibody responses include optimal activation of regulatory T cells, either through expression of autoimmune regulator or through interleukin-10 (IL-10) secretion, and relocation of autoreactive B cells to the periphery of germinal centers, thereby preventing the formation of follicular helper T–autoreactive B cell clusters (37–39). How these physiologic processes are subverted to generate pathogenic autoantibodies remains an area of considerable research interest and focus.

We have previously shown in our study population that anti-CCP and RF are detectable in the sera of ~10% of unaffected FDR and ~15% of RA patients. Importantly, titers of these RA-associated autoantibodies fluctuated, and, not uncommonly, they became undetectable over time, especially if the titers were low. This phenomenon may be reflective of the complex regulatory mechanisms described above, where most individuals do not develop pathogenic autoantibodies (40). Individuals who ultimately developed RA typically had increasing ACPA titers associated with epitope spreading, and were often positive for both anti-CCP and RF. In parallel studies, we and others have shown that ACPAs exhibiting highly glycosylated V-region domains, a feature that requires somatic hypermutation and T cell help, are predictive of future RA (41–43). In the present study, at-risk FDR demonstrated reactivity to multiple RA-associated and non-RA antigens, indicating the presence of a diverse autoantibody repertoire. Furthermore, HEp-2 IFA staining patterns and autoantibody titers were stable over time during the preclinical period, even in progressors with persistent seropositivity. Also, HEp-2 IFA titers and fine specificity did not appear to expand in parallel with the ACPA response in the individuals who ultimately developed RA. Taken together, these observations suggest that common immunologic processes involving interactions between autoreactive T cells and B cells are needed to generate pathogenic autoantibodies, but that distinct and unique factors are involved in driving the maturation of disease-specific autoantibodies and latent autoimmunity.

It seems likely that appropriate signals from follicular helper T cells are essential for pathogenic autoantibodies to develop through somatic hypermutation in autoreactive B cells (44). Global failure of autoreactive B cell clearance can also be an underlying cause of pathogenic autoantibody appearance in circulation, which is facilitated by differential expression of major histocompatibility complex class II haplotypes, the nature of RA- and SLE-associated antigens, and/or differences in epitope binding to HLA–DRB1, resulting in a bystander activation of autoreactive immune cells (45–47). Also, it is worth considering the role of intrinsic factors such as aberrant germinal center interactions mediated through BAFF and IL-21, deficiency of regulatory B cells, increased frequency of activation-induced cytidine deaminase–mediated somatic hypermutation, and reduced sialylation via an IL-23–mediated pathway (38,44,48–54). What is unknown is whether the altered tolerance mechanisms described above are specific to disease-associated autoantibodies or are at fault even for pathogenic alternative autoantibodies.

Our study has quite a few limitations. We studied FDR of First Nations RA patients, to understand the increased risk of RA development in a susceptible population, and to better understand the preclinical phase of this disease. Based on this, the generalizability of the observations to other populations can be questioned, although several other studies have demonstrated the expansion of the ACPA and other autoantibody responses during the preclinical stages of RA and SLE, respectively. We studied reactivity to a well-characterized panel of autoantigens that are commonly used in clinical practice to characterize specific patterns of autoimmunity and how these may relate to clinical features. The suitability of this platform to studying preclinical autoimmunity can be questioned, and there may be other autoreactivities that are more relevant to the preclinical stages of RA. Additional observations using high-density autoantibody arrays with an expanded coverage of self-antigen repertoire would be helpful in understanding

polyautoimmunity in preclinical RA, SLE, and other autoimmune diseases (55).

In conclusion, we presented evidence showing that the at-risk FDR of First Nations RA patients developed HEp-2 reactive autoantibodies along with RA-specific autoantibodies. We also demonstrated that the expansion of these alternative autoantibodies in FDR preceding RA onset does not follow a pattern similar to that observed in RA-specific autoantibodies. While expansion of alternative autoimmunity was observed only in patients with established RA, ACPA reactivity was separate from ANA reactivity. Overall, our findings support the notion of expanding preclinical autoantibody screening without being focused only on RA-specific autoantibodies to help us better understand their influence on RA onset and disease progression.

ACKNOWLEDGMENTS

We acknowledge the contribution of study participants from rural and urban First Nations people who participated in this study. We also appreciate the support of Chiefs and Band Councils of Norway House Cree Nation and St. Theresa Point First Nation. We acknowledge the laboratory assistance and expertise of Haiyan Hou and Meifeng Zhang in the MitogenDx Laboratory at the University of Calgary. The CTD Profile kit was a generous research gift in kind from Inova Diagnostics.

AUTHOR CONTRIBUTIONS

All authors were involved in drafting the article or revising it critically for important intellectual content, and all authors approved the final version to be published. Dr. Anaparti had full access to all of the data in the study and takes responsibility for the integrity of the data and the accuracy of the data analysis.

Study conception and design. Anaparti, El-Gabalawy.
Acquisition of data. Anaparti, Smolik, Meng, Jantz, Fritzler.
Analysis and interpretation of data. Anaparti, Smolik, O'Neil, Fritzler, El-Gabalawy.

REFERENCES

1. Scott DL, Wolfe F, Huizinga TW. Rheumatoid arthritis. Lancet 2010;376:1094–108.
2. Koppejan H, Trouw LA, Sokolove J, Lahey LJ, Huizinga TJ, Smolik IA, et al. Role of anti–carbamylated protein antibodies compared to anti–citrullinated protein antibodies in indigenous North Americans with rheumatoid arthritis, their first-degree relatives, and healthy controls. Arthritis Rheumatol 2016;68:2090–8.
3. Vencovsky J, Machacek S, Sedova L, Kafkova J, Gatterova J, Pesakova V, et al. Autoantibodies can be prognostic markers of an erosive disease in early rheumatoid arthritis. Ann Rheum Dis 2003;62:427–30.
4. Rantapää-Dahlqvist S, de Jong BA, Berglin E, Hallmans G, Wadell G, Stenlund H, et al. Antibodies against cyclic citrullinated peptide and IgA rheumatoid factor predict the development of rheumatoid arthritis. Arthritis Rheum 2003;48:2741–9.
5. Molano-Gonzalez N, Rojas M, Monsalve DM, Pacheco Y, Acosta-Ampudia Y, Rodriguez Y, et al. Cluster analysis of autoimmune rheumatic diseases based on autoantibodies: new insights for polyautoimmunity. J Autoimmun 2019;98:24–32.
6. James JA, Chen H, Young KA, Bemis EA, Seifert J, Bourn RL, et al. Latent autoimmunity across disease-specific boundaries in at-risk first-degree relatives of SLE and RA patients. EBioMedicine 2019;42:76–85.
7. Matusiewicz A, Strozynska-Byrska J, Olesinska M. Polyautoimmunity in rheumatological conditions. Int J Rheum Dis 2019; 22:386–91.
8. Ishikawa Y, Hashimoto M, Ito H, Tanaka M, Yukawa N, Fujii T, et al. Anti-nuclear antibody development is associated with poor treatment response to biological disease-modifying anti-rheumatic drugs in patients with rheumatoid arthritis. Semin Arthritis Rheum 2019;49:204–10.
9. Tanner S, Dufault B, Smolik I, Meng X, Anaparti V, Hitchon C, et al. A prospective study of the development of inflammatory arthritis in the family members of indigenous North American people with rheumatoid arthritis. Arthritis Rheumatol 2019;71:1494–503.
10. Hitchon CA, Khan S, Elias B, Lix LM, Peschken CA. Prevalence and incidence of rheumatoid arthritis in Canadian First Nations and non-First Nations people: a population-based study. J Clin Rheumatol 2019;26:169–75.
11. Ferucci ED, Darrah E, Smolik I, Choromanski TL, Robinson DB, Newkirk MM, et al. Prevalence of anti-peptidylarginine deiminase type 4 antibodies in rheumatoid arthritis and unaffected first-degree relatives in indigenous North American populations. J Rheumatol 2013;40:1523–8.
12. Peschken CA, Hitchon CA, Robinson DB, Smolik I, Barnabe CR, Prematilake S, et al. Rheumatoid arthritis in a North American Native population: longitudinal followup and comparison with a white population. J Rheumatol 2010;37:1589–95.
13. Johansson L, Pratesi F, Brink M, Arlestig L, D'Amato C, Bartaloni D, et al. Antibodies directed against endogenous and exogenous citrullinated antigens pre-date the onset of rheumatoid arthritis. Arthritis Res Ther 2016;18:127.
14. Pratesi F, Dioni I, Tommasi C, Alcaro MC, Paolini I, Barbetti F, et al. Antibodies from patients with rheumatoid arthritis target citrullinated histone 4 contained in neutrophils extracellular traps. Ann Rheum Dis 2014;73:1414–22.
15. Aletaha D, Neogi T, Silman AJ, Funovits J, Felson DT, Bingham CO III, et al. 2010 rheumatoid arthritis classification criteria: an American College of Rheumatology/European League Against Rheumatism collaborative initiative. Arthritis Rheum 2010;62:2569–81.
16. Mahler M, Betteridge Z, Bentow C, Richards M, Seaman A, Chinoy H, et al. Comparison of three immunoassays for the detection of myositis specific antibodies. Front Immunol 2019;10:848.
17. Troyanov Y, Targoff IN, Payette MP, Raynauld JP, Chartier S, Goulet JR, et al. Redefining dermatomyositis: a description of new diagnostic criteria that differentiate pure dermatomyositis from overlap myositis with dermatomyositis features. Medicine (Baltimore) 2014;93:318–32.
18. Damoiseaux J, Andrade LE, Carballo OG, Conrad K, Francescantonio PL, Fritzler MJ, et al. Clinical relevance of HEp-2 indirect immunofluorescent patterns: the International Consensus on ANA patterns (ICAP) perspective. Ann Rheum Dis 2019;78:879–89.
19. Sokolove J, Bromberg R, Deane KD, Lahey LJ, Derber LA, Chandra PE, et al. Autoantibody epitope spreading in the pre-clinical phase predicts progression to rheumatoid arthritis. PLoS One 2012;7:e35296.
20. Lloyd KA, Wigerblad G, Sahlstrom P, Garimella MG, Chemin K, Steen J, et al. Differential ACPA binding to nuclear antigens reveals a PAD-independent pathway and a distinct subset of acetylation cross-reactive autoantibodies in rheumatoid arthritis. Front Immunol 2018;9:3033.
21. Van der Woude D, Rantapaa-Dahlqvist S, Ioan-Facsinay A, Onnekink C, Schwarte CM, Verpoort KN, et al. Epitope spreading of the anti-citrullinated protein antibody response occurs before disease onset and is associated with the disease course of early arthritis. Ann Rheum Dis 2010;69:1554–61.
22. Rojas-Villarraga A, Toro CE, Espinosa G, Rodriguez-Velosa Y, Duarte-Rey C, Mantilla RD, et al. Factors influencing polyautoimmunity in systemic lupus erythematosus [review]. Autoimmun Rev 2010;9:229–32.

23. Grygiel-Gorniak B, Rogacka N, Puszczewicz M. Antinuclear antibodies in healthy people and non-rheumatic diseases: diagnostic and clinical implications [review]. Reumatologia 2018;56:243–8.
24. Dinse GE, Parks CG, Weinberg CR, Co CA, Wilkerson J, Zeldin DC, et al. Increasing prevalence of antinuclear antibodies in the United States. Arthritis Rheumatol 2020;72:1026–35.
25. Terao C, Ohmura K, Yamada R, Kawaguchi T, Shimizu M, Tabara Y, et al. Association between antinuclear antibodies and the HLA class II locus and heterogeneous characteristics of staining patterns: the Nagahama study. Arthritis Rheumatol 2014;66:3395–403.
26. Nagele EP, Han M, Acharya NK, DeMarshall C, Kosciuk MC, Nagele RG. Natural IgG autoantibodies are abundant and ubiquitous in human sera, and their number is influenced by age, gender, and disease. PLoS One 2013;8:e60726.
27. Pribylova J, Krausova K, Kocourkova I, Rossmann P, Klimesova K, Kverka M, et al. Colostrum of healthy mothers contains broad spectrum of secretory IgA autoantibodies. J Clin Immunol 2012;32:1372–80.
28. Cabiedes J, Cabral AR, Lopez-Mendoza AT, Cordero-Esperon HA, Huerta MT, Alarcon-Segovia D. Characterization of anti-phosphatidylcholine polyreactive natural autoantibodies from normal human subjects. J Autoimmun 2002;18:181–90.
29. Radic M, Marion T, Monestier M. Nucleosomes are exposed at the cell surface in apoptosis. J Immunol 2004;172:6692–700.
30. Chen Y, Khanna S, Goodyear CS, Park YB, Raz E, Thiel S, et al. Regulation of dendritic cells and macrophages by an anti-apoptotic cell natural antibody that suppresses TLR responses and inhibits inflammatory arthritis. J Immunol 2009;183:1346–59.
31. Chen Y, Park YB, Patel E, Silverman GJ. IgM antibodies to apoptosis-associated determinants recruit C1q and enhance dendritic cell phagocytosis of apoptotic cells. J Immunol 2009; 182:6031–43.
32. Culton DA, O'Conner BP, Conway KL, Diz R, Rutan J, Vilen BJ, et al. Early preplasma cells define a tolerance checkpoint for autoreactive B cells. J Immunol 2006;176:790–802.
33. Wardemann H, Yurasov S, Schaefer A, Young JW, Meffre E, Nussenzweig MC. Predominant autoantibody production by early human B cell precursors. Science 2003;301:1374–7.
34. Duty JA, Szodoray P, Zheng NY, Koelsch KA, Zhang Q, Swiatkowski M, et al. Functional anergy in a subpopulation of naive B cells from healthy humans that express autoreactive immunoglobulin receptors. J Exp Med 2009;206:139–51.
35. Thien M, Phan TG, Gardam S, Amesbury M, Basten A, Mackay F, et al. Excess BAFF rescues self-reactive B cells from peripheral deletion and allows them to enter forbidden follicular and marginal zone niches. Immunity 2004;20:785–98.
36. Smith MJ, Ford BR, Rihanek M, Coleman BM, Getahun A, Sarapura VD, et al. Elevated PTEN expression maintains anergy in human B cells and reveals unexpectedly high repertoire autoreactivity. JCI Insight 2019;4:e123384.
37. Cashman KS, Jenks SA, Woodruff MC, Tomar D, Tipton CM, Scharer CD, et al. Understanding and measuring human B-cell tolerance and its breakdown in autoimmune disease [review]. Immunol Rev 2019;292:76–89.
38. Sng J, Ayoglu B, Chen JW, Schickel JN, Ferre EM, Glauzy S, et al. AIRE expression controls the peripheral selection of autoreactive B cells. Sci Immunol 2019;4:eaav6778.
39. Maseda D, Smith SH, DiLillo DJ, Bryant JM, Candando KM, Weaver CT, et al. Regulatory B10 cells differentiate into antibody-secreting cells after transient IL-10 production in vivo. J Immunol 2012;188:1036–48.
40. Fritzler MJ. Toward a new autoantibody diagnostic orthodoxy: understanding the bad, good and indifferent [review]. Auto Immun Highlights 2012;3:51–8.
41. Lloyd KA, Steen J, Amara K, Titcombe PJ, Israelsson L, Lundstrom SL, et al. Variable domain N-linked glycosylation and negative surface charge are key features of monoclonal ACPA: implications for B-cell selection. Eur J Immunol 2018;48:1030–45.
42. Hafkenscheid L, de Moel E, Smolik I, Tanner S, Meng X, Jansen BC, et al. N-linked glycans in the variable domain of IgG anti–citrullinated protein antibodies predict the development of rheumatoid arthritis. Arthritis Rheumatol 2019;71:1626–33.
43. Rombouts Y, Willemze A, van Beers JJ, Shi J, Kerkman PF, van Toorn L, et al. Extensive glycosylation of ACPA-IgG variable domains modulates binding to citrullinated antigens in rheumatoid arthritis. Ann Rheum Dis 2016;75:578–85.
44. Wang Y, Lloyd KA, Melas I, Zhou D, Thyagarajan R, Lindqvist J, et al. Rheumatoid arthritis patients display B-cell dysregulation already in the naive repertoire consistent with defects in B-cell tolerance. Sci Rep 2019;9:19995.
45. Zhao Z, Ren J, Dai C, Kannapell CC, Wang H, Gaskin F, et al. Nature of T cell epitopes in lupus antigens and HLA-DR determines autoantibody initiation and diversification. Ann Rheum Dis 2019;78:380–90.
46. Pacheco Y, Acosta-Ampudia Y, Monsalve DM, Chang C, Gershwin ME, Anaya JM. Bystander activation and autoimmunity. J Autoimmun 2019;103:102301.
47. Yurasov S, Wardemann H, Hammersen J, Tsuiji M, Meffre E, Pascual V, et al. Defective B cell tolerance checkpoints in systemic lupus erythematosus. J Exp Med 2005;201:703–11.
48. Pfeifle R, Rothe T, Ipseiz N, Scherer HU, Culemann S, Harre U, et al. Regulation of autoantibody activity by the IL-23-TH17 axis determines the onset of autoimmune disease. Nat Immunol 2017;18:104–13.
49. Wang S, Wang J, Kumar V, Karnell JL, Naiman B, Gross PS, et al. IL-21 drives expansion and plasma cell differentiation of autoreactive CD11c(hi)T-bet(+) B cells in SLE. Nat Commun 2018;9:1758.
50. Cantaert T, Schickel JN, Bannock JM, Ng YS, Massad C, Delmotte FR, et al. Decreased somatic hypermutation induces an impaired peripheral B cell tolerance checkpoint. J Clin Invest 2016;126:4289–302.
51. Meyers G, Ng YS, Bannock JM, Lavoie A, Walter JE, Notarangelo LD, et al. Activation-induced cytidine deaminase (AID) is required for B-cell tolerance in humans. Proc Natl Acad Sci U S A 2011;108:11554–9.
52. Suurmond J, Atisha-Fregoso Y, Marasco E, Barlev AN, Ahmed N, Calderon SA, et al. Loss of an IgG plasma cell checkpoint in patients with lupus. J Allergy Clin Immunol 2019;143:1586–97.
53. Malkiel S, Jeganathan V, Wolfson S, Orduño NM, Marasco E, Aranow C, et al. Checkpoints for autoreactive B cells in the peripheral blood of lupus patients assessed by flow cytometry. Arthritis Rheumatol 2016;68:2210–20.
54. Zacca ER, Onofrio LI, Acosta CD, Ferrero PV, Alonso SM, Ramello MC, et al. PD-L1(+) regulatory B cells are significantly decreased in rheumatoid arthritis patients and increase after successful treatment. Front Immunol 2018;9:2241.
55. Fritzler MJ, Martinez-Prat L, Choi MY, Mahler M. The utilization of autoantibodies in approaches to precision health. Front Immunol 2018;9:2682.

Arthritis & Rheumatology
Vol. 73, No. 5, May 2021, pp 750–758
DOI 10.1002/art.41597

American College of Rheumatology
Empowering Rheumatology Professionals

Lifetime Risks, Life Expectancy, and Health Care Expenditures for Rheumatoid Arthritis: A Nationwide Cohort Followed Up From 2003 to 2016

Ying-Ming Chiu,[1] Yi-Peng Lu,[2] Joung-Liang Lan,[1] Der-Yuan Chen,[1] and Jung-Der Wang[3]

Objective. This study was undertaken to estimate the cumulative incidence rate of rheumatoid arthritis (RA) in the Taiwanese population ages 16–84 years, and life expectancy, loss of life expectancy, and lifetime health care expenditures for incident RA in Taiwan after 2003, when biologics began to be prescribed.

Methods. We obtained all claims data for the period 1999 to 2016 from the National Health Insurance program of Taiwan, and validated the data against the Catastrophic Illness Registry to establish the study cohort. We estimated the survival function for RA and extrapolated to lifetime using a rolling-over algorithm. For every RA case, we simulated sex-, age-, and calendar year–matched referents from vital statistics and estimated their life expectancy. The difference between the life expectancy of the referent and the life expectancy of the RA patient was the loss of life expectancy for the RA patient. Average monthly health care expenditures were multiplied by the corresponding survival rates and summed up throughout the lifetime to calculate the lifetime health care expenditures.

Results. A total of 29,352 new RA cases were identified during 2003–2016. There was a decreasing trend in cumulative incidence rate in those ages 16–84 for both sexes. Mean life expectancy after diagnosis of RA was 26.3 years, and mean lifetime cost was $72,953. RA patients had a mean loss of life expectancy of 4.97 years. Women with RA survived 1–2 years longer than men with RA of the same age, which resulted in higher lifetime expenditures for the former. Since the life expectancy for women in Taiwan was 6–7 years higher than that for men, the loss of life expectancy for women with RA was higher than that for men with RA. Annual health care expenditures were similar for both sexes.

Conclusion. Our findings indicate that since biologics became available, RA patients have lived longer and had higher lifetime expenditures, which should be monitored and evaluated for cost-effectiveness.

INTRODUCTION

Rheumatoid arthritis (RA) causes huge burdens of premature mortality and high medical expenditures (1). With advancements in treatment in recent decades, mortality has decreased, while medical expenditures have increased (2,3). Although investigators have used the standardized mortality rate to estimate the disease impact on patients conventionally, the impact of RA would be more easily understood by lay people if we could inform them of the life years lost due to the disease (4). In fact, several studies have reported the life years lost attributable to RA, but those studies generally showed large variations, ranging between 1 and 10 years (5–10). Possible reasons for this variation include cohorts collected before the launch of biologic agents (6–8), follow-up periods that covered the time both before and after important drugs (methotrexate or biologics) were launched (5,9,10), RA samples from a single hospital (5,6,8,9), and short follow-up periods (5,10). In addition, most studies were based on prevalent cases of RA (6,7,9,10). Alternatively, one may directly estimate the loss of life expectancy, which is the difference between the life expectancy of newly diagnosed RA patients (i.e., incident cases) and the life expectancy of their corresponding sex- and age-matched referents in the same calendar year, which could be estimated through life tables and real world data. Such a measure would provide

Supported by the Ministry of Science and Technology of Taiwan (grants MOST 107-2627-M-006-007 and MOST 108-2627-M-006-001) and by China Medical University Hospital (grant DMR-109-172).

[1]Ying-Ming Chiu, MD, PhD, Joung-Liang Lan, MD, Der-Yuan Chen, MD, PhD: China Medical University and China Medical University Hospital, Taichung, Taiwan; [2]Yi-Peng Lu, BS: National Cheng Kung University, Tainan, Taiwan; [3]Jung-Der Wang, MD, ScD: National Cheng Kung University and National Cheng Kung University Hospital, Tainan, Taiwan.

No potential conflicts of interest relevant to this article were reported.

Address correspondence to Jung-Der Wang, MD, ScD, National Cheng Kung University Hospital, Departments of Internal Medicine and Occupational and Environmental Medicine, 138 Sheng Li Road, North District, Tainan 704, Taiwan. Email: jdwang121@gmail.com.

Submitted for publication April 1, 2020; accepted in revised form November 17, 2020.

stakeholders with more direct information about disease impact to assist health policy decisions.

Moreover, previous studies of RA have usually used cross-sectional or short-term data to calculate health care expenditures, and most of them presented the expenditure as annual costs (11). Estimating long-term or lifetime costs could provide an overall estimate of the future impact on the health care system after disease occurrence, and would be useful for cost-effectiveness analysis. However, most previous studies that analyzed lifetime costs used Markov models (12,13). Markov models are useful for long-term predictions and policy decisions, but they are generally based on transitional probabilities and related costs extracted from short-term studies, which should be validated by real-world data after a long-term follow-up.

Hwang et al developed a novel semiparametric method to extrapolate the survival function at the end of follow-up, thereby improving the accuracy of estimates of life expectancy and loss of life expectancy from the date of diagnosis (14,15). The main principle of this method is to use data from age- and sex-matched referents simulated from vital statistics of the same calendar year for extrapolation. Using this novel method in a nationwide longitudinal cohort of incident cases of RA with up to 14 years of follow-up, we estimated the life expectancy, loss of life expectancy, and associated lifetime health care costs attributable to RA, with a particular focus on the period after 2003, when biologics began to be prescribed in Taiwan.

PATIENTS AND METHODS

Study approval. This study was approved by the Institutional Review Board of National Cheng Kung University Hospital (B-ER-105-386).

Data source. Taiwan launched the National Health Insurance (NHI) program in 1995. Since then, the public has received comprehensive medical care. The coverage rate of the NHI has been >99% since 2004. In this study, we abstracted claims data from the NHI program after creating interlinkages with the National Mortality Registry and Catastrophic Illness Registry. Data were obtained from the Health and Welfare Data Science Center of the Ministry of Health and Welfare of Taiwan.

Study cohort. Nationwide population-based data for the period from 1999 to 2016 were retrieved from the claims database of the NHI program. RA cases were defined according to the International Classification of Diseases, Ninth Revision (ICD-9) CM codes 714.0, 714.1, 714.2, and 714.81, and ICD-10 CM codes M05, M06.0, and M06.2–M06.9 (16,17). RA is included in the list of catastrophic illnesses and eligible for exemption from co-payments in Taiwan. According to NHI regulations, the approval of catastrophic illness status for RA requires clinical and laboratory findings fulfilling the American College of Rheumatology criteria (18,19). To prevent abuse, all registered cases must first be validated by 2 physicians for quality assurance. All RA cases detected in the NHI program were verified with the Catastrophic Illness Registry in this study. Since the cost of biologic agents has been reimbursed by the Taiwan NHI program since 2003, we included only RA cases newly diagnosed after 2003 in our study cohort. Patients <16 years old at the time of diagnosis were excluded (20). All patients were followed up to the end of 2016 or death. The patients' survival status was verified by linkage with the National Mortality Registry. The estimate of health care expenditures included both outpatient and inpatient costs related to RA. The analyses of life expectancy and lifetime costs were further stratified by sex and age at diagnosis of RA.

Estimation of the cumulative incidence rate of RA. The cumulative incidence rate can be used to estimate the lifetime risk, or probability that an individual will develop a disease at some point during the life span (21). Although some investigators have proposed defining the lifetime risk as the risk up to age 100 years (22,23), here we considered the risk from age 16 up to the life expectancy of women in Taiwan, or 84 years, to be the lifetime risk of RA in a general adult population for each calendar year from 2003 to 2016. Using the age- and sex-specific number of new cases abstracted from the NHI database for every 5 consecutive calendar years as the numerator, and the corresponding mid-year population at risk from vital statistics as the denominator, we calculated the age- and sex-specific incidence rates and cumulative incidence rate for RA. The cumulative incidence rate for the population ages 16–84 years was calculated to estimate the lifetime risk of RA, as follows:

$$CIR_{16-84} = 1 - \exp(-\Sigma i\,(IR_i)\,(\Delta t_i)),$$

where CIR_{16-84} is the cumulative incidence rate for the population ages 16–84 years, i = 16–19,20–24,…,80–84, IR_i is the incidence rate of the i-th age group, and Δt_i is the 5-year age range.

To compare the characteristics of incident RA populations diagnosed in different calendar years, prevalence rates of major comorbidities in the RA population were collected.

Table 1. Cumulative incidence rate of rheumatoid arthritis in the Taiwanese population ages 16–84 years, stratified by sex and calendar year of diagnosis*

Year	All	Women	Men
2003	1.24	1.90	0.59
2004	1.18	1.79	0.57
2005	1.12	1.68	0.55
2006	1.06	1.60	0.51
2007	1.00	1.44	0.55
2008	0.96	1.37	0.53
2009	0.94	1.34	0.52
2010	0.87	1.27	0.46
2011	0.83	1.16	0.49
2012	0.84	1.17	0.49
2013	0.73	1.04	0.41
2014	0.68	0.91	0.45
2015	0.64	0.89	0.38
2016	0.50	0.68	0.31

* Values are the percentage of subjects.

Table 2. Prevalence of major comorbidities in patients with rheumatoid arthritis, stratified by calendar period of disease diagnosis*

	2003–2007 (n = 12,190)	2008–2012 (n = 10,565)	2013–2016 (n = 6,597)
Age, mean ± SD years	52.48 ± 13.94	53.60 ± 14.16	54.37 ± 14.22
Sex			
No. (%) male	2,751 (22.57)	2,635 (24.94)	1,805 (27.36)
No. (%) female	9,439 (77.43)	7,930 (75.06)	4,792 (72.64)
Comorbidity, no. (%)			
Cancer	412 (3.4)	401 (3.8)	256 (3.9)
Cirrhosis of the liver	1,411 (11.6)	975 (9.2)	516 (7.8)
COPD	1,910 (15.7)	1,362 (12.9)	819 (12.4)
Diabetes	984 (8.1)	973 (9.2)	707 (10.7)
Cardiovascular disease	1,906 (15.6)	1,585 (15.0)	885 (13.4)
Hyperlipidemia	1,610 (13.2)	1,902 (18.0)	1,317 (20.0)
Stroke	506 (4.2)	431 (4.1)	253 (3.8)

* COPD = chronic obstructive pulmonary disease.

Estimation of life expectancy after diagnosis of RA. Estimates of life expectancy after the diagnosis of RA were obtained using the semiparametric survival extrapolation method proposed by Hwang and Wang (14,15) and verified mathematically by Fang et al (24). First, we created a reference population of subjects matched to the RA cohort with regard to age, sex, and calendar year according to the hazard function of the life table from Taiwan National Vital Statistics using Monte Carlo methods. Second, we took the logit transformation of the survival ratio of the RA cohort to the matched referents at each time point *t* and fitted a restricted cubic spline model, which was used to extrapolate the survival curve of the RA cohort for 1 month. Third, assuming the extrapolated 1 month to be the true observation, and omitting the data from the first month used for the previous extrapolation, we refitted the model again and extrapolated it to the next month. By performing the above procedure repeatedly, i.e., using a rolling-over algorithm (15), and extending the survival curve for the index cohort month-by-month, we reached a point where the survival rate was close to 0. For example, if the survival rate were extrapolated for 50 years, or 600 months, the software would repeatedly construct the restricted cubic spline model 600 times until all cases in the index cohort were deceased. Detailed methods and empirical examples have been published previously (4,15,25–30).

The area under the estimated lifetime survival curve is the life expectancy after the diagnosis of RA. The loss of life expectancy was thus the difference between the area of the mean survival curve for the RA cohort and the area of the mean survival curve for the matched referents. This parameter provided us with a measure of the loss of a patient's lifespan, which is also the burden of RA on the society.

Estimation of lifetime health care expenditures for patients with RA. Methods of estimating lifetime medical costs have been described previously (15,27). The total lifetime health care cost for RA patients refers to all direct health care expenditures paid by the NHI program from diagnosis of RA to death. We collected reimbursement data (inpatient and outpatient files) from the NHI database to estimate the average health care expenditure for

Table 3. Life expectancy, loss of life expectancy, lifetime health care expenditures, and cost per life year of RA, stratified by sex and age at diagnosis*

Sex and age at RA diagnosis	No. of deaths	Life expectancy, years	Loss of life expectancy, years	Loss of life expectancy/ life expectancy of matched referents, %†	Lifetime health care expenditures, dollars‡	Mean cost per life year, dollars‡
Both sexes						
Ages 16–49 years (n = 11,766)	297	29.37 ± 4.81	14.38 ± 4.81	33	77,917 ± 7,294	2,653
Ages 50–64 years (n = 11,477)	907	21.59 ± 1.50	6.01 ± 1.50	22	70,037 ± 3,429	3,244
Ages >65 years (n = 6,109)	2,011	11.82 ± 0.30	2.42 ± 0.31	17	43,649 ± 1,303	3,693
Men						
Ages 16–49 years (n = 2,324)	115	29.98 ± 6.28	8.50 ± 6.30	22	74,047 ± 7,969	2,470
Ages 50–64 years (n = 2,956)	364	22.26 ± 1.32	1.93 ± 1.33	8	68,068 ± 3,895	3,058
Ages >65 years (n = 1,911)	734	10.41 ± 0.43	2.16 ± 0.44	17	39,052 ± 1,895	3,751
Women						
Ages 16–49 years (n = 9,442)	182	31.92 ± 6.38	13.11 ± 6.38	29	81,832 ± 9,179	2,564
Ages 50–64 years (n = 8,521)	543	19.44 ± 1.82	9.36 ± 1.82	33	67,314 ± 4,144	3,463
Ages >65 years (n = 4,198)	1,277	12.35 ± 0.34	2.61 ± 0.34	17	45,269 ± 1,510	3,666

* Except where indicated otherwise, values are the mean ± SEM.
† The life expectancy of age-, sex-, and calendar year–matched referents was defined as the life expectancy after diagnosis of rheumatoid arthritis (RA) plus the loss of life expectancy for RA.
‡ $1 dollar (US) = $32.37 dollars (New Taiwan).

RA patients. We calculated total health care costs, including RA-related treatments, tests, and procedures, added up the monthly cost for all RA cases, and divided this by the total number of surviving cases in each month to estimate the average monthly health care cost. By multiplying the average monthly health care cost with the corresponding monthly mean probability of survival, we then obtained the lifetime health care cost. To accommodate for the possible increase in health care costs near the end of life, we estimated the monthly mean costs beyond the maximum follow-up using the mean expenditures of the patients in a specific number of months prior to their death with a weighted average. The number was determined according to the observed costs in the last several months of life of deceased patients with RA, where the weights were dependent on the extrapolated hazard rate of death. Monetary value was expressed in 2019 dollars (US) ($1 [US] = $32.37 [New Taiwan]). The estimates of lifetime costs were calculated using the iSQoL2 package.

Validation of the extrapolation method. We validated the accuracy of the extrapolation method by including only patients enrolled between 2003 and 2009 in the cohort to be extrapolated for 7 years, and compared the results with the 14 years of actual follow-up data estimated by the Kaplan-Meier method. Namely, we tested the validity of the extrapolation method by comparing the predicted estimation of 7 years of data with the actual observed data. Using the Kaplan-Meier estimates as the gold standard, we calculated the relative bias as follows: (estimate from extrapolation – Kaplan-Meier estimate at the end of 14 years)/Kaplan-Meier estimate.

RESULTS

Patient characteristics. A total of 29,352 RA cases newly diagnosed since 2003 were included. Three-fourths of the patients were women.

Cumulative incidence rate. The lifetime risk of RA, expressed as the cumulative incidence ratio in the general Taiwanese population ages 16–84 years, is shown in Table 1. There was a consistent declining trend from 2003 to 2016, with the incidence rate declining from 1.90% to 0.68% in women and from 0.59% to 0.31% in men. Prevalence rates of major comorbidities in RA patients are summarized in Table 2. There was no difference in the prevalence of comorbidities between different calendar periods of diagnosis, except for a mild increase in the prevalence of hyperlipidemia in more recent periods.

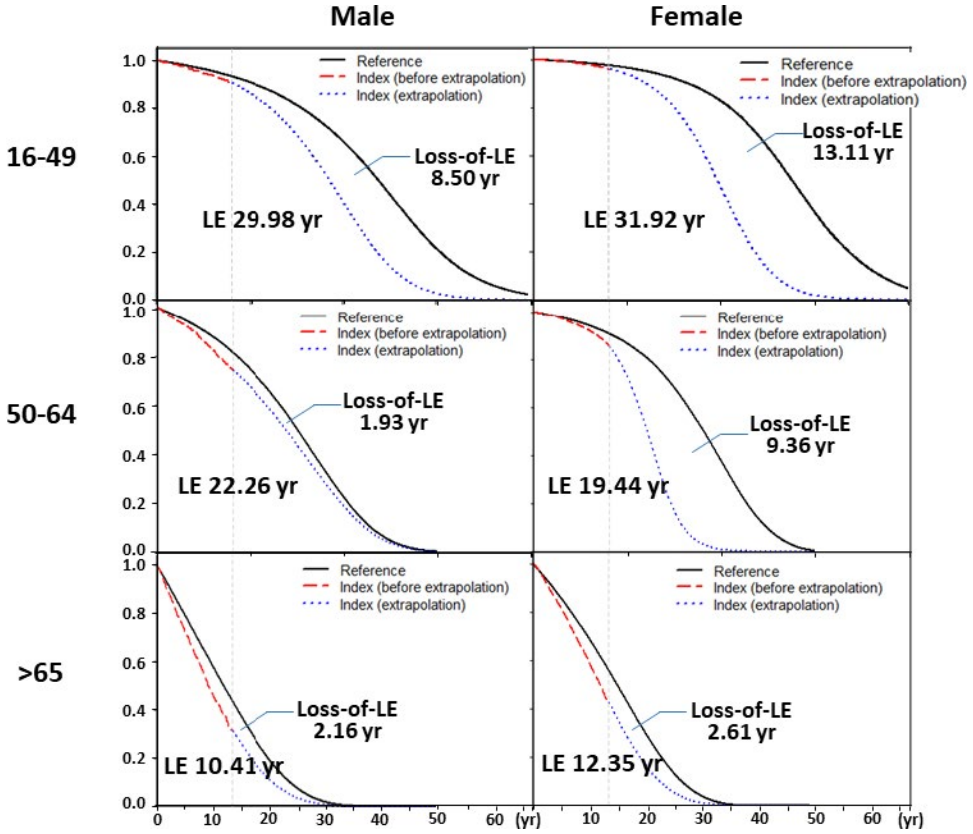

Figure 1. Life expectancy (LE) and loss of life expectancy after diagnosis of rheumatoid arthritis (RA), stratified by sex and age (in years) at diagnosis. Black lines represent sex- and age-matched referents simulated from Taiwanese national life tables; red lines represent data from the RA cohort; blue lines represent extrapolation from the RA cohort. The area between the curve for matched referents and that for the RA cohort is the loss of life expectancy.

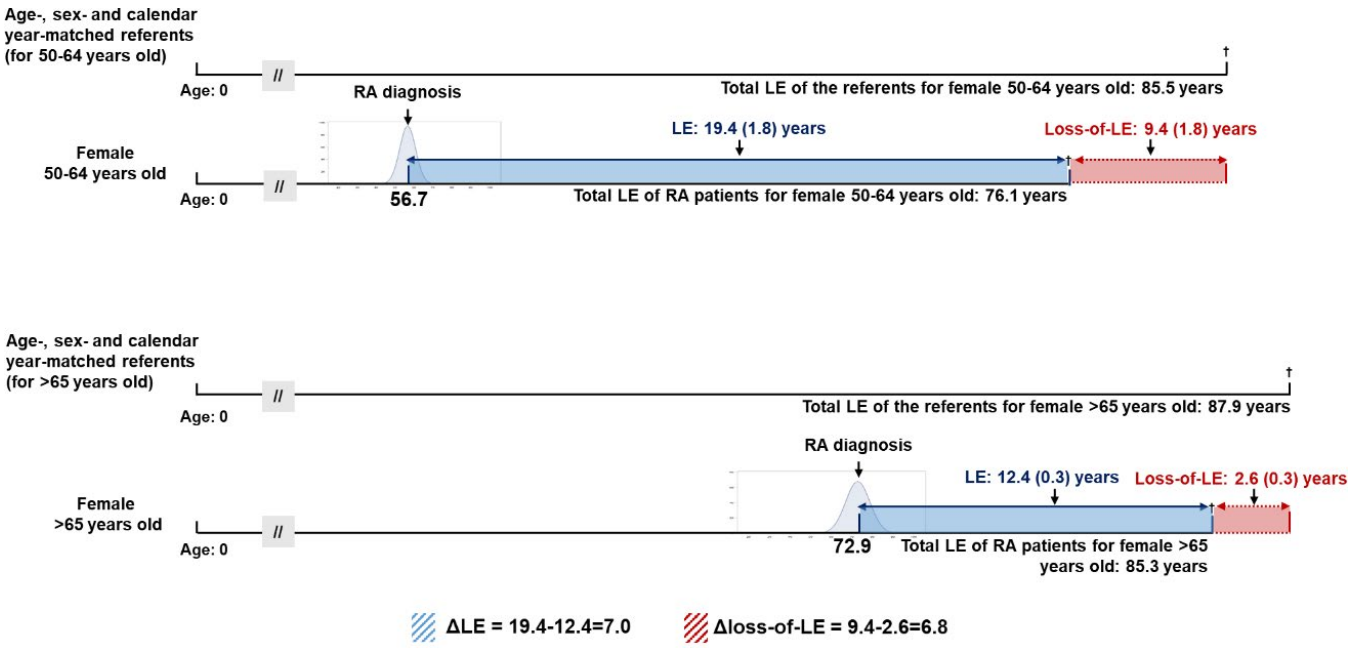

Figure 2. Comparison of loss of life expectancy (LE) estimates, adjusted for age, sex, and calendar year, in multiple cohorts. If a female patient with rheumatoid arthritis (RA) was diagnosed between 50 and 64 years of age, her life expectancy after diagnosis would be 19.4 years, or 7.0 years longer than that of a patient diagnosed at age >65 years (who had a life expectancy after diagnosis of 12.4 years). The loss of life expectancy was the difference between the life expectancy in the index cohort and that in the age-, sex-, and calendar year–matched referents simulated from life tables. Thus, the comparison of 2 loss of life expectancies, or Δloss of life expectancy (9.4–2.6 = 6.8), would be a difference-in-differences adjusted for the potential confounders. The apparent advantage of diagnosis at a younger age would be much less apparent after such an adjustment. Values are the mean ± SEM.

Estimation of life expectancy and loss of life expectancy. The estimated overall mean life expectancy after diagnosis of RA was 26.3 years, and the estimated mean loss of life expectancy was 4.97 years. The mean life expectancy and loss of life expectancy were 23.4 years and 9.68 years, respectively, for women, and 21.6 years and 4.11 years, respectively, for men. Table 3 summarizes the life expectancy and loss of life expectancy for RA patients stratified by sex and age at diagnosis, and Figure 1 shows the association between life expectancy and loss of life expectancy in these groups. Figure 2 shows changes in the estimated loss of life expectancy according to sex, age at diagnosis, and calendar year.

Lifetime health care expenditures and cost per life year. After biologic agents became available, the mean expected lifetime cost for RA patients was $72,953, which was higher for women than for men ($73,112 versus $63,557), and the mean cost per year was similar for women and men ($3,123 versus $2,942). Regardless of sex, the older the age at diagnosis of RA, the higher the average annual cost of treating RA (Table 3).

Validation of the extrapolation method. Table 4 indicates the differences between the month-by-month rolling-over extrapolation of 7 years based on the first 7 years of data and the observed 14-year real world estimates calculated by the Kaplan-Meier method. The relative biases were generally <5%.

DISCUSSION

This study estimated the lifetime risk, life expectancy, loss of life expectancy, and lifetime health care costs for RA. Before making more inferences, however, we must first demonstrate that these estimates are accurate. Our study had the following strengths. First, after excluding prevalent RA cases diagnosed before or during 1999–2002, we included only incident cases to establish a nationwide cohort and followed up the patients for 14 years. Therefore, we can be assured of the representativeness of our cases, and that the actual survival and health care costs were not confounded by different disease stages. Second, all RA cases included were validated through the Catastrophic Illness Registry. Thus, the cohort did not include patients with other types of inflammatory arthritis, and inpatient and outpatient costs were generally comprehensive and accurate. Moreover, since all RA patients can be waived from co-payment under our NHI system, they usually adhere to Taiwan NHI to minimize financial impact. Third, we validated our extrapolation method, using a cohort collected for the first 7 years, through comparison with an actual Kaplan-Meier estimate, by extrapolating to the 14th year. Given that censoring rates for all of the different age groups were >90% (except for those >65 years old), all relative biases were generally <5% (Table 4). We anticipate that our estimate of lifetime survival based on 14 years of follow-up is relatively accurate. Fourth, since our estimates of

Table 4. Validation of the extrapolated estimates of life expectancy after diagnosis of RA based on 7 years of follow-up of the RA cohort compared with 14 years of actual follow-up, calculated by the Kaplan-Meier method*

Sex and age at diagnosis	Age at diagnosis, mean ± SD years	Censoring rate at end of 7th year, %	Estimate using the extrapolation based on the first 7 years to the 14th year, months	Actual follow-up of 14 years by Kaplan-Meier estimate, months	Relative bias, %†
All					
Men (n = 3,824)	55.33 ± 14.14	92.5	143.40 ± 2.96	140.32 ± 0.80	2.2
Women (n = 12,718)	51.97 ± 13.86	96.8	155.97 ± 7.79	154.06 ± 0.37	1.2
Ages 16–49 years					
Men (n = 1,350)	40.27 ± 7.62	98.3	155.19 ± 14.29	159.83 ± 0.65	–2.9
Women (n = 5,599)	39.59 ± 7.94	99.2	164.02 ± 5.54	164.20 ± 0.24	–0.1
Ages 50–65 years					
Men (n = 1,459)	57.02 ± 4.27	95.1	150.76 ± 5.86	146.32 ± 1.19	3.0
Women (n = 4,800)	56.53 ± 4.24	98.1	152.33 ± 9.41	157.69 ± 0.46	–3.4
Ages >65 years					
Men (n = 1,015)	72.94 ± 5.75	81.2	104.42 ± 6.95	104.94 ± 1.89	–0.5
Women (n = 2,319)	72.43 ± 5.67	88.3	127.33 ± 8.13	121.62 ± 1.30	4.7

* Only data for rheumatoid arthritis (RA) cases diagnosed between 2003 and 2009 were included in the extrapolation. Except where indicated otherwise, values are the mean ± SEM.
† Relative bias = (extrapolated estimate – Kaplan-Meier estimate)/Kaplan-Meier estimate.

loss of life expectancy were based on referents matched to the RA patients for age, sex, and calendar year of diagnosis, the results were not confounded by these factors, including different medical technologies in use in different calendar years. Therefore, we tentatively conclude that our findings are generally accurate, and the possible pathophysiologic mechanisms should be explored further.

Because the cumulative incidence rate can be directly compared across different calendar years in populations in the same age range (31), we calculated the cumulative incidence rate instead of prevalence to explore the time trend of disease occurrence and its possible pathophysiology. Since the life expectancy in Taiwan has been approaching 80–84 years among women, we calculated the cumulative incidence rate in the population ages 16–84 years as an estimate of lifetime risk. Our results were much lower than those reported in the US, which were 3.6% and 1.7% for women and men, respectively (23). The major reason for such a difference is still unknown, but there are several possible explanations. First, there is temporal and geographic variability in the occurrence of RA (32). A previous study found that the incidence in Asia is lower than that in North America (33). Second, the RA incidence rates in high-income Asia have been on the decline, and our estimates were for the period from 2003 to 2016, which would be expected to be lower than the lifetime risk estimated in 2000 for the US population (23). Third, since our estimate of the cumulative incidence rate in the population ages 16–84 simply uses the mid-year population as the denominator for the calculation of the age-specific incidence rate, the age-specific incidence rates and lifetime risk would be slightly underestimated because of old age and competing risks of mortality due to other diseases. Thus, we only performed estimation up to the age of 84, or life expectancy in Taiwan, to minimize the aforementioned confounding. Since the estimate of the cumulative incidence rate in the population ages 16–84 years assumes that subjects do not die of other diseases before reaching the age of 85 years (21), caution must be used in counseling people, and the estimate is not useful for people >85 years old.

Our study also found that the occurrence of RA in Taiwan is declining, which deserves some exploration. The occurrence of RA may be affected by genetic and environmental factors (33), including smoking, periodontitis, hormone replacement therapy, and dietary patterns. From 2008 to 2017, the population of smokers in Taiwan decreased by 40% (34), which might partially explain the decline in RA incidence. However, since RA predominantly affects women, and cigarette consumption among women in Taiwan has remained at ~5% during the last 2 decades, we believe that changes in smoking habits cannot explain the declining trend in RA incidence in women. A study of periodontitis in Taiwan found that the disease prevalence increased from 1997 to 2013 (35). Because there are consistent decreasing trends in RA incidence rates among women >50 years of age (Supplementary Figure 1, available on the *Arthritis & Rheumatology* website at http://onlinelibrary.wiley.com/doi/10.1002/art.41597/abstract), increased rates of prescription for hormone replacement therapy cannot explain this tendency. In addition, healthy dietary patterns may reduce the incidence of RA, but the prevalence of metabolic syndrome in Taiwan has increased in the last 2 decades (36), implying that the decreasing occurrence of RA in Taiwan is unrelated to healthy dietary patterns.

Table 2 also shows that there were no major changes in the prevalence rates of comorbidities, including diabetes, in the newly diagnosed RA cases, except for a mild increase in the rate of hyperlipidemia in recent periods. A plausible reason may be the recently enhanced accessibility of rheumatology care. In fact, the number of board-certified rheumatologists in practice in Taiwan

increased from 151 in 2003 to 254 in 2016. The high accessibility of Taiwan's NHI, as well as the waived co-payments for patients with RA, make it easier for people with rheumatic symptoms to seek medical attention from a rheumatologist at a medical center without a referral (37). Thus, patients with early undifferentiated arthritis are usually more likely to receive disease-modifying antirheumatic drug treatment, which may stop the progression from preclinical RA to true RA. However, further studies are warranted to corroborate this hypothesis.

Previous studies used different methods of estimation of loss of life expectancy and showed that the life expectancy of RA patients decreased by 4–11 years for women and 1–10 years for men compared with the general population (5–8,10). However, many of those studies were conducted with small sample sizes. In addition, as follow-up periods increase, age- and sex-related factors, associated complications, and comorbidities may influence survival rates. So direct comparison may not be appropriate between different cohorts comprising patients of different ages and sex and between studies examining different calendar periods. Alternatively, we used national life tables to simulate referents matched for age, sex, and calendar year of diagnosis to estimate loss of life expectancy (Table 3), which would adjust for potential confounding by these factors (Figure 2) and could be used for the evaluation of outcomes of different medical technologies, including biosimilars. Our nationwide cohort followed up for 14 years showed loss of life expectancy ranging from 2 to 13 years for women with RA and from ~2 to 8 years for men with RA after adjustment for age, sex, and calendar year of diagnosis, which seems to corroborate previous results (10).

Although severe disease activity in RA can be well controlled by biologics, thus reducing mortality from severe RA (38), we still found some loss of life expectancy for patients with RA compared with the general population. Because of the limited financial resources in different insurance systems, there is still no consensus about how early or what amount of biologics can be prescribed and how long should they be continually prescribed after remission of RA. There may be adverse effects associated with the use of biologics. Thus, future studies are warranted to evaluate the cost-effectiveness of different reimbursement policies. Moreover, our study showed that women and those who had disease onset at a younger age had a higher loss of life expectancy when compared with matched referents (Table 3). Since cardiovascular disease probably accounts for premature mortality in these groups of RA patients (39,40), health care professionals should pay attention to patients' risk factors from the beginning of treatment.

Previous studies of the lifetime costs of RA have generally been based on the Markov model (41) and used short-term data, which might be confounded by different RA stages when making long-term predictions (11). Moreover, most of those studies were performed before biologic agents were launched, so their findings do not reflect the current real-world situation. Therefore, our method provides a viable alternative to estimate disease burden over the lifetime. We found that the average annual costs in different age groups of both sexes were similar, and the older the age at diagnosis, the higher the average annual costs (Table 3) (42). Thus, the longer life expectancy for women may be the major reason why their lifetime costs were higher than those for men.

The following limitations of this study must be acknowledged. First, the disease burden of RA, especially in the biologic era, should include effects on quality of life and functional disability. These data were not included in the present study and warrant further investigation. Second, although our cases came from the Catastrophic Illness Registry and may be accurate in diagnosis, there might be some delay from RA onset to diagnosis because of the caution taken to prevent abuse of co-payment waivers. Thus, the life expectancy may be a conservative estimate. However, such an effect would be cancelled out by comparison of loss of life expectancy between RA patients and the general population. Third, because the censoring rates of the youngest age group were all >98%, our estimation with 14 years of follow-up has limited accuracy, with high SEMs. Since biologic agents may further improve survival, longer periods of follow-up are warranted in the future to obtain a more accurate estimate. Fourth, this study only included direct medical costs and did not cover out-of-pocket expenditures and costs from loss of productivity and social services related to functional disability. Thus, the lifetime costs would be underestimated from a societal perspective, and future studies are warranted to quantify these issues. Fifth, since the mortality rate was low in men ages 16–49 years, the estimate of the confidence limits of loss of life expectancy may be highly inaccurate, and inferences regarding this group must be made with care. Finally, because the occurrence of RA has great geographic and ethnic variation, any generalization of our results for lifetime risk should be made with caution.

In conclusion, the mean life expectancy after diagnosis of RA was 26.3 years, and the lifetime cost was estimated to be $72,953 after biologics became available. However, there was still a mean loss of life expectancy of 4.97 years, indicating a health disparity that must be resolved. Future studies are needed to evaluate the effects of biologic agents on functional disability, quality of life, and cost-effectiveness from a societal perspective that includes productivity loss and/or social services (long-term care, etc.) and to provide evidence for reaching a consensus in the policy decision for RA treatment.

AUTHOR CONTRIBUTIONS

All authors were involved in drafting the article or revising it critically for important intellectual content, and all authors approved the final version to be published. Dr. Wang had full access to all of the data in the study and takes responsibility for the integrity of the data and the accuracy of the data analysis.

Study conception and design. Chiu, Lan, Chen, Wang.
Acquisition of data. Lu, Wang.
Analysis and interpretation of data. Chiu, Lu, Lan, Chen, Wang.

REFERENCES

1. Jonsson B, Kobelt G, Smolen J. The burden of rheumatoid arthritis and access to treatment: uptake of new therapies. Eur J Health Econ 2008;8:S61–86.
2. Choi HK, Hernán MA, Seeger JD, Robins JM, Wolfe F. Methotrexate and mortality in patients with rheumatoid arthritis: a prospective study. Lancet 2002;359:1173–7.
3. Jacobsson LT, Turesson C, Nilsson JA, Petersson IF, Lindqvist E, Saxne T, et al. Treatment with TNF blockers and mortality risk in patients with rheumatoid arthritis. Ann Rheum Dis 2007;66:670–5.
4. Liu PH, Wang JD, Keating NL. Expected years of life lost for six potentially preventable cancers in the United States. Prev Med 2013;56:309–13.
5. Lassere MN, Rappo J, Portek IJ, Sturgess A, Edmonds JP. How many life years are lost in patients with rheumatoid arthritis? Secular cause-specific and all-cause mortality in rheumatoid arthritis, and their predictors in a long-term Australian cohort study. Intern Med J 2013;43:66–72.
6. Mitchell DM, Spitz PW, Young DY, Bloch DA, McShane DJ, Fries JF. Survival, prognosis, and causes of death in rheumatoid arthritis. Arthritis Rheum 1986;29:706–14.
7. Gabriel SE, Crowson CS, O'Fallon WM. Mortality in rheumatoid arthritis: have we made an impact in 4 decades? J Rheumatol 1999;26:2529–33.
8. Minaur NJ, Jacoby RK, Cosh JA, Taylor G, Rasker JJ. Outcome after 40 years with rheumatoid arthritis: a prospective study of function, disease activity, and mortality. J Rheumatol Suppl 2004;69:3–8.
9. Shinomiya F, Mima N, Nanba K, Tani K, Nakano S, Egawa H, et al. Life expectancies of Japanese patients with rheumatoid arthritis: a review of deaths over a 20-year period. Mod Rheumatol 2008;18:165–9.
10. Mok CC, Kwok CL, Ho LY, Chan PT, Yip SF. Life expectancy, standardized mortality ratios, and causes of death in six rheumatic diseases in Hong Kong, China. Arthritis Rheum 2011;63:1182–9.
11. Kvien TK. Epidemiology and burden of illness of rheumatoid arthritis [review]. Pharmacoeconomics 2004;22 Suppl 1:1–12.
12. Rosery H, Bergemann R, Maxion-Bergemann S. International variation in resource utilisation and treatment costs for rheumatoid arthritis: a systematic literature review. Pharmacoeconomics 2005;23:243–57.
13. Stone C. The lifetime economic costs of rheumatoid arthritis. J Rheumatol 1984;11:819.
14. Hwang J. Monte Carlo estimation of extrapolation of quality-adjusted survival for follow-up studies. Stat Med 1999;18:1627–40.
15. Hwang JS, Hu TH, Lee LJ, Wang JD. Estimating lifetime medical costs from censored claims data. Health Econ 2017;26:e332–44.
16. Chung CP, Rohan P, Krishnaswami S, McPheeters ML. A systematic review of validated methods for identifying patients with rheumatoid arthritis using administrative or claims data [review]. Vaccine 2013;31:K41–61.
17. Nathan NO, Mørch LS, Wu CS, Olsen J, Hetland ML, Li J, et al. Rheumatoid arthritis and risk of spontaneous abortion: a Danish nationwide cohort study. Rheumatology (Oxford) 2020;59:1984–91.
18. Arnett FC, Edworthy SM, Bloch DA, McShane DJ, Fries JF, Cooper NS, et al. The American Rheumatism Association 1987 revised criteria for the classification of rheumatoid arthritis. Arthritis Rheum 1988;31:315–24.
19. Aletaha D, Neogi T, Silman AJ, Funovits J, Felson DT, Bingham CO III, et al. 2010 rheumatoid arthritis classification criteria: an American College of Rheumatology/European League Against Rheumatism collaborative initiative. Arthritis Rheum 2010;62:2569–81.
20. Alamanos Y, Voulgari PV, Drosos AA. Incidence and prevalence of rheumatoid arthritis, based on the 1987 American College of Rheumatology criteria: a systematic review. Semin Arthritis Rheum 2006;36:182–8.
21. Boyle P, Parkin DM. Statistical methods for registries. In: Jensen OM, Parkin DM, MacLennan R, Muir CS, Skeet RG, editors. Cancer registration: principles and methods. Lyon: International Agency for Research on Cancer; 1991. p. 147–8.
22. Hansen SN, Overgaard M, Andersen PK, Parner ET. Estimating a population cumulative incidence under calendar time trends. BMC Med Res Methodol 2017;17:7.
23. Crowson CS, Matteson EL, Myasoedova E, Michet CJ, Ernste FC, Warrington KJ, et al. The lifetime risk of adult-onset rheumatoid arthritis and other inflammatory autoimmune rheumatic diseases. Arthritis Rheum 2011;63:633–9.
24. Fang C, Chang Y, Hsu H, Twu S, Chen KT, Lin C, et al. Life expectancy of patients with newly-diagnosed HIV infection in the era of highly active antiretroviral therapy. QJM 2007;100:97–105.
25. Chu PC, Wang JD, Hwang JS, Chang YY. Estimation of life expectancy and the expected years of life lost in patients with major cancers: extrapolation of survival curves under high-censored rates. Value Health 2008;11:1102–9.
26. Hung MC, Liu MT, Cheng YM, Wang JD. Estimation of savings of life-years and cost from early detection of cervical cancer: a follow-up study using nationwide databases for the period 2002–2009. BMC Cancer 2014;14:505.
27. Wu TY, Chung CH, Lin CN, Hwang JS, Wang JD. Lifetime risks, loss of life expectancy, and health care expenditures for 19 types of cancer in Taiwan. Clin Epidemiol 2018;10:581.
28. Ou HT, Yang CY, Wang JD, Hwang JS, Wu JS. Life expectancy and lifetime health care expenditures for type 1 diabetes: a nationwide longitudinal cohort of incident cases followed for 14 years. Value Health 2016;19:976–84.
29. Kao TW, Huang JW, Hung KY, Chang YY, Chen PC, Yen CJ, et al. Life expectancy, expected years of life lost and survival of hemodialysis and peritoneal dialysis patients. J Nephrol 2010;23:677–82.
30. Lêng CH, Chou MH, Lin SH, Yang YK, Wang JD. Estimation of life expectancy, loss-of-life expectancy, and lifetime healthcare expenditures for schizophrenia in Taiwan. Schizophr Res 2016;171:97–102.
31. Rothman KJ, Greenland S. Measures of disease frequency. In: Rothman KJ, Greenland S, Lash TL, editors. Modern epidemiology. Philadelphia: Lippincott Williams & Wilkins; 2008. p. 37–40.
32. Minichiello E, Semerano L, Boissier MC. Time trends in the incidence, prevalence, and severity of rheumatoid arthritis: a systematic literature review. Joint Bone Spine 2016;83:625–30.
33. Safiri S, Kolahi AA, Hoy D, Smith E, Bettampadi D, Mansournia MA, et al. Global, regional and national burden of rheumatoid arthritis 1990–2017: a systematic analysis of the Global Burden of Disease study 2017. Ann Rheum Dis 2019;78:1463–71.
34. Health Promotion Administration. Ministry of Health and Welfare. Health education and tobacco control. URL: https://www.hpa.gov.tw/EngPages/List.aspx?nodeid=1054.
35. Yu HC, Su NY, Huang JY, Lee SS, Chang YC. Trends in the prevalence of periodontitis in Taiwan from 1997 to 2013: a nationwide population-based retrospective study. Medicine (Baltimore) 2017;96:e8585.
36. Yeh CJ, Chang HY, Pan WH. Time trend of obesity, the metabolic syndrome and related dietary pattern in Taiwan: from

NAHSIT 1993–1996 to NAHSIT 2005–2008. Asia Pac J Clin Nutr 2011;20:292.

37. Wu TY, Majeed A, Kuo KN. An overview of the healthcare system in Taiwan. London J Prim Care (Abingdon) 2010;3:115–9.
38. Puolakka K, Kautiainen H, Pohjolainen T, Virta L. No increased mortality in incident cases of rheumatoid arthritis during the new millennium [letter]. Ann Rheum Dis 2010;69:2057–8.
39. Naz SM, Farragher TM, Bunn DK, Symmons DP, Bruce IN. The influence of age at symptom onset and length of followup on mortality in patients with recent-onset inflammatory polyarthritis. Arthritis Rheum 2008;58:985–9.
40. Solomon DH, Goodson NJ, Katz JN, Weinblatt ME, Avorn J, Setoguchi S, et al. Patterns of cardiovascular risk in rheumatoid arthritis. Ann Rheum Dis 2006;65:1608–12.
41. Wong JB, Ramey DR, Singh G. Long-term morbidity, mortality, and economics of rheumatoid arthritis. Arthritis Rheum 2001;44:2746–9.
42. Yazici Y, Paget SA. Elderly-onset rheumatoid arthritis [review]. Rheum Dis Clin North Am 2000;26:517–26.

Arthritis & Rheumatology
Vol. 73, No. 5, May 2021, pp 759–768
DOI 10.1002/art.41589

American College of Rheumatology
Empowering Rheumatology Professionals

Etanercept or Methotrexate Withdrawal in Rheumatoid Arthritis Patients in Sustained Remission

Jeffrey R. Curtis,[1] Paul Emery,[2] Elaine Karis,[3] Boulos Haraoui,[4] Vivian Bykerk,[5] Priscilla K. Yen,[3] Greg Kricorian,[3] and James B. Chung[3]

Objective. Patients with rheumatoid arthritis (RA) in whom remission is achieved following combination therapy with methotrexate plus etanercept face an ongoing medication burden. This study was undertaken to investigate whether sustained remission achieved on combination therapy can be maintained with either methotrexate or etanercept monotherapy, as assessed following discontinuation of one or the other medication from the combination.

Methods. Of the 371 adult patients with RA who received combination therapy with methotrexate plus etanercept, remission (defined as a Simplified Disease Activity Index [SDAI] score of ≤3.3) was sustained in 253 patients through a 24-week open-label period. These 253 patients then entered a 48-week, double-blind period and were randomized to receive either 1) methotrexate monotherapy (n = 101), 2) etanercept monotherapy (n = 101), or 3) methotrexate plus etanercept combination therapy (n = 51). Patients who subsequently experienced disease-worsening received rescue therapy with the combination regimen at the same dosages as used in the initial run-in period. The primary end point was the proportion of patients in whom SDAI-defined remission was maintained without disease-worsening at week 48 in the etanercept monotherapy group as compared to the methotrexate monotherapy group. Secondary end points included time to disease-worsening, and the proportion of patients in whom SDAI-defined remission was recaptured after initiation of rescue therapy.

Results. Baseline demographic and clinical characteristics of the RA patients were similar across the treatment groups. At week 48, SDAI-defined remission was maintained in significantly more patients in the etanercept monotherapy group than in the methotrexate monotherapy group (49.5% versus 28.7%; $P = 0.004$). Moreover, as a secondary end point, sustained SDAI-defined remission was achieved in significantly more patients who received combination therapy than in those who received methotrexate monotherapy (52.9% versus 28.7%; $P = 0.006$). Time to disease-worsening was shorter in those who received methotrexate monotherapy than in those who received etanercept monotherapy or those who received combination therapy (each $P < 0.001$ versus methotrexate monotherapy). Among the patients who received rescue therapy, SDAI-defined remission was recaptured in 70–80% in each treatment group. No new safety signals were reported.

Conclusion. The efficacy of etanercept monotherapy was superior to that of methotrexate monotherapy and similar to that of combination therapy in maintaining remission in patients with RA. SDAI-defined remission was recaptured in most of the patients who were given rescue therapy. These data could inform decision-making when withdrawal of therapy is being considered to reduce treatment burden in patients with well-controlled RA.

ClinicalTrials.gov identifier: NCT02373813.

Supported by Amgen Inc.

[1]Jeffrey R. Curtis, MD: University of Alabama at Birmingham; [2]Paul Emery, MD: Leeds Institute of Rheumatic and Musculoskeletal Medicine, University of Leeds, NIHR Leeds Biomedical Research Centre, Leeds Teaching Hospitals NHS Trust, Leeds, UK; [3]Elaine Karis, MD, Priscilla K. Yen, PhD, Greg Kricorian, MD, James B. Chung, MD, PhD: Amgen Inc., Thousand Oaks, California; [4]Boulos Haraoui, MD: Centre Hospitalier de l'Université de Montréal, Montreal, Quebec, Canada; [5]Vivian Bykerk, MD: Hospital for Special Surgery, New York, New York.

Dr. Curtis has received consulting fees, speaking fees, and/or honoraria from Amgen, Corrona, Janssen, Myriad, and Pfizer (more than $10,000 each) and AbbVie, Bristol Myers Squibb, Gilead, Eli Lilly, Novartis, Sanofi, and Scipher Medicine (less than $10,000 each). Dr. Emery has received consulting fees, speaking fees, and/or honoraria from AbbVie, Amgen, Bristol Myers Squibb, Celltrion, Gilead, Eli Lilly, MSD, Novartis, Pfizer, Roche, Samsung, and Sanofi (less than $10,000 each). Drs. Karis, Yen, Kricorian, and Chung own stock or stock options in Amgen. Dr. Haraoui has received consulting fees, speaking fees, and/or honoraria from AbbVie, Gilead, and Pfizer (more than $10,000 each) and Amgen, Bristol Myers Squibb, Janssen, Eli Lilly, Merck, Roche, Sandoz, Sanofi-Genzyme, and UCB (less than $10,000 each). Dr. Bykerk has received consulting fees, speaking fees, and/or honoraria from Amgen, Bristol Myers Squibb, Gilead, Pfizer, Sanofi-Genzyme, Regeneron, Scipher Medicine, and UCB (less than $10,000 each).

Qualified researchers may request data from Amgen clinical studies. Complete details are available at https://wwwext.amgen.com/science/clinical-trials/clinical-data-transparency-practices/.

Address correspondence to Jeffrey R. Curtis, MD, University of Alabama at Birmingham, 510 20th Street South, Birmingham, AL 35294. Email: jrcurtis@uabmc.edu.

Submitted for publication July 28, 2020; accepted in revised form November 10, 2020.

INTRODUCTION

In patients with rheumatoid arthritis (RA), remission became a more realistic and achievable goal with the introduction of tumor necrosis factor inhibitors (TNFi) (1–3). Combining a TNFi (such as etanercept) with methotrexate in the treatment of RA patients has resulted in a greater reduction in disease activity and decreased radiographic progression, as well as improvement in physical function, when compared to either therapy alone. Combination therapy has accordingly been established as a commonly used and effective regimen for achieving sustained remission and/or lowering disease activity in patients with RA (4–6).

For patients in whom stringent remission has been achieved and sustained, important questions remain about the need to continue combination therapy to maintain good disease control (3). Guidelines from the American College of Rheumatology (ACR) and European League Against Rheumatism (EULAR) recommend carefully tapering (though not stopping all) RA therapy for patients whose disease is in remission (7,8), but clear data are lacking on how best to manage this process. Informed guidance on minimizing therapy while maintaining excellent disease control in RA would be of significant value for patients and physicians, especially considering the aging population whose disease may be associated with more comorbidities and complex medication regimens, and also the safety and tolerability issues associated with long-term methotrexate use (9,10).

Prior studies examining how withdrawal of methotrexate or TNFi therapy (11–16) can impact disease control have had key limitations, including varying and inconsistent definitions of adequate disease control/remission and lack of an initial observational period of sustained control (remission) prior to treatment reduction; both may be important factors for determining whether good disease control can be maintained after treatment withdrawal (17,18). In addition, previous studies in which either a TNFi or methotrexate was withdrawn did not examine monotherapy strategies with either medication in a single, comparative study.

The Study of Etanercept and Methotrexate in Combination or as Monotherapy in Subjects with Rheumatoid Arthritis (SEAM-RA) is a randomized, double-blind, controlled trial designed to study patients with RA whose disease is in stable, stringently defined remission after having received combination therapy with etanercept and methotrexate, and to rigorously investigate whether remission could be maintained with either etanercept or methotrexate monotherapy, as assessed after withdrawal of either treatment. This study aimed to directly address questions of practical importance to patients and physicians, with the goal of simplifying care and minimizing the medication burden in patients with RA.

PATIENTS AND METHODS

Trial design and oversight. This international, multicenter study (19) consisted of a 24-week open-label run-in period, a 48-week randomized, controlled double-blind period, and a 30-day safety follow-up period for all enrolled patients (see the Supplementary Notes for a list of the primary investigators and study sites, available on the *Arthritis & Rheumatology* website at http://onlinelibrary.wiley.com/doi/10.1002/art.41589/abstract). To be included in the SEAM-RA trial, patients with RA receiving combination therapy with methotrexate (dosage of 10–25 mg/week) plus etanercept (dosage of 50 mg/week) were required to have a score of ≤3.3 on the Simplified Disease Activity Index (SDAI; score range 0–86, with remission defined as ≤3.3, low disease activity as 3.4 to ≤11.0, moderate disease activity as 11.1 to 26, and high disease activity as >26) (20) at the time of screening, thereby satisfying the established ACR/EULAR criteria for remission (21). Once enrolled, patients continued combination therapy and entered a 24-week open-label run-in period, to identify patients whose disease remained stable and in remission. These patients were then selected for randomization into the subsequent double-blind, treatment-withdrawal period. Patients with an SDAI score of >3.3 and ≤11 on 2 or more visits or an SDAI score of >11 at any time during the run-in period were ineligible for the double-blind period.

Patients in whom SDAI-defined remission was achieved at the end of the run-in period and who met the above-described eligibility criteria at a subsequent baseline visit for the double-blind period were randomized 2:2:1 via an Interactive Voice and Web Response System to subsequently receive, on a weekly basis, either 1) oral methotrexate plus subcutaneous placebo (i.e., etanercept withdrawal), 2) subcutaneous etanercept plus oral placebo (i.e., methotrexate withdrawal), or 3) subcutaneous etanercept plus oral methotrexate (i.e., no change in therapy). During the double-blind period, patients and investigators were blinded with regard to the treatment assignments, and randomization was based on a computer-generated randomization schedule (prepared by staff at Amgen Inc.). During the double-blind period, patients randomized to receive methotrexate continued with the medication at the same dosage received during the screening and run-in period, and patients randomized to continue receiving etanercept received a dosage of 50 mg/week.

Randomized patients were considered to have disease-worsening if they had increased disease activity based on an SDAI score of >3.3 and ≤11 on 2 consecutive visits at least 2 weeks apart, an SDAI score of >3.3 and ≤11 at any time on 3 or more separate visits, or an SDAI score of >11 at any time. Patients with disease-worsening received weekly rescue treatment with the combination of etanercept plus methotrexate (i.e., reestablished or continued combination therapy using the same dosages received at the time of study enrollment).

During both the run-in and double-blind periods, etanercept (manufactured and supplied by Amgen Inc.) was administered using single-use, prefilled syringes in the dosages recommended in the prescribing information (22). Methotrexate (manufactured by Teva Pharmaceuticals and supplied by Amgen Inc.) was provided as 2.5-mg tablets during the run-in period and as 2.5-mg capsules

(to enable blinding) during the double-blind treatment period. Folic acid was prescribed at a dosage of 5–7 mg per week.

All patients provided written informed consent to participate in the trial, and each participating site obtained approval of the study protocol from an Institutional Review Board/Independent Ethics Committee. The statistical analyses were performed by the study sponsor.

Trial population. Key eligibility criteria at the time of screening included age ≥18 years, having a history of RA (consistent with the ACR/EULAR 2010 classification criteria [23]), having ≥6 months of good disease control (according to investigator opinion) before the run-in period, being in a state of disease remission based on an SDAI score of ≤3.3 at the time of screening (and at the end of the run-in period), having received etanercept at 50 mg weekly plus methotrexate at 10–25 mg weekly for ≥6 months, and having received a stable dose of oral methotrexate for ≥8 weeks prior to the first visit of the run-in period. Additional eligibility criteria are listed in the Supplementary Notes (http://onlinelibrary.wiley.com/doi/10.1002/art.41589/abstract).

End points for the double-blind period. During the double-blind period, patients were assessed on day 1 (baseline) and then at weeks 12, 24, 36, and 48. The primary end point was the proportion of patients having achieved SDAI-defined remission (an SDAI score of ≤3.3) without disease-worsening at week 48 in the etanercept monotherapy group as compared to the methotrexate monotherapy group. Secondary end points included the proportion of patients who experienced SDAI-defined remission without disease-worsening at week 48 in the combination therapy group as compared to the methotrexate monotherapy group. In those patients who experienced disease-worsening and were subsequently given rescue therapy, other secondary end points included the proportion of patients

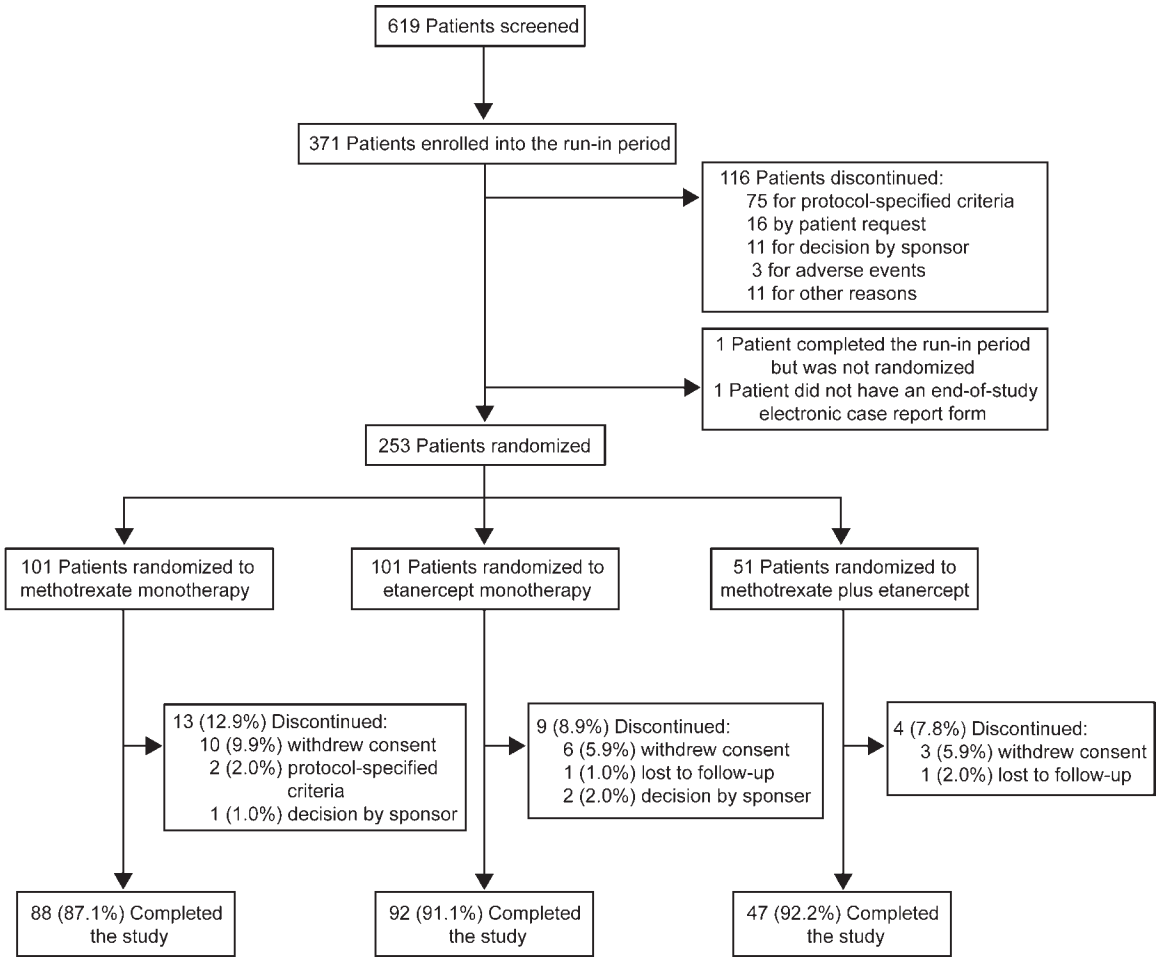

Figure 1. Flow chart of patient distribution in the study. At screening, patients with rheumatoid arthritis receiving methotrexate plus etanercept (combination therapy) were required to have a Simplified Disease Activity Index (SDAI) score of ≤3.3. After enrollment, patients continued receiving combination therapy and entered a 24-week open-label, run-in period to identify patients in whom stable remission was achieved for randomization into the subsequent double-blind, treatment-withdrawal period. Patients with an SDAI score of >3.3 and ≤11 on 2 or more visits or an SDAI score of >11 at any time during the run-in period were ineligible for the double-blind period. Patients with SDAI-defined remission at the end of the run-in period and who met eligibility for the double-blind period were randomized 2:2:1 into 1 of the 3 treatment groups.

in whom SDAI-defined remission was recaptured after initiation of rescue therapy, the SDAI scores in these patients over time after achievement of SDAI-defined remission, and the time to recapture SDAI-defined remission after initiation of rescue therapy. Safety end points included the percentage of patients who experienced adverse events, serious adverse events, fatal adverse events, and adverse events leading to withdrawal from the investigational product.

Statistical analysis. Data from prior treatment-withdrawal studies (12,16) were used to determine the SEAM-RA sample size. Based on a 2-sided chi-square test with 90% power to detect differences (at a significance level of 0.05) and assuming an effect size of 22% between the etanercept and methotrexate monotherapy groups, it was estimated that a sample size of 100 patients in the etanercept monotherapy group and 100 patients in the methotrexate monotherapy group would be required. Assuming a 30% attrition rate in the run-in period, it was estimated that ~358 patients were needed for enrollment, so that 250 patients could be randomized.

Analyses of the primary and secondary efficacy end points used the primary analysis set of all randomized patients, and these analyses were conducted according to treatment assignment. Analyses of safety end points used the safety analysis set of all randomized patients who received at least one dose of any investigational product, and these analyses were conducted according to the actual treatment received. Summary descriptive statistics were used for the baseline demographic and disease characteristics by treatment group.

For the primary end point, achievement of SDAI-defined remission at week 48 in patients in the etanercept monotherapy group was compared to that in the methotrexate monotherapy group, using a 2-sided chi-square test with a significance level of 0.05. Nonresponder imputation was used for missing values at week 48. Patients who dropped out of the study or experienced disease-worsening were considered nonresponders. Secondary end points were analyzed using the observed data set.

RESULTS

Patient characteristics. Between February 20, 2015 and June 26, 2018, the SEAM-RA study enrolled 371 patients into the 24-week, open-label run-in period, during which they continued combination therapy with methotrexate plus etanercept (Figure 1). The 253 patients eligible for the 48-week double-blind period were randomized from August 10, 2015 to December 5, 2018 to receive methotrexate monotherapy (101 patients), etanercept monotherapy (101 patients), or methotrexate plus etanercept (51 patients). The double-blind period was completed by 227 patients (89.7%); the most common reason for discontinuing was withdrawal of consent (Figure 1). The last day of the study was December 6, 2019. Among the 371 enrolled patients, 181 (49%) were from the US, and 62% of these patients were randomized to the treatment-withdrawal period. The overall percentage of

Table 1. Demographic and clinical characteristics of the RA patients at baseline*

Characteristic	Methotrexate monotherapy (n = 101)	Etanercept monotherapy (n = 101)	Combination therapy (n = 51)
Female sex, no. (%)	76 (75.2)	77 (76.2)	40 (78.4)
Age, years	56.2 ± 11.4	54.8 ± 12.8	55.9 ± 12.6
White, no. (%)	92 (91.1)	86 (85.1)	42 (82.4)
BMI, kg/m^2	27.8 ± 5.2	28.7 ± 5.7	28.7 ± 5.9
Duration of RA, years	9.7 ± 8.0	11.0 ± 7.4	10.3 ± 8.2
RF positive, no. (%)	59 (58.4)	64 (63.4)	35 (68.6)
Anti-CCP positive, no. (%)	66 (65.3)	67 (66.3)	35 (68.6)
Methotrexate dosage, mg/week	16.26 ± 4.56	15.97 ± 4.65	17.06 ± 4.99
Prednisone (≤5 mg daily), no. (%)	2 (2.0)	1 (1.0)	1 (2.0)
SDAI score	1.3 ± 1.0	1.3 ± 1.4	1.2 ± 1.2
Remission, no. (%)			
SDAI†	96 (95.0)	93 (92.1)	49 (96.1)
Boolean (in 28 joints)†	83 (82.2)	84 (83.2)	41 (80.4)
Tender joint count (of 28 joints)	0.1 ± 0.4	0.1 ± 0.4	0.2 ± 0.5
Swollen joint count (of 28 joints)	0.1 ± 0.4	0.0 ± 0.2	0.0 ± 0.2
Physician global assessment (scale 0–10)	0.30 ± 0.38	0.31 ± 0.91	0.17 ± 0.26
Patient global assessment (scale 0–10)	0.44 ± 0.58	0.45 ± 0.77	0.35 ± 0.55
CRP, mg/dl	0.27 ± 0.40	0.34 ± 0.54	0.47 ± 1.00
HAQ DI, mean ± SEM	0.32 ± 0.04	0.26 ± 0.04	0.28 ± 0.06

* Except where indicated otherwise, values are the mean ± SD. RA = rheumatoid arthritis; BMI = body mass index; RF = rheumatoid factor; anti-CCP = anti–cyclic citrullinated peptide; CRP = C-reactive protein; HAQ DI = Health Assessment Questionnaire disability index (score range 0–3).
† Clinical remission being defined as a Simplified Disease Activity Index (SDAI) score of ≤3.3 (score range 0–86) or meeting the Boolean criteria for remission according to the American College of Rheumatology/European League Against Rheumatism remission criteria (21).

enrolled patients who were randomized was 68%, and in some countries, as high as ~90% of their enrolled patients were randomized (in South Africa, 21 [91%] of 23 patients; in Poland, 19 [90%] of 21 patients).

The demographic and clinical characteristics of the patients at baseline were generally similar across the 3 randomized treatment groups (Table 1). Patients in each group were predominantly female and white, and the mean body mass index (BMI) of the study population was 28 kg/m^2 (Table 1). At the time of randomization, the overall mean age was 56 years, the mean duration of RA was 10.3 years, the mean dosage of methotrexate was 16.3 mg/week, the mean ± SD SDAI score was 1.3 ± 1.2, and the baseline mean ± SD Health Assessment Questionnaire disability index score (24) was 0.29 ± 0.03.

Maintenance of SDAI-defined remission. Analysis of the primary end point indicated that at week 48 of the double-blind period, SDAI-defined remission was maintained without disease-worsening in a significantly higher percentage of patients in the etanercept monotherapy group compared to the methotrexate monotherapy group (50 [49.5%] of 101 versus 29 [28.7%] of 101; P = 0.004) (Figure 2). Similarly, the disease remained in SDAI-defined remission by week 48 in a significantly higher percentage of patients in the continued combination therapy group compared to the methotrexate monotherapy group (27 [52.9%] of 51 versus 29 [28.7%] of 101; P = 0.006) (Figure 2).

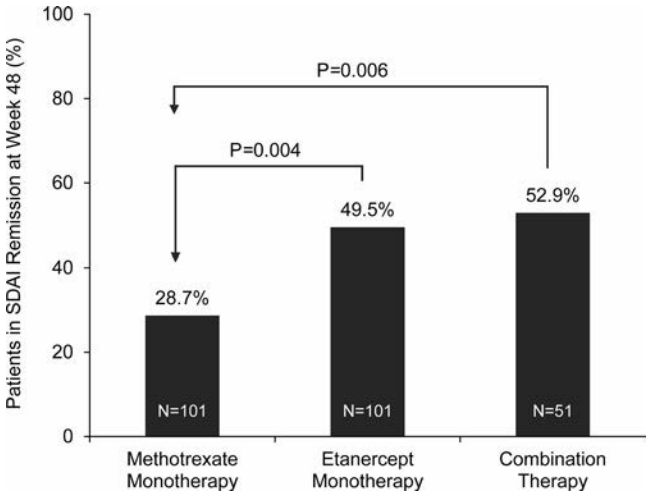

Figure 2. Patients in whom remission (as defined by a Simplified Disease Activity Index [SDAI] score of ≤3.3) was achieved without disease-worsening at week 48. The primary end point was comparison of the proportion of patients with SDAI-defined remission at week 48 between the etanercept and methotrexate monotherapy groups, among patients in the primary analysis set. A secondary end point was comparison of the methotrexate monotherapy and combination therapy groups. Missing data were imputed using nonresponder imputation (patients with disease-worsening were considered nonresponders). P values were estimated based on the chi-square test with continuity correction.

A univariate logistic regression analysis of selected covariates at baseline, in the data set including all patients, indicated potential predictors of remission maintenance. A higher baseline SDAI score was associated with a lower likelihood of maintaining remission, and a status of rheumatoid factor positivity was associated with a lower ability to maintain remission; positivity for anti–cyclic citrullinated peptide antibodies showed a similar trend.

The BMI of the patients at baseline had a slight impact on remission maintenance, with a higher baseline BMI correlating with a decreased ability to maintain remission. Disease duration or prior duration of etanercept or methotrexate treatment was not shown to be a predictor of remission maintenance in this analysis (data not shown).

Disease-worsening and recapture of remission. During the 48-week double-blind period, the percentage of patients with disease-worsening was 63 (62.4%) of 101 in the methotrexate monotherapy group, 40 (39.6%) of 101 in the etanercept monotherapy group, and 18 (35.3%) of 51 in the combination therapy group. The median SDAI score at initiation of rescue therapy in each group was as follows: median 25.3 (interquartile range [IQR] 15.0–35.0) in the methotrexate monotherapy group, median 15.8 (IQR 7.7–32.1) in the etanercept monotherapy group, and median 14.0 (IQR 12.0–24.5) in the combination therapy group. The majority of patients who met the criteria for disease-worsening during the 48-week double-blind period were identified based on having an SDAI score of >11 (84%, 75%, and 78% of patients in the methotrexate monotherapy, etanercept monotherapy, and combination therapy groups, respectively). The highest SDAI scores in all 3 treatment groups occurred during the first 24 weeks of the double-blind period (see results in Supplementary Figure 1, available on the *Arthritis & Rheumatology* website at http://onlinelibrary.wiley.com/doi/10.1002/art.41589/abstract).

The time to disease-worsening was shorter in the methotrexate monotherapy group compared to either the etanercept monotherapy group (P < 0.001) or the combination therapy group (P < 0.001) (Figure 3). The differences between the methotrexate monotherapy and etanercept monotherapy groups were discernible as early as 4 weeks.

The cumulative Kaplan-Meier estimate (with 95% confidence interval [95% CI]) for the probability of not experiencing disease-worsening by week 48 was 38.0% (95% CI 28.2–47.6) in the methotrexate monotherapy group, 59.6% (95% CI 49.2–68.5) in the etanercept monotherapy group, and 65.2% (95% CI 49.9–76.8) in the combination therapy group (see the Kaplan-Meier estimates at all time points in Supplementary Table 1, available on the *Arthritis & Rheumatology* website at http://onlinelibrary.wiley.com/doi/10.1002/art.41589/abstract).

During the double-blind period, rescue therapy was given to 52 (52%) of 101 patients in the methotrexate monotherapy group, 36 (36%) of 101 in the etanercept monotherapy group,

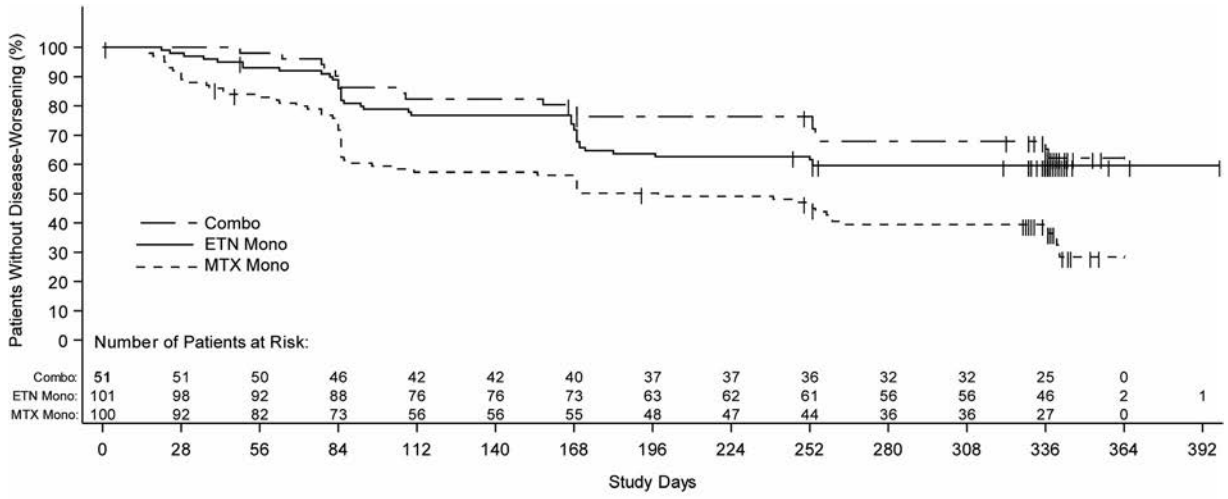

	MTX Mono (N = 101)	ETN Mono (N = 101)	Combo (N = 51)
Days to Disease-Worsening, Median (95% CI)	198 (96, 263)	NE (253, NE) P<0.001*	NE (336, NE) P<0.001*

Figure 3. Kaplan-Meier curves of time to disease-worsening in the 3 treatment groups (in the primary analysis set). The censor bars represent patients who did not have disease-worsening at their last Simplified Disease Activity Index–defined remission assessment date. One patient discontinued treatment with methotrexate (MTX) on study day 0, and thus was no longer at risk and was censored. The median time to disease-worsening in the etanercept (ETN) monotherapy (Mono) group and the combination (Combo) therapy group was not estimable (NE) because the cumulative event rate in these 2 groups at the end of the study period at 336 days (48 weeks) was 59.6% and 65.2%, respectively (i.e., did not reach or fall below 50%). **P* values are nominal and compare the etanercept-containing groups with the methotrexate monotherapy group using a 2-sided log-rank test. 95% CI = 95% confidence interval.

and 15 (29%) of 51 in the combination therapy group (a small number of patients who experienced disease-worsening withdrew from the study prior to receiving rescue therapy). Of the patients who received rescue therapy, 86 (83.5%) of 103 had ≥12 weeks of follow-up. The cumulative proportion of patients in whom SDAI-defined remission was recaptured after the initiation of rescue therapy (administered in response to disease-worsening) was 46%, 42%, and 47% by 12 weeks and 71%, 75%, and 80% by the end of the study in the methotrexate monotherapy, etanercept monotherapy, and combination therapy groups, respectively (Figure 4A). In comparison, the cumulative proportion of patients in whom SDAI-defined low disease activity was recaptured following rescue therapy was 71%, 81%, and 73% by 12 weeks and 96%, 92%, and 100% by the end of the study in the methotrexate monotherapy, etanercept monotherapy, and combination therapy groups, respectively (Figure 4B).

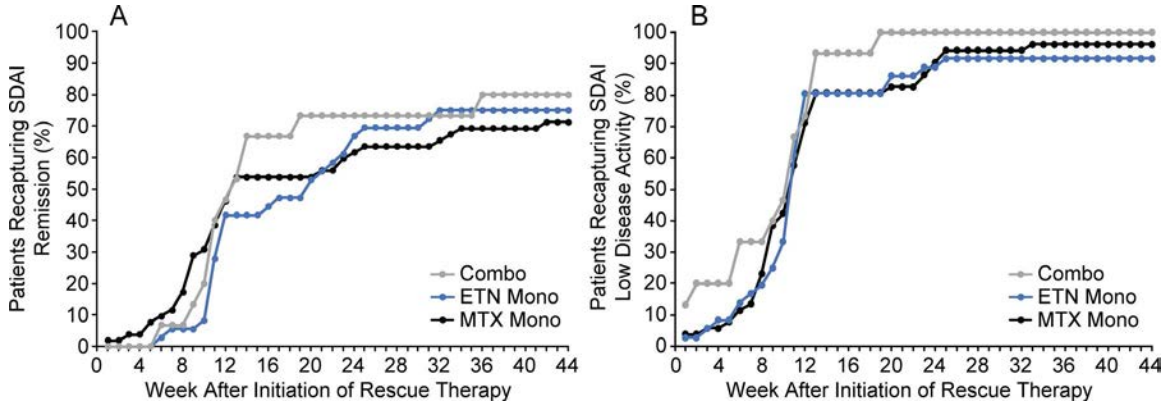

Figure 4. Cumulative proportion of patients in whom Simplified Disease Activity Index (SDAI)–defined remission (**A**) and low disease activity (**B**) were recaptured after initiation of rescue therapy (the rescue analysis set). The rescue analysis set consisted of 52 patients in the methotrexate (MTX) monotherapy (Mono) group, 36 patients in the etanercept (ETN) monotherapy group, and 15 patients in the combination (Combo) therapy group. On the X-axis, the value of 0 represents the time point of initiation of rescue therapy. Once SDAI-defined remission or low disease activity was recaptured, patient numbers remained as is for the subsequent weeks (even if remission or low disease activity status was lost at a later time).

Table 2. Summary of safety results from the double-blind period (safety analysis set)*

	Methotrexate monotherapy (n = 100)	Etanercept monotherapy (n = 99)	Combination therapy (n = 53)
All treatment-emergent AEs	63 (63.0)	55 (55.6)	33 (62.3)
Serious AEs	4 (4.0)	4 (4.0)	3 (5.7)
AEs leading to discontinuation of investigational product	3 (3.0)	2 (2.0)	0 (0.0)
Fatal AEs	0 (0.0)	0 (0.0)	0 (0.0)
AEs occurring in ≥5% of patients			
Infections	28 (28.0)	31 (31.3)	14 (26.4)
Musculoskeletal and connective tissue disorders	33 (33.0)	19 (19.2)	11 (20.8)
Injury and procedural complications	10 (10.0)	9 (9.1)	3 (5.7)
Respiratory, thoracic, and mediastinal disorders	6 (6.0)	4 (4.0)	3 (5.7)
Gastrointestinal disorders	4 (4.0)	6 (6.1)	2 (3.8)
Nervous system disorders	5 (5.0)	4 (4.0)	2 (3.8)

* Values are the number (%) of patients. The safety analysis set comprises patients in whom actual treatment was received. Patients in the monotherapy groups were included in the combination therapy group for the safety analysis set if they additionally received at least one dose of the other drug (i.e., nonassigned) during the double-blind period. Adverse events (AEs) were captured from randomization through the safety follow-up period (30 days after a patient's end of study) and were categorized using the Medical Dictionary for Regulatory Activities version 2.2. Serious AEs included aortic pseudoaneurysm, reactive arthritis, pneumonia, respiratory syncytial virus infection, concussion, spinal fracture, (worsening of) rheumatoid arthritis, gastric ulcer hemorrhage, ankle fracture, osteoarthritis, and herpes zoster.

There was no difference in the cumulative time to recapture SDAI-defined remission between the 3 treatment groups (see Supplementary Figure 2, available on the *Arthritis & Rheumatology* website at http://onlinelibrary.wiley.com/doi/10.1002/art.41589/abstract).

Safety outcomes. No new safety signals with the use of methotrexate or etanercept were observed (Table 2). Over the double-blind period, rates of treatment-emergent adverse events, serious adverse events, and events leading to discontinuation of the investigational product were similar across the 3 treatment groups. No fatal adverse events occurred. The most common adverse events were infections and musculoskeletal and connective tissue disorders.

DISCUSSION

Results from the SEAM-RA trial show that in patients in whom sustained SDAI-defined remission was achieved following treatment with the combination of methotrexate and etanercept, withdrawal of methotrexate resulted in a significantly greater ability to maintain remission over 1 year compared to withdrawal of etanercept. In addition, in patients in whom methotrexate was withdrawn (i.e., group receiving etanercept monotherapy), maintenance of remission was similar to that in the combination therapy group, and etanercept monotherapy was associated with a longer time to disease-worsening and a lower degree and proportion of patients with disease-worsening when compared to methotrexate monotherapy.

Disease flares in the setting of treatment withdrawal are a key concern. Though flares occurred with therapy withdrawal, these study results overall are reassuring, in that they demonstrate that when combination therapy was reinstituted following disease-worsening, remission was recaptured in the majority of patients in both treatment-withdrawal groups. Among all patients with disease-worsening, remission was recaptured in 70–80%, and low disease activity was recaptured in 90–100% by the end of the study. Patients receiving etanercept or methotrexate monotherapy achieved similar recapture rates to the combination therapy group. The high rate of recapture achieved in the combination therapy group without a change in treatment has been previously observed (13). Among those patients in whom remission was recaptured, the median time to fully recapture remission after initiation of rescue therapy was 11 weeks in the methotrexate monotherapy group, 12 weeks in the etanercept monotherapy group, and 11.4 weeks in the combination therapy group. SDAI-defined low disease activity was recaptured in even more patients, with ~70–80% of patients showing recapturing of low disease activity by 12 weeks after initiation of rescue therapy. Time to recapture remission may be shorter when these strategies are implemented in real-world clinical practice, as very few patients received prednisone for disease flares in this trial. These results provide a conservative estimate as to how methotrexate plus etanercept can induce recapture of remission without the use of steroids.

A univariate analysis of selected covariates provided insights into potential predictors of maintaining remission, with data suggesting that there is a greater potential likelihood of maintaining remission in seronegative patients with lower disease activity and

a lower BMI. However, further and more sophisticated analysis of factors associated with maintaining remission is beyond the scope of this report.

Several features of the study should be noted. The combination therapy group served as a comparator to the monotherapy groups, and also showed the extent to which patients with sustained remission can experience disease-worsening over an extended period of time because of the inherent variability in RA disease activity. Consistent with the findings in a previous study (17), remission was not maintained in approximately one-half of the patients in the combination therapy group over the 48-week double-blind period. The majority of these patients met the criteria for disease-worsening, with a meaningful increase in disease activity (75–84% of patients having an SDAI score of >11) as opposed to multiple smaller fluctuations around an SDAI score of 3.3.

The etanercept monotherapy and combination therapy groups were not formally compared against each other, as the anticipated modest difference would have required a prohibitive sample size to demonstrate definitively. By including the combination therapy group, the study does provide meaningful information about the relative ability of etanercept to maintain remission.

Radiographs were not collected in the SEAM-RA trial. In the COMET trial (Comparison of methotrexate monotherapy with a combination of methotrexate and etanercept in active, early, moderate to severe RA), a difference in the proportion of patients with radiographic nonprogression was observed between the etanercept and methotrexate combination groups compared to the etanercept monotherapy group (16). However, the patients enrolled in the COMET trial had early disease, at a stage when there is a higher rate of radiographic progression, and the trial targeted remission defined by the Disease Activity Score in 28 joints, a less stringent definition of remission compared to the SDAI definition of remission. Given that patients in the SEAM-RA trial had a relatively long duration of disease, a very good level of disease control, and rapid institution of rescue therapy upon disease-worsening, differences in radiographic progression between the 3 treatment groups would be small and challenging to detect. However, the inverse correlation between disease control and radiographic progression is well known (25), and etanercept monotherapy and etanercept plus methotrexate combination therapy have been shown to elicit better radiographic outcomes as compared to methotrexate monotherapy (26,27).

Randomized patients had sustained good disease control for at least 1 year (6-month history plus 24-week observed run-in period) prior to therapy withdrawal, a duration designed to reflect the real-world clinical setting. This trial used the stringent SDAI definition of remission, which along with Boolean-defined remission, is both widely accepted and recommended by the ACR and EULAR (7,8) and accepted by the US Food and Drug Administration (28). Although SDAI-defined remission may be achievable in a relatively small proportion of RA patients, by adopting such a stringent criterion and enrolling patients in whom very good disease control has been sustained, with a mean SDAI score of 1.3 prior to randomization, this study investigated the effects of treatment withdrawal in near-ideal conditions. The study did not address gradual drug tapering, but the treatment-withdrawal design in the setting of sustained stringent remission does provide a "best case" scenario for patients in whom reduction of therapy is being considered. Moreover, simply reducing therapy may not lessen the long-term safety concerns and the need for monitoring.

Overall, the results of the SEAM-RA study provide information on the likelihood of success of discontinuing methotrexate and can inform general decision-making around RA treatment strategies. These results may be of particular interest to physicians and patients concerned about adverse events, such as nausea and fatigue, and long-term safety issues associated with methotrexate (10,29). Differences among the various TNFi, in terms of the need for long-term administration of monotherapy as compared to combination therapy, have been reported and may be related, in part, to the differences in immunogenicity profiles, with etanercept showing potential benefits (30–34). Thus, sustained efficacy, tolerability, and possible safety risks should be carefully weighed in clinical decisions related to treatment choice and withdrawal. The results from the SEAM-RA trial have practical implications and may inform decision-making for patients and physicians when withdrawal of therapy is being considered to reduce treatment burden in the setting of well-controlled RA.

ACKNOWLEDGMENT

We thank Linda Rice, PhD, of Amgen Inc. for providing assistance with the drafting of the manuscript and for preparing the tables and figures.

AUTHOR CONTRIBUTIONS

All authors were involved in drafting the article or revising it critically for important intellectual content, and all authors approved the final version to be published. Dr. Curtis had full access to all of the data in the study and takes responsibility for the integrity of the data and the accuracy of the data analysis.

Study conception and design. Curtis, Haraoui, Kricorian, Chung.
Acquisition of data. Curtis, Haraoui, Bykerk, Karis, Yen, Kricorian, Chung.
Analysis and interpretation of data. Curtis, Emery, Karis, Haraoui, Bykerk, Yen, Kricorian, Chung.

ROLE OF THE STUDY SPONSOR

Amgen Inc., the sponsor of the SEAM-RA trial, designed the trial in collaboration with academic investigators, oversaw data collection, performed the data analyses, and supported the development of this manuscript. Data interpretation and writing of the manuscript were performed by both the Amgen and non-Amgen authors. The corresponding author had full access to all of the data in the study. The sponsor and the corresponding author had the final responsibility for the decision to submit this report for publication. Publication of this article was contingent upon approval by Amgen Inc. and all of the authors.

REFERENCES

1. Hamann P, Holland R, Hyrich K, Pauling JD, Shaddick G, Nightingale A, et al. Factors associated with sustained remission in rheumatoid arthritis in patients treated with anti–tumor necrosis factor. Arthritis Care Res (Hoboken) 2017;69:783–93.
2. Aletaha D, Smolen JS. Diagnosis and management of rheumatoid arthritis: a review. JAMA 2018;320:1360–72.
3. Edwards CJ, Galeazzi M, Bellinvia S, Ringer A, Dimitroulas T, Kitas G. Can we wean patients with inflammatory arthritis from biological therapies? [review]. Autoimmun Rev 2019;18:102399.
4. Klareskog L, van der Heijde D, de Jager JP, Gough A, Kalden J, Malaise M, et al. Therapeutic effect of the combination of etanercept and methotrexate compared with each treatment alone in patients with rheumatoid arthritis: double-blind randomised controlled trial. Lancet 2004;363:675–81.
5. Breedveld FC, Weisman MH, Kavanaugh AF, Cohen SB, Pavelka K, van Vollenhoven R, et al. The PREMIER study: a multicenter, randomized, double-blind clinical trial of combination therapy with adalimumab plus methotrexate versus methotrexate alone or adalimumab alone in patients with early, aggressive rheumatoid arthritis who had not had previous methotrexate treatment. Arthritis Rheum 2006;54:26–37.
6. Lipsky PE, van der Heijde DM, St Clair EW, Furst DE, Breedveld FC, Kalden JR, et al, on behalf of the Anti-Tumor Necrosis Factor Trial in Rheumatoid Arthritis with Concomitant Therapy Study Group. Infliximab and methotrexate in the treatment of rheumatoid arthritis. N Engl J Med 2000;343:1594–602.
7. Singh JA, Saag KG, Bridges SL Jr, Akl EA, Bannuru RR, Sullivan MC, et al. 2015 American College of Rheumatology guideline for the treatment of rheumatoid arthritis. Arthritis Rheumatol 2016; 68:1–26.
8. Smolen JS, Landewe RB, Bijlsma JW, Burmester GR, Dougados M, Kerschbaumer A, et al. EULAR recommendations for the management of rheumatoid arthritis with synthetic and biological disease-modifying antirheumatic drugs: 2019 update. Ann Rheum Dis 2020;79:685–99.
9. Treharne GJ, Douglas KM, Iwaszko J, Panoulas VF, Hale ED, Mitton DL, et al. Polypharmacy among people with rheumatoid arthritis: the role of age, disease duration and comorbidity. Musculoskeletal Care 2007;5:175–90.
10. Wang W, Zhou H, Liu L. Side effects of methotrexate therapy for rheumatoid arthritis: a systematic review. Eur J Med Chem 2018;158:502–16.
11. Pope JE, Haraoui B, Thorne JC, Vieira A, Poulin-Costello M, Keystone EC. The Canadian Methotrexate and Etanercept Outcome Study: a randomised trial of discontinuing versus continuing methotrexate after 6 months of etanercept and methotrexate therapy in rheumatoid arthritis. Ann Rheum Dis 2014;73:2144–51.
12. Smolen JS, Nash P, Durez P, Hall S, Ilivanova E, Irazoque-Palazuelos F, et al. Maintenance, reduction, or withdrawal of etanercept after treatment with etanercept and methotrexate in patients with moderate rheumatoid arthritis (PRESERVE): a randomised controlled trial. Lancet 2013;381:918–29.
13. Van Vollenhoven RF, Ostergaard M, Leirisalo-Repo M, Uhlig T, Jansson M, Larsson E, et al. Full dose, reduced dose or discontinuation of etanercept in rheumatoid arthritis. Ann Rheum Dis 2016; 75:52–8.
14. Emery P, Hammoudeh M, FitzGerald O, Combe B, Martin-Mola E, Buch MH, et al. Sustained remission with etanercept tapering in early rheumatoid arthritis. N Engl J Med 2014;371: 1781–92.
15. Emery P, Breedveld FC, Hall S, Durez P, Chang DJ, Robertson D, et al. Comparison of methotrexate monotherapy with a combination of methotrexate and etanercept in active, early, moderate to severe rheumatoid arthritis (COMET): a randomised, double-blind, parallel treatment trial. Lancet 2008;372:375–82.
16. Emery P, Breedveld F, van der Heijde D, Ferraccioli G, Dougados M, Robertson D, et al. Two-year clinical and radiographic results with combination etanercept–methotrexate therapy versus monotherapy in early rheumatoid arthritis: a two-year, double-blind, randomized study. Arthritis Rheum 2010;62:674–82.
17. Prince FH, Bykerk VP, Shadick NA, Lu B, Cui J, Frits M, et al. Sustained rheumatoid arthritis remission is uncommon in clinical practice. Arthritis Res Ther 2012;14:R68.
18. Ajeganova S, Huizinga T. Sustained remission in rheumatoid arthritis: latest evidence and clinical considerations. Ther Adv Musculoskelet Dis 2017;9:249–62.
19. Curtis JR, Trivedi M, Haraoui B, Emery P, Park GS, Collier DH, et al. Defining and characterizing sustained remission in patients with rheumatoid arthritis. Clin Rheumatol 2018;37:885–93.
20. Smolen JS, Breedveld FC, Schiff MH, Kalden JR, Emery P, Eberl G, et al. A simplified disease activity index for rheumatoid arthritis for use in clinical practice. Rheumatology (Oxford) 2003;42: 244–57.
21. Felson DT, Smolen JS, Wells G, Zhang B, van Tuyl LH, Funovits J, et al. American College of Rheumatology/European League Against Rheumatism provisional definition of remission in rheumatoid arthritis for clinical trials. Arthritis Rheum 2011;63:573–86.
22. Enbrel (etanercept) prescribing information. Thousand Oaks (CA): Immunex; 2017.
23. Aletaha D, Neogi T, Silman AJ, Funovits J, Felson DT, Bingham CO III, et al. 2010 rheumatoid arthritis classification criteria: an American College of Rheumatology/European League Against Rheumatism collaborative initiative. Arthritis Rheum 2010;62: 2569–81.
24. Fries JF, Spitz P, Kraines RG, Holman HR. Measurement of patient outcome in arthritis. Arthritis Rheum 1980;23:137–45.
25. Van der Heijde D. Radiographic progression in rheumatoid arthritis: does it reflect outcome? Does it reflect treatment? Ann Rheum Dis 2001;60 Suppl 3:iii47–50.
26. Genovese MC, Bathon JM, Martin RW, Fleischmann RM, Tesser JR, Schiff MH, et al. Etanercept versus methotrexate in patients with early rheumatoid arthritis: two-year radiographic and clinical outcomes. Arthritis Rheum 2002;46:1443–50.
27. Van der Heijde D, Klareskog L, Landewé R, Bruyn GA, Cantagrel A, Durez P, et al. Disease remission and sustained halting of radiographic progression with combination etanercept and methotrexate in patients with rheumatoid arthritis. Arthritis Rheum 2007;56: 3928–39.
28. US Food and Drug Administration. Guidance document: rheumatoid arthritis–developing drug products for treatment. May 2013. URL: https://www.fda.gov/regulatory-information/search-fda-guidance-documents/rheumatoid-arthritis-developing-drug-products-treatment.
29. Ridker PM, Everett BM, Pradhan A, MacFadyen JG, Solomon DH, Zaharris E, et al. Low-dose methotrexate for the prevention of atherosclerotic events. N Engl J Med 2019;380:752–62.
30. Jani M, Barton A, Warren RB, Griffiths CE, Chinoy H. The role of DMARDs in reducing the immunogenicity of TNF inhibitors in chronic inflammatory diseases. Rheumatology (Oxford) 2014; 53: 213–22.
31. Fagerli KM, Lie E, van der Heijde D, Heiberg MS, Lexberg AS, Rodevand E, et al. The role of methotrexate co-medication in TNF-inhibitor treatment in patients with psoriatic arthritis: results from 440 patients included in the NOR-DMARD study. Ann Rheum Dis 2014;73:132–7.

32. Favalli EG, Pregnolato F, Biggioggero M, Becciolini A, Penatti AE, Marchesoni A, et al. Twelve-year retention rate of first-line tumor necrosis factor inhibitors in rheumatoid arthritis: real-life data from a local registry. Arthritis Care Res (Hoboken) 2016; 68:432–9.
33. Emery P, Vlahos B, Szczypa P, Thakur M, Jones HE, Woolcott J, et al. Longterm drug survival of tumor necrosis factor inhibitors in patients with rheumatoid arthritis. J Rheumatol 2020;47: 493–501.
34. Pappas DA, Litman HJ, Lesperance T, Kricorian G, Karis E, Rebello S, et al. Persistence on biologic DMARD monotherapy after achieving rheumatoid arthritis disease control on combination therapy: retrospective analysis of CORRONA registry data. Rheumatol Int 2021;41: 381–90.

Arthritis & Rheumatology
Vol. 73, No. 5, May 2021, pp 769–778
DOI 10.1002/art.41585

American College of Rheumatology
Empowering Rheumatology Professionals

Suppression of Rheumatoid Arthritis by Enhanced Lymph Node Trafficking of Engineered Interleukin-10 in Murine Models

Eiji Yuba,[1] Erica Budina,[2] Kiyomitsu Katsumata,[2] Ako Ishihara,[2] Aslan Mansurov,[2] Aaron T. Alpar,[2] Elyse A. Watkins,[2] Peyman Hosseinchi,[2] Joseph W. Reda,[2] Abigail L. Lauterbach,[2] Mindy Nguyen,[2] Ani Solanki,[2] Takahiro Kageyama,[3] Melody A. Swartz,[2] Jun Ishihara,[4] and Jeffrey A. Hubbell[2]

Objective. Rheumatoid arthritis (RA) is a major autoimmune disease that causes synovitis and joint damage. Although clinical trials have been performed using interleukin-10 (IL-10), an antiinflammatory cytokine, as a potential treatment of RA, the therapeutic effects of IL-10 have been limited, potentially due to insufficient residence in lymphoid organs, where antigen recognition primarily occurs. This study was undertaken to engineer an IL-10–serum albumin (SA) fusion protein and evaluate its effects in 2 murine models of RA.

Methods. SA-fused IL-10 (SA–IL-10) was recombinantly expressed. Mice with collagen antibody–induced arthritis (n = 4–7 per group) or collagen-induced arthritis (n = 9–15 per group) were injected intravenously with wild-type IL-10 or SA–IL-10, and the retention of SA–IL-10 in the lymph nodes (LNs), immune cell composition in the paws, and therapeutic effect of SA–IL-10 on mice with arthritis were assessed.

Results. SA fusion to IL-10 led to enhanced accumulation in the mouse LNs compared with unmodified IL-10. Intravenous SA–IL-10 treatment restored immune cell composition in the paws to a normal status, elevated the frequency of suppressive alternatively activated macrophages, reduced IL-17A levels in the paw-draining LN, and protected joint morphology. Intravenous SA–IL-10 treatment showed similar efficacy as treatment with an anti–tumor necrosis factor antibody. SA–IL-10 was equally effective when administered intravenously, locally, or subcutaneously, which is a benefit for clinical translation of this molecule.

Conclusion. SA fusion to IL-10 is a simple but effective engineering strategy for RA therapy and has potential for clinical translation.

INTRODUCTION

Rheumatoid arthritis (RA) is an autoimmune disease that is currently controlled through treatment with inhibitors of inflammatory pathways. Pathologic features of RA are synovitis and joint destruction, which cause severe pain and joint dysfunction (1,2). Although the causal antigen for RA has not been fully elucidated, collagen recognition by immune cells plays a key role. During RA progression, autoantigen-specific T cells, especially Th17 cells, are activated and produce inflammatory cytokines including interleukin-17 (IL-17). Inflammatory cytokines in the joint, such as tumor necrosis factor (TNF) and IL-6, induce activation of macrophages and neutrophils as mediators of the inflammatory response. These inflammatory cells infiltrate the joints and cause various inflammatory responses, including activation of osteoclasts that destroy the bones in the joint (3). The current strategy for RA treatment is symptomatic, and, considering that many inflammatory cytokines are involved in RA progression, various biologic therapies such as antibodies or soluble receptors for TNF have been developed and approved for clinical use (4).

Supported by the University of Chicago.

[1]Eiji Yuba, PhD: University of Chicago, Chicago, Illinois, and Osaka Prefecture University, Osaka, Japan; [2]Erica Budina, BS, Kiyomitsu Katsumata, PhD, Ako Ishihara, MD, Aslan Mansurov, BS, Aaron T. Alpar, BS, Elyse A. Watkins, PhD, Peyman Hosseinchi, BS, Joseph W. Reda, BS, Abigail L. Lauterbach, BS, Mindy Nguyen, BS, Ani Solanki, BS, Melody A. Swartz, PhD, Jeffrey A. Hubbell, PhD: University of Chicago, Chicago, Illinois; [3]Takahiro Kageyama, PhD, MD: University of Illinois at Chicago; [4]Jun Ishihara, PhD: University of Chicago, Chicago, Illinois, and Imperial College London, London, UK.

Drs. Katsumata, A. Ishihara, J. Ishihara, and Hubbell and Mr. Mansurov are inventors on patent application PCT/US20/19668. Drs. Yuba, A. Ishihara, Watkins, J. Ishihara, and Hubbell are inventors on US provisional patent application 63/083,722, which covers the technology described in this article. No other disclosures relevant to this article were reported.

Address correspondence to Jun Ishihara, PhD, 86 Woodlane, London W12 0BZ UK (email: j.ishihara@imperial.ac.uk); or to Jeffrey A. Hubbell, PhD, 5640 S Ellis Ave, Chicago, IL 60636 (email: jhubbell@uchicago.edu).

Submitted for publication April 7, 2020; accepted in revised form November 5, 2020.

As another type of biologic therapy, administration of antiinflammatory cytokines has been studied for the treatment of RA to induce systemic suppression of inflammation or tolerance. IL-10 is one such antiinflammatory cytokine (5–7), and various attempts have been made to explore IL-10–based autoimmune disease therapies (6–8). However, the therapeutic effect of IL-10 in autoimmune disease is still a subject of controversy, possibly because of its short circulating half-life and its uncontrolled biodistribution after systemic administration (8). To address these drawbacks of IL-10 treatment, molecular engineering of IL-10 has been employed. Polyethylene glycol (PEG) has been grafted to IL-10 to prolong circulation (9); however, PEGylation generally induces significant decreases in protein bioactivity, since controlling the extent of modification and the modification site is challenging.

An IL-10 variant that targets an extracellular matrix protein splice variant that is present in sites of chronic inflammation has been produced by fusion of an antibody fragment to promote accumulation of IL-10 within the site of inflammation, showing enhanced function in the active collagen-induced arthritis (CIA) model (10–12). IL-10 accumulation at the site of inflammation directly suppresses inflammation at the disease site, whereas IL-10 also binds to IL-10 receptor–expressing cells such as macrophages, dendritic cells, and Th17 (13,14) present in secondary lymphoid organs, which induces various biologic responses, including differentiation of T cells, polarization of antigen-presenting cells (APCs), decrease in CD86 expression on APCs, and suppression of inflammatory responses (15). Therefore, IL-10 delivery to the secondary lymphoid organs would be a promising approach to induce systemic suppression of inflammation or tolerance. However, successful candidates have not yet been developed.

In the present study, we engineered IL-10 by fusion to serum albumin (SA), seeking to explore if the therapeutic effects of IL-10 in RA would be improved. We observed that SA fusion to IL-10 enhanced not only circulation time but also accumulation in the lymph nodes (LNs). The suppressive effects of engineered IL-10 on arthritis were evaluated using a passive collagen antibody–induced arthritis (CAIA) mouse model and an active CIA mouse model. We found that SA fusion to IL-10 enhanced accumulation of IL-10 in the mouse LNs after intravenous injection. SA-fused IL-10 significantly improved the antiinflammatory effects of IL-10 in the 2 murine models of RA and functioned similarly to TNF blockade.

MATERIALS AND METHODS

Production and purification of recombinant proteins. The sequences encoding for mouse SA without propeptide (amino acids 25–608 of whole SA), mouse IL-10, and a $(GGGS)_2$ linker (Supplementary Table 1, available on the Arthritis & Rheumatology website at http://onlinelibrary.wiley.com/doi/10.1002/art.41585/abstract) were synthesized and subcloned into the mammalian expression vector pcDNA3.1(+) by GenScript. A sequence encoding for 6 His was added at the C-terminus for further purification of the recombinant protein. Suspension-adapted HEK 293F cells were routinely maintained in serum-free FreeStyle 293 expression medium (Gibco). On the day of transfection, cells were inoculated into fresh medium at a density of 1×10^6 cells/ml, and 2 μg/ml plasmid DNA, 2 μg/ml 25-kd linear polyethyleneimine (Polysciences), and OptiPRO SFM media (4% final concentration; ThermoFisher) were sequentially added. The culture flask was agitated by orbital shaking at 135 rpm at 37°C in the presence of 5% CO_2. Seven days after transfection, the cell culture medium was collected by centrifugation and filtered through a 0.22-μm filter. Culture media were loaded into a HisTrap HP 5-ml column (GE Healthcare), using an ÄKTA pure 25 system (GE Healthcare). After washing the column with wash buffer (20 m*M* NaH_2PO_4, 0.5*M* NaCl, pH 8.0), protein was eluted with a gradient of 500 m*M* imidazole (in 20 m*M* NaH_2PO_4, 0.5*M* NaCl, pH 8.0). The protein was further purified with size-exclusion chromatography using a HiLoad Superdex 200 PG column (GE Healthcare) using phosphate buffered saline (PBS) as an eluent. All purification steps were carried out at 4°C.

Protein expression was verified as >90% pure by sodium dodecyl sulfate–polyacrylamide gel electrophoresis (SDS-PAGE). Purified proteins were tested for endotoxin via a HEK-Blue TLR4 reporter cell line, and endotoxin levels were confirmed to be <0.01 endotoxin units/ml. Protein concentration was determined by measuring the absorbance at 280 nm using a NanoDrop spectrophotometer (Thermo Scientific).

Mice. Seven-week-old female BALB/c mice and 8-week-old male DBA/1J mice were obtained from The Jackson Laboratory. Experiments were approved by the Institutional Animal Care and Use Committee of the University of Chicago.

CAIA model. Arthritis was induced in female BALB/c mice by intraperitoneal injection of anticollagen antibody cocktail (1.0 mg/mouse; Chondrex) on day 0, followed by intraperitoneal injection of lipopolysaccharide (LPS) (25 μg/mouse; Chondrex) on day 3. On day 3, mice were injected either intravenously, subcutaneously (in the mid-back), or via the footpad with PBS, wild-type IL-10, or SA–IL-10 (each equivalent to 43.5 μg of IL-10), or 200 μg of rat anti-mouse TNF antibody (clone XT3.11; Bio X Cell) before LPS injection. Joint swelling was scored every day according to the manufacturer's protocol (Chondrex). On the last day of scoring, the hind paws were fixed in 10% neutral formalin (Sigma-Aldrich), decalcified in Decalcifer II (Leica), and then subjected to histologic analysis. Paraffin-embedded paws were sliced into 5-μm–thick sections and stained with hematoxylin and eosin. The images were scanned with a Pannoramic digital slide scanner and analyzed using Pannoramic Viewer software. The severity of synovial hyperplasia and bone resorption in the arthritis model was scored on a scale of 0–2 according to previously reported criteria (16), with slight modifications as follows: 0 = normal to minimal infiltration of pannus in the cartilage and subchondral bone of

the marginal zone, 1 = mild to moderate infiltration of the marginal zone with minor cortical and medullary bone destruction, and 2 = severe infiltration associated with total or near total destruction of joint architecture. The scores in both hind paws were summed for each mouse (total score range per mouse 0–4). The histopathologic analyses were performed in a blinded manner.

CIA model. Male DBA/1J mice (8 weeks old) were immunized by subcutaneous injection of bovine collagen/Freund's complete adjuvant emulsion (Hooke Kit; Hooke Laboratories) into the base of the tail. Three weeks later, mice were given a booster injection of bovine collagen/Freund's incomplete adjuvant emulsion (Hooke Kit; Hooke Laboratories). After the booster injection, mice were examined every day, and joint swelling was scored according to the manufacturer's protocol (Hooke Laboratories). On the day mice had a total score of 2–4 (defined as day 0), they were intravenously injected with PBS or SA–IL-10 (each equivalent to 43.5 μg of IL-10), or 200 μg of rat anti-mouse TNF antibody (clone XT3.11; Bio X Cell). On the last day of scoring, hind paws were collected and histologic analysis was performed as described above.

LN microscopy. BALB/c mice were intravenously injected with wild-type IL-10 labeled with DyLight 594 (43.5 μg) or SA–IL-10 labeled with equimolar amounts of dye. Twenty-four hours after injection, mouse popliteal LNs were harvested and frozen in dry ice with OCT compound. Tissue slices (10 μm) were obtained by cryosectioning. The tissues were fixed with 2% paraformaldehyde in PBS for 15 minutes at room temperature. After washing with PBS–Tween (PBST), the tissues were blocked with 2% bovine serum albumin in PBST for 1 hour at room temperature. Tissues were stained with anti-mouse CD3 antibody (1:100) (145-2C11; BioLegend) or anti-mouse peripheral lymph node addressin (PNAd) antibody (1:200) (MECA79; BioLegend) and Alexa Fluor 488–conjugated donkey anti-rat antibody (1:400; Jackson ImmunoResearch). Tissues were washed 3 times and then covered with ProLong Gold antifade mountant with DAPI (ThermoFisher Scientific). An IX83 microscope (Olympus) with 10× magnification was used for imaging for CD3 staining, and a Leica SP8 3D confocal laser scanning microscope with 20× magnification was used for PNAd staining. Images were processed using ImageJ software (National Institutes of Health).

LN pharmacokinetics. Wild-type IL-10 or SA–IL-10 (each equivalent to 35 μg of IL-10) was injected intravenously into mice with CAIA. Popliteal, mesenteric, and cervical LNs were collected 30 minutes and 1, 4, 8, 24, 32, 48, and 72 hours after injection, and were subsequently homogenized using Lysing Matrix D and FastPrep-24 5G (MP Biomedical) for 40 seconds at 5,000 beats per minute in T-PER tissue protein extraction reagent (Thermo Scientific) with cOmplete protease inhibitor cocktail (Roche). After homogenization, samples were incubated overnight at 4°C. Samples were centrifuged (at 5,000*g* for 5 minutes), and total protein concentration and IL-10 concentration were analyzed using a BCA assay kit (Thermo Fisher) and IL-10 Mouse Uncoated enzyme-linked immunosorbent assay (ELISA) kit (Invitrogen), respectively. Simultaneously, cytokine levels in the LN extract were measured using a Mouse Uncoated ELISA kit (Invitrogen) or Ready-SET-Go! ELISA kits (eBioscience) according to the manufacturer's protocol. For detection of granulocyte–macrophage colony-stimulating factor (GM-CSF), wild-type IL-10 or SA–IL-10 (each equivalent to 35 μg of IL-10) was injected intravenously twice, with 3 days between injections, into mice with CAIA. The day following the last injection, mouse popliteal LNs were collected for detection of GM-CSF.

Flow cytometric analysis. Mice with CAIA were intravenously injected with PBS, wild-type IL-10, or SA–IL-10 (each equivalent to 43.5 μg of IL-10). Eight days after injection, blood and hind paws were harvested. Red blood cells were lysed with ACK lysing buffer (Quality Biological), followed by antibody staining for flow cytometric analysis. Paws were digested in Dulbecco's modified Eagle's medium supplemented with 2% fetal bovine serum, 2 mg/ml collagenase D, and 40 μg/ml DNase I (Roche) for 60 minutes at 37°C. Single-cell suspensions were obtained by gentle disruption through a 70-μm cell strainer. Antibodies against the following molecules were used: anti-mouse CD3 (145-2C11; BD Biosciences), CD4 (RM4-5; BD Biosciences), anti-mouse CD8α (53–6.7; BD Biosciences), anti-mouse CD25 (PC61; BD Biosciences), anti-mouse CD45 (30-F11; BD Biosciences), CD44 (IM7; BD Biosciences), CD62L (MEL-14; BD Biosciences), PD-1 (29F.1A12; BD Biosciences), NK1.1 (PK136; BD Biosciences), FoxP3 (MF23; BD Biosciences), F4/80 (T45-2342; BD Biosciences), MHCII (M5/114.15.2; BioLegend), CD206 (C068C2; BioLegend), Ly6G (1A8; BioLegend), Ly-6C (HK1.4; BioLegend), CD11b (M1/70; BioLegend), CD11c (HL3; BD Biosciences), and B220 (RA3-6B2; BioLegend).

Fixable live/dead cell discrimination was performed using Fixable Viability Dye eFluor 455 (eBioscience) according to the manufacturer's instructions. Staining was carried out on ice for 20 minutes, unless indicated otherwise, and intracellular staining was performed using a FoxP3 staining kit according to the manufacturer's instructions (BioLegend). Following a washing step, cells were stained with specific antibodies for 20 minutes on ice prior to fixation. All flow cytometric analyses were done using a Fortessa flow cytometer (BD Biosciences) and analyzed using FlowJo software (Tree Star).

RESULTS

Binding of SA-fused IL-10 to neonatal Fc receptor (FcRn) and APCs and accumulation of SA–IL-10 within the mouse LNs. Wild-type mouse IL-10 and SA-fused mouse IL-10 were recombinantly expressed, and the molecular weight of the fusion protein was higher than that of wild-type IL-10, as determined by SDS-PAGE; in addition, most of the SA–IL-10 existed

as a monomer under nonreducing conditions (Figure 1a). Surface plasmon resonance analysis revealed that SA–IL-10 binds to FcRn with micromolar order of K_d (Figure 1b). The ability of these proteins to bind to splenocytes and single cells isolated from the popliteal LN was further evaluated by flow cytometry (Figure 1c). SA-fused IL-10 exhibited high binding to macrophages and dendritic cells in both splenocytes and LN-derived cells. After intravenous injection of fluorescently labeled wild-type IL-10 or SA–IL-10, significantly higher fluorescence signals for SA–IL-10 than for wild-type IL-10 were observed within the mouse popliteal LN (Figure 1d). Interestingly, higher fluorescence signals were located surrounding high endothelial venules (HEVs), where APCs reside (17).

Prolonged blood circulation of SA–IL-10. SA is known to demonstrate long circulation via FcRn-mediated recycling on vascular endothelial cells (18,19). As expected, SA–IL-10 showed significantly prolonged blood circulation compared with wild-type IL-10 (Supplementary Figure 1a, available on the *Arthritis & Rheumatology* website at http://onlinelibrary.wiley.com/doi/10.1002/art.41585/abstract). Supplementary Figure 1b shows the fluorescence signals from major organs of mice intravenously injected with DyLight 800–labeled proteins. Reflecting its long circulation properties, SA–IL-10 showed higher signals in the mouse heart, lungs, and spleen than wild-type IL-10.

Reduced immune activity after accumulation of SA–IL-10 within the mouse LNs. SA-fused IL-10 showed micromolar affinity to FcRn (Figure 1b) and accumulation within the mouse LNs after intravenous injection (Figure 1d). Next, the amounts of IL-10 and its pharmacokinetics in the mouse LNs were quantitatively evaluated (Figures 2a–c). After intravenous injection of wild-type IL-10 or SA–IL-10 into mice with CAIA, IL-10 concentrations in the LNs at various time points were detected using ELISAs. SA–IL-10 showed significantly higher IL-10 signals in the joint-draining (popliteal) LN and the mesenteric LN and relatively high signals in a nondraining (cervical) LN compared with wild-type IL-10 at 4 hours after injection (Figure 2a). SA–IL-10–injected mice showed peak IL-10 concentration ~1 hour after injection (Figure 2b) and 5–18 times higher areas under the curve (AUCs) than wild-type IL-10 in the LNs (Figure 2c). Notably, SA–IL-10 was detectable in mouse

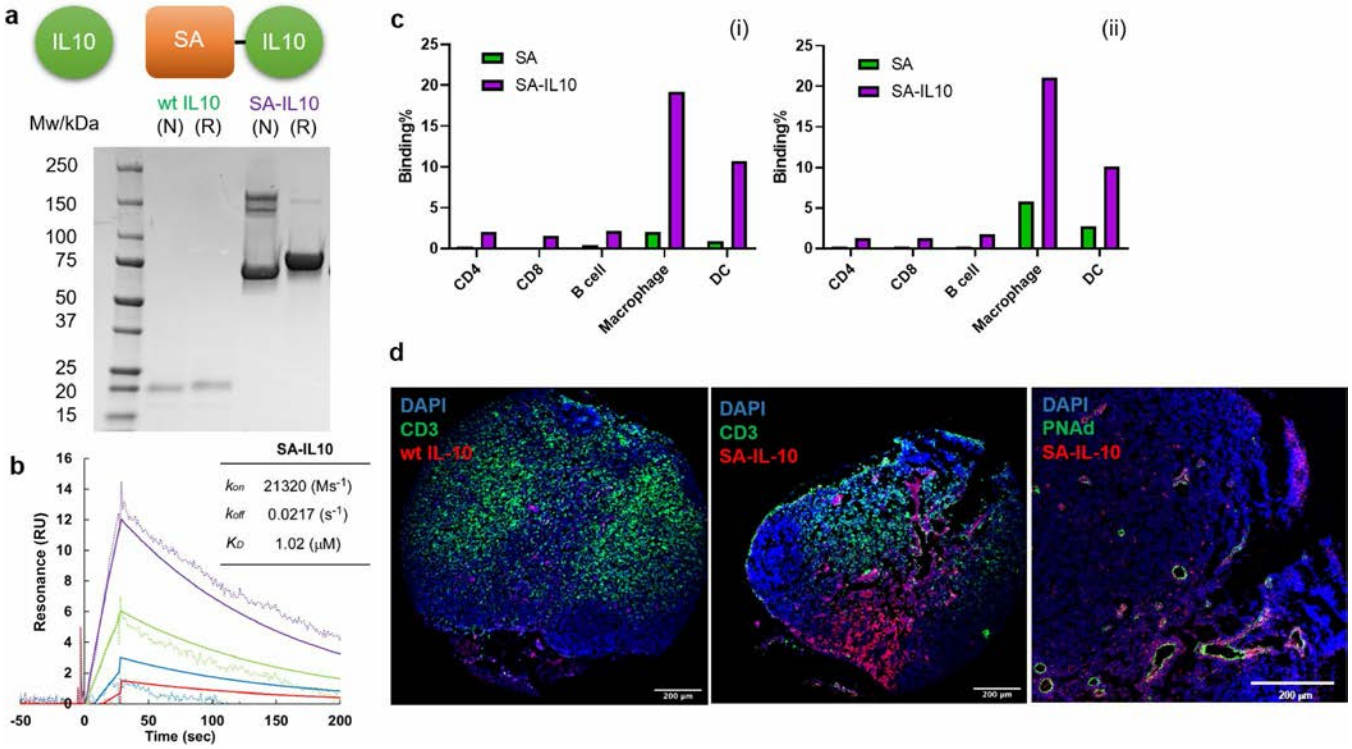

Figure 1. Fusion of serum albumin (SA) to interleukin-10 (IL-10) induces neonatal Fc receptor (FcRn) binding and results in accumulation of IL-10 in the mouse lymph nodes (LNs). **a**, Sodium dodecyl sulfate–polyacrylamide gel electrophoresis analysis of wild-type (WT) IL-10 and SA–IL-10. N = nonreducing; R = reducing. **b**, Surface plasmon resonance analysis of the binding of SA–IL-10 to FcRn. RU = resonance unit. **c**, Binding of SA and SA–IL-10 to CD4+ cells, CD8+ cells, B cells, macrophages, and dendritic cells (DCs) in splenocytes (i) and single cells from the mouse popliteal LN (ii). Splenocytes or single cells from the popliteal LN were incubated with SA or SA–IL-10 for 30 minutes on ice. Binding of each protein to immune cells was detected by co-staining with an anti-SA antibody and antibodies for specific markers of each immune cell population. **d**, Immunofluorescence images of the mouse popliteal LN after intravenous injection of DyLight 594–labeled wild-type IL-10 or SA–IL-10. T cells and high endothelial venules were stained with anti-CD3 antibody or anti–peripheral lymph node addressin (anti-PNAd) antibody, respectively.

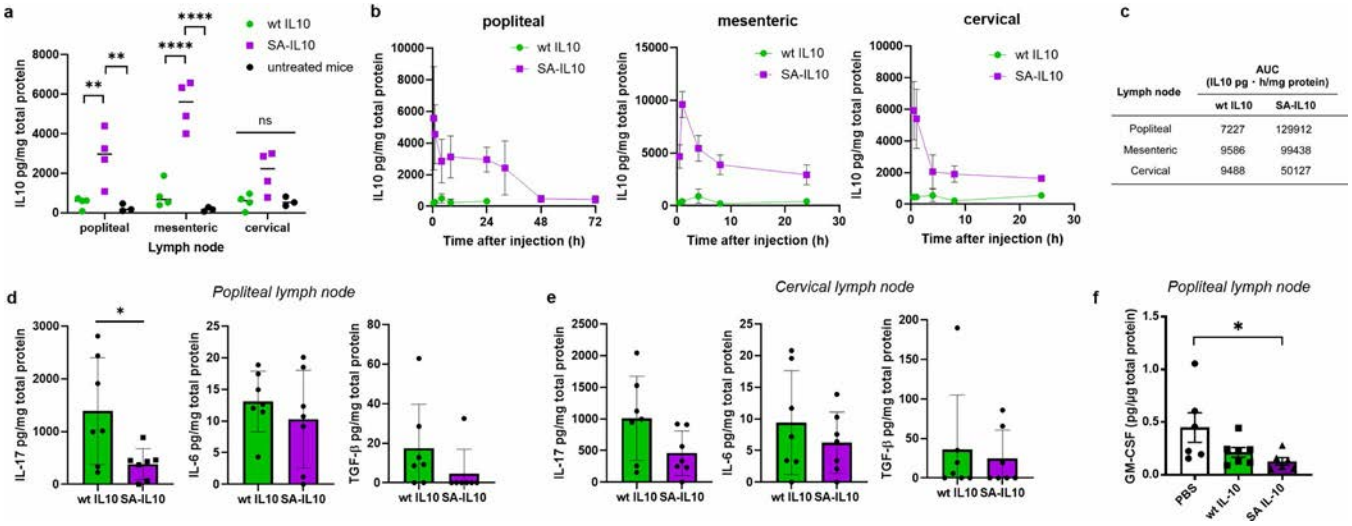

Figure 2. SA-fused IL-10 accumulates within mouse LNs and suppresses Th17 activation. Collagen antibody–induced arthritis was induced in mice by passive immunization with anticollagen antibodies, followed by intraperitoneal injection of lipopolysaccharide (LPS; defined as day 3). On the day of LPS injection, wild-type IL-10 or SA–IL-10 was intravenously injected into arthritic mice. Levels of IL-10 and Th17-related cytokines in mouse LNs were measured using enzyme-linked immunosorbent assay. **a**, IL-10 levels in mouse popliteal, mesenteric, and cervical LNs 4 hours after injection of wild-type IL-10 or SA–IL-10. Symbols represent individual mice; horizontal lines show the mean. **b**, Pharmacokinetics of wild-type IL-10 and SA–IL-10 in mouse popliteal, mesenteric, and cervical LNs after intravenous injection. Values are the mean ± SEM (n = 4 mice per group). **c**, Area under the curve (AUC) for wild-type IL-10 and SA–IL-10 in the indicated mouse LNs. **d** and **e**, Th17-related cytokine levels in the joint-draining (popliteal) LNs (**d**) and nondraining (cervical) LNs (**e**) of mice treated with wild-type IL-10 or SA–IL-10. **f**, Granulocyte–macrophage colony-stimulating factor (GM-CSF) levels in the popliteal LNs of mice treated with phosphate buffered saline (PBS), wild-type IL-10, or SA–IL-10. In **d**–**f**, symbols represent individual mice (n = 7 per group); bars show the mean ± SEM. * = $P < 0.05$; ** = $P < 0.01$; **** = $P < 0.0001$, by analysis of variance with Tukey's test in **a** and **f**; by Student's 2-tailed *t*-test in **d** and **e**. TGFβ = transforming growth factor β; NS = not significant (see Figure 1 for other definitions). Color figure can be viewed in the online issue, which is available at http://onlinelibrary.wiley.com/doi/10.1002/art.41585/abstract.

popliteal LNs even after 3 days (Figure 2b). These data indicate that SA–IL-10 immediately accumulated within mouse LNs after intravenous injection and showed higher retention in the LNs than wild-type IL-10.

High concentrations and AUCs of SA–IL-10 in the LNs may affect the phenotypes of various immune cells in LNs and other secondary lymphoid organs. Therefore, immune cell populations in the spleen and popliteal LN were analyzed by flow cytometry (Supplementary Figure 2, available on the *Arthritis & Rheumatology* website at http://onlinelibrary.wiley.com/doi/10.1002/art.41585/abstract). Intravenous injection of SA–IL-10 induced a significant decrease in the frequency of CD3+ T cells and CD45+ lymphocytes in the mouse spleen (Supplementary Figure 2a). In addition, the frequencies of CD86+ dendritic cells, granulocytic myeloid-derived suppressor cells (MDSCs), and CD86+ classically activated (M1) macrophages decreased and that of CD206+ alternatively activated (M2) macrophages increased after injection of SA–IL-10 compared with PBS or wild-type IL-10. A similar tendency was observed within the mouse popliteal LNs (Supplementary Figure 2b). These data suggest that SA–IL-10 suppressed the activity of APCs and simultaneously activated immunosuppressive M2 macrophages.

Deactivation of APCs, and accumulation of high levels of IL-10, in the mouse LNs might suppress the activity of Th17 cells, which play a crucial role in the development of RA (20,21). We measured the levels of Th17-related cytokines (IL-17, IL-6, and transforming growth factor β) in the joint-draining (popliteal) LN and a nondraining (cervical) LN. Compared with treatment with wild-type IL-10, IL-17 levels were significantly reduced in the mouse popliteal LN after treatment with SA–IL-10, and levels in the cervical LN were not significantly reduced by either IL-10 variant (Figures 2d and e). Treatment with SA–IL-10 reduced the concentration of GM-CSF in the popliteal LN, whereas wild-type IL-10 did not (Figure 2f).

Suppression of the development of RA in mice treated with SA–IL-10. The therapeutic effects of engineered IL-10 in the passive CAIA model were evaluated (Figure 3). Intravenous injection of SA–IL-10 significantly suppressed the development of arthritis, whereas mice injected with PBS or wild-type IL-10 exhibited severe inflammation in the paws (Figure 3a). Histologic analysis indicated that intravenous administration of SA–IL-10 significantly suppressed inflammatory responses in the mouse paws and reduced joint pathology compared with PBS (Figure 3b). The effect of the administration route on therapeutic efficacy was also investigated, comparing intravenous, local (footpad), and subcutaneous (at a distant site, the mid-back) administration (Figure 3c). Notably, SA–IL-10 showed quite high

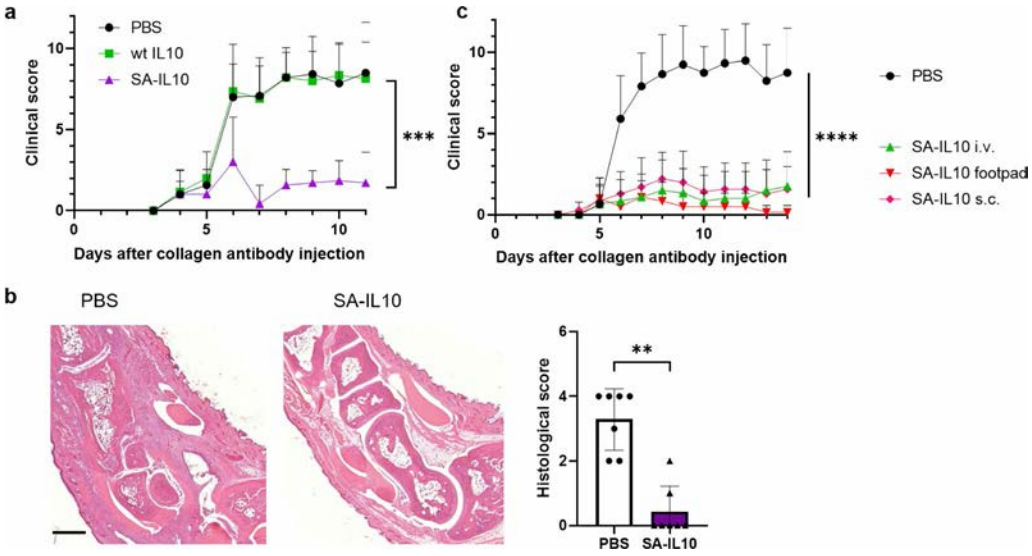

Figure 3. SA-fused IL-10 suppresses arthritis development more effectively than wild-type IL-10. **a**, Arthritis scores in mice with collagen antibody–induced arthritis (CAIA) treated with phosphate buffered saline (PBS), wild-type IL-10, or SA–IL-10. CAIA was induced by passive immunization with anticollagen antibodies, followed by intraperitoneal injection of lipopolysaccharide (LPS). On the day of LPS injection, PBS, wild-type IL-10, or SA–IL-10 (equivalent to 43.5 μg of IL-10) was injected intravenously into arthritic mice. Values are the mean ± SEM (n = 7 mice per group). **b**, Left, Representative images of mouse joints stained with hematoxylin and eosin on day 14 in each treatment group. Bar = 500 μm. Right, Histologic scores in mice with CAIA treated with PBS or SA–IL-10. The severity of synovial hyperplasia and bone resorption was scored on a scale of 0–4 as described in Materials and Methods. Symbols represent individual mice (n = 7 per group); bars show the mean ± SEM. **c**, Therapeutic effects of SA–IL-10 administered by different routes. Arthritis scores in mice treated with SA–IL-10 intravenously (IV), in the footpad, or subcutaneously (SC) are shown. Values are the mean ± SEM (n = 7 mice per group). ** = $P < 0.01$; *** = $P < 0.001$; **** = $P < 0.0001$, by analysis of variance with Tukey's test in **a** and **c**; by Student's 2-tailed *t*-test in **b**. See Figure 1 for other definitions. Color figure can be viewed in the online issue, which is available at http://onlinelibrary.wiley.com/doi/10.1002/art.41585/abstract.

suppressive effects on CAIA by all of the administration routes tested (Figure 3c).

A second arthritis model, the active CIA model, was used to evaluate the effects of SA–IL-10 on RA. A single injection of SA–IL-10 in mice with CIA induced significant suppression of arthritis development compared with PBS (Figure 4a). Most mice treated with PBS showed severe inflammation of the paws, as indicated by histologic analysis and the histologic score (Figure 4b). In contrast, the paws of SA–IL-10-treated mice exhibited almost identical status to the paws of naive mice, and most mice treated with SA–IL-10 had a histologic score of ≤1 (Figure 4b). Treatment with anti-TNF antibody, a mouse model of an antibody drug used to treat RA, also suppressed the increase in clinical scores compared with treatment with PBS in mice with CIA (Figure 4c); however, 2 injections of anti-TNF antibody did not reverse the histologic damage in the mouse joints or significantly decrease the histologic score, although there was a nonsignificant decrease in the histologic score in mice treated with anti-TNF antibody compared with those treated with PBS ($P = 0.1008$) (Figure 4d). Taken together, these results indicate the highly suppressive effect on inflammation of local, intravenous, or subcutaneous administration of SA–IL-10. The therapeutic effect of SA–IL-10 was comparable to or greater than that of anti-TNF antibody treatment.

Suppression of inflammatory responses in the paws of mice treated with SA–IL-10. Next, immune cell populations in the mouse hind paws were analyzed using flow cytometry (Figure 5a). Frequencies of CD45+ immune cells were significantly decreased in mice treated with intravenous injection of SA–IL-10 compared with those treated with PBS or wild-type IL-10. Within CD45+ cells, the frequencies of B cells and dendritic cells in SA–IL-10–treated mice became comparable to those in healthy mice, and CD11b+ cell frequency decreased to the level in healthy mice as well. Among CD11b+ cells, the granulocytic MDSC population was reduced, and macrophage frequency was recovered to near the level in healthy mice compared with PBS- or wild-type IL-10–treated mice. In addition, the frequency of CD206+ M2 macrophages was significantly increased by injection of SA–IL-10 compared with PBS or wild-type IL-10, even exceeding that in healthy mice. An analysis of T cell populations in the paws revealed that SA–IL-10 suppressed the change in CD4+ cells and FoxP3+ Treg cells in mice with CAIA (Supplementary Figure 3a, available on the *Arthritis & Rheumatology* website at http://onlinelibrary.wiley.com/doi/10.1002/art.41585/abstract). Furthermore, SA–IL-10 suppressed a decrease in Treg cell frequency in the blood (Supplementary Figure 3b). Reflecting these changes in immune cell populations, the levels of various inflammatory cytokines in the mouse paws were significantly decreased

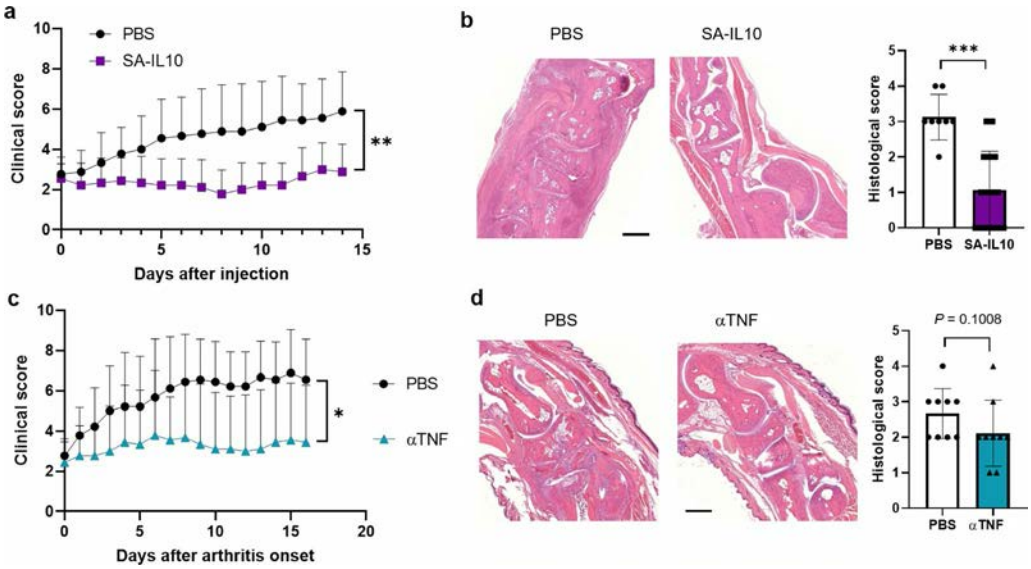

Figure 4. SA-fused IL-10 shows an improved therapeutic effect on established arthritis. Male DBA/1J mice were subcutaneously injected with bovine collagen/Freund's complete adjuvant emulsion in the tail base. After 3 weeks, bovine collagen/Freund's incomplete adjuvant emulsion was injected as a boost. When arthritis scores were 2–4 (defined as day 0), mice were intravenously injected with phosphate buffered saline (PBS), SA–IL-10 (each equivalent to 43.5 μg of IL-10), or 200 μg of anti–tumor necrosis factor (anti-TNF) antibody. In **c** and **d**, mice received the same treatments again on day 3. **a** and **c**, Arthritis scores in mice treated with PBS or SA–IL-10 (**a**) and mice treated with PBS or anti-TNF (αTNF) antibody (**c**). Values are the mean ± SEM (n = 9–15 mice per group). **b** and **d**, Left, Representative images of hematoxylin and eosin–stained mouse joints on day 16 after treatment with PBS or SA–IL-10 (**b**) or treatment with PBS or anti-TNF antibody (**d**). Bars = 500 μm. Right, Histologic scores in mice treated with PBS or SA–IL-10 (**b**) and in mice treated with PBS or anti-TNF antibody (**d**). The severity of synovial hyperplasia and bone resorption was scored on a scale of 0–4 as described in Materials and Methods. * = $P < 0.05$; ** = $P < 0.01$; *** = $P < 0.001$, by Student's 2-tailed *t*-test. See Figure 1 for other definitions. Color figure can be viewed in the online issue, which is available at http://onlinelibrary.wiley.com/doi/10.1002/art.41585/abstract.

by intravenous injection of SA–IL-10, to levels comparable with those in healthy mice (Figure 5b).

Albumin-fused IL-10 shows no toxicity and no immunosuppression after injection. Finally, safety assessments were performed to investigate whether engineered IL-10 demonstrates any adverse effects. Representative blood parameters measured by a hematology analyzer and spleen weights did not show any significant changes among the treatment groups (Supplementary Figure 4, available on the *Arthritis & Rheumatology* website at http://onlinelibrary.wiley.com/doi/10.1002/art.41585/abstract). Various biochemical markers in serum were also investigated using a biochemistry analyzer (Supplementary Figure 4b). For the groups treated with engineered IL-10, most markers, except for amylase (the levels of which were not increased, but rather slightly decreased), showed similar levels to those in the group treated with PBS. Furthermore, in a model of vaccination to ovalbumin (OVA), neither injection of SA-IL-10 nor injection of anti-TNF affected anti-OVA IgG titers, whereas FTY720 (fingolimod), a clinically approved drug for the treatment of multiple sclerosis, showed some immunosuppressive trend (although not statistically significant) under these experimental conditions (Supplementary Figure 5, available on the *Arthritis & Rheumatology* website at http://onlinelibrary.wiley.com/doi/10.1002/art.41585/abstract). These results indicate that engineered IL-10 possesses high safety and does not lead to broad immunosuppression after systemic administration.

DISCUSSION

Current treatment of RA is based on symptomatic therapy that relieves pain, controls synovitis, and suppresses joint injury. Antibody drugs or competitive soluble receptors that neutralize inflammatory cytokines, especially TNF, have provided high therapeutic efficacy for patients with RA (4). These biotherapeutics mainly act at the inflamed joints to capture the inflammatory cytokines. However, these inhibitory drugs are known to increase the risk of infection, because their targets are pleiotropic in immune function and these drugs are repeatedly administered to provide their antiinflammatory effect at the disease site (22–25). In addition, administration of antibody drugs can cause the induction of neutralizing antidrug antibodies, which decreases therapeutic efficiency (26). Therefore, development of an alternative approach with a structurally different molecular class and with a different immunosuppressive molecular mechanism such as tolerance is desired.

In this study, we explored a novel approach to treat RA through enhanced LN trafficking using engineered IL-10, which is a representative antiinflammatory cytokine and modulates

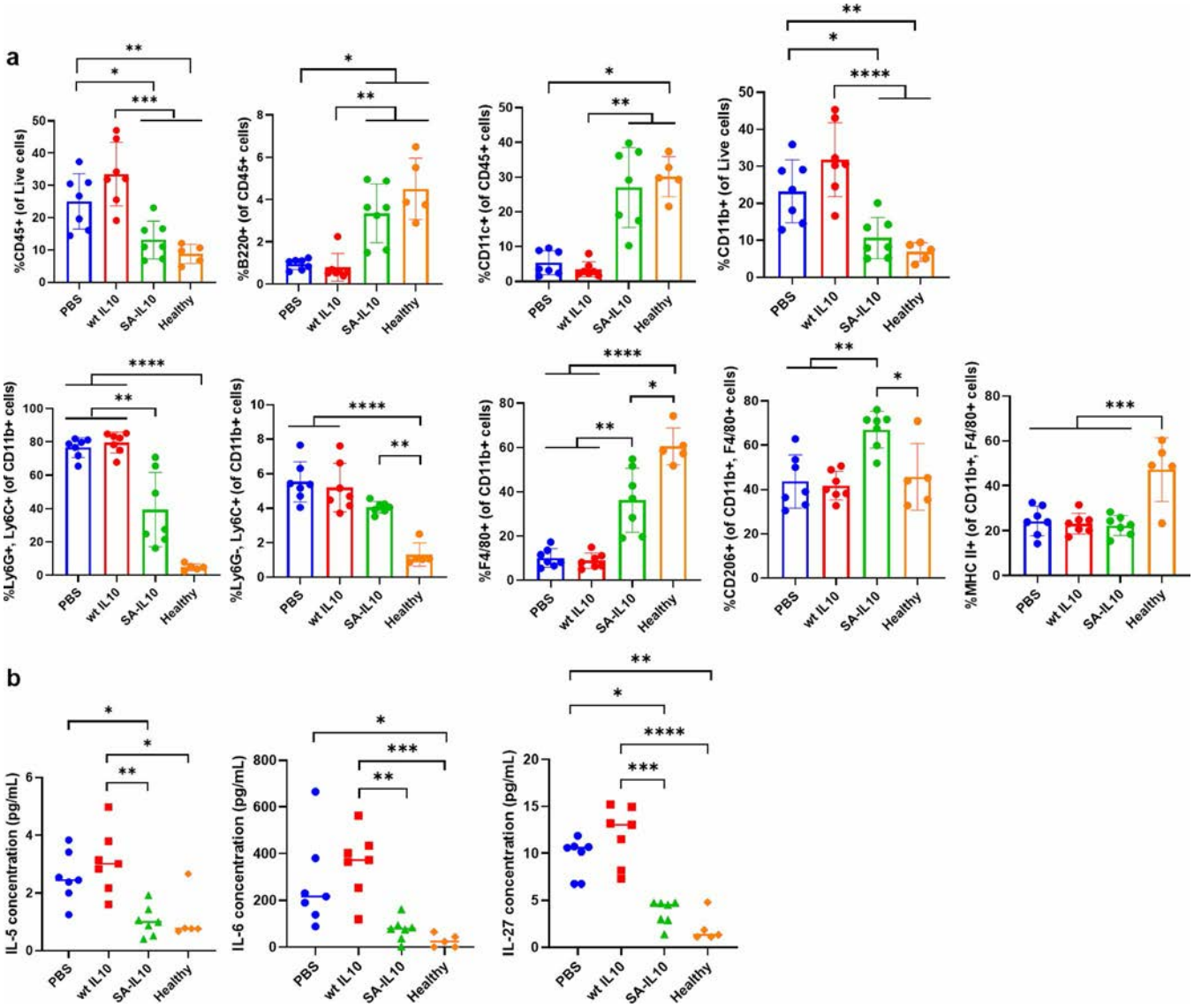

Figure 5. SA-fused IL-10 suppresses inflammatory responses in the mouse paws. Collagen antibody–induced arthritis was induced in mice by passive immunization with anticollagen antibodies, followed by intraperitoneal injection of lipopolysaccharide (LPS). On the day of LPS injection (defined as day 3), phosphate buffered saline (PBS), wild-type IL-10, or SA–IL-10 was intravenously injected into arthritic mice. **a**, Frequency of CD45+ cells, B cells (B220+ cells within CD45+ lymphocytes), dendritic cells (CD11c+ cells within CD45+ lymphocytes), monocytes (CD11b+ cells within CD45+ lymphocytes), granulocytic myeloid-derived suppressor cells (MDSCs)/neutrophils (Ly-6G+Ly-6C+CD11b+CD45+), monocytic MDSCs (Ly-6G–Ly-6C+CD11b+CD45+), macrophages (F4/80+CD11b+CD45+), alternatively activated macrophages (CD206+ F4/80+CD11b+CD45+), and classically activated macrophages (MHCII+F4/80+CD11b+CD45+) determined by flow cytometry of single cells extracted on day 11 from the hind paws of mice treated with PBS, wild-type IL-10, or SA–IL-10, or healthy mice. Symbols represent individual mice (n = 7 per group); bars show the mean ± SEM. **b**, Cytokine levels on day 11 in the hind paws of mice treated with PBS, wild-type IL-10, or SA–IL-10, and healthy mice. Symbols represent individual mice (n = 5–7 per group); horizontal lines show the mean. * = $P < 0.05$; ** = $P < 0.01$; *** = $P < 0.001$; **** = $P < 0.0001$, by Kruskal-Wallis test followed by Dunn's multiple comparison test for the comparison of the frequency of CD11c+ in **a**; by analysis of variance with Tukey's test for all other comparisons. See Figure 1 for other definitions. Color figure can be viewed in the online issue, which is available at http://onlinelibrary.wiley.com/doi/10.1002/art.41585/abstract.

the phenotypes of RA-related immune cells toward immunosuppressive states. Clinical trials of recombinant IL-10 for the treatment of autoimmune diseases including RA have already been performed (6–8,27). One of the drawbacks of IL-10 is its short half-life in the blood (8). In this study, we genetically fused SA to IL-10 to extend its retention in the secondary lymphoid organs. We evaluated SA–IL-10, in comparison with wild-type IL-10, for the amelioration of arthritis in 2 mouse models. CAIA is a macrophage- and neutrophil-mediated model of acute RA, whereas CIA is a T cell–mediated, and especially Th17-mediated, RA model. Given that RA is a heterogeneous disease in the clinic and the models complement each other, it

is encouraging that SA-fused IL-10 suppressed disease severity in both models. SA fusion to IL-10 is crucial for obtaining a marked therapeutic effect, which is comparable to or relatively greater than that achieved with anti-TNF antibody, a common therapy in the clinic. Additionally, to the best of our knowledge, this study is the first to show a therapeutic effect of IL-10 in the CAIA model.

Compared with wild-type IL-10, SA fusion to IL-10 resulted in enhanced accumulation of IL-10 and prolonged duration of high IL-10 concentrations in the LNs after intravenous injection in mice (Figure 2a). So far, LN trafficking of SA or albumin-binding nanoparticles has mainly been achieved by intradermal or subcutaneous administration, where the LN is accessed via the afferent lymphatic vessel downstream of the collecting lymphatic vessels at the injection site (28–31). In the context of a biodistribution study of inflammatory cytokines, a previous study showed high localization of human SA–fused IL-2 after intravenous injection into the mouse spleen, liver, and LNs, where IL-2 receptor–expressing T cells exist, but the precise mechanism of this high localization has not been elucidated (32).

In this study, we showed enhanced trafficking of SA-fused IL-10 into mouse LNs after intravenous injection, where the SA enters the LN via the blood vasculature. SA–IL-10 exhibited high binding affinity (micromolar K_d, as expected) to FcRn (Figure 1b), which provides prolonged blood circulation properties to proteins via recycling mediated via FcRn expressed in vascular endothelial cells (Supplementary Figure 1a). Recycling via transcytosis (from the basal side back to the lumenal side) of IgG via FcRn is a well-established phenomenon, whereas the same phenomenon for SA has been reported more recently (18,19). In the LN, FcRn-mediated molecular transport would seem to lead to accumulation there. Interestingly, histologic analysis revealed the accumulation of SA–IL-10 surrounding the HEVs of the LNs (Figure 1d). Further experiments are needed to reveal a more detailed mechanism of enhanced LN accumulation and the relationship with FcRn, such as LN accumulation analysis using mutated SA-fused IL-10 to abrogate FcRn binding.

SA–IL-10 showed high binding to APCs in the spleen and the joint-draining LN (Figure 1b). After accumulation within the LNs, SA–IL-10 molecules are taken up by APCs resident within the LNs, leading to the suppression of dendritic cell and M1 macrophage activities and the induction of M2 macrophages (Supplementary Figure 2). M2 macrophages can change the differentiation fate of Th0 cells to Treg cells in the LNs (33). Furthermore, the immunosuppressive environment created by high concentrations of IL-10 in the LNs may cause the further polarization of macrophages to an M2 phenotype and the suppression of Th17 differentiation (34,35), resulting in the decrease in the levels of IL-17, GM-CSF, and other cytokines that we observed in the mouse LNs (Figures 2d and f). GM-CSF is a cytokine that is a marker for pathogenic Th17, and its inhibitory antibody is currently being tested in clinical trials (36). Thus, the decrease in GM-CSF levels upon SA–IL-10 treatment indicates decreased immunoactivation in the joint-draining LN. Th17 cells reportedly express IL-10 receptor, and IL-10 binding suppresses IL-17 expression and secretion (14,37). Because Th17 cell antigen recognition primarily occurs in the lymphoid tissue, SA–IL-10 may bind to Th17 cells directly to suppress the IL-17 pathway. These changes in the LNs also suppressed the infiltration of immune cells, especially granulocytic MDSCs and monocytes, into the paws (Figure 5a) and induced an increase in M2 macrophages (Figure 5a), resulting in a decrease in the levels of inflammatory cytokines (Figure 5b) and the suppression of joint inflammation (Figures 3 and 4).

SA–IL-10 induced high antiinflammatory responses after administration by any of the routes tested, namely, intravenous, subcutaneous (at a distant site), or footpad (local) injections (Figure 3c), suggesting that SA–IL-10 can enter the LNs systemically after uptake by a local injection-site draining lymphatic vessel and transit through the lymphatic system back into the systemic circulation via the thoracic duct. The high therapeutic effect of subcutaneous injection suggests a particular clinical benefit of SA–IL-10. Therefore, SA fusion is a simple but effective way to prepare engineered cytokines to achieve enhanced LN trafficking.

In this study, SA fusion to IL-10 achieved increased persistence within the LNs, where autoimmunity-related immune recognition develops and persists. As a result, SA–IL-10 suppressed the main inflammatory pathway of RA progression, without inhibition of a pleiotropic inflammatory cytokine such as TNF. In addition, SA–IL-10 did not show any notable toxicities or immunosuppressive effects in preliminary safety assessments (Supplementary Figures 4 and 5). SA–IL-10 exhibited marked therapeutic effects in both the CIA and CAIA models. Therefore, our data suggest the potential of SA–IL-10 for clinical application for the suppression of RA, and our findings more broadly suggest the ability to modulate immunity through systemic tolerogenic manipulation of the LNs in other autoimmune and inflammatory diseases.

ACKNOWLEDGMENTS

We thank the staff of the Human Tissue Resource Center of the University of Chicago for histologic analysis. We thank the staff of the Integrated Light Microscopy Core of the University of Chicago for imaging. We thank S. Gomes for assistance with SDS-PAGE and experiments and W. Hou for assistance with subcutaneous injection into the mouse tail and experiments. We thank Professor T. Sano (University of Illinois at Chicago) for experimental advice and helpful discussions.

AUTHOR CONTRIBUTIONS

All authors were involved in drafting the article or revising it critically for important intellectual content, and all authors approved the final version to be published. Dr. Yuba had full access to all of the data in the study and takes responsibility for the integrity of the data and the accuracy of the data analysis.

Study conception and design. Yuba, J. Ishihara, Hubbell.

Acquisition of data. Yuba, Budina, Katsumata, A. Ishihara, Mansurov, Alpar, Watkins, Hosseinchi, Reda, Lauterbach, Nguyen, Solanki, J. Ishihara, Hubbell.
Analysis and interpretation of data. Yuba, Kageyama, Swartz, J. Ishihara, Hubbell.

REFERENCES

1. Firestein GS. Evolving concepts of rheumatoid arthritis [review]. Nature 2003;423:356–61.
2. McInnes IB, Schett G. The pathogenesis of rheumatoid arthritis. N Engl J Med 2011;365:2205–19.
3. Guon Q, Wang Y, Xu D, Johannes N, Pavlos NJ, Xu J. Rheumatoid arthritis: pathological mechanisms and modern pharmacologic therapies [review]. Bone Res 2018;6:15.
4. Weinblatt ME, Keystone EC, Furst DE, Moreland LW, Weisman MH, Birbara CA, et al. Adalimumab, a fully human anti–tumor necrosis factor α monoclonal antibody, for the treatment of rheumatoid arthritis in patients taking concomitant methotrexate: the ARMADA trial. Arthritis Rheum 2003;48:35–45.
5. Couper KN, Blount DG, Riley EM. IL-10: the master regulator of immunity to infection. J Immunol 2008;180:5771–7.
6. Asadullah K, Sterry W, Volk HD. Interleukin-10 therapy: review of a new approach. Pharmacol Rev 2003;55:241–69.
7. Ouyang W, O'Garra A. IL-10 family cytokines IL-10 and IL-22: from basic science to clinical translation. Immunity 2019;50:871–91.
8. Saxena A, Khosraviani S, Noel S, Mohan D, Donner T, Hamad AR. Interleukin-10 paradox: a potent immunoregulatory cytokine that has been difficult to harness for immunotherapy. Cytokine 2015;74:27–34.
9. Alvarez HM, So OY, Hsieh S, Shinsky-Bjorde N, Ma H, Song Y, et al. Effects of PEGylation and immune complex formation on the pharmacokinetics and biodistribution of recombinant interleukin 10 in mice. Drug Metab Dispos 2012;40:360–73.
10. Schwager K, Kaspar M, Bootz F, Marcolongo R, Paresce E, Neri D, et al. Preclinical characterization of DEKAVIL (F8-IL10), a novel clinical-stage immunocytokine which inhibits the progression of collagen-induced arthritis. Arthritis Res Ther 2009;11:R142.
11. Doll F, Schwager K, Hemmerle T, Neri D. Murine analogues of etanercept and of F8-IL10 inhibit the progression of collagen-induced arthritis in the mouse. Arthritis Res Ther 2013;15:R138.
12. Bruijnen ST, Chandrupatla DM, Giovanonni L, Neri D, Vugts DJ, Huisman MC, et al. F8-IL10: a new potential antirheumatic drug evaluated by a PET-guided translational approach. Mol Pharm 2019;16:273–81.
13. Ruffell B, Strachan DC, Chan V, Rosenbusch A, Ho CM, Pryer N, et al. Macrophage IL10 blocks $CD8^+$ T cell-dependent responses to chemotherapy by suppressing IL-12 expression in intratumoral dendritic cells. Cancer Cell 2014;26:623–37.
14. Huber S, Gagliani N, Esplugues E, O'Connor W Jr, Huber FJ, Shaudhry A, et al. Th17 cells express interleukin-10 receptor and are controlled by $Foxp3^-$ and $Foxp3^+$ regulatory $CD4^+$ T cells in an interleukin-10-dependent manner. Immunity 2011;34:554–65.
15. Mittal SK, Cho KJ, Ishido S, Roche PA. Interleukin 10 (IL-10)-mediated immunosuppression: MARCH-I induction regulates antigen presentation by macrophages but not dendritic cells. J Biol Chem 2015;290:27158–67.
16. Khachigian LM, Collagen antibody-induced arthritis. Nat Protoc 2006; 1:251216.
17. Miyasaka M, Tanaka T. Lymphocyte trafficking across high endothelial venules: dogmas and enigmas [review]. Nat Rev Immunol 2004; 4:360–70.
18. Pyzik M, Rath T, Kuo TT, Win S, Baker K, Hubbard JJ, et al. Hepatic FcRn regulates albumin homeostasis and susceptibility to liver injury. Proc Natl Acad Sci U S A 2017;114:E2862–71.
19. Pyzik M, Sand KM, Hubbard JJ, Andersen JT, Sandlie I, Blumbert RS. The neonatal Fc receptor (FcRn): a misnomer? [review]. Front Immunol 2019;10:1540.
20. Kotake S, Yago T, Kobashigawa T, Nanke Y. The plasticity of Th17 cells in the pathogenesis of rheumatoid arthritis. J Clin Med 2017;6:E67.
21. Van Hamburg JP, Tas SW. Molecular mechanisms underpinning T helper 17 cell heterogeneity and functions in rheumatoid arthritis. J Autoimmun 2018;87:69–81.
22. Chiang YC, Kuo LN, Yen YH, Tang CH, Chen HY. Infection risk in patients with rheumatoid arthritis treated with etanercept or adalimumab. Comput Methods Programs Biomed 2014;116:319–27.
23. Downey C. Serious infection during etanercept, infliximab and adalimumab therapy for rheumatoid arthritis: a literature review. Int J Rheum Dis 2016;19:536–50.
24. Reid JD, Bressler B, English J. A case of adalimumab-induced pneumonitis in a 45-year-old man with Crohn's disease. Can Respir J 2011;18:262–4.
25. Zalevsky J, Chamberlain AK, Horton HM, Karki S, Leung IW, Sproule TJ, et al. Enhanced antibody half-life improves in vivo activity. Nat Biotechnol 2010;28:157–9.
26. Cludts I, Spinelli FR, Morello F, Hockley J, Valesini G, Wadhwa M. Anti-therapeutic antibodies and their clinical impact in patients treated with the TNF antagonist adalimumab. Cytokine 2017;96:16–23.
27. Wang X, Wong K, Ouyang W, Rutz S. Targeting IL-10 family cytokines for the treatment of human diseases. Cold Spring Harb Perspect Biol 2019;11:a028548.
28. Liu H, Moynihan KD, Zhen Y, Szeto GL, Li AV, Huang B, et al. Structure-based programming of lymph-node targeting in molecular vaccines. Nature 2017;507:519–22.
29. Wang P, Zhao P, Dong S, Xu T, He X, Chen M, et al. An albumin-binding polypeptide both targets cytotoxic T lymphocyte vaccines to lymph nodes and boosts vaccine presentation by dendritic cells. Theranostics 2018;8:223–36.
30. Zhu G, Lynn GM, Jacobson O, Chen K, Liu Y, Zhang H, et al. Albumin/vaccine nanocomplexes that assemble in vivo for combination cancer immunotherapy. Nat Commun 2017;8:1954.
31. Vandoorne K, Addadi Y, Neeman M. Visualizing vascular permeability and lymphatic drainage using labeled serum albumin. Angiogenesis 2010;13:75–85.
32. Yao Z, Dai W, Perry J, Brechbiel MW, Sung C. Effect of albumin fusion on the biodistribution of interleukin-2. Cancer Immunol Immunother 2004;53:404–10.
33. Li J, Hsu HC, Mountz JD. The dynamic duo-inflammatory M1 macrophages and Th17 cells in rheumatic diseases. J Orthop Rheumatol 2013;1:4.
34. Guo B. IL-10 modulates Th17 pathogenicity during autoimmune diseases. J Clin Cell Immunol 2016;7:400.
35. Degboé Y, Rauwel B, Baron M, Boyer JF, Ruyssen-Witrand A, Constantin A, et al. Polarization of rheumatoid macrophages by TNF targeting through an IL-10/STAT3 mechanism. Front Immunol 2019;10:3.
36. Avci AB, Feist E, Burmester GR. Tagering GM-CSF in rheumatoid arthritis. Clin Exp Rheumatol 2016;34:S39–44.
37. Schwager S, Detmar M. Inflammation and lymphatic function [review]. Front Immunol 2019;10:308.

Arthritis & Rheumatology
Vol. 73, No. 5, May 2021, pp 779–788
DOI 10.1002/art.41580

American College of Rheumatology
Empowering Rheumatology Professionals

Venous Thromboembolism Risk With JAK Inhibitors: A Meta-Analysis

Mark Yates, Amanda Mootoo, Maryam Adas, Katie Bechman, Sanketh Rampes, Vishit Patel, Sumera Qureshi, Andrew P. Cope, Sam Norton, and James B. Galloway

Objective. JAK inhibitor therapies are effective treatment options for immune-mediated inflammatory diseases (IMIDs), but their use has been limited by venous thromboembolism (VTE) risk warnings from licensing authorities. We undertook this study to evaluate the VTE risk of JAK inhibitors in patients with IMIDs.

Methods. Systematic searches of Medline and Embase databases from inception to September 30, 2020 were conducted. Phase II and phase III double-blind, randomized controlled trials (RCTs) of JAK inhibitors at licensed doses were included in our analyses. RCTs with no placebo arm, long-term extension studies, post hoc analyses, and pooled analyses were excluded. Three researchers independently extracted data on exposure to JAK inhibitors or placebo and VTE events (e.g., pulmonary embolism [PE] and deep vein thrombosis [DVT]) and assessed study quality.

Results. A total of 42 studies were included, from an initial search that yielded 619. There were 6,542 JAK inhibitor patient exposure years (PEYs) compared to 1,578 placebo PEYs. There were 15 VTE events in the JAK inhibitor group and 4 in the placebo group. The pooled incidence rate ratios (IRRs) of VTE, PE, and DVT in patients receiving JAK inhibitors were 0.68 (95% confidence interval [95% CI] 0.36–1.29), 0.44 (95% CI 0.28–0.70), and 0.59 (95% CI 0.31–1.15), respectively.

Conclusion. This meta-analysis of RCT data defines the VTE risk with JAK inhibitors as a class in IMID patients. The pooled IRRs do not provide evidence that support the current warnings of VTE risk for JAK inhibitors. These findings will aid continued development of clinical guidelines for the use of JAK inhibitors in IMIDs.

INTRODUCTION

The introduction of biologic therapies in the early 2000s led to a phase change in the management of immune-mediated inflammatory diseases (IMIDs) including inflammatory arthropathies, psoriasis, and inflammatory bowel disease. More recently, small molecule inhibitors have been added to the growing list of therapeutic methods (1). The JAK/STAT pathway is a key modulator of the inflammatory response (2). To date, 4 JAK inhibitors have been licensed for the treatment of rheumatoid arthritis (RA) and/or psoriatic arthritis (PsA) in North America and/or Europe: tofacitinib (RA, PsA), baricitinib (RA), upadacitinib (RA), and filgotinib (RA). Licensing for other IMID indications will likely follow.

Concerns have been raised regarding the risk of venous thromboembolism (VTE) with JAK inhibitor therapy. In 2017, the Food and Drug Administration (FDA) added a black box warning to the Summary of Product Characteristics (SPC) for baricitinib, stating that it should be used with caution in patients at increased risk for VTE (3). This was followed by a similar warning from the FDA and the European Medicines Agency (EMA) in 2019 for tofacitinib 10 mg prescribed twice daily for the treatment of ulcerative colitis (UC). It was recommended that clinicians avoid prescribing these medications to patients at a higher risk for VTE (4,5). These warnings were based upon a small number of randomized controlled trials (RCTs). Given the rarity of VTEs, individual trials had insufficient power to confirm or exclude a significant difference in risk (6).

Supported in part by the British Society for Rheumatology, Versus Arthritis.

Mark Yates, PhD, Amanda Mootoo, MBBS, Maryam Adas, MBBS, Katie Bechman, PhD, Sanketh Rampes, MA, Vishit Patel, MSc, Sumera Qureshi, BM, BCh, Andrew P. Cope, PhD, Sam Norton, PhD, James B. Galloway, PhD: King's College London, London, UK.

Drs. Yates and Mootoo contributed equally to this work.

Dr. Yates has received honoraria from UCB and AbbVie (less than $10,000). Dr. Galloway has received honoraria from AbbVie, Celgene, Gilead, Janssen, Eli Lilly, Novartis, Pfizer, Roche, and UCB (less than $10,000 each). Drs. Cope and Dr. Galloway are co–principal investigators on a COVID-19 interventional study (TACTIC-R) that is funded in part by Eli Lilly, through a grant awarded to the University of Cambridge. No other disclosures relevant to this article were reported.

Address correspondence to Mark Yates, PhD, Centre for Rheumatic Diseases, King's College London, Weston Education Centre, Cutcombe Road, London SE5 9RJ, UK. Email: mark.yates@kcl.ac.uk.

Submitted for publication August 12, 2020; accepted in revised form November 23, 2020.

Previous studies have demonstrated an increased risk of VTE events in patients with an IMID diagnosis (7), with a biologic explanation that the inflammatory burden creates a prothrombotic state. Consequently, controlling inflammation with effective IMID treatment could reduce VTE risk. JAK inhibitors may be a special case, as this class of therapy modulates the JAK2 receptor, which is involved in myelopoiesis and the production of platelets (8). Transient increases in platelet counts have been observed following JAK inhibitor therapy initiation, although these were not predictive of VTE (9). There remains considerable uncertainty about any link between JAK inhibitor therapy and VTE events.

Clarification of VTE risk with JAK inhibitor therapy is crucial to informing physicians who are considering this strategy, given that these drugs offer to patients clinically meaningful improvements in disease activity. Accordingly, we set out to evaluate the VTE risk with JAK inhibitors in patients with IMIDs by undertaking a meta-analysis based on pooled findings from published RCTs.

METHODS

Databases and search strategy. We performed a systematic search of studies in humans up to November 30, 2019, with no specified start date. The following search was performed using the Medline and Embase databases: "tofacitinib or baricitinib or upadacitinib or filgotinib" and "rheumatoid or psoriatic arthritis or psoriasis or ankylosing spondylitis or axial spondyloarthritis or ulcerative colitis or crohns." The search was limited by the following constraints: RCTs, English language, and human study participants. The initial search was conducted by 2 researchers (MY and AM) with verification from a third (MA). The study was registered with an international prospective register of systematic reviews (Prospero 2020 CRD42020161645).

Eligibility criteria. Eligible studies were original reports of phase II and phase III RCTs of JAK inhibitor therapy, with a placebo comparator arm. Studies were excluded if they were not double-blind. Long-term extension (LTE) studies, post hoc analyses, and pooled analyses were excluded after checking to ensure that the original reports had been included in the search. Conference abstracts, case reports, letters to the editor, review articles, case–control studies, and cohort studies were all excluded. Doses of JAK inhibitors (tofacitinib 5 mg and 10 mg twice daily, baricitinib 2 mg and 4 mg once daily, upadacitinib 15 mg once daily) that were licensed when the literature search was performed (September 2020) were considered. Doses of filgotinib (200 mg and 100 mg) were also included, having just received marketing authorization from the European Commission for the treatment of RA.

Study selection. Two researchers independently screened study titles and abstracts and selected eligible studies. Disagreement was discussed, with a third researcher resolving any differences over a study's inclusion. Data were extracted from eligible studies into a data collection table by 3 researchers. Studies that were subsequently found to be ineligible after a full transcript review were excluded. National clinical trial numbers of included studies were compared to ensure that there was no duplication.

Data extraction. The following information was extracted from each study: citation details, author list, study design, underlying condition, study duration, study location, number of patients, inclusion/exclusion criteria, drug doses, patient characteristics, adverse events (AEs), and serious AEs (SAEs). Deep vein thrombosis (DVT) and pulmonary embolism (PE) were considered VTE events. Details about these events were extracted from full-text articles, supplementary materials, and appendices. To ensure that all VTE events were identified, an additional review of the tabular summary of original RCT data in the ClinicalTrials.gov database was performed. All data included in the meta-analysis were checked by 3 independent researchers.

Assessment of bias. Each study undergoing data extraction was assessed for quality using the Cochrane risk-of-bias tool (10).

Statistical analysis. Analyses were performed using Stata 16 software. Patient exposure years (PEYs) were calculated using sample size and study duration for the treatment and placebo groups, assuming a per-protocol model. Per-protocol analyses are generally considered more appropriate for safety outcomes.

Crude incidence rates of PE, DVT, and overall VTE events were calculated for each study. Overall VTE event numbers were calculated as a sum of PE and DVT events. In RCTs, reported PEs are coded as SAEs; therefore, complete reporting was assumed. DVTs may be coded as an AE or SAE. Most RCTs have an AE reporting threshold. This can lead to VTE events not being reported. For example, in an RCT with an AE reporting threshold of 5%, where 2 DVT events occurred in 100 patients receiving a study drug, these would not be included in the trial findings on ClinicalTrials.gov.

For the primary analyses of VTE and DVT event rates, only studies with an explicit publication of VTE/DVT event rates were included. To address the reporting threshold issue, the impact of DVT reporting uncertainty was explored with 2 sensitivity analyses. In the first analysis, it was assumed that 0 DVT events had occurred when the number of events was not explicitly reported due to falling below the threshold. In the second analysis, it was assumed that the maximum number of DVTs could have occurred and remained under the reporting threshold in the treatment arm only. A further sensitivity analysis was conducted to identify differences between diagnostic groups.

The pooled relative risk of VTE with JAK inhibitor therapy versus placebo was estimated with incidence rate ratios (IRRs) and 95% confidence intervals (95% CIs), using the Mantel-Haenszel

random-effects method for binary data. Estimates are graphically displayed in forest plots.

RESULTS

Study screening. The electronic database search identified 619 articles. Following a title and abstract review, 513 articles were excluded for not meeting eligibility criteria. A total of 106 articles underwent a full-text review. This led to a further 64 articles being excluded for not meeting eligibility criteria, leaving a total of 42 eligible articles. The systematic literature review flow diagram is detailed in Figure 1.

Study characteristics. A total of 42 studies were included in this meta-analysis, of which 20 were phase II and 20 were phase III RCTs. Two studies were described as phase II/III. Articles were published from 2009 to 2020, with 12,207 patients receiving JAK inhibitor therapy and 5,062 receiving a placebo. Twenty-nine studies were RCTs of patients with inflammatory arthropathies (RA, PsA, ankylosing spondylitis), 6 focused on inflammatory bowel disease (UC, Crohn's disease), and 7 focused on psoriasis. Of the 42 studies, 31 (74%) included patients with previous or current exposure to other immunosuppressive therapies. Details about all included RCTs can be found in Table 1. AE reporting thresholds ranged from 0% to 5%.

Risk of bias. Risk of bias for this sample of studies was typically low. Forty studies (95%) were randomized and double-blind (with regard to participants and assessors), with 33 studies (79%) considered to have an overall low risk of bias. Further details on individual study bias assessment can be found in Supplementary Table 1 (available on the *Arthritis & Rheumatology* website at http://onlinelibrary.wiley.com/doi/10.1002/art.41580/abstract).

Meta-analysis. A total of 15 VTE events (10 PEs, 5 DVTs) were reported in patients receiving JAK inhibitor therapy over 6,542 PEYs, equivalent to a rate of 0.23 per 100 PEYs (95% CI 0.12–0.38). In comparison, we observed a rate of 4 VTE events (2 PEs, 2 DVTs) in patients receiving placebo over 1,578 PEYs, equivalent to a rate of 0.25 per 100 PEYs (95% CI 0.07–0.73).

The pooled IRRs of VTE, PE, and DVT events in patients receiving JAK inhibitors were 0.68 (95% CI 0.36–1.29), 0.44 (95%

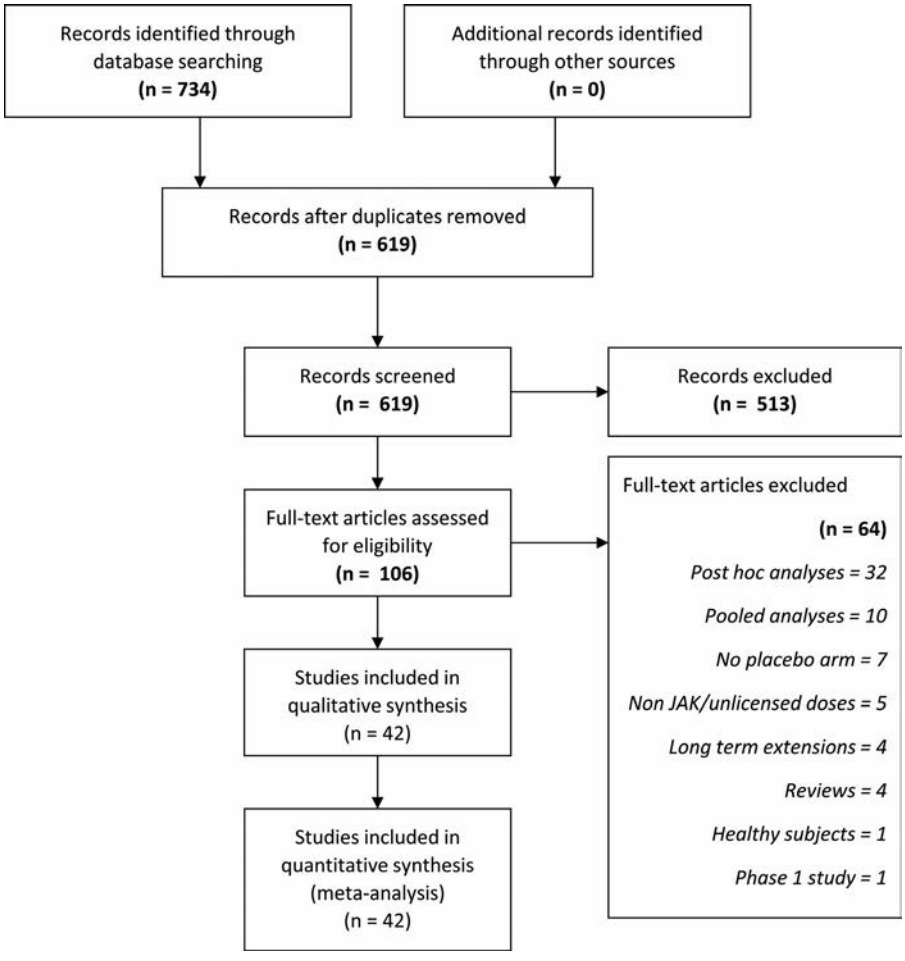

Figure 1. Flow diagram of the systematic search.

Table 1. All eligible RCTs*

Author, year, study name (ref.)	Study location	Dose included in analyses, mg	Phase of study	Disease	No. of subjects receiving JAK inhibitors	No. of subjects receiving placebo	Age, mean ± SD years
Tofacitinib							
Gladman et al, 2017, OPAL Beyond (11)	Worldwide	5, 10	III	PsA	263	131	50 ± 12
Sandborn et al, 2012 (12)	Worldwide	10	II	UC	33	48	43.2 ± 12.8†
Tanaka et al, 2015 (13)	Japan	5, 10	II	RA	105	53	52.6 ± 10.9†
Sandborn et al, 2014 (14)	Worldwide	5	II	CD	20	34	37 ± 12
Panes et al, 2017 (15)	Worldwide	5, 10	II	CD	172	92	39 ± 12
Sandborn et al, 2017, OCTAVE Induction 1 (16)	Worldwide	10	III	UC	476	122	41.3 ± 14.1†
Sandborn et al, 2017, OCTAVE Induction 2 (16)	Worldwide	10	III	UC	429	112	41.1 ± 13.5†
Bechelez et al, 2015 (17)	Worldwide	5, 10	III	Psoriasis	662	108	44 ± 12
Papp et al, 2015, OPT Pivotal 1 (18)	Worldwide	5, 10	III	Psoriasis	723	177	45 ± 13
Papp et al, 2015, OPT Pivotal 2 (18)	Worldwide	5, 10	III	Psoriasis	763	196	45 ± 13
Van Vollenhoven et al, 2012 (19)	Worldwide	5, 10	III	RA	513	108	53 ± 12
Van der Heijde et al, 2019, ORAL Scan (20)	Worldwide	5, 10	III	RA	797	160	53 ± 12
Kremer et al, 2009 (21)	Worldwide	5	II	RA	61	65	51 ± 12
Mease et al, 2017, OPAL Broaden (22)	Worldwide	5, 10	III	PsA	316	105	48 ± 12
Zhang et al, 2017 (23)	Asia	5, 10	III	Psoriasis	178	88	41 ± 12
Winthrop et al, 2017 (24)	US	5	II	RA	55	57	62 ± 8
Van der Heijde et al, 2017 (25)	Worldwide	5, 10	II	AS	104	51	42 ± 12
Burmester et al, 2013 (26)	Worldwide	5, 10	III	RA	267	132	55.0 ± 11.3
Kremer et al, 2013 (27)	Worldwide	5, 10	III	RA	633	159	52.3 ± 11.6
Papp et al, 2012 (28)	US, Canada	5	IIb	Psoriasis	147	50	44 ± 12.6†
Fleischmann et al, 2012 (29)	Worldwide	5, 10	IIb	RA	272	59	53.3 ± 12.6
Kremer et al, 2012 (30)	Worldwide	5, 10	IIb	RA	438	69	52 ± 12.8†
Fleischmann et al, 2012 (31)	Worldwide	5, 10	III	RA	488	122	51.8 ± 11.8
Tanaka et al, 2011 (32)	Japan	5, 10	II	RA	108	28	51.3 ± 10.7
Krueger et al, 2016 (33)	US	10	II	Psoriasis	9	3	45.6 ± 13.3
Baricitinib							
Keystone et al, 2015 (34)	Worldwide	2, 4	IIb	RA	203	98	51.2 ± 11.71
Taylor et al, 2017, RA-BEAM (35)	Worldwide	4	III	RA	487	488	53.3 ± 12.1
Papp et al, 2016 (36)	US, Canada, Japan	2, 4	IIb	Psoriasis	237	34	47.3 ± 13.3
Tanaka et al, 2016 (37)	Japan	2, 4	IIb	RA	96	49	53.6 ± 11.8
Genovese et al, 2016, RA-BEACON (38)	Worldwide	2, 4	III	RA	351	176	55.7 ± 11.0
Dougados et al, 2017, RA-BUILD (39)	Worldwide	2, 4	III	RA	456	228	51.8 ± 12.3

(Continued)

Table 1. *(Cont'd)*

Author, year, study name (ref.)	Study location	Dose included in analyses, mg	Phase of study	Disease	No. of subjects receiving JAK inhibitors	No. of subjects receiving placebo	Age, mean ± SD years
Upadacitinib							
Van der Heijde et al, 2019, SELECT-AXIS 1 (40)	Worldwide	15	II/III	AS	93	94	47 ± 12.8†
Fleischmann et al, 2019, SELECT-COMPARE (41)	Worldwide	15	III	RA	651	651	53.9 ± 12.07
Genovese et al, 2018, SELECT-BEYOND (42)	Worldwide	15	III	RA	329	169	57.1 ± 11.42
Burmester et al, 2018, SELECT-NEXT (43)	Worldwide	15	III	RA	440	221	55.7 ± 11.65
Sandborn et al, 2020, U-ACHIEVE (44)	Worldwide	15	IIb	UC	49	46	47 (range 22–71)
Kameda et al, 2020, SELECT-SUNRISE (45)	Japan	15	IIb/III	RA	49	49	56.0 ± 12.5
Filgotinib							
Westhovens et al, 2017, DARWIN 1 (46)	Worldwide	100, 200	IIb	RA	171	86	52 ± 1.4†
Kavanaugh et al, 2017 DARWIN 2 (47)	Worldwide	100, 200	II	RA	139	72	53 ± 1.4†
Genovese et al, 2019, FINCH 2 (48)	Worldwide	100, 200	III	RA	301	148	55 ± 11.9‡
Mease et al, 2018, EQUATOR (49)	Worldwide	200	II	PsA	65	66	49 ± 12.2
Van der Heijde et al, 2018, TORTUGA (50)	Worldwide	200	II	AS	58	58	41 ± 11.6†

* RCTs = randomized controlled trials; PsA = psoriatic arthritis; UC = ulcerative colitis; RA = rheumatoid arthritis; CD = Crohn's disease; AS = ankylosing spondylitis.
† For treatment group.
‡ For most populous region.

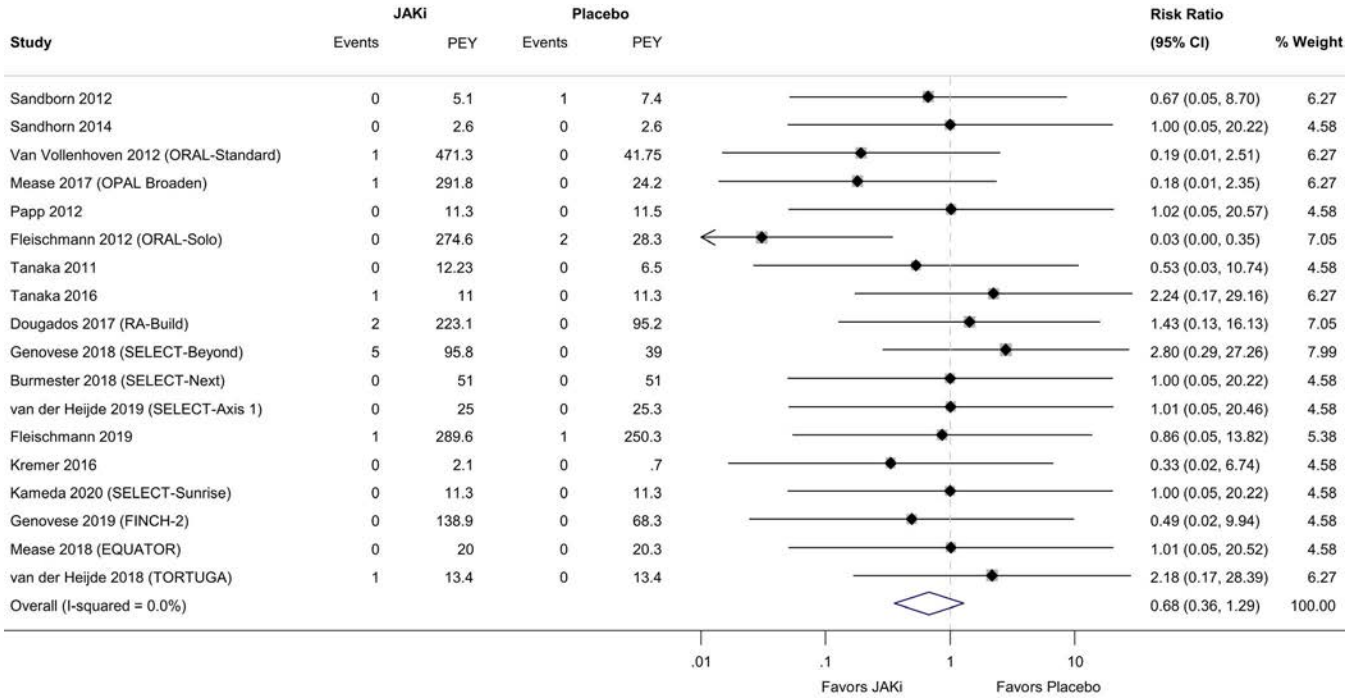

Figure 2. Forest plot of overall venous thromboembolism events. JAKi = JAK inhibitors; PEY = patient exposure years; 95% CI = 95% confidence interval. Color figure can be viewed in the online issue, which is available at http://onlinelibrary.wiley.com/doi/10.1002/art.41580/abstract.

CI 0.28–0.70), and 0.59 (95% CI 0.31–1.15), respectively. Further details about the individual studies can be found in Figures 2–4.

Sensitivity analyses explored the impact of missing data due to reporting thresholds. If it was assumed that there were 0 events for which no information on DVT was reported, the odds ratio was 0.42 (95% CI 0.26–0.65). Conversely, if it was assumed that the maximum number of DVTs occurred in the treatment arm (while remaining below the reporting threshold), the odds ratio increased to 1.34 (95% CI 0.91–1.97). Additional details are shown in Supplementary Figures 1 and 2 (on the *Arthritis & Rheumatology* website at http://onlinelibrary.wiley.com/doi/10.1002/art.41580/abstract). Repeat analyses stratified by diagnosis did not identify any differences from the overall analysis.

DISCUSSION

This meta-analysis defines the risk of VTE with JAK inhibitor therapy in IMID patients across a large number of RCTs. Overall, the pooled-effect estimates confirm that VTE risk is unlikely to be substantially increased in those receiving JAK inhibitors compared to those receiving placebo. However, given the low event rates, and thus less precise data, a true effect involving a small increase in risk cannot be ruled out, nor can small-to-large protective effects.

Currently, a product warning is in place for JAK inhibitors regarding VTE risk (3–5). For baricitinib, this was based on regulatory review of RCTs and an LTE study, which identified an imbalance in the number of events in JAK inhibitor therapy arms (51), whereas for tofacitinib, it was based upon interim findings from an as-yet-unpublished LTE (52). Our findings do not confirm this association.

The likely explanation for the discrepancy in findings is the exclusion of LTEs from our meta-analysis and the pooling of results across different JAK inhibitor therapies. We intentionally excluded LTE studies as they are open-label trials with no placebo arm. This widens the discrepancy between placebo and treatment arm PEYs, which is relevant due to the rarity of VTE as an outcome. Even with LTE study data excluded, our meta-analysis provided 4,780 more PEYs in treatment arms compared to placebo. Adding LTE study data amplifies this difference substantially.

It is important to consider the context within which the excess VTE risk has been observed. The mechanism by which JAK inhibitors could lead to an altered VTE risk is difficult to reconcile biologically. IMIDs confer an increased risk of VTE, a relationship that is associated with disease severity (53). Controlling the inflammatory burden should theoretically offset any excess VTE risk attributable to the disease. In polycythemia rubra vera, a condition associated with significantly increased rates of VTE, ruxolitinib (a JAK2 inhibitor) was associated with a reduced VTE rate, according to a recent meta-analysis (54).

However, it may be that there are 2 effects present, operating in different directions. The JAK signaling pathways encompass a series of homodimer and heterodimer transmembrane receptors that have a broad range of activating ligands and downstream

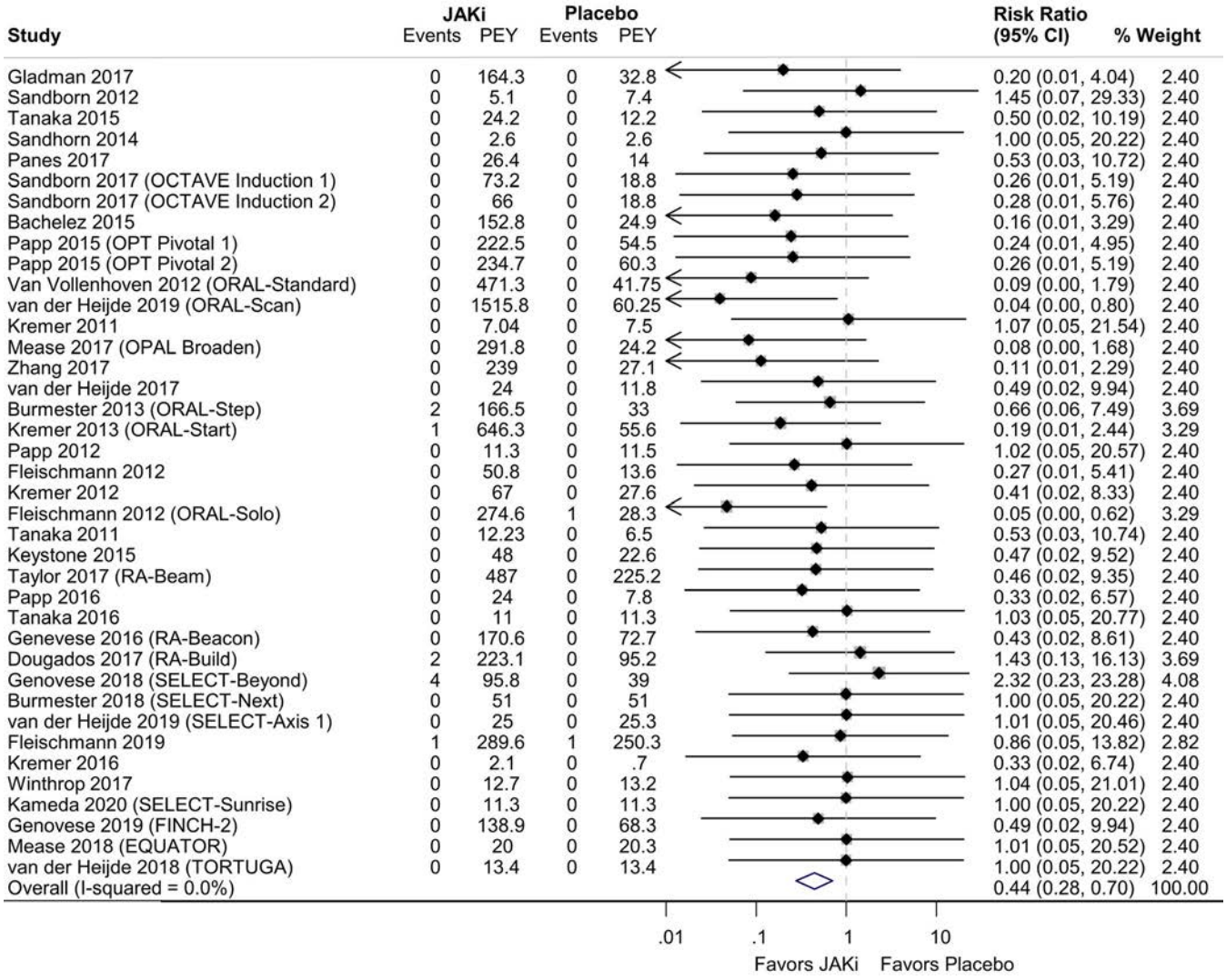

Figure 3. Forest plot of pulmonary embolism events. See Figure 2 for definitions. Color figure can be viewed in the online issue, which is available at http://onlinelibrary.wiley.com/doi/10.1002/art.41580/abstract.

signaling effects. From a hematopoiesis perspective, blocking JAK2 in particular could be expected to suppress platelet growth by the inhibition of thrombopoietin signaling (55). Paradoxically, platelet counts transiently increase in the first weeks of baricitinib treatment (9).

A further consideration is that we are assuming that the mechanistic explanation for a link between JAK inhibitor therapy and VTE risk would be mediated by the JAK/STAT signaling pathway. In the era of biologic therapies, where target specificity is perfect, this would be a reasonable assumption. In contrast, the modulation of the JAK pathway uses small-molecule inhibitors, and it is possible that there are off-target effects on other signaling pathways that are as yet unknown.

An important additional study that examines the long-term safety of tofacitinib in patients at increased risk for cardiovascular disease is ongoing. Interim analysis of the data resulted in an FDA and EMA advisory warning regarding the use of tofacitinib at a higher dose (10 mg twice daily) because of an increased risk of infection and VTE (52). Caveats about this research include that there is selection bias toward high-risk patients, and the dose tested is greater than the licensed dose for some indications, including RA. This study is powered based on an event-driven sample size (i.e., the study will terminate only after a predetermined number of people have experienced the primary end point, as opposed to studies that have fixed sample sizes for a predefined follow-up period). When the full study is published, it will provide important additional information pertaining to the risk of VTE with JAK inhibitor therapy. Future registry data will also be critical.

The present study is the most extensive meta-analysis, to date, of VTE risk with JAK inhibitor therapy, spanning licensed doses across multiple IMIDs. A further strength of this work was the ability to identify granular data on both AEs and SAEs from all studies in ClinicalTrials.gov, providing confidence in event ascertainment.

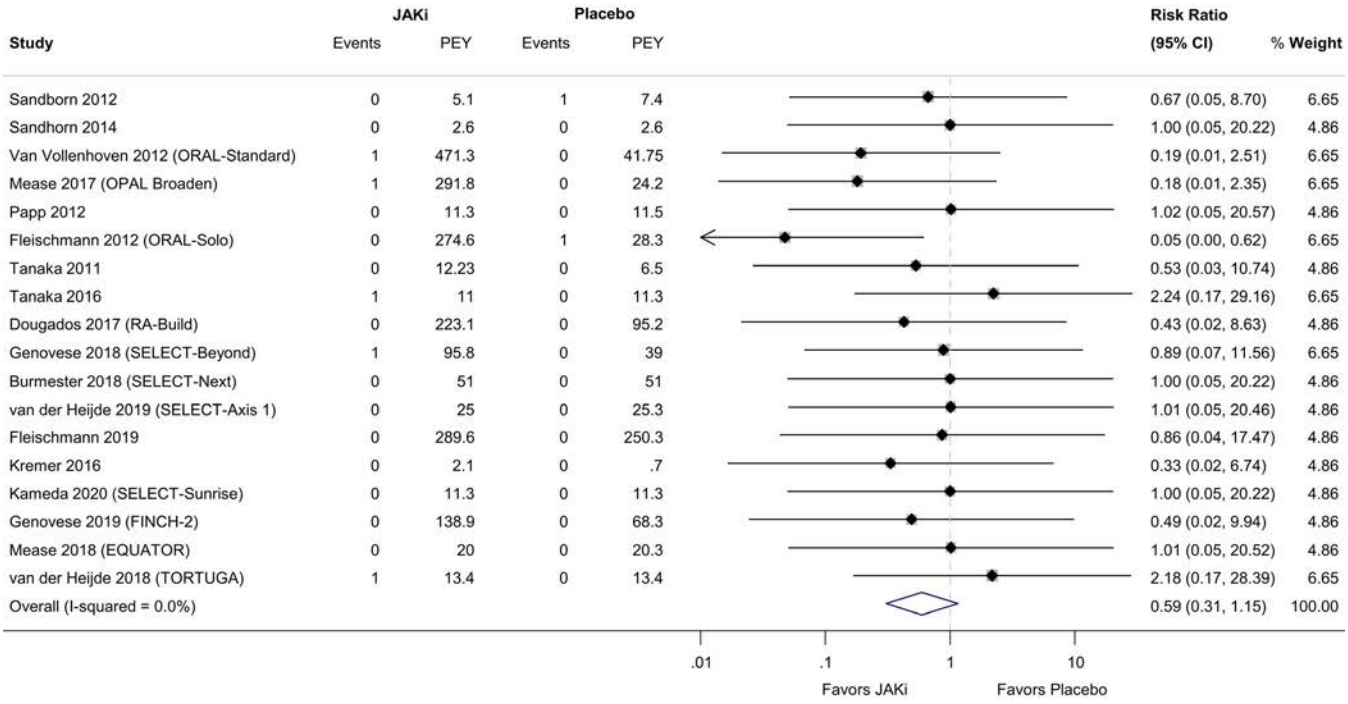

Figure 4. Forest plot of deep vein thrombosis events. See Figure 2 for definitions. Color figure can be viewed in the online issue, which is available at http://onlinelibrary.wiley.com/doi/10.1002/art.41580/abstract.

There were limitations to our study, as well. The studies included in this meta-analysis are RCTs with tight inclusion/exclusion criteria that limit the external validity of findings. Patients at the highest risk for VTE, such as older patients and those with multiple morbidities, may be underrepresented in the RCTs, so the extrapolation of findings among these populations must be done cautiously. This could explain the lower rate of VTEs in the placebo group (0.25 per 100 PEYs) compared to that reported in IMID observational studies (0.35 per 100 PEYs) (56).

Our analyses used aggregate data, and it was not possible to adopt a full survival model approach using individual patient–level data and time to event analyses, which would have added power and potentially allowed for additional subanalyses exploring differences between drugs and doses.

Reports from a number of studies did not explicitly show event rates for DVT. We modeled this in sensitivity analyses, by comparing the 0-event rate and the maximum-event rate that would have remained under the reporting threshold on ClinicalTrials.gov. The former offers the most conservative estimate of risk, suggesting that JAK inhibitor therapy reduces DVT risk by >60%, and the latter offers the most punitive estimate, suggesting a 30% increase in DVT risk with JAK inhibitors. These estimates are extreme, with the true value likely lying between the two. The width between these estimates (IRR 0.42 and IRR 1.34, respectively) highlights the importance of RCTs publishing full data sets with no reporting threshold for AEs. It is important to acknowledge uncertainty, particularly when considering earlier RCTs published prior to the scientific community's awareness of a possible link between JAK inhibitors and VTE.

The RCTs included have relatively short durations of follow-up, with a notably shorter exposure window for patients receiving placebo compared to those receiving JAK inhibitors, as illustrated by the total PEYs: 1,578 versus 6,542. In pharmacovigilance studies, AEs and SAEs typically follow an exponential decay distribution, with event frequencies higher shortly after drug initiation. Occasionally, events do not follow this pattern and increase in frequency with cumulative drug exposure. As we do not know the time-varying nature of VTE risk, it is possible—if there is a cumulative effect with JAK inhibitor therapy—that we would not have observed this.

Our analyses were unable to include consideration for concomitant medication, such as glucocorticoids. There is an established risk between glucocorticoid therapy and VTE risk (57), and it is possible that there are associations between glucocorticoids and other AEs, as has been described with infections (58). We did not have access to patient-level data (including markers of disease activity and individual treatment modifications) and could not adjust for these in our analyses. It is plausible that patients receiving placebo had higher disease activity and ongoing active inflammation, increasing their VTE risk compared to patients receiving JAK inhibitors.

The data presented here do not provide evidence in support of the current warnings of VTE risk for typical trial patients offered JAK inhibitors. These findings will aid in the continued development of clinical guidelines for the use of JAK inhibitor therapies in IMIDs. VTE represents only one aspect of the safety profile of this class of

therapy, and these results should be considered in the wider context of the risk and benefit of JAK inhibitors in different therapeutic areas.

AUTHOR CONTRIBUTIONS

All authors were involved in drafting the article or revising it critically for important intellectual content, and all authors approved the final version to be published. Dr. Yates had full access to all of the data in the study and takes responsibility for the integrity of the data and the accuracy of the data analysis.

Study conception and design. Yates, Mootoo, Cope, Norton, Galloway.
Acquisition of data. Yates, Mootoo, Adas, Rampes, Patel, Qureshi.
Analysis and interpretation of data. Yates, Adas, Bechman, Cope, Norton, Galloway.

REFERENCES

1. Bechman K, Yates M, Galloway JB. The new entries in the therapeutic armamentarium: the small molecule JAK inhibitors [review]. Pharmacol Res 2019;147:104392.
2. Renauld JC. Class II cytokine receptors and their ligands: key antiviral and inflammatory modulators [review]. Nat Rev Immunol 2003;3:667–76.
3. Olumiant (baricitinib) prescribing information. Indianapolis (IN): Lilly; 2018. URL: https://www.accessdata.fda.gov/drugsatfda_docs/label/2018/207924s000lbl.pdf.
4. US Food and Drug Administration. FDA approves boxed warning about increased risk of blood clots and death with higher dose of arthritis and ulcerative colitis medicine tofacitinib (Xeljanz, Xeljanz XR). August 2019. URL: https://www.fda.gov/drugs/drug-safety-and-availability/fda-approves-boxed-warning-about-increased-risk-blood-clots-and-death-higher-dose-arthritis-and.
5. European Medicines Agency. EMA confirms Xeljanz to be used with caution in patients at high risk of blood clots. November 2019. URL: https://www.ema.europa.eu/en/news/ema-confirms-xeljanz-be-used-caution-patients-high-risk-blood-clots#:~:text=EMA%20has%20concluded%20that%20Xeljanz,high%20risk%20of%20blood%20clots.
6. Scott IC, Hider SL, Scott DL. Thromboembolism with janus kinase (JAK) inhibitors for rheumatoid arthritis: how real is the risk? Drug Saf 2018;41:645–53.
7. Zöller B, Li X, Sundquist J, Sundquist K. Autoimmune diseases and venous thromboembolism: a review of the literature. Am J Cardiovasc Dis 2012;2:171–83.
8. Tang Y, Liu W, Wang W, Fidler T, Woods B, Levine RL, et al. Inhibition of JAK2 suppresses myelopoiesis and atherosclerosis in Apoe$^{-/-}$ mice. Cardiovasc Drugs Ther 2020;34:145–52.
9. Kremer J, Huizinga T, Chen L, Saifan C, Issa M, Witt S, et al. FRI0090 Analysis of neutrophils, lymphocytes, and platelets in pooled phase 2 and phase 3 studies of baricitinib for rheumatoid arthritis. Ann Rheum Dis 2017;76 Suppl:512.
10. Higgins JP, Savovic J, Page MJ, Sterne JA, on behalf of the RoB2 Development Group. Revised Cochrane risk-of-bias tool for randomized trials (RoB 2). URL: https://sites.google.com/site/riskofbiastool/welcome/rob-2-0-tool/current-version-of-rob-2. August 2019.
11. Gladman D, Rigby W, Azevedo VF, Behrens F, Blanco R, Kaszuba A, et al. Tofacitinib for psoriatic arthritis in patients with an inadequate response to TNF inhibitors. N Engl J Med 2017;377:1525–36.
12. Sandborn WJ, Ghosh S, Panes J, Vranic I, Su C, Rousell S, et al. Tofacitinib, an oral Janus kinase inhibitor, in active ulcerative colitis. N Engl J Med 2012;367:616–24.
13. Tanaka Y, Takeuchi T, Yamanaka H, Nakamura H, Toyoizumi S, Zwillich S. Efficacy and safety of tofacitinib as monotherapy in Japanese patients with active rheumatoid arthritis: a 12-week, randomized, phase 2 study. Mod Rheumatol 2015;25:514–21.
14. Sandborn WJ, Ghosh S, Panes J, Vranic I, Wang W, Niezychowski W, et al. A phase 2 study of tofacitinib, an oral Janus kinase inhibitor, in patients with Crohn's disease. Clin Gastroenterol Hepatol 2014;12:1485–93.
15. Panés J, Sandborn WJ, Schreiber S, Sands BE, Vermeire S, D'Haens G, et al. Tofacitinib for induction and maintenance therapy of Crohn's disease: results of two phase IIb randomised placebo-controlled trials. Gut 2017;66:1049–59.
16. Sandborn WJ, Su C, Sands BE, D'Haens GR, Vermeire S, Schreiber S, et al. Tofacitinib as induction and maintenance therapy for ulcerative colitis. N Engl J Med 2017;376:1723–36.
17. Bachelez H, van de Kerkhof PC, Strohal R, Kubanov A, Valenzuela F, Lee JH, et al. Tofacitinib versus etanercept or placebo in moderate-to-severe chronic plaque psoriasis: a phase 3 randomised non-inferiority trial. Lancet 2015;386:552–61.
18. Papp KA, Menter MA, Abe M, Elewski B, Feldman SR, Gottlieb AB, et al. Tofacitinib, an oral Janus kinase inhibitor, for the treatment of chronic plaque psoriasis: results from two randomized, placebo-controlled, phase III trials. Br J Dermatol 2015;173:949–61.
19. Van Vollenhoven RF, Fleischmann R, Cohen S, Lee EB, Meijide JA, Wagner S, et al. Tofacitinib or adalimumab versus placebo in rheumatoid arthritis. N Engl J Med 2012;367:508–19.
20. Van der Heijde D, Strand V, Tanaka Y, Keystone E, Kremer J, Zerbini CA, et al. Tofacitinib in combination with methotrexate in patients with rheumatoid arthritis: clinical efficacy, radiographic, and safety outcomes from a twenty-four–month, phase III study. Arthritis Rheumatol 2019;71:878–91.
21. Kremer JM, Bloom BJ, Breedveld FC, Coombs JH, Fletcher MP, Gruben D, et al. The safety and efficacy of a JAK inhibitor in patients with active rheumatoid arthritis: results of a double-blind, placebo-controlled phase IIa trial of three dosage levels of CP-690,550 versus placebo [published erratum appears in Arthritis Rheum 2012;64:1487]. Arthritis Rheum 2009;60:1895–905.
22. Mease P, Hall S, FitzGerald O, van der Heijde D, Merola JF, Avila-Zapata F, et al. Tofacitinib or adalimumab versus placebo for psoriatic arthritis. N Engl J Med 2017;377:1537–50.
23. Zhang J, Tsai TF, Lee MG, Zheng M, Wang G, Jin H, et al. The efficacy and safety of tofacitinib in Asian patients with moderate to severe chronic plaque psoriasis: a phase 3, randomized, double-blind, placebo-controlled study. J Dermatol Sci 2017;88:36–45.
24. Winthrop KL, Wouters AG, Choy EH, Soma K, Hodge JA, Nduaka CI, et al. The safety and immunogenicity of live zoster vaccination in patients with rheumatoid arthritis before starting tofacitinib: a randomized phase II trial. Arthritis Rheumatol 2017;69:1969–77.
25. Van der Heijde D, Deodhar A, Wei JC, Drescher E, Fleishaker D, Hendrikx T, et al. Tofacitinib in patients with ankylosing spondylitis: a phase II, 16-week, randomised, placebo-controlled, dose-ranging study. Ann Rheum Dis 2017;76:1340–7.
26. Burmester GR, Blanco R, Charles-Schoeman C, Wollenhaupt J, Zerbini C, Benda B, et al. Tofacitinib (CP-690,550) in combination with methotrexate in patients with active rheumatoid arthritis with an inadequate response to tumour necrosis factor inhibitors: a randomised phase 3 trial. Lancet 2013;381:451–60.
27. Kremer J, Li ZG, Hall S, Fleischmann R, Genovese M, Martin-Mola E, et al. Tofacitinib in combination with nonbiologic disease-modifying antirheumatic drugs in patients with active rheumatoid arthritis: a randomized trial. Ann Intern Med 2013;159:253–61.
28. Papp KA, Menter A, Strober B, Langley RG, Buonanno M, Wolk R, et al. Efficacy and safety of tofacitinib, an oral Janus kinase inhibitor, in the treatment of psoriasis: a phase 2b randomized placebo-controlled dose-ranging study. Br J Dermatol 2012;167:668–77.
29. Fleischmann R, Cutolo M, Genovese MC, Lee EB, Kanik KS, Sadis S, et al. Phase IIb dose-ranging study of the oral JAK inhibitor tofacitinib

(CP-690,550) or adalimumab monotherapy versus placebo in patients with active rheumatoid arthritis with an inadequate response to disease-modifying antirheumatic drugs. Arthritis Rheum 2012;64:617–29.
30. Kremer JM, Cohen S, Wilkinson BE, Connell CA, French JL, Gomez-Reino J, et al. A phase IIb dose-ranging study of the oral JAK inhibitor tofacitinib (CP-690,550) versus placebo in combination with background methotrexate in patients with active rheumatoid arthritis and an inadequate response to methotrexate alone. Arthritis Rheum 2012;64:970–81.
31. Fleischmann R, Kremer J, Cush J, Schulze-Koops H, Connell CA, Bradley JD, et al. Placebo-controlled trial of tofacitinib monotherapy in rheumatoid arthritis. N Engl J Med 2012;367:495–507.
32. Tanaka Y, Suzuki M, Nakamura H, Toyoizumi S, Zwillich SH, Tofacitinib Study Investigators. Phase II study of tofacitinib (CP-690,550) combined with methotrexate in patients with rheumatoid arthritis and an inadequate response to methotrexate. Arthritis Care Res (Hoboken) 2011;63:1150–8.
33. Krueger J, Clark JD, Suárez-Fariñas M, Fuentes-Duculan J, Cueto I, Wang CQ, et al. Tofacitinib attenuates pathologic immune pathways in patients with psoriasis: a randomized phase 2 study. J Allergy Clin Immunol 2016;137:1079–90.
34. Keystone EC, Taylor PC, Drescher E, Schlichting DE, Beattie SD, Berclaz PY, et al. Safety and efficacy of baricitinib at 24 weeks in patients with rheumatoid arthritis who have had an inadequate response to methotrexate. Ann Rheum Dis 2015;74:333–40.
35. Taylor PC, Keystone EC, van der Heijde D, Weinblatt ME, del Carmen Morales L, Gonzaga JR, et al. Baricitinib versus placebo or adalimumab in rheumatoid arthritis. N Engl J Med 2017;376:652–62.
36. Papp KA, Menter MA, Raman M, Disch D, Schlichting DE, Gaich C, et al. A randomized phase 2b trial of baricitinib, an oral Janus kinase (JAK) 1/JAK2 inhibitor, in patients with moderate-to-severe psoriasis. Br J Dermatol 2016;174:1266–76.
37. Tanaka Y, Emoto K, Cai Z, Aoki T, Schlichting D, Rooney T, et al. Efficacy and safety of baricitinib in Japanese patients with active rheumatoid arthritis receiving background methotrexate therapy: a 12-week, double-blind, randomized placebo-controlled study. J Rheumatol 2016;43:504–11.
38. Genovese MC, Kremer J, Zamani O, Ludivico C, Krogulec M, Xie L, et al. Baricitinib in patients with refractory rheumatoid arthritis. N Engl J Med 2016;374:1243–52.
39. Dougados M, van der Heijde D, Chen YC, Greenwald M, Drescher E, Liu J, et al. Baricitinib in patients with inadequate response or intolerance to conventional synthetic DMARDs: results from the RA-BUILD study. Ann Rheum Dis 2017;76:88–95.
40. Van der Heijde D, Song IH, Pangan AL, Deodhar A, van den Bosch F, Maksymowych WP, et al. Efficacy and safety of upadacitinib in patients with active ankylosing spondylitis (SELECT-AXIS 1): a multicentre, randomised, double-blind, placebo-controlled, phase 2/3 trial. Lancet 2019;394:2108–17.
41. Fleischmann R, Pangan AL, Song IH, Mysler E, Bessette L, Peterfy C, et al. Upadacitinib versus placebo or adalimumab in patients with rheumatoid arthritis and an inadequate response to methotrexate: results of a phase III, double-blind, randomized controlled trial. Arthritis Rheumatol 2019;71:1788–800.
42. Genovese MC, Fleischmann R, Combe B, Hall S, Rubbert-Roth A, Zhang Y, et al. Safety and efficacy of upadacitinib in patients with active rheumatoid arthritis refractory to biologic disease-modifying anti-rheumatic drugs (SELECT-BEYOND): a double-blind, randomised controlled phase 3 trial. Lancet 2018;391:2513–24.
43. Burmester GR, Kremer JM, van den Bosch F, Kivitz A, Bessette L, Li Y, et al. Safety and efficacy of upadacitinib in patients with rheumatoid arthritis and inadequate response to conventional synthetic disease-modifying anti-rheumatic drugs (SELECT-NEXT): a randomised, double-blind, placebo-controlled phase 3 trial. Lancet 2018;391:2503–12.
44. Sandborn WJ, Ghosh S, Panes J, Schreiber S, D'Haens G, Tanida S, et al. Efficacy of upadacitinib in a randomized trial of patients with active ulcerative colitis. Gastroenterology 2020;158:2139–49.
45. Kameda H, Takeuchi T, Yamaoka K, Oribe M, Kawano M, Zhou Y, et al. Efficacy and safety of upadacitinib in Japanese patients with rheumatoid arthritis (SELECT-SUNRISE): a placebo-controlled phase IIb/III study. Rheumatology (Oxford) 2020;59:3303–13.
46. Westhovens R, Taylor PC, Alten R, Pavlova D, Enríquez-Sosa F, Mazur M, et al. Filgotinib (GLPG0634/GS-6034), an oral JAK1 selective inhibitor, is effective in combination with methotrexate (MTX) in patients with active rheumatoid arthritis and insufficient response to MTX: results from a randomised, dose-finding study (DARWIN 1). Ann Rheum Dis 2017;76:998–1008.
47. Kavanaugh A, Kremer J, Ponce L, Cseuz R, Reshetko OV, Stanislavchuk M, et al. Filgotinib (GLPG0634/GS-6034), an oral selective JAK1 inhibitor, is effective as monotherapy in patients with active rheumatoid arthritis: results from a randomised, dose-finding study (DARWIN 2). Ann Rheum Dis 2017;76:1009–19.
48. Genovese MC, Kalunian K, Gottenberg JE, Mozaffarian N, Bartok B, Matzkies F, et al. Effect of filgotinib vs placebo on clinical response in patients with moderate to severe rheumatoid arthritis refractory to disease-modifying antirheumatic drug therapy: the FINCH 2 randomized clinical trial. JAMA 2019;322:315–25.
49. Mease P, Coates LC, Helliwell PS, Stanislavchuk M, Rychlewska-Hanczewska A, Dudek A, et al. Efficacy and safety of filgotinib, a selective Janus kinase 1 inhibitor, in patients with active psoriatic arthritis (EQUATOR): results from a randomised, placebo-controlled, phase 2 trial. Lancet 2018;392:2367–77.
50. Van der Heijde D, Baraliakos X, Gensler LS, Maksymowych WP, Tseluyko V, Nadashkevich O, et al. Efficacy and safety of filgotinib, a selective janus kinase 1 inhibitor, in patients with active ankylosing spondylitis (TORTUGA): results from a randomised, placebo-controlled, phase 2 trial. Lancet 2018;392:2378–87.
51. US Food and Drug Administration. FDA briefing information for the April 23, 2018 meeting of the Arthritis Advisory Committee. URL: https://www.fda.gov/media/112372/download.
52. Pfizer, sponsor. Safety study of tofacitinib versus tumor necrosis factor (TNF) inhibitor in subjects with rheumatoid arthritis. ClinicalTrials.gov identifier: NCT02092467; 2020.
53. Davies R, Galloway JB, Watson KD, Lunt M, Symmons DP, Hyrich KL. Venous thrombotic events are not increased in patients with rheumatoid arthritis treated with anti-TNF therapy: results from the British Society for Rheumatology Biologics Register. Ann Rheum Dis 2011;70:1831–4.
54. Samuelson BT, Vesely SK, Chai-Adisaksopha C, Scott BL, Crowther M, Garcia D. The impact of ruxolitinib on thrombosis in patients with polycythemia vera and myelofibrosis: a meta-analysis. Blood Coagul Fibrinolysis 2016;27:648–52.
55. Miyakawa Y, Oda A, Druker B, Kato T, Miyazaki H, Handa M, et al. Recombinant thrombopoietin induces rapid protein tyrosine phosphorylation of Janus kinase 2 and Shc in human blood platelets. Blood 1995;86:23–7.
56. Galloway J, Barrett K, Irving P, Khavandi K, Nijher M, Nicholson R, et al. Risk of venous thromboembolism in immune-mediated inflammatory diseases: a UK matched cohort study. RMD Open 2020;6:e001392.
57. Johannesdottir SA, Horváth-Puhó E, Dekkers OM, Cannegieter SC, Jørgensen JO, Ehrenstein V, et al. Use of glucocorticoids and risk of venous thromboembolism: a nationwide population-based case-control study. JAMA Intern Med 2013;173:743–52.
58. Strangfeld A, Listing J, Herzer P, Liebhaber A, Rockwitz K, Richter C, et al. Risk of herpes zoster in patients with rheumatoid arthritis treated with anti-TNF-α agents. JAMA 2009;301:737–44.

Arthritis & Rheumatology
Vol. 73, No. 5, May 2021, pp 789–799
DOI 10.1002/art.41600

American College of Rheumatology
Empowering Rheumatology Professionals

RNA Sequencing Reveals Interacting Key Determinants of Osteoarthritis Acting in Subchondral Bone and Articular Cartilage: Identification of *IL11* and *CHADL* as Attractive Treatment Targets

Margo Tuerlings, Marcella van Hoolwerff, Evelyn Houtman, Eka H. E. D. Suchiman, Nico Lakenberg, Hailiang Mei, Enrike H. M. J. van der Linden, Rob R. G. H. H. Nelissen, Yolande Y. F. M. Ramos, Rodrigo Coutinho de Almeida, and Ingrid Meulenbelt

Objective. To identify key determinants of the interactive pathophysiologic processes in subchondral bone and cartilage in osteoarthritis (OA).

Methods. We performed RNA sequencing on macroscopically preserved and lesional OA subchondral bone from patients in the Research Arthritis and Articular Cartilage study who underwent joint replacement surgery due to OA (n = 24 sample pairs: 6 hips and 18 knees). Unsupervised hierarchical clustering and differential expression analyses were conducted. Results were combined with data on previously identified differentially expressed genes in cartilage (partly overlapping samples) as well as data on recently identified OA risk genes.

Results. We identified 1,569 genes that were significantly differentially expressed between lesional and preserved subchondral bone, including *CNTNAP2* (fold change [FC] 2.4, false discovery rate [FDR] 3.36×10^{-5}) and *STMN2* (FC 9.6, FDR 2.36×10^{-3}). Among these 1,569 genes, 305 were also differentially expressed, and with the same direction of effect, in cartilage, including the recently recognized OA susceptibility genes *IL11* and *CHADL*. Upon differential expression analysis with stratification for joint site, we identified 509 genes that were exclusively differentially expressed in subchondral bone of the knee, including *KLF11* and *WNT4*. These genes that were differentially expressed exclusively in the knee were enriched for involvement in epigenetic processes, characterized by, e.g., *HIST1H3J* and *HIST1H3H*.

Conclusion. *IL11* and *CHADL* were among the most consistently differentially expressed genes OA pathophysiology–related genes in both bone and cartilage. As these genes were recently also identified as robust OA risk genes, they classify as attractive therapeutic targets acting on 2 OA-relevant tissues.

INTRODUCTION

Osteoarthritis (OA) represents multiple subtypes of degenerative joint diseases, characterized by progressive and irreversible degeneration of articular cartilage and structural changes in subchondral bone. Globally, OA is a highly prevalent and disabling disease that results in high social and economic burdens to society (1). Yet, there is no proven therapy to prevent OA or slow its progression. Development of OA is dependent on multiple factors, with both environmental and genetic components (2,3). To discover genes and underlying disease pathways, genetic investigations, such as large genome-wide association studies, have been performed, identifying compelling OA risk single-nucleotide polymorphisms (SNPs) (4–6). Functional follow-up studies involve exploring the expression patterns in disease-relevant tissues, behavior with pathophysiology, and/or expression quantitative trait locus (eQTL) or cis-eQTL analysis. To date, major efforts have been made to characterize pathophysiologic processes of OA in

Supported by the Dutch Scientific Research Council (NOW/ZonMW Vici grant 91816631/528), the European Union Seventh Framework Programme (project TREAT-OA; 200800), and the Dutch Arthritis Society (grant DAA_10_1-402). The RAAK study is supported by Leiden University Medical Center.

Margo Tuerlings, MSc, Marcella van Hoolwerff, MSc, Evelyn Houtman, MSc, Eka H. E. D. Suchiman, MSc, Nico Lakenberg, MSc, Hailiang Mei, PhD, Enrike H. M. J. van der Linden, MD, Rob R. G. H. H. Nelissen, MD, PhD, Yolande Y. F. M. Ramos, PhD, Rodrigo Coutinho de Almeida, PhD, Ingrid Meulenbelt, PhD: Leiden University Medical Center, Leiden, The Netherlands.

No potential conflicts of interest relevant to this article were reported.

Address correspondence to Ingrid Meulenbelt, PhD, Leiden University Medical Center, Department of Biomedical Data Sciences, Section of Molecular Epidemiology, LUMC Post-zone S-05-P, PO Box 9600, 2300 RC Leiden, The Netherlands. Email: i.meulenbelt@lumc.nl.

Submitted for publication June 4, 2020; accepted in revised form November 24, 2020.

articular cartilage. However, only a few studies have focused on OA pathophysiologic processes in the underlying bone (7,8).

In recent decades, there has been accumulating evidence that subchondral bone contributes to both onset and progression of OA (9–12). In healthy bone there is a balanced process between bone resorption and bone deposition, as a consequence of dynamic adaptation to mechanical load. In OA this balance is disturbed, which results in changes in the architecture of the subchondral trabecular bone, increased thickness of the subchondral bone plate, formation of new bony structures, called osteophytes, at the joint margins, and development of subchondral bone cysts (2,13,14). In addition, studies have shown an association between bone mineral density and OA development, which suggests that subchondral bone is involved in the early stages of OA (13,15). This was also suggested in studies of subchondral bone marrow lesions, showing these to be very early markers of OA (8,16).

In contrast to cartilage and despite its relevance, only a limited number of studies have focused on the characterization of OA disease processes at the gene expression level in subchondral bone. Chou et al (7) performed whole-genome expression profiling of non-OA and OA subchondral bone using microarray analysis, which led to identification of genes involved in pathways such as lipid metabolism and mineral metabolism. Kuttapitiya et al (8) used microarray analysis to identify genes involved in bone remodeling, pain sensitization, and matrix turnover that were differentially expressed between OA bone marrow lesional tissue and control tissue. However, both of these studies included samples from the knee only.

In the present study, we explored RNA sequencing data on preserved and lesional OA subchondral bone to identify genes that change with progression of OA. The samples used were obtained from the joints of patients in the Research Arthritis and Articular Cartilage (RAAK) study who underwent total joint replacement surgery due to OA. In total, we compared paired subchondral bone samples (preserved and lesional) from 24 OA patients from whom preserved and lesional cartilage was also collected. The results presented here contribute to further understanding of the ongoing OA process in the subchondral bone and provide insight into the pathophysiology of the disease in bone relative to cartilage.

MATERIALS AND METHODS

Sample description. The current investigation included 26 patients from the RAAK study who underwent joint replacement surgery due to OA. Macroscopically preserved and lesional OA subchondral bone was collected from the joints of these patients. Of note, classification of OA subchondral bone as preserved or lesional was based on classification of its overlying cartilage as preserved or lesional, as described previously (17). The results reported here were compared to the results of our earlier study of macroscopically preserved and lesional OA articular cartilage from 35 patients from the RAAK study (18). Fourteen of these 35 patients were included in the present study, as samples of both preserved and lesional subchondral bone and preserved and lesional articular cartilage were available. The sample size for the current study was determined using the R package ssize.fdr, version 1.2 (19), with parameters based on our previous similar analysis of articular cartilage (18) and a desired power of 0.8 (see Supplementary Figure 1, on the *Arthritis & Rheumatology* website at http://onlinelibrary.wiley.com/doi/10.1002/art.41600/abstract). Since the parameters were based on cartilage, whereas bone is known to be more heterogeneous, we decided to include an excess of samples. The samples were either randomly selected or selected based on their overlap with the cartilage data. Informed consent was obtained from all participants in the RAAK study, and ethical approval for the RAAK study was granted by the medical ethics committee of Leiden University Medical Center (P08.239/P19.013).

RNA sequencing. RNA was isolated from subchondral bone using an RNeasy Mini kit (Qiagen). Paired-end 2 × 100–bp RNA sequencing (Illumina TruSeq RNA Library Prep Kit, Illumina HiSeq2000, and Illumina HiSeq4000) was performed. Strand-specific RNA sequencing libraries were generated, which yielded a mean of 20 million reads per sample. Data from both Illumina platforms were integrated and analyzed with the same in-house pipeline. RNA sequencing reads were aligned using GSNAP (20) against GRCh38, with default parameters. Read abundance per sample was estimated using HTSeq count, version 0.11.1 (21). Only uniquely mapping reads were used for estimating expression. The quality of the raw reads for RNA sequencing was checked using MultiQC, version 1.7 (22). The adaptors were clipped using Cutadapt version 1.1 (23), applying default settings (minimum overlap length of 3). To identify outliers, principal components analysis and hierarchical clustering of the samples were applied, and 1 extreme outlier was identified. A sensitivity analysis was performed, which showed that the outlier had a large effect on the results in the overall data set. Based on this, the outlier was removed from the data set. There was 1 sample without paired data, which was also removed from the data set. After removal of these samples, only 24 participants were included for further analysis. The RNA sequencing data are deposited at the European Genome-Phenome Archive (www.ega-archive.org; accession no. EGAS00001004476).

Cluster analysis. Prior to the cluster analysis, variance stabilizing transformation was performed on the data, and 1,000 genes were selected based on the highest coefficient of variation (24,25). To identify the optimal number of clusters in the unsupervised hierarchical clustering the silhouette width score approach was used, with a higher average silhouette width score indicating a more optimal number of clusters (26). Details on the cluster

analyses and the stability of cluster solutions have been reported previously (25).

Differential expression analysis and pathway enrichment. Differential expression analysis was performed on paired lesional and preserved subchondral bone samples, using the DESeq2 R package, version 1.24.0 (27). A general linear model assuming a negative binomial distribution was applied, followed by a paired Wald test between lesional and preserved OA samples, with the preserved samples set as a reference. The Benjamini-Hochberg method was used to correct for multiple testing, as indicated by the false discovery rate (FDR), with a significance cutoff value of 0.05. Gene enrichment was performed using the online functional annotation tool DAVID, selecting for the gene ontology (GO) terms Biological Processes (GOTERM_BP_DIRECT), Cellular Component (GOTERM_CC_DIRECT), and Molecular Function (GOTERM_MF_DIRECT) and for the Reactome Homo Sapiens (R-HSA) and the KEGG pathways (28). Moreover, the protein–protein interactions were analyzed using the online tool STRING, version 11.0 (29). An analysis summary scheme is shown in Figure 1.

Quantitative reverse transcriptase–polymerase chain reaction (qRT-PCR) validation. Complementary DNA synthesis was performed with a Transcriptor First Strand cDNA Synthesis Kit (Roche), using 400 ng of RNA. We used qRT-PCR to quantitatively determine gene expression of *FRZB*, *CNTNAP2*, *STMN2*, *CHRDL2*, *POSTN*, and *ASPN*. Relative gene expression was evaluated using $-\Delta C_t$ values, with *GAPDH* and *SDHA* as internal controls. Generalized estimating equation analysis was performed to calculate the significance of differences between the lesional and preserved samples.

Comparison of subchondral bone and articular cartilage. The 1,569 genes that were significantly differentially expressed (by FDR) between preserved and lesional OA subchondral bone (24 paired samples) reported here were compared to the 2,387 genes that were significantly differentially expressed between preserved and lesional OA articular cartilage (35 paired samples) as determined in our earlier study (18). Genes that were significantly differentially expressed in both tissues were selected, and the directions of effect were explored.

RESULTS

Sample characteristics. To characterize the pathophysiologic process in subchondral bone with ongoing OA, we performed RNA sequencing on macroscopically preserved and lesional OA subchondral bone samples from patients in the RAAK study who underwent joint replacement surgery due to

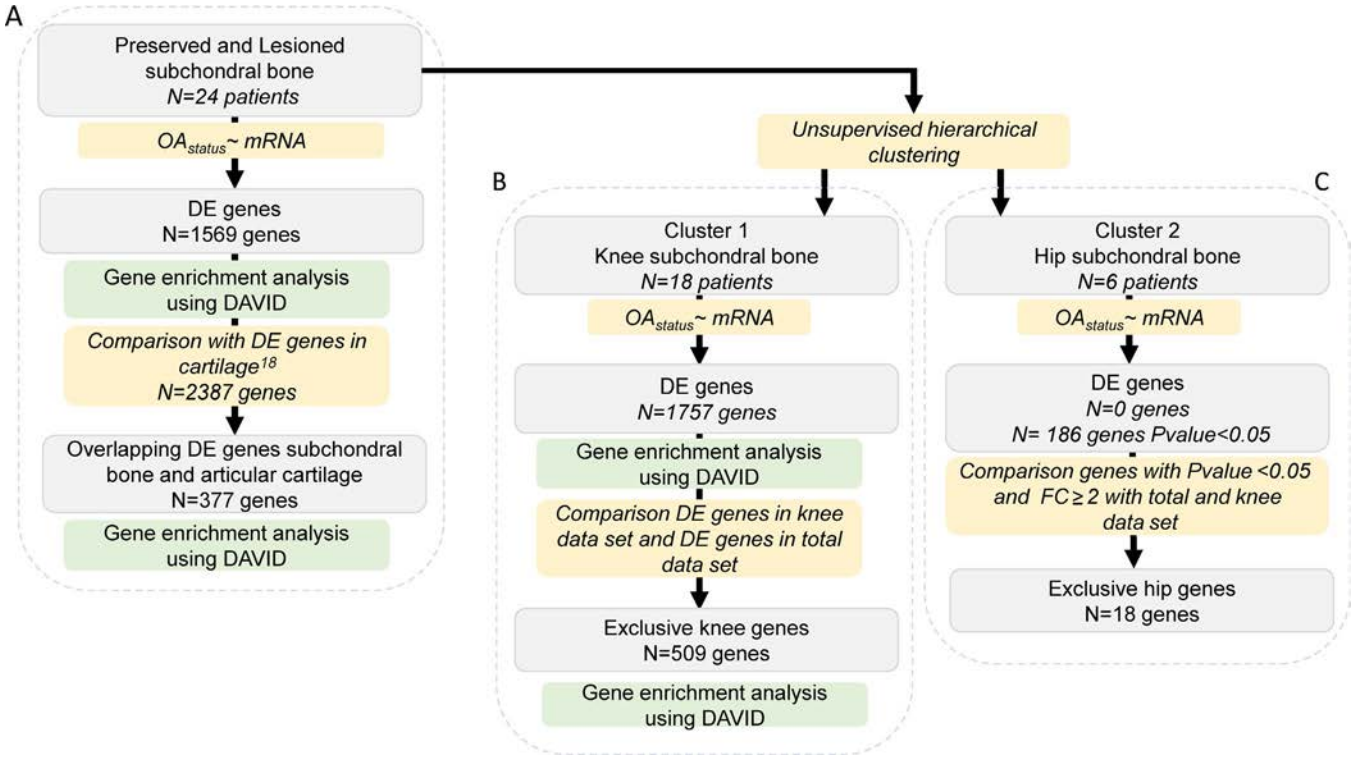

Figure 1. Overview of the study strategy. **A**, Determination of genes that were consistently differentially expressed (DE) between preserved and lesional osteoarthritis (OA) subchondral bone in the overall data set. **B**, Determination of genes that were differentially expressed in knee subchondral bone. **C**, Determination of genes that were differentially expressed in hip subchondral bone. Number of genes represents the significantly differentially expressed genes (according to the false discovery rate method), excluding those that were differentially expressed only in hip samples. FC = fold change.

OA. The RNA sequencing was performed on 24 paired samples (6 from hips and 18 from knees (Supplementary Table 1, on the *Arthritis & Rheumatology* website at http://onlinelibrary.wiley.com/doi/10.1002/art.41600/abstract).

Prior to the differential expression analysis, we tested for possible contamination by cartilage tissue in the subchondral bone samples. We used RNA sequencing data on both tissue types from the same joint and evaluated the relative difference in expression levels of 3 cartilage-specific genes (*COL2A1*, *COMP*, and *CRTAC1*) and 3 bone-specific genes (*COL1A1*, *SPP1*, and *BGLAP*), as described previously (30). As shown in Supplementary Table 2 (http://onlinelibrary.wiley.com/doi/10.1002/art.41600/abstract), we observed relatively low levels of cartilage-specific genes and high levels of bone-specific genes in the subchondral bone data set under study, suggesting no-to-minimal cross-contamination. Next, we explored whether the expression pattern in subchondral bone was associated with any baseline characteristics of the patients (Supplementary Table 1), by performing unsupervised hierarchical clustering. To include the most informative genes in the cluster analysis, 1,000 genes were selected based on the highest coefficient of variation in the total data set (preserved and lesional; n = 24 pairs). As shown in Figure 2 and Supplementary Figure 2 (http://onlinelibrary.wiley.com/doi/10.1002/art.41600/abstract), we identified 2 clusters. These appeared to be based on joint site, indicating an inherent difference between hip and knee subchondral bone.

Differential expression analysis and pathway enrichment. We first determined the genes that were consistently differentially expressed between preserved and lesional OA subchondral bone in the overall data set, to explore the most consistent OA pathways (Figure 1A). Upon differential expression analysis in the 24 sample pairs, we identified 1,569 genes that were genome-wide significantly differentially expressed between lesional and preserved OA subchondral bone tissue. Of these differentially expressed genes, 750 were up-regulated and 819 were down-regulated (Figure 3 and Supplementary Table 3, on the *Arthritis & Rheumatology* website at http://onlinelibrary.wiley.com/doi/10.1002/art.41600/abstract). The most significantly down-regulated gene was *FRZB* (fold change [FC] 0.53, FDR 3.99×10^{-7}), encoding Frizzled-related protein, which is a well-known OA gene showing consistently lower expression in lesional relative

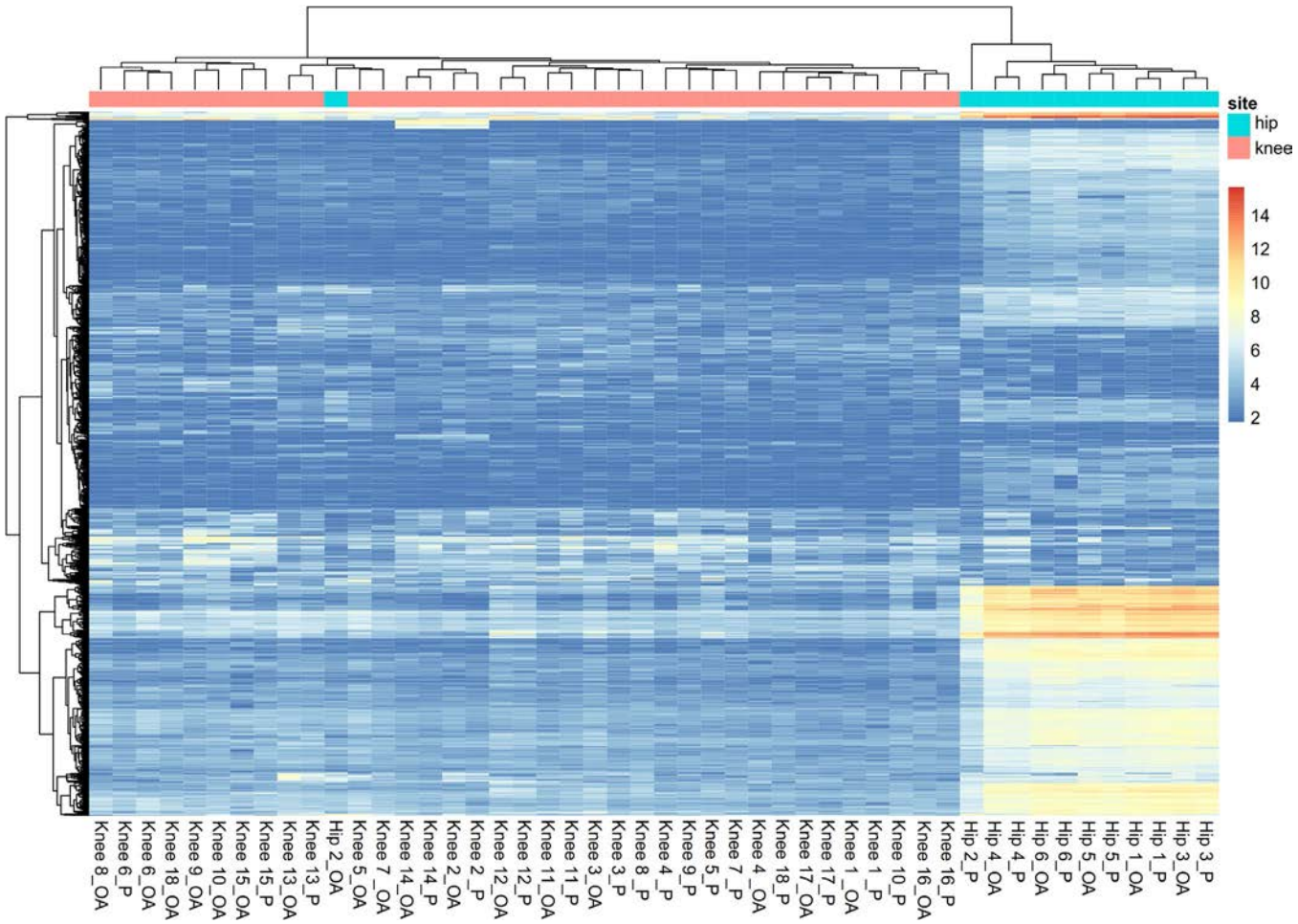

Figure 2. Cluster analysis using the 1,000 genes selected for their highest coefficient of variation. Two clusters based on joint site (knee or hip) were identified. OA = osteoarthritic; P = preserved.

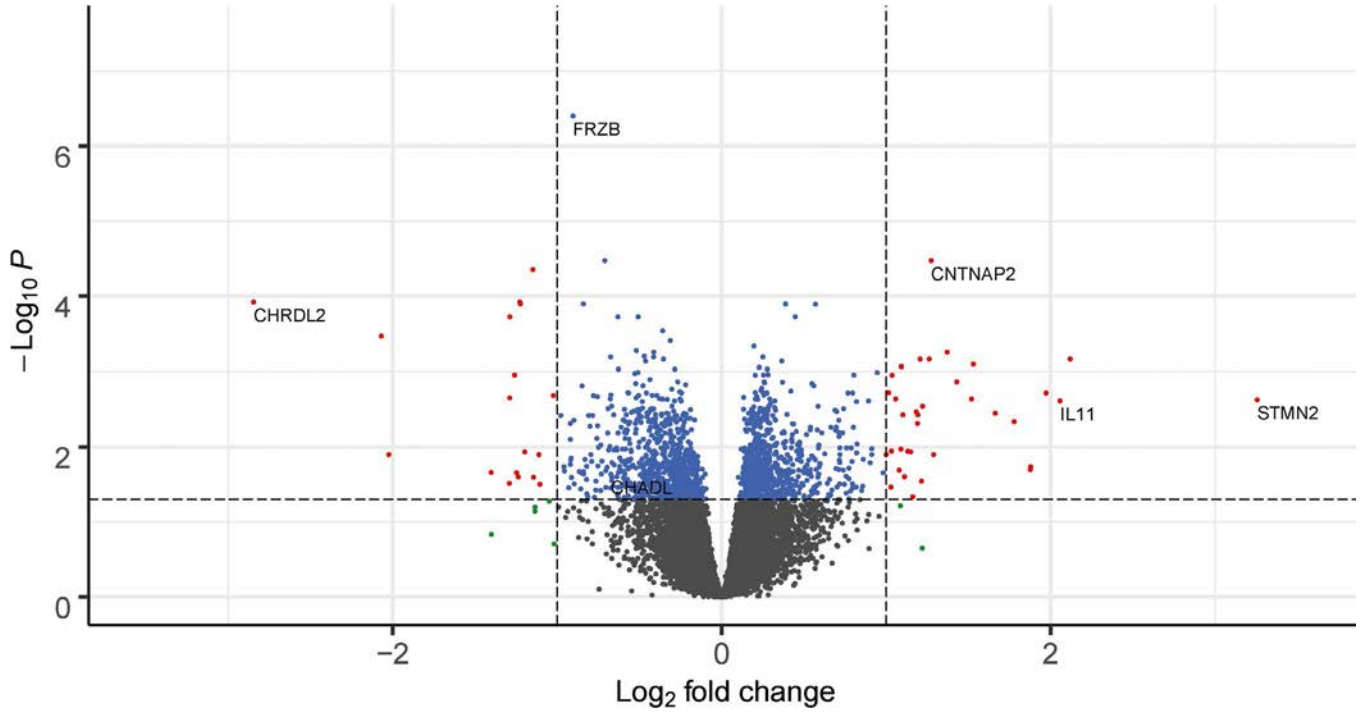

Figure 3. Volcano plot of differentially expressed genes in the subchondral bone. Blue dots represent genes that were significantly differentially expressed, red dots represent genes that were significantly differentially expressed and had an absolute fold change (FC) of ≥2, and green dots represent genes with an absolute FC of ≥2 that were not significantly differentially expressed.

to preserved OA articular cartilage (17,18). The most significantly up-regulated gene was *CNTNAP2* (FC 2.42, FDR 3.36 × 10^{-5}), encoding the contactin-associated protein-like 2 protein (CASPR2). Among the 1,569 differentially expressed genes, 53 had an absolute FC of ≥2 (35 up-regulated and 18 down-regulated). The most highly up-regulated gene was *STMN2* (FC 9.56, FDR 2.36 × 10^{-3}), encoding stathmin 2, while the most down-regulated gene was *CHRDL2* (FC 0.14, FDR 1.20 × 10^{-4}), encoding chordin-like protein 2.

Next, we explored whether the 1,569 significantly differentially expressed genes were enriched in relation to particular pathways or processes, using DAVID. The results demonstrated significantly enriched Gene Ontology (GO) terms regarding processes involved in translational and posttranslational processes, such as signal recognition particle–dependent cotranslational protein targeting to membrane (GO 0006614; 33 genes) (FDR 4.27 × 10^{-7}) and translational initiation (GO 0006413; 36 genes) (FDR 1.95 × 10^{-4}). These processes were both mainly characterized by ribosomal proteins such as *RPS24*, *RPS4X*, and *RPS18* (Supplementary Table 4, http://onlinelibrary.wiley.com/doi/10.1002/art.41600/abstract). Gene enrichment analysis of the genes selected for the highest FC (FC ≥2; n = 53 genes) showed significant enrichment of processes regarding the extracellular matrix (GO 0005615; 16 genes) (FDR 1.19 × 10^{-5}), characterized by up-regulation of *WNT16* (FC 4.35, FDR 6.88 × 10^{-4}), *CRLF1* (FC 2.32, FDR 2.86 × 10^{-2}), and *OGN* (FC 3.43, FDR 4.62 × 10^{-3}), and the proteinaceous extracellular matrix (GO 0005578; 7 genes) (FDR 4.50 × 10^{-2}), characterized by up-regulation of *POSTN* (FC 2.04, FDR 3.44 × 10^{-2}), *ASPN* (FC 3.17, FDR 3.56 × 10^{-3}), and *CTHRC1* (FC 2.15, FDR 3.75 × 10^{-3}) (Supplementary Table 5, http://onlinelibrary.wiley.com/doi/10.1002/art.41600/abstract). To explore interactions between proteins encoded by the 53 differentially expressed genes with an FC of ≥2, we used the online tool STRING. We identified significant enrichment for protein–protein interactions among 22 of 44 proteins (P = 3.20 × 10^{-9}) (Figure 4).

Comparison of subchondral bone and articular cartilage. To investigate interacting OA pathophysiologic processes in subchondral bone and articular cartilage, we compared the differentially expressed genes identified in bone with our previously reported results on differentially expressed genes in articular cartilage (18) (Figure 1A) (24 sample pairs from bone and 35 from cartilage; 14 patients with available sample pairs from both bone and cartilage). This analysis revealed 337 genes that were differentially expressed in both subchondral bone and articular cartilage (Supplementary Figure 3, on the *Arthritis & Rheumatology* website at http://onlinelibrary.wiley.com/doi/10.1002/art.41600/abstract). Of these 337 overlapping genes, the majority (305 genes) showed similar directions of effect in cartilage and bone (Supplementary Table 6, http://onlinelibrary.wiley.com/doi/10.1002/art.41600/abstract), while 32 genes showed opposite directions of effect between the 2 tissue types (Supplementary Table 7, http://onlinelibrary.wiley.com/doi/10.1002/art.41600/abstract). *ALX4*, encoding aristaless-like homeobox 4, was notable among the genes showing opposite

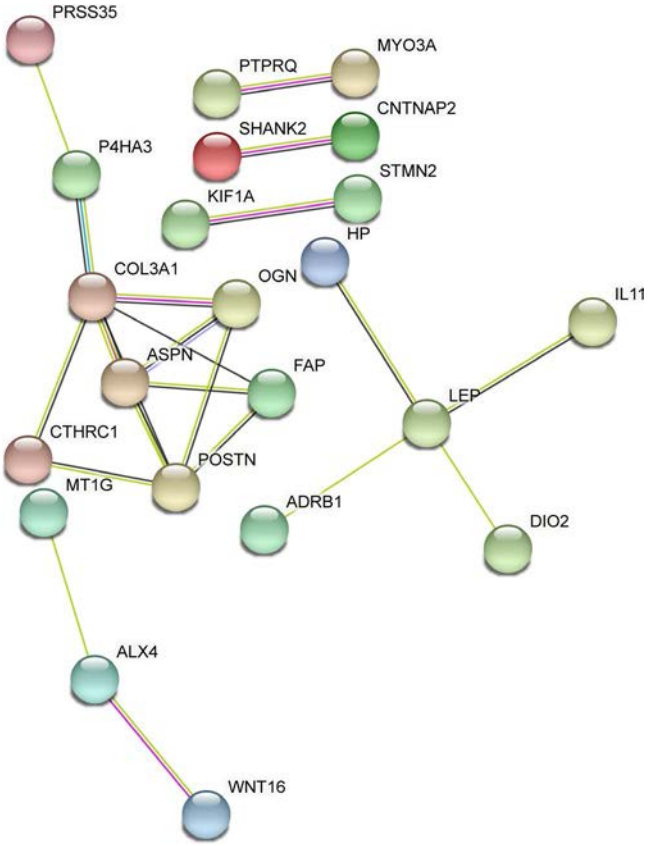

Figure 4. Protein–protein interaction network of proteins encoded by genes that showed an absolute fold change of ≥2 (n = 53 genes), created with the tool STRING.

directions of effect. *ALX4* is known to be involved in osteogenesis and was one of the most highly up-regulated genes in bone (Table 1). Among the 305 genes showing a similar direction of effect, 14 were among the top 25 genes with the highest FC in both tissues, such as *WNT16*, *IL11*, *CRLF1*, and *FRZB* (Table 1).

To explore common underlying pathways in subchondral bone and articular cartilage, we performed gene enrichment analysis with the 305 genes that showed similar directions of effect in cartilage and bone. We found significant enrichment for the GO terms extracellular region (GO 0005576; 36 genes) (FDR 4.56×10^{-3}), characterized by the expression of, for example, *COL6A3*, *FGF14*, and *GDF6*, proteinaceous extracellular matrix (GO 0005578; 17 genes) (FDR 7.98×10^{-3}), characterized by the expression of, for example, *CHADL*, *ADAMTS17*, and *SPOCK3,* and extracellular space (GO 0005615; 37 genes) (FDR 4.42×10^{-3}), characterized by the expression of, for example, *CD63*, *SPP1*, and *RELN* (Supplementary Table 8, on the *Arthritis & Rheumatology* website at http://onlinelibrary.wiley.com/doi/10.1002/art.41600/abstract).

Differential expression analysis stratified by joint site. Since hip and knee samples showed different gene expression profiles in the cluster analysis (Figure 2), we repeated the differential expression analysis with stratification by joint site to explore whether we could identify exclusive OA pathways that occur in subchondral bone of knees only or hips only. Differential expression analysis of the 18 knee sample pairs revealed 1,757 genes that were significantly differentially expressed (Figure 1B), of which 902 genes were up-regulated and 855 were down-regulated in lesional compared to preserved OA subchondral bone (Supplementary Table 9, http://onlinelibrary.wiley.com/doi/10.1002/art.41600/abstract). Moreover, we identified 509 genes that were differentially expressed exclusively in the knee (Supplementary Table 10, http://onlinelibrary.wiley.com/doi/10.1002/art.41600/abstract), i.e., these genes were not differentially expressed in an analysis of the total data set (Supplementary Table 3, http://onlinelibrary.wiley.com/doi/10.1002/art.41600/abstract) or the hip data set (Supplementary Table 11, http://onlinelibrary.wiley.com/doi/10.1002/art.41600/abstract). Enrichment analysis of these genes that were differentially expressed exclusively in the knee showed significant enrichment for processes involved in epigenetic regulation, such as nucleosome (GO 0000786; 20 genes) (FDR 1.81×10^{-9}), DNA methylation (R-HSA 5334118; 15 genes) (FDR 2.48×10^{-6}), and regulation of gene silencing (GO 0060968; 6 genes) (FDR 1.90×10^{-2}), all characterized by members of the histone H3 family, such as *HIST1H3J* and *HIST1H3H* (Supplementary Table 12, http://onlinelibrary.wiley.com/doi/10.1002/art.41600/abstract).

Differential expression analysis using only the hip samples (6 pairs) did not reveal any genes that were significantly differentially expressed by the FDR method when comparing preserved and lesional subchondral bone. However, among the genes with a *P* value of <0.05 and an absolute FC of ≥2 (Supplementary Table 11), 18 genes appeared to be differentially expressed exclusively in the hip (Figure 1C); i.e., not differentially expressed in an analysis of the total data set (Supplementary Table 3) or the knee data set (Supplementary Table 9). Included among these genes with differential expression exclusively in the hip were *CALCR*, *LGR5*, and *COL2A1* (Supplementary Table 13, http://onlinelibrary.wiley.com/doi/10.1002/art.41600/abstract).

Validation of differentially expressed genes. To validate and replicate the findings of the differential expression analysis performed using RNA sequencing, we used a set of 20 samples to conduct both technical replication (10 samples) and biologic replication (10 samples) by qRT-PCR. Validation analysis of 6 genes, *FRZB*, *CNTNAP2*, *STMN2*, *CHRDL2*, *POSTN*, and *ASPN*, showed significant differences between preserved and lesional subchondral bone, with directions of effect similar to those found by RNA sequencing. Replication analysis also showed significant differences, with the same directions of effects as shown by RNA sequencing (Supplementary Table 14, on the *Arthritis & Rheumatology* website at http://onlinelibrary.wiley.com/doi/10.1002/art.41600/abstract).

Table 1. Genes classified as the top 25 genes based on the highest absolute FC in either bone or cartilage, 14 of which were among the top 25 with the highest FC in both tissues*

Ensemble ID/ gene name	Subchondral bone		Articular cartilage		Top 25 absolute FC	
	FC	FDR	FC	FDR	SB	AC
WNT16	4.35	6.88×10^{-4}	8.48	1.10×10^{-13}	x	x
IL11	4.16	2.44×10^{-3}	22.8	1.53×10^{-20}	x	x
GDF6	3.67	2.02×10^{-2}	1.58	3.19×10^{-2}	x	
OGN	3.43	4.62×10^{-3}	2.00	1.02×10^{-3}	x	
ASPN	3.17	3.56×10^{-3}	1.65	3.04×10^{-2}	x	
MYO3A	2.44	1.27×10^{-2}	2.25	1.16×10^{-4}	x	
CRLF1	2.32	2.86×10^{-2}	3.04	2.96×10^{-10}	x	x
GPR158	2.31	6.88×10^{-4}	2.73	3.63×10^{-3}	x	x
PPP1R14C	2.19	1.14×10^{-2}	2.52	1.33×10^{-11}	x	
MT1G	2.16	2.50×10^{-2}	1.97	1.72×10^{-4}	x	
ALX4	2.08	2.30×10^{-3}	0.55	2.75×10^{-2}	x	
P4HA3	2.05	1.12×10^{-3}	1.84	1.49×10^{-5}	x	
FAP	2.05	1.14×10^{-2}	1.69	1.09×10^{-3}	x	
POSTN	2.04	3.44×10^{-2}	2.06	3.20×10^{-2}	x	
HOXB-AS1	2.00	1.27×10^{-2}	1.64	4.86×10^{-2}	x	
KIF20A	1.97	2.22×10^{-2}	1.59	4.44×10^{-2}	x	
TNFAIP	1.93	1.03×10^{-3}	3.58	2.48×10^{-8}	x	x
ERFE	1.87	1.63×10^{-2}	3.44	8.82×10^{-12}	x	x
PTGES	1.64	1.63×10^{-2}	3.06	3.61×10^{-12}		x
TNFRSF12A	1.50	2.31×10^{-2}	2.68	1.14×10^{-8}		x
WNT10B	1.49	3.25×10^{-2}	3.47	1.52×10^{-6}		x
COCH	1.46	4.21×10^{-2}	3.30	1.01×10^{-8}		x
CD55	1.46	2.48×10^{-2}	2.96	1.05×10^{-14}		x
P3H2	1.37	1.14×10^{-2}	3.23	4.71×10^{-18}		x
NGF	1.36	3.26×10^{-2}	4.91	2.53×10^{-14}		x
SPP1	1.36	4.81×10^{-2}	3.14	8.98×10^{-7}		x
NTRK3	0.70	3.56×10^{-3}	0.31	2.64×10^{-5}		x
LMO3	0.58	3.82×10^{-3}	0.28	1.67×10^{-5}		x
FRZB	0.53	3.99×10^{-7}	0.27	1.87×10^{-9}	x	x
RELN	0.53	2.56×10^{-2}	0.22	7.37×10^{-12}	x	x
SLC14A1	0.53	1.71×10^{-2}	0.51	7.05×10^{-6}	x	
CRISPLD1	0.51	1.84×10^{-2}	0.36	9.29×10^{-6}	x	x
ZNF385C	0.51	3.82×10^{-3}	0.43	2.30×10^{-6}	x	
HIF3A	0.49	2.07×10^{-3}	0.58	2.72×10^{-2}	x	
AL845331.2	0.46	3.16×10^{-2}	0.34	3.50×10^{-2}	x	x
GPC5	0.43	1.27×10^{-4}	0.36	1.47×10^{-8}	x	x
AC005165.1	0.43	1.20×10^{-4}	0.45	5.31×10^{-4}	x	
FGF14	0.41	1.89×10^{-4}	0.58	2.01×10^{-4}	x	
AC084816.1	0.38	2.20×10^{-2}	0.45	2.20×10^{-5}	x	
KIF1A	0.25	1.27×10^{-2}	0.37	8.64×10^{-8}	x	x
SPOCK3	0.24	3.41×10^{-4}	0.22	1.56×10^{-9}	x	x
CHRDL2	0.14	1.20×10^{-4}	0.13	7.07×10^{-9}	x	x

* FC = fold change; FDR = false discovery rate; SB = subchondral bone; AC = articular cartilage.

Differential expression of previously identified risk genes. In recent genome-wide association studies of hip and knee OA (5,6), 27 loci conferring risk to OA were identified (Table 2). To assess whether those OA susceptibility genes are also involved in OA pathophysiology in articular cartilage, subchondral bone, or both, we explored their expression levels and differential expression between lesional and preserved tissue in our data sets. As shown in Table 2, we identified 2 risk genes, *IL11* and *CHADL*, that were differentially expressed in both subchondral bone and articular cartilage. In addition, *IL11* showed both significant differential expression in knee subchondral bone (FC 4.07, FDR 7.00×10^{-3}) and a high FC (FC 4.77, $P = 4.43 \times 10^{-2}$) in hip subchondral bone. This indicates that, based on our data set, *IL11* has an effect in both tissues and at both joint sites, albeit not significant according to FDR in hip subchondral bone.

DISCUSSION

Differential expression analysis of gene expression levels in preserved and lesional OA subchondral bone (n = 24 paired samples) revealed 1,569 genes that were significantly differentially expressed, including *CNTNAP2* and *STMN2*. Upon comparing these 1,569 differentially expressed genes with the 2,387 genes with OA pathophysiology previously shown to be differentially expressed in cartilage, we found an overlap of 305 genes that had the same direction of effect. These 305 overlapping genes

Table 2. Expression levels and differential expression of OA risk genes identified in recent genome-wide association studies*

Gene	Bone, total data set			Cartilage, total data set		
	Expression†	FC, preserved vs. OA	FDR	Expression†	FC, preserved vs. OA	FDR
COL11a1	1	1.19	6.21×10^{-1}	1	1.07	7.59×10^{-1}
HDAC9	2	0.97	6.75×10^{-1}	1	0.59	9.10×10^{-6}
SMO	2	1.00	9.91×10^{-1}	1	0.69	7.85×10^{-5}
TNC	1	1.18	2.58×10^{-1}	1	1.41	1.09×10^{-2}
LMX1B	NE	NA	NA	3	0.99	9.80×10^{-1}
LTBP3	1	0.87	3.08×10^{-1}	1	1.08	6.95×10^{-1}
FAM101A (*RFLNA*)	4	0.99	9.77×10^{-1}	2	0.49	6.48×10^{-5}
IL11	3	4.16	2.44×10^{-3}	1	22.80	1.53×10^{-20}
ITIH1	NE	NA	NA	NE	NA	NA
FILIP1	2	0.84	7.07×10^{-2}	3	1.23	2.38×10^{-1}
RUNX2	1	1.07	4.75×10^{-1}	2	0.93	7.79×10^{-1}
ASTN2	4	0.87	2.42×10^{-1}	4	0.82	2.43×10^{-1}
SMAD3	1	0.93	3.74×10^{-1}	1	0.84	2.83×10^{-2}
HFE	3	1.01	9.07×10^{-1}	2	0.88	1.32×10^{-1}
CHADL	4	0.63	2.33×10^{-2}	1	0.63	1.29×10^{-1}
LTBP1	1	0.97	6.91×10^{-1}	1	1.15	1.70×10^{-1}
SBNO1	1	0.98	6.79×10^{-1}	1	1.10	3.94×10^{-1}
WWP2	1	0.82	2.47×10^{-1}	1	0.79	3.43×10^{-2}
GDF5	4	0.92	8.08×10^{-1}	1	1.23	3.09×10^{-1}
TGFB1	NE	NA	NA	NE	NA	NA
TNFSF15	4	1.23	2.42×10^{-1}	3	1.00	9.91×10^{-1}
FGF18	NE	NA	NA	2	1.58	9.51×10^{-4}
CTSK	1	1.41	3.23×10^{-1}	1	1.03	8.91×10^{-1}
DPEP1 (*MBD1*)	1	0.95	2.83×10^{-1}	1	0.96	6.20×10^{-1}
DIABLO	4	0.95	7.37×10^{-1}	3	1.08	6.46×10^{-1}
CRHR1	NE	NA	NA	4	0.62	5.10×10^{-1}
MAPT	3	0.61	3.47×10^{-2}	4	0.70	1.56×10^{-1}

* OA = osteoarthritis; FC = fold change; FDR = false discovery rate; NE = not expressed; NA = not applicable.
† In quartiles, with 1 being the highest expressed quartile and 4 being the lowest expressed quartile.

were enriched for processes related to the extracellular matrix, characterized by the expression of, among others, *COL6A3, GDF6*, and *SPP1*. Moreover, among the 305 overlapping genes were *IL11* and *CHADL* (Table 2 and Supplementary Table 6, on the *Arthritis & Rheumatology* website at http://onlinelibrary.wiley.com/doi/10.1002/art.41600/abstract), which were previously identified as being OA risk genes (5,6). By applying hierarchical clustering on the overall RNA sequencing data set from subchondral bone, we observed 2 clusters based on joint site (knee and hip). When stratifying the analysis for joint site, we identified 1,757 genes that were differentially expressed between preserved and lesional knee OA bone, 509 of which were differentially expressed in the knee exclusively, including genes such as *WNT4* and *KLF11*. These OA genes that were differentially expressed exclusively in the knee were enriched for regulation of gene silencing by epigenetic processes such as DNA methylation and histone modification, characterized by genes such as *HIST1H3J* and *HIST1H3H*, as well as being enriched for other processes.

Among the 1,569 genes that were significantly differentially expressed between lesional and preserved OA subchondral bone using the FDR method in the complete data set, we identified *CNTNAP2* (FC 2.42, FDR 3.36×10^{-5}) and *STMN2* (FC 9.56, FDR 2.36×10^{-3}) as the most significantly up-regulated gene and the gene with the highest FC, respectively. *CNTNAP2*, encoding CASPR2, is known for its effect on cell–cell interactions in the nervous system, synapse development, neural migration, and neural connectivity (31,32). Neither *CNTNAP2* nor its encoded protein were previously identified as being related to OA. *STMN2* also plays a role in the control of neuronal differentiation. Moreover, *STMN2* is expressed during osteogenesis, and it was previously shown to be highly up-regulated in OA bone marrow lesions as compared to control bone samples (8,33). In addition, we found other neural markers to be up-regulated in lesional compared to preserved OA subchondral bone, such as *NGF* and *THBS3* (Supplementary Table 3, http://onlinelibrary.wiley.com/doi/10.1002/art.41600/abstract). Based on these findings, we hypothesize that the formation of new neuronal structures in bone is increased with ongoing OA, which might suggest that OA-related pain originates from bone (8). However, functional follow-up research is needed to confirm this hypothesis.

The hierarchical clustering was done on the top 1,000 genes that showed the highest coefficient of variation between samples; hence, the clusters reflect particularly large differences. Based on the results observed here, it could thus be concluded that these highly variable genes reflect consistent differences between subchondral bone in the knee and subchondral bone in the hip, which was not previously seen in similar analyses of cartilage (25). Consequently, the fact that neither preserved and lesional samples from the same individual nor preserved samples or lesional samples as a group cluster together indicated that the 1,000

genes with the highest coefficient of variation are marking differences between knees and hips only. This does not rule out the relevance of the highly consistently differentially expressed genes reflecting OA subchondral bone pathology described here.

Upon differential expression analysis with stratification by joint site, we discovered 509 genes that were unique to the knee compared to the complete data set, which were significantly enriched for epigenetic processes such as DNA methylation, reflected by the expression of, among others, *HIST1H3J* and *HIST1H3H*. The significant enrichment of these epigenetic processes among the knee-exclusive genes indicates a change in epigenetics with ongoing knee OA, which is not seen with ongoing hip OA. This was also previously demonstrated in articular cartilage, where hip and knee methylation profiles clustered apart irrespective of OA status. However, this was characterized by the expression of different genes, such as the homeobox genes (34,35). We did not find FDR-significant genes when selecting the hip samples, which is likely due to the small sample size (n = 6 sample pairs). Nonetheless, we identified 18 genes that were exclusively differentially expressed in the hip based on the nominal *P* value and an absolute FC of ≥2, including genes such as *CALCR*, *LGR5*, and *COL2A1*. However, replication is needed to confirm our findings regarding these genes differentially expressed exclusively in the hip.

Given the accumulating awareness of cross-talk between articular cartilage and subchondral bone in OA (10,36), we compared RNA sequencing data from subchondral bone and from articular cartilage (24 sample pairs, and 35 sample pairs, respectively, with an overlap of 14 patients). Compared to the number of genes identified as being significantly differentially expressed between preserved and lesional OA articular cartilage based on FDR (n = 2,387 genes), we found fewer genes that were significantly differentially expressed by FDR between preserved and lesional OA subchondral bone (n = 1,569 genes). This difference might be due to the difference in sample size. However, it could also reflect the fact that bone as multicellular tissue is more heterogeneous. The relatively small overlap in genes that were differentially expressed in the same direction in both subchondral bone and cartilage (305 of 3,619; 8.43%) subchondral bone and cartilage suggests that there is a difference in OA pathophysiology between the 2 tissues.

To find genes that are most likely causal in OA, we explored 27 previously published genes with SNPs that were identified as being genome-wide significantly associated with OA (Table 2), suggesting that those genes have a more causal relationship to OA and making them attractive potential treatment targets (5,6). To examine whether the previously identified OA risk genes are involved in the OA pathophysiologic process in both cartilage and subchondral bone, we compared the expression levels and the differential expression between preserved and lesional samples (Table 2). We found that the OA risk genes *IL11* and *CHADL* were differentially expressed in both cartilage and subchondral bone and with the same direction of effect, thus making them attractive potential therapeutic targets with effects in both tissue types. *CHADL*, encoding chondroadherin-like protein, is involved in collagen binding and is a negative modulator of chondrocyte differentiation. The OA susceptibility allele rs117018441-T, located in an intron of *CHADL*, marks higher expression of *CHADL* compared to rs117018441-G in skeletal muscle and adipose tissue according to the Genotype-Tissue Expression Project (5,37). This may indicate that increased expression of *CHADL* has a negative regulatory role in both bone and cartilage and that inhibition of this gene could be a therapeutic strategy. However, when stratifying by joint site, we found *CHADL* to be differentially expressed specifically in the knee subchondral bone, suggesting that it is a treatment target for knee OA exclusively.

IL11, encoding interleukin-11 (IL-11), is known for its role in bone remodeling, and lack of IL-11 function is associated with impaired bone formation (38). Notably, *IL11* was recently proposed as a potential therapeutic target for OA in cartilage (6), since the OA risk allele rs4252548-T, a missense variant p.Arg112His, acts via reduced function of the IL-11 protein. As such, increasing IL-11 protein levels was proposed as a strategy for treatment of OA. In this study we have again shown that *IL11* is highly up-regulated in lesional versus preserved OA tissue in both subchondral bone and articular cartilage (FC 4.16 and 22.8, respectively). Taken together, these data indicate that reduced function of IL-11 predisposes to OA onset and that the up-regulation of *IL11* with OA pathophysiology could be considered an attempt of chondrocytes to enhance extracellular matrix integrity. Nonetheless, the consistent and considerable up-regulation of *IL11* in both subchondral bone and articular cartilage may not necessarily reflect a lack of potency to produce IL-11, unless translation of the protein is hampered. This requires further functional investigation, preferably in an in vitro model of OA. *CHADL* and *IL11* could both be highly suitable treatment targets with effects in both bone and cartilage. However, further functional research is needed to confirm the effects of these genes on bone and cartilage metabolism.

The classification of OA subchondral bone as preserved or lesional is derived from its overlying cartilage. We acknowledge that this ascertainment strategy is bound to introduce heterogeneity between samples. Nonetheless, we identified FDR-significant, and hence very consistent, differentially expressed genes. In other words, despite the fact that there may be heterogeneity in the preserved cartilage, we found consistent markers of the OA pathophysiologic process in subchondral bone.

To our knowledge, this is the first reported study of large-scale differential gene expression patterns in OA subchondral bone, performed using RNA sequencing in both hip and knee samples. We identified distinct differences in expression patterns between hips and knees. Moreover, we identified multiple genes that were previously demonstrated in OA articular cartilage, in addition to genes that were subchondral bone specific. These results will contribute to a better understanding of the pathophysiologic processes underlying the development of OA.

ACKNOWLEDGMENTS

We thank all of the participants of the RAAK study. We also thank Demien Broekhuis, Robert van der Wal, Peter van Schie, Shaho Hasan, Maartje Meijer, Daisy Latijnhouwers, and Geert Spierenburg for collecting the study samples. We thank the personnel of the Sequence Analysis Support Core of Leiden University Medical Center for their support. Data were generated within the scope of the Medical Delta Regenerative Medicine 4D programs Generating Complex Tissues with Stem Cells and Printing Technology and Improving Mobility with Technology.

AUTHOR CONTRIBUTIONS

All authors were involved in drafting the article or revising it critically for important intellectual content, and all authors approved the final version to be published. Ms Tuerlings had full access to all of the data in the study and takes responsibility for the integrity of the data and the accuracy of the data analysis.

Study conception and design. Tuerlings, Ramos, Coutinho de Almeida, Meulenbelt.

Acquisition of data. Tuerlings, van Hoolwerff, Houtman, Suchiman, Lakenberg, Mei, van der Linden, Nelissen, Ramos, Coutinho de Almeida, Meulenbelt.

Analysis and interpretation of data. Tuerlings, Ramos, Coutinho de Almeida, Meulenbelt.

REFERENCES

1. Woolf AD, Erwin J, March L. The need to address the burden of musculoskeletal conditions. Best Pract Res Clin Rheumatol 2012;26:183–224.
2. Goldring MB, Goldring SR. Articular cartilage and subchondral bone in the pathogenesis of osteoarthritis. Ann N Y Acad Sci 2010;1192:230–7.
3. Vina ER, Kwoh CK. Epidemiology of osteoarthritis: literature update [review]. Curr Opin Rheumatol 2018;30:160–7.
4. Zeggini E, Panoutsopoulou K, Southam L, Rayner NW, Day-Williams AG, Lopes MC, et al, for the arcOGEN Consortium and the arcOGEN Collaborators. Identification of new susceptibility loci for osteoarthritis (arcOGEN): a genome-wide association study. Lancet 2012;380:815–23.
5. Styrkarsdottir U, Lund SH, Thorleifsson G, Zink F, Stefansson OA, Sigurdsson JK, et al. Meta-analysis of Icelandic and UK data sets identifies missense variants in SMO, IL11, COL11A1 and 13 more new loci associated with osteoarthritis. Nat Genet 2018;50:1681–7.
6. Tachmazidou I, Hatzikotoulas K, Southam L, Esparaza-Gordillo J, Haberland V, Zheng J, et al. Identification of new therapeutic targets for osteoarthritis through genome-wide analyses of UK Biobank data. Nat Genet 2019;51:230–6.
7. Chou CH, Wu CC, Song IW, Chuang HP, Lu SL, Chang JH, et al. Genome-wide expression profiles of subchondral bone in osteoarthritis. Arthritis Res Ther 2013;15:R190.
8. Kuttapitiya A, Assi L, Laing K, Hing C, Mitchell P, Whitley G, et al. Microarray analysis of bone marrow lesions in osteoarthritis demonstrates up-regulation of genes implicated in osteochondral turnover, neurogenesis and inflammation. Ann Rheum Dis 2017;76:1764–73.
9. Fellows CR, Matta C, Mobasheri A. Applying proteomics to study crosstalk at the cartilage-subchondral bone interface in osteoarthritis: current status and future directions. EBioMedicine 2016;11:2–4.
10. Goldring SR, Goldring MB. Changes in the osteochondral unit during osteoarthritis: structure, function and cartilage-bone crosstalk [review]. Nat Rev Rheumatol 2016;12:632–44.
11. Funck-Brentano T, Cohen-Solal M. Crosstalk between cartilage and bone: when bone cytokines matter. Cytokine Growth Factor Rev 2011;22:91–7.
12. Pan J, Wang B, Li W, Zhou X, Scherr T, Yang Y, et al. Elevated crosstalk between subchondral bone and cartilage in osteoarthritic joints. Bone 2012;51:212–7.
13. Funck-Brentano T, Cohen-Solal M. Subchondral bone and osteoarthritis. Curr Opin Rheumatol 2015;27:420–6.
14. Loeser RF, Goldring SR, Scanzello CR, Goldring MB. Osteoarthritis: a disease of the joint as an organ [review]. Arthritis Rheum 2012;64:1697–707.
15. Barbour KE, Murphy LB, Helmick CG, Hootman JM, Renner JB, Jordan JM. Bone mineral density and the risk of hip and knee osteoarthritis: the Johnston County Osteoarthritis Project. Arthritis Care Res (Hoboken) 2017;69:1863–70.
16. Roemer FW, Guermazi A, Javaid MK, Lynch JA, Niu J, Zhang Y, et al. Change in MRI-detected subchondral bone marrow lesions is associated with cartilage loss: the MOST Study. A longitudinal multicentre study of knee osteoarthritis. Ann Rheum Dis 2009;68:1461–5.
17. Ramos YF, den Hollander W, Bovée JV, Bomer N, van der Breggen R, Lekenberg N, et al. Genes involved in the osteoarthritis process identified through genome wide expression analysis in articular cartilage: the RAAK study. PLoS One 2014;9:e103056.
18. Coutinho de Almeida R, Ramos YF, Mahfouz A, den Hollander W, Lakenberg N, Houtman E, et al. RNA sequencing data integration reveals an miRNA interactome of osteoarthritis cartilage. Ann Rheum Dis 2019;78:270–7.
19. Liu P, Hwang JT. Quick calculation for sample size while controlling false discovery rate with application to microarray analysis. Bioinformatics 2007;23:739–46.
20. Wu TD, Watanabe CK. GMAP: a genomic mapping and alignment program for mRNA and EST sequences. Bioinformatics 2005;21:1859–75.
21. Anders S, Pyl PT, Huber W. HTSeq: a Python framework to work with high-throughput sequencing data. Bioinformatics 2015;31:166–9.
22. Ewels P, Magnusson M, Lundin S, Käller M. MultiQC: summarize analysis results for multiple tools and samples in a single report. Bioinformatics 2016;32:3047–8.
23. Martin M. Cutadapt removes adapter sequences from high-throughput sequencing reads. EMBnet J 2011;17:10–2.
24. Li W, Fan M, Xiong M. SamCluster: an integrated scheme for automatic discovery of sample classes using gene expression profile. Bioinformatics 2003;19:811–7.
25. Coutinho de Almeida R, Mahfouz A, Mei H, Houtman E, den Hollander W, Soul J, et al. Identification and characterization of two consistent osteoarthritis subtypes by transcriptome and clinical data integration. Rheumatology (Oxford) 2021;60:1166–75.
26. Charrad M, Ghazzali N, Boiteau V, Niknafs A. NbClust: an R package for determining the relevant number of clusters in a data set. J Stat Softw 2014;61:1–36.
27. Love MI, Huber W, Anders S. Moderated estimation of fold change and dispersion for RNA-seq data with DESeq2. Genome Biol 2014;15:550.
28. Huang DW, Sherman BT, Lempicki RA. Systematic and integrative analysis of large gene lists using DAVID bioinformatics resources. Nat Protoc 2009;4:44–57.
29. Szklarczyk D, Gable AL, Lyon D, Junge A, Wyder S, Huerta-Cepas J, et al. STRING v11: protein-protein association networks with increased coverage, supporting functional discovery in genome-wide experimental datasets. Nucleic Acids Res 2019;47:D607–13.
30. Chou CH, Lee CH, Lu LS, Song IW, Chuang HP, Kuo SY, et al. Direct assessment of articular cartilage and underlying subchondral bone reveals a progressive gene expression change in human osteoarthritic knees. Osteoarthritis Cartilage 2013;21:450–61.
31. Lu Z, Reddy MV, Liu J, Kalichava A, Liu J, Zhang L, et al. Molecular architecture of contactin-associated protein-like 2 (CNTNAP2) and its interaction with contactin 2 (CNTN2). J Biol Chem 2016;291:24133–47.
32. Rodenas-Cuadrado P, Ho J, Vernes SC. Shining a light on CNTNAP2: complex functions to complex disorders. Eur J Hum Genet 2014;22:171–8.
33. Chiellini C, Grenningloh G, Cochet O, Scheideler M, Trajanoski Z, Ailhaud G, et al. Stathmin-like 2, a developmentally-associated

neuronal marker, is expressed and modulated during osteogenesis of human mesenchymal stem cells. Biochem Biophys Res Commun 2008;374:64–8.
34. Reynard LN. Analysis of genetics and DNA methylation in osteoarthritis: what have we learnt about the disease? [review]. Semin Cell Dev Biol 2017;62:57–66.
35. Den Hollander W, Ramos YF, Bos SD, Bomer N, van der Breggen R, Lakenberg N, et al. Knee and hip articular cartilage have distinct epigenomic landscapes: implications for future cartilage regeneration approaches. Ann Rheum Dis 2014;73:2208–12.
36. Tat SK, Lajeunesse D, Pelletier JP, Martel-Pelletier J. Targeting subchondral bone for treating osteoarthritis: what is the evidence? Best Pract Res Clin Rheumatol 2010;24:51–70.
37. Styrkarsdottir U, Helgason H, Sigurdsson A, Norddahl GL, Agustsdottir AB, Reynard LN, et al. Whole-genome sequencing identifies rare genotypes in COMP and CHADL associated with high risk of hip osteoarthritis. Nat Genet 2017;49:801–5.
38. Lokau J, Göttert S, Arnold P, Düsterhöft S, López DM, Grötzinger J, et al. The SNP rs4252548 (R112H) which is associated with reduced human height compromises the stability of IL-11. Biochim Biophys Acta Mol Cell Res 2018;1865:496–506.

Errata

DOI 10.1002/art.41755

In the article by Rodríguez-Carrio et al in the March 2021 issue of *Arthritis & Rheumatology* (Profiling of Serum Oxylipins During the Earliest Stages of Rheumatoid Arthritis [pages 401–413]), the academic degree listed for one of the authors, Dr. Roxana Coras, was incorrect and the institutional affiliation listed for two of the authors, Dr. Coras and Dr. Mónica Guma, was incomplete. The text in the title-page footnotes should have read "[2]Roxana Coras, MD, Mónica Guma, MD, PhD: University of California School of Medicine, San Diego, and Department of Medicine, Autonomous University of Barcelona, Barcelona, Spain."

DOI 10.1002/art.41761

In the article by Kolasinski et al in the February 2020 issue of *Arthritis & Rheumatology* (2019 American College of Rheumatology/Arthritis Foundation Guideline for the Management of Osteoarthritis of the Hand, Hip, and Knee [pages 220–233]), there was an error in Figure 2B: Chondroitin should not have been included among the pharmacologic therapies recommended against for hand osteoarthritis. The corrected Figure 2B is shown below.

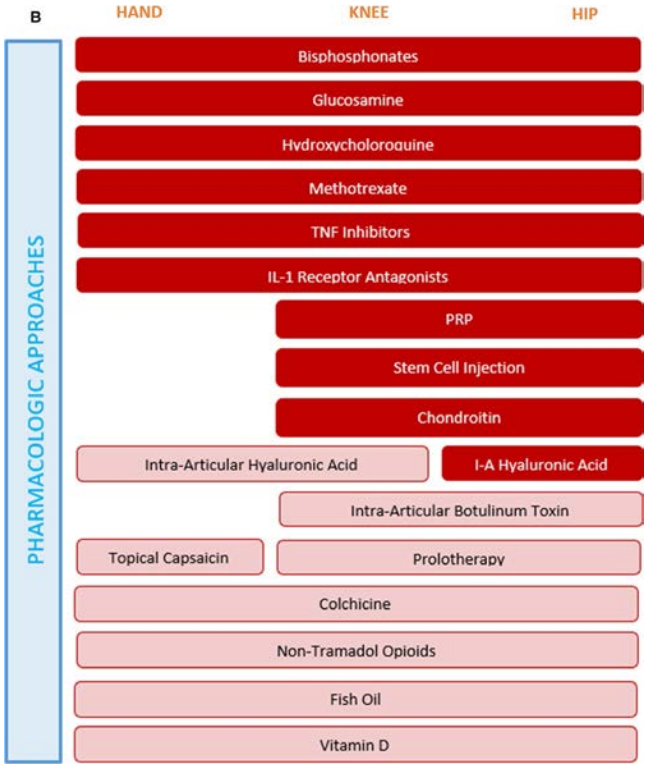

We regret the errors.

American College of Rheumatology
Empowering Rheumatology Professionals

Arthritis & Rheumatology
Vol. 73, No. 5, May 2021, pp 800–805
DOI 10.1002/art.41595

Which Magnetic Resonance Imaging Lesions in the Sacroiliac Joints Are Most Relevant for Diagnosing Axial Spondyloarthritis? A Prospective Study Comparing Rheumatologists' Evaluations With Radiologists' Findings

X. Baraliakos,[1] A. Ghadir,[2] M. Fruth,[2] U. Kiltz,[1] I. Redeker,[3] and J. Braun[1]

Objective. Pathologic sacroiliac (SI) joint changes on magnetic resonance imaging (MRI) are important for the classification of axial spondyloarthritis (SpA). In daily practice, radiologists play a major role in interpreting imaging findings. This study was undertaken to evaluate the impact of MRI SI joint findings on the identification of axial SpA by radiologists, in comparison to diagnosis by rheumatologists.

Methods. Patients age ≤45 years were prospectively included when referred for clinical suspicion of axial SpA and underwent a complete diagnostic evaluation including STIR- and T1-weighted MRI of the SI joint. Diagnosis made by an experienced rheumatologist with access to all relevant information was considered the gold standard. MRIs were evaluated by 2 experienced radiologists who were unaware of the clinical data, who indicated which MRI lesions were "critical" to the decision for or against axial SpA.

Results. Of the 300 patients included, 132 (44%) were diagnosed as having axial SpA. Mean age was comparable between the 2 groups, but patients with axial SpA and those with non–axial SpA differed with regard to symptom duration (58.6 ± 69.5 versus 33.9 ± 45.1 months, respectively; $P = 0.003$) and HLA–B27 positivity (75.6% versus 19%, respectively; $P < 0.001$). Rheumatologists and radiologists agreed on the diagnosis in 262 cases (87.3%), while 34 patients (11.3%) were diagnosed as having axial SpA by rheumatologists only (clinically), and 4 cases (1.3%) were judged as suggestive of axial SpA by radiologists only. Bone marrow edema (BME) and sclerosis showed the highest sensitivity, while erosions and fatty lesions showed the highest specificity, for axial SpA diagnosis. The combination of BME with erosions had the highest positive predictive value (86.5%).

Conclusion. The MRI findings with the highest diagnostic value in patients in whom axial SpA is suspected are structural changes in the SI joint, alone or in combination with BME. Our findings indicate that while the absence of BME is usually not compatible with a diagnosis of axial SpA, the presence of BME does not necessarily confirm a diagnosis of axial SpA.

INTRODUCTION

Axial spondyloarthritis (SpA) is a chronic inflammatory disease that mainly affects the axial skeleton. The prevalence of axial SpA has been estimated to be between 0.1% and 1.4% (1). For classification of patients with axial SpA, the Assessment of SpondyloArthritis international Society (ASAS) classification criteria (2) are now well established. Based on these criteria, patients diagnosed as having axial SpA can be classified for participation in clinical trials for axial SpA when they have chronic back pain, symptom onset at age <45 years, and either inflammatory changes or structural changes, detected by magnetic resonance imaging (MRI) or conventional radiographs, respectively, in the area of the sacroiliac (SI) joint (imaging arm). In addition, in the absence of positive imaging, positive findings on laboratory tests for HLA–B27 are required (clinical arm). The frequency of using imaging for the identification of patients with axial SpA has been reported to be higher than that of using genetic background (3) in routine daily practice.

Typical MRI findings that represent axial inflammation indicative of active disease are changes with high water content called

[1]X. Baraliakos, MD, U. Kiltz, MD, J. Braun, MD: Rheumazentrum Ruhrgebiet, Herne, Germany, and Ruhr-Universität Bochum, Bochum, Germany; [2]A. Ghadir, MD, M. Fruth, MD: Radiologie Herne, Herne, Germany; [3]I. Redeker, MD: German Rheumatism Research Center Berlin, Berlin, Germany.

No potential conflicts of interest relevant to this article were reported.

Address correspondence to Xenofon Baraliakos, MD, Rheumazentrum Ruhrgebiet, Ruhr-University Bochum, Claudiussstrasse 45, Herne 44649, Germany. Email: xenofon.baraliakos@elisabethgruppe.de.

Submitted for publication June 17, 2020; accepted in revised form November 17, 2020.

bone marrow edema (BME). Typical MRI findings that represent structural lesions are changes with abnormal fat signals indicative of fat metaplasia, i.e., fatty lesions, but also include bony changes indicative of sclerosis, erosions, and ankylosis (4). BME especially has been proposed and used for the diagnosis, classification, and assessment of disease activity (5), although structural changes have also been found useful for the diagnosis of axial SpA, and especially for differentiation of axial SpA from other causes of back pain. However, structural changes have not been accepted as good enough for classification purposes to date (6). In a recent update of the ASAS definition of a positive MRI of the SI joint for classification as axial SpA, the role of structural SI joint lesions located periarticularly at the SI joint was recognized as an additional feature of axial SpA, but this has not yet become part of official recommendations (7).

On the other hand, recent studies of populations with no evidence of axial SpA (healthy volunteers, military recruits, runners, patients with chronic back pain, and postpartum women) have suggested that a substantial proportion of these individuals may present with BME lesions on MRI of the SI joints (8–10). These findings have led to increased skepticism regarding the role of BME lesions in the diagnosis of SpA, due to the fear of too many false-positive or false-negative evaluations of patients in whom axial SpA is suspected and, hence, misclassifications and misdiagnoses (11).

In the present study, we prospectively investigated the impact of different MRI lesions in the SI joint for a diagnosis of axial SpA beyond classification, in order to compare the findings of radiologists with the clinical diagnosis made by rheumatologists.

PATIENTS AND METHODS

Patient recruitment and diagnosis. Consecutive patients age ≤45 years who were referred to our outpatient clinic by nonrheumatologists due to suspicion of axial SpA were prospectively included. A total of 5 rheumatologists with >10 years of clinical experience examined all study patients (and all patients were planned to be seen by the same rheumatologist). All patients received a complete diagnostic evaluation, including laboratory tests of C-reactive protein level and HLA–B27 status. Complete imaging of the SI joint (conventional radiographs and MRI in the STIR and T1-weighted sequence in the semicoronal and semiaxial orientation [5]), was performed in the same radiology department for all patients, routinely by the same personnel and with the same imaging protocol. After evaluation of all examinations by the rheumatologist without having the radiologist's report yet available, a diagnosis of axial SpA (with differentiation as non–axial SpA) was made by the rheumatologist. The differentiation between nonradiographic axial SpA and radiographic axial SpA was determined based on the ASAS classification criteria using conventional radiographs. The study was approved by the ethics committee of the Medical Council Muenster, Westfalia-Lippe, Germany (2017-696-f-S).

Imaging evaluation. All MRIs were extracted from the hospital's database, and all demographic information was removed by an individual not associated with the present study. After anonymization, all MRIs were given to 2 different experienced radiologists (AG and MF) who specialized in the evaluation of imaging of patients with low back pain and rheumatic conditions, and who had not previously seen the images. The radiologists, who had only been informed that the patients were young (≤45 years old) and had chronic back pain, evaluated the MRIs independently and judged whether or not each individual MRI was compatible with a diagnosis of axial SpA. Furthermore, the radiologists documented which lesions they considered "critical" for the decision for or against axial SpA. The radiologists documented the presence of critical lesions on MRI as inflammatory lesions (BME) only, chronic lesions (erosions, fat metaplasia, sclerosis, or ankylosis), or a combination of BME and any of the chronic lesions. The identification of a positive BME or chronic lesion was based on ASAS definitions (12). In addition, and independent of lesion identification, all lesions were quantified using the Berlin SI joint MRI scoring system (13). Briefly, this scoring system quantifies BME, erosions, sclerosis, fat, and ankylosis based on assessment of SI joint quadrants. All lesions are evaluated separately, with a total score for all items calculated per patient.

For the final evaluation and comparison between rheumatologists' diagnosis and radiologists' findings, and for calculation of the Berlin SI joint MRI score, only the lesions on which the 2 radiologists agreed were taken into account. The radiologists who participated in this evaluation did not have access to any other imaging results, including conventional radiographs of the SI joints.

Statistical analysis. Continuous data are shown as the mean ± SD, and categorical data are shown as percentages. Descriptive statistics were compared between groups using the Mann-Whitney U test for continuous variables or the chi-square test for categorical variables. All tests were 2-sided, with a significance level set at 0.05. The associations between MRI lesions detected by the radiologists and the diagnosis made by the rheumatologist were assessed by calculation of odds ratios (ORs) for single lesions or combinations of lesions. Ankylosis was not included in this particular analysis as a chronic lesion because of the high specificity but low sensitivity and low expected prevalence in this population. Interobserver reliability (agreement between radiologists) for the identification of active lesions (BME), chronic lesions, and combinations of the 2 lesion types was calculated by intraclass correlation coefficients (ICCs) (95% confidence interval [95% CI]). Finally, the mean or median (where appropriate) Berlin SI joint MRI scores for all patients diagnosed as having axial SpA were compared with the scores for patients without this diagnosis.

RESULTS

Patient characteristics. Overall, 300 patients were included. Of those, 132 patients (44.0%) were diagnosed as having axial SpA by the rheumatologist, while in 168 patients (56.0%) axial SpA was not diagnosed by the rheumatologist. The mean ± SD age was 34.5 ± 7.2 years in the axial SpA group and 34.5 ± 7.4 years in the non–axial SpA group. The mean ± SD symptom duration was 58.6 ± 69.5 months in the axial SpA group versus 33.9 ± 45.1 months in the non–axial SpA group ($P = 0.003$), and 101 (75.6%) of the patients with axial SpA versus 32 (19%) of the patients with non–axial SpA were positive for HLA–B27 ($P < 0.001$). The ASAS classification criteria were fulfilled by 100 (75.8%) of the patients in the axial SpA group and by 67 (39.9%) of the patients in the non–axial SpA group ($P = 0.01$), both mainly due to MRI findings (BME).

Agreement between rheumatologists and radiologists. Of the 132 patients diagnosed as having axial SpA by the rheumatologist, 98 (74.2%) were also identified as having axial SpA by the radiologists (based on imaging), while among the 168 patients who were not diagnosed as having axial SpA, the radiologists did not find imaging signs indicative of axial SpA in 164 (97.6%), indicating good agreement. This resulted in an overall agreement between rheumatologists and radiologists regarding the diagnosis of axial SpA in 262 of 300 patients (87.3%). The ICCs were 0.99 for BME (95% CI 0.99–0.99), 0.92 for chronic lesions (95% CI 0.91–0.94), and 0.87 for the combination of BME and chronic lesions (95% CI 0.84–0.89). However, 34 patients (11.3%) were diagnosed as having axial SpA by the rheumatologists on a clinical basis only, meaning that they did not have positive imaging findings but presented with suggestive clinical symptoms beyond inflammatory back pain at a young age and were HLA–B27 positive. These cases were not considered as being disagreed upon between rheumatologists and radiologists, since they were diagnosed on clinical grounds without the potential help of imaging.

Assessment of lesions by radiologists and relationship of imaging findings to clinical diagnosis. In the 98 patients for whom the rheumatologist and radiologist agreed on a diagnosis of axial SpA, the "critical" lesion most frequently identified by the radiologist was the combination of BME with a concomitant chronic lesion, while BME without concomitant chronic lesions was the least frequent "critical" lesion in this group (Table 1). Of the 164 patients for whom the radiologist and rheumatologist agreed on non–axial SpA, no patient was found to have a chronic lesion, while all of them had BME alone (Table 1).

In contrast, of the 4 patients in whom rheumatologists did not diagnose axial SpA but radiologists suggested axial SpA, none was found to have BME alone, but all of them had chronic changes, either alone or in combination with BME (Table 1). All of these patients were women, had given birth to children, reported high levels of back pain (≥5 on a scale of 0–10), and were HLA–B27 negative. All of them were diagnosed as having osteitis condensans ilii by the rheumatologist.

The proportions of patients with BME, chronic lesions, or a combination of BME and chronic lesions who had axial SpA in different stages (radiographic versus nonradiographic) or non–axial SpA are shown in Table 1.

Table 1. Diagnosis of axial SpA by rheumatologists and radiologists, and distribution of SI joint lesion types on MRI in patients without axial SpA and patients with axial SpA by subtype (nonradiographic or radiographic)*

Rheumatologist diagnosis/radiologist diagnosis and MRI lesion judged critical for diagnosis by the radiologist	No. (%) of patients (n = 300)	Interpretation of MRIs by the radiologist			
		Non–axial SpA	Axial SpA	Nonradiographic axial SpA†	Radiographic axial SpA†
Axial SpA/axial SpA	98 (32.7)				
BME (n = 8)	–	0 (0)	8 (8.2)	3 (37.5)	5 (62.5)
Chronic lesions (n = 24)	–	0 (0)	24 (24.7)	10 (41.7)	14 (58.3)
BME and chronic lesions (n = 66)	–	0 (0)	66 (67.0)	32 (48.5)	34 (51.5)
Axial SpA/no axial SpA	34 (11.3)				
BME (n = 0)	–	0 (0)	0 (0)	0 (0)	0 (0)
Chronic lesions (n = 0)	–	0 (0)	0 (0)	0 (0)	0 (0)
BME and chronic lesions (n = 0)	–	0 (0)	0 (0)	0 (0)	0 (0)
No axial SpA/axial SpA	4 (1.3)				
BME (n = 0)	–	0 (0)	0 (0)	0 (0)	0 (0)
Chronic lesions (n = 3)	–	0 (0)	3 (75)	1 (33.3)	2 (66.7)
BME and chronic lesions (n = 1)	–	0 (0)	1 (25)	1 (100)	0 (0)
No axial SpA/no axial SpA	164 (54.7)				
BME (n = 164)	–	164 (100)	0 (0)	0 (0)	0 (0)
Chronic lesions (n = 0)	–	0 (0)	0 (0)	0 (0)	0 (0)
BME and chronic lesions (n = 0)	–	0 (0)	0 (0)	0 (0)	0 (0)

* Values are the number (%). SI = sacroiliac; MRI = magnetic resonance imaging; BME = bone marrow edema.
† The differentiation between nonradiographic axial spondyloarthritis (SpA) and radiographic axial SpA was based on an evaluation of conventional radiographs performed by the rheumatologist, as described in Patients and Methods.

Table 2. Comparison of the diagnostic value of different lesions on MRI of the SI joints for the diagnosis of axial SpA compared to non–axial SpA in daily practice, based on the diagnostic decision of rheumatologists and the lesions identified by radiologists*

Lesion type	Sensitivity, %	Specificity, %	Positive LR	Negative LR	OR (95% CI)	PPV, %	NPV,%
BME	72.5	63.3	1.98	0.43	4.6 (2.8–7.5)	60.5	74.8
Fatty lesion	56.5	89.3	5.30	0.49	10.9 (6.0–19.8)	80.4	72.6
Erosion	59.5	88.8	5.30	0.46	11.6 (6.4–21.0)	80.4	73.9
Sclerosis	81.7	43.2	1.44	0.42	3.4 (2.0–5.8)	52.7	75.3
BME + any chronic lesion	71.8	72.8	2.64	0.39	16.0 (7.5–34.0)	67.1	76.9
BME + fatty lesion	36.6	95.3	7.74	0.67	11.6 (5.3–25.7)	85.7	66.0
BME + erosion	48.9	94.1	8.26	0.54	15.2 (7.4–31.4)	86.5	70.4
BME + sclerosis	64.1	75.1	2.58	0.48	5.4 (3.3–8.9)	66.7	73.0

* MRI = magnetic resonance imaging; SI = sacroiliac; SpA = spondyloarthritis; LR = likelihood ratio; OR = odds ratio; 95% CI = 95% confidence interval; PPV = positive predictive value; NPV = negative predictive value; BME = bone marrow edema.

Association between lesion types identified by radiologists and clinical diagnosis. The sensitivity and specificity of all single lesions or combinations of lesions, together with the ORs for all lesion types, are shown in Table 2. In the analysis of single lesions, sensitivity was highest for BME (72.5%) and sclerosis (81.7%), while specificity was highest for erosions (88.8%) and fatty lesions (89.3%). Overall, erosions (OR 11.6 [95% CI 6.4–21]) and fatty lesions (10.9 [95% CI 6.0–19.8]) had the highest ORs for identifying axial SpA patients, while the ORs for BME and sclerosis were low (Table 2).

The combination of BME with any chronic change showed an increase in the specificity of BME lesions (72.8%) without loss of sensitivity (71.8%). Similar trends of improvement were also found for the OR for identification of the correct diagnosis when using combinations of lesions, especially for the combination of BME with erosions (OR 15.2 [95% CI 7.4–31.4]) and the combination of BME with fatty lesions (OR 11.6 [95% CI 5.3–25.7]) (Table 2). Similarly, the positive predictive values were highest for erosions and fatty lesions or their combinations with BME, respectively (Table 2).

Quantification of MRI lesions in axial SpA patients versus non–axial SpA patients. Overall, patients diagnosed as having axial SpA showed significantly higher mean total Berlin SI joint MRI scores for the quantification of lesions. In addition, those with axial SpA had higher scores for BME, erosions, and fatty lesions, while there was no difference between groups in the score for sclerosis or ankylosis (Table 3).

Table 3. Berlin SI joint MRI scores in the patients with axial SpA and patients with non–axial SpA*

Lesion type	Axial SpA (n = 132)	Non–axial SpA (n = 168)	*P*
Total score	14.8 ± 10.8	2.7 ± 3.4	<0.001
BME score (range 0–24)	3.3 ± 3.6	0.8 ± 1.3	–
Fatty lesions (range 0–24)	5.2 ± 6.8	0.5 ± 1.9	–
Erosion score (range 0–24)	4.5 ± 5.4	0.4 ± 1.4	–
Median sclerosis or ankylosis score (range 0–2)	0	0	–

* Except where indicated otherwise, value are the mean ± SD. SI = sacroiliac; MRI = magnetic resonance imaging; SpA = spondyloarthritis; BME = bone marrow edema.

DISCUSSION

Ever since the original publication of the ASAS classification criteria in 2009 (2), together with the first definition of a "positive" MRI of the SI joint (14), there has been a constant effort to increase experience with the use of MRI and the quality of judging the different types of lesions in patients with axial SpA. Recently, ASAS has gone beyond defining a "positive MRI" for axial SpA solely based on the presence of BME, and chronic structural changes have been incorporated to reach a better sensitivity and specificity of those imaging findings (8). However, the high sensitivity but low specificity of BME in SI joint MRIs has become a constant problem for the evaluation of patients with low back pain (15). In addition, if classification criteria are misused for diagnostic purposes, a high chance of overdiagnosis (8–10) and overtreatment has been reported (7).

In this study, we found that in the interpretation of MRIs of the SI joint, the combination of BME with chronic lesions such as erosions, fatty lesions, or sclerosis was associated with an increase in specificity without loss in sensitivity for the diagnosis of axial SpA, as compared to BME lesions alone, which are rather used for classification purposes. Beyond sensitivity and specificity, both positive and negative likelihood ratios increased when BME and chronic lesions were found in combination, while the likelihood ratios for chronic lesions (especially fatty lesions and erosions) alone were also higher than those for BME alone. These results confirm earlier findings that were based on the quantification of lesions found in SI joint quadrants and compared to a more global assessment by expert readers (16). However, that study included a much smaller sample size than the present study, evaluated the MRIs for use in the context of classification and not for diagnosis, and did not incorporate fatty lesions or sclerosis as possible chronic MRI changes. In comparison, in another evaluation of patients with axial SpA in the nonradiographic stage compared with only a small control group, fatty

lesions showed no clinical utility in the recognition of this axial SpA stage, which might also be explained by the fact that such lesions may take time to develop. Nevertheless, the use of fatty lesions in the contextual interpretation of SI joint MRI was confirmed when BME or erosions were concomitantly assessed (7). Furthermore, and, although similar conclusions were recently reached in a systematic literature review (17), all studies published to date have been performed on the basis of identification of the most appropriate lesions to confirm the clinician's diagnosis, whereas our analysis had the a priori target of the identification of the "critical" lesions and combinations of lesions to differentiate between axial SpA and non–axial SpA based on the expert's clinical judgment.

Another interesting aspect of our study was the analysis of the probability of detection of different MRI lesions in patients clinically diagnosed as having axial SpA as compared to patients in whom axial SpA was not diagnosed. In this context, detection of single lesions was, again, superior to chronic lesions and especially erosions and fatty lesions. However, the highest OR for lesions to be found in axial SpA patients was observed for the combination of BME and (any) chronic lesion, confirming the importance of structural lesions for the interpretation of BME and differentiation from BME associated with diagnoses other than axial SpA (18,19) or even in healthy volunteers (20). This finding is of major clinical relevance related to the ASAS definition of BME when interpreting MRI findings in the context of a diagnosis of axial SpA (7).

Finally, the probability of an occurrence of the above-mentioned lesions in patients diagnosed as having axial SpA provides reassurance that using MRI as the major diagnostic imaging method in this disease is appropriate. The positive predictive values for fatty lesions and erosions were >80%, indicating that a "positive MRI" based on these findings is associated with a very high probability that the rheumatologist will, in the clinical context, also diagnose axial SpA. On the other hand, overinterpretation of these lesions by radiologists may occur, but is much less common, as seen by the very low proportion of patients identified by radiologists as having lesions suggestive of axial SpA but who were not diagnosed as having axial SpA by the rheumatologists. Obviously, and similar to what has been described above, in these cases the radiologic findings need to be interpreted in the clinical context of the patients. In comparison, the positive predictive value of BME alone was almost 61%. The negative predictive value of almost 77% for the combination of BME and (any) chronic lesion indicated that an MRI that is "negative" for this combination is also associated with a very high probability of exclusion of axial SpA in patients in whom SpA is clinically suspected.

The overall agreement between rheumatologists and radiologists was high in our study, which may well be due to the fact that we have been working together for many years. Indeed, when patients who were diagnosed on a clinical basis only were excluded, agreement was close to 99%. Although this finding can be seen as reassuring that, in specialized centers, collaboration between rheumatologists and radiologists may improve the level of care for patients who have symptoms indicative of axial SpA, it may also represent a limitation since the results are likely to be different in other settings. The expertise of both rheumatologists and radiologists may differ substantially in different settings, and not all of them have undergone specialized imaging training. Similar problems were reported in a study comparing the performance of untrained (local) investigators with trained (central) readers in recognizing structural MRI lesions of the SI joint in patients with recent inflammatory back pain (21). However, the same data set showed that the interreader agreement was better when fatty lesions were scored, and, in another analysis of patients from the same cohort, there was only minor disagreement regarding the recognition of BME (16). Nevertheless, this limitation should be regarded as an indication of a strong need for appropriate training in the interpretation of axial SpA–associated MRI lesions for both radiologists and rheumatologists.

Another limitation of our study is the fact that we used T1-weighted sequences for the identification of erosions. It has recently been shown that, for good (22) and earlier (23) identification of erosions, more advanced MRI sequences, such as 3-dimensional volumetric interpolated breath-hold examination (VIBE), may be more appropriate. We assume that when VIBE sequences are applied in daily practice instead of T1-weighted sequences, the diagnostic value of erosions will be even higher than reported here. The diagnosis of axial SpA in daily practice is a complex, multistep approach, and MRI has a rather established role in a previously proposed diagnostic algorithm (24). In the daily practice of some institutions, SI joint MRI may be an adjunct examination that follows a thorough clinical evaluation only when the pretest probability for a diagnosis of axial SpA is relatively high. It would indeed be interesting to explore the impact of SI joint MRI findings by radiologists and rheumatologists on the preimaging clinical evaluation. In our practice we very much appreciate the "independent" assessment of experienced musculoskeletal radiologists because it provides a more neutral view of what is really reflected on the MRI, in contrast to our clinical view, which may well be influenced by expectations, emotions, and prejudices. Nevertheless, the clinically essential issue is the step-by-step pattern recognition process that finally matters for a diagnosis of axial SpA. Therefore, it is essential to understand the impact of the different steps and especially the value and validity of the interpretation of SI joint MRI findings.

In conclusion, we show that the MRI lesions in the SI joint with the highest diagnostic value for the identification of axial SpA are structural lesions, alone or in combination with BME. While the presence of BME did not necessarily confirm a diagnosis of axial SpA, the absence of BME was associated with the absence of axial SpA, indicating that chronic changes such as erosions and fatty lesions are most relevant for a diagnosis of axial SpA in daily practice, but the presence of such lesions alone was not sufficient

for that diagnosis according to the rheumatologist. However, sclerosis and small erosions do also occur in other diseases such as osteitis condensans.

AUTHOR CONTRIBUTIONS

All authors were involved in drafting the article or revising it critically for important intellectual content, and all authors approved the final version to be published. Dr. Baraliakos had full access to all of the data in the study and takes responsibility for the integrity of the data and the accuracy of the data analysis.

Study conception and design. Baraliakos, Braun.
Acquisition of data. Baraliakos, Ghadir, Fruth.
Analysis and interpretation of data. Baraliakos, Fruth, Kiltz, Redeker, Braun.

REFERENCES

1. Braun J, Sieper J. Ankylosing spondylitis. Lancet 2007;369: 1379–90.
2. Rudwaleit M, van der Heijde D, Landewe R, Listing J, Akkoc N, Brandt J, et al. The development of Assessment of SpondyloArthritis international Society classification criteria for axial spondyloarthritis. Part II. Validation and final selection. Ann Rheum Dis 2009;68:777–83.
3. Moltó A, Paternotte S, Claudepierre P, Breban M, Dougados M. Effectiveness of tumor necrosis factor α blockers in early axial spondyloarthritis: data from the DESIR cohort. Arthritis Rheumatol 2014;66:1734–44.
4. Mandl P, Navarro-Compan V, Terslev L, Aegerter P, van der Heijde D, D'Agostino MA, et al. EULAR recommendations for the use of imaging in the diagnosis and management of spondyloarthritis in clinical practice. Ann Rheum Dis 2015;74:1327–39.
5. Sieper J, Rudwaleit M, Baraliakos X, Brandt J, Braun J, Burgos-Vargas R, et al. The Assessment of SpondyloArthritis international Society (ASAS) handbook: a guide to assess spondyloarthritis. Ann Rheum Dis 2009;68 Suppl 2:ii1–44.
6. Bakker PA, van den Berg R, Lenczner G, Thevenin F, Reijnierse M, Claudepierre P, et al. Can we use structural lesions seen on MRI of the sacroiliac joints reliably for the classification of patients according to the ASAS axial spondyloarthritis criteria? Data from the DESIR cohort. Ann Rheum Dis 2017;76:392–8.
7. Lambert RG, Bakker PA, van der Heijde D, Weber U, Rudwaleit M, Hermann KG, et al. Defining active sacroiliitis on MRI for classification of axial spondyloarthritis: update by the ASAS MRI working group. Ann Rheum Dis 2016;75:1958–63.
8. De Winter J, de Hooge M, van de Sande M, de Jong H, van Hoeven L, de Koning A, et al. Magnetic resonance imaging of the sacroiliac joints indicating sacroiliitis according to the Assessment of SpondyloArthritis international Society definition in healthy individuals, runners, and women with postpartum back pain. Arthritis Rheumatol 2018;70:1042–8.
9. Varkas G, de Hooge M, Renson T, de Mits S, Carron P, Jacques P, et al. Effect of mechanical stress on magnetic resonance imaging of the sacroiliac joints: assessment of military recruits by magnetic resonance imaging study. Rheumatology (Oxford) 2018;57:508–13.
10. Baraliakos X, Richter A, Feldmann D, Ott A, Buelow R, Schmidt CO, et al. Frequency of MRI changes suggestive of axial spondyloarthritis in the axial skeleton in a large population-based cohort of individuals aged <45 years. Ann Rheum Dis 2020;79:186–92.
11. Braun J, Baraliakos X, Kiltz U. Non-radiographic axial spondyloarthritis: a classification or a diagnosis? [letter]. Clin Exp Rheumatol 2016;34 Suppl 95:S5–6.
12. Weber U, Ostergaard M, Lambert RG, Pedersen SJ, Chan SM, Zubler V, et al. Candidate lesion-based criteria for defining a positive sacroiliac joint MRI in two cohorts of patients with axial spondyloarthritis. Ann Rheum Dis 2015;74:1976–82.
13. Haibel H, Rudwaleit M, Brandt HC, Grozdanovic Z, Listing J, Kupper H, et al. Adalimumab reduces spinal symptoms in active ankylosing spondylitis: clinical and magnetic resonance imaging results of a fifty-two–week open-label trial. Arthritis Rheum 2006; 54:678–81.
14. Rudwaleit M, Jurik AG, Hermann KG, Landewe R, van der Heijde D, Baraliakos X, et al. Defining active sacroiliitis on magnetic resonance imaging (MRI) for classification of axial spondyloarthritis: a consensual approach by the ASAS/OMERACT MRI group. Ann Rheum Dis 2009;68:1520–7.
15. Weber U, Hodler J, Kubik RA, Rufibach K, Lambert RG, Kissling RO, et al. Sensitivity and specificity of spinal inflammatory lesions assessed by whole-body magnetic resonance imaging in patients with ankylosing spondylitis or recent-onset inflammatory back pain. Arthritis Rheum 2009;61:900–8.
16. Van den Berg R, Lenczner G, Thevenin F, Claudepierre P, Feydy A, Reijnierse M, et al. Classification of axial SpA based on positive imaging (radiographs and/or MRI of the sacroiliac joints) by local rheumatologists or radiologists versus central trained readers in the DESIR cohort. Ann Rheum Dis 2015;74:2016–21.
17. Jones A, Bray TJ, Mandl P, Hall-Craggs MA, Marzo-Ortega H, Machado PM. Performance of magnetic resonance imaging in the diagnosis of axial spondyloarthritis: a systematic literature review. Rheumatology (Oxford) 2019;58:1955–65.
18. Weber U, Pedersen SJ, Zubler V, Rufibach K, Chan SM, Lambert RG, et al. Fat infiltration on magnetic resonance imaging of the sacroiliac joints has limited diagnostic utility in nonradiographic axial spondyloarthritis. J Rheumatol 2014;41:75–83.
19. Braun J, Baraliakos X. Active and chronic sacroiliitis, spondylitis and enthesitis. How specific are imaging findings for axial spondyloarthritis? [editorial]. Rheumatology (Oxford) 2019;58:1321–4.
20. Braun J, Baraliakos X, Buehring B, Fruth M, Kiltz U. Differential diagnosis of axial spondyloarthritis-axSpA mimics. Z Rheumatol 2019;78:31–42. In German.
21. Jacquemin C, Vargas RR, van den Berg R, Thevenin F, Lenczner G, Reijnierse M, et al. What is the reliability of non-trained investigators in recognising structural MRI lesions of sacroiliac joints in patients with recent inflammatory back pain? Results of the DESIR cohort. RMD Open 2016;2:e000303.
22. Diekhoff T, Greese J, Sieper J, Poddubnyy D, Hamm B, Hermann KA. Improved detection of erosions in the sacroiliac joints on MRI with volumetric interpolated breath-hold examination (VIBE): results from the SIMACT study. Ann Rheum Dis 2018;77:1585–9.
23. Baraliakos X, Hoffmann F, Deng X, Wang YY, Huang F, Braun J. Detection of erosions in sacroiliac joints of patients with axial spondyloarthritis using the magnetic resonance imaging volumetric interpolated breath-hold examination. J Rheumatol 2019; 46:1445–9.
24. Van den Berg R, de Hooge M, Rudwaleit M, Sieper J, van Gaalen F, Reijnierse M, et al. ASAS modification of the Berlin algorithm for diagnosing axial spondyloarthritis: results from the SPondyloArthritis Caught Early (SPACE)-cohort and from the Assessment of SpondyloArthritis international Society (ASAS)-cohort. Ann Rheum Dis 2013;72:1646–53.

Arthritis & Rheumatology
Vol. 73, No. 5, May 2021, pp 806–815
DOI 10.1002/art.41607

American College of Rheumatology
Empowering Rheumatology Professionals

Is Treatment in Patients With Suspected Nonradiographic Axial Spondyloarthritis Effective? Six-Month Results of a Placebo-Controlled Trial

Tamara Rusman,[1] Mignon A. C. van der Weijden,[1] Michael T. Nurmohamed,[2] Robert B. M. Landewé,[3] Janneke J. H. de Winter,[3] Bouke J. H. Boden,[4] Pierre M. Bet,[1] Carmella M. A. van der Bijl,[1] Conny van der Laken,[1] and Irene E. van der Horst-Bruinsma[1]

Objective. To investigate the efficacy of 16-week treatment with etanercept (ETN) in patients with suspected nonradiographic axial spondyloarthritis (SpA).

Methods. Tumor necrosis factor inhibitor–naive patients with inflammatory back pain with at least 2 SpA features and high disease activity (Bath Ankylosing Spondylitis Disease Activity Index score ≥4), without the requirement of a positive finding on magnetic resonance imaging (MRI) of the sacroiliac (SI) joint and/or elevated C-reactive protein (CRP) level, were randomized (1:1) to receive ETN (n = 40) or placebo (n = 40) for 16 weeks and subsequently were followed up for a further 8 weeks (to 24 weeks from baseline) without study medication. The primary end point was the Assessment of SpondyloArthritis international Society 20 (ASAS20) response at 16 weeks. Secondary end points included the Ankylosing Spondylitis Disease Activity Score (ASDAS) and changes in disease parameters, including the Bath Ankylosing Spondylitis Metrology Index (BASMI), CRP level, erythrocyte sedimentation rate (ESR), and Spondyloarthritis Research Consortium of Canada index scores (MRI of the SI joint), after 16 and 24 weeks.

Results. Patient characteristics at baseline were comparable between the ETN and placebo groups. At 16 weeks, there was no significant difference in the percentage of patients exhibiting ASAS20 response between the ETN group (6 patients [16.7%]) and the placebo group (4 patients [11.1%]) (relative risk 0.7 [95% confidence interval 0.2–2.2], $P = 0.5$). Only the ESR showed more improvement in the ETN group compared to the placebo group at 16 weeks (decreases of 2.2 mm/hour and 1.4 mm/hour, respectively), but the difference did not reach statistical significance. Between 16 and 24 weeks, without study medication, the BASMI, CRP level, and ESR had worsened to a greater extent in the ETN group compared to the placebo group, with the difference being significant for the CRP level.

Conclusion. This study shows that in patients with suspected nonradiographic axial SpA with high disease activity but without the requirement of a positive finding on SI joint MRI and/or elevated CRP level, treatment with ETN is not effective.

INTRODUCTION

According to the Assessment of SpondyloArthritis international Society (ASAS) classification criteria, axial spondyloarthritis (SpA) can be divided in 2 groups: patients with radiographic signs of sacroiliitis (radiographic axial SpA; ankylosing spondylitis [AS]) and patients without radiographic sacroiliitis (nonradiographic axial SpA) (1). Despite the availability of these classification criteria, there is still a lack of understanding of disease presentation and progression, especially in patients with nonradiographic axial SpA (2–5).

EudraCT database no. 2009-015515-40.
Supported by an unrestricted grant from Pfizer and ReumaNederland.
[1]Tamara Rusman, MSc, Mignon A. C. van der Weijden, MD, PhD, Carmella M. A. van der Bijl, MD, Conny van der Laken, MD, PhD, Irene E. van der Horst-Bruinsma, MD, PhD, Pierre M. Bet, PhD: VU University Medical Center, Amsterdam, The Netherlands; [2]Michael T. Nurmohamed, MD, PhD: VU University Medical Center and Reade, Amsterdam, The Netherlands; [3]Robert B. M. Landewé, MD, PhD, Janneke J. H. de Winter, MD, PhD: AMC University Medical Center, Amsterdam, The Netherlands; [4]Bouke J. H. Boden, MD: Onze Lieve Vrouwe Gasthuis (OLVG), Amsterdam, The Netherlands.

Dr. Landewé has received consulting fees and/or honoraria from AbbVie, Bristol Myers Squibb, Celgene, GlaxoSmithKline, UCB, Amgen, Lilly, Pfizer, Novartis, Galápagos, Gilead, and Janssen (less than $10,000 each) and research grants from AbbVie, Centocor, Novartis, Pfizer, and UCB. Dr. van der Horst-Bruinsma has received consulting fees or speaking fees from AbbVie, Bristol Myers Squibb, Pfizer, UCB, MSD, Lilly, and Novartis (less than $10,000 each) and unrestricted research grants from MSD, Pfizer, and AbbVie for investigator-initiated studies. No other disclosures relevant to this article were reported.

Address correspondence to Irene E. van der Horst-Bruinsma, MD, PhD, Amsterdam UMC VUMC, PO Box 7057, Amsterdam 1007 MB, The Netherlands. Email: ie.vanderhorst@amsterdamumc.nl.

Submitted for publication July 8, 2020; accepted in revised form December 1, 2020.

Inflammatory back pain is present in ~70% of patients diagnosed as having axial SpA, and therefore is an important clinical symptom of axial involvement (5,6). An algorithm described by Rudwaleit et al showed a high probability that AS could be diagnosed at the preradiographic stage in patients with chronic back pain with inflammatory back pain as the primary presenting symptom (7). Based on this algorithm, the probability that the patient has AS is at least 90% if inflammatory back pain plus 2 or 3 other features are present (8).

Currently, the ASAS classification criteria are widely accepted for use in clinical practice, although they were developed for the purpose of classification for study eligibility and not for clinical diagnosis (1,9–11). In order to classify axial SpA at an early stage of the disease, the ASAS classification criteria divide patients in 2 groups: patients who meet the "clinical arm" and patients who meet the "imaging arm." The "clinical arm" includes patients who are HLA–B27 positive and have 2 additional features of SpA, and the "imaging arm" includes patients with active inflammatory lesions of the sacroiliac (SI) joints as seen on magnetic resonance imaging (MRI) along with 1 additional feature of SpA (1,10).

In many reported studies, a positive SI joint finding on MRI has been one of the prerequisites for starting tumor necrosis factor inhibitor (TNFi) treatment in patients with nonradiographic axial SpA. The other criteria for starting TNFi therapy in nonradiographic axial SpA are unsuccessful treatment with at least 2 different nonsteroidal antiinflammatory drugs (NSAIDs) and increased C-reactive (CRP) levels in the setting of negative MRI findings (12,13). Increased CRP levels, however, were found in only 30% of patients with nonradiographic axial SpA (9,14), and in 59–64% of patients with nonradiographic axial SpA with high disease activity, inflammatory lesions of the SI joint are not detected on MRI. A patient population selected based on the ASAS classification criteria may therefore be different from the population seen in daily clinical practice (6,14).

In addition, in several studies MRI has shown false-positive results of bone marrow edema at the SI joint (not related to axial SpA disease). This is the case in ~23% of healthy individuals, 57% of postpartum women, and in recreational runners, professional athletes, and military recruits undergoing physical training. In all of these cases the MRI component of the ASAS classification criteria was fulfilled (15–17).

In most studies a higher rate of response to TNFi was observed in nonradiographic axial SpA patients who had elevated CRP levels and/or MRI-detected inflammatory lesions compared to patients without these factors (13,18–20). Only 2 randomized clinical trials on the efficacy of TNFi included patients with nonradiographic axial SpA without the abovementioned requirements (21,22), 1 of which did not include an objective scoring method for MRI-detected SI joint lesions (21). Both studies revealed a significant difference in response according to the ASAS criteria for 40% improvement (ASAS40) (23) between the placebo group (12.5–15%) and the treatment group (36–54.5%).

Data are lacking on the indications for biologic treatment in patients with suspected nonradiographic axial SpA who have low CRP levels and do not have active lesions seen on SI joint MRI. Therefore, a double blind, placebo-controlled clinical trial with the TNFi etanercept (ETN) was initiated. The primary aim of this proof-of-concept study was to assess the short-term efficacy of TNFi treatment, according to the ASAS20 response over 16 weeks, in patients with inflammatory back pain and suspected nonradiographic axial SpA with high disease activity, regardless of the CRP level or the presence of SI joint inflammation seen on MRI. "Disease activity" was used in this study as terminology by default, since there is no validation for the Bath Ankylosing Spondylitis Disease Activity Index (BASDAI) (24) in this patient group (25); we actually investigated the "level of symptoms" at 16 and 24 weeks. Secondary aims were to investigate the number of AS Disease Activity Score (ASDAS) (26) responders after 16 weeks, change from baseline in mean disease status, and the proportion of patients with inflammatory lesions of the SI joints seen on MRI at 16 and 24 weeks.

PATIENTS AND METHODS

Study population. Patients with chronic back pain and a suspicion of nonradiographic axial SpA were recruited from November 11, 2009 through August 29, 2014 at the rheumatology outpatient clinics of the VU University Medical Center (VUMC) and Reade/Jan van Breemen Research Institute, and via the website of the Dutch AS patient society (Dutch Axial Spondyloarthritis Foundation). Patients were eligible for inclusion if they were at least 18 years of age and fulfilled the Calin criteria for inflammatory back pain (27). Patients were enrolled based on the algorithm of Rudwaleit et al (7), with at least 2 SpA features according to the European Spondylarthropathy Study Group classification criteria (28) if HLA–B27 negative, and at least 1 SpA feature if B27 positive. In addition, patients had to have a high disease activity score (BASDAI ≥4) and insufficient response to at least 2 different NSAIDs. Patients were excluded if they had definite AS according to the modified New York criteria (29) or had received biologic treatment in the past (Table 1). Detailed descriptions of the inclusion and exclusion criteria have been published previously (30). Because of a slow enrollment rate in the first study period, adaptations of the inclusion criteria were made in the second half of 2011, allowing patients without inflammatory lesions seen on MRI to be included in the study. The study was approved by the local ethical review board, and all patients provided written informed consent prior to screening.

Treatment allocation and methods. The Prevention of the Progression of Very Early Symptoms in Ankylosing Spondylitis study was a randomized, double blind, placebo-controlled trial performed at VUMC (EudraCT number 2009-015515-40). Patients were randomly assigned (1:1) to receive ETN (25 mg twice weekly) or placebo. After 16 weeks, patients were followed up without study treatment for up to 3 years. Radiographs were obtained at baseline and after 1 year and 3 years of follow-up (only baseline data provided in the present report).

Table 1. PrevAS study inclusion and exclusion criteria*

Inclusion criteria	Exclusion criteria
Age ≥18 years	Diagnosis of radiographic axial SpA/AS according to the modified New York criteria (29)
Inflammatory back pain meeting the Calin criteria (27)†	
HLA–B27 positive with ≥1 SpA feature *or* HLA–B27 negative with ≥2 SpA features (1)‡	Previous treatment with a biologic agent
High disease activity score (BASDAI ≥4)	Contraindications to treatment with a TNFi
Insufficient response to ≥2 different NSAIDs	

* PrevAS = Prevention of the Progression of Very Early Symptoms in Ankylosing Spondylitis; BASDAI = Bath Ankylosing Spondylitis Disease Activity Index; TNFi = tumor necrosis factor inhibitor.
† Back pain with an insidious onset before the age of 45 years, chronic back pain persistence for at least 3 months, morning stiffness, improvement with exercise, pain at night.
‡ Spondyloarthritis (SpA) features include asymmetric arthritis, alternating buttock pain, dactylitis, enthesitis of the Achilles tendon or the plantar fascia, presence or history of psoriasis, inflammatory bowel disease (IBD), or acute anterior uveitis (AAU), first- or second-degree relative with ankylosing spondylitis (AS)/psoriasis/AAU/IBD, positive response to nonsteroidal antiinflammatory drugs (NSAIDs), and increased C-reactive protein level (≥10.0 mg/liter) or erythrocyte sedimentation rate (≥15 mm/hour).

The study drug ETN was supplied by Pfizer. Placebo ETN was developed and validated at the clinical pharmacology department of VUMC. The study medication was labeled at the VUMC central pharmacy and distributed to the VUMC outpatient pharmacy department for dispensing to study subjects. The pharmacist randomized the patients and provided the masked study medication to the study personnel. All investigators, including the study physician and research nurse, remained blinded with regard to the treatment until the last patient had completed the study. The study drug was self-administrated twice weekly with a subcutaneous injection that contained 25 mg of ETN or placebo. The normally distributed injections of ETN, in a dose of 50 mg administered once a week, were not feasible for this study because the placebo could only be produced in a 25-mg formulation.

Patients were allowed to continue taking analgesics, NSAIDs, disease-modifying antirheumatic drugs (DMARDs), and/or oral glucocorticoids (≤10 mg/day). The dosage had to be stable for 2 weeks prior to the baseline evaluation in the case of NSAIDs and oral glucocorticoids, and 4 weeks in the case of DMARDs; during the study, the dosage could be reduced or the treatment temporarily discontinued. Patients were allowed to receive intraarticular glucocorticoid injections. Treatment with any cytotoxic drugs, investigational drugs, or agents targeted at reducing TNF was not allowed during the first 16 weeks. All concomitant medication used during the study or changes in medication dosage were reported during each study visit.

Assessments. All study personnel and patients were blinded with regard to the randomization schedule and to treatment assignments until the last patient had completed the 3-year follow-up. In order to prevent influencing the study visit assessments (due to events caused by the medication such as injection site reactions), assessors who were not involved in the study performed the physical examinations and evaluated laboratory results.

Data collection. Demographic data were recorded, and disease-specific variables were assessed, including disease duration (duration of back pain at baseline), inflammatory back pain, SpA features, family history and presence of extraarticular manifestations such as uveitis, inflammatory bowel disease (IBD), and psoriasis, and use of concomitant medication (NSAIDs, DMARDs). Questionnaires on pain, overall well-being (Bath Ankylosing Spondylitis patient global score [31]), and quality of life (Short Form 36 health survey [32]) were administered during each visit. In addition, physical examinations were performed during each visit, including assessments to determine the Maastricht Ankylosing Spondylitis Enthesitis Score (MASES) (33) and swollen and tender joint counts (of 44 joints).

Time on study treatment (ETN or placebo) and compliance were determined. Compliance was calculated based on the number of injections taken divided by the number of injections expected. Safety parameters, such as adverse events, were registered during the follow-up visits. Safety analyses included all patients who had received ≥1 dose of study treatment.

Clinical efficacy parameters. Clinical efficacy was assessed based on the numbers of patients who met the ASAS20/40 response criteria and the ASDAS using the C-reactive protein level (ASDAS-CRP) response criteria (with clinically important improvement defined as a decrease in the ASDAS-CRP to ≤1.1 and major improvement defined as a decrease in the ASDAS-CRP to ≤2.0) (34) and based on the frequency of low disease activity (ASDAS-CRP <2.1) and inactive disease status according to the ASDAS-CRP criteria (ASDAS-CRP <1.3). Efficacy was measured throughout the first 16 weeks of treatment and at 24 weeks, i.e., 8 weeks after study-related treatment was discontinued. Other clinical outcome parameters were the Bath AS Functional Index (35), the Bath AS Metrology Index (BASMI [35]), global pain, and measures of inflammation, i.e., CRP (median value and proportion of patients with values exceeding the upper limit of normal [10.0 mg/liter]) and erythrocyte sedimentation rate (ESR).

MRI outcome measures. MR images were independently assessed by 2 expert readers (RBML and JJHdW), who were blinded with regard to treatment, patient characteristics, and sequence of the different MRIs. Potential reader discrepancies were resolved by consultation with a third reviewer (BJHB).

SI joint MRIs were assessed according to the ASAS definition (37,38). To quantify the extent of and evaluate the changes in active inflammation seen on SI joint MRI, the Spondyloarthritis Research Consortium of Canada (SPARCC) MRI Indices for Assessment of Spinal and SI Joint Inflammation in AS (SPARCC scores) (39,40) were used. A score of ≥2 was considered an indicator of SI joint inflammation shown on MRI. The mean

score from the 2 independent readers (or 3 readers if a third observer was needed) was used. Minimally important change in the SI joints was defined as a change in the SPARCC score of ≥2.5 (40). Intraclass correlation coefficients (ICCs) were calculated for change scores and presented as scores for absolute agreement.

Statistical analysis. The primary outcome measure of this trial was the ASAS20 response. It was assumed that 50% of the patients treated with ETN (intervention group) and 20% of the patients treated with placebo (control group) would experience an ASAS20 response. In order to statistically support a real difference of 30%, 40 patients per arm were required ($\alpha = 0.05$, $\beta = 0.20$). Data were presented as the mean ± SD or, in cases of skewed distribution, as the median and interquartile range (IQR).

The analysis included the intent-to-treat population, with baseline, 16-week, and 24-week clinical outcome measurements. All patients who received at least 1 dose of the study drug were included in the intent-to-treat analysis. Data up to the last known data point for a study patient were included for analyses.

The primary outcome ASAS20 response and secondary outcomes ASAS40 and ASDAS-CRP response according to clinically important improvement and major improvement were assessed by chi-square test or, if the data were skewed, by nonparametric tests, such as the Mann-Whitney U test. Categorical data were assessed by chi-square test. Post hoc analyses were performed for ASAS20 and ASDAS-CRP response at 16 weeks, according to baseline CRP levels (normal CRP/elevated CRP [>10.0 mg/liter]), SI joint inflammation based on SPARCC score (yes/no), HLA–B27 status (positive/negative), sex (male/female), and NSAID use (yes/no). ICC between readers' scores for change in inflammation parameters on MRI, between baseline and 16 weeks and between 16 weeks and 24 weeks, was calculated. Relative risks (RRs) and 95% confidence intervals (95% CIs) were calculated.

All statistical analyses were performed using SPSS for Windows version 26.0. Two-sided *P* values less than 0.05 were considered significant.

RESULTS

Patients and baseline characteristics. One hundred six consecutive patients were screened for this 16-week placebo-controlled trial. Twenty-six patients (24.5%) did not meet entry criteria, and 80 were enrolled (40 in the ETN group and 40 in the placebo group) (Figure 1).

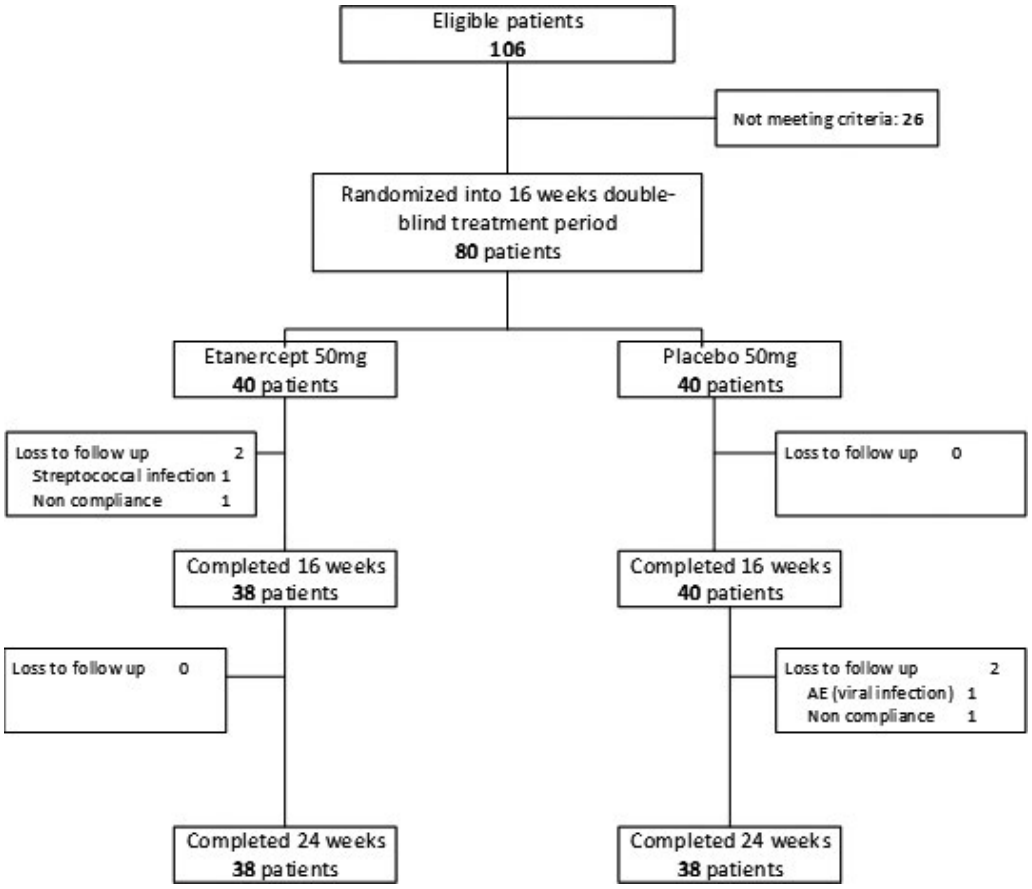

Figure 1. Flow chart showing disposition of the patients. AE = adverse event.

Table 2. Baseline demographic and clinical characteristics of the study population (n = 80)*

	Total	Etanercept (n = 40)	Placebo (n = 40)
Demographics			
Female	51 (64)	27 (68)	24 (60)
Age, mean ± SD years	34 ± 10	36 ± 10	33 ± 9
Clinical characteristics and extraarticular manifestations			
Disease duration, median (IQR) years	4.0 (2–9)	5.0 (2.5–14)	3.5 (2–8)
HLA–B27 positive	48 (60)	25 (63)	23 (58)
No. of SpA features, mean ± SD†	3 ± 1	3 ± 1	3 ± 2
Uveitis	15 (19)	10 (25)	5 (13)
Psoriasis	30 (38)	15 (38)	15 (38)
IBD	30 (38)	13 (33)	17 (43)
Concomitant medications			
NSAIDs	54 (68)	26 (65)	28 (70)
DMARDs	9 (11)	6 (15)	3 (8)

* There were no statistically significant differences between groups. Except where indicated otherwise, values are the number (%). IQR = interquartile range; DMARDs = disease-modifying antiinflammatory drugs.
† Spondyloarthritis (SpA) features include asymmetric arthritis, alternating buttock pain, dactylitis, enthesitis of the Achilles tendon or the plantar fascia, presence or history of psoriasis, inflammatory bowel disease (IBD), or acute anterior uveitis (AAU), first- or second-degree relative with ankylosing spondylitis (AS)/psoriasis/AAU/IBD, positive response to nonsteroidal antiinflammatory drugs (NSAIDs), and increased C-reactive protein level (≥10.0 mg/liter) or erythrocyte sedimentation rate (≥15 mm/hour).

HLA–B27 status, number of SpA features, and other baseline patient characteristics were comparable between the ETN and placebo groups (Tables 2 and 3). The majority of the patients were female (63.8%). The mean ± SD age was 34.5 ± 9.6 years, and 60.0% (48 of 80) were HLA–B27 positive. NSAIDs were used by 67.5% and DMARDs by 11.3% (most commonly methotrexate [n = 3] and sulfasalazine [n = 3]). The median CRP level was 2.5 mg/liter (IQR 2.5–6.0). The mean ± SD BASDAI was 5.1 ± 2.4, and the mean ± SD ASDAS-CRP was 2.8 ± 1.1, which indicates moderate-to-severe disease activity. The median SPARCC-SI joint score at baseline was 0.0 (IQR 0.0–3.1).

Exposure and compliance. Within the 16-week double-blind period, 2 patients, both in the ETN group, discontinued the study (1 had an unrelated adverse event [AE] [streptococcal infection] and the other patient was lost to follow-up) and 78 (97.5%) completed the treatment. Compliance with the study medication, i.e., the percentage of patients who took the medication according to the study protocol in the first 16 weeks, was 72.1%. There were no significant differences between the 2 treatment groups. In the follow-up period without treatment (week 16 to week 24), 2 patients, both in the placebo group, discontinued (1 had a viral infection and the other found the study visits too burdensome), which resulted in an analyzable population of 76 patients (95.0%) at 24 weeks (Figure 1). No patients initiated or restarted ETN or another biologic treatment during the week 16–24 follow-up period without study medication.

Clinical efficacy. At week 16, 10 of 72 patients (13.9%) had achieved an ASAS20 response: 6 (16.7%) in the ETN group and 4 (11.1%) in the placebo group. This difference was not statistically significant (RR 0.7 [95% CI 0.2–2.2], $P = 0.5$) (Table 4). ASAS40 response at 16 weeks was achieved in 6 of 72 patients (8.3%): 3 (8.3%) in each treatment group. An ASDAS-CRP response (clinically important improvement and major improvement) was achieved in 12 of 62 patients (19.4%): 8 (25.0%) in the ETN group and 4 (13.3%) in the placebo group. This difference was also not statistically significant (RR 0.5 [95% CI 0.2–1.6], $P = 0.2$) (Table 4). Separate assessments of clinically important improvement and major improvement showed no significant differences between the 2 treatments at 16 weeks (RR 0.3 [95% CI 0.1–1.4], $P = 0.1$ and RR 2.1 [95% CI 0.2–22], $P = 0.5$, respectively) (Table 4). Low disease activity according to the ASDAS-CRP at 16 weeks was achieved in 30 of 70 patients (42.9%): 44.1% in the ETN group and 41.7% in the placebo group (RR:0.9 [95% CI 0.6–1.6], $P = 0.8$). Inactive disease according to the ASDAS-CRP was achieved in 13 of 70 patients (18.6%): 20.6% in the ETN group and 16.7% in the placebo group (RR 0.8 [95% CI 0.3–2.2], $P = 0.7$). During the first 16 weeks, both the ESR and the pain score showed more improvement in the ETN group than in the placebo group (mean ± SD change –2.2 ± 5.2 mm/hour versus –1.4 ± 7.4 mm/hour and –1.4 ± 2.7 versus –0.8 ± 2.7, respectively).

Between 16 weeks and 24 weeks, without study medication, the mean BASMI, CRP level, and ESR worsened more in the ETN group compared to the placebo group (mean ± SD change 1.6 ± 9.9 versus –0.3 ± 1.6, 1.8 ± 5.3 mg/liter versus –0.4 ± 2.7 mg/liter [$P = 0.02$], and 3.2 ± 9.8 mm/hour versus 0.03 ± 8.2 mm/hour, respectively) (see Supplementary Table 1, on the *Arthritis & Rheumatology* website at http://onlinelibrary.wiley.com/doi/10.1002/art.41607/abstract). Mean disease activity scores are presented in Figure 2.

Table 3. Baseline data on the disease outcomes assessed in the study population (n = 80)*

	Total	Etanercept (n = 40)	Placebo (n = 40)
ASDAS-CRP	2.8 ± 1.1	2.8 ± 0.8	2.8 ± 1.4
BASDAI, 0–10 NRS	5.1 ± 2.4	4.8 ± 2.2	5.4 ± 2.3
BASFI, 0–10 NRS	3.8 ± 2.5	3.8 ± 2.6	3.9 ± 2.4
CRP, median (IQR) mg/liter	2.5 (2.5–6.0)	2.5 (2.5–5.5)	2.5 (2.5–6.5)
CRP >ULN, no. (%)	9.0 (13)	6 (17)	3 (9)
ESR, median (IQR) mm/hour	6.0 (2.0–11)	8.0 (2.5–14)	4.5 (2.0–9.0)
$BASMI_{lin}$, 0–10 NRS	2.6 ± 1.1	2.4 ± 1.1	2.7 ± 0.9
MASES, 0–13	7.9 ± 3.1	7.9 ± 2.6	7.9 ± 2.6
SJC (44 joints), median (IQR)	0.0 (0.0–0.0)	0.0 (0.0–0.0)	0.0 (0.0–0.0)
TJC (44 joints), median (IQR)	2.0 (0.0–5.0)	1.0 (0.0–4.0)	2.5 (0.0–6.8)
TJC >1, no. (%)	42 (53)	18 (45)	24 (60)
Patient global well-being, NRS	5.4 ± 2.4	5.2 ± 2.4	5.5 ± 2.5
Patient pain, NRS	5.2 ± 2.4	5.4 ± 2.5	5.1 ± 2.3
SF-36 PCS, 0–100 NRS	40.8 ± 6.6	40.6 ± 6.9	41.0 ± 6.4
SF-36 MCS, 0–010 NRS	40.0 ± 6.9	40.1 ± 7.0	39.9 ± 6.8
MRI			
SPARCC SI joint score (0–72), median (IQR)	0.0 (0.0–3.1)	0.0 (0.0–3.0)	0.0 (0.0–3.3)
SPARCC SI joint positive (≥2.0), no. (%)	18 (23)	8 (21)	10 (26)
ASAS positive, no. (%)	14 (18)	8 (21)	6 (15)
Conventional radiography			
BASRI (0–8), median (IQR)	0.3 (0.0–0.5)	0.3 (0.0–0.8)	0.1 (0.0–0.5)
BASRI positive (≥2.0), no. (%)	2 (3)	2 (5)	0 (0)
mSASSS (0–72), median (IQR)	2.0 (0.0–3.0)	2.0 (0.0–2.0)	2.0 (1.0–5.0)
mSASSS positive (≥2.0), no. (%)	41 (60)	23 (68)	18 (53)

* There were no statistically significant differences between groups. For all parameters except the swollen joint count (SJC) and tender joint count (TJC), data were not available from all 80 patients, as follows: For the Ankylosing Spondylitis Disease Activity Score using the C-reactive protein level (ASDAS-CRP), n = 67 (35 etanercept, 32 placebo). For the Bath Ankylosing Spondylitis Disease Activity Index (BASDAI), n = 78 (39 etanercept, 39 placebo). For the Bath Ankylosing Spondylitis Functional Index ($BASMI_{lin}$), n = 74 (38 etanercept, 36 placebo). For CRP, n = 69 (36 etanercept, 33 placebo). For erythrocyte sedimentation rate (ESR), n = 69 (33 etanercept, 36 placebo). For the Bath Ankylosing Spondylitis Metrology Index (linear measure) ($BASMI_{lin}$), (BASMI), n = 77 (38 etanercept, 39 placebo). For the Maastricht Ankylosing Spondylitis Enthesitis Score (MASES), n = 29 (9 etanercept, 20 placebo). For patient global well-being and patient pain assessments, n = 78 (39 etanercept, 39 placebo). For the Short Form 36 (SF-36) physical component score (PCS) and mental component score (MCS), n = 78 (39 etanercept, 39 placebo). For magnetic resonance imaging (MRI)–based Spondyloarthritis Research Consortium of Canada (SPARCC) sacroiliac (SI) joint findings and positive diagnosis of spondyloarthritis according to the Assessment of SpondyloArthritis international Society (ASAS) criteria, n = 78 (39 etanercept, 39 placebo). For the Bath Ankylosing Spondylitis Radiology Index (BASRI), n = 77 (39 etanercept, 38 placebo). For the modified Stoke Ankylosing Spondylitis Spine Score (mSASSS), n = 68 (34 etanercept, 34 placebo). Except where indicated otherwise, values are the mean ± SD. NRS = numerical rating scale; IQR = interquartile range; ULN = upper limit of normal.

MRI findings. Reliability of results between MRI readers was confirmed by ICC analysis. ICCs at baseline, 16 weeks, and 24 weeks were 0.76, 0.72, and 0.70, respectively. Positive SI joint MRI findings according to the ASAS definition were observed in 14 of 78 patients (17.9%) at baseline, 7 of 72 (9.7%) at 16 weeks, and 9 of 73 (12.3%) at 24 weeks. Comparison of the percentage

Table 4. Rates of treatment response at 16 weeks*

	Etanercept group, no. (%)	Placebo group, no. (%)	RR (95% CI)
Clinical response			
ASAS20	6 (17)	4 (11)	0.7 (0.2–2.2)
ASAS40	3 (8)	3 (8)	1.00 (0.2–4.6)
ASDAS-CRP response (CII and MI)	8 (25)	4 (13)	0.5 (0.2–1.6)
ASDAS-CRP (CII ≤1.1)	7 (22)	2 (7)	0.3 (0.1–1.4)
ASDAS-CRP (MI ≤2.0)	1 (3)	2 (7)	2.1 (0.2–22)
ASDAS-CRP (LDA <2.1)	15 (44)	15 (42)	0.9 (0.6–1.6)
ASDAS-CRP (ID <1.3)	7 (21)	6 (17)	0.8 (0.3–2.2)
Imaging response			
SPARCC SI joint MRI response (change ≥2.5)	8 (24)	7 (19)	0.8 (0.3–2.0)

* None of the relative risk (RR) values were statistically significant. For ASAS response, n = 72 (36 etanercept, 36 placebo). For ASDAS-CRP clinically important improvement (CII) and major improvement (MI), n = 62 (32 etanercept, 30 placebo). For ASDAS-CRP low disease activity (LDA) and inactive disease (ID), n = 70 (34 etanercept, 36 placebo). For SPARCC SI joint MRI response, n = 72 (35 etanercept, 37 placebo). 95% CI = 95% confidence interval (see Table 3 for other definitions).

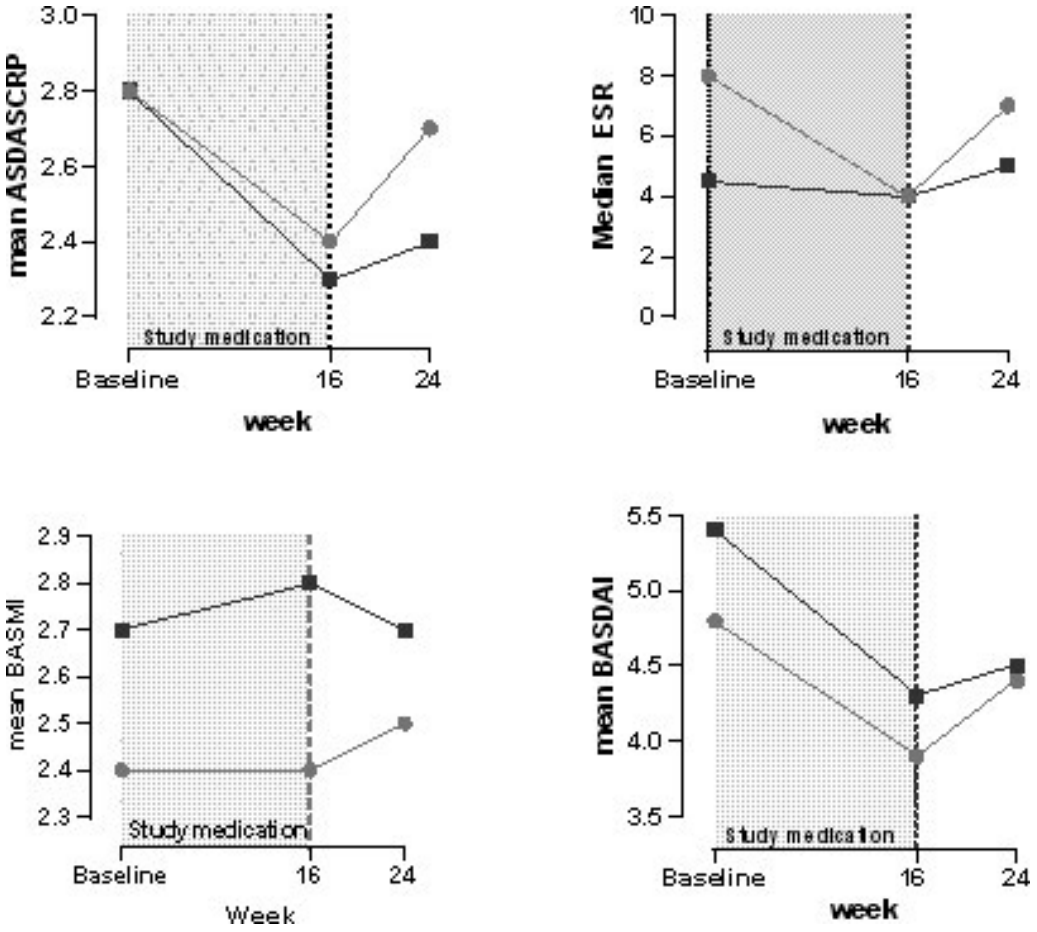

Figure 2. Disease activity by treatment group. Patients were treated for 16 weeks with etanercept (light gray circles) or placebo (dark gray squares). ASDAS-CRP = Ankylosing Spondylitis Disease Activity Score using the C-reactive protein level; ESR = erythrocyte sedimentation rate (mm/hour); BASMI = Bath Ankylosing Spondylitis Metrology Index; BASDAI = Bath Ankylosing Spondylitis Disease Activity Index.

of patients with positive SI joint MRI findings by treatment group revealed no significant differences (at baseline 20.5% in the ETN group versus 15.4% in the placebo group, at 16 weeks 8.6% in the ETN group versus 10.8% in the placebo group, and at 24 weeks 14.3% in the ETN group versus 10.5% in the placebo group; RR [95% CI] 0.8 [0.3–2.0], 1.3 [0.3–5.2], and 0.7 [0.2–2.5], respectively).

Median SPARCC scores in the total study population were 0.0 (IQR 0.0–3.1), 0.0 (IQR 0.0–0.0), and 0.0 (IQR 0.0–1.5) at baseline, 16 weeks, and 24 weeks, respectively. Differences between groups were negligible and not statistically significant at baseline and 16 weeks. At 24 weeks, the difference in the change in SPARCC score (median 0.0 [IQR 0.0–1.0] in the ETN group versus 0.0 [IQR 0.0–0.0] in the placebo group) appeared statistically significant (P = 0.03). Positive SI joint MRI findings according to the SPARCC score (score ≥2.0) were observed in 18 of 78 patients (23.1%) at baseline, 10 of 72 (13.9%) at 16 weeks, and 9 of 73 (12.3%) at 24 weeks. Comparison of the percentage of patients with positive SI joint MRI findings according to SPARCC score by treatment group revealed no significant differences (at baseline 20.5% in the ETN group versus 25.6% in the placebo group, at 16 weeks 8.6% in the ETN group versus 10.8% in the placebo group, and at 24 weeks 10.5% in the ETN group versus 14.3% in the placebo group; RR [95% CI] 1.3 [0.6–2.8], 0.9 [0.8–1.2], and 0.7 [0.2–2.5], respectively).

At 16 weeks, a minimally important change in the SPARCC-score (decrease of ≥ 2.5) had been achieved in 8 patients (23.5%) in the ETN group and 7 patients (19.4%) in the placebo group (RR 0.8 [95% CI 0.3–2.0], P = 0.7) (Table 4).

Subgroup analyses. Fulfillment of the ASAS20 response after 16 weeks was not related to an elevated CRP level (≥10.0 mg/liter) or a positive finding on SI joint MRI according to the SPARCC score or ASAS definition, or to both an elevated CRP level and a positive finding on SI joint MRI. Of the 10 patients who had achieved an ASAS20 response at 16 weeks, 2 had an elevated CRP level at baseline: 1 of 4 in the placebo group (25.0%) and 1 of 6 in the ETN group (16.7%). Comparison between patients with a positive finding on SI joint MRI according to the ASAS definition revealed no differences between treatment groups. Three patients with a positive finding on SI joint MRI according to the ASAS definition achieved an ASAS20 response: 1 of 4 in the placebo group

(25.0%) and 2 of 6 in the ETN group (33.3%). Results were similar when a positive finding on SI joint MRI was assessed using the SPARCC score. In both the ETN group and the placebo group, only 1 patient with both an elevated CRP level and a positive finding on SI joint MRI achieved an ASAS20 response. In addition, ASAS20 response at 16 weeks was not influenced by sex, age, NSAID use, DMARD use, HLA–B27 status, or history of IBD, uveitis, or psoriasis.

Safety. At 16 weeks, AEs were reported in 30 of 78 patients (38.5%): 15 of 38 (39.5%) in the ETN group and 15 of 40 (37.5%) in the placebo group. Observed AEs were mainly diarrhea (20.0%), colds, and flu (both 10.0%). One patient was diagnosed as having a serious infection (streptococcal infection) and was withdrawn from the study. In 8 of 30 cases (26.7%) a possible relationship to the study drug was considered, and in 4 of 30 cases (13.3%) the AE was classified as being probably related to the drug. A higher proportion of patients in the ETN group had an AE that was possibly or probably related to the study drug compared to the placebo group (7 [50%] versus 5 [31.0%]). In 6 of 30 cases (20.0%), treatment for the AE was needed. Study drug was temporarily stopped in only 2 of the 30 cases (6.7%), both in the placebo group. At 24 weeks, 21 of 76 patients (27.6%) reported having had an AE; these were probably not related to study treatment since no patient received a biologic between week 16 and week 24. However, 1 patient experienced a viral infection that was serious enough for the patient to discontinue study participation. One patient experienced an exacerbation of IBD.

DISCUSSION

In this study, 16 weeks of treatment with ETN in patients with suspected nonradiographic axial SpA and reportedly high disease activity, but without the requirement of a positive MRI finding and/or elevated CRP level, did not result in significant improvement of disease activity compared to placebo. To date there have been only 2 other published placebo-controlled trials that included patients with nonradiographic axial SpA with high disease activity without the requirement of elevated CRP level and/or inflammatory lesions seen on SI joint MRI (21,22). Both studies had a slightly higher proportion of HLA–B27–positive patients compared to our study (75% versus 60%). One study had a high percentage of patients with active MRI lesions at baseline (63% of the 46 patients) whereas the other had a lower percentage of patients with positive findings (32% of 200 patients), as in our study (23% of 80 patients). The numbers of patients with an increased CRP level are difficult to compare between studies, as each study used a different definition of elevated CRP level, ranging from ≥6 mg/liter to ≥10 mg/liter.

In the earlier studies a significantly higher rate of ASAS20 response was observed in the groups treated with TNFi compared to placebo (54.5–71.1% versus 12.5–40.0%), which contrasts with our present findings. In our study, the frequency of improvement in disease activity scores (ASAS20 and ASDAS-CRP) was not significantly different in the ETN group compared to the placebo group. Comparison of the ASAS20 and ASDAS-CRP response within the ETN group showed a slightly higher percentage of responders according to the ASDAS-CRP (25%) than according to the ASAS20 (17%). This might reflect the influence of TNFi on CRP levels rather than on other outcome parameters.

In the study by Haibel and colleagues (21), the proportion of patients with positive SI joint MRI findings at baseline was much higher than was observed in the present study (63% versus 32%). Being HLA–B27 positive and/or having active inflammatory lesions seen on SI joint MRI at baseline were predictors of an ASAS20 response in previous studies (20,21,41,42). Subanalyses by HLA–B27 status in our study revealed that B27-positive patients slightly more frequently had a positive SI joint MRI result according to the SPARCC score (26% versus 19%) and/or an elevated CRP level (≥10.0 mg/liter) compared to B27-negative patients. Due to the small number of patients in our study who had positive SI joint MRI findings at baseline, we were unable to detect differences in treatment efficacy between patients with and those without a positive SI joint MRI result and/or increased CRP levels. The relatively low number of patients with either a positive SI joint MRI finding (23%) and/or elevated CRP level (13%) at baseline in our study could be an explanation for the absence of an observed treatment effect in favor of ETN.

In addition, features of the patients included in this study might have more overlap with the "axial SpA group with peripheral signs," as described in a recent publication by Sepriano and colleagues (43), than with "pure axial SpA." This assumption is based on the low prevalence of positive SI joint MRI findings, high MASES scores, high number of patients with a tender joint count of >1 (52%), high proportion of female patients (64%), and high prevalence of psoriasis (38%) and IBD (38%), which are often associated with peripheral symptoms.

Our study cohort was relatively unique compared to most populations used in clinical trials of biologic treatments in axial SpA. With this unique study population some limitations emerged. For example, according to the algorithm described by Rudwaleit et al (7), many of the patients in our study population had a high probability (up to 90%) of developing a form of axial SpA, and this may be one of the reasons we did not demonstrate significant results regarding efficacy of ETN treatment. A longer-term study (3-year follow-up) is underway, which should allow us to further characterize the disease progression in this population. Questions could be raised as to whether our inclusion and exclusion criteria captured patients with true nonradiographic axial SpA. Although our patients are typical of those commonly seen in clinical practice, published scientific data are scant. This study adds to the body of evidence and provides some direction with regard to prescription of TNFi treatment in this patient group. The terminology "disease activity" was used by default, although we realize the disease

activity outcome measures used have not been validated for this study population, and what we actually measured was the "level of symptoms" (25). Another limitation is that we learned, during analysis of the data, that the study was underpowered to compare patients with versus those without a positive SI joint MRI finding and/or elevated CRP level, although the data were sufficient to analyze differences in disease activity between the 2 treatment groups. Furthermore, there was a long period of enrollment, due to the use of only one study center. The fact that we included only one center might, however, increase the reliability of the results by limiting the number of observers, and we have no reason to believe a faster enrollment rate would have influenced the study results.

In conclusion, the present results indicate that early treatment with ETN is not effective in patients with suspected nonradiographic axial SpA without the requirement of a positive MRI result or increased CRP level. It would be of interest to know whether our findings can be replicated in future investigations with comparable study populations and equal proportions of patients with and without positive SI joint MRI findings and elevated CRP levels.

AUTHOR CONTRIBUTIONS

All authors were involved in drafting the article or revising it critically for important intellectual content, and all authors approved the final version to be published. Ms Rusman had full access to all of the data in the study and takes responsibility for the integrity of the data and the accuracy of the data analysis.

Study conception and design. Van der Weijden, Bet, van der Horst-Bruinsma.

Acquisition of data. Rusman, van der Weijden, Landewé, de Winter, Boden, van der Bijl, van der Horst-Bruinsma.

Analysis and interpretation of data. Rusman, van der Weijden, Nurmohamed, Landewé, de Winter, Boden, van der Laken, van der Horst-Bruinsma.

REFERENCES

1. Rudwaleit M, van der Heijde D, Landewé R, Listing J, Akkoc N, Brandt J, et al. The development of Assessment of SpondyloArthritis international Society classification criteria for axial spondyloarthritis. Part II. Validation and final selection. Ann Rheum Dis 2009;68:777–83.
2. Deodhar A, Reveille JD, van den Bosch F, Braun J, Burgos-Vargas R, Caplan L, et al. The concept of axial spondyloarthritis: joint statement of the Spondyloarthritis Research and Treatment Network and the Assessment of SpondyloArthritis international Society in response to the US Food and Drug Administration's comments and concerns. Arthritis Rheumatol 2014;66:2649–56.
3. Kiltz U, Baraliakos X, Karakostas P, Igelmann M, Kalthoff L, Klink C, et al. Do patients with non-radiographic axial spondylarthritis differ from patients with ankylosing spondylitis? Arthritis Care Res (Hoboken) 2012;64:1415–22.
4. Robinson PC, Bird P, Lim I, Saad N, Schachna L, Taylor AL, et al. Consensus statement on the investigation and management of non-radiographic axial spondyloarthritis (nr-axSpA). Int J Rheum Dis 2014;17:548–56.
5. Rudwaleit M, Sieper J. Referral strategies for early diagnosis of axial spondyloarthritis [review]. Nat Rev Rheumatol 2012;8:262–8.
6. Rudwaleit M, Haibel H, Baraliakos X, Listing J, Märker-Hermann E, Zeidler H, et al. The early disease stage in axial spondylarthritis: results from the German Spondyloarthritis Inception Cohort. Arthritis Rheum 2009;60:717–27.
7. Rudwaleit M, van der Heijde D, Khan MA, Braun J, Sieper J. How to diagnose axial spondyloarthritis early. Ann Rheum Dis 2004;63:535–43.
8. Sieper J, Rudwaleit M. Early referral recommendations for ankylosing spondylitis (including pre-radiographic and radiographic forms) in primary care. Ann Rheum Dis 2005;64:659–63.
9. Proft F, Poddubnyy D. Ankylosing spondylitis and axial spondyloarthritis: recent insights and impact of new classification criteria. Ther Adv Musculoskelet Dis 2018;10:129–39.
10. Rudwaleit M, van der Heijde D, Landewe R, Akkoc N, Brandt J, Chou CT, et al. The Assessment of SpondyloArthritis international Society classification criteria for peripheral spondyloarthritis and for spondyloarthritis in general. Ann Rheum Dis 2011;70:25–31.
11. Gazeau P, Cornec D, Timsit MA, Dougados M, Saraux A. Classification criteria versus physician's opinion for considering a patient with inflammatory back pain as suffering from spondyloarthritis. Joint Bone Spine 2018;85:85–91.
12. Deodhar A, Reveille JD, van den Bosch F, Braun J, Burgos-Vargas R, Caplan L, et al. The concept of axial spondyloarthritis: joint statement of the spondyloarthritis research and treatment network and the Assessment of SpondyloArthritis international Society in response to the US Food and Drug Administration's comments and concerns. Arthritis Rheumatol 2014;66:2649–56.
13. Sieper J, van der Heijde D, Dougados M, Mease PJ, Maksymowych WP, Brown MA, et al. Efficacy and safety of adalimumab in patients with non-radiographic axial spondyloarthritis: results of a randomised placebo-controlled trial (ABILITY-1). Ann Rheum Dis 2013;72:815–22.
14. Braun J, Baraliakos X, Kiltz U, Heldmann F, Sieper J. Classification and diagnosis of axial spondyloarthritis: what is the clinically relevant difference? J Rheumatol 2015;42:31–8.
15. De Winter J, de Hooge M, van de Sande M, de Jong H, van Hoeven L, de Koning A, et al. Magnetic resonance imaging of the sacroiliac joints indicating sacroiliitis according to the Assessment of SpondyloArthritis international Society definition in healthy individuals, runners, and women with postpartum back pain. Arthritis Rheumatol 2018;70:1042–8.
16. Varkas G, de Hooge M, Renson T, De Mits S, Carron P, Jacques P, et al. Effect of mechanical stress on magnetic resonance imaging of the sacroiliac joints: assessment of military recruits by magnetic resonance imaging study [published erratum appears in Rheumatology (Oxford) 2018;57:588]. Rheumatology (Oxford) 2018;57:508–13.
17. Weber U, Jurik AG, Zejden A, Larsen E, Jørgensen SH, Rufibach K, et al. Frequency and anatomic distribution of magnetic resonance imaging features in the sacroiliac joints of young athletes: exploring "background noise" toward a data-driven definition of sacroiliitis in early spondyloarthritis. Arthritis Rheumatol 2018;70:736–45.
18. Moltó A, Paternotte S, Claudepierre P, Breban M, Dougados M. Effectiveness of tumor necrosis factor α blockers in early axial spondyloarthritis: data from the DESIR cohort. Arthritis Rheumatol 2014;66:1734–44.
19. Van der Heijde D, Baraliakos X, Hermann KA, Landewé RB, Machado PM, Maksymowych WP, et al. Limited radiographic progression and sustained reductions in MRI inflammation in patients with axial spondyloarthritis: 4-year imaging outcomes from the RAPID-axSpA phase III randomised trial. Ann Rheum Dis 2018;77:699–705.
20. Gulfe A, Kapetanovic MC, Kristensen LE. Efficacy and drug survival of anti-tumour necrosis factor-α therapies in patients with non-radiographic axial spondyloarthritis: an observational cohort study from Southern Sweden. Scand J Rheumatol 2014;43:493–7.

21. Haibel H, Rudwaleit M, Listing J, Heldmann F, Wong RL, Kupper H, et al. Efficacy of adalimumab in the treatment of axial spondylarthritis without radiographically defined sacroiliitis: results of a twelve-week randomized, double-blind, placebo-controlled trial followed by an open-label extension up to week fifty-two. Arthritis Rheum 2008;58:1981–91.
22. Sieper J, van der Heijde D, Dougados M, Maksymowych WP, Scott BB, Boice JA, et al. A randomized, double-blind, placebo-controlled, sixteen-week study of subcutaneous golimumab in patients with active nonradiographic axial spondyloarthritis. Arthritis Rheumatol 2015;67:2702–12.
23. Anderson JJ, Baron G, van der Heijde D, Felson DT, Dougados M. Ankylosing Spondylitis Assessment Group preliminary definition of short-term improvement in ankylosing spondylitis. Arthritis Rheum 2001;44:1876–86.
24. Garrett S, Jenkinson T, Kennedy LG, Whiteloc H, Gaisford P, Calin A. A new approach to defining disease status in ankylosing spondylitis: the Bath Ankylosing Spondylitis Disease Activity Index. J Rheumatol 1994;21:2286–91.
25. Kilic E, Kilic G, Akgul O, Ozgocmen S. Discriminant validity of the Ankylosing Spondylitis Disease Activity Score (ASDAS) in patients with non-radiographic axial spondyloarthritis and ankylosing spondylitis: a cohort study. Rheumatol Int 2015;35:981–9.
26. Lukas C, Landewé R, Sieper J, Dougados M, Davis J, Braun J, et al, for the Assessment of SpondyloArthritis international Society. Development of an ASAS-endorsed disease activity score (ASDAS) in patients with ankylosing spondylitis. Ann Rheum Dis 2009;68:18–24.
27. Calin A, Porta J, Fries JF, Schurman DJ. Clinical history as a screening test for ankylosing spondylitis. JAMA 1977;237:2613–4.
28. Dougados M, van der Linden S, Juhlin R, Huitfeldt B, Amor B, Calin A, et al. The European Spondylarthropathy Study Group preliminary criteria for the classification of spondylarthropathy. Arthritis Rheum 1991;34:1218–27.
29. Van der Linden S, Valkenburg HA, Cats A. Evaluation of diagnostic criteria for ankylosing spondylitis: a proposal for modification of the New York criteria. Arthritis Rheum 1984;27:361–8.
30. Rusman T, John MB, van der Weijden MA, Boden BJ, van der Bijl CM, Bruijnen ST, et al. Presence of active MRI lesions in patients suspected of non-radiographic axial spondyloarthritis with high disease activity and chance at conversion after a 6-month follow-up period. Clin Rheumatol 2020;39:1521–9.
31. Jones SD, Steiner A, Garrett SL, Calin A. The Bath Ankylosing Spondylitis Patient Global Score. Rheumatology (Oxford) 1996;35: 66–71.
32. Ware JE Jr, Snow KK, Kosinski M, Gandek B. SF-36 health survey: manual and interpretation guide. Boston: The Health Institute, New England Medical Center; 1993.
33. Heuft-Dorenbosch L, Spoorenberg A, van Tubergen A, Landewé R, van der Tempel H, Mielants H, et al. Assessment of enthesitis in ankylosing spondylitis. Ann Rheum Dis 2003;62:127–32.
34. Machado P, Landewé R, Lie E, Kvien TK, Braun J, Baker D, et al. Ankylosing Spondylitis Disease Activity Score (ASDAS): defining cut-off values for disease activity states and improvement scores. Ann Rheum Dis 2011;70:47–53.
35. Calin A, Garrett S, Whitelock H, Kennedy LG, O'Hea J, Mallorie P, et al. A new approach to defining functional ability in ankylosing spondylitis: the development of the Bath Ankylosing Spondylitis Functional Index. J Rheumatol 1994;21:2281–5.
36. Jenkinson TR, Mallorie PA, Whitelock HC, Kennedy LG, Garrett SL, Calin A. Defining spinal mobility in ankylosing spondylitis (AS): the Bath AS Metrology Index. J Rheumatol 1994;21:1694–8.
37. Maksymowych WP, Lambert RG, Ostergaard M, Pedersen SJ, Machado PM, Weber U, et al. MRI lesions in the sacroiliac joints of patients with spondyloarthritis: an update of definitions and validation by the ASAS MRI working group. Ann Rheum Dis 2019;78: 1550–8.
38. Rudwaleit M, Jurik AG, Hermann KG, Landewe R, van der Heijde D, Baraliakos X, et al. Defining active sacroiliitis on magnetic resonance imaging (MRI) for classification of axial spondyloarthritis: a consensual approach by the ASAS/OMERACT MRI group. Ann Rheum Dis 2009;68:1520–7.
39. Maksymowych WP, Inman RD, Salonen D, Dhillon SS, Williams M, Stone M, et al. Spondyloarthritis Research Consortium of Canada magnetic resonance imaging index for assessment of sacroiliac joint inflammation in ankylosing spondylitis. Arthritis Rheum 2005;53:703–9.
40. Maksymowych WP, Inman RD, Salonen D, Dhillon SS, Williams M, Stone M, et al. Spondyloarthritis Research Consortium of Canada magnetic resonance imaging index for assessment of sacroiliac joint inflammation in ankylosing spondylitis. Arthritis Rheum 2005;53:703–9.
41. Marzo-Ortega H, McGonagle D, O'Connor P, Hensor EM, Bennett AN, Green MJ, et al. Baseline and one year magnetic resonance imaging of the sacroiliac joint and lumbar spine in very early inflammatory back pain: relationship between symptoms, HLA-B27, and disease extent and persistence. Ann Rheum Dis 2008;68:1721–7.
42. Van Onna M, Jurik AG, van der Heijde D, van Tubergen A, Heuft-Dorenbosch L, Landewé R. HLA-B27 and gender independently determine the likelihood of a positive MRI of the sacroiliac joints in patients with early inflammatory back pain: a 2-year MRI follow-up study. Ann Rheum Dis 2011;70:1981–5.
43. Sepriano A, Ramiro S, van der Heijde D, van Gaalen F, Hoonhout P, Molto A, et al. What is axial spondyloarthritis? A latent class and transition analysis in the SPACE and DESIR cohorts [published erratum appears in Ann Rheum Dis 2020;79:e78]. Ann Rheum Dis 2020;79:324–31.

Arthritis & Rheumatology
Vol. 73, No. 5, May 2021, pp 816–825
DOI 10.1002/art.41598

American College of Rheumatology
Empowering Rheumatology Professionals

Long-Term Safety and Efficacy of Anifrolumab in Adults With Systemic Lupus Erythematosus: Results of a Phase II Open-Label Extension Study

W. Winn Chatham,[1] Richard Furie,[2] Amit Saxena,[3] Philip Brohawn,[4] Erik Schwetje,[4] Gabriel Abreu,[5] and Raj Tummala[4]

Objective. To investigate long-term safety and tolerability of anifrolumab, a human monoclonal antibody to the type I interferon (IFN) receptor subunit 1, in patients with moderate-to-severe systemic lupus erythematosus (SLE).

Methods. This 3-year, multinational, open-label extension study included adult patients who completed treatment (48 weeks of anifrolumab or placebo; 12-week follow-up) in the MUSE phase IIb randomized controlled trial (RCT). Patients initially received 1,000 mg of anifrolumab intravenously every 4 weeks, which was reduced to 300 mg every 4 weeks based on the benefit/risk profile established in the MUSE trial. Adverse events (AEs) were assessed monthly. Exploratory end points included the SLE Disease Activity Index 2000 (SLEDAI-2K), Systemic Lupus International Collaborating Clinics/American College of Rheumatology Damage Index (SDI), pharmacodynamics, and health-related quality of life (HRQoL).

Results. Of the 246 patients who completed the RCT, 218 (88.6%) enrolled in the open-label extension study, of which 139 (63.8%) completed 3 years of treatment. Approximately 69.7% of patients reported ≥1 AE during the first year of open-label extension treatment. Frequency and patterns of serious AEs and AEs of special interest over 3 years were consistent with those reported for 1 year of treatment in the RCT. Few patients (6.9%) discontinued treatment due to AEs. No new safety signals were identified. Improvement in the SLEDAI-2K was sustained over 3 years. SDI and Short Form 36 health survey scores remained stable. Neutralization of type I IFN gene signatures was maintained in the IFN-high population, and C3, C4, and anti–double-stranded DNA showed trends toward sustained improvement.

Conclusion. Long-term anifrolumab treatment demonstrates an acceptable safety profile with sustained improvement in SLE disease activity, HRQoL, and serologic measures.

INTRODUCTION

Systemic lupus erythematosus (SLE) is a chronic, clinically heterogeneous autoimmune disease that affects multiple organ systems (1,2). Despite the introduction of glucocorticoids and immunosuppressive drugs, there remains a major unmet need for more efficacious therapies (3,4); additionally, glucocorticoids and immunosuppressive drugs can have poor tolerability. Moreover, long-term use of standard SLE treatments, especially steroids, can contribute to subsequent morbidity (4). Given the necessity for long-term disease management in patients with SLE (2), novel treatments are needed to reduce overall disease activity, prevent organ damage, and reduce the concomitant use of steroids.

Anifrolumab is a fully human IgG1κ monoclonal antibody that binds to the type I interferon (IFN) receptor with high specificity and affinity, and inhibits activity of all type I IFNs (5,6). High serum levels and gene signature overexpression of type I IFN have been associated with SLE disease activity, severity, and clinical manifestations (7–11). Because the type I IFN

ClinicalTrials.gov identifier: NCT01753193.
Supported by AstraZeneca.
[1]W. Winn Chatham, MD: University of Alabama at Birmingham; [2]Richard Furie, MD: Zucker School of Medicine at Hofstra/Northwell, Great Neck, New York; [3]Amit Saxena, MD: New York University, New York; [4]Philip Brohawn, BS (current address: Immunocore LTD, Rockville, Maryland), Erik Schwetje, BS, Raj Tummala, MD: AstraZeneca, Gaithersburg, Maryland; [5]Gabriel Abreu, PhD: AstraZeneca, Gothenburg, Sweden.

Dr. Chatham has received research support from AstraZeneca. Dr. Furie has received consulting fees from AstraZeneca (more than $10,000) and research support from AstraZeneca. Dr. Saxena has received consulting fees from AstraZeneca (less than $10,000) and research support from AstraZeneca. Mr. Schwetje and Dr. Tummala own stock or stock options in AstraZeneca.
Address correspondence to Raj Tummala, MD, One MedImmune Way, Gaithersburg, MD 20878. Email: raj.tummala@astrazeneca.com.
Submitted for publication February 12, 2020; accepted in revised form November 17, 2020.

receptor mediates signaling by all type I IFNs, blockade with anifrolumab inhibits IFN-responsive gene expression and downstream inflammatory and immunologic processes (5,6,12). Thus, anifrolumab has potential as a targeted treatment for patients with SLE.

Anifrolumab demonstrated efficacy in the MUSE phase IIb randomized controlled trial (RCT; Study 1013) (13), with improvement in a range of clinical end points, including the SLE Responder Index (14), British Isles Lupus Assessment Group (BILAG)–based Composite Lupus Assessment (15), Cutaneous Lupus Erythematosus Disease Area and Severity Index (16,17), and swollen and tender joint counts (13). Anifrolumab treatment also resulted in sustained neutralization of the type I IFN gene signature throughout the 1-year study, and very few patients developed antidrug antibodies to anifrolumab (13). In addition, anifrolumab had an acceptable safety profile, with similar frequency and patterns of serious adverse events (SAEs) across treatment groups, although patients receiving anifrolumab experienced a dose-dependent increase in herpes zoster reactivation (13).

Here we report results of an extension of the phase IIb RCT, which included open-label anifrolumab treatment for up to 3 years. The primary objective was to evaluate the long-term safety and tolerability of anifrolumab. A secondary objective was to evaluate the immunogenicity of anifrolumab, and exploratory objectives were to evaluate efficacy, SLE-related biomarkers, and health-related quality of life (HRQoL).

PATIENTS AND METHODS

Study design and treatment. The MUSE open-label extension (Study 1145, ClinicalTrials.gov identifier: NCT01753193, and protocol: CD-IA-MEDI-546-1145) was a 3-year, multinational, multicenter study of adults with moderate-to-severe SLE who completed randomized treatment with anifrolumab 300 mg or 1,000 mg or placebo given intravenously in the MUSE RCT. Patients were eligible for the open-label extension if they completed RCT treatment and follow-up, met the open-label extension inclusion criteria, and had no safety issues that led to exclusion (Figure 1). This study was conducted from March 28, 2013 to July 18, 2018.

All patients initially received intravenous (IV) anifrolumab 1,000 mg every 4 weeks in the open-label extension. Based on the benefit/risk profile from the RCT, the 300-mg dose was selected for phase III studies, and the dosage in the open-label extension was subsequently reduced from 1,000 mg to 300 mg every 4 weeks. Patients received their last dose of RCT treatment on day 337, had their last study assessment visit on day 365, and had their last follow-up visit on day 422 of the RCT. The first dose of open-label anifrolumab treatment was generally administered within 28 days of the last follow-up visit of the RCT (i.e., within 85–113 days of the last dose in the RCT). Baseline was day 1 of the open-label extension (RCT day 422), prior to anifrolumab administration. Patients received anifrolumab over 156 weeks, with the final open-label dose administered at week 156. There was an

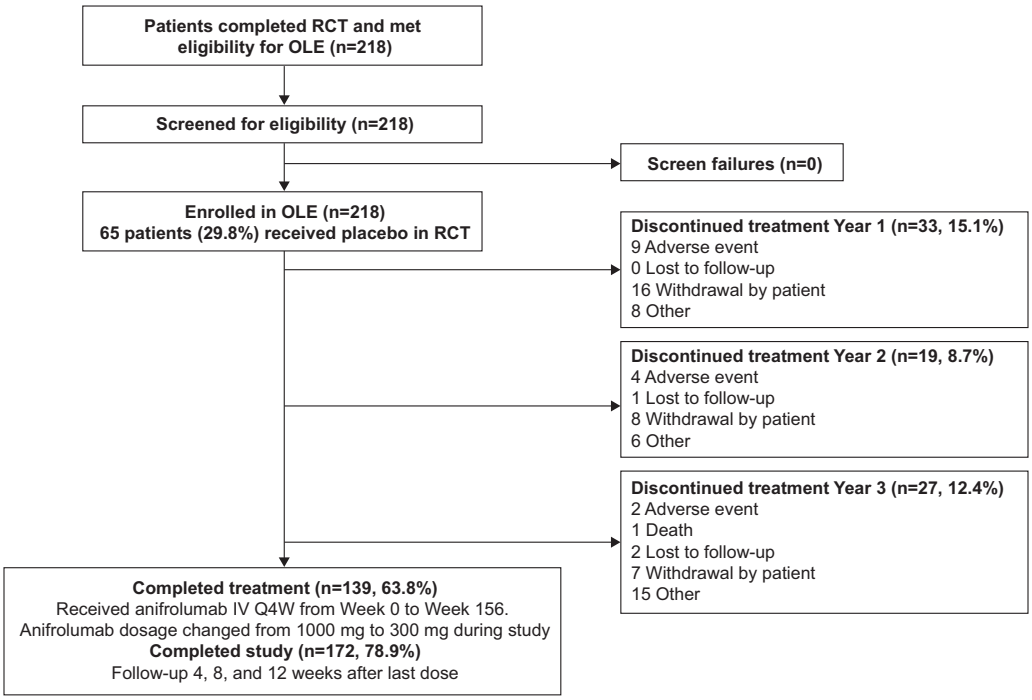

Figure 1. Flow chart of the open-label extension (OLE) study design and patient disposition. RCT = randomized controlled trial; IV = intravenous; Q4W = every 4 weeks.

85-day follow-up period that included an end-of-treatment period visit at week 160 and final follow-up visit at week 168.

This study was approved by the research ethics committees at each study site and was performed in accordance with the Declaration of Helsinki, the International Conference on Harmonisation Note for Guidance on Good Clinical Practice, and applicable regulatory requirements. All patients provided written informed consent to participate.

Patients. All patients in the open-label extension had completed the RCT. Patients ages 18–65 years at screening were enrolled in the RCT only if they fulfilled ≥4 of the 11 1997 American College of Rheumatology (ACR) classification criteria for SLE (13,18). Other inclusion criteria for the RCT included an SLE Disease Activity Index 2000 (SLEDAI-2K) score of ≥6 (19), ≥1 A or ≥2 B BILAG-2004 items (20), a clinical SLEDAI-2K score of ≥4, and a physician's global assessment of disease activity of ≥1 on a visual analog scale from 0 (no disease) to 3 (severe disease) during screening. In the RCT, patients were excluded if they had active and severe lupus nephritis or neuropsychiatric SLE (13).

For inclusion in the open-label extension, patients must have completed RCT treatment with anifrolumab or placebo to day 337 and attended the last study assessment visit (day 365) and follow-up visit (day 422). Patients were excluded if they underwent major surgery within 8 weeks before enrollment in the open-label extension or elective major surgery planned during the study period or if they received azathioprine (>200 mg/day), mycophenolate mofetil/mycophenolic acid (>2.0 gm/day), methotrexate (>25 mg/week), any vaccine within 4 weeks prior to enrollment, or BCG vaccine within 1 year of enrollment.

Standard-of-care treatments for SLE were allowed throughout the open-label extension and were modified at the discretion of the investigator within protocol-defined limits. Permitted SLE medications included oral glucocorticoids (up to 40 mg/day of prednisone or equivalent), intramuscular glucocorticoids, intraarticular/tendon sheath/bursa glucocorticoid injections, antimalarials, immunosuppressants (methotrexate, mycophenolate mofetil/mycophenolic acid, and azathioprine), nonsteroidal anti-inflammatory drugs (NSAIDs), analgesics, and topical therapy.

Safety and efficacy assessments. Safety and tolerability of anifrolumab were assessed by monitoring AEs, serious AEs, serious AEs of special interest, clinical laboratory tests, and immunogenicity throughout the study. Nonserious AEs were recorded at each monthly visit only during the first year of the study. SAEs, including those of special interest, were recorded at each visit throughout the 3-year period. AEs of special interest were defined as abnormal hepatic function, new or reactivated tuberculosis (TB) infection, herpes zoster infection, malignant neoplasms, infusion, hypersensitivity and anaphylactic reactions, and vasculitis.

Efficacy was assessed periodically during visits throughout the treatment and follow-up periods. Disease activity was measured with SLEDAI-2K (19) every 3 months. The Systemic Lupus International Collaborative Clinics/ACR Damage Index (SDI) (21), measured every 6 months, was used to evaluate organ damage. Impact on HRQoL was assessed every 6 months using the

Table 1. Baseline characteristics of the patients in the open-label extension and the RCT*

	Open-label extension (n = 218)	RCT (n = 307)
Age, mean ± SD years	40.8 ± 12.2	39.8 ± 12.2
Female	203 (93.1)	287 (93.5)
Body mass index, mean ± SD kg/m^2	27.3 ± 6.8†	26.5 ± 6.2
Race		
White	87 (39.9)	128 (41.7)
Other‡	85 (39.0)	109 (35.5)
African American	29 (13.3)	41 (13.4)
Asian	11 (5.0)	22 (7.2)
American Indian/Alaskan Native	4 (1.8)	5 (1.6)
Multiple	2 (0.9)	2 (0.7)
Ethnicity		
Hispanic or Latino	104 (47.7)	129 (42.0)
Not Hispanic or Latino	114 (52.3)	178 (58.0)
SLEDAI-2K global score		
Mean ± SD	4.9 ± 3.9	10.9 ± 4.1
Median (range)	4.0 (0–22)	10.0 (4–29)
SDI score		
Mean ± SD	0.6 ± 1.0	0.7 ± 1.1
Median (range)	0.0 (0–5)	0.0 (0–7)
4-gene IFN gene signature		
High	143/213 (67.1)	231 (75.2)
Low	70/213 (32.9)	76 (24.8)
ANA positive	203/212 (95.8)	299 (98.0)
Anti-dsDNA positive	57/205 (27.8)§	185 (76.8)/79 (25.9)¶
Abnormal (low) complement C3	61/206 (29.6)	119 (39.0)
Abnormal (low) complement C4,	49/206 (23.8)	74 (24.3)
SLE medication#		
Glucocorticoids	159 (72.9)	258 (84.0)
Oral glucocorticoid dosage ≥10 mg/dl (prednisone or equivalent)	60 (37.7)	182 (59.3)
Antimalarial	149 (68.3)	219 (71.3)
Other immunosuppressants		
Methotrexate	45 (20.6)	60 (19.5)
Azathioprine	34 (15.6)	63 (20.5)
Mycophenolate	25 (11.5)	33 (10.7)
Leflunomide	1 (0.5)	0

* Except where indicated otherwise, values are the number (%). RCT = randomized controlled trial; SLEDAI-2K = Systemic Lupus Erythematosus Disease Activity Index 2000; SDI = Systemic Lupus International Collaborative Clinics/American College of Rheumatology Damage Index; IFN = interferon; ANA = antinuclear antibody; anti-dsDNA = anti–double-stranded DNA; SLE = systemic lupus erythematosus.
† n = 166.
‡ Includes patients from Latin America who could not identify with the race definitions provided (e.g., Mestizo).
§ Multiple assays.
¶ Farr/multiplex immunoassays.
# Patients may have received >1 drug.

Short Form 36 version 2 (SF-36v2) health survey (22,23) physical component summary, mental component summary, and domain scores.

Serologic measures, including C3, C4, CH50, and anti–double-stranded DNA (anti-dsDNA), were assessed every 12 weeks (as part of the SLEDAI-2K assessment) during treatment and on days 28 and 85 of the follow-up period. Anti-dsDNA was initially measured using a Farr assay. Due to the discontinuation of the assay during the study, an enzyme-linked immunosorbent assay (ELISA) was used for the remainder of the study. Blood samples were collected for pharmacodynamic and immunogenicity assessments. A 4-gene test was used at open-label extension baseline to classify patients as type I IFN gene signature high or low. A 21-gene assay was used to determine type I IFN gene signature expression as a pharmacodynamic marker at baseline, every 12 weeks from week 12 to week 48, every 24 weeks starting at week 72 through the end of treatment, and again on days 28 and 85 of the follow-up period. Other safety assessments included urinalysis, measurement of vital signs, physical examination, monitoring for Cushingoid features, and electrocardiography (ECG).

Statistical analysis. No formal statistical hypothesis testing was performed; all analyses were descriptive. Analyses included all patients who received ≥1 dose of anifrolumab in the open-label extension. Data from day 396 of the RCT were used as baseline data for patients with missing baseline data from the open-label extension (open-label extension day 1/RCT day 422). Efficacy was evaluated descriptively by visit using raw scores and change from baseline. The last observation carried forward approach was used to impute missing SLEDAI-2K component scores if ≥1 component of the SLEDAI-2K was missing. AEs were reported by preferred term and coded according to the Medical Dictionary for Regulatory Activities version 21.0.

RESULTS

Patient disposition and baseline characteristics. In the RCT, 305 patients were randomized to receive placebo (n = 102), anifrolumab 300 mg (n = 99), or anifrolumab 1,000 mg (n = 104). Of the 246 patients who completed the RCT, 218 (88.6%) met the eligibility criteria, were enrolled, and received treatment in the open-label extension (Figure 1) at 59 sites across 13 countries. Of the patients in the open-label extension, 153 (70.2%) had received anifrolumab and 65 (29.8%) had received placebo in the RCT. A total of 139 of 218 patients (63.8%) completed open-label extension treatment, and 172 of 218 patients (78.9%) completed the study procedures after treatment completion or discontinuation. The most common reason for treatment discontinuation was patient withdrawal of consent (31 of 218; 14.2%); 15 patients (6.9%) discontinued treatment due to an AE. Of the 31 patients who withdrew consent, 9 had ongoing AEs at the end of the study; the majority of cases were considered by the investigator to be not related to the drug. It should be noted that these AEs may not have been the cause for withdrawal of consent. In 29 additional patients (13.3%), treatment was discontinued for other reasons, including pregnancy, sponsor closing site, investigator decision, receipt of medication prohibited by the protocol, missed visits/doses, patient relocation, and patient not adhering to protocol. Nine of these 29 patients had ongoing AEs at the end of the open-label extension. Three patients (1.4%) were lost to follow-up, and 1 (0.5%) died prior to study completion.

The majority of patients (64.2%) received ≥35 doses of anifrolumab in the open-label extension (not including exposure in the RCT). Of the 218 patients, 154 (70.6%) were treated for ≥30 months, for a total of 542 patient-years of exposure. All 218 patients received ≥1 dose of anifrolumab 1,000 mg before the dose was modified to 300 mg, and 191 of 218 patients (87.6%) received ≥1 dose of anifrolumab 300 mg (i.e., 27 patients discontinued treatment before the anifrolumab dose was reduced to 300 mg, after

Table 2. Adverse events during anifrolumab treatment in the first year of the 3-year open-label extension and during the 1-year RCT

Adverse event category, no. (%)	Anifrolumab treatment in open-label extension (n = 218)	Anifrolumab treatment (both dosages) in RCT (n = 204)*
Any adverse event	152 (69.7)	174 (85.3)
Adverse events in ≥5% of patients		
Nasopharyngitis	24 (11.0)	24 (11.8)
Bronchitis	21 (9.6)	16 (7.8)
Headache	14 (6.4)	24 (11.8)
Upper respiratory tract infection	14 (6.4)	24 (11.8)
Diarrhea	10 (4.6)	12 (5.9)
Urinary tract infection	9 (4.1)	22 (10.8)
Influenza	6 (2.8)	14 (6.9)
Sinusitis	6 (2.8)	12 (5.9)
Cough	4 (1.8)	11 (5.4)
Herpes zoster	3 (1.4)	15 (7.4)

* From ref. 13. Data from 101 patients who received placebo during the randomized controlled trial (RCT) were not included.

receiving 1–17 doses of anifrolumab 1,000 mg). Of the 218 patients, 126 (57.8%) received ≥10 doses of anifrolumab 1,000 mg, and 172 (78.9%) received ≥10 doses of anifrolumab 300 mg.

Baseline characteristics of the patients in the open-label extension population were similar to those of patients in the RCT. Most patients were female (93.1%); 39.9% were white, 13.3% were African American, and 5.0% were Asian. The mean age was 40.8 years (range 19–66 years) (Table 1). At open-label extension baseline, 159 of 218 patients (72.9%) were receiving glucocorticoids, 60 (37.7%) of which were receiving prednisone or equivalent glucocorticoids ≥10 mg/day. Additionally, the majority of patients were receiving antimalarials (149 of 218; 68.3%) (Table 1).

The mean ± SD baseline SDI score in the open-label extension (0.6 ± 1.0) was similar to the baseline SDI score in the RCT (0.7 ± 1.1). The mean ± SD baseline SLEDAI-2K global score, however, was lower in the open-label extension (4.9 ± 3.9) than at baseline of the RCT (10.9 ± 4.1) (Table 1), reflecting decreased disease activity. At open-label extension baseline, ~25% of patients had abnormal levels of anti-dsDNA (57 of 205; 27.8%) and C4 (49 of 206; 23.8%). These values for serologic measures were comparable to those at RCT baseline. However, the percentage of patients with abnormal C3 levels at baseline was lower in the open-label extension (61 of 206; 29.6%) than in the RCT (119 of 307; 39.0%) (Table 1). Most patients in the open-label extension had high type I IFN gene signature at baseline (143 of 213; 67.1%); the percentage of RCT patients with high type I IFN gene signature at baseline was 75.2% (231 of 307). Anifrolumab-treated patients who completed the RCT and did not enroll in the open-label extension had demographic and disease characteristics (e.g., SLEDAI-2K, IFN gene signature, C3, C4) similar to those who continued in the open-label extension.

Table 3. All serious adverse events, including serious adverse events of special interest, during the 3-year open-label extension and during the 1-year RCT

	Anifrolumab treatment in open-label extension (n = 218)*	Anifrolumab treatment (both dosages) in RCT (n = 204)†
Patients with ≥1 serious adverse event, no. (%)	50 (22.9)	34 (16.7)
Serious adverse events in ≥2 patients, no. (%)		
Systemic lupus erythematosus flares	5 (2.3)	6 (2.9)
Pneumonia	4 (1.8)	4 (2.0)
Bronchitis	2 (0.9)	0 (0.0)
Chikungunya virus infection	2 (0.9)	0 (0.0)
Gastroenteritis	2 (0.9)	1 (0.5)
Post-procedural infection	2 (0.9)	0 (0.0)
Urinary tract infection	2 (0.9)	1 (0.5)
Femur fracture	2 (0.9)	0 (0.0)
Osteonecrosis	2 (0.9)	0 (0.0)
Spinal column stenosis	2 (0.9)	0 (0.0)
Nephrotic syndrome	2 (0.9)	0 (0.0)
Dysfunctional uterine bleeding	2 (0.9)	0 (0.0)
Pleural effusion	2 (0.9)	0 (0.0)
Herpes zoster	1 (0.5)	2 (1.0)
Chest pain	0 (0.0)	3 (1.5)
Influenza	0 (0.0)	3 (1.5)
Appendicitis	0 (0.0)	2 (1.0)
Headache	0 (0.0)	2 (1.0)
Patients with ≥1 serious adverse event of special interest, no. (%)	25 (11.5)	25 (12.3)
Herpes zoster infection	11 (5.0)	15 (7.4)
Infusion-related reaction	4 (1.8)	6 (2.9)
Hypersensitivity	2 (0.9)	0 (0.0)
Drug hypersensitivity	1 (0.5)	0 (0.0)
Infusion-related nausea	1 (0.5)	0 (0.0)
Latent tuberculosis	6 (2.8)	2 (1.0)
Vasculitis	2 (0.9)	0 (0.0)
Malignancies	1 (0.5)‡	2 (1.0)§
Varicella	0 (0.0)	1 (0.5)
Mycobacterium tuberculosis complex test positive	0 (0.0)	1 (0.5)

***** Events occurred from the date of the first dose of anifrolumab in the open-label extension (i.e., not including the randomized controlled trial [RCT]) until the last dose plus 85 days.
† Some data from ref. 13. Data from 101 patients who received placebo during the RCT were not included.
‡ Event of Hodgkin's disease.
§ Events of invasive ductal breast carcinoma and malignant lung neoplasm.

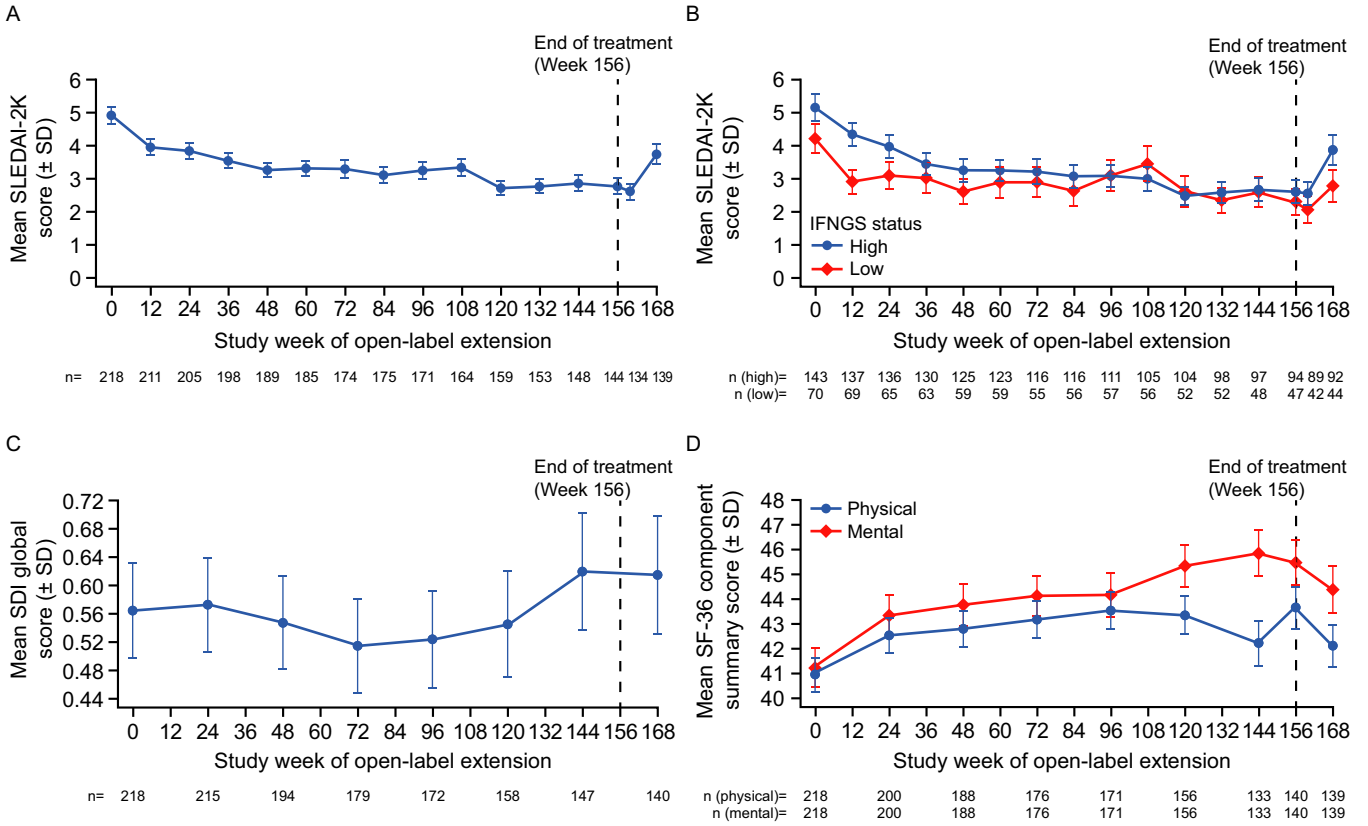

Figure 2. Mean Systemic Lupus Erythematosus Disease Activity Index 2000 (SLEDAI-2K), Systemic Lupus International Collaborative Clinics/American College of Rheumatology Damage Index (SDI) global score, and Short Form 36 health survey (SF-36) component summary scores from baseline to week 168. **A** and **B**, SLEDAI-2K score in all patients (**A**) and by type I interferon gene signature (IFNGS) status (**B**) during open-label treatment with anifrolumab. **C** and **D**, SDI global score (**C**) and SF-36 physical and mental component summary scores (**D**) during treatment with anifrolumab.

Safety. AEs that occurred during the first year of the 3-year open-label extension and during the 1-year RCT (in the anifrolumab treatment group) are shown in Table 2. During year 1 of the open-label extension, 152 of 218 patients (69.7%) experienced ≥1 AE. The most frequent AEs were nasopharyngitis (11.0%), bronchitis (9.6%), headache (6.4%), and upper respiratory tract infection (6.4%). Severe AEs (grade ≥3) were reported by 30 of 218 patients (13.8%) in year 1. The most frequent severe AEs included bronchitis (3 patients; 1.4%), gastroenteritis (2 patients; 0.9%), pharyngitis (2 patients; 0.9%), osteonecrosis (2 patients; 0.9%), and SLE flares (2 patients; 0.9%). The overall frequency of AEs was lower during the first year of the 3-year open-label extension than during the year-long RCT period (69.7% versus 85.3%).

All SAEs, including those of special interest, throughout the 3-year open-label extension and 1-year RCT are shown in Table 3. Over the entire open-label extension period, 50 of 218 patients (22.9%) had ≥1 SAE. The most common SAEs were SLE flares (5 patients; 2.3%) and pneumonia (4 patients; 1.8%). One patient (0.5%) died due to pneumonia after receiving 32 doses of anifrolumab (16 1,000-mg doses and 16 300-mg doses); the patient had received placebo in the RCT. Throughout the open-label extension, 138 of 218 patients (63.3%) had infections and infestations, of whom 24 (17.4%) were considered to have SAEs. Regarding AEs of special interest, herpes zoster infection was reported in 11 of 218 patients (5.0%); 2 events were disseminated, and neither event was serious. Few patients experienced infusion-related reactions (4 of 218; 1.8%) or hypersensitivity including drug hypersensitivity (3 of 218; 1.4%). No patients experienced anaphylaxis. Overall, 6 of 218 patients (2.8%) experienced latent tuberculosis (TB) infection, including 1 serious case. Latent TB infection in this study was defined as a new positive and confirmed QuantiFERON-TB Gold in-tube test result with no evidence of active TB. There were no events of new or reactivated TB reported in the study. Vasculitis was reported in 2 of 218 patients (0.9%), with 1 event of grade 3 severity.

Efficacy. The mean ± SD SLEDAI-2K global score was 4.9 ± 3.9 at baseline and 2.5 ± 2.7 at week 160, with a mean change of –2.1 from baseline to week 160. By week 168 (12 weeks after last dose), the mean change from baseline was –0.9 (Figure 2A). Approximately 64.9% of patients (37 of 57 patients with available data) with a baseline SLEDAI-2K score ≥6 achieved a ≥4-point reduction, and 27.9% (31 of 111 patients with available data) with a baseline SLEDAI-2K score >0 achieved a SLEDAI-2K

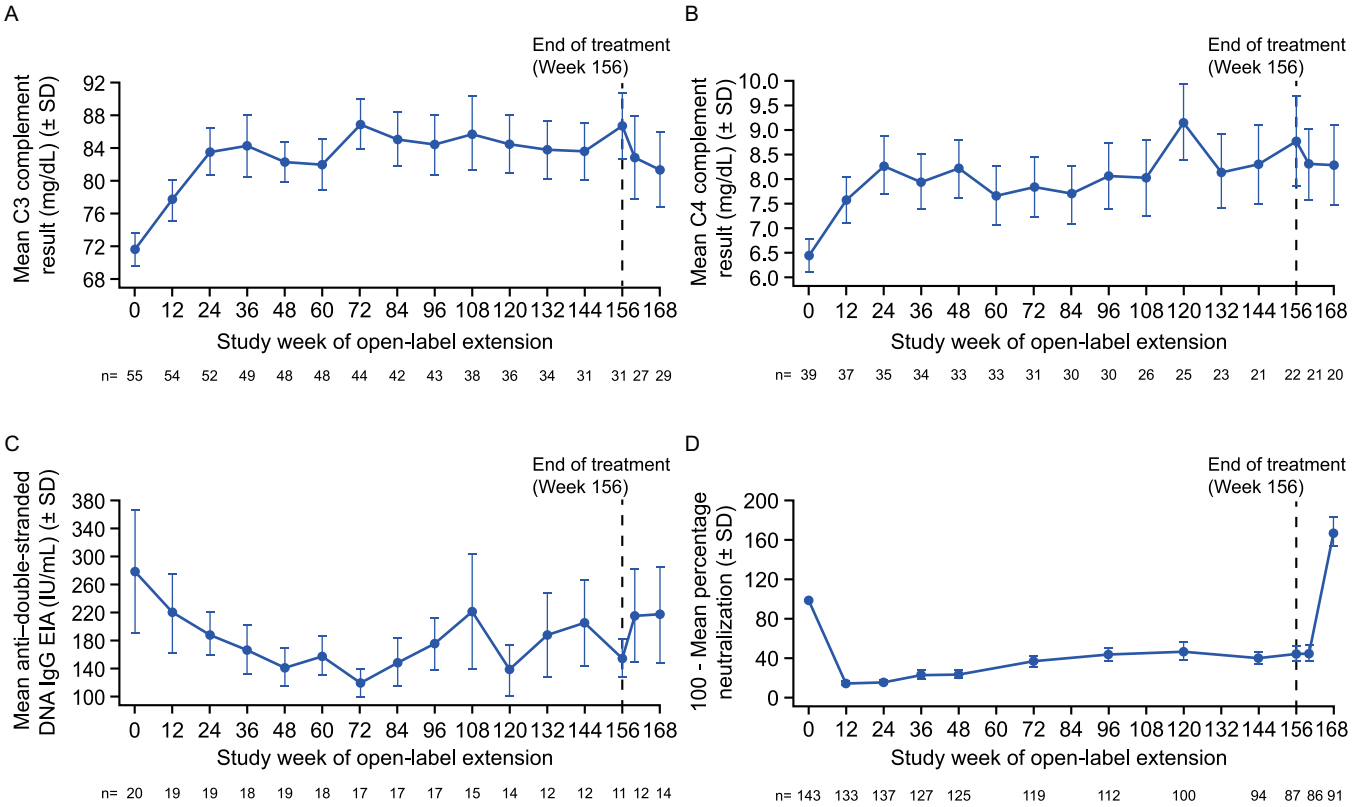

Figure 3. **A** and **B**, Mean complement C3 levels (**A**) and C4 levels (**B**) over time in the open-label extension, in patients with abnormal levels at baseline. **C**, Mean levels of anti–double-stranded DNA (anti-dsDNA) by immunoglobulin G enzyme immunoassay (IgG EIA) over time in the open-label extension, in patients positive for anti-dsDNA antibodies at baseline. **D**, Neutralization of type I interferon (IFN) gene signature over time in the open-label extension, in patients with high IFN gene signature expression at baseline. Color figure can be viewed in the online issue, which is available at http://onlinelibrary.wiley.com/doi/10.1002/art.41598/abstract.

score of 0 at week 160. Furthermore, baseline mean ± SD SLE-DAI-2K global scores were slightly greater for patients with high IFN gene signature than for patients with low IFN gene signature (5.2 ± 4.2 and 4.3 ± 3.1, respectively) and remained slightly greater throughout the study. At week 160, the mean ± SD change from baseline was –2.2 ± 3.8 for patients with high IFN gene signature expression and –1.9 ± 2.5 for patients with low IFN gene signature expression; by week 168, the mean ± SD change from baseline was –0.7 ± 4.3 and –1.6 ± 3.5, respectively (Figure 2B).

The mean SDI global score was generally stable over time (Figure 2C). SF-36 physical and mental component summary scores increased over time, with mean ± SD changes from baseline to week 156 of 2.1 ± 6.3 and 2.9 ± 10.1, respectively; mean ± SD changes from baseline to week 168 were 0.9 ± 7.1 and 2.0 ± 10.6, respectively (Figure 2D).

Serologic measures. Long-term anifrolumab treatment was associated with a trend toward a sustained increase in mean C3 levels, as well as a trend toward shifts from abnormal to normal C3 levels (Figure 3A) (mean ± SD change in C3 levels from baseline to week 168 of 8.54 ± 17.5 mg/dl). C4 levels also showed trends toward sustained improvement (Figure 3B), with a mean ± SD change from baseline to week 168 of 1.98 ± 3.5 mg/dl. The assay used to measure anti-dsDNA in this study changed over the course of the open-label extension. Therefore, analysis of the mean change over time for anti-dsDNA was limited to patients who had both baseline and post-baseline results evaluated using the same assay (n = 20). In this group of patients, anti-dsDNA displayed a trend toward improvement (Figure 3C), from a mean of 278.2 IU/ml at baseline to a mean of 216.7 IU/ml at week 168.

Immunogenicity. Five patients (2.3%) had antidrug antibodies at any time during this study, 3 of whom were antidrug antibody positive only at open-label extension baseline. The other 2 patients were positive at ≥2 post-baseline assessments (with ≥16 weeks between first and last positive result); only 1 patient was considered persistently antidrug antibody positive, as the other patient was antidrug antibody positive at baseline and had no increase in titer over baseline levels. Two antidrug antibody–positive patients received immunosuppressants during the study. No hypersensitivity reactions were reported among antidrug antibody–positive patients during the study. One antidrug antibody–positive patient, who was antidrug antibody negative in the RCT and at open-label extension baseline, had decreased

exposure to anifrolumab and reduced pharmacodynamic suppression at week 48. The reduction in serum concentrations of anifrolumab as well as the decrease in IFN gene signature suppression may be attributed to the reduction in anifrolumab dose from 1,000 mg to 300 mg at week 44.

Type I IFN gene signature. Neutralization of IFN gene signature expression was sustained (mean percentage of baseline signature at week 156 was 44.4%) in patients with high baseline IFN gene signature expression (Figure 3D). By week 168, following treatment cessation, neutralization had reversed (mean percentage of baseline signature was 167.6%).

Clinical laboratory evaluations and vital signs. Ten patients (4.7%) had increases in the urinary protein/creatinine ratio (defined as ≥395 gm/mole) at any time post-baseline. These changes were transient, and patients continued treatment with anifrolumab. No clinically relevant trends were observed for mean vital sign values, physical findings, or Cushingoid features over time. No patients had shifts in ECG from normal results at baseline to clinically important abnormalities during the study.

DISCUSSION

Anifrolumab treatment was associated with an acceptable safety profile and sustained improvements in disease activity and HRQoL in patients receiving up to 3 years of treatment in the MUSE open-label extension study. To date, this is the longest study of continuous anifrolumab exposure in patients with SLE.

Irreversible organ damage that accumulates due to long-term SLE disease activity underscores the importance of developing therapeutic approaches that can be administered continuously for long-term disease management (2,4). Furthermore, morbidity from the long-term use of standard-of-care therapies, such as steroids and immunosuppressive agents (4,24), emphasizes the need for safer therapies. At baseline of the RCT, ~60% of patients were receiving prednisone or equivalent glucocorticoids ≥10 mg/day, whereas at baseline of the open-label extension, 38% of patients were receiving steroids ≥10 mg/day (prednisone or equivalent). The ability to taper oral glucocorticoids during the RCT was at least in part related to the beneficial effects of anifrolumab treatment during the year-long study (13).

Safety profiles of AEs, serious AEs, and serious AEs of special interest in the open-label extension were consistent with previous observations (13). Overall, the frequency of AEs during the first year of the open-label extension was lower than during the first year of the RCT, likely because the majority of patients in the open-label extension (70.2%) were previously treated with anifrolumab during the RCT. Few patients discontinued treatment due to an AE. In the 4 pneumonia cases, most patients were able to continue in the study with or without anifrolumab treatment interruptions, and most events resolved without sequelae. With the exception of 1 patient, all pneumonia cases were considered by the investigator to be not related to treatment. In addition, 1 patient who received placebo in the RCT died of community-acquired pneumonia. The death occurred 19 days after the previous anifrolumab dose and was assessed by the investigator to be related to treatment. Moreover, no increases in the frequency of herpes zoster reactivation occurred over the course of the open-label extension compared with the RCT, suggesting no association between treatment duration and frequency of herpes zoster events. The number of doses before an event of herpes zoster ranged from 1 to 39. There were also no differences in the occurrence of herpes zoster reactivation between patients who had previously taken anifrolumab and those who were receiving it for the first time in this study. All herpes zoster events were cutaneous, and few were disseminated. Although some patients had treatment interruptions, all patients with herpes zoster events recovered without discontinuing treatment with anifrolumab because of the event.

Efficacy measures showed improvements over the first several study visits, and those improvements were maintained for up to 3 years of anifrolumab treatment. Disease activity, as reflected by SLEDAI-2K global scores, was lower at the start of the open-label extension than at the start of the RCT. Moreover, a decrease in disease activity was observed early in the open-label extension and was maintained throughout 156 weeks of treatment, with an increase occurring following treatment cessation. In the RCT, a greater effect size was observed in patients with high type I IFN gene signatures than in patients with low type I IFN gene signatures (13). In the open-label extension, patients with both low and high baseline type I IFN gene signatures showed similar trends in SLEDAI-2K scores. It was not possible to compare the efficacy trends observed in patients with high IFN gene signature versus low IFN gene signature between the RCT and open-label extension because there was no placebo group in the open-label extension to determine treatment differences. The similar SLEDAI-2K trends in patients in the open-label extension with high and low IFN gene signatures may be attributed to prior RCT treatment with anifrolumab, which may have lowered the disease activity baseline for most patients in the open-label extension and minimized differences in disease improvement between the high IFN gene signature and low IFN gene signature groups.

HRQoL and permanent organ damage, measured by SDI, generally remained stable over 3 years. The decrease in mean SDI score observed from week 48 to week 120 may be attributed to patients dropping out of the study over time. In addition, the incidence of antidrug antibody development was low during open-label extension treatment, as it had been in the RCT (13). Patients who were type I IFN gene signature high at baseline had sustained neutralization of the IFN gene signature (~55% mean neutralization), followed by a rebound after completion of treatment.

Strengths of this study included the 3-year duration with a high treatment completion rate of ~80%. The open-label study design has limitations, including the lack of a placebo group, which

prevents treatment comparisons. The unblinded design may introduce bias in the outcome. The study is also subject to selection bias, as the patients who received anifrolumab and completed the RCT may have enriched the open-label extension population with patients who were more likely to tolerate anifrolumab. Additionally, because some patients received anifrolumab (~70%) during the RCT and some received placebo (~30%), patients had varying amounts of exposure to anifrolumab, but the impact of differential exposure remains unknown. Exposure also varied among patients because of the switch in anifrolumab dosage (1,000 mg to 300 mg every 4 weeks) during the open-label extension study.

Despite the introduction of belimumab to the SLE treatment landscape (25), an unmet need for safer and more efficacious therapeutics remains. Based on the prominent role of IFN pathway activation in SLE pathogenesis (7–9), a few studies have attempted to explore its potential as a therapeutic target. A phase II clinical trial evaluated the efficacy and safety of the anti-IFNα monoclonal antibody sifalimumab (26). Although sifalimumab demonstrated clinical efficacy with an acceptable safety profile (26), development of this drug was not pursued given the superior pharmacodynamic and clinical effects of anifrolumab (25). A phase II clinical trial of rontalizumab, a humanized IgG1 anti-IFNα antibody capable of neutralizing all 12 subtypes of IFNα, failed to meet primary and secondary end points (25,27). While blocking IFN signaling was mixed in the studies described above, inhibition of the IFN receptor with anifrolumab was successful in the MUSE phase II RCT (13).

In conclusion, this open-label extension reaffirmed the safety profile observed in the 1-year parent study and, more importantly, showed that these results were maintained with long-term exposure to anifrolumab. These findings suggest that long-term inhibition of the type I IFN pathway with anifrolumab may provide a promising novel therapeutic strategy in addition to currently available treatments for patients with SLE.

ACKNOWLEDGMENTS

We thank the investigators, research staff, health care providers, patients, and caregivers who contributed to this study. We also thank Maria Prada, PhD (JK Associates, Inc., part of Fishawack Health) for medical writing assistance.

AUTHOR CONTRIBUTIONS

All authors were involved in drafting the article or revising it critically for important intellectual content, and all authors approved the final version to be published. Dr. Chatham had full access to all of the data in the study and takes responsibility for the integrity of the data and the accuracy of the data analysis.

Study conception and design. Chatham, Furie, Brohawn, Tummala.
Acquisition of data. Chatham, Brohawn, Tummala.
Analysis and interpretation of data. Chatham, Furie, Saxena, Brohawn, Schwetje, Abreu, Tummala.

ROLE OF THE STUDY SPONSOR

AstraZeneca provided funding and medical writing assistance for the study. AstraZeneca employees were involved in the design and conduct of the study; contributed to the collection, analysis, and interpretation of the data; and supported the authors in the development of the manuscript. All authors approved the content of the submitted manuscript and were involved in the decision to submit the manuscript for publication. Publication of this article was contingent upon approval by AstraZeneca.

REFERENCES

1. La Paglia GM, Leone MC, Lepri G, Vagelli R, Valentini E, Alunno A, et al. One year in review 2017: systemic lupus erythematosus. Clin Exp Rheumatol 2017;35:551–61.
2. Manson JJ, Rahman A. Systemic lupus erythematosus [review]. Orphanet J Rare Dis 2006;1:6.
3. Petri M. Long-term outcomes in lupus. Am J Manag Care 2001; 7:S480–5.
4. Ruiz-Irastorza G, Danza A, Khamashta M. Glucocorticoid use and abuse in SLE. Rheumatology (Oxford) 2012;51:1145–53.
5. Peng L, Oganesyan V, Wu H, Dall'Acqua WF, Damschroder MM. Molecular basis for antagonistic activity of anifrolumab, an anti-interferon-α receptor 1 antibody. MAbs 2015;7:428–39.
6. Riggs JM, Hanna RN, Rajan B, Zerrouki K, Karnell JL, Sagar D, et al. Characterisation of anifrolumab, a fully human anti-interferon receptor antagonist antibody for the treatment of systemic lupus erythematosus. Lupus Sci Med 2018;5:e000261.
7. Baechler EC, Batliwalla FM, Karypis G, Gaffney PM, Ortmann WA, Espe KJ, et al. Interferon-inducible gene expression signature in peripheral blood cells of patients with severe lupus. Proc Natl Acad Sci U S A 2003;100:2610–5.
8. Kirou KA, Lee C, George S, Louca K, Peterson MG, Crow MK. Activation of the interferon-α pathway identifies a subgroup of systemic lupus erythematosus patients with distinct serologic features and active disease. Arthritis Rheum 2005;52:1491–503.
9. Postal M, Sinicato NA, Pelicari KO, Marini R, Costallat LT, Appenzeller S. Clinical and serological manifestations associated with interferon-α levels in childhood-onset systemic lupus erythematosus. Clinics (Sao Paulo) 2012;67:157–62.
10. Lichtman EI, Helfgott SM, Kriegel MA. Emerging therapies for systemic lupus erythematosus: focus on targeting interferon-α. Clin Immunol 2012;143:210–21.
11. Crow MK. Advances in understanding the role of type I interferons in systemic lupus erythematosus. Curr Opin Rheumatol 2014;26:467–74.
12. Ivashkiv LB, Donlin LT. Regulation of type I interferon responses [review]. Nat Rev Immunol 2014;14:36–49.
13. Furie R, Khamashta M, Merrill JT, Werth VP, Kalunian K, Brohawn P, et al. Anifrolumab, an anti–interferon-α receptor monoclonal antibody, in moderate-to-severe systemic lupus erythematosus. Arthritis Rheumatol 2017;69:376–86.
14. Furie RA, Petri MA, Wallace DJ, Ginzler EM, Merrill JT, Stohl W, et al. Novel evidence-based systemic lupus erythematosus responder index. Arthritis Rheum 2009;61:1143–51.
15. Wallace DJ, Kalunian K, Petri MA, Strand V, Houssiau FA, Pike M, et al. Efficacy and safety of epratuzumab in patients with moderate/severe active systemic lupus erythematosus: results from EMBLEM, a phase IIb, randomised, double-blind, placebo-controlled, multicentre study. Ann Rheum Dis 2014;73:183–90.
16. Klein R, Moghadam-Kia S, LoMonico J, Okawa J, Coley C, Taylor L, et al. Development of the CLASI as a tool to measure disease severity and responsiveness to therapy in cutaneous lupus erythematosus. Arch Dermatol 2011;147:203–8.
17. Albrecht J, Taylor L, Berlin JA, Dulay S, Ang G, Fakharzadeh S, et al. The CLASI (Cutaneous Lupus Erythematosus Disease Area and Severity Index): an outcome instrument for cutaneous lupus erythematosus. J Invest Dermatol 2005;125:889–94.

18. Hochberg MC, for the Diagnostic and Therapeutic Criteria Committee of the American College of Rheumatology. Updating the American College of Rheumatology revised criteria for the classification of systemic lupus erythematosus [letter]. Arthritis Rheum 1997;40:1725.
19. Gladman DD, Ibanez D, Urowitz MB. Systemic Lupus Erythematosus Disease Activity Index 2000. J Rheumatol 2002;29:288–91.
20. Yee CS, Farewell V, Isenberg DA, Prabu A, Sokoll K, Teh LS, et al. Revised British Isles Lupus Assessment Group 2004 index: a reliable tool for assessment of systemic lupus erythematosus activity. Arthritis Rheum 2006;54:3300–5.
21. Gladman DD, Goldsmith CH, Urowitz MB, Bacon P, Fortin P, Ginzler E, et al. The Systemic Lupus International Collaborating Clinics/American College of Rheumatology (SLICC/ACR) Damage Index for systemic lupus erythematosus international comparison. J Rheumatol 2000;27:373–6.
22. Ware JE Jr, Gandek B. Overview of the SF-36 Health Survey and the International Quality of Life Assessment (IQOLA) project. J Clin Epidemiol 1998;51:903–12.
23. Ware J, Kosinski M, Dewey J. How to score version 2 of the SF-36 Health Survey. Lincoln (RI): QualityMetric, Inc.; 2000.
24. Amissah-Arthur MB, Gordon C. Contemporary treatment of systemic lupus erythematosus: an update for clinicians. Ther Adv Chronic Dis 2010;1:163–75.
25. Vukelic M, Li Y, Kyttaris VC. Novel treatments in lupus [review]. Front Immunol 2018;9:2658.
26. Khamashta M, Merrill JT, Werth VP, Furie R, Kalunian K, Illei GG, et al. Sifalimumab, an anti-interferon-α monoclonal antibody, in moderate to severe systemic lupus erythematosus: a randomised, double-blind, placebo-controlled study. Ann Rheum Dis 2016;75:1909–16.
27. Kalunian KC, Merrill JT, Maciuca R, McBride JM, Townsend MJ, Wei X, et al. A phase II study of the efficacy and safety of rontalizumab (rhuMAb interferon-α) in patients with systemic lupus erythematosus (ROSE). Ann Rheum Dis 2016;75:196–202.

American College of Rheumatology
Empowering Rheumatology Professionals

Arthritis & Rheumatology
Vol. 73, No. 5, May 2021, pp 826–836
DOI 10.1002/art.41608

The Type II Anti-CD20 Antibody Obinutuzumab (GA101) Is More Effective Than Rituximab at Depleting B Cells and Treating Disease in a Murine Lupus Model

Anthony D. Marinov,[1] Haowei Wang,[2] Sheldon I. Bastacky,[1] Erwin van Puijenbroek,[3] Thomas Schindler,[4] Dario Speziale,[3] Mario Perro,[3] Christian Klein,[3] Kevin M. Nickerson,[1] and Mark J. Shlomchik[1]

Objective. Depleting pathogenic B cells could treat systemic lupus erythematosus (SLE). However, depleting B cells in an inflammatory setting such as lupus is difficult. This study was undertaken to investigate whether a type II anti-CD20 monoclonal antibody (mAb) with a different mechanism of action, obinutuzumab (GA101), is more effective than a type I anti-CD20 mAb, rituximab (RTX), in B cell depletion in lupus, and whether efficient B cell depletion results in amelioration of disease.

Methods. We treated lupus-prone MRL/lpr mice expressing human CD20 on B cells (hCD20 MRL/lpr mice) with either RTX or GA101 and measured B cell depletion under various conditions, as well as multiple clinical end points.

Results. A single dose of GA101 was markedly more effective than RTX in depleting B cells in diseased MRL/lpr mice ($P < 0.05$). RTX overcame resistance to B cell depletion in diseased MRL/lpr mice with continuous treatments. GA101 was more effective in treating hCD20 MRL/lpr mice with early disease, as GA101-treated mice had reduced glomerulonephritis ($P < 0.05$), lower anti-RNA autoantibody titers ($P < 0.05$), and fewer activated CD4+ T cells ($P < 0.0001$) compared to RTX-treated mice. GA101 also treated advanced disease, and continual treatment prolonged survival. Using variants of GA101, we also elucidated B cell depletion mechanisms in vivo in mice with lupus.

Conclusion. Albeit both anti-CD20 antibodies ameliorated early disease, GA101 was more effective than RTX in important parameters, such as glomerulonephritis score. GA101 proved beneficial in an advanced disease model, where it prolonged survival. These data support clinical testing of GA101 in SLE and lupus nephritis.

INTRODUCTION

Systemic lupus erythematosus (SLE) is a systemic autoimmune disease characterized by activated autoreactive B and T cells, which lead to the production of autoantibodies and immune complexes, infiltration of lymphocytes into target tissues, and production of inflammatory cytokines (1). Whereas patients typically present with skin and oral lesions, the autoimmune process can damage various organs, such as the kidney, skin, lungs, brain, and heart (2). A serious and common complication of SLE is glomerulonephritis.

B cells play a key role and serve multiple functions in the mediation and progression of autoimmune diseases, including SLE in mice and humans, by both producing autoantibodies against nuclear antigens and acting as antigen-presenting cells to activate pathogenic T cells (3). We previously created B cell–deficient lupus-prone mouse strains, which failed to develop activated CD8 and CD4+ T cells, and in which dermatitis and nephritis were abrogated (4,5). Similar findings have been obtained in multiple murine models of lupus (6–8).

B cell–targeted therapy for the treatment of SLE has been extensively investigated. Indeed, belimumab, which targets BAFF, showed clinical efficacy in patients with SLE, leading to its approval by the Food and Drug Administration in 2011. However, 2 trials of rituximab (RTX), a well-established anti-CD20 chimeric monoclonal antibody (mAb) that depletes B cells, in patients with SLE and lupus nephritis failed to meet their respective primary end points (9–11). This led to multiple theories to explain the failure, ranging from suboptimal trial

Supported by grants R01-AR-044077 and 1S10-OD-011925-01 from the NIH and by a grant from Roche to the University of Pittsburgh.

[1]Anthony D. Marinov, MS, Sheldon I. Bastacky, MD, Kevin M. Nickerson, PhD, Mark J. Shlomchik, MD, PhD: University of Pittsburgh School of Medicine, Pittsburgh, Pennsylvania; [2]Haowei Wang, MD: Yale University, New Haven, Connecticut; [3]Erwin van Puijenbroek, MSc, Dario Speziale, MSc, Mario Perro, PhD, Christian Klein, PhD: Roche, Zurich, Switzerland; [4]Thomas Schindler, PhD: Hoffmann-La Roche, Basel, Switzerland.

Mr. van Puijenbroek, Drs. Schindler, Perro, and Klein, and Mr. Speziale own stock or stock options in Roche. No other disclosures relevant to this article were reported.

Address correspondence to Mark J. Shlomchik, MD, PhD, University of Pittsburgh School of Medicine, Department of Immunology, W1052 Biomedical Science Tower, 200 Lothrop Street, Pittsburgh, PA 15261. Email: mshlomch@pitt.edu.

Submitted for publication January 1, 2020; accepted in revised form December 1, 2020.

design to the notion that B cells were not in fact critical for lupus pathogenesis.

Prior to those studies, we had created a murine model of anti-CD20 treatment of lupus by introducing a bacterial artificial chromosome transgene that expresses human CD20 into the mouse germline and then fully backcrossing it on both normal and autoimmune-prone genetic backgrounds. We then used conventional murine anti-CD20 antibodies to deplete B cells. These agents successfully depleted B cells in the spleens of BALB/c mice, but were notably ineffective in the lymphoid tissues of MRL/lpr mice (12). Nonetheless, we found that by delivering very high doses of anti-CD20 for multiple weeks, we could eventually deplete B cells and mitigate disease (13). Similar findings were obtained by others and us in additional murine lupus strains, using either anti-human CD20 (anti-hCD20) antibodies or murine anti-mouse CD20 (8). We then showed that the presence of IgG immune complexes in the serum of autoimmune mice was sufficient to block IgG anti-CD20–mediated B cell depletion in vivo (12); further, lupus patients are known to be unable to clear IgG-opsonized red blood cells (14), presumably for similar reasons. Since only limited doses, sufficient to deplete B cell lymphoma in individuals without autoimmune disease, were used in the clinical studies (9,11), we thus proposed that insufficient tissue B cell depletion in at least a subset of lupus patients could explain why RTX failed to reach clinical end points (12).

We hypothesized that a second class of anti-CD20 antibody, called a "type II anti-CD20," which was postulated to have a different mechanism of action of depletion, could be more efficacious. Compared with type I anti-CD20 antibodies like RTX, type II antibodies like obinutuzumab (GA101) are reported to exhibit more direct B cell–killing effects, and rely less on complement-dependent cytotoxicity (15). Furthermore, the Fc part of GA101 is glycoengineered, enhancing its affinity for Fcγ receptor IIIa (FcγRIIIa) on natural killer cells and monocyte/macrophages and as a consequence antibody-dependent cellular cytotoxicity and antibody-dependent cellular phagocytosis (15,16). GA101 is only one of two such antibodies in common use (17,18) and has been developed and approved under the tradename Gazyva/Gazyvaro for the treatment of chronic lymphocytic leukemia (CLL) (19,20) and follicular lymphoma (21,22).

In this study, we used our hCD20-transgenic murine lupus model to compare the B cell depletion efficiency of GA101 and RTX in MRL/lpr mice. We then further evaluated the B cell depletion efficiency of GA101 and its therapeutic effect in MRL/lpr mice treated at disease onset, after disease establishment, or continuously. We also used a mutant of GA101 with abolished effector functions (23) along with a non-glycoengineered version of GA101 (wild-type GA101) to help elucidate the context of lupus. Our overall conclusion is that GA101 is indeed a more potent B cell–depleting agent in lupus, even though its mechanism of action at least partly overlaps with that of type I antibodies in vivo, and moreover, that GA101 is an effective treatment for murine SLE. GA101 is more effective than RTX at acute B cell depletion, which leads to better clinical response in some contexts.

MATERIALS AND METHODS

Mice. A BAC-transgenic mouse expressing human CD20 on B cells was generated (13) and backcrossed >10 generations onto the MRL/lpr background to produce MRL/lpr mice expressing human CD20 (hCD20 MRL/lpr mice). Mice were euthanized by CO_2 inhalation. All mice were housed under specific pathogen–free conditions, and all experiments were performed with the approval of the University of Pittsburgh Institutional Animal Care and Use Committees.

Antibody reagents for in vivo studies. Antibodies used are described in Supplementary Table 1, available on the *Arthritis & Rheumatology* website at http://onlinelibrary.wiley.com/doi/10.1002/art.41608/abstract. To reduce immunogenicity in long-term experiments, murinized GA101 bearing a human Fab region of GA101 and a murine IgG2a Fc portion, and murinized RTX based on 2B8 antibody, were generated according to standard procedures as glycoengineered (GA101) or wild-type non-glycoengineered (wild-type GA101) antibodies. GA101 P329G-LALA mutant (mutant GA101) was used to investigate the role of Fc-mediated effector function (23,24). Isotype control IgG2a was purchased from Bio X Cell (clone C1.18.4; catalog no. BE0085).

B cell depletion. B cells were depleted by intraperitoneal (IP) injection of female hCD20 MRL/lpr mice with the indicated amounts of antibody. Unless otherwise specified, in long-term treatment experiments mice were initially given 2 mg of RTX, GA101, or isotype control (mouse IgG2a) IP, then treated twice weekly with 1 mg for the indicated time periods.

Flow cytometric analysis. Preparation of splenocytes has been described previously (25). The following antibodies were produced in the laboratory or purchased as indicated: phycoerythrin (PE)–Cy7–conjugated anti-mouse CD11c (N418; BioLegend); PerCP–Cy5.5–conjugated anti-mouse T cell receptor β (H57-597; BioLegend); BUV395-conjugated anti-mouse CD19 (1D3; Becton Dickinson), Alexa Fluor 488–conjugated anti-mouse CD19 (1D3.2); BV605-conjugated anti-mouse CD4 (RM4; Becton Dickinson), PE-conjugated anti-mouse CD4 (GK1.5; BioLegend); PE–Cy7–conjugated anti-mouse CD62L (MEL-14; BioLegend); BV605-conjugated anti-mouse CD44 (1M7; Becton Dickinson), allophycocyanin (APC)–Cy7–conjugated anti-mouse CD44 (IM7; BioLegend); APC–Cy7–conjugated anti-mouse I-A/I-E (M5/114.15.2; BioLegend); BV605-conjugated anti-mouse CD138 (281-2; Becton Dickinson), PE-conjugated anti-mouse CD138 (281-2; BioLegend); Pacific Blue–conjugated anti-mouse CD8 (TIB-105); Alexa Fluor 680–conjugated anti-mouse CD38 (90),

Pacific Blue–conjugated anti-mouse CD38 (90); Alexa Fluor 488–conjugated peanut agglutinin; Pacific Blue–conjugated anti-mouse kappa (187.1); PE-conjugated anti-mouse CD11b (M1/70; Becton Dickinson); Alexa Fluor 647–conjugated anti-mouse CD35 (8C12); PE–Cy7–conjugated anti-mouse CD23 (B3B4; BioLegend); Alexa Fluor 647–conjugated anti-mouse IgM (B7-6); PE-conjugated anti-mouse IgG2a (goat polyclonal; SouthernBiotech). Flow cytometry data were collected on a BD LSR II or BD LSRFortessa and analyzed using FlowJo software (TreeStar).

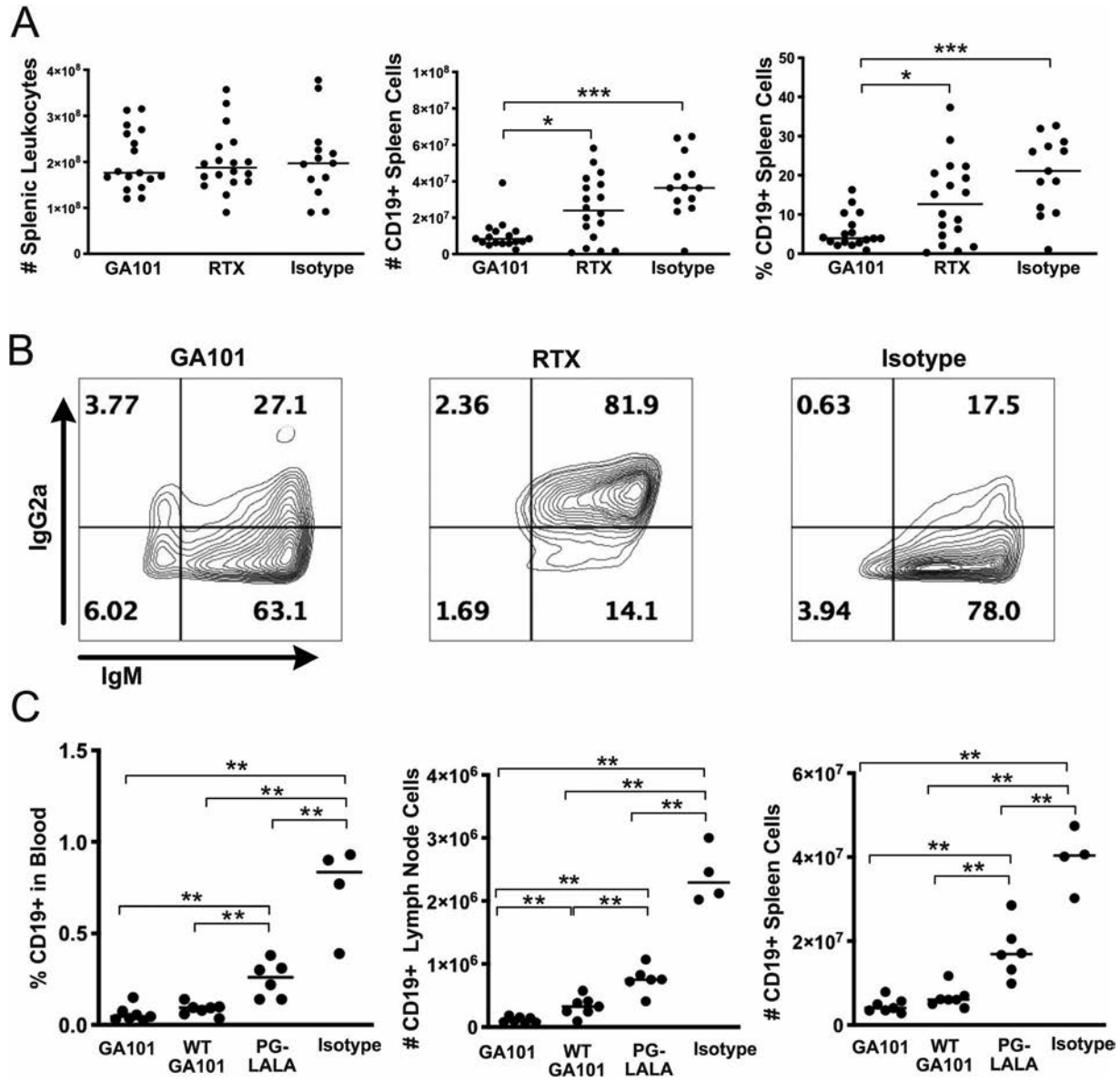

Figure 1. GA101 depletes B cells more efficiently than rituximab (RTX) in MRL/lpr mice, and B cell depletion is not entirely dependent on the Fc portion of GA101. **A**, Numbers of splenic leukocytes, numbers of CD19+ spleen cells, and percentage of CD19+ spleen cells in MRL/lpr mice expressing human CD20 on B cells (hCD20 MRL/lpr mice) treated intraperitoneally (IP) with 1 mg of GA101, RTX, or isotype control antibody (mouse IgG2a). Two days after injection, B cell depletion in the mouse spleen was measured by flow cytometry. Data were pooled from 5 independent experiments. Each symbol represents an individual mouse; horizontal lines show the median. **B**, Staining of residual B cells with anti-IgG2a and anti-IgM antibodies to determine if cells were coated with the injected anti-CD20. Residual B cells were highly antibody positive in RTX-treated mice but not in GA101-treated mice. Values are the percent of positive cells. Results are representative of experiments with at least 6 mice per group. **C**, Percentage of CD19+ cells in the blood, number of CD19+ lymph node cells, and number of CD19+ spleen cells in hCD20 MRL/lpr mice treated with GA101, wild-type (WT) GA101 (not glycoengineered), P329G-LALA mutant GA101 that lacks Fc-mediated effector functions and disrupts antibody-mediated phagocytosis (PG-LALA), or isotype control. Mice were injected IP with 2 mg of the indicated treatment on day 0, then 1 mg on days 2 and 4, and euthanized on day 7. Each symbol represents an individual mouse; horizontal lines show the median. * = $P < 0.05$; ** = $P < 0.01$; *** = $P < 0.001$, by Mann-Whitney 2-tailed test.

Evaluation of disease. Mice were evaluated for skin disease, and dorsal lesions were scored on a scale of 0–5 as previously described (5), based on lesion area, with up to an additional 0.5 points for facial rash/loss of whiskers and 0.25 points for dermatitis of each ear. Spleens and axillary lymph nodes were weighed. For analysis of renal disease, mouse kidneys were bisected and fixed in 10% formalin. Kidneys were embedded in paraffin, sectioned, and stained with hematoxylin and eosin (H&E) at Histo-Scientific Research Laboratories (Mount Jackson, VA). H&E-stained sections were scored for interstitial nephritis on a scale of 0–4 and for glomerulonephritis on a scale of 0–6, as previously described (26,27). Proteinuria was assayed using Albustix (Siemens).

Enzyme-linked immunosorbent assays (ELISAs). ELISAs were performed to measure antinucleosome, anti-RNA, and anti-Sm antibodies in the serum. Antinucleosome and anti-RNA ELISAs were performed as previously described (28). The lower limits of detection were 0. 02 μg/ml and 0.02 μg/ml, respectively. Anti-RNA ELISAs were performed as previously described (29). The lower limit of detection for the anti-RNA ELISA was 0.1 μg/ml.

Serum RTX and GA101 concentrations were measured by C2D1 sandwich ELISA. A biotin-conjugated anti-rabbit IgG (Fc-specific) antibody produced in goat (SAB3700856-2MG; Sigma-Aldrich) was used as first capture antibody in streptavidin-precoated 96-well plates and incubated for 1 hour at room temperature. Coated plates were washed 3 times with 200 μl wash buffer (10% fetal calf serum in phosphate buffered saline) and incubated for 1 hour at room temperature with the second capture antibody, an anti-RTX (antiidiotype) antibody (MAB9630; R&D Systems) or a MonoRab anti-obinutuzumab (169F10) rabbit mAb (A01967;GenScript). Serum samples were collected preinjection (control), and at 1 hour, 6 hours, 24 hours, and 48 hours after antibody treatment. Serum samples were then diluted in wash buffer at a concentration of 1:40,000. Coated plates were washed 3 times with 200 μl wash buffer and incubated for 1 hour at room temperature with the sera samples. Known concentrations of RTX or GA101 (ranging from 10 ng/ml to 0.15 ng/ml) were included to generate a standard curve. The plates were then washed 3 times with 200 μl wash buffer and incubated for 1 hour at room temperature with a horseradish peroxidase–conjugated goat polyclonal antibody to mouse IgG (ab97040; Abcam). Plates were then washed 3 times with 200 μl wash buffer and developed for 15 minutes at room temperature with ABTS solution (ID 11684302001; Roche), and signal was detected in an ELISA plate reader (Infinite M Plex; Tecan) using a wavelength of 405 nm and a reference wavelength of 490 nm.

Statistical analysis. Statistical analysis was performed using 2-tailed Mann-Whitney test. *P* values less than 0.05 were considered significant. For survival analysis, the Kaplan-Meier method was used to determine statistical significance. Data were analyzed using GraphPad version 7.0a.

RESULTS

More efficient depletion of B cells with GA101 treatment than RTX treatment in hCD20 MRL/lpr mice. MRL/lpr mice in our colony start to develop disease at 10 weeks old, and by 16 weeks of age they have late-stage disease with high titers of circulating autoantibodies and immune complexes in the serum (refs. 30 and 31, and Marinov AD: unpublished observations). To determine how, in the setting of established disease, GA101 depletes B cells compared to RTX, 16-week-old transgenic hCD20 MRL/lpr mice were given a single 1 mg dose of GA101, RTX, or isotype control (mouse IgG2a) IP. Two days after treatment, splenic CD19+ B cell populations were enumerated. GA101 depleted splenic B cells in 16-week-old MRL/lpr mice more efficiently than RTX or control (Figure 1A).

The reduced efficiency of RTX to deplete splenic B cells could have been due to failure of the antibody to bind to B cells or due to poor clearance of anti-CD20–bound cells. To determine if residual B cells were bound by RTX or GA101, we stained cells with anti-mouse IgG2a. Residual B cells were highly antibody positive in RTX-treated mice but not in GA101-treated mice (Figure 1B). This finding indicates that the RTX antibodies bound to the B cells, but the RTX-opsonized cells were not being phagocytized by macrophages, whereas the GA101-coated B cells were being more rapidly removed.

We also determined the pharmacokinetics of both murinized molecules in a dose-response single administration in both 6-week-old and 13-week-old MRL/lpr mice. Both RTX and GA101 had similar kinetics over 48 hours, and a dose-dependent peak serum concentration (Supplementary Figure 1, available on the *Arthritis & Rheumatology* website at http://onlinelibrary.wiley.com/doi/10.1002/art.41608/abstract). Notably, therapeutic exposure in the mouse was in the range of several hundred micrograms per milliliter, as is observed with GA101 in the clinic (32). Thus, we conclude that differences in in vivo exposure to drug cannot account for differences in the ability of RTX versus GA101 to deplete B cells.

B cell depletion by GA101 in hCD20 MRL/lpr mice is not entirely dependent on the Fc effector function of the antibody. We further wanted to gain insight into the role of the glycoengineering of GA101 and whether the Fc portion of the GA101 antibody plays a role in B cell depletion (Figure 1C). Optimal B cell depletion occurred with an intact Fc and glycoengineered GA101. Depletion with the P329G-LALA mutant that lacks Fc-mediated effector functions left 3 times as many residual B cells in the mouse spleen compared to native glycoengineered GA101. However, it still reduced splenic B cells by 55% compared to the isotype control. The effect of the non-glycoengineered wild-type version of GA101 was more subtle, as it caused B cell depletion in mice comparable to that caused by glycoengineered GA101 in most settings. Nonetheless, it was significantly inferior

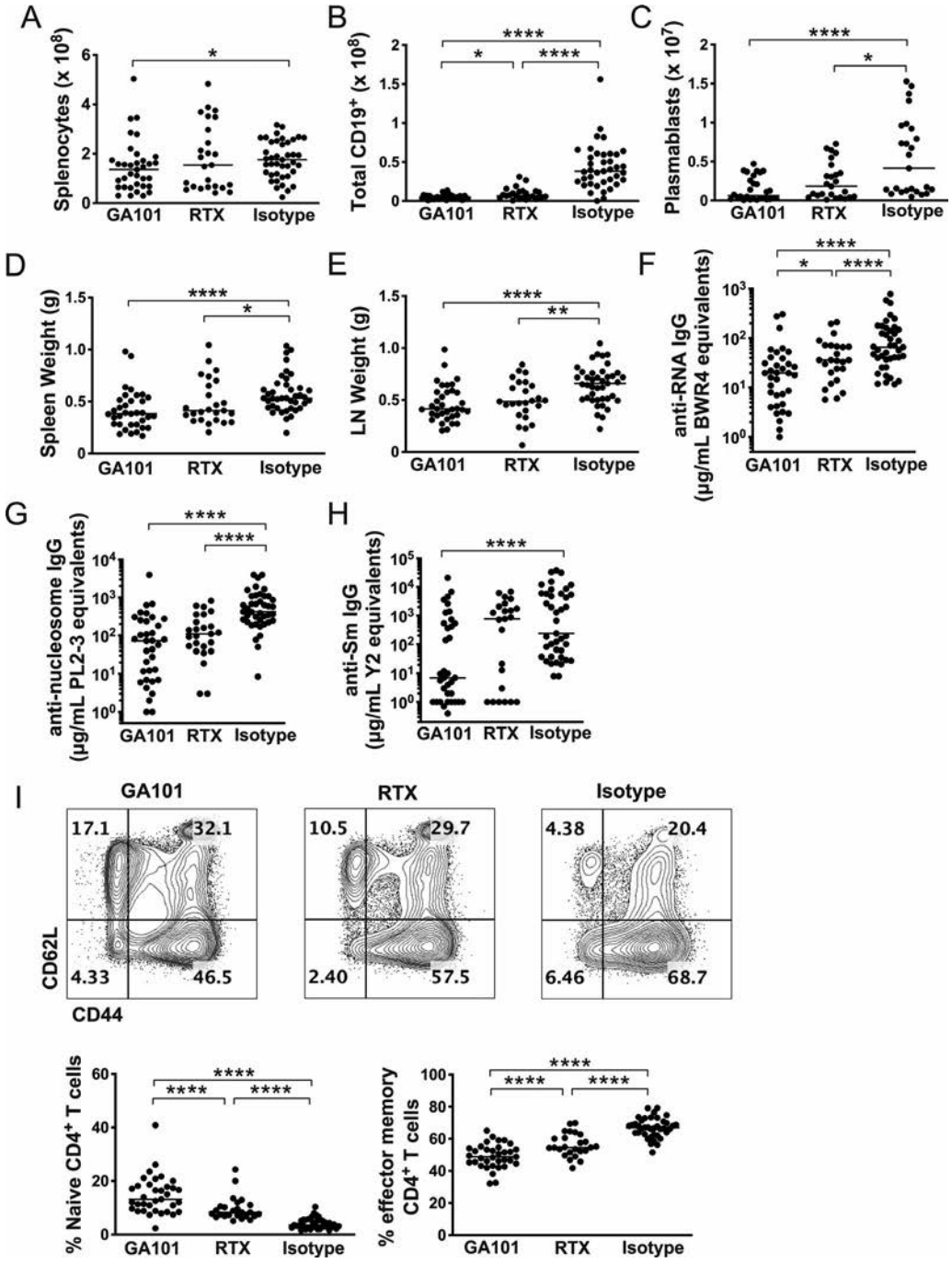

Figure 2. Comparison of GA101-mediated and rituximab (RTX)–mediated B cell depletion in mice with early disease. Ten-week-old MRL/lpr mice expressing human CD20 on B cells with early lupus disease were treated with GA101, RTX, or isotype control for 6 weeks. **A**–**C**, Numbers of splenocytes (**A**), total CD19+ cells (**B**), and plasmablasts (**C**) in the spleens of mice treated as indicated, determined by flow cytometry. **D** and **E**, Spleen (**D**) and axillary lymph node (LN) (**E**) weights in mice treated as indicated. **F**–**H**, Serum levels of anti-RNA (**F**), antinucleosome (**G**), and anti-Sm (**H**) autoantibodies in mice treated as indicated, measured by enzyme-linked immunosorbent assay. **I**, Flow cytometry representative gating (top) and quantitation (bottom) showing the percentages of naive CD4+ T cells and effector memory ($CD44^{high}CD62L^{low}$) CD4+ T cells in mice treated as indicated. Data were pooled from 3 independent experiments. In **A**–**H**, each symbol represents an individual mouse; horizontal lines show the median. * = $P < 0.05$; ** = $P < 0.01$; **** = $P < 0.0001$, by Mann-Whitney 2-tailed test.

to GA101 in depleting lymph node B cells, and there was a similar trend in blood and spleen. These findings indicate that GA101 has multiple mechanisms of B cell depletion in vivo in the context of lupus, which include Fc receptor (FcR)–independent mechanisms, as has been postulated for type II antibodies based on in vitro studies (33).

Modest increase in effectiveness of GA101 versus RTX for longer-term treatment of early disease in hCD20 MRL/lpr mice. Although GA101 depleted B cells more efficiently than RTX after a one-time treatment in older hCD20 MRL/lpr mice, we wanted to determine if GA101, compared to RTX, would be able to overcome inhibition of B cell depletion with continued treatment over a 6-week period when started in younger mice, and if so, if this would modify disease. To this end, we began treating hCD20 MRL/lpr mice at 10 weeks of age, a time at which disease is initiating (early disease; Supplementary Figure 2, available on the *Arthritis & Rheumatology* website at http://onlinelibrary.wiley.com/doi/10.1002/art.41608/abstract). After mice received 6 weeks of treatment, proteinuria and skin disease were measured; spleen and axillary lymph nodes were weighed; serum was obtained for antinuclear, anti-RNA, and anti-Sm ELISAs; splenocytes were stained for B cells, plasmablasts, and T cell activation markers; and kidneys were processed and histologic sections scored for kidney infiltrates and glomerulonephritis.

GA101 treatment slightly reduced spleen cell numbers (Figure 2A), an effect attributable to B cell depletion. Notably, GA101 depleted B cells in the mouse spleen more efficiently than RTX (Figure 2B). Both RTX and GA101 treatment depleted plasmablasts (Figure 2C), an effect likely due to depletion of the CD20+ B cell precursors of short-lived plasmablasts (13). Treatment with either antibody resulted in lower spleen and lymph node weights (Figures 2D and E) and disease improvement in several surrogate markers of autoimmunity, compared to controls. Both groups demonstrated lower anti-RNA and antinucleosome levels, while only GA101-treated mice had lower anti-Sm autoantibody levels (Figures 2F–H). In both GA101-treated mice and RTX-treated mice, T cell activation, a B cell–driven phenomenon (34), was ameliorated, with fewer activated and more naive T cells compared to controls (Figure 2I).

Critically, both RTX treatment and GA101 treatment resulted in reduced proteinuria (Figure 3A) and lower interstitial nephritis scores (Figure 3B); only GA101 treatment resulted in reduced glomerulonephritis scores compared to control treatment (Figure 3C). Skin disease was not affected (Figure 3D), possibly due to the early initiation of treatment and the relatively younger age at which the mice were analyzed, since skin disease is a late manifestation; more than half of control-treated mice had no detectable skin disease. Despite the fact that both treatments showed an effect in several pharmacodynamic readouts, GA101 treatment led to an even lower glomerulonephritis score than did RTX treatment (Figure 3C). In addition, compared to RTX-treated mice, GA101-treated mice had fewer activated CD4+

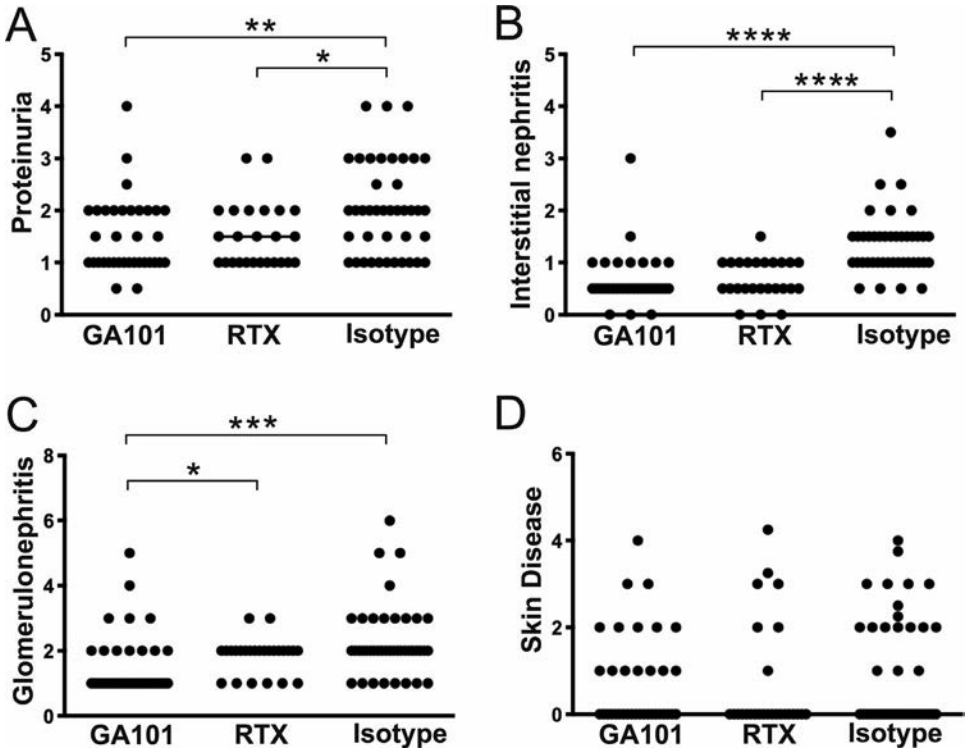

Figure 3. Effects of GA101-mediated and rituximab (RTX)–mediated B cell depletion on target organ disease in mice with early autoimmunity. Ten-week-old MRL/lpr mice expressing human CD20 on B cells were treated with GA101, RTX, or isotype control for 6 weeks. **A**, Proteinuria in mice treated as indicated, evaluated by dipstick assay the day before mice were euthanized. **B** and **C**, Interstitial nephritis (**B**) and glomerulonephritis (**C**) scores for hematoxylin and eosin–stained kidney sections from mice treated as indicated. **D**, Skin disease scores for mice treated as indicated. Data were pooled from 3 independent experiments. Each symbol represents an individual mouse; horizontal lines show the median. * = $P < 0.05$; ** = $P < 0.01$; *** = $P < 0.001$; **** = $P < 0.0001$, by Mann-Whitney 2-tailed test.

T cells (Figure 2I), with a greater proportion of phenotypically naive T cells. Finally, anti-RNA antibody levels were significantly reduced in GA101-treated mice compared to RTX-treated mice (Figure 2F).

GA101 treatment of established disease in hCD20 MRL/lpr mice. Given that extended treatment with either GA101 or RTX ameliorated disease when started early in the disease course, we next wanted to determine if GA101 would successfully deplete B cells and ameliorate disease in mice when treatment was started during established disease, a setting that had not been tested in this model using any other B cell depletion reagent. We thus began treatment of additional cohorts of 13-week-old hCD20 MRL/lpr mice (established disease; Supplementary Figure 2). After 6 weeks, mice were euthanized and tissues were processed as described above. Even though there was more advanced disease at the start of therapy, B cells were successfully depleted by GA101 (Figures 4A and B). As in the early disease treatment cohorts, plasmablasts were reduced, as was spleen weight (Figures 4C and D), while lymph node weight was unaffected in this protocol (Figure 4E). Levels of all autoantibodies measured were also significantly reduced by GA101 treatment (Figures 4F–H). Again, similar to the early disease cohort, GA101 treatment reduced T cell activation (Figure 4I). Most importantly, GA101 treatment of mice with established disease still ameliorated many aspects of clinical disease, including proteinuria,

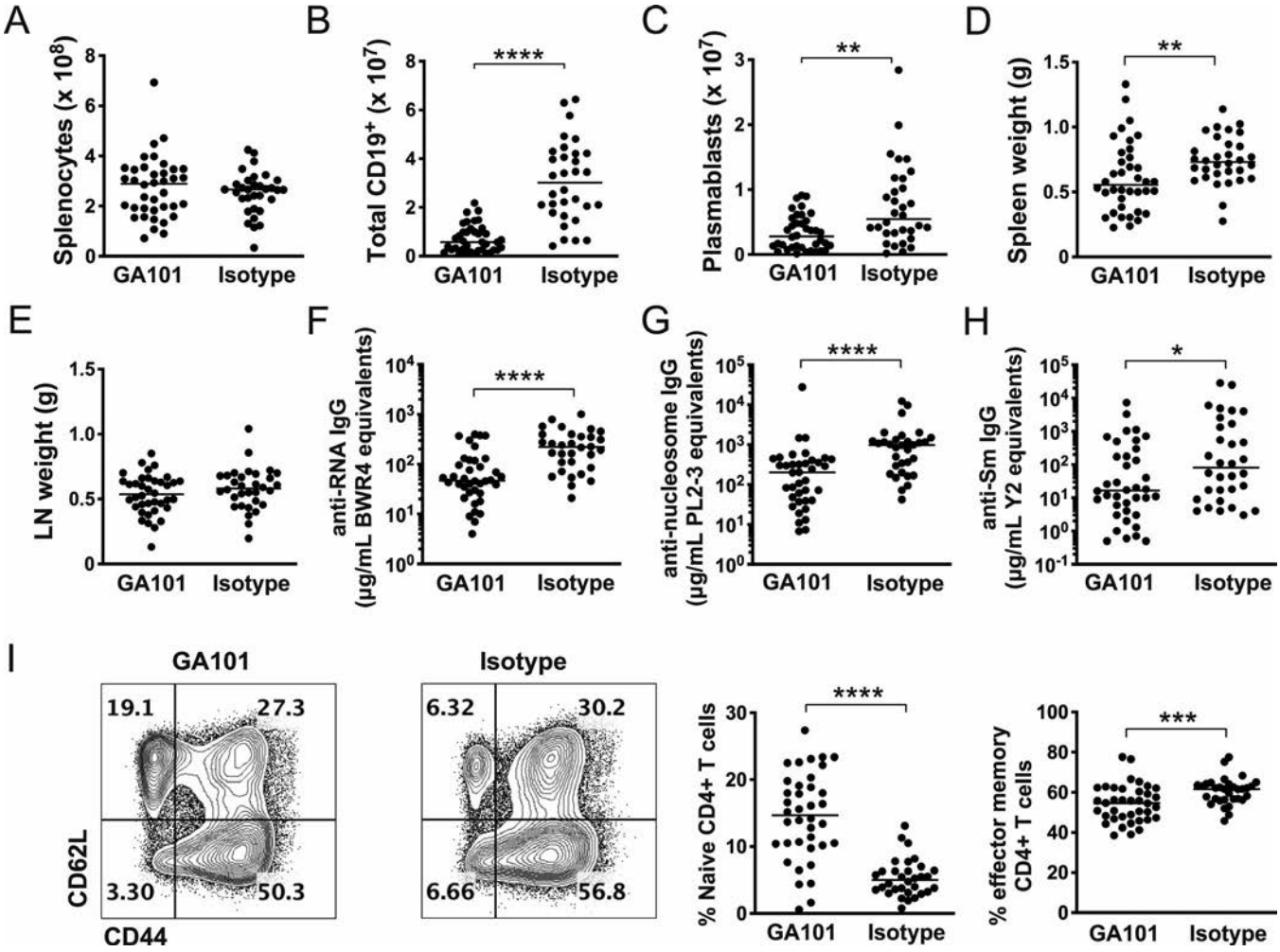

Figure 4. Effects of GA101 treatment on immunologic parameters when initiated in mice with established autoimmunity. Thirteen-week-old MRL/lpr mice expressing human CD20 on B cells with established disease were treated with GA101 or isotype control for 6 weeks. **A**–**C**, Numbers of splenocytes (**A**), total CD19+ cells (**B**), and plasmablasts (**C**) in the spleens of mice treated as indicated, determined by flow cytometry and cell counting. **D** and **E**, Spleen (**D**) and axillary lymph node (LN) (**E**) weights in mice treated as indicated. **F–H**, Serum levels of anti-RNA (**F**), antinucleosome (**G**), and anti-Sm (**H**) autoantibodies in mice treated as indicated, measured by enzyme-linked immunosorbent assay. **I**, Flow cytometry representative gating (left) and quantitation (right) showing the percentages of naive CD4+ T cells and effector memory ($CD44^{high}CD62L^{low}$) CD4+ T cells in mice treated as indicated. Data are pooled from 3 independent experiments. Each symbol represents an individual mouse; horizontal lines show the median. * = $P < 0.05$; ** = $P < 0.01$; *** = $P < 0.001$; **** = $P < 0.0001$, by Mann-Whitney 2-tailed test.

interstitial nephritis, and skin disease (Figure 5); the latter was not affected in the early disease cohort, probably because there was little disease in the control group (Figure 3D). In the mice with established disease, only glomerulonephritis was not significantly reduced in the treatment group, although there was a trend in that direction.

Sustained B cell depletion is necessary and sufficient to prolong survival in hCD20 MRL/lpr mice. Given the efficacy of GA101 in treating both early and established disease, we wanted to determine whether a 6-week treatment that was initiated early would be sufficient to alter the course of disease, potentially conferring a longer-term benefit. Alternatively, it was possible that sustained GA101 treatment would be needed for prolonged benefit. We therefore designed an experiment to compare one 6-week course with continuing treatment. Ten-week-old hCD20 MRL/lpr mice were treated with either GA101 or isotype control for 6 weeks; then in one group GA101 was discontinued, while in another GA101 was continued until the mice reached 31 weeks of age. Survival was the end point.

Continual B cell depletion with GA101 resulted in significantly extended survival, as assessed at 20 weeks of age, compared to controls, while GA101 treatment for only 6 weeks did not significantly prolong survival compared to controls (Figure 6). Though there was a trend toward improved survival, treatment for only 6 weeks followed by discontinuation did not significantly increase survival compared to controls. This finding suggests that while there may be some benefit of transient treatment, B cell depletion likely would need to be sustained for long-term survival benefit in this lupus mouse model.

DISCUSSION

Despite clear biologic evidence that B cells are centrally involved in lupus pathogenesis, depletion of B cells using the chimeric type I anti-CD20 mAb, RTX, failed to meet end points in 2 randomized clinical trials (9,11). We have proposed that a major reason for this failure, despite B cells being a valid target in SLE, is that standard agents and treatment protocols are relatively ineffective at depleting B cells (12,13). We hypothesized that type II anti-CD20 antibodies might be more effective for B cell depletion, and that they could be a more efficacious means to achieve clinical responses. In this study we tested these ideas in a relevant model of preclinical lupus.

We found that GA101 was superior to RTX in depleting B cells in lupus-prone mice. This advantage was most evident in

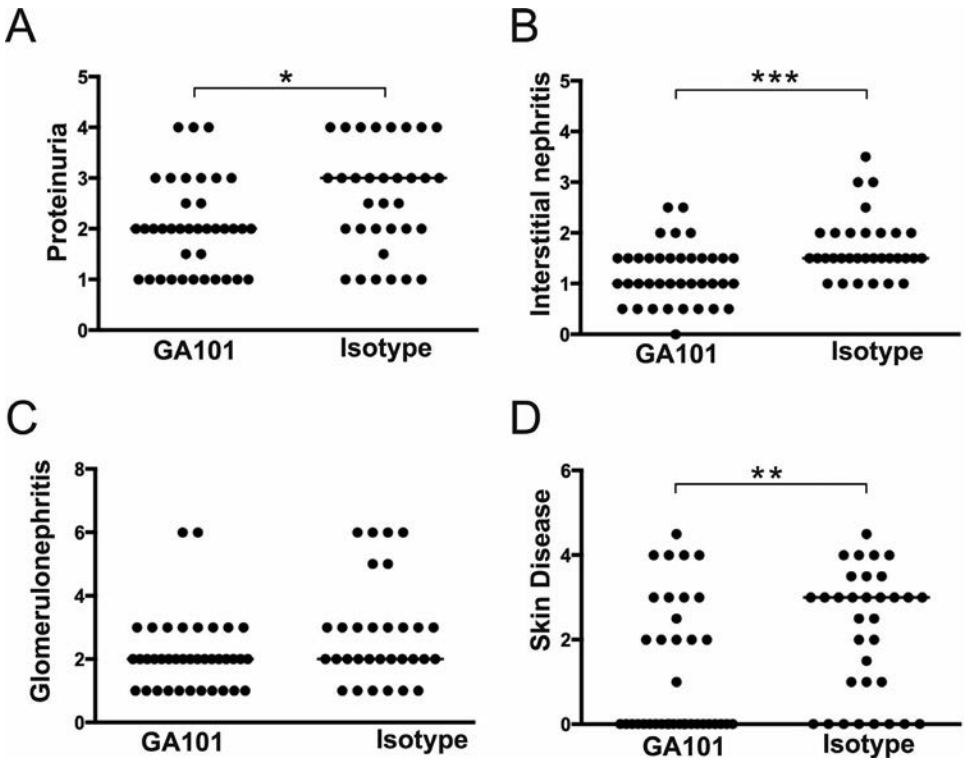

Figure 5. Effects of GA101 treatment on clinical disease when initiated in mice with established autoimmunity. Thirteen-week-old old MRL/lpr mice expressing human CD20 on B cells with established disease were treated with GA101 or isotype control for 6 weeks. **A**, Proteinuria in mice treated as indicated, evaluated by dipstick assay the day before mice were euthanized. **B** and **C**, Interstitial nephritis (**B**) and glomerulonephritis (**C**) scores for hematoxylin and eosin–stained kidney sections from mice treated as indicated. **D**, Skin disease scores for mice treated as indicated. Data were pooled from 3 independent experiments. Each symbol represents an individual mouse; horizontal lines show the median. * = $P < 0.05$; ** = $P < 0.01$; *** = $P < 0.001$, by Mann-Whitney 2-tailed test.

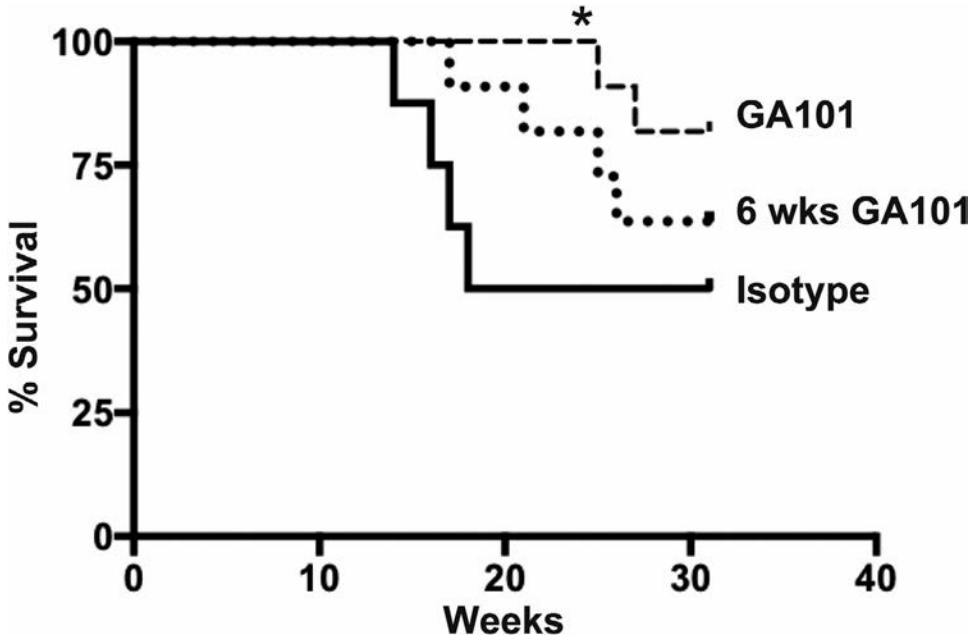

Figure 6. Effect of treatment with GA101 on survival in lupus-prone mice. Beginning at 10 weeks of age, one group of MRL/lpr mice expressing human CD20 on B cells (hCD20 MRL/lpr mice) was treated continuously with GA101 (n = 11) or isotype control (n = 8), and one group of hCD20 MRL/lpr mice was treated for 6 weeks with GA101 and then treatment was discontinued (n = 11). Censoring the data at 20 weeks of age, at which point 50% of the control animals had died, showed that continuous treatment with GA101 significantly improved survival compared to treatment with isotype control. * = P = 0.018 versus control, by Fisher's exact test.

short-term depletion experiments, which can reveal inherent differences in depletion efficacy. Over time, RTX was able to deplete B cells, as predicted in earlier studies (12,13), although it never achieved the same extent of depletion as GA101. The superior depleting ability of GA101 is consistent with findings in patients with CLL, resulting in improved progression-free survival in a head-to-head comparison with RTX (20) and could be important when translated to other clinical settings, where cost and feasibility limit the amount and duration of treatment or where type I anti-CD20 antibodies show limited efficacy.

Both RTX and GA101 ameliorated early disease in hCD20 MRL/lpr mice; however, GA101 was more effective in certain readouts, suggesting better overall efficacy. Earlier studies in this model had shown that conventional type I anti-CD20 mAb could treat early disease if applied continuously for weeks (13). Similar data were obtained in NZB/NZW mice by Bekar et al (8).

More importantly, we found that GA101 could treat more established disease. Although we did not directly compare GA101 to RTX in this model due to logistical reasons (long-term experiments requiring many mice in each group and biologic replicates to ensure reproducibility), we predict that GA101 would again be more effective than RTX under these even more challenging conditions based on its differentiated mechanism resulting in superiority in acute depletion, as was seen in early disease cohorts.

These findings extend our previous murine model work and that of others in several ways. Treatment of truly established disease is possible. We previously only treated early disease in the MRL/lpr model, while Bekar et al also treated mice that had just obtained 2+ but did not achieve 3+ proteinuria (8). Though Bekar et al referred to "established disease" in their report, in the NZB/NZW model, first detection of 2+ proteinuria is best considered new-onset disease, as can be discerned from the incidence of proteinuria as reported by Bekar et al (8).

By comparing GA101 and RTX, we also learned that small differences in B cell depletion, when measured in tissues, can be associated with meaningful differences in preclinical end points in hCD20 MRL/lpr mice. Glomerulonephritis scores were significantly lower and there were significantly fewer activated T cells in the mice with early disease treated with GA101 than in those treated with RTX, and this was associated with fewer total CD19+ cells in the spleen in the GA101-treated mice than in the RTX-treated mice, even though both treatments resulted in extensive B cell depletion.

Finally, from these experiments we learned that effective B cell depletion in murine models can extend survival, which had not been tested previously. Nonetheless, a single course of treatment did not induce a state of immune tolerance or remission, suggesting that a clinical approach of sustained treatment with GA101 is needed. While the findings of the present study are not definitive in this regard, they do provide evidence that continued suppression of B cells can treat disease for extended periods of time in preclinical models.

It is not clear which of the several engineered features of GA101 give it unique depleting properties, but our data support the

hypothesis that it is a combination of several properties. Based on a series of in vitro studies, the depletion mechanisms of anti-CD20 could include complement fixation, antibody-dependent cellular cytotoxicity, opsonization for FcR-mediated clearance by phagocytes such as macrophages, and direct apoptosis-inducing effects on target B cells (33). Classic type I antibodies, such as RTX, were thought to be superior at complement-mediated lysis, while type II antibodies were uniquely effective at inducing cell death. However, in vivo, in hCD20-transgenic mice or using murine anti-CD20 (35), depletion by type I antibodies was attributed chiefly to FcR-mediated cell clearance, independent of complement fixation or potential direct effects on CD20+ B cells (36). While a type II antibody (B1; tositumomab) was reported to be more efficacious than isotype-matched type I antibodies in depleting B cells in normal mice after a single low-dose injection, the mechanism of action was not determined (18).

Here we have investigated the in vivo mechanisms of depletion by GA101 in the challenging setting of lupus, using mutant versions of the antibody. Results of depletion experiments using the "P329G-LALA" version of GA101, which is completely inactivated with respect to FcR-mediated effector function (23), indicate that these FcR-mediated functions *do* contribute to B cell depletion in the lupus setting in vivo. However, this mutant antibody still mediated some B cell depletion, demonstrating that FcR-mediated clearance is not the only important mechanism. The non-glycoengineered version of GA101 showed only slightly less efficacy compared to GA101 itself in this model, suggesting only a small contribution of glycoengineering to B cell depletion in hCD20 MRL/lpr mice. The mechanisms by which glycoengineered production, resulting in enhanced affinity for the human FcγRIII, enhances in vivo efficacy, e.g., through antibody-dependent cell-mediated cytotoxicity or antibody-dependent cellular phagocytosis, are not entirely clear. B cell depletion may vary in different compartments (15) and may differ between mice and humans. Increased efficacy may therefore be limited in mice, due to differences in FcRs between species, or the in vivo setting of lupus may provide unique barriers to depletion. GA101 has shown superior efficacy in vivo in humans but so far only in the setting of B cell malignancy, particularly with malignancies such as CLL that have relatively low CD20 expression, and in follicular non-Hodgkin lymphoma (20,21).

It is tempting to speculate that GA101 is particularly efficacious in more challenging depletion settings due at least in part to its higher affinity for FcRs, mediated by both glycoengineering and its enhanced capability to elicit direct cell death, in part as a consequence of being a type II CD20 antibody, due to its unique hinge region mutation. The reduced dependency of GA101 on complement may be advantageous in the human autoimmune diseases where depletion by type I antibodies may be limited due to hypocomplementemia. Conversely, enhanced direct cell death could be beneficial in diseases that are driven by pathogenic tissue-resident B cells.

Insights from this work into the efficacy and mechanisms of GA101 in a preclinical lupus model, as well as the use of CD19 chimeric antigen receptor T cells for enhanced B cell depletion in lupus models (6), could have implications for clinical translation. With a more efficacious depletion tool, B cells might be revisited as a target in SLE. Indeed, the initial data that were generated for this article helped to motivate the NOBILITY clinical trial of GA101 in patients (ClinicalTrials.gov identifier: NCT02550652) (37) as well as the pivotal REGENCY study (ClinicalTrials.gov identifier: NCT NCT04221477).

ACKNOWLEDGMENTS

We would like to thank Jeremy Tilstra for insights and useful discussions. We thank the Division of Laboratory Animal Resources staff at the University of Pittsburgh for excellent mouse husbandry.

AUTHOR CONTRIBUTIONS

All authors were involved in drafting the article or revising it critically for important intellectual content, and all authors approved the final version to be published. Dr. Shlomchik had full access to all of the data in the study and takes responsibility for the integrity of the data and the accuracy of the data analysis.

Study conception and design. Marinov, Wang, Klein, Shlomchik.
Acquisition of data. Marinov, Wang, Bastacky, van Puijenbroek, Schindler, Speziale, Perro, Klein, Shlomchik.
Analysis and interpretation of data. Marinov, Wang, Klein, Nickerson, Shlomchik.

ADDITIONAL DISCLOSURES

Authors van Puijenbroek, Speziale, Perro, and Klein are employees of Roche. Author Schindler is an employee of Hoffmann-La Roche.

REFERENCES

1. Shlomchik MJ. Activating systemic autoimmunity: B's, T's, and tolls. Curr Opin Immunol 2009;21:626–33.
2. Tsokos GC. Systemic lupus erythematosus [review]. N Engl J Med 2011;365:2110–21.
3. Foster MH. T cells and B cells in lupus nephritis. Semin Nephrol 2007;27:47–58.
4. Chan OT, Madaio MP, Shlomchik MJ. The central and multiple roles of B cells in lupus pathogenesis. Immunol Rev 1999;169:107–21.
5. Chan OT, Madaio MP, Shlomchik MJ. B cells are required for lupus nephritis in the polygenic, Fas-intact MRL model of systemic autoimmunity. J Immunol 1999;163:3592–6.
6. Kansal R, Richardson N, Neeli I, Khawaja S, Chamberlain D, Ghani M, et al. Sustained B cell depletion by CD19-targeted CAR T cells is a highly effective treatment for murine lupus. Sci Transl Med 2019;11:eaav1648.
7. Li Y, Chen F, Putt M, Koo YK, Madaio M, Cambier JC, et al. B cell depletion with anti-CD79 mAbs ameliorates autoimmune disease in MRL/lpr mice. J Immunol 2008;181:2961–72.
8. Bekar KW, Owen T, Dunn R, Ichikawa T, Wang W, Wang R, et al. Prolonged effects of short-term anti-CD20 B cell depletion therapy in murine systemic lupus erythematosus. Arthritis Rheum 2010;62:2443–57.
9. Merrill J, Buyon J, Furie R, Latinis K, Gordon C, Hsieh HJ, et al. Assessment of flares in lupus patients enrolled in a phase II/III study of rituximab (EXPLORER). Lupus 2011;20:709–16.

10. Sanz I, Lee FE. B cells as therapeutic targets in SLE [review]. Nat Rev Rheumatol 2010;6:326–37.
11. Rovin BH, Furie R, Latinis K, Looney RJ, Fervenza FC, Sanchez-Guerrero J, et al. Efficacy and safety of rituximab in patients with active proliferative lupus nephritis: the Lupus Nephritis Assessment with Rituximab study. Arthritis Rheum 2012;64:1215–26.
12. Ahuja A, Teichmann LL, Wang H, Dunn R, Kehry MR, Shlomchik MJ. An acquired defect in IgG-dependent phagocytosis explains the impairment in antibody-mediated cellular depletion in lupus. J Immunol 2011;187:3888–94.
13. Ahuja A, Shupe J, Dunn R, Kashgarian M, Kehry MR, Shlomchik MJ. Depletion of B cells in murine lupus: efficacy and resistance. J Immunol 2007;179:3351–61.
14. Frank MM, Hamburger MI, Lawley TJ, Kimberly RP, Plotz PH. Defective reticuloendothelial system Fc-receptor function in systemic lupus erythematosus. N Engl J Med 1979;300:518–23.
15. Mossner E, Brunker P, Moser S, Puntener U, Schmidt C, Herter S, et al. Increasing the efficacy of CD20 antibody therapy through the engineering of a new type II anti-CD20 antibody with enhanced direct and immune effector cell-mediated B-cell cytotoxicity. Blood 2010;115:4393–402.
16. Ferrara C, Brünker P, Suter T, Moser S, Püntener U, Umaña P. Modulation of therapeutic antibody effector functions by glycosylation engineering: Influence of Golgi enzyme localization domain and co-expression of heterologous β1, 4-N-acetylglucosaminyltransferase III and Golgi α-mannosidase II. Biotechnol Bioeng 2006;93:851–61.
17. Tobinai K, Klein C, Oya N, Fingerle-Rowson G. A review of obinutuzumab (GA101), a novel type II anti-CD20 monoclonal antibody, for the treatment of patients with B-cell malignancies. Adv Ther 2017;34:324–56.
18. Beers SA, Chan CH, James S, French RR, Attfield KE, Brennan CM, et al. Type II (tositumomab) anti-CD20 monoclonal antibody out performs type I (rituximab-like) reagents in B-cell depletion regardless of complement activation. Blood 2008;112:4170–7.
19. Fischer K, Al-Sawaf O, Bahlo J, Fink AM, Tandon M, Dixon M, et al. Venetoclax and obinutuzumab in patients with CLL and coexisting conditions. N Engl J Med 2019;380:2225–36.
20. Goede V, Fischer K, Busch R, Engelke A, Eichhorst B, Wendtner CM, et al. Obinutuzumab plus chlorambucil in patients with CLL and coexisting conditions. N Engl J Med 2014;370:1101–10.
21. Marcus R, Davies A, Ando K, Klapper W, Opat S, Owen C, et al. Obinutuzumab for the first-line treatment of follicular lymphoma. N Engl J Med 2017;377:1331–44.
22. Cheson BD, Chua N, Mayer J, Dueck G, Trněný M, Bouabdallah K, et al. Overall survival benefit in patients with rituximab-refractory indolent non-Hodgkin lymphoma who received obinutuzumab plus bendamustine induction and obinutuzumab maintenance in the GADOLIN study. J Clin Oncol 2018;36:2259–66.
23. Herter S, Herting F, Muth G, van Puijenbroek E, Schlothauer T, Ferrara C, et al. GA101 P329GLALA, a variant of obinutuzumab with abolished ADCC, ADCP and CDC function but retained cell death induction, is as efficient as rituximab in B-cell depletion and antitumor activity. Haematologica 2018;103:e78–81.
24. Schlothauer T, Herter S, Koller CF, Grau-Richards S, Steinhart V, Spick C, et al. Novel human IgG1 and IgG4 Fc-engineered antibodies with completely abolished immune effector functions. Protein Eng Des Sel 2016;29:457–66.
25. Shlomchik MJ, Zharhary D, Saunders T, Camper SA, Weigert MG. A rheumatoid factor transgenic mouse model of autoantibody regulation. Int Immunol 1993;5:1329–41.
26. Nickerson KM, Cullen JL, Kashgarian M, Shlomchik MJ. Exacerbated autoimmunity in the absence of TLR9 in MRL.Fas(lpr) mice depends on Ifnar1. J Immunol 2013;190:3889–94.
27. Campbell A, Kashgarian M, Shlomchik M. NADPH oxidase inhibits the pathogenesis of systemic lupus erythematosus. Sci Transl Med 2012;4:157ra41.
28. Nickerson KM, Christensen SR, Shupe J, Kashgarian M, Kim D, Elkon K, et al. TLR9 regulates TLR7- and MyD88-dependent autoantibody production and disease in a murine model of lupus. J Immunol 2010;184:1840–8.
29. Blanco F, Kalsi J, Isenberg DA. Analysis of antibodies to RNA in patients with systemic lupus erythematosus and other autoimmune rheumatic diseases. Clin Exp Immunol 1991;86:66–70.
30. Tilstra JS, Avery L, Menk AV, Gordon RA, Smita S, Kane LP, et al. Kidney-infiltrating T cells in murine lupus nephritis are metabolically and functionally exhausted. J Clin Invest 2018;128:4884–97.
31. Gordon RA, Herter JM, Rosetti F, Campbell AM, Nishi H, Kashgarian M, et al. Lupus and proliferative nephritis are PAD4 independent in murine models. JCI Insight 2017;2:e92926.
32. Salles GA, Morschhauser F, Solal-Céligny P, Thieblemont C, Lamy T, Tilly H, et al. Obinutuzumab (GA101) in patients with relapsed/refractory indolent non-Hodgkin lymphoma: results from the phase II GAUGUIN study. J Clin Oncol 2013;31:2920–6.
33. Glennie MJ, French RR, Cragg MS, Taylor RP. Mechanisms of killing by anti-CD20 monoclonal antibodies [review]. Mol Immunol 2007;44:3823–37.
34. Chan O, Shlomchik MJ. A new role for B cells in systemic autoimmunity: B cells promote spontaneous T cell activation in MRL-lpr/lpr mice. J Immunol 1998;160:51–9.
35. Uchida J, Hamaguchi Y, Oliver JA, Ravetch JV, Poe JC, Haas KM, et al. The innate mononuclear phagocyte network depletes B lymphocytes through Fc receptor-dependent mechanisms during anti-CD20 antibody immunotherapy. J Exp Med 2004;199:1659–69.
36. Gong Q, Ou Q, Ye S, Lee WP, Cornelius J, Diehl L, et al. Importance of cellular microenvironment and circulatory dynamics in B cell immunotherapy. J Immunol 2005;174:817–26.
37. Hoffmann-La Roche, sponsor. A randomized, double-blind, placebo-controlled, multi-center study to evaluate the safety and efficacy of obinutuzumab in patients with ISN/RPS 2003 class III or IV lupus nephritis. ClinicalTrials.gov identifier: NCT02550652.

Arthritis & Rheumatology
Vol. 73, No. 5, May 2021, pp 837–847
DOI 10.1002/art.41669

American College of Rheumatology
Empowering Rheumatology Professionals

Long-Term Outcomes in Patients With Connective Tissue Disease–Associated Pulmonary Arterial Hypertension in the Modern Treatment Era: Meta-Analyses of Randomized, Controlled Trials and Observational Registries

Dinesh Khanna,[1] Carol Zhao,[2] Rajan Saggar,[3] Stephen C. Mathai,[4] Lorinda Chung,[5] J. Gerry Coghlan,[6] Mehul Shah,[2] John Hartney,[2] and Vallerie McLaughlin[1]

Objective. Data on the magnitude of benefit of modern therapies for pulmonary arterial hypertension (PAH) in connective tissue disease (CTD)–associated PAH are limited. In this study, we performed meta-analyses of randomized, controlled trials (RCTs) and registries to quantify the benefit of these modern therapies in patients with CTD-PAH.

Methods. The PubMed and Embase databases were searched for articles reporting data from RCTs or registries published between January 1, 2000 and November 25, 2019. Eligibility criteria included multicenter studies with ≥30 CTD-PAH patients. For an RCT to be included, the trial had to evaluate an approved PAH therapy, and long-term risks of clinical morbidity and mortality or 6-minute walk distance had to be reported. For a registry to be included, survival rates had to be reported. Random-effects models were used to pool the data.

Results. Eleven RCTs (total of 4,329 patients; 1,267 with CTD-PAH) and 19 registries (total of 9,739 patients; 4,008 with CTD-PAH) were included. Investigational therapy resulted in a 36% reduction in the risk of clinical morbidity/mortality events both in the overall PAH population (hazard ratio [HR] 0.64, 95% confidence interval [95% CI] 0.54, 0.75; $P < 0.001$) and in CTD-PAH patients (HR 0.64, 95% CI 0.51, 0.81; $P < 0.001$) as compared to control subjects. The survival rate was lower in CTD-PAH patients compared to all PAH patients (survival rate 62%, 95% CI 57, 67% versus 72%, 95% CI 69, 75% at 3 years). The survival rate in CTD-PAH patients treated primarily after 2010 was higher than that in CTD-PAH patients treated before 2010 (survival rate 73%, 95% CI 62, 81% versus 65%, 95% CI 59, 71% at 3 years).

Conclusion. Modern therapy provides a similar reduction in morbidity/mortality risk in patients with CTD-PAH when compared to the PAH population overall. Risk of death is higher in CTD-PAH patients than in those with PAH overall, but survival has improved in the last 10 years, which may be related to increased screening and/or new treatment approaches. Early detection of PAH in patients with CTD and up-front intensive treatment are warranted.

Supported by Actelion Pharmaceuticals US, Inc.

[1]Dinesh Khanna, MD, MSc, Vallerie McLaughlin, MD, FACC, FCCP: University of Michigan, Ann Arbor; [2]Carol Zhao, MS, Mehul Shah, MD, PhD, John Hartney, PhD: Actelion Pharmaceuticals US, Inc., South San Francisco, California; [3]Rajan Saggar, MD: David Geffen School of Medicine, University of California, Los Angeles; [4]Stephen C. Mathai, MD, MHS: Johns Hopkins University School of Medicine, Baltimore, Maryland; [5]Lorinda Chung, MD, MS: Stanford University and Palo Alto VA Health Care System, Palo Alto, California; [6]J. Gerry Coghlan, MD: Royal Free Hospital London, London, UK.

Dr. Khanna has received consulting fees from Acceleron, Bristol Myers Squibb, Gilead, Genentech/Roche, GlaxoSmithKline, Mitsubishi Tanabe, and Sanofi Aventis/Genzyme (less than $10,000 each) and from Actelion, Bayer, Boehringer Ingelheim, Corbus, CSL Behring, and Horizon (more than $10,000 each) and holds stock in Eicos Sciences. Ms Zhao and Drs. Shah and Hartney are employees of Actelion and own stock or stock options in Johnson & Johnson, the parent company of Janssen Pharmaceuticals. Dr. Saggar has received consulting fees, speaking fees, and/or honoraria from Actelion, Gilead, and United Therapeutics (more than $10,000 each) and research support from those companies. Dr. Mathai has received consulting fees from Arena and Liquidia (less than $10,000 each) and from Actelion and United Therapeutics (more than $10,000 each). Dr. Chung has received consulting fees from Bristol Myers Squibb, Eicos Sciences, and Mitsubishi Tanabe (less than $10,000 each) and from Boehringer Ingelheim (more than $10,000), has received research support from Boehringer Ingelheim and United Therapeutics, and has served on a data safety monitoring board for Reata. Dr. Coghlan has received consulting fees, speaking fees, and/or honoraria from Bayer and GlaxoSmithKline (less than $10,000 each) and from Johnson & Johnson (more than $10,000) and research support from Johnson & Johnson. Dr. McLaughlin has received consulting fees from Altavant, CVC Caremark, CiVi Biopharma, and Gossamer Bio (less than $10,000 each) and from Actelion, Acceleron, Arena, Bayer, and United Therapeutics (more than $10,000 each) and research support from Acceleron, Actelion, Bayer, Reata, SoniVie, and United Therapeutics.

Address correspondence to Dinesh Khanna, MD, MSc, University of Michigan, Division of Rheumatology, Department of Internal Medicine, 300 North Ingalls Street, SPC 542, Suite 7C27, Ann Arbor, MI 48109. Email: khannad@med.umich.edu.

Submitted for publication August 18, 2020; accepted in revised form January 26, 2021.

INTRODUCTION

Pulmonary arterial hypertension (PAH) leads to right ventricular dysfunction and failure, with a median survival of ~3 years from the time of diagnosis (1,2). Connective tissue disease (CTD)–associated PAH is historically associated with shortened survival compared to idiopathic PAH (IPAH) (3–6). Early detection of PAH with established methods among patients with CTDs, such as those with systemic sclerosis (SSc) (7), and subsequent early treatment may improve survival outcomes (8). Rheumatologists are in a unique and critical position to identify these patients.

Availability of new and combination therapy approaches targeting multiple pathophysiologic pathways have led to improved outcomes in PAH (9–16). However, trials of PAH therapies generally enroll patients with different etiologies of PAH, and trials devoted solely to those with CTD-PAH are rare; therefore, the magnitude of treatment effect in CTD-PAH is poorly defined, as these patients represent a subgroup in most trials, albeit a large one. Furthermore, data on whether new treatment approaches have resulted in improved survival in CTD-PAH are lacking.

For the present study, we conducted 2 meta-analyses. In one meta-analysis, we analyzed randomized, controlled trials (RCTs) to evaluate the magnitude of benefit of US Food and Drug Administration (FDA)–approved PAH therapies in patients with CTD-PAH. In the other meta-analysis, we analyzed real-world observational disease registries to compare survival outcomes between patients with CTD-PAH and the overall PAH population, and between patients treated mostly before 2010 and those treated mostly after 2010. Compared to prior meta-analyses that have evaluated outcomes in RCTs among patients with CTD-PAH (17,18), our RCT meta-analysis provides a more contemporary data set that includes modern agents and treatment paradigms, as well as a larger sample size. Our second meta-analysis extends these findings by evaluating long-term survival outcomes, an end point that is not typically included in RCTs because of their shorter duration. We also investigated survival over time, to determine whether the availability of newer therapies and treatment approaches has translated into improved survival in real-world settings.

PATIENTS AND METHODS

Study design. These meta-analyses were conducted in accordance with the Preferred Reporting Items for Systematic Review and Meta-Analysis guidelines (19), with a modification suited to the rare disease state of PAH. Specifically, we conducted a comprehensive literature search, instead of a systematic review, to identify peer-reviewed reports of RCTs evaluating new therapies and disease registries. We did not expand the search to databases beyond PubMed and Embase, nor did we examine reference lists and non-database sources for additional information, because of the very low likelihood of this method yielding additional articles in this rare disease. The protocol was registered with the International Prospective Register of Systematic Reviews (PROSPERO registration no. CRD42020167119) (20).

Search strategy and selection criteria. PubMed and Embase (Elsevier) were searched for English-only articles reporting data from RCTs or registries and published between January 1, 2000 and November 25, 2019. Specific parameters (search terms, Boolean operators, and filters) were applied. To identify RCTs, we searched in PubMed for the term "pulmonary arterial hypertension" in the title along with "AND (randomized OR randomised)" and restricted the search to human subjects; in Embase, we searched for "('pulmonary hypertension'/exp OR 'pulmonary hypertension')" and restricted the search to phase III or phase IV RCTs. To identify registries, we searched in PubMed for the term "pulmonary arterial hypertension" in the title along with "AND (registry OR observation OR consecutive OR multicenter OR multicentre)" and restricted the search to human subjects; in Embase, we searched for "pulmonary hypertension" in the title along with "AND ('observational study'/exp OR 'observational study')."

RCTs and registries had to meet the following inclusion criteria. 1) The RCT or registry was conducted at multiple centers. 2) Enrolled patients were adult patients with World Health Organization (WHO) group 1 pulmonary hypertension (i.e., PAH) (21). 3) The RCT or registry included ≥30 patients with CTD-PAH. 4) Publicly available CTD-PAH–specific outcomes data were provided for the CTD-PAH subgroup. 5) Enrollment of patients began in 2000 or later. 6) Long-term incidence rates of clinical morbidity and/or mortality were reported (median enrollment time ≥6 months).

Only peer-reviewed data were included. Additional inclusion criteria for RCTs were as follows: the RCT was a phase III or phase IV study; the evaluated PAH therapy had received current approval from the FDA; patients were exposed to the study drug for PAH treatment for at least 3 months; and one of the defined primary or secondary end points was time to clinical morbidity/mortality, time to clinical worsening, or 6-minute walk distance (6MWD) measured 3–6 months from baseline.

To minimize the risk of bias in study selection, we utilized the above-noted strict prespecified inclusion/exclusion criteria. This involved a detailed review of each study design, patient inclusion and exclusion criteria, and definition of study end points. Studies not meeting the prespecified criteria were excluded. In addition, at least 2 reviewers independently verified the studies that were to be included in the analyses, with any disagreements arbitrated by the lead author (DK) and senior author (VM).

Publications providing the same data from the same RCT or registry were removed. For multiple publications from a single study, the most recent publication containing data on the CTD-PAH population was utilized. Data from all primary reports of RCTs were included in the analyses of all PAH patients and CTD-PAH patients, unless more detailed information for CTD-PAH patients

were included in later post hoc analyses. When we extracted data from the post hoc analyses of the CTD-PAH subgroup, we ensured that the number of patients in the CTD-PAH subgroup and the statistical analysis method were consistent with that described in the primary report. If multiple registries were conducted in a single country, only studies that did not substantially overlap in enrollment period were included, to avoid capturing data from the same patient in multiple registries.

Data were extracted from RCT and registry publications separately by 2 team members (with medical, science, or statistical expertise) under the leadership of statisticians at Actelion Pharmaceuticals. Extracted data were verified by a third team member independently. In the event of a discrepancy, a statistician verified the data prior to the final statistical analysis, and one of the authors (JH) arbitrated any disagreements.

Data were extracted separately for patients with any of the PAH etiologies and for patients with CTD-PAH. Baseline data extracted for both RCTs and registries were the 6MWD, age, sex, WHO functional class, and PAH etiology. Data extracted after baseline were the change in the 6MWD from baseline to between 3 and 6 months, number of clinical morbidity/mortality events, and hazard ratio (HR) (with 95% confidence interval [95% CI]) for the long-term risk of morbidity/mortality in RCTs. In addition, data from the registries included the survival rates at 1, 2, and 3 years, as reported in the registry or as determined from Kaplan-Meier survival curves using a graph digitizer.

Statistical analysis. The meta-analysis of RCTs evaluated the effect of PAH therapies on time to clinical morbidity and/or mortality in all patients and in patients with CTD-PAH, as well as the effect on the 6MWD measured between 3 and 6 months after initiation of study treatment. The components of the clinical morbidity/mortality end points varied among the studies (see Supplementary Table 1, available on the *Arthritis & Rheumatology* website at http://onlinelibrary.wiley.com/doi/10.1002/art.41669/abstract). The meta-analysis of registries evaluated survival outcomes in all patients and in patients with CTD-PAH. Analysis populations are defined in Supplementary Table 2, available on the *Arthritis & Rheumatology* website at http://onlinelibrary.wiley.com/doi/10.1002/art.41669/abstract.

To assess heterogeneity among studies, we calculated the I^2 value associated with the fixed-effects meta-analysis models. These values indicated that most analyses using fixed-effects models had high heterogeneity, whereas analyses using random-effects meta-analysis models had I^2 values that were considered to be within the acceptable range of heterogeneity (I^2 lower than 50%) (see Supplementary Table 3, available on the *Arthritis & Rheumatology* website at http://onlinelibrary.wiley.com/doi/10.1002/art.41669/abstract). Thus, we controlled for heterogeneity among studies by consistently using random-effects meta-analysis models to pool results, using inverse variance weighting followed by unweighting with application of a random-effects variance component. The overall treatment effect estimate was calculated using the DerSimonian and Laird random-effects method (22).

Time-to-event end points were estimated using the Kaplan-Meier method. Survival rates at 1, 2, and 3 years in the registries were extracted from Kaplan-Meier curves and were stratified by study period mostly before or after 2010, to assess the impact of newer treatment approaches. Outcomes were analyzed for the overall PAH population and stratified by disease etiology (all CTD-PAH patients and CTD-PAH subtypes [SSc or systemic lupus erythematosus (SLE) or IPAH]). Registries with ≥50% of the study period in 2010 or later were classified as the after-2010 group.

Sensitivity analyses included analysis of treatment effect in RCTs in patients with IPAH compared to patients with CTD-PAH. In the registries, analysis of survival rate in selected studies containing both CTD-PAH and other etiologies was performed to confirm the historical difference between etiologies.

A forest plot showing the effect size and associated variability in each study, as well as the combined effect, was created to examine the consistency of results. If any outliers were apparent, the data extraction was verified from the original source and the units were confirmed to ensure that no unit conversion was necessary. If, after this, an outlier was detected, a sensitivity analysis removing the outlier could be conducted to assess the impact on the overall analysis. However, no such outliers were found in our analysis.

Statistical analyses were performed using Comprehensive Meta-Analysis version 3 software (Biostat).

RESULTS

Study and patient characteristics. With regard to RCTs, a total of 801 articles were identified through our comprehensive search strategy (see Supplementary Figure 1, available on the *Arthritis & Rheumatology* website at http://onlinelibrary.wiley.com/doi/10.1002/art.41669/abstract) and 11 studies were ultimately included in the meta-analysis (as listed in Supplementary Table 4 on the *Arthritis & Rheumatology* website at http://onlinelibrary.wiley.com/doi/10.1002/art.41669/abstract). Among those that met the criteria for one of the defined primary end points, 5 RCTs reported time to clinical morbidity/mortality events (12–16,23,24) (specifically defined in Supplementary Table 1 [http://onlinelibrary.wiley.com/doi/10.1002/art.41669/abstract]), and 6 RCTs reported change in the 6MWD (10,11,25–30). The 11 RCTs enrolled a total of 4,329 patients with PAH, including 1,267 patients with CTD-PAH (29.3%). Each RCT evaluated the addition of a PAH-specific therapy to a patient's current care, so that patients were stratified according to whether they received no PAH-specific treatment, monotherapy, or dual combination therapy.

With regard to observational registries, a total of 1,389 articles were identified through our search (see Supplementary Figure 2,

Table 1. Baseline characteristics of all patients with PAH in the randomized, controlled trials*

	Investigational treatment group				Control group			
Study (ref.)	No. of patients	Age, mean ± SD years	Female, %	WHO functional class I–II, %	No. of subjects	Age, mean ± SD years	Female, %	WHO functional class I–II, %
AMBITION (12)	253	55 ± 14	74	30	247	54 ± 15	81	32
GRIPHON (15)	574	48 ± 15	80	48	582	48 ± 16	80	45
SERAPHIN (14)	242	45 ± 15	80	50	250	47 ± 17	74	52
PHIRST (10)	79	53 ± 15	75	35	82	55 ± 15	79	29
ARIES-1 (28)	67	49 ± 16	79	36	67	48 ± 16	88	37
ARIES-2 (28)	63	50 ± 16	81	46	65	51 ± 14	68	40
PATENT (11)	254	51 ± 17	80	45	126	51 ± 17	78	51
SUPER-1 (9)	71	48 ± 15	79	39	70	49 ± 17	81	47
BREATHE-1 (25)	144	49 ± 16	79	0	69	47 ± 16	78	0
COMPASS-2 (13)	159	53 ± 15	79	45	175	55 ± 16	73	39
FREEDOM-EV (16)	346	46 ± 16	80	62	344	45 ± 15	78	70
All studies	2,252	50 ± 1.1†	79	41	2,077	50 ± 1.2†	78	43

* PAH = pulmonary arterial hypertension; WHO = World Health Organization; AMBITION = Ambrisentan plus Tadalafil in PAH; GRIPHON = Prostacyclin Receptor Agonist (Prostaglandin I_2) in PAH; SERAPHIN = Study with an Endothelin Receptor Antagonist in PAH to Improve Clinical Outcome; PHIRST = PAH and Response to Tadalafil; ARIES = Randomized, Double-blind, Placebo-controlled, Multicenter, Efficacy Study of Ambrisentan for PAH (1 and 2); PATENT = PAH Soluble Guanylate Cyclase–Stimulator Trial 1; SUPER-1 = Sildenafil Use in PAH; BREATHE-1 = Bosentan Randomized Trial of Endothelin Antagonist Therapy; COMPASS-2 = Combination of Bosentan and Sildenafil Versus Sildenafil Monotherapy on PAH; FREEDOM-EV = International, Multicenter, Randomized, Double-blind, Placebo-controlled Event-driven Trial of Oral Treprostinil in Subjects with PAH.
† Values are the estimated mean ± SEM from the random-effects model.

available on the *Arthritis & Rheumatology* website at http://onlinelibrary.wiley.com/doi/10.1002/art.41669/abstract) and 19 registries were ultimately included in the meta-analysis (as listed in Supplementary Table 5, available on the *Arthritis & Rheumatology* website at http://onlinelibrary.wiley.com/doi/10.1002/art.41669/abstract): in 9 of the registries, patients with PAH of all etiologies were enrolled (4,5,31–37), and in 10 registries, only patients with CTD-PAH were enrolled (38–47). The 19 registries enrolled 9,739 patients with PAH, including 4,008 patients with CTD-PAH (41.2%).

At baseline both in the RCTs and in the registries, patients with CTD-PAH were older and had a lower mean 6MWD compared to the overall PAH population. In RCTs, patients with PAH of any etiology had a mean age of 50 years, 78–79% were female, and 41–43% had WHO functional class I or II disease (Table 1). Patients with CTD-PAH in the RCTs had a mean age of 55–56 years, compared to a mean age of 50 years among patients of all PAH etiologies, and had a mean 6MWD of 337–339 meters, compared to a mean 6MWD of 355–357 meters among patients of all PAH etiologies (see Supplementary Tables 6 and 7 on the *Arthritis & Rheumatology* website at http://onlinelibrary.wiley.com/doi/10.1002/art.41669/abstract).

In all 16 registries in which baseline characteristics were reported separately for the CTD-PAH population, patients with

Table 2. Baseline characteristics of the registry patients with PAH of any etiology and patients with CTD-PAH*

	All patients (n = 7,844)					Patients with CTD-PAH (n = 2,113)			
Registry (ref.)	Age, mean ± SD years	Female, %	WHO functional class I–II, %	6MWD, mean ± SD meters	CTD, %	Age, mean ± SD years	Female, %	WHO functional class I–II, %	6MWD, mean ± SD meters
REHAP (31)	45 ± 17	71	31	363 ± 120	18	54 ± 15	90	21	309 ± 115
PAH-QuERI (32)	55 ± 16	77	47	NR	29	NR	NR	NR	NR
COMPERA (5)	64 ± 16	64	11	298 ± 126	22	66 ± 13	78	11	273 ± 130
French PAH Network Registry (4)	50 ± 15	66	25	329 ± 109	15	56 ± 15	80	26	315 ± 111
REVEAL (33)	50 ± 17	77	NR	NR	28	NR	NR	NR	NR
Turkish registry (34)	46 ± 17	77	21	NR	22	NR	NR	NR	NR
Chinese Registry-PAH (35)	36 ± 15	76	46	390 ± 111	37	42 ± 14	85	45	384 ± 107
BPR (36)	59 ± 17	77	11	NR	42	62 ± 11	85	6	NR
KORPAH (37)	50 ± 17	78	53	363 ± 116	58	54 ± 17	85	63	358 ± 114
All registries	51 ± 2.7†	74	28	348 ± 16.4†	29	56 ± 3.3†	84	24	328 ± 20.1†

* PAH = pulmonary arterial hypertension; CTD-PAH = connective tissue disease–associated PAH; WHO = World Health Organization; 6MWD = 6-minute walk distance; REHAP = Spanish Registry of PAH; PAH-QuERI = PAH Quality Enhancement Research Initiative; NR = not reported; COMPERA = Comparative, Prospective Registry of Newly Initiated Therapies for Pulmonary Hypertension; REVEAL = Registry to Evaluate Early and Long-term PAH Disease Management; BPR = Bosentan Patient Registry; KORPAH = Korean Registry of PAH.
† Values are the estimated mean ± SEM from the random-effects model.

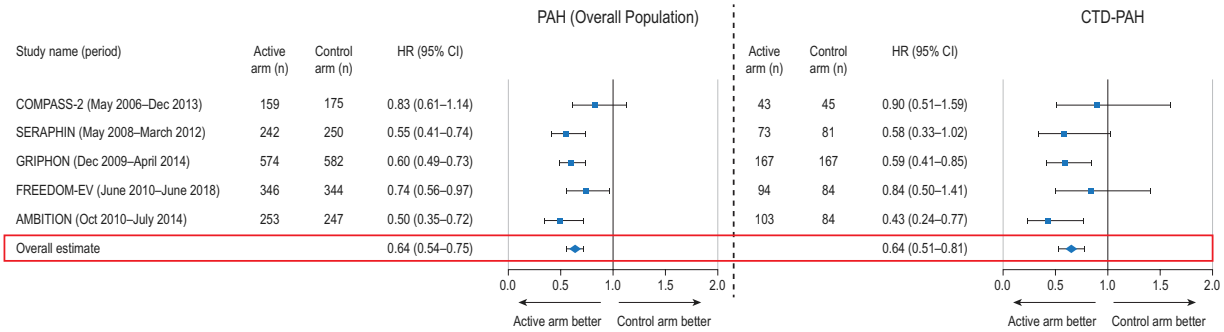

Figure 1. Time to clinical morbidity/mortality event for all patients with pulmonary arterial hypertension (PAH) (left) and patients with connective tissue disease (CTD)–associated PAH (right) in randomized, controlled trials that evaluated time to clinical morbidity/mortality event as a primary end point (5 trials). Results are depicted as forest plots, showing the hazard ratio (HR) with 95% confidence interval (95% CI) in the active treatment group relative to the control group. Overall HRs were estimated using random-effects models. COMPASS-2 = Combination of Bosentan and Sildenafil Versus Sildenafil Monotherapy on PAH; SERAPHIN = Study with an Endothelin Receptor Antagonist in PAH to Improve Clinical Outcome; GRIPHON = Prostacyclin Receptor Agonist (Prostaglandin I_2) in PAH; FREEDOM-EV = International, Multicenter, Randomized, Double-blind, Placebo-controlled Event-driven Trial of Oral Treprostinil in Subjects with PAH; AMBITION = Ambrisentan plus Tadalafil in PAH.

CTD-PAH had a mean age of 55 years, 87% were female, 30% had WHO functional class I or II disease, and the mean 6MWD was 327 meters (see Supplementary Table 8 on the *Arthritis & Rheumatology* website at http://onlinelibrary.wiley.com/doi/10.1002/art.41669/abstract). In the 9 registries in which patients with all PAH etiologies were enrolled, the patients had a mean age of 51 years, 74% were female, 28% had WHO functional class I or II disease, and the mean 6MWD was 348 meters. Patients with CTD-PAH in these 9 registries had a mean age of 56 years, 84% were female, 24% had WHO functional class I or II disease, and the mean 6MWD was 328 meters (Table 2). Baseline data from the registries for the CTD-PAH subgroups treated before 2010 and those treated after 2010 are shown in Supplementary Table 9, and baseline data from the registries for the CTD-PAH subgroups of SSc and SLE are shown in Supplementary Table 10 (available on the *Arthritis & Rheumatology* website at http://onlinelibrary.wiley.com/doi/10.1002/art.41669/abstract).

Outcomes from RCTs. Among the 5 RCTs in which time to clinical morbidity/mortality events was reported as the primary end point, 3,172 patients were enrolled (941 with CTD-PAH [30%]) (12–16,23,24). Additional PAH therapy resulted in a 36% reduction in the risk of morbidity/mortality events in the overall PAH population compared to that in control subjects (HR 0.64, 95% CI 0.54, 0.75; $P < 0.001$), and a 36% reduction in the risk of morbidity/mortality events in patients with CTD-PAH compared to controls (HR 0.64, 95% CI 0.51, 0.81; $P < 0.001$) (Figure 1).

In the overall PAH population, additional PAH therapy led to a placebo- or monotherapy-corrected increase in the 6MWD (mean increase of 28.6 meters, 95% CI 19.2, 38.0; $P < 0.001$) (Figure 2A). In 8 RCTs (total of 2,874 patients; 882 with CTD-PAH [31%]), this end point was reported according to CTD-PAH etiology (9–12,15,23–30). Additional PAH therapy led to an increase in the 6MWD in the overall PAH population (mean increase of 34.6 meters, 95% CI 22.1, 47.1; $P < 0.001$) and in patients with CTD-PAH (mean increase of 20.4 meters, 95% CI 10.9, 29.9; $P < 0.001$) (Figures 2B and C).

Sensitivity analyses were performed to compare outcomes between patients with CTD-PAH and patients with IPAH among the subset of trials in which outcomes were reported separately in the IPAH subpopulation. Results from patients with IPAH trended similar to those in the overall PAH population (HR for risk of morbidity/mortality events 0.63, 95% CI 0.54, 0.73; $P < 0.001$).

Outcomes from registries. Among the 9 registries in which patients with PAH were included irrespective of etiology (4,5,31,32–37), survival rates in the 2,113 patients with CTD-PAH were lower than in the 7,829 patients in the overall PAH population (Figure 3A).

Among all CTD-PAH patients with available data, including those from both the all-PAH registries and the CTD-PAH–specific registries (19 registries, 3,978 patients), survival rates in patients with CTD-PAH in the registries in which treatment was received within ≥50% of the study period during or after 2010 (n = 1,819) were higher than in patients with CTD-PAH in the registries in which treatment was received within ≥50% of the study period occurring before 2010 (n = 2,159) (Figure 3B).

Among all patients with CTD-PAH, survival rates were lower for those with SSc (n = 1,485) (36,38,41,43,44,46,47) compared to those with SLE (n = 456) (39,40,42,45) (Figure 3C).

DISCUSSION

Our meta-analysis of RCTs demonstrated that patients with CTD-PAH derive a clinically significant benefit from currently available PAH therapies, which, in many patients, comprises the addition of a drug targeting a second or third pathway involved in the

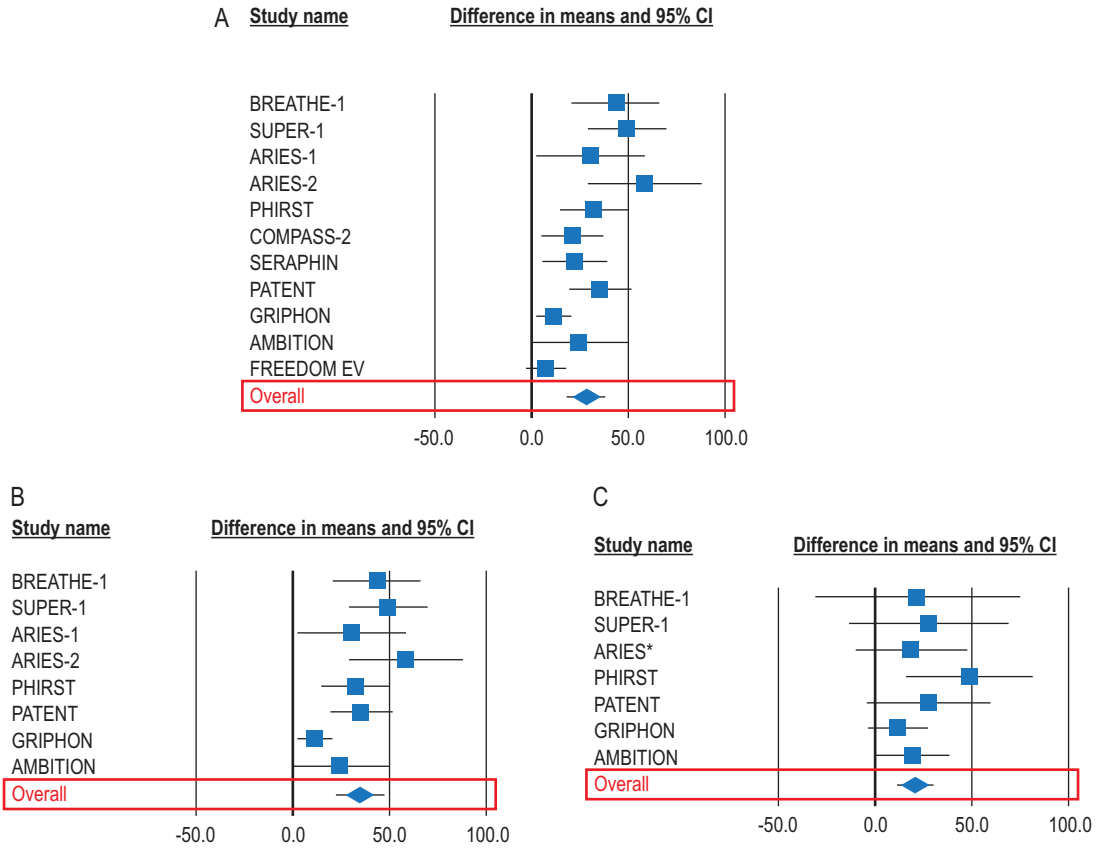

Figure 2. Change in the 6-minute walk distance (6MWD) for all patients with pulmonary arterial hypertension (PAH) of any etiology in all randomized, controlled trials (RCTs) (11 trials) (**A**), for all patients in RCTs that reported 6MWD in patients with connective tissue disease (CTD)–associated PAH (8 trials) (**B**), and for patients with CTD-PAH (8 trials) (**C**). Results are depicted as forest plots, showing the mean change in the 6MWD from baseline to between 3 and 6 months, with 95% confidence interval (95% CI). *Combined data from the Randomized, Double-blind, Placebo-controlled, Multicenter, Efficacy Study of Ambrisentan for PAH 1 and 2 (ARIES-1 and ARIES-2, respectively). BREATHE-1 = Bosentan Randomized Trial of Endothelin Antagonist Therapy; SUPER-1 = Sildenafil Use in PAH; PHIRST = PAH and Response to Tadalafil; COMPASS-2 = Combination of Bosentan and Sildenafil Versus Sildenafil Monotherapy on PAH; SERAPHIN = Study with an Endothelin Receptor Antagonist in PAH to Improve Clinical Outcome; PATENT = PAH Soluble Guanylate Cyclase–Stimulator Trial 1; GRIPHON = Prostacyclin Receptor Agonist (Prostaglandin I2) in PAH; AMBITION = Ambrisentan plus Tadalafil in PAH; FREEDOM-EV = International, Multicenter, Randomized, Double-blind, Placebo-controlled Event-driven Trial of Oral Treprostinil in Subjects with PAH.

pathophysiology of PAH. Our meta-analysis of registries showed that patients with CTD-PAH have a higher risk of death than the overall PAH population; however, survival has improved among the CTD-PAH population treated mostly in the last 10 years compared to earlier patient populations.

Two other relatively recent meta-analyses have also evaluated the benefit of PAH-specific therapy in patients with CTD-PAH (17,18). Rhee and colleagues (17) evaluated individual patient data from 11 RCTs published between 2002 and 2013 (total of 2,762 patients; 827 with CTD-PAH [30%]). Most of the trials (59% of patients) evaluated endothelin receptor antagonists (ERAs). Similar to our findings based on the 6MWD, patients with CTD-PAH experienced less benefit than patients with IPAH. The mean placebo-corrected treatment effect, measured as the change in 6MWD from baseline to 3 months, was 23.1 meters in patients with CTD-PAH versus 40.4 meters in patients with IPAH (adjusted treatment effect difference −17.3 meters, 90% CI −31.3, −3.3; *P* for interaction = 0.043). We reported a similar placebo- or monotherapy-corrected mean change in the 6MWD of 20.4 meters in patients with CTD-PAH. Our reference population included patients with all PAH etiologies, which may explain the lower benefit (difference of 34.6 meters for the change in the 6MWD) observed in our study compared to that observed in patients with IPAH reported by Rhee and colleagues (17). However, earlier meta-analyses of RCTs reporting change in the 6MWD are also conflicting, with one study showing a similar treatment benefit between patients with CTD-PAH and those with PAH of all etiologies (48) and another showing no treatment benefit in patients with CTD-PAH (49). Time to clinical worsening was not significantly prolonged among patients with CTD-PAH in the meta-analysis by Rhee and colleagues (17), as the odds ratio for the likelihood of a longer time to clinical worsening was 0.72

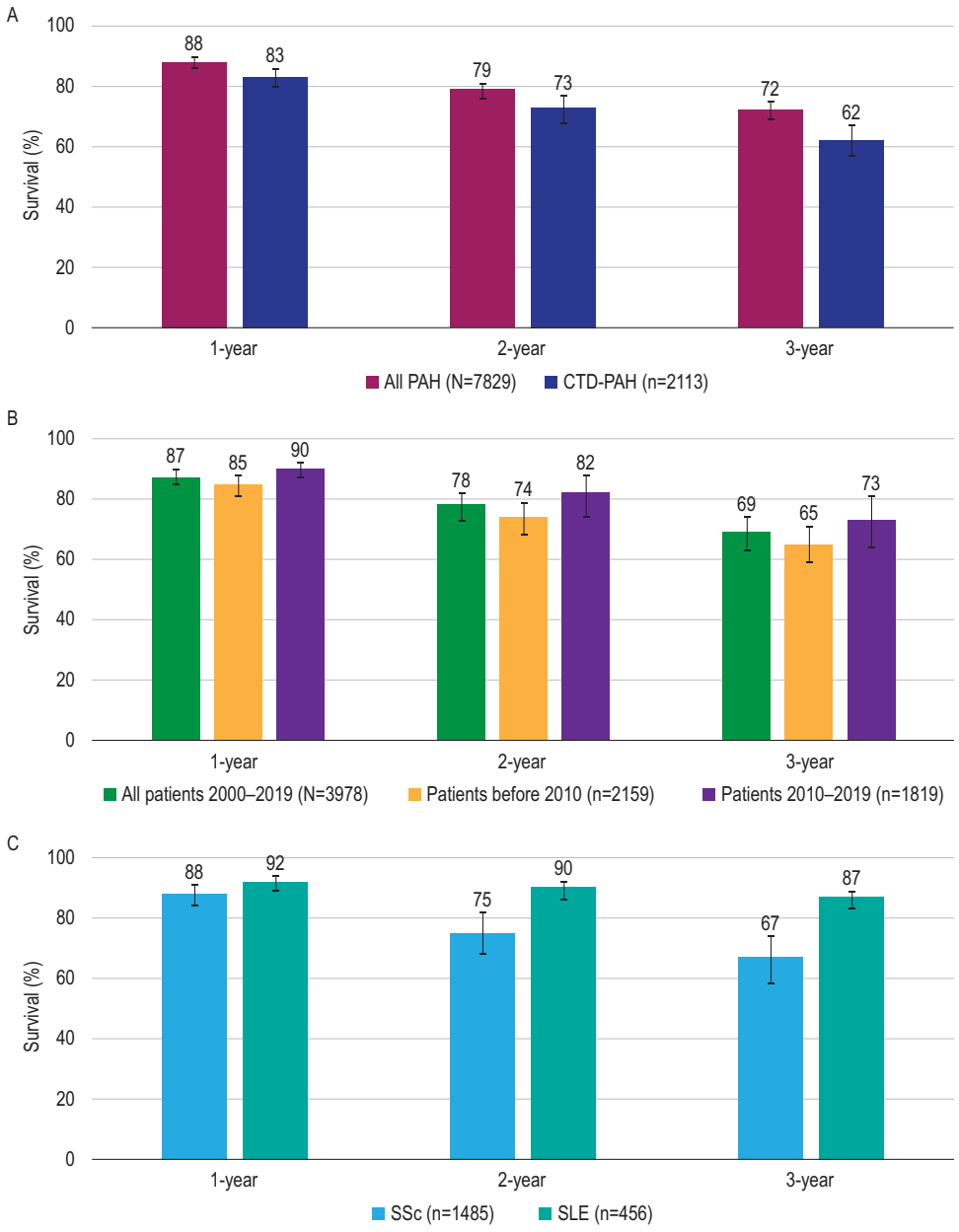

Figure 3. Survival estimates at 1 year, 2 years, and 3 years in all patients with pulmonary arterial hypertension (PAH) and patients with connective tissue disease (CTD)–associated PAH from the registries in which all PAH etiologies were included (9 registries) (**A**), in patients with CTD–associated PAH from all registries (19 registries) by enrollment period (**B**), and by CTD subtype from disease-specific registries or registries that included disease-specific outcomes (8 registries for systemic sclerosis [SSc] and 4 registries for systemic lupus erythematosus [SLE]) (**C**). Results are shown as the survival rates with 95% confidence intervals.

(95% CI 0.45, 1.16), whereas we demonstrated a reduction in the risk of a morbidity/mortality event with PAH-specific therapy (HR 0.64, 95% CI 0.51, 0.80).

The difference between meta-analyses may result from several factors. We believe that our analysis provides a more precise estimate of treatment effect because we applied more stringent statistical methods to pool the studies. Specifically, we measured the time to a clinical morbidity/mortality event by using the HR, which averages the treatment effect over the entire study period. Rhee and colleagues measured clinical worsening events using an odds ratio, which is affected by differences in study duration. Further, our study required a median study duration of ≥6 months to capture long-term clinical morbidity and mortality (current standards to assess overall benefit), whereas ~50% of the trials included in the meta-analysis by Rhee and colleagues (17) were of 12 weeks to 18 weeks in duration (i.e., a previous standard to assess PAH therapy efficacy). Finally, we used a more contemporary data set, which included trials of the most recently available PAH therapies, comprising oral ERAs, phosphodiesterase type 5 inhibitors, oral prostacyclin pathway agents, and riociguat, as well

as more use of combination therapy. This data set, thus, more accurately reflects current treatment approaches. This approach also resulted in a larger patient population (1,267 CTD-PAH patients from RCTs, compared to 827 patients in the analysis by Rhee and colleagues), which increases the precision of the statistical estimates.

Pan and colleagues (18) analyzed data extracted from 6 RCTs published between 2011 and 2017 (total of 3,262 patients; 963 with CTD-PAH [30%]). These trials evaluated ERAs, tadalafil, selexipag, and riociguat. This meta-analysis aimed to compare combination therapy to monotherapy; however, background therapy varied among studies and patients within the studies. Among 4 RCTs in the CTD-PAH subset included in the analysis, additional PAH therapy led to a 27% reduction in relative risk for clinical worsening (pooled relative risk 0.73, 95% CI 0.60, 0.89; $P = 0.002$). These data are consistent with our finding of a 36% reduction in risk of a clinical morbidity/mortality event in the CTD-PAH population. There were differences in methodology between the 2 analyses. In our study, for clinical relevance, only those treatment groups receiving FDA-approved doses were analyzed. Additionally, our meta-analysis included the more recently published FREEDOM-EV trial (International, Multicenter, Randomized, Double-blind, Placebo-controlled Event-driven Trial of Oral Treprostinil in Subjects with PAH) (16), the results of which were published after completion of the meta-analysis by Pan and colleagues (18). Pan and colleagues also found no statistically significant benefit from additional therapy in terms of improvement in the 6MWD among patients with CTD-PAH (mean change 21.38 meters, 95% CI −20.38, 63.14; $P = 0.32$). This end point was derived from 3 RCTs. Our meta-analysis, which included 8 trials in which this end point was evaluated, demonstrated a similar benefit (measured numerically as change in the 6MWD) that was statistically significant in patients with CTD-PAH (mean change 20.4 meters, 95% CI 10.9, 29.9; $P < 0.001$), perhaps reflecting greater statistical power due to increased sample size. Overall, compared to the meta-analysis by Pan and colleagues (18), our study provides an expanded evaluation, including the FREEDOM-EV trial, with an additional meta-analysis of survival rates in registries, because data on long-term survival outcomes and longitudinal analysis of survival outcomes over decades cannot be feasibly obtained from RCTs.

Patients with CTD-PAH have a substantial risk of death; however, patients with CTD-PAH who were treated within the last 10 years have numerically higher survival rates than those treated earlier. This difference may be related to increased screening for PAH, especially in those with SSc. Increased screening leads to earlier diagnosis, which provides the opportunity for earlier management (8) but also introduces lead-time bias (50). If lead-time bias is present, patients in later registries would be expected to be younger and to have less severe disease. Our analysis found that in the later registries, patients were older than those in the earlier registries (mean age 57 years versus 54 years), but had less severe disease (as defined by the proportion of patients with WHO functional class I or II disease) (40% versus 23%) and had a higher 6MWD (336 meters versus 321 meters) (see Supplementary Table 9, available on the *Arthritis & Rheumatology* website at http://onlinelibrary.wiley.com/doi/10.1002/art.41669/abstract). Whether lead-time bias is playing a substantial role in our results cannot be definitively determined from the current analysis.

The difference in survival over time also may reflect the availability of new treatment approaches. The improvement in survival is likely underestimated, since just 6 registries (32%) enrolled patients in 2015 or later, when all currently available treatments were in use and early combination therapy became more prevalent (5,34,39,41,46,47). More recent data are available from the United Kingdom Pulmonary Hypertension Audit (51). The most recent peer-reviewed published data from this database (38) are included in our meta-analysis; however, the latest report available (data from 2009–2019) is not included due to lack of peer review. Published data from 2001–2007 reported 1-, 2-, and 3-year survival rates among patients with SSc-associated PAH of 78%, 58%, and 47%, respectively. Corresponding survival rates from 2009–2019 were 81%, 61%, and 55%, respectively. These data corroborate the improved survival rates observed over time in our meta-analysis. Consistent with clinical observations and published data (6,38,52), our meta-analysis demonstrated that patients with SSc have worse survival rates than those with SLE. It should be noted, however, that patients with SSc in our analysis were older than those with SLE and appeared to have more severe disease, as indicated by fewer patients with WHO functional class I or II disease and a shorter 6MWD (see Supplementary Table 10, available on the *Arthritis & Rheumatology* website at http://onlinelibrary.wiley.com/doi/10.1002/art.41669/abstract), which likely also contributed to their poorer survival. We were not able to use meta-analysis to compare the treatment effect in RCTs between patients with SSc and those with SLE since only 2 RCTs provided sufficient data on patients with SSc (23,24) and only 1 provided sufficient data on patients with SLE (24).

Because all-cause mortality was evaluated, we may have overestimated the incidence of death due to PAH among patients with CTD-PAH. These patients were older and experienced a greater comorbidity burden compared to the overall PAH population. As such, these patients were possibly frailer and may have died from causes other than PAH. Although registries are subject to bias, these sources of long-term data and larger sample size were deemed important to include in order to provide prolonged survival data unavailable from RCTs. Current guidelines now recommend combination therapy and more intensive therapy regardless of PAH etiology (53), and our meta-analysis of registries provides evidence suggesting that the modern approach to treatment focuses on improving survival in CTD-PAH. Nonetheless, survival remains lower for these patients, highlighting the need for continued research into the best treatment approaches and screening programs to promote early diagnosis and prompt management.

Additional avenues for research to improve outcomes in this population include standardized reporting of comorbidities, which can substantially impact outcomes in CTD-PAH as well as in PAH of other etiologies (54). Identification of comorbidities is further complicated by the lack of a consensus definition for significant interstitial lung disease in SSc. An additional area of focus should be standardized reporting of baseline risk profiles, since data suggest that patients with CTD-PAH are at greater risk of death despite a less severe hemodynamic phenotype (5,55). Identification of clinically relevant changes in outcome measures, which may differ among PAH subtypes, would also be helpful. Finally, the era of personalized medicine may enable smaller study sizes and, ultimately, facilitate the discovery of treatment approaches that would yield a greater benefit within CTD-PAH populations.

A strength of our meta-analyses is the inclusion of only trials evaluating therapies that are approved for PAH treatment. By limiting the RCTs to only those with approved therapies, the results better reflect the benefit that can be observed in real-world settings. In addition, our meta-analysis of RCTs assessed the impact of current PAH treatments on morbidity and mortality, as endorsed by the 6th World Symposium on Pulmonary Hypertension (53). A limitation of our meta-analysis of RCTs was that definitions of a clinical morbidity/mortality event (as listed in Supplementary Table 1 [http://onlinelibrary.wiley.com/doi/10.1002/art.41669/abstract]) varied to a limited extent across studies.

A limitation of our meta-analysis of registries was the limited availability of studies that enrolled patients from 2015 onward, which would provide a survival estimate consistent with that observed in modern clinical practice. In all analyses, the overall PAH population to which we compared the CTD-PAH population included patients with CTD-PAH, because not all studies provided IPAH-specific data. However, sensitivity analyses of RCTs that provided IPAH-specific data demonstrated similar trends in patients with IPAH compared to those with CTD-PAH as had been observed for the comparison between all PAH etiologies and CTD-PAH.

An additional limitation is that it is unknown to what extent the treatment effect is influenced by different background therapies, potential variability in exposure to therapies, concomitant medications (such as immunosuppressants), as well as different proportions of newly and previously diagnosed patients in the study populations. Finally, the diagnosis of PAH was accepted on the basis of the criteria used in each study or registry; it is possible that underlying conditions, such as pulmonary veno-occlusive disease and concomitant interstitial lung disease, were present and to differing degrees among the various studies. A limitation of our search methodology was that we did not search additional databases beyond PubMed and Embase. As noted, however, we do not expect any differences in outcomes as a result of this, given the parameters of our meta-analyses, the rarity of this disease state, and the relatively small number of studies reporting data separately for the subset of patients with CTD-PAH.

In conclusion, these complementary meta-analyses of RCTs and observational disease registries demonstrated that with modern PAH treatments, patients with CTD-PAH had a similar reduction in the risk of clinical morbidity and mortality events when compared to the overall PAH population. The improvement in the 6MWD in patients with CTD-PAH appeared smaller than in those with other types of PAH, perhaps reflecting comorbidities (such as musculoskeletal involvement), independent of their cardiopulmonary capacity. Patients with CTD-PAH have a higher risk of death than the overall PAH population; however, survival has improved among this subgroup treated in the last 10 years compared to earlier cohorts. Patients with SSc have worse survival rates than those with SLE. Given the high risk of mortality in these patients, early detection and up-front aggressive treatment are warranted (56).

ACKNOWLEDGMENTS

The authors would like to thank Saling Huang, PhD, for consulting on the statistical analysis, and Kristine Jermakian for her contributions to the comprehensive review and data extraction.

AUTHOR CONTRIBUTIONS

All authors were involved in drafting the article or revising it critically for important intellectual content, and all authors approved the final version to be published. Dr. Khanna had full access to all of the data in the study and takes responsibility for the integrity of the data and the accuracy of the data analysis.

Study conception and design. Khanna, Zhao, Mathai, Coghlan, Shah, Hartney, McLaughlin.

Acquisition of data. Zhao, Shah, Hartney.

Analysis and interpretation of data. Khanna, Zhao, Saggar, Mathai, Chung, Coghlan, Shah, Hartney, McLaughlin.

ROLE OF THE STUDY SPONSOR

Funding for this analysis was provided by Actelion Pharmaceuticals US, Inc., a Janssen Pharmaceutical Company of Johnson & Johnson. Medical writing support was provided by Holly Strausbaugh, PhD, and Laura Evans, PharmD, on behalf of Twist Medical, LLC, which was funded by Actelion Pharmaceuticals. Data were collected and analyzed by some of the authors who are employees of Actelion Pharmaceuticals. All authors had full access to the data, contributed to data interpretation, contributed to manuscript writing, and had final responsibility for the decision to submit for publication. The publication of this article was not contingent upon approval by anyone from Actelion Pharmaceuticals except for authors who are employees of Actelion Pharmaceuticals, who, like all authors regardless of affiliation, are ethically required to approve of an article before it is submitted for publication.

REFERENCES

1. Galiè N, Humbert M, Vachiery JL, Gibbs S, Lang I, Torbicki A, et al. 2015 ESC/ERS guidelines for the diagnosis and treatment of pulmonary hypertension: the Joint Task Force for the Diagnosis and Treatment of Pulmonary Hypertension of the European Society of Cardiology (ESC) and the European Respiratory Society (ERS): endorsed by: Association for European Paediatric and Congenital Cardiology (AEPC), International Society for Heart and Lung Transplantation (ISHLT). Eur Heart J 2016;37:67–119.

2. D'Alonzo GE, Barst RJ, Ayres SM, Bergofsky EH, Brundage BH, Detre KM, et al. Survival in patients with primary pulmonary hypertension: results from a national prospective registry. Ann Intern Med 1991;115:343–9.
3. Simonneau G, Gatzoulis MA, Adatia I, Celermajer D, Denton C, Ghofrani A, et al. Updated clinical classification of pulmonary hypertension. J Am Coll Cardiol 2013;62:D34–41.
4. Humbert M, Sitbon O, Yaïci A, Montani D, O'Callaghan DS, Jaïs X, et al. Survival in incident and prevalent cohorts of patients with pulmonary arterial hypertension. Eur Respir J 2010;36:549–55.
5. Hoeper MM, Kramer T, Pan Z, Eichstaedt CA, Spiesshoefer J, Benjamin N, et al. Mortality in pulmonary arterial hypertension: prediction by the 2015 European pulmonary hypertension guidelines risk stratification model. Eur Respir J 2017;50:1700740.
6. Chung L, Liu J, Parsons L, Hassoun PM, McGoon M, Badesch DB, et al. Characterization of connective tissue disease-associated pulmonary arterial hypertension from REVEAL: identifying systemic sclerosis as a unique phenotype. Chest 2010;138: 1383–94.
7. Young A, Nagaraja V, Basilious M, Habib M, Townsend W, Gladue H, et al. Update of screening and diagnostic modalities for connective tissue disease-associated pulmonary arterial hypertension. Semin Arthritis Rheum 2019;48:1059–67.
8. Humbert M, Yaici A, de Groote P, Montani D, Sitbon O, Launay D, et al. Screening for pulmonary arterial hypertension in patients with systemic sclerosis: clinical characteristics at diagnosis and long-term survival. Arthritis Rheum 2011;63:3522–30.
9. Galiè N, Ghofrani HA, Torbicki A, Barst RJ, Rubin LJ, Badesch D, et al. Sildenafil citrate therapy for pulmonary arterial hypertension. N Engl J Med 2005;353:2148–57.
10. Galiè N, Brundage BH, Ghofrani HA, Oudiz RJ, Simonneau G, Safdar Z, et al. Tadalafil therapy for pulmonary arterial hypertension. Circulation 2009;119:2894–903.
11. Ghofrani HA, Galiè N, Grimminger F, Grünig E, Humbert M, Jing ZC, et al. Riociguat for the treatment of pulmonary arterial hypertension. N Engl J Med 2013;369:330–40.
12. Galiè N, Barberà JA, Frost AE, Ghofrani HA, Hoeper MM, McLaughlin VV, et al. Initial use of ambrisentan plus tadalafil in pulmonary arterial hypertension. N Engl J Med 2015;373:834–44.
13. McLaughlin V, Channick RN, Ghofrani HA, Lemarié JC, Naeije R, Packer M, et al. Bosentan added to sildenafil therapy in patients with pulmonary arterial hypertension. Eur Respir J 2015;46: 405–13.
14. Pulido T, Adzerikho I, Channick RN, Delcroix M, Galiè N, Ghofrani HA, et al. Macitentan and morbidity and mortality in pulmonary arterial hypertension. N Engl J Med 2013;369:809–18.
15. Sitbon O, Channick R, Chin KM, Frey A, Gaine S, Galiè N, et al. Selexipag for the treatment of pulmonary arterial hypertension. N Engl J Med 2015;373:2522–33.
16. White RJ, Jerjes-Sanchez C, Bohns Meyer GM, Pulido T, Sepulveda P, Wang KY, et al. Combination therapy with oral treprostinil for pulmonary arterial hypertension: a double-blind placebo-controlled clinical trial. Am J Respir Crit Care Med 2020;201:707–17.
17. Rhee RL, Gabler NB, Sangani S, Praestgaard A, Merkel PA, Kawut SM. Comparison of treatment response in idiopathic and connective tissue disease-associated pulmonary arterial hypertension. Am J Respir Crit Care Med 2015;192:1111–7.
18. Pan J, Lei L, Zhao C. Comparison between the efficacy of combination therapy and monotherapy in connective tissue disease associated pulmonary arterial hypertension: a systematic review and meta-analysis. Clin Exp Rheumatol 2018;36:1095–102.
19. Moher D, Liberati A, Tetzlaff J, Altman DG, PRISMA Group. Preferred Reporting Items for Systematic Reviews and Meta-Analyses: the PRISMA statement. J Clin Epidemiol 2009;62:1006–12.
20. National Institute for Health Research. PROSPERO: international prospective register of systematic reviews. URL: https://www.crd.york.ac.uk/prospero/.
21. Simonneau G, Montani D, Celermajer DS, Denton CP, Gatzoulis MA, Krowka M, et al. Haemodynamic definitions and updated clinical classification of pulmonary hypertension. Eur Respir J 2019;53: 1801913.
22. DerSimonian R, Laird N. Meta-analysis in clinical trials. Control Clin Trials 1986;7:177–88.
23. Coghlan JG, Galiè N, Barberà JA, Frost AE, Ghofrani HA, Hoeper MM, et al. Initial combination therapy with ambrisentan and tadalafil in connective tissue disease-associated pulmonary arterial hypertension (CTD-PAH): subgroup analysis from the AMBITION trial. Ann Rheum Dis 2017;76:1219–27.
24. Gaine S, Chin K, Coghlan G, Channick R, Di Scala L, Galiè N, et al. Selexipag for the treatment of connective tissue disease-associated pulmonary arterial hypertension. Eur Respir J 2017;50:1602493.
25. Rubin LJ, Badesch DB, Barst RJ, Galiè N, Black CM, Keogh A, et al. Bosentan therapy for pulmonary arterial hypertension. N Engl J Med 2002;346:896–903.
26. Denton CP, Humbert M, Rubin L, Black CM. Bosentan treatment for pulmonary arterial hypertension related to connective tissue disease: a subgroup analysis of the pivotal clinical trials and their open-label extensions. Ann Rheum Dis 2006;65:1336–40.
27. Badesch DB, Hill NS, Burgess G, Rubin LJ, Barst RJ, Galiè N, et al. Sildenafil for pulmonary arterial hypertension associated with connective tissue disease. J Rheumatol 2007;34:2417–22.
28. Galiè N, Olschewski H, Oudiz RJ, Torres F, Frost A, Ghofrani HA, et al. Ambrisentan for the treatment of pulmonary arterial hypertension: results of the ambrisentan in pulmonary arterial hypertension, randomized, double-blind, placebo-controlled, multicenter, efficacy (ARIES) study 1 and 2. Circulation 2008;117:3010–9.
29. Badesch DB. Ambrisentan therapy for pulmonary arterial hypertension: a comparison by PAH etiology [abstract]. Chest 2007;132 Suppl:488b–9.
30. Galiè N, Denton CP, Dardi F, Manes A, Mazzanti G, Li B, et al. Tadalafil in idiopathic or heritable pulmonary arterial hypertension (PAH) compared to PAH associated with connective tissue disease. Int J Cardiol 2017;235:67–72.
31. Escribano-Subias P, Blanco I, López-Meseguer M, Lopez-Guarch CJ, Roman A, Morales P, et al. Survival in pulmonary hypertension in Spain: insights from the Spanish registry. Eur Respir J 2012;40:596–603.
32. McLaughlin VV, Langer A, Tan M, Clements PJ, Oudiz RJ, Tapson VF, et al. Contemporary trends in the diagnosis and management of pulmonary arterial hypertension: an initiative to close the care gap. Chest 2013;143:324–32.
33. Benza RL, Miller DP, Barst RJ, Badesch DB, Frost AE, McGoon MD. An evaluation of long-term survival from time of diagnosis in pulmonary arterial hypertension from the REVEAL Registry. Chest 2012;142:448–56.
34. Yaylalı YT, Başarıcı I, Avcı BK, Meriç M, Sinan UY, Şenol H, et al. Risk assessment and survival of patients with pulmonary hypertension: multicenter experience in Turkey. Anatol J Cardiol 2019;21:322–30.
35. Zhang R, Dai LZ, Xie WP, Yu ZX, Wu BX, Pan L, et al. Survival of Chinese patients with pulmonary arterial hypertension in the modern treatment era. Chest 2011;140:301–9.
36. Keogh A, Strange G, McNeil K, Williams TJ, Gabbay E, Proudman S, et al. The Bosentan Patient Registry: long-term survival in pulmonary arterial hypertension. Intern Med J 2011;41:227–34.
37. Chung WJ, Park YB, Jeon CH, Jung JW, Ko KP, Choi SJ, et al. Baseline characteristics of the Korean registry of pulmonary arterial hypertension. J Korean Med Sci 2015;30:1429–38.

38. Condliffe R, Kiely DG, Peacock AJ, Corris PA, Gibbs JS, Vrapi F, et al. Connective tissue disease-associated pulmonary arterial hypertension in the modern treatment era. Am J Respir Crit Care Med 2009;179:151–7.
39. Qian J, Li M, Zhang X, Wang Q, Zhao J, Tian Z, et al. Long-term prognosis of patients with systemic lupus erythematosus-associated pulmonary arterial hypertension: CSTAR-PAH cohort study. Eur Respir J 2019;53:1800081.
40. Kang KY, Jeon CH, Choi SJ, Yoon BY, Choi CB, Lee CH, et al. Survival and prognostic factors in patients with connective tissue disease-associated pulmonary hypertension diagnosed by echocardiography: results from a Korean nationwide registry. Int J Rheum Dis 2017;20:1227–36.
41. Kolstad KD, Li S, Steen V, Chung L, on behalf of the PHAROS Investigators. Long-term outcomes in systemic sclerosis-associated pulmonary arterial hypertension from the Pulmonary Hypertension Assessment and Recognition of Outcomes in Scleroderma Registry (PHAROS). Chest 2018;154:862–71.
42. Hao YJ, Jiang X, Zhou W, Wang Y, Gao L, Wang Y, et al. Connective tissue disease-associated pulmonary arterial hypertension in Chinese patients. Eur Respir J 2014;44:963–72.
43. Ngian GS, Stevens W, Prior D, Gabbay E, Roddy J, Tran A, et al. Predictors of mortality in connective tissue disease-associated pulmonary arterial hypertension: a cohort study. Arthritis Res Ther 2012;14:R213.
44. Launay D, Humbert M, Berezne A, Cottin V, Allanore Y, Couderc LJ, et al. Clinical characteristics and survival in systemic sclerosis-related pulmonary hypertension associated with interstitial lung disease. Chest 2011;140:1016–24.
45. Hachulla E, Jais X, Cinquetti G, Clerson P, Rottat L, Launay D, et al. Pulmonary arterial hypertension associated with systemic lupus erythematosus: results from the French pulmonary hypertension registry. Chest 2018;153:143–51.
46. Morrisroe K, Stevens W, Huq M, Prior D, Sahhar J, Ngian GS, et al. Survival and quality of life in incident systemic sclerosis-related pulmonary arterial hypertension. Arthritis Res Ther 2017;19:122.
47. Weatherald J, Boucly A, Launay D, Cottin V, Prévot G, Bourlier D, et al. Haemodynamics and serial risk assessment in systemic sclerosis associated pulmonary arterial hypertension. Eur Respir J 2018; 52:1800678.
48. Kuwana M, Watanabe H, Matsuoka N, Sugiyama N. Pulmonary arterial hypertension associated with connective tissue disease: meta-analysis of clinical trials. BMJ Open 2013;3:e003113.
49. Avouac J, Wipff J, Kahan A, Allanore Y. Effects of oral treatments on exercise capacity in systemic sclerosis related pulmonary arterial hypertension: a meta-analysis of randomised controlled trials. Ann Rheum Dis 2008;67:808–14.
50. Weatherald J, Montani D, Jevnikar M, Jaïs X, Savale L, Humbert M. Screening for pulmonary arterial hypertension in systemic sclerosis. Eur Respir Rev 2019;28:190023.
51. NHS Digital. National audit of pulmonary hypertension: Great Britain, 2018-19. October 24, 2019. URL: https://files.digital.nhs.uk/BA/4EF20E/NAPH%2010AR%20-%20Main%20Report.pdf.
52. Sobanski V, Giovannelli J, Lynch BM, Schreiber BE, Nihtyanova SI, Harvey J, et al. Characteristics and survival of anti–U1 RNP antibody–positive patients with connective tissue disease–associated pulmonary arterial hypertension. Arthritis Rheumatol 2016;68:484–93.
53. Galiè N, Channick RN, Frantz RP, Grünig E, Jing ZC, Moiseeva O, et al. Risk stratification and medical therapy of pulmonary arterial hypertension. Eur Respir J 2019;53:1801889.
54. Lewis RA, Thompson AA, Billings CG, Charalampopoulos A, Elliot CA, Hamilton N, et al. Mild parenchymal lung disease and/or low diffusion capacity impacts survival and treatment response in patients diagnosed with idiopathic pulmonary arterial hypertension. Eur Respir J 2020;55:2000041.
55. Peacock AJ, Ling Y, Johnson MK, Kiely DG, Condliffe R, Elliot CA, et al. Idiopathic pulmonary arterial hypertension and co-existing lung disease: is this a new phenotype? Pulm Circ 2020;10:2045894020914851.
56. Nagaraja V, Cerinic MM, Furst DE, Kuwana M, Allanore Y, Denton CP, et al. Current and future outlook on disease modification and defining low disease activity in systemic sclerosis. Arthritis Rheumatol 2020;72:1049–58.

American College of Rheumatology
Empowering Rheumatology Professionals

Arthritis & Rheumatology
Vol. 73, No. 5, May 2021, pp 848–857
DOI 10.1002/art.41594

Eccentric Resistance Training Ameliorates Muscle Weakness in a Mouse Model of Idiopathic Inflammatory Myopathies

Koichi Himori,[1] Yuki Ashida,[1] Daisuke Tatebayashi,[2] Masami Abe,[2] Yuki Saito,[2] Takako Chikenji,[3] Håkan Westerblad,[4] Daniel C. Andersson,[5] and Takashi Yamada[2]

Objective. High-force eccentric contractions (ECCs) have traditionally been excluded from rehabilitation programs that include patients with idiopathic inflammatory myopathies (IIMs) due to unverified fear of causing muscle damage and inflammation. In an IIM animal model that used mice with experimental autoimmune myositis (EAM), we undertook this study to investigate whether ECC training can safely and effectively be used to counteract muscle weakness in IIM.

Methods. EAM was induced in BALB/c mice by immunization with 3 injections of myosin emulsified in Freund's complete adjuvant. Controls (n = 12) and mice with EAM (n = 12) were exposed to either an acute bout of 100 ECCs or 4 weeks of ECC training (20 ECCs every other day). To induce ECCs, plantar flexor muscles were electrically stimulated while the ankle was forcibly dorsiflexed.

Results. Less cell damage, as assessed by Evans blue dye uptake, was observed in the muscles of mice with EAM, compared to controls, after an acute bout of 100 ECCs ($P < 0.05$). Maximum Ca^{2+}-activated force was decreased in skinned gastrocnemius muscle fibers from mice with EAM, and this was accompanied by increased expression of endoplasmic reticulum (ER) stress proteins, including Gsp78 and Gsp94 ($P < 0.05$). ECC training prevented the decrease in force and the increase in ER stress proteins and also enhanced the expression and myofibrillar binding of small heat-shock proteins (HSPs) ($P < 0.05$), which can stabilize myofibrillar structure and function.

Conclusion. ECC training protected against the reduction in myofibrillar force–generating capacity in an IIM mouse model, and this occurred via inhibition of ER stress responses and small HSP–mediated myofibrillar stabilization.

INTRODUCTION

Patients with idiopathic inflammatory myopathies (IIMs), including polymyositis (PM), dermatomyositis (DM), and juvenile DM, experience muscle weakness, which often results in disability and decreased quality of life (1). Progressive proximal muscle weakness is common in patients with PM and DM, although these patients also have an impairment of distal lower muscles (2). The mechanisms underlying muscle weakness associated with IIMs are still poorly understood, although the notion that contractile dysfunctions intrinsic to the muscle fibers play a role is supported by findings showing reduced force per cross-sectional area (i.e., specific force) in fast- and slow-twitch muscle in a mouse model of inflammatory myositis (3).

IIMs are histologically characterized by inflammatory cell infiltration in skeletal muscle and persisting major histocompatibility complex (MHC) class I expression in muscle fibers (4). Current treatment includes glucocorticoids combined with other immunosuppressive agent(s), but some patients are left with muscle weakness despite this treatment (5,6). Moreover, several studies show poor correlation between the severity of muscle weakness and the degree of inflammatory cell infiltration (5,7). The exact molecular mechanisms behind this "noninflammatory" component in myositis-induced muscle weakness remain unclear.

Dr. Himori's work was supported by the Japan Society for the Promotion of Science (grant JP20J01754). Dr. Westerblad's work was supported by the Swedish Research Council (grant 2018-02576). Dr. Andersson's work was supported by the Swedish Heart-Lung Foundation (grants 20160741 and 20180803), the Harald and Greta Jeansson Foundation, the Swedish Society for Medical Research (grant S16-0159), and the Swedish Medical Association (grant SLS-891461).

[1]Koichi Himori, PhD, Yuki Ashida, MSc: Sapporo Medical University, Sapporo, Japan, and the Japan Society for the Promotion of Science, Tokyo, Japan; [2]Daisuke Tatebayashi, PhD, Masami Abe, MSc, Yuki Saito, PhD, Takashi Yamada, PhD: Sapporo Medical University, Sapporo, Japan; [3]Takako Chikenji, PhD: Sapporo Medical University and Hokkaido University, Sapporo, Japan; [4]Håkan Westerblad, MD, PhD: Karolinska Institutet, Stockholm, Sweden; [5]Daniel C. Andersson, MD, PhD: Karolinska Institutet, Stockholm, Sweden, and Karolinska University Hospital, Solna, Sweden.

No potential conflicts of interest relevant to this article were reported.

Address correspondence to Takashi Yamada, PhD, Graduate School of Health Sciences, Sapporo Medical University, South 1 West 17, Chuo-ku Sapporo, Japan 060-8556. Email: takashi.yamada1976@sapmed.ac.jp.

Submitted for publication May 4, 2020; accepted in revised form November 10, 2020.

It has been proposed that an increase of MHC class I on myositis muscle fibers results in the activation of the endoplasmic reticulum (ER) stress response (8). Indeed, muscles from IIM patients and mouse models have shown that ER stress proteins, including Grp78 and Grp94, are up-regulated and colocalized to muscle fibers overexpressing MHC class I (9). Data from nonmuscle cell lines demonstrated that reactive oxygen species (ROS) are generated in response to ER stress (10). We and others have shown that inflammatory conditions cause oxidation-dependent modifications of contractile proteins and impair myofibrillar function (11–13). Thus, ER stress–induced ROS can be one of the main factors reducing the specific force production in skeletal muscle from IIM patients (14).

Historically, it has been recommended that IIM patients refrain from active exercise due to fear of increased muscle inflammation and disease progression, but this viewpoint has been refuted in recent years (15). The safety and the beneficial effects of exercise in IIM patients were first reported in 1993 (16,17). Since then, there has been mounting evidence showing that resistive training combined with immunosuppressive drugs improves muscle strength without signs of increased disease activity in patients with acute or chronic IIMs (16,18–23). Notably, none of these studies showed elevations in serum creatine phosphokinase levels following physical training, indicating that susceptibility of sarcolemma to mechanical stress–induced damage is not increased in muscles from patients with IIMs.

The absolute mechanical load imposed during eccentric contraction (ECC)–mode training is generally substantially greater than that imposed in concentric- or isometric-mode training. Given that signaling promoting muscle hypertrophy and strength is positively related to the mechanical load, ECC training is regarded as an effective way to enhance muscle strength in normal subjects (24). Conversely, it is well known that unaccustomed exercise with intense ECCs causes a prolonged force depression and muscle damage (25,26). In patients with Duchenne muscular dystrophy (DMD) and in the mdx mouse model, a lack of dystrophin disrupts the link between the cytoskeleton and the extracellular matrix, leading to the loss of sarcolemmal integrity, especially when muscles are exposed to ECCs (27,28). However, little is known as to whether the susceptibility to ECC-induced muscle damage is increased in IIMs.

ECCs, but not concentric contractions, have been shown to result in partial translocation of small heat-shock proteins (HSPs) from cytosol to myofibrils (29). Small HSPs have the ability to stabilize myofibrillar proteins, such as myosin (30) and actin (31), thereby assisting in the maintenance of myofibrillar structure and function; however, accumulation of small HSPs in myofibrillar structures might also be a sign of increased myofibrillar negative stress (32). Accordingly, ECC training has been shown to enhance binding of the small HSP αB-crystallin to the myofibrils and therefore prevent myofibrillar dysfunction in skeletal muscle from rats with adjuvant-induced arthritis, an animal model for rheumatoid arthritis (33).

One widely used animal model of IIMs is experimental autoimmune myositis (EAM), which resembles the human disease in several aspects, including necrotic and regenerating fibers and endomysial infiltrates with invaded fibers (34). In this study, we used mice with EAM as a model for acute IIMs and tested the following principal hypotheses: 1) myofibrillar force production is decreased in muscle fibers from mice with EAM; 2) susceptibility to ECC-induced damage is not increased in muscles from mice with EAM; and 3) ECC training counteracts the EAM-induced muscle weakness via ER stress–dependent and small HSP–dependent pathways.

MATERIALS AND METHODS

Ethical approval. All experimental procedures were approved by the Committee on Animal Experiments of Sapporo Medical University (no. 18-030). Animal care was conducted in accordance with institutional guidelines.

Induction of experimental autoimmune myositis. Female BALB/c mice (8 weeks old; n = 24) and 1 male Wistar rat (9 weeks old) as a source of skeletal muscle for EAM induction were supplied by Sankyo. Mice were given food and water ad libitum and housed in an environmentally controlled room (24°C, ± 2°C) with a 12-hour light/dark cycle. EAM was induced by immunizing mice with partially purified rat myosin, including myosin-binding protein C, as previously reported (34). Further details can be found in Supplementary Methods (available on the *Arthritis & Rheumatology* website at http://onlinelibrary.wiley.com/doi/10.1002/art.41594/abstract).

Experimental design. We performed 2 separate experiments to examine whether ECC resistance exercise can be a safe and effective intervention counteracting the muscle weakness in mice with EAM.

Experiment 1. We first assessed whether muscles from mice with EAM were weaker than those from control mice, and whether there was a difference between the 2 groups in susceptibility to damage caused by ECCs. Female BALB/c mice were randomly assigned to a control group (n = 6) or an EAM group (n = 6). Mice were anesthetized by isoflurane inhalation, and the in vivo plantar flexor torque was measured. Mice were placed in a supine position on a platform, and each foot was secured in a foot plate at right angle (0° dorsiflexion) and connected to a torque sensor (S-14154; Takei Scientific Instruments). Plantar flexor muscles (including the gastrocnemius [GAS], plantaris, and soleus muscles) were exposed to supramaximal neuromuscular electrical stimulation (NMES) using a pair of surface electrodes, which were strapped with tape to the posterior surface of the calf. The maximum isometric torque was measured at a stimulation frequency of 100 Hz (duration 600 msec) with supramaximal square-wave current pulses (SEN-3401; Nihon Kohden).

In control experiments, we confirmed that the maximum isometric torque of plantar flexion is comparable between NMES with surface electrodes and direct sciatic nerve stimulation (Supplementary Figure 1, http://onlinelibrary.wiley.com/doi/10.1002/art.41594/abstract). The NMES protocol used in this study activates both the dorsiflexors and plantar flexors. The antagonistic actions of the dorsiflexors might counter some of the force produced by the plantar flexors. However, it has been reported that plantar flexor torque was increased by only ~10% after tenotomy of the dorsiflexors (35). During ECCs, the ankle was dorsiflexed by a servomotor (S-14154; Takei Scientific Instruments) from 0° to 40° dorsiflexion at a constant speed during the NMES at 100 Hz. ECCs were produced every 6 seconds. Muscle damage was shown to increase progressively with the number of ECCs (36), and the velocity of muscle stretch was a critical determinant of the degree of damage (37). We have previously demonstrated in normal rats that muscle damage is not induced by repeated sessions of NMES training with 20 ECCs at 20°/second (38), whereas a single bout of 100 ECCs at 150°/second causes major muscle damage (26).

Based on these results, the left and right plantar flexor muscles in each animal were subjected to either 20 presumably nondamaging ECCs (20°/second, duration 2 seconds) or 100 presumably damaging ECCs (150°/second, duration 267 msec), 24 hours after the last immunization. Histologic parameters of muscle damage and the expression levels of dystrophin and dysferlin were assessed in the middle belly of the medial GAS muscles 48 hours following the ECCs, because histopathologic changes are the most severe after a few days in skeletal muscles from mice (39) and rats (26).

Experiment 2. To examine whether ECC training improves EAM-induced muscle weakness, female BALB/c mice were randomly assigned to a control group (n = 6) or an EAM group (n = 6). In the mice with EAM, ECC training was performed on the left leg (referred to as the EAM + ECC group), and the right leg served as a nontraining EAM control. The ECC training was initiated 24 hours after the last immunization and was carried out every other day for a total of 14 sessions. Each session consisted of 4 sets, given at 5-minute intervals, of 5 ECCs (20°/second, duration 2 seconds) produced every 6 seconds.

In control experiments, we confirmed that the maximum isometric torque of the plantar flexor muscles was fully recovered 48 hours after an ECC session, i.e., at the time of the next ECC session (data not shown). Twenty-four hours after the last ECC exercise, in vivo isometric contractile properties were measured at stimulation frequencies ranging from 1 to 120 Hz (duration 600 msec), produced at 1-minute intervals. Due to practical limitations, we could not evaluate cross-sectional area for lateral GAS muscles or muscle length for GAS muscles, and thus the torque was normalized by whole GAS muscle weight instead. During 100-Hz contractions, the peak rates of torque development (dP/dt; maximum positive slope during a 10-msec moving window) and torque decline (–dP/dt; maximum negative slope during a 10-msec moving window) were determined and normalized by isometric torque. Thereafter, mice were euthanized by cervical dislocation under isoflurane anesthesia, and the plantar flexor muscles were dissected from each mouse. The medial GAS muscles were used for skinned muscle fiber experiments and biochemical analyses.

Measurement of Ca^{2+}-activated force in skinned muscle fibers. Chemically skinned muscle fibers were prepared and Ca^{2+}-activated force was measured according to methods described by Mollica et al (40), with some modifications. Further details can be found in Supplementary Methods (http://onlinelibrary.wiley.com/doi/10.1002/art.41594/abstract).

Histopathologic analyses. Images stained with hematoxylin and eosin and Evans blue dye (EBD) were obtained from the serial sections as previously described (26). Further details about histopathologic analyses, including immunostaining, can be found in Supplementary Methods (http://onlinelibrary.wiley.com/doi/10.1002/art.41594/abstract).

Immunoblotting. Protein extraction and immunoblotting were performed as previously described (26). Further details about immunoblotting can be found in Supplementary Methods (http://onlinelibrary.wiley.com/doi/10.1002/art.41594/abstract).

Myosin heavy chain (MyHC) isoform separation. Aliquots of the whole muscle homogenates (5 μg) were applied for MyHC electrophoresis as previously described in detail (41). Using a 6% polyacrylamide slab gel, electrophoresis was run at 4ºC for 24 hours at 160V and stained with Coomassie brilliant blue. Images of gels were densitometrically evaluated with ImageJ.

Determination of MyHC, actin, αB-crystallin, and Hsp25 content in skinned fiber. At the completion of the force measurements, MyHC, actin, αB-crystallin, and Hsp25 content were measured in skinned fiber (33). Further details can be found in Supplementary Methods and Supplementary Figure 2 (http://onlinelibrary.wiley.com/doi/10.1002/art.41594/abstract).

Statistical analysis. Data are presented as the mean ± SEM. Student's unpaired *t*-test, one-way analysis of variance (ANOVA), and two-way repeated measures ANOVA were used to determine statistically significant differences, as appropriate. A Bonferroni post hoc test was used when significant differences were determined using ANOVA. *P* values less than 0.05 were considered significant. Further details can be found in Supplementary Methods (http://onlinelibrary.wiley.com/doi/10.1002/art.41594/abstract).

RESULTS

Muscles from mice with EAM are weaker but potentially less susceptible to ECC training–induced damage compared to those from control mice. The EAM model was created by immunizing mice with partially purified myosin, including myosin-binding protein C, resulting in the expression of MHC

class I and the infiltration of CD8+ cells in GAS muscles (Supplementary Figure 3, http://onlinelibrary.wiley.com/doi/10.1002/art.41594/abstract). In experiment 1, there was no difference in body weight between controls (n = 6) and mice with EAM (n = 6) (mean ± SEM 19.0 ± 0.8 gm versus 18.0 ± 0.7 gm, respectively; $P > 0.05$). In contrast, spleen weight was 5.7-fold higher in mice with EAM than in controls (mean ± SEM 502 ± 27 mg versus 88 ± 3 mg; $P < 0.05$). GAS muscle weight was 30% lower in the EAM group than in the control group (mean ± SEM 64.9 ± 4.6 mg versus 93.0 ± 3.3 mg; $P < 0.05$). The in vivo maximum isometric absolute torque and specific torque (maximum isometric torque/GAS muscle weight) were, respectively, 45% and 21% lower in the muscles from mice with EAM compared to those from controls (mean ± SEM maximum isometric torque 4.3 ± 0.3 mNm versus 7.8 ± 0.4 mNm [$P < 0.05$]; mean ± SEM specific torque 66.5 ± 2.5 mNm/gm versus 83.9 ± 2.9 mNm/gm [$P < 0.05$]).

To examine whether muscles in mice with EAM become more fragile and susceptible to ECC-induced damage, plantar flexor muscles were exposed to 20 or 100 ECCs (Figures 1A–D). The relative maximum isometric torque, expressed as the maximum isometric torque immediately after 20 or 100 ECCs a percentage of the maximum isometric torque before ECCs, was not different between muscles from the control group and those from the EAM group (Supplementary Figure 4, http://onlinelibrary.wiley.com/doi/10.1002/art.41594/abstract). In both groups, there was little histologic damage (Figures 1E and F), and the area of EBD-positive fibers was small (mean ± SEM percentage of total area 0.9 ± 0.6% in controls versus 0.6 ± 0.1% in mice with EAM; $P > 0.05$) 48 hours after 20 ECCs (Figures 1I and J). In contrast, degenerative changes and inflammatory cell infiltration (Figures 1G and H, and Supplementary Figure 5, http://onlinelibrary.wiley.com/doi/10.1002/art.41594/abstract) and EBD-positive fibers (Figure 1K and L) were found 48 hours after receiving 100 ECCs. Surprisingly, the proportion of EBD-positive area was significantly lower in the EAM group than in the control group after 100 ECCs (mean ± SEM 24 ± 2% versus 44 ± 8%; $P < 0.05$) (Figure 1M). In resting muscles (i.e., those not exposed to ECCs), there was no difference in dystrophin expression between the groups, whereas the expression level of dysferlin was markedly higher in the mice with EAM than in the controls (Figures 1N and O).

ECC training–induced prevention of force depression in skinned fibers from mice with EAM. In experiment 2, there was no difference in body weight between controls (n = 6) and mice with EAM (n = 6) (mean ± SEM 21.0 ± 0.4 gm versus 20.9 ± 0.4 gm, respectively; $P > 0.05$). The weight of the spleen was 2.9-fold higher in mice with EAM than in controls (mean ± SEM 341 ± 22 mg versus 116 ± 5 mg; $P < 0.05$). The GAS muscle weight was significantly lower in the EAM group than in the control group (mean ± SEM 80.5 ± 1.6 mg versus 92.6 ± 3.8 mg; $P < 0.05$), and this was not restored by ECC training (mean ± SEM 82.9 ± 3.1 mg; $P > 0.05$).

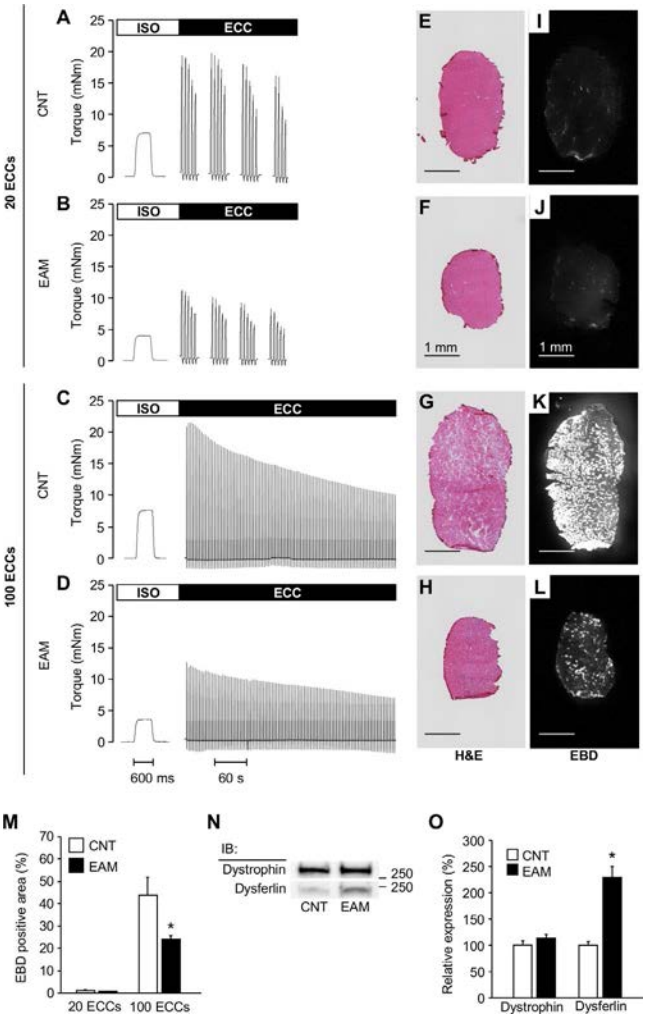

Figure 1. Susceptibility to eccentric contraction (ECC)–induced damage is not increased in the gastrocnemius (GAS) muscle from mice with experimental autoimmune myositis (EAM). **A–D**, Representative original records of maximal isometric (ISO) contractions and 20 or 100 ECCs in the plantar flexor muscle from controls (CNT) (**A** and **C**) and mice with EAM (**B** and **D**). Each vertical line represents 1 ECC. **E–L**, Representative images of serial transverse sections of medial GAS muscles stained with hematoxylin and eosin (H&E) (**E–H**) and Evans blue dye (EBD) (**I–L**) 48 hours after 20 or 100 ECCs. Bars = 1 mm. **M**, Quantification of the EBD-positive area compared to the total muscle cross-sectional area. Bars show the mean ± SEM results from 6 muscles per group. **N**, Representative Western immunoblots (IB) illustrating the levels of dystrophin and dysferlin. **O**, Relative expression of dystrophin and dysferlin. Bars show the mean ± SEM normalized to the total proteins from the stain-free image. The mean in muscles from controls was set at 100% (n = 3–5 muscles per group). * = $P < 0.05$ versus control.

In vivo isometric specific torque at a relatively high-frequency stimulation (50–120 Hz) was lower in the EAM and EAM + ECC groups than in the control group ($P < 0.05$) (Figures 2A and B). Notably, isometric specific torque at 70, 100, and 120 Hz stimulation frequencies was higher in the EAM + ECC group compared

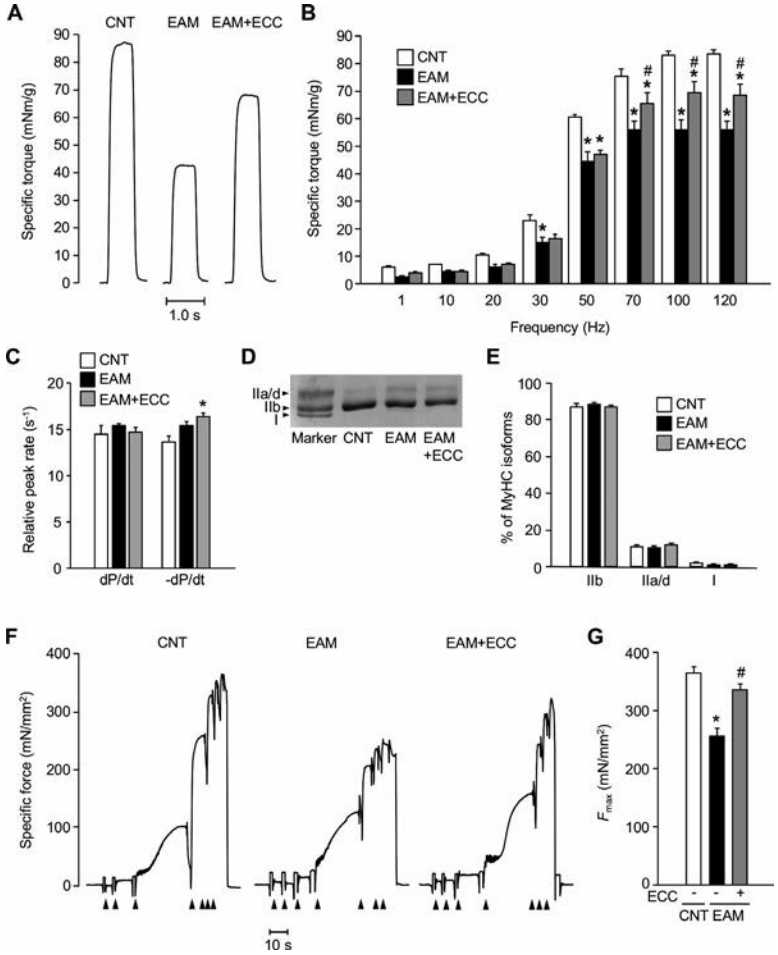

Figure 2. ECC training protects against the decrease in myofibrillar force production in GAS muscle from mice with EAM. **A**, Representative original records of in vivo specific torque (determined as the ratio of isometric torque to GAS muscle weight) in plantar flexor muscles from controls and mice with EAM, with or without ECC training. **B**, Specific torque–frequency relationships. **C**, Peak rates of force development (dP/dt) and relaxation (–dP/dt) in 100-Hz contractions. **D** and **E**, Electrophoretically separated myosin heavy chain (MyHC) isoforms (**D**) and percentage distribution of MyHC isoforms (**E**) (n = 6 mice per group). I represents a slow isoform, and IIa/d and IIb represent fast isoforms. **F**, Ca^{2+}-activated force in chemically skinned fibers from GAS muscles (n = 14–21 fibers per group). Fibers were exposed to solutions at progressively higher free Ca^{2+} concentrations: pCa 6.4, 6.2, 6.0, 5.8, 5.6, 5.4, and 4.7. **G**, Maximum Ca^{2+}-activated force per cross-sectional area (F_{max}) (n = 14–21 fibers per group). In **B**, **C**, **E**, and **G**, bars show the mean ± SEM. * = $P < 0.05$ versus controls; # = $P < 0.05$ versus mice with EAM. See Figure 1 for other definitions.

to the EAM group ($P < 0.05$). We observed no significant difference between groups regarding the peak rates of force development in 100-Hz tetanic contractions (Figure 2C). Similarly, there was no difference in the peak rates of force relaxation between controls and mice with EAM, but force relaxation was higher in the EAM + ECC group compared to controls. The GAS muscles were composed mainly of fast-twitch fibers (Figure 2D), and there were no significant differences in the distribution of MyHC isoforms between the groups (Figure 2E). Figure 2F shows the typical traces of Ca^{2+}-activated force in skinned fibers from GAS muscles in each group. The fiber diameter was smaller in the EAM group (mean ± SEM 36.1 ± 0.7 μm [n = 14 fibers]; $P < 0.05$) and the EAM + ECC group (mean ± SEM 37.3 ± 1.5 μm [n = 15 fibers]; $P < 0.05$), compared to the control group (mean ± SEM 41.5 ± 1.0 μm [n = 21 fibers]). The maximum Ca^{2+}-activated force per cross-sectional area (F_{max}) was ~30% lower in EAM muscle fibers than in control muscle fibers (mean ± SEM 256 ± 13 mN/mm^2 versus 365 ± 11 mN/mm^2; $P < 0.05$) (Figure 2G). Importantly, ECC training restored F_{max} to the control level in skinned fibers from EAM muscles (mean ± SEM 334 ± 12 mN/mm^2; $P > 0.05$). On the other hand, there was no alteration in pCa_{50} in muscle fibers from mice with EAM (mean ± SEM 5.83 ± 0.01 pCa units), or those from mice in the EAM + ECC group (mean ± SEM 5.81 ± 0.02 pCa units), compared to controls (mean ± SEM 5.86 ± 0.02 pCa units).

No alteration in MyHC or actin content in skinned fibers from mice with EAM. The decrease in F_{max} in skinned EAM muscle fibers can, in principle, be due to a decreased number of force-producing myosin cross-bridges and/or impaired

cross-bridge function with decreased force per cross-bridge. Therefore, we assessed whether the expression levels of MyHC and actin are decreased in skeletal muscles from mice with EAM. Neither MyHC nor actin content was altered in skinned fibers from mice with EAM compared to controls (Figures 3A and B). Moreover, ECC training had no effect on the expression levels of these proteins in muscle fibers from mice with EAM. Thus, these data suggest that EAM-induced decrease in F_{max} is not caused by a decreased number of myosin cross-bridges but may be due to impaired cross-bridge function with decreased force per cross-bridge.

ECC training–induced suppression of up-regulation of ER stress proteins in GAS muscles from mice with EAM. Compared to muscles from controls, the levels of Grp78, Grp94, high mobility group box chromosomal protein 1 (HMGB-1), and NADPH oxidase 2 (NOX-2)/gp91^{phox} were significantly increased, by 6.1-, 3.2-, 3.3-, and 1.3-fold, respectively, in EAM muscles ($P < 0.05$) (Figures 4A–D). ECC training prevented an increase in expression of Grp78 and Grp94 in EAM muscles ($P < 0.05$), but it had no effect on the increase in expression of HMGB-1 and NOX-2/gp91^{phox} ($P > 0.05$).

ECC training–induced increase in expression of small HSPs and their binding to myofibrillar proteins in GAS muscles from mice with EAM. Catalase expression was 1.7-fold higher in the EAM + ECC group than in the control group ($P < 0.05$) (Figures 5A and B). Expression levels of the small HSP αB-crystallin and Hsp25 in whole GAS muscles were 10-fold and 5.6-fold higher in the EAM + ECC group compared to the control group, respectively ($P < 0.05$) (Figures 5C and D).

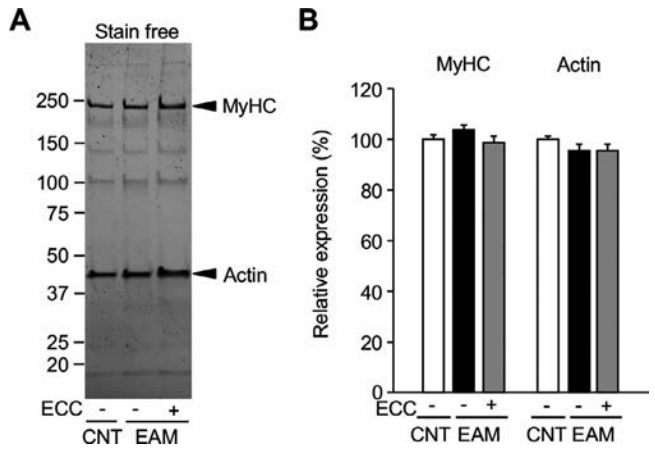

Figure 3. Neither myosin heavy chain (MyHC) nor actin content is altered in skinned fibers from mice with EAM. **A**, Representative stain-free gel of myofibrillar proteins in skinned fibers from GAS muscles from controls and mice with EAM (n = 14–21 fibers per group), with or without ECC training. **B**, Relative expression of MyHC and actin. Bars show the mean ± SEM. Data were normalized to the total proteins from the stain-free image, and the mean in muscles from controls was set at 100%. See Figure 1 for other definitions.

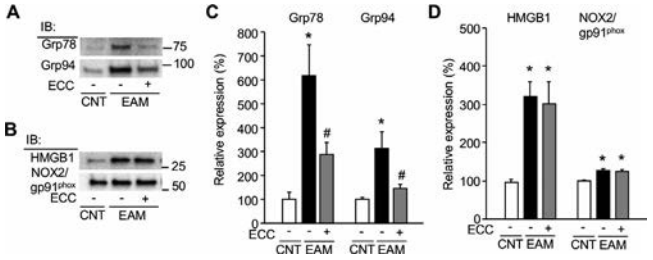

Figure 4. ECC training suppresses the up-regulation of endoplasmic reticulum stress proteins but not of inflammation–redox stress proteins in GAS muscle from mice with EAM. **A** and **B**, Representative Western immunoblots illustrating the levels of Grp78 and Grp94 (**A**) and high mobility group box protein 1 (HMGB-1) and NADPH oxidase (NOX-2/gp91^{phox}) (**B**) in GAS muscles from controls and mice with EAM (n = 6 muscles per group), with or without ECC training. **C** and **D**, Relative expression of these proteins. Bars show the mean ± SEM. Data were normalized to the total proteins from the stain-free image, and the mean in muscles from controls was set at 100%. * = $P < 0.05$ versus controls; # = $P < 0.05$ versus mice with EAM. See Figure 1 for other definitions.

In addition, immunoblot analysis using skinned muscle fiber segments revealed that the amount of αB-crystallin and Hsp25 binding to myofibrils was 23-fold and 3.0-fold higher in the EAM + ECC group compared to the control group, respectively (n = 10 fibers per group; $P < 0.05$) (Figures 5E and F).

DISCUSSION

Mice with EAM, an animal model for acute IIM, display severe muscle weakness due to a reduction in muscle weight combined with decreased muscle quality (i.e., decreased myofibrillar force–generating capacity resulting in decreased force production per cross-sectional area). Importantly, we have shown here that muscles from mice with EAM are not more susceptible to ECC training–induced damage than muscles from controls. In fact, our findings in skinned fiber preparations, in which plasma membrane was chemically permeabilized and myofibrils were directly activated by exogenous Ca^{2+} to evoke force, suggest that ECC training effectively counteracts the decline in myofibrillar force production in EAM muscles. On the other hand, GAS muscle weight in the mice with EAM was not restored by ECC training, which differs from our previous findings on normal mice in which GAS muscle weight was slightly increased (~6%) after 4 weeks of ECC training, assessed using the same protocol as in the present study (42).

Numerous studies have shown an increased susceptibility to ECC-induced muscle damage in patients with DMD and in the mdx mouse model (28). Mechanisms underlying this increased susceptibility are not completely understood, but a potential explanation could be that a lack of dystrophin and dystrophin-associated protein complex may lead to the severe loss of force triggered by increased Ca^{2+} entry, possibly through

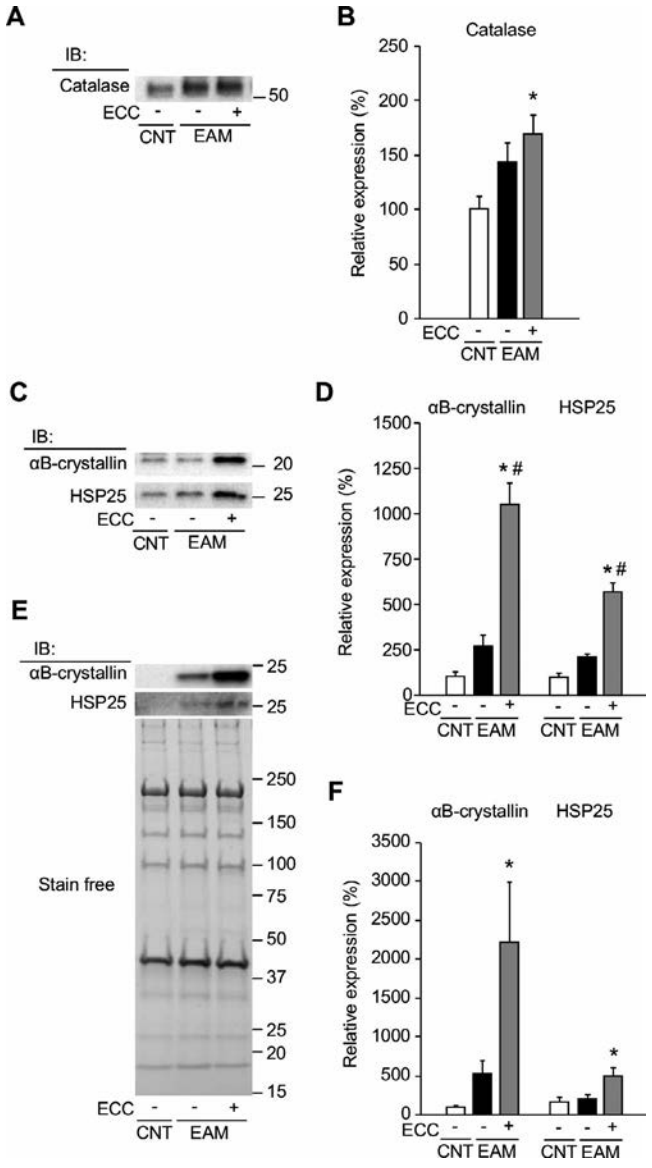

Figure 5. ECC training increases the expression levels of small heat-shock proteins (HSPs) and their binding to myofibrillar proteins in GAS muscle from mice with EAM. **A** and **B**, Representative Western immunoblot showing catalase levels (**A**) and relative expression (**B**) in GAS muscles from controls and mice with EAM, with or without ECC training. **C** and **D**, Representative Western immunoblots showing αB-crystalline and Hsp25 levels (**C**) and relative expression (**D**) in GAS muscles from controls and mice with EAM, with or without ECC training. **E** and **F**, Typical immunoblot images of small HSPs and stain-free images in skinned fibers from each group (n = 10 fibers per group) (**E**) and relative expression of αB-crystallin and Hsp25 content, normalized by total myofibrillar proteins in each fiber (**F**). In **B**, **D**, and **F**, bars show the mean ± SEM. Data were normalized to the total proteins from the stain-free image, and the mean in muscles from controls was set at 100%. * = $P < 0.05$ versus controls; # = $P < 0.05$ versus mice with EAM. See Figure 1 for other definitions.

transient receptor potential channels (28). Importantly, it has been shown that a force loss after in vivo ECCs is detectable in muscles from mdx mice but not from myopathic mice with type VI collagen deficiency (43), which indicates that increased susceptibility to ECC-induced muscle damage is not a common feature in myopathies. Nevertheless, until relatively recently, it was common to advise IIM patients not to perform high-intensity contractions and ECCs due to fear of aggravating the damage to the inflamed muscle. There is now a growing body of evidence demonstrating that resistance training improves muscle strength without inducing muscle fiber damage (16,18–23).

Importantly, our data suggest that skeletal muscles from mice with EAM might be less susceptible to ECC-induced muscle damage compared to controls, as less uptake of membrane-impermeable EBD was observed after damaging ECCs (Figure 1M). However, this decrease in uptake might also reflect the fact that force, and hence the mechanical stress, was lower in muscles from mice with EAM compared to controls. Nevertheless, it appears unlikely that sarcolemmal integrity was reduced in muscle fibers from mice with EAM, which is supported by preserved protein expression of dystrophin, an important stabilizer for sarcolemmal structure (44), in skeletal muscles from mice with EAM (Figure 1O). Furthermore, EAM muscles not exposed to ECCs showed a markedly higher expression level of dysferlin compared to controls. Since dysferlin mediates sarcolemmal repair (45), this finding indicates an improved membrane repair capacity and/or an increased susceptibility to membrane damage in EAM muscles.

In contrast to the remarkable increase in EBD-positive fibers observed 48 hours after damaging ECCs in the control group, a previous study showed few EBD-positive fibers immediately after damaging ECCs (46). This inconsistency can be explained by the different time points, as we and others have shown that membrane damage requires a few days to develop after damaging ECCs (26,39). In contrast, the relative maximum isometric torque was markedly depressed immediately after ECCs were applied to muscles from both mice with EAM and controls (Supplementary Figure 4, http://onlinelibrary.wiley.com/doi/10.1002/art.41594/abstract). These findings are consistent with the notion that the primary mechanism of strength loss immediately after damaging ECCs is excitation–contraction coupling failure and, to a lesser extent, muscle damage (47).

A previous study on a mouse model of inflammatory myositis demonstrated impaired contractile function in both fast- and slow-twitch skeletal muscle, with a large loss of force per cross-sectional area in the fast-twitch muscle (3). This is consistent with our findings of reduced in vivo specific torque in EAM mouse plantar flexor muscles, which are preferentially composed of fast-twitch muscle fibers. Using the skinned fiber preparation, we showed that F_{max}, but not myofibrillar Ca^{2+} sensitivity, is severely reduced in the fast-twitch GAS muscle fibers from mice with EAM. The decline in tetanic force was not accompanied by any significant change in contraction kinetics, as judged from unaltered peak rates of force development and relaxation in 100-Hz tetanic contractions. Thus, a dominant component of the in vivo

contractile dysfunction in EAM muscles appears to be myofibrillar dysfunction with decreased cross-bridge force production, without any major effect on cross-bridge kinetics. This is in slight contrast to previous results obtained in mice with collagen-induced arthritis in which the muscle weakness was accompanied by decreased myofibrillar force production and rate of force development (13). Impaired excitation–contraction coupling, resulting in reduced Ca^{2+} activation of myofibrillar force production, may also contribute to the muscle weakness in IIM (48,49). However, this seems to be of minor importance in EAM muscles, because reduced Ca^{2+} activation has the largest effect on force at low stimulation frequencies, and EAM muscles displayed significant force decreases only at high stimulation frequencies (50).

It has been proposed that during ER stress, accumulation of misfolded proteins induces ROS production as a result of a persistent protein refolding process (10). Further support for a ROS-dependent mechanism underlying the muscle weakness in IIM is demonstrated in a recent study in which the ROS scavenger *N*-acetylcysteine was found to protect against muscle weakness in mice with EAM (51). In the present study, we showed that ECC resistance training counteracted the myofibrillar dysfunction in EAM muscles, and this was accompanied by attenuated expression of the ER stress proteins Grp78 and Grp94 and increased catalase protein expression. Increased expression of MHC class I can activate ER stress and thereby contribute to muscle dysfunction (8,9), and MHC class I expression can be induced by HMGB-1 acting via the Toll-like receptor 4 (49). In the present study, however, the ECC training–induced protection against increased ER stress protein expression and myofibrillar weakness in EAM muscles occurred without attenuating the up-regulation of HMGB-1 expression.

Despite remaining uncertainties regarding the molecular mechanisms underlying the observed effects of ECC training on the ER stress response in EAM muscles, the lower expression of the ER-located chaperones Grp78 and Grp94 in the EAM + ECC group compared to the EAM group may reflect a training-induced upstream inhibition of the unfolded protein response. In any case, our data suggest that ECC training might reduce ER stress–induced ROS production and thereby improve contractile function in skeletal muscle from mice with EAM, although further studies are required to confirm this suggestion and to define the precise mechanisms involved.

Our findings revealed that ECC training increases the expression of small HSP αB-crystallin and Hsp25 in EAM muscles. Importantly, we observed a significant ECC-induced increase in the binding of αB-crystallin and Hsp25 to myofibrillar proteins in muscle fibers from mice with EAM. It has been demonstrated that a single bout of ECC exercise results in the up-regulation of small HSP as well as their translocation to myofibrils in skeletal muscle (52–54). Small HSP have been shown to protect enzymatic activity of myosin (30) and stabilize actin filaments (31) under stress conditions. Moreover, transgenic overexpression of αB-crystallin has been shown to protect myocardial function against ischemia/reperfusion-induced oxidative injury (55). It has also been demonstrated that αB-crystallin can prevent oxidative stress–induced apoptosis in mouse neonatal cardiomyocytes (56). Thus, ECC training of EAM muscles resulted in enhanced expression levels of small HSP, which may contribute to protection against muscle weakness by preserving myofibrillar structure and function, as well as protecting against oxidative stress insults.

In conclusion, we used a mouse IIM model with skeletal muscle weakness due to impaired myofibrillar force generation. Muscles from IIM mice were, if anything, less susceptible to damage induced by high-force ECCs compared to controls. In fact, ECC training protected against muscle weakness in IIM mice via ER stress–dependent and small HSP–dependent pathways. Our findings suggest that resistance training involving high-force ECC can be a safe and effective method to combat muscle weakness in patients with IIM. Indeed, a case report has shown that a submaximal eccentric training regimen can improve strength and sit-to-stand performance without incurring an exacerbation of disease activity in a patient with IIM (57). On the other hand, high-force ECC exercise to which the subject is unaccustomed may lead to extensive muscle damage, and in some cases rhabdomyolysis, even in normal subjects (58). Consequently, further studies should be conducted in patients with IIMs to define exercise protocols (i.e., contraction modes, exercise intensity, volume, frequency, and duration) that maximize the benefits of exercise while minimizing the risk of exacerbated muscle problems.

AUTHOR CONTRIBUTIONS

All authors were involved in drafting the article or revising it critically for important intellectual content, and all authors approved the final version to be published. Dr. Yamada had full access to all of the data in the study and takes responsibility for the integrity of the data and the accuracy of the data analysis.

Study conception and design. Yamada.

Acquisition of data. Himori, Ashida, Tatebayashi, Abe, Saito, Chikenji, Yamada.

Analysis and interpretation of data. Himori, Westerblad, Andersson, Yamada.

REFERENCES

1. Harris-Love MO, Shrader JA, Koziol D, Pahlajani N, Jain M, Smith M, et al. Distribution and severity of weakness among patients with polymyositis, dermatomyositis and juvenile dermatomyositis. Rheumatology (Oxford) 2009;48:134–9.
2. Alexanderson H, Broman L, Tollbäck A, Josefson A, Lundberg IE, Stenström CH. Functional index-2: validity and reliability of a disease-specific measure of impairment in patients with polymyositis and dermatomyositis. Arthritis Rheum 2006;55:114–22.
3. Coley W, Rayavarapu S, Pandey GS, Sabina RL, van der Meulen JH, Ampong B, et al. The molecular basis of skeletal muscle weakness in a mouse model of inflammatory myopathy. Arthritis Rheum 2012;64:3750–9.
4. Lundberg IE, de Visser M, Werth VP. Classification of myositis [review]. Nat Rev Rheumatol 2018;14:269–78.

5. Englund P, Lindroos E, Nennesmo I, Klareskog L, Lundberg IE. Skeletal muscle fibers express major histocompatibility complex class II antigens independently of inflammatory infiltrates in inflammatory myopathies. Am J Pathol 2001;159:1263–73.
6. Barsotti S, Lundberg IE. Current treatment for myositis. Curr Treatm Opt Rheumatol 2018;4:299–315.
7. Li CK, Varsani H, Holton JL, Gao B, Woo P, Wedderburn LR. MHC class I overexpression on muscles in early juvenile dermatomyositis. J Rheumatol 2004;31:605–9.
8. Henriques-Pons A, Nagaraju K. Nonimmune mechanisms of muscle damage in myositis: role of the endoplasmic reticulum stress response and autophagy in the disease pathogenesis. Curr Opin Rheumatol 2009;21:581–7.
9. Nagaraju K, Casciola-Rosen L, Lundberg I, Rawat R, Cutting S, Thapliyal R, et al. Activation of the endoplasmic reticulum stress response in autoimmune myositis: potential role in muscle fiber damage and dysfunction. Arthritis Rheum 2005;52:1824–35.
10. Haynes CM, Titus EA, Cooper AA. Degradation of misfolded proteins prevents ER-derived oxidative stress and cell death. Mol Cell 2004;15:767–76.
11. Yamada T, Place N, Kosterina N, Östberg T, Zhang SJ, Grundtman C, et al. Impaired myofibrillar function in the soleus muscle of mice with collagen-induced arthritis. Arthritis Rheum 2009;60:3280–9.
12. Supinski GS, Callahan LA. Free radical-mediated skeletal muscle dysfunction in inflammatory conditions. J Appl Physiol 2007; 102:2056–63.
13. Yamada T, Fedotovskaya O, Cheng AJ, Cornachione AS, Minozzo FC, Aulin C, et al. Nitrosative modifications of the Ca^{2+} release complex and actin underlie arthritis-induced muscle weakness. Ann Rheum Dis 2015;74:1907–14.
14. Lightfoot AP, McArdle A, Jackson MJ, Cooper RG. In the idiopathic inflammatory myopathies (IIM), do reactive oxygen species (ROS) contribute to muscle weakness? Ann Rheum Dis 2015;74:1340–6.
15. Alexanderson H, Lundberg IE. Exercise as a therapeutic modality in patients with idiopathic inflammatory myopathies. Curr Opin Rheumatol 2012;24:201–7.
16. Escalante A, Miller L, Beardmore TD. Resistive exercise in the rehabilitation of polymyositis/dermatomyositis. J Rheumatol 1993;20:1340–4.
17. Hicks JE, Miller F, Plotz P, Chen TH, Gerber L. Isometric exercise increases strength and does not produce sustained creatinine phosphokinase increases in a patient with polymyositis. J Rheumatol 1993;20:1399–401.
18. Varjú C, Pethö E, Kutas R, Czirják L. The effect of physical exercise following acute disease exacerbation in patients with dermato/polymyositis. Clin Rehabil 2003;17:83–7.
19. Alexanderson H, Stenström CH, Lundberg I. Safety of a home exercise programme in patients with polymyositis and dermatomyositis: a pilot study. Rheumatology (Oxford) 1999;38:608–11.
20. Alexanderson H, Stenström CH, Jenner G, Lundberg I. The safety of a resistive home exercise program in patients with recent onset active polymyositis or dermatomyositis. Scand J Rheumatol 2000;29:295–301.
21. Wiesinger GF, Quittan M, Graninger M, Seeber A, Ebenbichler G, Sturm B, et al. Benefit of 6 months long-term physical training in polymyositis/dermatomyositis patients. Br J Rheumatol 1998;37:1338–42.
22. Alexanderson H, Dastmalchi M, Esbjörnsson-Liljedahl M, Opava CH, Lundberg IE. Benefits of intensive resistance training in patients with chronic polymyositis or dermatomyositis. Arthritis Rheum 2007;57:768–77.
23. Nader GA, Dastmalchi M, Alexanderson H, Grundtman C, Gernapudi R, Esbjörnsson M, et al. A longitudinal, integrated, clinical, histological and mRNA profiling study of resistance exercise in myositis. Mol Med 2010;16:455–64.
24. Hortobágyi T, Hill JP, Houmard JA, Fraser DD, Lambert NJ, Israel RG. Adaptive responses to muscle lengthening and shortening in humans. J Appl Physiol (1985) 1996;80:765–72.
25. Kamandulis S, de Souza Leite F, Hernandez A, Katz A, Brazaitis M, Bruton JD, et al. Prolonged force depression after mechanically demanding contractions is largely independent of Ca^{2+} and reactive oxygen species. FASEB J 2017;31:4809–20.
26. Yamada R, Himori K, Tatebayashi D, Ashida Y, Ikezaki K, Miyata H, et al. Preconditioning contractions prevent the delayed onset of myofibrillar dysfunction after damaging eccentric contractions. J Physiol 2018;596:4427–42.
27. Lindsay A, Baumann CW, Rebbeck RT, Yuen SL, Southern WM, Hodges JS, et al. Mechanical factors tune the sensitivity of mdx muscle to eccentric strength loss and its protection by antioxidant and calcium modulators. Skelet Muscle 2020;10:3.
28. Allen DG, Whitehead NP, Froehner SC. Absence of dystrophin disrupts skeletal muscle signaling: roles of Ca^{2+}, reactive oxygen species, and nitric oxide in the development of muscular dystrophy [review]. Physiol Rev 2016;96:253–305.
29. Frankenberg NT, Lamb GD, Overgaard K, Murphy RM, Vissing K. Small heat shock proteins translocate to the cytoskeleton in human skeletal muscle following eccentric exercise independently of phosphorylation. J Appl Physiol (1985) 2014;116:1463–72.
30. Melkani GC, Cammarato A, Bernstein SI. AlphaB-crystallin maintains skeletal muscle myosin enzymatic activity and prevents its aggregation under heat-shock stress. J Mol Biol 2006;358:635–45.
31. Wang K, Spector A. Alpha-crystallin stabilizes actin filaments and prevents cytochalasin-induced depolymerization in a phosphorylation-dependent manner. Eur J Biochem 1996;242:56–66.
32. Unger A, Beckendorf L, Bohme P, Kley R, von Frieling-Salewsky M, Lochmuller H, et al. Translocation of molecular chaperones to the titin springs is common in skeletal myopathy patients and affects sarcomere function. Acta Neuropathol Commun 2017;5:72.
33. Himori K, Tatebayashi D, Ashida Y, Yamada T. Eccentric training enhances the αB-crystallin binding to the myofibrils and prevents skeletal muscle weakness in adjuvant-induced arthritis rat. J Appl Physiol (1985) 2019;127:71–80.
34. Allenbach Y, Solly S, Gregoire S, Dubourg O, Salomon B, Butler-Browne G, et al. Role of regulatory T cells in a new mouse model of experimental autoimmune myositis. Am J Pathol 2009;174:989–98.
35. Garma T, Kobayashi C, Haddad F, Adams GR, Bodell PW, Baldwin KM. Similar acute molecular responses to equivalent volumes of isometric, lengthening, or shortening mode resistance exercise. J Appl Physiol (1985) 2007;102:135–43.
36. Hesselink MK, Kuipers H, Geurten P, van Straaten H. Structural muscle damage and muscle strength after incremental number of isometric and forced lengthening contractions. J Muscle Res Cell Motil 1996;17:335–41.
37. Mori T, Agata N, Itoh Y, Miyazu-Inoue M, Sokabe M, Taguchi T, et al. Stretch speed-dependent myofiber damage and functional deficits in rat skeletal muscle induced by lengthening contraction. Physiol Rep 2014;2:e12213.
38. Ashida Y, Himori K, Tatebayashi D, Yamada R, Ogasawara R, Yamada T. Effects of contraction mode and stimulation frequency on electrical stimulation-induced skeletal muscle hypertrophy. J Appl Physiol (1985) 2018;124:341–8.
39. Sacco P, Jones DA, Dick JR, Vrbová G. Contractile properties and susceptibility to exercise-induced damage of normal and mdx mouse tibialis anterior muscle. Clin Sci (Lond) 1992;82:227–36.

40. Mollica JP, Dutka TL, Merry TL, Lamboley CR, McConell GK, McKenna MJ, et al. S-glutathionylation of troponin I (fast) increases contractile apparatus Ca2+ sensitivity in fast-twitch muscle fibres of rats and humans. J Physiol 2012;590:1443–63.
41. Wada M, Okumoto T, Toro K, Masuda K, Fukubayashi T, Kikuchi K, et al. Expression of hybrid isomyosins in human skeletal muscle. Am J Physiol Cell Physiol 1996;271:C1250–5.
42. Tatebayashi D, Himori K, Yamada R, Ashida Y, Miyazaki M, Yamada T. High-intensity eccentric training ameliorates muscle wasting in colon 26 tumor-bearing mice. PLoS One 2018;13:e0199050.
43. Blaauw B, Agatea L, Toniolo L, Canato M, Quarta M, Dyar KA, et al. Eccentric contractions lead to myofibrillar dysfunction in muscular dystrophy. J Appl Physiol (1985) 2010;108:105–11.
44. Petrof BJ, Shrager JB, Stedman HH, Kelly AM, Sweeney HL. Dystrophin protects the sarcolemma from stresses developed during muscle contraction. Proc Natl Acad Sci U S A 1993;90:3710–4.
45. Roche JA, Tulapurkar ME, Mueller AL, van Rooijen N, Hasday JD, Lovering RM, et al. Myofiber damage precedes macrophage infiltration after in vivo injury in dysferlin-deficient A/J mouse skeletal muscle. Am J Pathol 2015;185:1686–98.
46. Olthoff JT, Lindsay A, Abo-Zahrah R, Baltgalvis KA, Patrinostro X, Belanto JJ, et al. Loss of peroxiredoxin-2 exacerbates eccentric contraction-induced force loss in dystrophin-deficient muscle. Nat Commun 2018;9:5104.
47. Warren GL, Ingalls CP, Lowe DA, Armstrong RB. Excitation-contraction uncoupling: major role in contraction-induced muscle injury [review]. Exerc Sport Sci Rev 2001;29:82–7.
48. Grundtman C, Bruton J, Yamada T, Östberg T, Pisetsky DS, Harris HE, et al. Effects of HMGB1 on in vitro responses of isolated muscle fibers and functional aspects in skeletal muscles of idiopathic inflammatory myopathies. FASEB J 2010;24:570–8.
49. Zong M, Bruton JD, Grundtman C, Yang H, Li JH, Alexanderson H, et al. TLR4 as receptor for HMGB1 induced muscle dysfunction in myositis. Ann Rheum Dis 2013;72:1390–9.
50. Allen DG, Lamb GD, Westerblad H. Skeletal muscle fatigue: cellular mechanisms. Physiol Rev 2008;88:287–332.
51. Meyer A, Laverny G, Allenbach Y, Grelet E, Ueberschlag V, Echaniz-Laguna A, et al. IFN-β-induced reactive oxygen species and mitochondrial damage contribute to muscle impairment and inflammation maintenance in dermatomyositis. Acta Neuropathol 2017;134:655–66.
52. Féasson L, Stockholm D, Freyssenet D, Richard I, Duguez S, Beckmann JS, et al. Molecular adaptations of neuromuscular disease-associated proteins in response to eccentric exercise in human skeletal muscle. J Physiol 2002;543:297–306.
53. Koh TJ, Escobedo J. Cytoskeletal disruption and small heat shock protein translocation immediately after lengthening contractions. Am J Physiol Cell Physiol 2004;286:C713–22.
54. Paulsen G, Vissing K, Kalhovde JM, Ugelstad I, Bayer ML, Kadi F, et al. Maximal eccentric exercise induces a rapid accumulation of small heat shock proteins on myofibrils and a delayed HSP70 response in humans. Am J Physiol Regul Integr Comp Physiol 2007;293:R844–53.
55. Ray PS, Martin JL, Swanson EA, Otani H, Dillmann WH, Das DK. Transgene overexpression of αB crystallin confers simultaneous protection against cardiomyocyte apoptosis and necrosis during myocardial ischemia and reperfusion. FASEB J 2001;15:393–402.
56. Chis R, Sharma P, Bousette N, Miyake T, Wilson A, Backx PH, et al. Alpha-crystallin B prevents apoptosis after H_2O_2 exposure in mouse neonatal cardiomyocytes. Am J Physiol Heart Circ Physiol 2012;303:H967–78.
57. Harris-Love MO. Safety and efficacy of submaximal eccentric strength training for a subject with polymyositis. Arthritis Rheum 2005;53:471–4.
58. Kim J, Lee J, Kim S, Ryu HY, Cha KS, Sung DJ. Exercise-induced rhabdomyolysis mechanisms and prevention: a literature review. J Sport Health Sci 2016;5:324–33.

American College of Rheumatology
Empowering Rheumatology Professionals

Arthritis & Rheumatology
Vol. 73, No. 5, May 2021, pp 858–865
DOI 10.1002/art.41602

Study of Tofacitinib in Refractory Dermatomyositis: An Open-Label Pilot Study of Ten Patients

Julie J. Paik,[1] Livia Casciola-Rosen,[1] Joseph Yusup Shin,[1] Jemima Albayda,[1] Eleni Tiniakou,[1] Doris G. Leung,[1] Laura Gutierrez-Alamillo,[1] Jamie Perin,[1] Liliana Florea,[1] Corina Antonescu,[1] Sherry G. Leung,[1] Grazyna Purwin,[1] Andrew Koenig,[2] and Lisa Christopher-Stine[1]

Objective. This open-label 12-week study was conducted to evaluate the efficacy and safety of tofacitinib, a JAK inhibitor, in treatment-refractory active dermatomyositis (DM).

Methods. Tofacitinib in extended-release doses of 11 mg was administered daily to 10 subjects with DM. Prior to treatment, a complete washout of all steroid-sparing agents was performed. The primary outcome measure was assessment of disease activity improvement based on the International Myositis Assessment and Clinical Studies group definition of improvement. Response rate was measured as the total improvement score according to the 2016 American College of Rheumatology (ACR)/European League Against Rheumatism (EULAR) myositis response criteria. Secondary outcome measures included Cutaneous Dermatomyositis Disease Area and Severity Index (CDASI) scores, chemokine levels, immunohistochemical analysis of STAT1 expression in the skin, RNA sequencing analysis, and safety.

Results. At 12 weeks, the primary outcome was met in all 10 subjects. Five (50%) of 10 subjects experienced moderate improvement in disease activity, and the other 50% experienced minimal improvement according to the 2016 ACR/EULAR myositis response criteria. The secondary outcome of the mean change in the CDASI activity score over 12 weeks was statistically significant (mean ± SD 28 ± 15.4 at baseline versus 9.5 ± 8.5 at 12 weeks) (P = 0.0005). Serum chemokine levels of CXCL9/CXCL10 showed a statistically significant change from baseline. A marked decrease in STAT1 signaling in association with suppression of interferon target gene expression was demonstrated in 3 of 9 skin biopsy samples from subjects with dermatomyositis. The mean ± SD level of creatine kinase in the 10 subjects at baseline was 82 ± 34.8 IU/liter, highlighting that disease activity was predominantly located in the skin.

Conclusion. This is the first prospective, open-label clinical trial of tofacitinib in DM that demonstrates strong clinical efficacy of a pan-JAK inhibitor, as measured by validated myositis response criteria. Future randomized controlled trials using JAK inhibitors should be considered for treating DM.

INTRODUCTION

Dermatomyositis (DM) is an idiopathic inflammatory myopathy that primarily affects the muscle and skin. We previously reported a case of refractory DM and inflammatory arthritis treated with tofacitinib, a pan-JAK inhibitor, in which clinical improvement of disease activity in the skin, muscle, and joints was observed (1). Other small case reports and series have demonstrated that this class of medications may be helpful in treating refractory DM and polymyositis (2–4). In particular, the first case report of a JAK

ClinicalTrials.gov identifier: NCT03002649.

The Rheumatic Diseases Research Core Center was supported by the NIH (grant P30-AR-070254). Dr. Casciola-Rosen's work was supported in part by the Donald B. and Dorothy L. Stabler Foundation. Drs. Albayda and Tiniakou's work was supported by the Jerome L. Greene Foundation. Dr. Florea's work was supported in part by the NIH (grant R01-GM-129085). Dr. D. Leung's work was supported by the National Institute of Neurological Disorders and Stroke, NIH (Mentored Patient-Oriented Research Career Development award 5K23-NS-091379).

[1]Julie J. Paik, MD, MHS, Livia Casciola-Rosen, PhD, Joseph Yusup Shin, BS, Jemima Albayda, MD, Eleni Tiniakou, MD, Doris G. Leung, MD, PhD, Laura Gutierrez-Alamillo, MD, Jamie Perin, PhD, Liliana Florea, PhD, Corina Antonescu, BS, Sherry G. Leung, BA, Grazyna Purwin, BA, Lisa Christopher-Stine, MD, MPH: Johns Hopkins University School of Medicine, Baltimore, Maryland; [2]Andrew Koenig, DO: Pfizer, Inc., New York, New York.

Drs. Paik and Casciola-Rosen received research support from Pfizer, Inc. Dr. Koenig owns stock or stock options in Pfizer, Inc. Dr. Christopher-Stine has received consulting fees and/or honoraria from AbbVie (less than $10,000). No other disclosures relevant to this article were reported.

Address correspondence to Julie J. Paik, MD, MHS, 5200 Eastern Avenue, Mason F. Lord, Center Tower, Suite 4500, Baltimore, MD 21224. Email: jpaik1@jhmi.edu.

Submitted for publication June 12, 2020; accepted in revised form November 24, 2020.

inhibitor, ruxolitinib, which demonstrated efficacy in recalcitrant DM, was thought to be mediated by blocking interferon (IFN)–regulated proinflammatory cytokines such as CXCL9/CXCL10, thereby making JAK inhibitors an attractive therapeutic agent in the treatment of DM (3). This 12-week, open-label, proof-of-concept study was conducted to evaluate the efficacy and safety of tofacitinib in active, treatment-refractory DM. We hypothesized that JAK inhibition would reduce the activation of type I IFN–regulated proteins and key chemokines (CXCL9/CXCL10) that would correspond to biologic activity before and after treatment with tofacitinib.

PATIENTS AND METHODS

Study population. This study was conducted at the Johns Hopkins Myositis Center. Thirteen subjects were screened for eligibility, and 10 were enrolled in the study. Written informed consent was obtained from each study subject. Eligible subjects included adults 18 years and older with a diagnosis of definite or probable DM as defined by Bohan and Peter (5,6). Eligibility for study enrollment also included a Cutaneous Dermatomyositis Disease Area and Severity Index (CDASI) score (7) of ≥5 (range 0–100), a prior skin or muscle biopsy diagnostic finding of DM, or a prior positive finding of ≥1 myositis-specific antibody (MSA). Although not mandatory, subjects with muscle weakness were eligible for study enrollment and required a score of ≤142 of 150 on a Manual Muscle Testing in 8 muscles (MMT-8) assessment.

Refractory disease was defined as active disease that persisted despite a 12-week trial of steroid therapy as well as lack of response to at least prednisone and 1 other first-line immunosuppressive agent such as methotrexate (MTX), mycophenolate mofetil (MMF), or azathioprine (AZA). The maximum daily dose of prednisone allowed at time of study entry was 20 mg, and the dose amount had to be stable for >2 weeks prior to the baseline visit. Treatment with steroids was not required before study initiation and was only used if subjects were not tolerating the washout of steroid-sparing agents.

To minimize confounding, subjects with the following conditions were excluded from the study: juvenile DM, myositis overlapping with other autoimmune diseases, history of hypersensitivity to any study drugs, cancer-associated myositis, or other types of myositis or myopathies. Subjects with hypersensitivity to the study drug, pregnant or lactating women, and any subject with concomitant illnesses including severe cardiopulmonary disease, active infections, inflammatory bowel disease, or history of bowel rupture were also excluded from study enrollment. Subjects with a history of any malignancy (other than localized basal cell carcinoma of the skin), treated or untreated, within the past 5 years were excluded. Individuals with late-stage DM wherein muscle weakness, according to the investigator (JJP), could be attributable to muscle damage, rather than myositis disease activity, were also excluded.

Study design. This was a proof-of-concept study to evaluate the efficacy and safety of tofacitinib in refractory DM using a prospective open-label design over the course of 12 weeks. Washout of immunosuppressive or immunomodulatory agents was required prior to subjects receiving the first dose of study drug as follows: MTX, AZA, MMF, tacrolimus, and hydroxychloroquine (12–16 weeks prior to first dose); rituximab and cyclophosphamide (12 months prior to first dose); and intravenous immunoglobulin (IVIG) (3 months prior to first dose). Study subjects self-administered 11 mg of extended-release tofacitinib by mouth daily for 12 weeks. A forced prednisone taper was instituted at 8 weeks if subjects were receiving prednisone at study entry. Rescue prednisone, not to exceed a daily dose of 20 mg, was allowed at the discretion of the investigator if there was any disease flare. Clinical assessments and safety analyses based on laboratory data were performed every 4 weeks for 12 weeks, with an optional 4-week extension. Skin biopsy of unaffected and affected skin was performed (by JJP) using a 4-mm punch technique at baseline and 12 weeks, and needle muscle biopsy samples were performed (by DGL) at baseline and 12 weeks in a manner as previously described (8), using a Pro-Mag Ultra Automatic Biopsy instrument (Argon Medical Devices). Magnetic resonance imaging (MRI) of the thigh muscles was performed bilaterally at baseline and 12 weeks.

Adverse events (AEs). Occurrence of AEs and serious AEs (SAEs) were monitored and reported in a standardized manner using the Common Terminology Criteria of the National Cancer Institute version 4.03. One of the study investigators (JJP) determined whether the AEs or SAEs were associated with the study drug.

Primary and secondary end points. The primary end point for the trial was improvement in disease activity as defined by the International Myositis Assessment and Clinical Studies (IMACS) group, which includes improvement of 3 of any 6 core set measures by >20% with no more than 2 core set measures worsening by >25% (not including the MMT in the assessment of worsening) (9). Response rate was determined according to the total improvement score based on the 2016 American College of Rheumatology (ACR)/European League Against Rheumatism (EULAR) myositis response criteria (10).

Secondary outcome measures included safety measures and change from baseline in the following measures (assays used are described below): CDASI, STAT1 expression in the skin, CXCL9 and CXCL10 levels, MRI assessment of the thighs bilaterally, and RNA sequencing (RNA-Seq) of blood, skin, and muscle biopsy samples.

Immunohistochemical analysis. Paraffin-embedded skin sections, obtained from biopsy samples of uninvolved and involved skin at baseline and 12 weeks after treatments start, were immunostained with 6.7 μg/ml of anti-STAT1 mouse monoclonal

antibody (Novus Biologicals) at a temperature of 4°C overnight followed by incubation with horseradish peroxidase–conjugated anti-mouse secondary antibody (Dako) at a 1:500 dilution as previously described (11). Control staining of sections was performed with an equivalent concentration of isotype-matched mouse IgG, or in the absence of primary antibody (Supplementary Figure 1, available on the *Arthritis & Rheumatology* website at http://onlinelibrary.wiley.com/doi/10.1002/art.41602/abstract). Staining was visualized using the diaminobenzidine substrate chromagen system (Dako), with the reaction time held constant for all immunostaining. Nuclei were stained using Mayer's hematoxylin solution (Dako).

Light microscopy images were obtained using a Zeiss Axioskop 50 with a Zeiss AxioCam HRC camera and performed with AxioVision 4.9.1 software. Camera settings were held constant for all images, enabling a semiquantitative comparison of staining intensity to be assessed across sections. Two investigators (LCR and LGA) independently examined the staining. Skin biopsy samples were obtained from 9 subjects pretreatment and posttreatment. One subject declined the skin biopsy at week 12.

Measurement of CXCL9 and CXCL10. Sera from all study subjects were obtained at 4-week intervals, aliquoted, and banked at a temperature of –80°C. Levels of CXCL9 and CXCL10 in these banked sera were assayed using commercially available enzyme-linked immunosorbent assay kits according to the manufacturer's instructions (R&D Systems).

Autoantibody assays. Autoantibodies were assayed on banked sera using a commercially available line immunoblot platform (Myositis profile; Euroimmun).

RNA-Seq library preparation and sequencing. RNA sequencing was performed in the blood, skin, and muscle of subjects. NEBNext Poly(A) Magnetic Isolation Module (NEB product no. E7490) and NEBNext Ultra II Directional RNA Library Prep kit for Illumina (product no. E7765) were used to generate libraries. The procedure included poly(A) RNA isolation and fragmentation, complementary DNA synthesis and end repair, sequencing adapter ligation, and polymerase chain reaction amplification to prepare the libraries. The resulting library insert size was 200–500 bp that peaked around 300 bp. Libraries were uniquely barcoded and pooled for NovaSeq6000 sequencing. Pooled libraries were sequenced on an Illumina NovaSeq6000 instrument using standard protocols for S2 50-bp paired-end sequencing. We multiplexed 112 samples for an estimated 75 million reads per sample. Illumina sequencing was conducted at the Genetic Resources Core Facility at Johns Hopkins Institute of Genetic Medicine (Baltimore, Maryland).

Bioinformatics analysis. RNA sequencing data were analyzed to determine the genes present in each subject, their expression levels, and the differences between expression levels at different time points during treatment. Genes with a ≥ 1.5 $\log_2$ fold change in expression were considered to be significantly differentially expressed (at $P < 0.05$). In all available samples, the down-regulated genes were compared from 12 weeks (primary outcome measure) to baseline (an overview of the numbers of down-regulated and up-regulated genes for each comparison is presented in Supplementary Table 1, available on the *Arthritis & Rheumatology* website at http://onlinelibrary.wiley.com/doi/10.1002/art.41602/abstract). Samples were analyzed separately by tissue type (blood, skin, and muscle). Following quality checking, sequencing reads were aligned to the human genome GRCh38 with TopHat2 software version 2.1.0 (12), and then assembled into genes and transcripts using the program CLASS2 version 2.1.7 (13). Transcripts from all samples were further merged and mapped to the Gencode version 27 gene models to create a unified set of gene annotations for gene quantification and differential analyses. Differentially expressed genes were determined with the DESeq2 tool (14) and used for subsequent pathway analysis with Ingenuity Pathway Analysis (Qiagen). Lastly, IFN gene scores, as previously reported (15), were computed separately in blood and muscle by calculating the IFN scores for the median log fold change in expression of 15 IFN signature genes (EPSTI1, HERC5, IFI27, IFI44, IFI44L, IFI6, IFIT1, IFIT3, ISG15, MX1, OAS1, OAS3, and RSAD2) from baseline to 12 weeks, relative to that in normal samples of blood and muscle (SRR607219 and ERR030876, respectively). A median log fold

Table 1. Demographic and clinical characteristics of the 10 study subjects at baseline*

Age, mean ± SD years	45.6 ± 10.6
Female sex	7 (70)
Race	
White	9 (90)
African American	1 (10)
Disease duration, mean ± SD years	6.45 ± 4.55
Prednisone usage at study entry†	4 (40)
CDASI, mean ± SD score	28 ± 15.4
CDASI, median (IQR) score	21 (18–30)
MMT, mean ± SD score	147 ± 5.06
MMT, median (IQR) score	150 (145–150)
Creatine kinase, mean ± SD IU/liter	82 ± 34.8
Creatine kinase, median (IQR) IU/liter	97 (53–116)
Myositis autoantibody	
TIF1γ	7 (70)
Mi-2	1 (10)
NXP-2	2 (20)
Prior immunosuppressive treatment‡	
Methotrexate	9 (90)
Azathioprine	2 (20)
Mycophenolate mofetil	5 (50)
Intravenous immunoglobulin	6 (60)
Rituximab	1 (10)

* Except where indicated, values are the number (%). CDASI = Cutaneous Dermatomyositis Disease Area and Severity Index; IQR = interquartile range; MMT = Manual Muscle Testing; TIF1γ = transcription intermediary factor 1γ; NXP-2 = nuclear matrix protein 2.
† Maximum daily dose of prednisone allowed at study entry was 20 mg.
‡ Prior immunosuppressive treatments were not mutually exclusive, as patients may have been receiving more than one type of immunosuppressive agent at once prior to study enrollment.

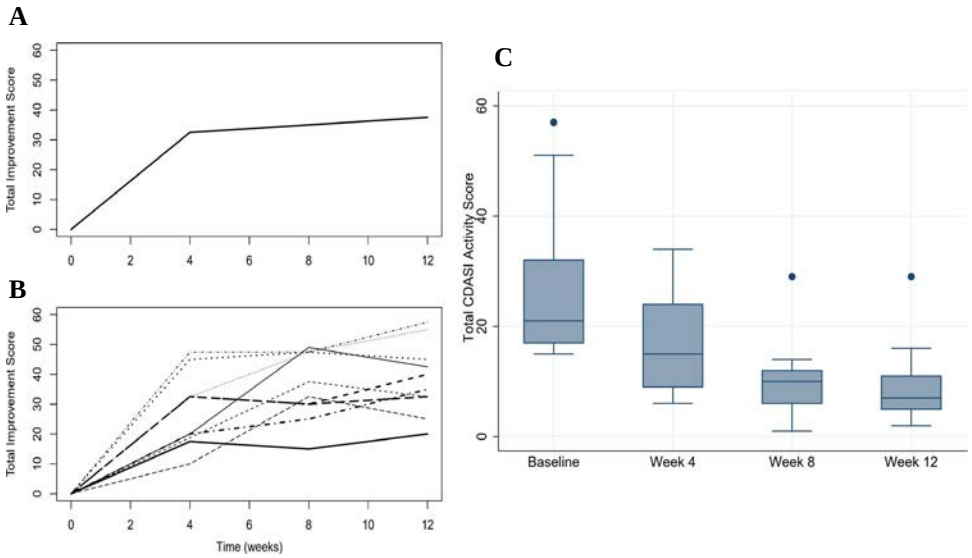

Figure 1. Key outcome measures determined in the 10 study subjects with active dermatomyositis included the median total improvement score over the 12-week study period in all 10 subjects (**A**) and in each individual subject (**B**), and the Cutaneous Dermatomyositis Disease Area and Severity Index (CDASI) scores from baseline to week 12 (**C**). Values in **C** are shown as box plots. Each box represents the 25th to 75th percentiles. Lines inside the boxes represent the median. Whiskers show the spread of the scores. Circles indicate outliers.

change of ≥1.5 was defined as significant when comparing IFN scores in the muscle from baseline to 12 weeks.

Statistical analysis. Baseline demographic, clinical, and laboratory variables were evaluated with descriptive statistics. Continuous variables were summarized as the mean ± SD, and categorical variables were summarized as proportions in each category. Median total improvement scores were compared to baseline values using Wilcoxon's rank sum test. CDASI values were compared to baseline values using paired *t*-tests and Wilcoxon's rank sum test. Change in chemokine levels over time was assessed using Wilcoxon's rank sum test for paired data. To test the correlation between changes in expression (log 2-fold change) from baseline to week 12 in each marker gene identified by RNA-Seq analysis and total improvement scores or CDASI scores, Pearson's correlation coefficients were calculated across all subjects.

RESULTS

Demographic and clinical characteristics of the study subjects. Ten subjects completed the study without any experiencing any SAEs. Baseline clinical features of all 10 subjects enrolled in the study are summarized in Table 1. The mean ± SD age was 45.6 ± 10.6 years with a mean ± SD disease duration of 6.5 ± 4.6 years. Seventy percent of subjects were female, and 90% were white. Skin disease

Figure 2. Assessment of skin symptoms in a representative subject with dermatomyositis shows cutaneous improvements in the chest and back (upper and lower panels, respectively) from baseline (left) to 4 weeks (middle) and 12 weeks (right) after treatment with tofacitinib.

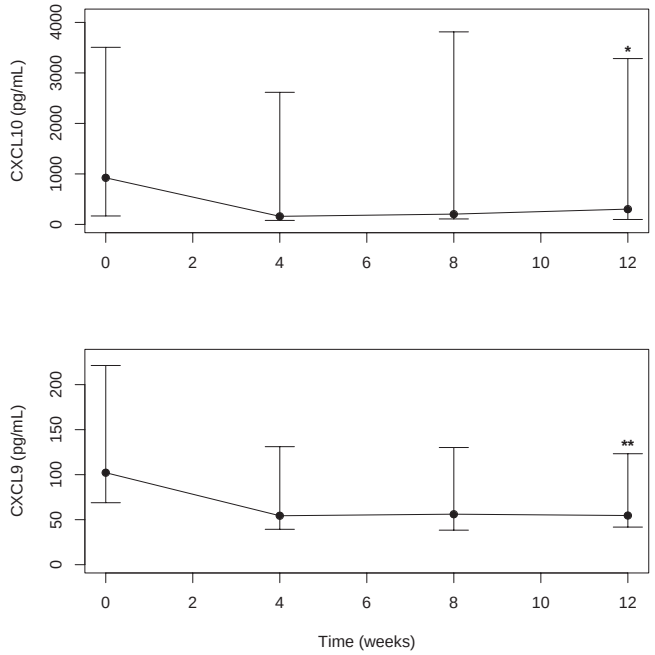

Figure 3. Serum levels of chemokines CXCL9 and CXCL10 in subjects with dermatomyositis from baseline (0 weeks) to 12 weeks after treatment wiith tofacitinib. Results are the median with 95% confidence intervals at each time point. * = $P = 0.013$; ** = $P = 0.049$ versus baseline, by Wilcoxon's rank sum test.

activity as measured by a mean CDASI score at study entry was 28 ± 15.4, without significant overall muscle involvement observed at study entry. All study subjects had disease activity that was refractory to prior treatment with ≥2 steroid-sparing agents for skin or muscle disease. At the time of study entry, all 10 subjects had treatment-refractory skin disease, whereas 1 of 10 subjects had moderate muscle weakness. Other than rash and muscle weakness, additional clinical features included calcinosis (n = 3 subjects). No subjects were observed to have interstitial lung disease.

Primary outcome measure. All 10 subjects who completed the study met the primary outcome measure of interest, the IMACS group definition of improvement, at 12 weeks. These subjects also met the outcome measure of minimal improvement using the 2016 ACR/EULAR myositis response criteria. The median total improvement score was 40 (interquartile range 32.5–47.5) (Figure 1A). Seven (70%) of 10 subjects had at least minimal improvement based on the change in total improvement score at 4 weeks, which was sustained until the primary end point at 12 weeks.

Secondary outcome measures. *Improvement in cutaneous disease activity as measured by the validated CDASI.* All 10 subjects had at least moderate skin disease activity as validated by the CDASI, with a mean ± SD CDASI score of 28 ± 15 at study entry that improved to 9.5 ± 8.5 by 12 weeks, which was considered statistically significant ($P = 0.0005$) (Figures 1C and Figure 2). Furthermore, the mean change in the CDASI was 18.5, a 66% decrease from baseline. A >40% change in the CDASI has been reported to indicate a meaningful change in quality of life (16). Based on the definition of a CDASI score of ≤14 indicating mild skin disease (7), 7 (70%) of 10 subjects improved from having moderate-to-severe skin disease activity to mild disease activity.

Levels of chemokines and findings of immunohistochemical analysis. Median serum levels of CXCL9/CXCL10 in all subjects demonstrated a statistically significant change from baseline to 12 weeks with treatment ($P = 0.049$ and $P = 0.013$ for CXCL9 and CXCL10, respectively) (Figure 3). To explore the efficacy of tofacitinib in inhibiting STAT1 expression in the skin, a semiquantitative approach was used to assess change in STAT1 staining. STAT1 immunostaining performed on these paraffin-embedded skin sections showed that STAT1 levels were lower in affected skin biopsy samples in 3 of 9 subjects from baseline to week 12 (Figure 4). Control immunostaining performed on these skin sections confirmed specificity of the STAT1 staining (Supplementary Figure 1, available on the *Arthritis & Rheumatology* website at http://onlinelibrary.wiley.com/doi/10.1002/art.41602/abstract). Interestingly, of these 3 subjects, 2 (67%) of 3 were moderate responders on the total improvement score, and the mean change ± SD in CDASI

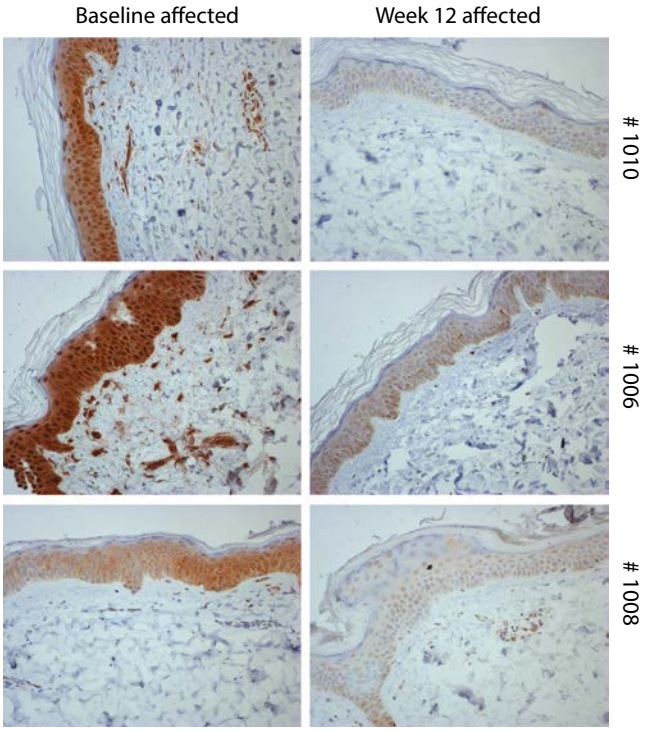

Figure 4. Biopsy samples were obtained from the affected skin of subjects with dermatomyositis. Paraffin-embedded skin sections were immunostained for STAT1 at baseline and 12 weeks after treatment. Samples from 3 representative subjects are shown.

scores of all 3 subjects was 14 ± 3.6. In the other 6 subjects, the following STAT1 staining patterns were observed: no STAT1 staining seen both at baseline and at week 12 in 4 subjects, high STAT1 levels at baseline and at week 12 in 1 subject, and no STAT1 baseline staining but variable STAT1 levels at week 12 in 1 subject. Of note, minimal staining was observed in unaffected skin at baseline (Supplementary Figure 2, available on the *Arthritis & Rheumatology* website at http://onlinelibrary.wiley.com/doi/10.1002/art.41602/abstract).

Muscle involvement. The mean ± SD MMT score of all 10 subjects was 147 ± 5.06, which is indicative of only very mild muscle weakness at study entry. Two subjects had an MMT score of <140 at entry, with 1 subject having an MMT score of 127. The subject with an MMT score of 127 demonstrated a 9-point improvement in the MMT-8 assessment at 12 weeks. This subject also had objective evidence of edema on muscle MRI, which improved from baseline to 12 weeks (Supplementary Figure 3, available on the *Arthritis & Rheumatology* website at http://onlinelibrary.wiley.com/doi/10.1002/art.41602/abstract).

RNA-Seq analysis in the blood, skin, and muscle. In all available samples, genes found to be down-regulated at 12 weeks compared to baseline were assessed (primary outcome measure). In the blood, the genes of interest that were down-regulated were C1QB and C1QC, which are both involved in the complement pathway. In the skin, the predominant gene of interest that was down-regulated was CXCL9. Notably, RNA-Seq analysis of the 3 subjects who also had STAT1 inhibition on immunohistochemical analysis revealed that skin biopsy samples obtained at week 12 exhibited significant gene expression differences in comparison to baseline, with enrichment of IFN target genes that were found to be suppressed at 12 weeks (Figure 5). Lastly, in the muscle, the genes of interest that were down-regulated were C1QB and C1QC, CXCL9, and type I IFN–related genes such as IFI27, MX2, ISG15, and IFI16. The IFN score was down-regulated in the muscle of 5 of 8 subjects with an average change of 6.86 ± 4.32. Overall, the CXCL9 and CXC10 and complement pathway were highly down-regulated across all tissue types (blood, skin, and muscle) (Supplementary

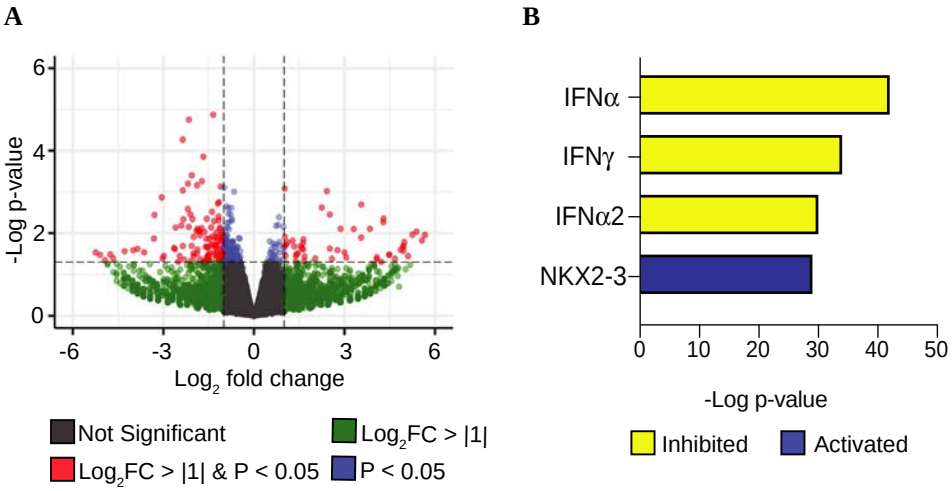

C

Ingenuity Pathway Analysis: top upstream regulators	Gene members
IFNα	*FOS, B2M, SP100, RNF213, NMI, LAP3,TNFSF10, GBP5, ADAR, TRIM21, WARS, PARP14, ITGA4, IL10RA, SOCS1, C19orf66, PARP10, GIMAP4, SP110, PARP12, PLSCR1, APOBEC3G, SAMD9, HELZ2, STAT1, IL32, TRANK1, PARP9, IFIH1, ID01, DHX58, LILRB4, IL7R,IFIT3, GBP1, HERC5, RTP4, CCR5, IFI35, CCR1, USP18, CD8, C3AR1, FCGR1A, PRF1, TBX21, NKG7, GZMB, GZMH, CXCL10.*
IFNγ	*CHAC1, TP73, GLIS1, FOS, PMEL, TYRP1, VIPR1, TGFBR2,B2M, LIFR, CTSS, SP100, ADM, KLF2, GLUL, THBS1, NMI, ODC1, TNFSF10, AGTR1, PSME2, GBP5, CORO1A, TRIM21, WARS, LCP2, DDX60, PARP14, ITGA4, A2M, TSC22D3, IL10RA, SOCS1, CTGF, ALOX5AP, SERPINE1, IFIT5, SP110, DDX60L, PLSCR1, SAMD9, APOBEC3G, RAC2, STAT1, IL32, LY6E, PARP9, IFIH1, IDO1*
IFNα2	*B2M, SP100, TNFSF10, TRIM21, DDX60, SOCS1, C19orf66, IFIT5, SP110, LGALS3BP, TRIM14, PARP12, PLSCR1, SAMD9, STAT1, LY6E, PARP9, IFIH1, IDO1, LILRB4, MMP9, IFIT3, GBP1, HERC5, LILRB2, SLC15A3, SAMHD1, IFI35, USP18, TBX21, CXCL10, CXCR3, TGM2, CXCL11, CXCL9*
NKX2-3	*CSRNP1, SYT11, ADM, KLF2, ZNFX1, RNF213, LAP3, TRIM21, DDX60, PARP14, PLEKHA4, MEDAG, C19orf66, PARP10, SP110, PARP12, DCLK1, DDX60L, PLSCR1, APOBEC3G, SAMD9, TRPC6, HELZ2, STAT1, LY6E, PARP9, IDO1, DHX58, IL7R, GBP1, RTP4, USP41, USP18*

Figure 5. Suppression of interferon (IFN) target gene expression by tofacitinib in skin biopsy samples. **A**, Volcano plots of differentially expressed genes (dots) at baseline and at 12 weeks following tofacitinib treatment. FC = fold change. **B**, Top Ingenuity Pathway Analysis predictions of upstream regulators of differentially expressed genes assessed by RNA sequencing. Adjusted *P* values <0.05 were considered significant. **C**, List of differentially expressed genes targeted by each upstream regulator.

Figure 4, available on the *Arthritis & Rheumatology* website at http://onlinelibrary.wiley.com/doi/10.1002/art.41602/abstract).

In correlation studies performed with our clinical outcome measures, the total improvement score was not correlated with any gene expression in the blood, skin, or muscle. However, there was a moderate correlation between the MX2 gene in the muscle and CDASI score (r^2 = 0.56) as well as between CXCL10 in the blood and CDASI score (r^2 = 0.53) (Supplementary Table 2, http://onlinelibrary.wiley.com/doi/10.1002/art.41602/abstract).

Steroid tapering. Four (40%) of 10 subjects were receiving 20 mg of prednisone daily at study entry, of whom 3 (75%) required prednisone for active skin disease and 1 (25%) required prednisone for active skin and muscle disease. Three (75%) of the 4 subjects were able to completely discontinue treatment with all steroids.

Safety and tolerability. Over the 12-week study period, 11 mg of daily extended-release tofacitinib was well-tolerated and safe. There were no SAEs observed over the course of the study. There was one recurrent AE, a urinary tract infection (UTI) that required 2 courses of antibiotics. This subject also had a history of recurrent UTIs prior to entry into the study but did not have a UTI at screening. There were no significant changes in levels of white blood cell count, hemoglobin, platelet count, creatine kinase, or serum creatine over the 12-week trial period. No deep vein thromboses or venous thromboembolisms were observed over the course of the study.

DISCUSSION

This is the first proof-of-concept, open-label, prospective clinical trial of tofacitinib, a pan-JAK inhibitor, in DM that has demonstrated strong clinical efficacy as measured by validated myositis response criteria. Enrolled subjects were those with refractory disease, among whom treatment with ≥2 steroid-sparing agents had failed, and who were not permitted to receive concurrent steroid-sparing immunosuppressant therapies, thereby demonstrating the efficacy of tofacitinib monotherapy. Tofacitinib was well-tolerated with no major AEs observed requiring study discontinuation. All subjects in the study met the ACR/EULAR myositis response criteria at the primary end point of 12 weeks, with 50% having shown moderate improvement and 50% showing at least minimal improvement of disease activity.

The overall clinical phenotype of the 10 subjects were skin-predominant refractory DM and only 1 subject with significant muscle weakness. Demonstrated improvement in the total improvement score was largely driven by the patient and physician global assessments of disease activity and the Health Assessment Questionnaire disability index as many subjects did not have a low MMT score or high creatine kinase values at study entry. Improvement in skin disease was quite striking and evident as early as 4 weeks (Figures 2 and 3). Since there was only 1 subject with moderate muscle weakness, meaningful conclusions cannot be made regarding muscle strength improvement; however, this subject did have an improvement in strength, with concurrent improvement in muscle edema on muscle MRI.

The a priori hypothesis was that key chemokines such as CXCL9 and CXCL10 would be inhibited via the JAK/STAT pathway and that type I IFN–related pathways would also be down-regulated in the skin, muscle, and blood. There have been multiple studies demonstrating that CXCL9 and CXCL10 are strong biomarkers in DM (17,18). Similarly, prior studies have established that there is preferential activation of the type I IFN pathway in DM (19–21). Interestingly, our investigations demonstrate that CXCL9 and CXCL10 were both down-regulated in the blood, skin, and muscle. In particular, biochemical assays of both CXCL9 and CXCL10 showed a statistically significant decrease at 12 weeks compared to baseline. The importance of the key chemokines being down-regulated with treatment was also further supported by the RNA-Seq results in the skin, blood, and muscle. However, when evaluating the IFN signature of all 10 study subjects, significant inhibition of specific IFN-related genes was only demonstrated in the muscle tissue. Previous studies have shown that expression of the IFN signature is much higher in diseased muscle than in blood in DM and may provide an explanation for this finding (19). Nonetheless, the fact that the serum levels of CXCL9 and CXCL10 were down-regulated is both clinically and mechanistically meaningful given that these chemokines may be strong biomarkers of disease activity in adult DM. Thus, type II IFN or IFNγ, in conjunction with type I IFN–related pathways, may be playing an important role in the pathogenesis of DM.

The remarkable benefit of tofacitinib in skin disease activity was measured clinically by an improvement in the validated CDASI activity score. Of the 9 subjects in whom skin biopsies were performed pretreatment and posttreatment, 3 had immunohistochemical results that demonstrated decreased staining of STAT1 at 12 weeks compared to baseline. This was coupled with a marked improvement in their CDASI activity score (mean improvement of 72.3%), thereby highlighting that there was evidence of efficacy mediated through the JAK/STAT pathway. RNA-Seq analysis of skin biopsy samples obtained from these 3 subjects also showed marked inhibition of IFN target genes, further supporting the a priori hypothesis that tofacitinib would be effective by blocking this pathway. Of note, NKX2-3 was predicted among the top activated upstream regulators. Although polymorphisms of NKX2-3 have been associated with inflammatory bowel disease (22), its precise functional role in inflammation remains unclear.

MSAs were assayed in all 10 subjects using a myositis antibody panel (Euroimmun platform). Seven subjects had anti–transcription intermediary factor 1γ (anti-TIF1γ) antibodies, 2 were positive for anti–nuclear matrix protein 2 antibodies, and 1 subject was positive for anti–Mi-2 antibodies. Interestingly, the antibody titers remained unchanged after treatment for 12 weeks. Notably, 5 (71%) of 7 subjects positive for anti-TIF1γ antibodies were moderate responders, with the other 2 subjects showing minimal responses to treatment.

In our trial, tofacitinib was well-tolerated, with no subject discontinuing the therapy. While it has been reported that JAK inhibitors are associated with a higher risk of herpes zoster, this was not seen in any of the 10 study subjects. Furthermore, there were no other serious infections that required hospitalization during the trial. There was 1 subject who required 2 rounds of antibiotics due to recurrent UTIs, and though she did not have a UTI at study entry, the subject did have a history of recurrent infections in the past 5 years intermittently.

The limitations of this study include the lack of a control group or randomization. Furthermore, there was no separate arm to study a higher dose for efficacy. Lastly, only 1 subject had moderate muscle weakness, making it difficult to reach any robust clinical conclusions about the effects of the study treatment on muscle. Therefore, the primary end point, the total improvement score, was not driven by the MMT-8 or creatine kinase values. Despite these limitations, this open-label, prospective clinical trial is the first in its class to show efficacy using validated response criteria in refractory DM. Additionally, the extensive studies done on blood, skin, and muscle tissue have allowed us to explore the mechanisms by which tofacitinib may be exerting its therapeutic effect. Tofacitinib was well-tolerated with minimal AEs, highlighting the importance of further investigations on JAK inhibitors in a larger randomized controlled trial in patients with DM.

AUTHOR CONTRIBUTIONS

All authors were involved in drafting the article or revising it critically for important intellectual content, and all authors approved the final version to be published. Dr. Paik had full access to all the study data and takes responsibility for the integrity of the data and the accuracy of the data analysis.

Study conception and design. Paik, S. Leung, Christopher-Stine.

Acquisition of data. Paik, Casciola-Rosen, Albayda, Tiniakou, D. Leung, Gutierrez-Alamilo, S. Leung, Purwin, Koenig

Analysis and/or interpretation of data. Paik, Casciola-Rosen, Shin, D. Leung, Gutierrez-Alamilo, Perin, Florea, Antonescu, Koenig, Christopher-Stine.

REFERENCES

1. Paik JJ, Christopher-Stine L. A case of refractory dermatomyositis responsive to tofacitinib. Semin Arthritis Rheum 2017;46:e19.
2. Kurtzman DJ, Wright NA, Lin J, Femia AN, Merola JF, Patel M, et al. Tofacitinib citrate for refractory cutaneous dermatomyositis: an alternative treatment [letter]. JAMA Dermatol 2016;152:944–5.
3. Hornung T, Janzen V, Heidgen FJ, Wolf D, Bieber T, Wenzel J. Remission of recalcitrant dermatomyositis treated with ruxolitinib [letter]. N Engl J Med 2014;371:2537–8.
4. Ladislau L, Suárez-Calvet X, Toquet S, Landon-Cardinal O, Amelin D, Depp M, et al. JAK inhibitor improves type I interferon induced damage: proof of concept in dermatomyositis. Brain 2018;141:1609–21.
5. Bohan A, Peter JB. Polymyositis and dermatomyositis. Part I. N Engl J Med 1975;292:344–7.
6. Bohan A, Peter JB. Polymyositis and dermatomyositis. Part II. N Engl J Med 1975;292:403–7.
7. Anyanwu CO, Fiorentino DF, Chung L, Dzuong C, Wang Y, Okawa J, et al. Validation of the Cutaneous Dermatomyositis Disease Area and Severity Index: characterizing disease severity and assessing responsiveness to clinical change. Br J Dermatol 2015;173:969–74.
8. Wagner KR, Hamed S, Hadley DW, Gropman AL, Burstein AH, Escolar DM, et al. Gentamicin treatment of Duchenne and Becker muscular dystrophy due to nonsense mutations. Ann Neurol 2001;49:706–11.
9. Rider LG, Giannini EH, Brunner HI, Ruperto N, James-Newton L, Reed AM, et al. International consensus on preliminary definitions of improvement in adult and juvenile myositis. Arthritis Rheum 2004;50:2281–90.
10. Aggarwal R, Rider LG, Ruperto N, Bayat N, Erman B, Feldman BM, et al. 2016 American College of Rheumatology/European League Against Rheumatism criteria for minimal, moderate, and major clinical response in adult dermatomyositis and polymyositis: an International Myositis Assessment and Clinical Studies Group/Paediatric Rheumatology International Trials Organisation collaborative initiative. Arthritis Rheumatol 2017;69:898–910.
11. Fiorentino DF, Presby M, Baer AN, Petri M, Rieger KE, Soloski M, et al. PUF60: a prominent new target of the autoimmune response in dermatomyositis and Sjögren's syndrome. Ann Rheum Dis 2016;75:1145–51.
12. Kim D, Pertea G, Trapnell C, Pimentel H, Kelley R, Salzberg SL. TopHat2: accurate alignment of transcriptomes in the presence of insertions, deletions and gene fusions. Genome Biol 2013;14:R36.
13. Song L, Sabunciyan S, Florea L. CLASS2: accurate and efficient splice variant annotation from RNA-seq reads. Nucleic Acids Res 2016;44:e98.
14. Love MI, Huber W, Anders S. Moderated estimation of fold change and dispersion for RNA-seq data with DESeq2. Genome Biol 2014;15:550.
15. Greenberg SA, Higgs BW, Morehouse C, Walsh RJ, Kong SW, Brohawn P, et al. Relationship between disease activity and type 1 interferon- and other cytokine-inducible gene expression in blood in dermatomyositis and polymyositis. Genes Immun 2012;13:207–13.
16. Ahmed S, Chakka S, Concha J, Krain R, Feng R, Werth VP. Evaluating important change in cutaneous disease activity as an efficacy measure for clinical trials in dermatomyositis. Br J Dermatol 2020;182:949–54.
17. Wienke J, Enders FB, Lim J, Mertens JS, van den Hoogen LL, Wijngaarde CA, et al. Galectin-9 and CXCL10 as biomarkers for disease activity in juvenile dermatomyositis: a longitudinal cohort study and multicohort validation. Arthritis Rheumatol 2019;71:1377–90.
18. Chen M, Quan C, Diao L, Xue F, Xue K, Wang B, et al. Measurement of cytokines and chemokines and association with clinical severity of dermatomyositis and clinically amyopathic dermatomyositis. Br J Dermatol 2018;179:1334–41.
19. Greenberg SA, Pinkus JL, Pinkus GS, Burleson T, Sanoudou D, Tawil R, et al. Interferon-α/β-mediated innate immune mechanisms in dermatomyositis. Ann Neurol 2005;57:664–78.
20. Baechler EC, Bauer JW, Slattery CA, Ortmann WA, Espe KJ, Novitzke J, et al. An interferon signature in the peripheral blood of dermatomyositis patients is associated with disease activity. Mol Med 2007;13:59–68.
21. Pinal-Fernandez I, Casal-Dominguez M, Derfoul A, Pak K, Plotz P, Miller FW, et al. Identification of distinctive interferon gene signatures in different types of myositis. Neurology 2019;93:e1193–204.
22. Lu X, Tang L, Li K, Zheng J, Zhao P, Tao Y, et al. Contribution of NKX2-3 polymorphisms to inflammatory bowel diseases: a meta-analysis of 35358 subjects. Sci Rep 2014;4:3924.

American College of Rheumatology
Empowering Rheumatology Professionals

Arthritis & Rheumatology
Vol. 73, No. 5, May 2021, pp 866–874
DOI 10.1002/art.41604

Inflammatory Myositis in Cancer Patients Receiving Immune Checkpoint Inhibitors

Jeffrey Aldrich,[1] Xerxes Pundole,[1] Sudhakar Tummala,[1] Nicolas Palaskas,[1] Clark R. Andersen,[1] Mahran Shoukier,[1] Noha Abdel-Wahab,[2] Anita Deswal,[1] and Maria E. Suarez-Almazor[1]

Objective. To estimate the incidence of immune checkpoint inhibitor–related myositis (ICI-myositis) in cancer patients receiving ICIs, and to report associated clinical manifestations, patterns of care, and outcomes.

Methods. We identified a retrospective cohort of patients receiving ICIs between 2016 and 2019 seen at the University of Texas MD Anderson Cancer Center. Cases of ICI-myositis were identified using International Classification of Disease codes and confirmed by reviewing medical records and pathology, as available.

Results. A total of 9,088 patients received an ICI. Thirty-six patients (0.40%) were identified as having ICI-myositis: 17 patients (47%) with ICI-myositis alone and 19 (53%) with overlap manifestations (5 patients with myocarditis, 5 with myasthenia gravis, and 9 with both). The incidence of ICI-myositis was 0.31% in those receiving ICI monotherapy and 0.94% in those receiving combination ICI therapy (relative risk 3.1 [95% confidence interval 1.5–6.1]). Twenty-five patients (69%) received ≥1 treatment in addition to glucocorticoids: plasmapheresis in 17 patients (47%), intravenous immunoglobulin in 12 (33%), and biologics in 11 (31%). Patients with overlap conditions had worse outcomes than those with myositis alone, and 79% of them developed respiratory failure. Eight patients died as a result of ICI-myositis, and all had overlap syndrome with myasthenia gravis or myocarditis ($P < 0.05$); 75% of these patients had a concomitant infection.

Conclusion. ICI-myositis is a rare but severe adverse event. More than half of the patients presented with overlap manifestations and had deleterious outcomes, including respiratory failure and death. None of the patients with ICI-myositis alone died as a result of adverse events. Optimal treatment strategies have yet to be determined.

INTRODUCTION

Immune checkpoint inhibitors (ICIs) have revolutionized cancer care. Currently approved ICIs include antibodies that target CTLA-4, programmed death 1 (PD-1) on T cells, or programmed death ligand 1 (PD-L1) on tumor cells. These therapies are indicated as a single agent or in combination (anti–CTLA-4 and anti–PD-1) (1–3). The ability of ICIs to stimulate the immune system provides a powerful antitumor effect, but these benefits can be hindered by the development of immune-related adverse events (IRAEs). Neuromuscular IRAEs have rarely been reported in clinical trials, with an incidence of ICI-related myositis (ICI-myositis) of <1% (4,5). However, as the use of ICIs has grown, an increasing number of articles describing ICI-myositis have been published, primarily as case reports and small case series (6–10). Importantly, cases of ICI-myositis with concomitant myasthenia gravis (MG), myocarditis, or both have been reported, often with poor outcomes (11–13). Rheumatologists may often be confronted with such cases of overlap syndromes. This is the largest reported institutional case series on the incidence, clinical characteristics, disease course, treatment patterns, and prognosis of ICI-myositis presenting alone or in combination with MG and/or myocarditis.

PATIENTS AND METHODS

Patients. We conducted a retrospective cohort study of patients seen at our institution between March 2016 and September 2019 who had received ≥1 of the following ICIs:

Supported by the National Cancer Institute, NIH (grant P30-CA-016672).

[1]Jeffrey Aldrich, MD, Xerxes Pundole, MD, PhD, Sudhakar Tummala, MD, Nicolas Palaskas, MD, Clark R. Andersen, MS, Mahran Shoukier, MD, Anita Deswal, MD, MPH, Maria E. Suarez-Almazor, MD, PhD: University of Texas MD Anderson Cancer Center, Houston; [2]Noha Abdel-Wahab, MD, PhD: University of Texas MD Anderson Cancer Center, Houston, and Assiut University Hospitals, Assiut, Egypt.

Dr. Suarez-Almazor has received consulting fees, speaking fees, and/or honoraria from Pfizer, AbbVie, Gilead, AMAG, Agile Therapeutics, Eli Lilly, and Avenue Therapeutics (less than $10,000 each) and research support from Pfizer. No other disclosures relevant to this article were reported.

Address correspondence to Maria E. Suarez-Almazor, MD, PhD, University of Texas MD Anderson Cancer Center, Department of Health Services Research, Unit 1444, 1515 Holcombe Boulevard, Houston, TX 77030. Email: msalmazor@mdanderson.org.

Submitted for publication April 28, 2020; accepted in revised form November 24, 2020.

pembrolizumab, nivolumab, cemiplimab-rwlc, atezolizumab, avelumab, durvalumab, or ipilimumab. Patients with ICI-myositis were identified from electronic health records (EHRs) using the International Statistical Classification of Diseases and Related Health Problems, Tenth Revision codes: M60.* (myositis), M33.* (dermatopolymyositis), M36.0 (dermatopolymyositis in neoplastic disease), and M62.83 (rhabdomyolysis). We also examined M62.89 (other specified disorders of muscle) and a random sample of 100 patients with claims for M63 (other disease of muscle) and M79.1 (myalgia) (n = 50 patients each). None of the latter 3 codes identified patients with ICI-myositis. The EHRs of selected patients were reviewed.

There are no published diagnostic criteria for ICI-myositis, and the current criteria for primary polymyositis/dermatomyositis are not entirely adequate for ICI-myositis, as they include features such as autoantibodies and histology findings not applicable for this ICI-induced AE (14). We therefore used a case definition on the basis of patient symptoms suggestive of myositis (fatigue, myalgia, or muscle weakness) with ≥1 of the following: an elevation in creatinine kinase (CK) or aldolase (≥2× the upper limit of normal), or inflammatory infiltrate detected on skeletal muscle biopsy. ICI-myositis was graded using Common Terminology Criteria for Adverse Events version 5.0 and classified as either mild (symptoms grade 1–2) or severe (symptoms grade 3–4) (15). A diagnosis of overlapping MG was made if a patient had evidence of muscle weakness with a positive anti–acetylcholine receptor (anti-AChR) antibody result. A patient with a negative AChR antibody result was also considered to have MG in the setting of fatigable ptosis or diplopia. Patients with fixed ptosis or weak extraocular muscles without diplopia were considered to have myositis with myasthenia-like features in the setting of a negative AChR antibody result. Overlapping myocarditis was identified as definite, probable, or possible based on previously proposed case definitions (16).

To assess outcomes, we reviewed the EHR until November 2019 or until patient death, if earlier. We attributed death to ICI-myositis if death was directly caused by myositis and overlap syndrome or caused by infection related to myositis treatment. Infections were considered treatment-related if the patient was receiving glucocorticoids for ICI-myositis at the time of a positive isolate. Symptom burden was assessed at the time of hospital discharge or first follow-up visit and categorized as resolved, improved, stabilized, or worsened.

Statistical analysis. We used chi-square tests or Fisher's exact tests for comparison of categorical variables, and 2-sided *t*-tests or Mann-Whitney tests for continuous variables. Survival analysis was performed using Kaplan-Meier methods and log rank tests. *P* values less than 0.05 were considered significant. The study was approved by the MD Anderson Cancer Center Institutional Review Board prior to any data collection.

RESULTS

Of the 9,088 patients who received ≥1 ICI, 36 patients (0.40%) were identified as having ICI-myositis. Ten of these patients have previously been described in the literature: 4 patients in a cases series of myositis and 6 in a case series of MG, both published by our group (17,18). Baseline characteristics of the patients with ICI-myositis are shown in Table 1. The median age was 69 years, and most patients (86%) were male. Of the 1,278 patients who received combination ICI therapy, 12 patients (0.94%) developed ICI-myositis, compared to 24 of 7,810 patients (0.31%) who received ICI monotherapy (relative risk 3.1 [95% confidence interval 1.5–6.1]). One of the 383 patients who received ipilimumab alone and 23 of the 7,427 patients who received anti–PD-1/PD-L1 monotherapy developed ICI-myositis (0.26% and 0.31%, respectively). Seventeen ICI-myositis patients (47%) had myositis alone and 19 (53%) had overlap syndrome (5 patients [26%] with myocarditis, 5 [26%] with MG, and 9 [47%] with both myocarditis and MG). The patient treated with ipilimumab monotherapy was excluded from the comparative analyses.

No patients had a history of inflammatory myositis prior to ICI therapy. One patient with melanoma developed a skin rash diagnosed as amyopathic dermatomyositis after nivolumab treatment, with positive serum antinuclear antibody results and normal CK levels. The patient then received pembrolizumab and developed weakness with worsening rash and CK elevation consistent with myositis.

Clinical presentation. The median time to symptom onset was 27 days from ICI initiation, following a median of 2 doses (range 1–6) (Table 2). Patients with overlap syndrome had more severe symptoms, including ptosis, bulbar dysfunction, and dyspnea, compared to those with ICI-myositis alone. Thirty-four

Table 1. Baseline characteristics of the patients with ICI-myositis (n = 36)*

Age at diagnosis, median (range) years	69 (40–95)
Male	31 (86)
Underlying cancer	
Melanoma	9 (25)
Renal cell carcinoma	5 (14)
Other	22 (61)
ICI monotherapy	24 (67)
Anti–PD-1/PD-L1	23 (96)
Anti–CTLA-4	1 (4)
ICI combination therapy	12 (33)
Myositis alone	17 (47)
Overlap syndrome	19 (53)
MG and myocarditis	9 (47)
MG	5 (26)
Myocarditis	5 (26)

* Except where indicated otherwise, values are the number (%) of patients. ICI-myositis = immune checkpoint inhibitor–related myositis; anti–PD-1/PD-L1 = anti–programmed death 1/programmed death ligand 1; MG = myasthenia gravis.

Table 2. Clinical presentation and diagnostic testing of the patients with ICI-myositis alone and those with overlap syndrome*

	All patients (n = 36)†	ICI-myositis alone (n = 16)	Overlap syndrome (n = 19)	*P*
Time to symptom onset after initial ICI, median (range) days	27 (7–161)	36 (7–161)	21 (9–149)	0.21
No. of ICI doses prior to symptom presentation, median (range)	2 (1–6)	2 (1–6)	2 (1–6)	0.20
Symptoms/signs				
Fatigue	33 (92)	16 (100)	16 (84)	0.23
Weakness	27 (75)	12 (75)	15 (79)	1.00
Myalgia	28 (78)	14 (88)	14 (74)	0.42
Bulbar symptoms	17 (47)	3 (19)	13 (68)	0.006
Dyspnea	15 (42)	3 (19)	12 (63)	0.02
CTCAE grade 3–4	20 (56)	5 (31)	15 (79)	0.006
Laboratory results				
CK elevation	34 (94)	14 (88)	19 (100)	0.20
Maximum CK, median (range) units/liter	2,299 (23–24,485)	1,735 (23–11,274)	3,519 (555–24,485)	0.17
Aldolase elevation	26/27 (96)	14/14 (100)	11/12 (92)	0.46
Aldolase, median (range) units/liter	26 (7–147)	17 (8–147)	36 (7–145)	0.35
Troponin T elevation	19/24 (83)	7/10 (70)	12/14 (86)	0.61
Troponin I elevation	14/18 (78)	3/7 (43)	11/11 (100)	0.01
Myositis-specific antibody positivity	4/21 (19)‡	0/7 (0)	4/13 (31)	0.16
AChR-positive	7/25 (28)	1/7 (14)§	6/17 (35)	0.62
Anti-striational–positive	11/24 (46)	2/7 (29)	9/16 (56)	0.37
Rhabdomyolysis	10 (28)	3 (19)	6 (32)	0.46
Imaging				
MRI				
Cardiac irregularities	0/10 (0)	0/6 (0)	0/4 (0)	–
Soft tissue irregularities	2/3 (67)	2/3 (67)	0/0 (0)	1.00
EMG	15 (42)	4 (25)	11 (58)	0.09
Evidence of myopathy	13 (87)	3 (75)	10 (91)	0.48
Evidence of neuromuscular junction disorder	5/14 (36)¶	0 (0)	5/10 (50)	1.00

* Except where indicated otherwise, values are the number (%) of patients. ICI-myositis = immune checkpoint inhibitor–related myositis; CTCAE = Common Terminology Criteria for Adverse Events; CK = creatinine kinase; MRI = magnetic resonance imaging.
† One patient treated with ipilimumab monotherapy was included in the total patients group but excluded in comparison groups.
‡ Two of 12 were positive for anti-SSA, 1 of 21 positive for anti-Ku, 1 of 21 positive for anti-PM/Scl, 0 of 11 positive for anti–nuclear matrix protein 2, 0 of 13 positive for anti–transcription intermediary factor 1γ, and 0 of 1 positive for anti–hydroxymethylglutaryl-coenzyme.
§ One patient who was positive for acetylcholine receptor antibody (AChR) had no clinical myasthenia gravis symptoms and was diagnosed as having myositis alone.
¶ For 1 patient, neuromuscular junction dysfunction could not be assessed on electromyography (EMG) due to sedation.

patients (94%) had CK elevation. Two patients had normal CK levels, of whom 1 had an elevated aldolase level (19.5 units/liter), and the other had both an elevated aldolase level (14 units/liter) and skeletal muscle biopsy results consistent with ICI-myositis.

Myositis-specific autoantibodies were evaluated in 21 patients, and 4 patients were positive: 2 for anti-SSA and 1 each for anti-Ku and anti-PM/Scl. AChR antibodies were positive in 28% of patients. One patient with profound weakness and respiratory failure who required intubation had negative AChR antibody results on 3 occasions, which became positive 6 days after admission. Patients with positive anti-striational antibody results had similar symptom severity at presentation as those who tested negative (see Supplementary Table 1, on the *Arthritis & Rheumatology* website at http://onlinelibrary.wiley.com/doi/10.1002/art.41604/abstract).

Three patients underwent soft tissue magnetic resonance imaging (MRI) that showed muscle enhancement in 2 and normal imaging in 1. Fifteen patients were evaluated with repetitive nerve stimulation and electromyography (EMG): 13 patients (87%) showed features consistent with myopathy, and 5 of 14 (36%) showed neuromuscular junction dysfunction suggestive of MG.

Patients treated with combination ICI therapy developed symptoms earlier than patients treated with anti–PD-1/PD-L1 monotherapy (32 days versus 14 days; $P = 0.003$), but no other significant differences were found (Supplementary Table 2, http://onlinelibrary.wiley.com/doi/10.1002/art.41604/abstract).

Histopathology. Twelve patients underwent skeletal muscle biopsy (Supplementary Table 3, http://onlinelibrary.wiley.com/doi/10.1002/art.41604/abstract). Ten biopsy specimens (83%) showed lymphocytic infiltration, with a majority (71%) having both CD8+ and CD4+ T cells. One patient without lymphocytic cell infiltration demonstrated sarcolemmal immunoreactivity with major histocompatibility complex class I consistent with inflammatory myopathy. Four patients had muscle necrosis. Nine patients

Table 3. Treatments used in ICI-myositis alone and in overlap syndrome*

	All patients (n = 36)†	ICI-myositis alone (n = 16)	Overlap syndrome (n = 19)	*P*
Initial steroid dose, median (range) mg/kg/day‡	1.8 (0.1–18)	1.7 (0.1–3)	1.9 (0.3–18)	0.17
Other agents	25 (69)	8 (50)	17 (89)	0.02
Treated initially with other agent§	10 (40)	2 (25)	8 (47)	0.07
Time to second agent, median (range) days	2 (0–59)	14 (1–59)	2 (0–10)	0.15
Plasmapheresis	17 (47)	4 (25)	13 (68)	0.02
IVIG	12 (33)	1 (8)	11 (65)	0.002
Biologic agents	11 (31)	5 (31)	6 (32)	1.00
Rituximab	7 (19)	3 (19)	4 (21)	1.00
Infliximab	6 (17)	3 (19)	3 (16)	1.00
Tocilizumab	3 (8)	1 (6)	2 (11)	1.00
Other treatments	12 (33)	3 (23)	8 (47)	0.26
Tacrolimus	6 (17)	1 (6)	5 (26)	0.19
MMF	5 (14)	1 (6)	5 (26)	0.19

* Except where indicated otherwise, values are the number (%) of patients. ICI-myositis = immune checkpoint inhibitor–related myositis; IVIG = intravenous immunoglobulin; MMF = mycophenolate mofetil.
† One patient treated with ipilimumab monotherapy was included in the total patients group but excluded in comparison groups.
‡ All steroid doses were converted to methylprednisolone for dosing comparison.
§ Given on the same day or the day after initial steroid dose.

underwent endomyocardial biopsy, of whom 7 (78%) had lymphocytic infiltration consistent with myocarditis (Supplementary Table 4, http://onlinelibrary.wiley.com/doi/10.1002/art.41604/abstract).

Myocarditis and MG. Fourteen patients were diagnosed as having concurrent myocarditis; 7 patients were diagnosed as having definite myocarditis, based on endomyocardial biopsy, and 7 were diagnosed as having possible myocarditis. Most patients had dyspnea (64%), while only 2 patients (14%) presented with chest pain; electrocardiogram (EKG) changes were frequent (64%) (Supplementary Table 5, http://onlinelibrary.wiley.com/doi/10.1002/art.41604/abstract).

Fourteen patients were diagnosed as having concurrent MG; 6 had a positive AChR antibody result. Eight patients with

Table 4. Outcomes in the patients with ICI-myositis alone and those with overlap syndrome*

	All patients (n = 36)†	ICI-myositis alone (n = 16)	Overlap syndrome (n = 19)	*P*
Severity				
Patients requiring hospitalization	34 (94)	16 (100)	18 (95)	1.00
Total hospital stay, median (range) days	14 (2–105)	6 (2–50)	24 (5–105)	0.008
Respiratory failure	15 (42)	0 (0)	15 (79)	<0.001
Time to respiratory failure, median (range) days‡	12 (4–26)	NA	12 (4–26)	–
Myositis outcome				
Total steroid time, median (range) days	45 (1–250)§	43 (1–220)	44 (4–250)	0.99
Time to CK normalization, median (range) days	11 (2–112)¶	7 (3–112)	18 (2–105)	0.73
Symptoms at end of hospitalization				
Improved or resolved	22 (61)	13 (81)	8 (42)	0.04
Stabilized	6 (17)	3 (19)	3 (16)	1.00
Worsened	8 (22)	0 (0)	8 (42)	0.004
ICI rechallenge	5 (14)	2 (13)	3 (16)	1.00
Myositis flare	1 (20)	0 (0)	1 (33)	1.00
No ICI rechallenge	31 (86)	14 (88)	16 (84)	1.00
Myositis flare	2 (6)	2 (13)	0 (0)	0.21
Patient outcome				
Overall death	24 (67)	9 (56)	14 (74)	0.31
Death from myositis or overlap syndrome	8 (22)	0 (0)	8 (42)	0.004
Death from cancer progression	16 (44)	9 (56)	6 (32)	0.18
Infection	10 (28)	1 (6)	9 (47)	0.01

* Except where indicated otherwise, values are the number (%) of patients. NA = not applicable (see Table 2 for other definitions).
† One patient treated with ipilimumab monotherapy was included in the total patients group but excluded in comparison groups.
‡ From symptom onset to respiratory failure.
§ Steroid treatment was extended in 6 patients for other reasons (i.e., other immune-related adverse events, cancer progression).
¶ Total of 25 patients. CK never normalized in 5 patients, 4 patients did not have follow-up data on CK, and 2 patients did not have elevated CK levels.

negative AChR antibody results were diagnosed as having MG based on fatigable ocular features (Supplementary Table 6, http://onlinelibrary.wiley.com/doi/10.1002/art.41604/abstract). An additional 6 patients who had negative diagnostic evaluations for MG were described as having "myasthenia-like features" with the presence of fixed ptosis. Nine patients had myositis, myocarditis, and MG; 8 patients presented with grade 3–4 symptoms with a median CK level of 3,797 units/liter (range 2,147–19,794 units/liter). Most patients did not undergo skeletal or endomyocardial biopsy.

Treatment. All patients had discontinued ICIs, and all but 1 were treated initially with glucocorticoids, most at a dose equivalent to >1 mg/kg day of methylprednisolone (Table 3). The median initial glucocorticoid dose was similar in patients with ICI-myositis alone and those with overlap syndrome. Six patients received intravenous pulse methylprednisolone (500–1,000 mg/day): 3 patients received it as treatment for myocarditis, 2 for severe weakness, and 1 for respiratory failure. Additional therapies were utilized in 25 of the 36 patients, most commonly plasmapheresis and intravenous immunoglobulin (IVIG), in 17 patients (47%) and 12 patients (33%), respectively. Other agents included rituximab (19%), infliximab (17%), tocilizumab (8%), tacrolimus (17%), and mycophenolate mofetil (14%). These therapies were more common in patients with overlap syndrome compared to those with myositis alone (89% versus 50%; P = 0.02). Heatmaps of therapies used in relation to overlap syndrome or myositis alone are shown in Supplementary Figures 1 and 2 (http://onlinelibrary.wiley.com/doi/10.1002/art.41604/abstract).

Outcomes. Most patients with ICI-myositis (94%) required hospitalization (Table 4). Patients with overlap syndrome had significantly longer hospitalizations, were more likely to experience respiratory failure, and were more frequently transferred to the intensive care unit. The 9 patients with the triad of ICI-myositis, MG, and myocarditis had the worst outcomes, with respiratory failure occurring in all, and more than half died as a result of their IRAEs.

In patients who developed respiratory failure, the median time from symptom onset to ventilation being needed was 12 days. Of the 15 patients with respiratory failure, 12 cases were attributed primarily to neuromuscular dysfunction, with pneumonia as a contributing factor in several patients. Of the remaining 3 patients, 1 had metastatic pleural and lung disease, 1 had pulmonary embolism and possible pneumonia, and 1 had concomitant immune-related pneumonitis as seen on computed tomography (CT). For 1 patient, a CT scan that was obtained several months before immunotherapy showed mild pulmonary fibrosis. All patients underwent chest radiography during the myositis episode, and 8 patients had CT scans. Of these 8 patients, only 1 showed ground-glass opacities, but these were attributed to possible pneumonia.

At the time of discharge, patients with ICI-myositis alone were more likely to have improved or resolved symptoms compared to those with overlap syndrome (81% versus 42%; P = 0.04). The median overall survival was longer in patients with ICI-myositis alone (2.5 years) compared to those with overlap syndrome (0.5 years), but the difference was not statistically significant (Figure 1).

Eight patients (22%) experienced worsening symptoms with persistent respiratory failure and died. All had overlap syndrome. Culture-positive infections likely contributed to 3 deaths. Seven additional patients had documented infections during therapy with glucocorticoids, including 3 patients treated with IV pulse glucocorticoids. Organisms isolated are listed in Supplementary Table 7 (http://onlinelibrary.wiley.com/doi/10.1002/art.41604/abstract). Differences between patients who died as a result of ICI-myositis and those who did not are shown in Table 5. None of the patients with myositis alone died because of their IRAE, while 42% of the patients with overlap syndrome died as a consequence of their IRAE (P = 0.004). Patients who died of myositis were older than those who did not (median age 77 years versus 69 years). All patients who died of ICI-myositis had developed respiratory failure, and most (75%) developed an infection.

After resolution of the ICI-myositis, 5 patients were rechallenged with ICI treatment (3 with the same agent) (Table 4). One patient had recurrent myositis and MG with respiratory failure requiring mechanical ventilation and recovered. The other 4 patients did not have a subsequent flare. Of the 31 patients who were not rechallenged, only 2 experienced a mild flare during follow-up.

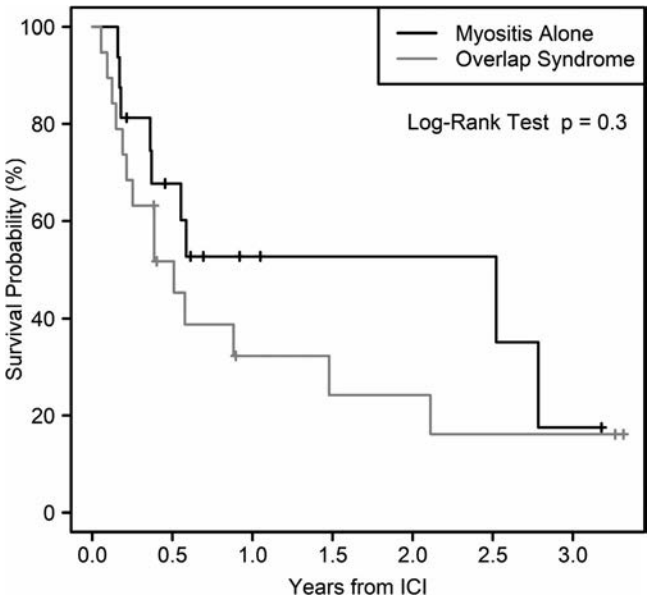

Figure 1. Kaplan-Meier curve for overall survival with immune checkpoint inhibitor (ICI) treatment in patients diagnosed as having myositis alone versus those diagnosed as having myositis with myocarditis, myasthenia gravis, or both (overlap syndrome).

Table 5. Clinical characteristics and outcomes in the patients who died as a result of myositis versus those who did not*

	Patients with myositis-related death (n = 8)	Remaining patients (n = 27)†	*P*
Diagnosis			0.004
Myositis alone	0 (0)	16 (59)	
Overlap syndrome	8 (100)	11 (41)	
Demographic data			
Age at myositis diagnosis, median (range) years	77 (65–87)	69 (40–94)	0.04
Time to symptom onset, median (range) days	19 (9–149)	29 (7–161)	0.80
Symptoms/signs			
Fatigue	8 (100)	24 (89)	1.00
Weakness	6 (75)	21 (78)	1.00
Myalgia	7 (88)	21 (78)	1.00
Ptosis	8 (100)	12 (44)	0.006
Bulbar symptoms	6 (75)	10 (37)	0.16
Dyspnea	7 (88)	8 (30)	0.01
CTCAE grade 3–4	6 (75)	14 (52)	0.42
Other IRAEs	0 (0)	11 (41)	0.04
Laboratory results			
CK elevation	7 (88)	25 (93)	0.55
Maximum CK, median (range) units/liter	3,038 (555–12,706)	2,233 (23–24,485)	1.00
Aldolase elevation	6 (86)	19 (100)	0.27
Aldolase, median (range) units/liter	29 (7–145)	19 (8–147)	0.41
Troponin T elevation	6 (86)	13 (76)	1.00
Troponin I elevation	5 (100)	9 (69)	1.00
AChR-positive	4 (50)	3 (19)	0.17
Anti-striational–positive	3 (38)	8 (53)	0.67
Treatment			
Initial glucocorticoid dose, median (range) mg/kg/day	2 (0.9–9.5)	1.8 (0.1–18)	0.66
Total glucocorticoid duration, median (range) days	23.5 (4–70)	52 (1–250)	<0.001
Other agents	8 (100)	17 (63)	0.07
Plasmapheresis	7 (88)	10 (37)	0.02
Outcome			
Total hospital stay, median (range) days	27 (5–59)	12 (2–105)	0.71
Respiratory failure	8 (100)	7 (26)	<0.001
Infection	6 (75)	4 (15)	0.003

* Except where indicated otherwise, values are the number (%) of patients. IRAEs = immune-related adverse events (see Table 2 for other definitions).
† One patient treated with ipilimumab monotherapy was included in the total patients group but excluded in comparison groups.

DISCUSSION

We report the largest single-center series of cancer patients receiving ICIs who developed myositis. In the present study, the overall limited incidence of ICI-myositis was 0.40%. In comparison, the estimated incidence of biopsy-proven ICI-myositis in a single-center study was 0.76% (8), and a pharmacovigilance safety analysis estimated the incidence at 0.17% (19). Only 1 patient in our study was treated with single-agent ipilimumab, and few case reports exist in the literature, but this could be a result of the declining use of ipilimumab as monotherapy (20,21). In patients receiving combination ICI therapy, the incidence of myositis was close to 3 times higher than that in patients receiving monotherapy, with earlier onset of symptoms. Similarly, studies have demonstrated earlier onset and increased severity of other IRAEs in patients receiving combination therapy (22,23).

Onset of myositis occurred soon after ICI exposure, with half of the cases occurring within 1 month. Only 1 patient had a skin rash consistent with dermatomyositis, suggesting that in most patients, myositis is a de novo event, and not a subclinical paraneoplastic syndrome revealed after ICI therapy. The most common presenting symptoms included myalgia, proximal limb weakness, and ocular/bulbar symptoms, as has been reported in smaller case series (10,24,25). The quickly progressing weakness

with prominent myalgia that is characteristic of ICI-myositis contrasts with the typically slower onset of symptoms in primary autoimmune polymyositis (26). Several of our patients developed necrotizing myositis and rhabdomyolysis, highlighting the acute and severe nature of ICI-myositis.

Two patients had normal CK levels and elevated aldolase. There have been other reports of CK-negative ICI-myositis (8,27). In a case series of 12 patients with symptomatic idiopathic myopathy and elevated serum aldolase levels (but normal CK), 11 had abnormal findings on muscle biopsy (28). Murine models have shown that aldolase level/CK level discordance may be due to high aldolase levels in regenerating myocytes preferentially targeted during myositis (29). Therefore, when ICI-myositis is being considered, aldolase levels should be evaluated if CK levels are normal.

Approximately 40% of the patients in this study had concomitant myocarditis. Given the high prevalence and potential for poor outcomes, all patients with ICI-myositis should be evaluated for myocarditis by assessing troponin levels and EKG. If they have cardiac symptoms or abnormal test results, they should be further evaluated by a cardiologist.

In idiopathic myositis, troponin T is frequently elevated in the absence of clinical myocarditis (30). While our results showed only a moderate specificity advantage for troponin I, we agree that it should be utilized when myocarditis is suspected, given the cross-reactivity of troponin T with skeletal muscle. Only 2 patients with myocarditis had reduced left ventricular ejection fraction according to transthoracic echocardiography, in contrast to a case–control study in which it was frequently reduced in ICI-related myocarditis (31). Recent reports have suggested that >50% of patients with ICI-related myocarditis may have normal left ventricular ejection fraction (32). Additionally, cardiac MRI was not sensitive in our cohort compared to other reports, although new studies show significantly lower sensitivity of cardiac MRI in ICI-related myocarditis (32,33). Therefore, while transthoracic echocardiography and cardiac MRI may assist in diagnosis, negative results cannot exclude myocarditis, and cardiac biopsy should be considered when myocarditis is suspected. Furthermore, in our study, patients may have had myocarditis diagnosed at an earlier stage given that they presented first with concurrent myositis; cardiac MRI has been demonstrated to have an even lower sensitivity if performed early in the presentation of ICI-related myocarditis (32).

Thirty-nine percent of patients developed MG. Important signs and symptoms that should raise suspicion for MG include ptosis, diplopia, visual changes, bulbar symptoms, and shortness of breath. Given the high prevalence of concomitant MG in ICI-myositis, we recommend AChR antibody testing and neurology consultation, with EMG as needed. While AChR antibodies are specific, reports have shown reduced sensitivity in ICI-related MG compared to idiopathic MG (18,34,35). If clinical suspicion of MG remains high despite a negative AChR antibody result, repeat testing should be considered (1 patient in our cohort tested positive after 6 days). Testing for other MG antibodies (muscle-specific kinase, lipoprotein receptor–related protein 4) can be considered; however, no cases have been reported in the literature. Repetitive nerve conduction studies and single-fiber EMG can also aid in diagnosis, but both can be abnormal in isolated myositis. The degree of symptoms and pathology (necrotic) can make diagnosis of accompanying MG a challenge in the absence of antibodies. Therefore, we believe these entities should be considered the same from a management standpoint, with aggressive treatment directed to those with respiratory or bulbar involvement.

Nearly half of the patients tested were positive for anti-striational antibodies in high titers, more commonly in those with concomitant MG. It is unclear whether these antibodies are pathogenic or the result of an immune response to exposed intracellular antigens (17,36). Studies on idiopathic MG show that anti-striational antibodies occur more frequently in severe disease, and changes in titer correlated with severity over the disease course in an individual patient (37). In our study, while patients had similar initial severity grades regardless of anti-striational antibody status, those who tested positive for the antibodies appeared to have more complications. Given the limited size of our cohort, we were unable to draw conclusions about the benefit of serial titer measurement. However, we recommend testing for anti-striational antibodies, as this can assist in diagnosis and may indicate concomitant MG and more severe disease (38). None of the patients had circulating antibodies against transcription intermediary factor 1γ or nuclear matrix protein 2, which have frequently been reported in paraneoplastic myositis (39), but not all patients were tested.

Nearly all patients were treated with glucocorticoids, consistent with current guidelines (40). Plasmapheresis and IVIG were the next most commonly used therapies, an approach also reported in smaller series (8,10). Given the lack of data, it is unclear whether therapies such as plasmapheresis and IVIG should be used initially or deferred until a response to initial glucocorticoids can be observed. In our study, approaches to the timing of treatment (early versus delayed) appeared to be independent of symptom grade and were mostly determined according to preference of the treating team. Our prior data on ICI-related MG suggest that patients may benefit from early IVIG or plasmapheresis, regardless of initial severity (18). Similarly, use of biologic agents in our cohort seemed largely dictated by physician preferences. While their efficacy and safety in idiopathic forms of myositis have been studied, evidence for their role in ICI-myositis is lacking, and a recent Dutch study showed a deleterious effect on survival for patients with melanoma who received tumor necrosis factor inhibitors to treat IRAEs (41–43).

Patients who developed ICI-myositis without overlap syndrome had favorable outcomes, including short hospitalizations with CK level normalization and symptom improvement or resolution over days to weeks. However, >50% of our patients developed overlapping MG and/or myocarditis, leading to extended

hospitalizations, respiratory failure, and death. Forty-two percent of patients with overlap syndrome died as a consequence of their IRAEs, compared to 0% of those with myositis alone. Respiratory failure was primarily attributed to neuromuscular dysfunction, often associated with pneumonia. The observed death rate was comparable to the findings in a recent pharmacovigilance study that showed a mortality rate of 52% in patients with ICI-myositis and concomitant myocarditis, compared to 15% in patients with myositis alone ($P < 0.001$) (44). The high mortality rate associated with myocarditis emphasizes the need for new treatment approaches. The predominance of T cells on endomyocardial biopsy specimens supports recent efforts to utilize T cell–targeted approaches in glucocorticoid-refractory myocarditis (45,46).

As infection frequently contributed to mortality in our patients, the risks of immunosuppression should be highlighted. A single-center study showed that in patients with IRAEs, use of glucocorticoids and infliximab was associated with serious infection (47). As patients with ICI-myositis are frequently treated with long courses of glucocorticoids, preventive measures such as *Pneumocystis jiroveci* prophylaxis should be considered (48).

Rechallenge with ICI in our study largely followed current guidelines (49). In patients with ICI-myositis alone, ICI treatment can reasonably be restarted after myositis resolution. However, guidelines suggest that patients with concurrent MG or a myocarditis grade of ≥2 should not be rechallenged with ICIs. One of the patients in the present study, who had severe overlap syndrome and experienced a flare after reexposure to ICI treatment, demonstrates the risk of rechallenge.

To our knowledge, this study includes the largest cohort of patients with ICI-myositis. As a single-center study, it was possible to obtain detailed information on disease presentation, course, and outcomes, which is often not possible with population- or pharmacy-based data sources. While this study provides key details on the current practices for ICI-myositis, which we believe are essential for practicing rheumatologists, it also has limitations. Our study was too small to draw conclusions on management or make additional recommendations regarding ICI rechallenge. Larger studies are needed to establish best practices, as our study shows that even in a single center, treatment is often guided by physician preferences.

In conclusion, this study shows that ICI-myositis alone can be successfully treated. However, in more than half of patients, overlapping MG and/or myocarditis results in significant morbidity and mortality. Concomitant use of multiple agents targeting B cells, T cells, and cytokines may be needed in severe cases, which could result in reduced duration of glucocorticoid treatment. As death was frequently attributed to infection, the risks and benefits of immunosuppression will need to be weighed. Future progress will require translational research to elucidate the underlying mechanisms of ICI-myositis. Large multicenter studies are needed to identify predictive biomarkers and determine optimal treatments that minimize risk of infection.

ACKNOWLEDGMENT

The authors would like to thank Yimin Geng at the Research Medical Library at MD Anderson Cancer Center for her assistance with the literature review.

AUTHOR CONTRIBUTIONS

All authors were involved in drafting the article or revising it critically for important intellectual content, and all authors approved the final version to be published. Dr. Aldrich had full access to all of the data in the study and takes responsibility for the integrity of the data and the accuracy of the data analysis.

Study conception and design. Aldrich, Pundole, Suarez-Almazor.
Acquisition of data. Aldrich.
Analysis and interpretation of data. Aldrich, Pundole, Tummala, Palaskas, Andersen, Shoukier, Abdel-Wahab, Deswal, Suarez-Almazor.

REFERENCES

1. Yervoy (ipilimumab). Prescribing information. Princeton (NJ): Bristol Myers Squibb; 2011. URL: https://packageinserts.bms.com/pi/pi_yervoy.pdf.
2. Keytruda (pembrolizumab). Prescribing information. Whitehouse Station (NJ): Merck Sharp & Dohme Corp; 2014. URL: https://www.merck.com/product/usa/pi_circulars/k/keytruda/keytruda_pi.pdf.
3. Opdivo (nivolumab). Prescribing information. Princeton (NJ): Bristol Myers Squibb; 2014. URL: https://packageinserts.bms.com/pi/pi_opdivo.pdf.
4. Wang Y, Zhou S, Yang F, Qi X, Wang X, Guan X, et al. Treatment-related adverse events of PD-1 and PD-L1 inhibitors in clinical trials: a systematic review and meta-analysis. JAMA Oncol 2019;5:1008–19.
5. Khoja L, Day D, Chen TW, Siu LL, Hansen AR. Tumour- and class-specific patterns of immune-related adverse events of immune checkpoint inhibitors: a systematic review. Ann Oncol 2017;28:2377–85.
6. Haslam A, Prasad V. Estimation of the percentage of US patients with cancer who are eligible for and respond to checkpoint inhibitor immunotherapy drugs. JAMA Network Open 2019;2:e192535.
7. Kimura T, Fukushima S, Miyashita A, Aoi J, Jinnin M, Kosaka T, et al. Myasthenic crisis and polymyositis induced by one dose of nivolumab. Cancer Science 2016;107:1055–8.
8. Liewluck T, Kao JC, Mauermann ML. PD-1 Inhibitor-associated myopathies: emerging immune-mediated myopathies. J Immunother 2018;41:208–11.
9. Kao JC, Liao B, Markovic SN, Klein CJ, Naddaf E, Staff NP, et al. Neurological complications associated with anti-programmed death 1 (PD-1) antibodies. JAMA Neurol 2017;74:1216–22.
10. Seki M, Uruha A, Ohnuki Y, Kamada S, Noda T, Onda A, et al. Inflammatory myopathy associated with PD-1 inhibitors. J Autoimmun 2019;100:105–13.
11. Fazel M, Jedlowski PM. Severe myositis, myocarditis, and myasthenia gravis with elevated anti-striated muscle antibody following single dose of ipilimumab-nivolumab therapy in a patient with metastatic melanoma. Case Reports Immunol 2019;2019:2539493.
12. Kang KH, Grubb W, Sawlani K, Gibson MK, Hoimes CJ, Rogers LR, et al. Immune checkpoint-mediated myositis and myasthenia gravis: a case report and review of evaluation and management. Am J Otolaryngol 2018;39:642–5.
13. Petitpain N, Garon J, Degiorgis M, Swiegot D, Ries F, Gillet P. Pembrolizumab induced fatal myositis and myocarditis. Fundamd Clin Pharmacol 2019;33 Suppl 1:68.
14. Lundberg IE, Tjärnlund A, Bottai M, Werth VP, Pilkington C, de Visser M, et al. 2017 European League Against Rheumatism/American College of Rheumatology classification criteria for adult and juvenile

idiopathic inflammatory myopathies and their major subgroups. Arthritis Rheumatol 2017;69:2271–82.

15. National Cancer Institute: National Institutes of Health. Common Terminology Criteria for Adverse Events (CTCAE). September 2017. URL: https://ctep.cancer.gov/protocoldevelopment/electronic_applications/ctc.htm.
16. Bonaca M, Olenchock B, Salem JE, Wiviott S, Ederhy S, Cohen A, et al. Myocarditis in the setting of cancer therapeutics: proposed case definitions for emerging clinical syndromes in cardio-oncology [review]. Circulation 2019;140:80–91.
17. Shah M, Tayar JH, Abdel-Wahab N, Suarez-Almazor ME. Myositis as an adverse event of immune checkpoint blockade for cancer therapy. Semin Arthritis Rheum 2019;48:736–40.
18. Safa H, Johnson DH, Trinh VA, Rodgers TE, Lin H, Suarez-Almazor ME, et al. Immune checkpoint inhibitor related myasthenia gravis: single center experience and systematic review of the literature. J Immunother Cancer 2019;7:319.
19. Johnson DB, Balko JM, Compton ML, Chalkias S, Gorham J, Xu Y, et al. Fulminant myocarditis with combination immune checkpoint blockade. N Engl J Med 2016;375:1749–55.
20. Hunter G, Voll C, Robinson CA. Autoimmune inflammatory myopathy after treatment with ipilimumab. Can J Neurol Sci 2009;36:518–20.
21. Ali SS, Goddard AL, Luke JJ, Donahue H, Todd DJ, Werchniak A, et al. Drug-associated dermatomyositis following ipilimumab therapy: a novel immune-mediated adverse event associated with cytotoxic T-lymphocyte antigen 4 blockade. JAMA Dermatol 2015;151:195–9.
22. Kanjanapan Y, Day D, Butler MO, Wang L, Joshua AM, Hogg D, et al. Delayed immune-related adverse events in assessment for dose-limiting toxicity in early phase immunotherapy trials. Eur J Cancer 2019;107:1–7.
23. Martins F, Sofiya L, Sykiotis GP, Lamine F, Maillard M, Fraga M, et al. Adverse effects of immune-checkpoint inhibitors: epidemiology, management and surveillance [review]. Nat Rev Clin Oncol 2019; 16:563–80.
24. Touat M, Maisonobe T, Knauss S, Salem OB, Hervier B, Auré K, et al. Immune checkpoint inhibitor-related myositis and myocarditis in patients with cancer. Neurology 2018;91:e985–94.
25. Kao JC, Brickshawana A, Liewluck T. Neuromuscular complications of programmed cell death-1 (PD-1) inhibitors [review]. Curr Neurol Neurosci Rep 2018;18:63.
26. Dalakas MC. Polymyositis, dermatomyositis and inclusion-body myositis. N Engl J Med 1991;325:1487–98.
27. Moreira A, Loquai C, Pföhler C, Kähler KC, Knauss S, Heppt MV, et al. Myositis and neuromuscular side-effects induced by immune checkpoint inhibitors. Eur J Cancer 2019;106:12–23.
28. Nozaki K, Pestronk A. High aldolase with normal creatine kinase in serum predicts a myopathy with perimysial pathology. J Neurol Neurosurg Psychiatry 2009;80:904–8.
29. Casciola-Rosen L, Hall JC, Mammen AL, Christopher-Stine L, Rosen A. Isolated elevation of aldolase in the serum of myositis patients: a potential biomarker of damaged early regenerating muscle cells. Clin Exp Rheumatol 2012;30:548–53.
30. Erlacher P, Lercher A, Falkensammer J, Nassonov EL, Samsonov MI, Shtutman VZ, et al. Cardiac troponin and β-type myosin heavy chain concentrations in patients with polymyositis or dermatomyositis. Clin Chim Acta 2001;306:27–33.
31. Mahmood SS, Fradley MG, Cohen JV, Nohria A, Reynolds KL, Heinzerling LM, et al. Myocarditis in patients treated with immune checkpoint inhibitors. J Am Coll Cardiol 2018;71:1755–64.
32. Zhang L, Awadalla M, Mahmood SS, Nohria A, Hassan MZ, Thuny F, et al. Cardiovascular magnetic resonance in immune checkpoint inhibitor-associated myocarditis. Eur Heart J 2020;41:1733–43.
33. Zhang L, Awadalla M, Mahmood SS, Groarke JD, Nohria A, Liu S, et al. Late gadolinium enhancement in patients with myocarditis from immune checkpoint inhibitors. J Am Coll Cardiol 2019;73 Suppl 1:675.
34. Vincent A, Newsom-Davis J. Acetylcholine receptor antibody as a diagnostic test for myasthenia gravis: results in 153 validated cases and 2967 diagnostic assays. J Neurol Neurosurg Psychiatry 1985;48:1246–52.
35. Chan KH, Lachance DH, Harper CM, Lennon VA. Frequency of seronegativity in adult-acquired generalized myasthenia gravis. Muscle Nerve 2007;36:651–8.
36. Bilen MA, Subudhi SK, Gao J, Tannir NM, Tu SM, Sharma P. Acute rhabdomyolysis with severe polymyositis following ipilimumab-nivolumab treatment in a cancer patient with elevated anti-striated muscle antibody. J Immunother Cancer 2016;4:36.
37. Romi F, Skeie GO, Aarli JA, Gilhus NE. The severity of myasthenia gravis correlates with the serum concentration of titin and ryanodine receptor antibodies. Arch Neurol 2000;57:1596–600.
38. Kufukihara K, Watanabe Y, Inagaki T, Takamatsu K, Nakane S, Nakahara J, et al. Cytometric cell-based assays for anti-striational antibodies in myasthenia gravis with myositis and/or myocarditis. Sci Rep 2019;9:5284.
39. Fiorentino DF, Chung LS, Christopher-Stine L, Zaba L, Li S, Mammen AL, et al. Most patients with cancer-associated dermatomyositis have antibodies to nuclear matrix protein NXP-2 or transcription intermediary factor 1γ. Arthritis Rheum 2013;65:2954–62.
40. Brahmer JR, Lacchetti C, Schneider BJ, Atkins MB, Brassil KJ, Caterino JM, et al. Management of immune-related adverse events in patients treated with immune checkpoint inhibitor therapy: American Society of Clinical Oncology clinical practice guideline. J Clin Oncol 2018;36:1714–68.
41. Oddis CV, Reed AM, Aggarwal R, Rider LG, Ascherman DP, Levesque MC, et al. Rituximab in the treatment of refractory adult and juvenile dermatomyositis and adult polymyositis: a randomized, placebo-phase trial. Arthritis Rheum 2013;65:314–24.
42. De Souza FH, Miossi R, de Moraes JC, Bonfá E, Shinjo SK. Favorable rituximab response in patients with refractory idiopathic inflammatory myopathies. Adv Rheumatol 2018;58:31.
43. Verheijden RJ, May AM, Blank CU, Aarts MJ, van den Berkmortel FW, van den Eertwegh AJ, et al. Association of anti-TNF with decreased survival in steroid refractory ipilimumab and anti-PD1 treated patients in the Dutch Melanoma Treatment Registry. Clin Cancer Res 2020;26:2268–74.
44. Anquetil BC, Salem LJ, Lebrun-Vignes JB, Johnson JD, Mammen JA, Stenzel JW, et al. Immune checkpoint inhibitor–associated myositis: expanding the spectrum of cardiac complications of the immunotherapy revolution [letter]. Circulation 2018;138:743–5.
45. Esfahani K, Buhlaiga N, Thébault P, Lapointe R, Johnson NA, Miller WH Jr. Alemtuzumab for immune-related myocarditis due to PD-1 therapy. N Engl J Med 2019;380:2375–6.
46. Salem JE, Allenbach Y, Vozy A, Brechot N, Johnson DB, Moslehi JJ, et al. Abatacept for severe immune checkpoint inhibitor-associated myocarditis [letter]. N Engl J Med 2019;380:2377–9.
47. Del Castillo M, Romero FA, Arguello E, Kyi C, Postow MA, Redelman-Sidi G. The spectrum of serious infections among patients receiving immune checkpoint blockade for the treatment of melanoma. Clin Infect Dis 2016;63:1490–3.
48. Cooley L, Dendle C, Wolf J, Teh BW, Chen SC, Boutlis C, et al. Consensus guidelines for diagnosis, prophylaxis and management of Pneumocystis jirovecii pneumonia in patients with haematological and solid malignancies, 2014 [review]. Intern Med J 2014;44:1350–63.
49. Thompson JA, Schneider BJ, Brahmer J, Andrews S, Armand P, Bhatia S, et al. Management of immunotherapy-related toxicities 1.2019. J Natl Comp Canc Netw 2019;17:255–89.

Arthritis & Rheumatology
Vol. 73, No. 5, May 2021, pp 875–884
DOI 10.1002/art.41605

American College of Rheumatology
Empowering Rheumatology Professionals

Synovial Fluid Neutrophils From Patients With Juvenile Idiopathic Arthritis Display a Hyperactivated Phenotype

Mieke Metzemaekers,[1] Bert Malengier-Devlies,[1] Karen Yu,[1] Sofie Vandendriessche,[1] Jonas Yserbyt,[2] Patrick Matthys,[1] Lien De Somer,[3] Carine Wouters,[3] and Paul Proost[1]

Objective. Juvenile idiopathic arthritis (JIA) is the most common rheumatic disease in childhood. The predominant subtypes, oligoarticular and polyarticular JIA, are traditionally considered to be autoimmune diseases with a central role for T cells and autoantibodies. Mounting evidence suggests an important role for neutrophils in JIA pathogenesis. We undertook this study to investigate the phenotypic features of neutrophils present in the blood and inflamed joints of patients.

Methods. JIA synovial fluid (SF) and parallel blood samples from JIA patients and healthy children were collected. SF-treated neutrophils from healthy donors and pleural neutrophils from patients with pleural effusion were investigated as controls for SF exposure and extravasation. Multicolor flow cytometry panels allowed for in-depth phenotypic analysis of neutrophils, focusing on the expression of adhesion molecules, activation, and maturation markers and chemoattractant receptors. Multiplex technology was used to quantify cytokines in plasma and SF.

Results. SF neutrophils displayed an activated, hypersegmented phenotype with decreased CD62L expression, up-regulation of adhesion molecules CD66b, CD11b, and CD15, and down-regulation of CXCR1/2. An elevated percentage of CXCR4-positive neutrophils was detected in SF from patients. Pleural neutrophils showed less pronounced maturation differences. Strikingly, significant percentages of SF neutrophils showed a profound up-regulation of atypical neutrophil markers, including CXCR3, intercellular adhesion molecule 1, and HLA–DR.

Conclusion. Our data show that neutrophils in inflamed joints of JIA patients have an activated phenotype. This detailed molecular analysis supports the notion that a complex intertwining between these innate immune cells and adaptive immune events drives JIA.

INTRODUCTION

Juvenile idiopathic arthritis (JIA) is the most common rheumatic disease in childhood and an important cause of disability when patients are not treated appropriately (1). By definition, JIA clinically presents with peripheral joint inflammation of unknown origin, persisting for ≥6 weeks and starting before 16 years of age. The disease is categorized into distinct subclasses, with oligoarticular and polyarticular JIA being most prevalent. Apart from the number of inflamed joints during the first 6 months of disease, some mechanistic and immunologic overlap exists between these two JIA subtypes. Consistently, there is growing consensus that oligoarticular JIA and, in particular, rheumatoid factor–negative polyarticular JIA may represent a continuum of a single disease entity rather than distinct diseases.

Oligoarticular and polyarticular JIA are traditionally considered to be multifactorial autoimmune diseases that may start when a rather innocuous environmental trigger evokes an autoreactive insult in genetically predisposed individuals (2,3). The strong association with HLA variants and profound accumulation of Th1 cells in affected joints underscore the pivotal role of adaptive immunity in these JIA subtypes (1,4). Nevertheless, the full spectrum

Supported by FWO Vlaanderen (grant G.0808.18N), Katholieke University Leuven (C1 grant C16/17/010), the Rega Foundation, and the European Union Horizon 2020 program (grant 779295). Ms Metzemaekers's work was supported by a L'Oréal-UNESCO for Women in Science PhD Fellowship and by FWO Vlaanderen. Ms Vandendriessche's work was supported by FWO Vlaanderen Strategic Basic Research PhD Fellowship.

[1]Mieke Metzemaekers, MSc, Bert Malengier-Devlies, MSc, Karen Yu, MSc, Sofie Vandendriessche, MSc, Patrick Matthys, MSc, PhD, Paul Proost, MSc, PhD: Katholieke University Leuven, Leuven, Belgium; [2]Jonas Yserbyt, MD, PhD: University Hospitals Leuven, Leuven, Belgium; [3]Lien De Somer, MD, PhD, Carine Wouters, MD, PhD: European Reference Network for Rare Immunodeficiency, Autoinflammatory and Autoimmune Diseases (RITA), University Hospitals Leuven, and Katholieke University Leuven, Leuven, Belgium.

Drs. De Somer, Wouters, and Proost contributed equally to this work.

Dr. Wouters has received unrestricted grants paid to Katholieke University Leuven from Novartis, Roche, GlaxoSmithKline, and Pfizer. No other disclosures relevant to this article were reported.

Address correspondence to Paul Proost, MSc, PhD, Molecular Immunology Lab, Rega Institute, Katholieke University Leuven, Herestraat 49, Box 1042, Leuven, Belgium. Email: paul.proost@kuleuven.be.

Submitted for publication April 24, 2020; accepted in revised form November 24, 2020.

of immunopathologic manifestations observed in patients most likely involves both innate and adaptive immunity (4,5). Previous research efforts have shown that peripheral blood neutrophils from JIA patients display transcriptional abnormalities and remain in an activated state even during remission, suggesting a role for neutrophils in JIA pathophysiology (6–8). This hypothesis is further supported by the presence of S100A12 in the serum and synovial fluid (SF) of patients (9).

Neutrophils are armed with oxidative and nonoxidative defense mechanisms, including the capacity to release reactive oxygen species (ROS) and the ability to engulf and destroy foreign material (phagocytosis) (10). These innate leukocytes were initially considered simple and mere servile phagocytes, acting as nonspecific pathogen exterminators only. With the appearance of sophisticated technologies, a more refined model of neutrophil function has evolved. Mounting evidence suggests that neutrophils display phenotypic and functional heterogeneity and may contribute to the initiation, modulation, and resolution of inflammation, either directly or indirectly, via instructing innate as well as adaptive immune cells (11–18). Moreover, strongly activated neutrophils may eventually acquire the capacity to present antigens (19,20). The precise phenotypic features of neutrophils from JIA patients, in particular those present in the SF of inflamed joints, are currently unknown. We therefore aimed to extensively characterize the circulating and synovial neutrophils from oligoarticular and polyarticular JIA patients.

PATIENTS AND METHODS

Patients. Twenty-three JIA patients with a median age of 11 years (range 4–17) and a female:male ratio of 15:8 were recruited at the University Hospital Leuven. SF was collected only when joint aspiration was required for treatment. Blood and SF samples were collected in BD Vacutainer tubes treated with EDTA (BD Biosciences) and processed within 30 minutes of withdrawal. Pleural fluids were collected from 5 patients who required local aspiration, with a median age of 68 years (range 41–81) and a female:male ratio of 2:3, and were studied as controls for neutrophil extravasation. In addition, blood samples were collected from 12 healthy children (median age 10 years [range 4–18], female:male ratio 7:5) and 18 adult volunteers (median age 28 years [range 24–64], female:male ratio 12:6). Informed consent was obtained according to the ethical guidelines of the Declaration of Helsinki. Parents or legal guardians signed the informed consent on behalf of patients who were legal minors. The Ethics Committee of the University Hospital Leuven approved this study (S59874). For detailed patient characteristics, please refer to Supplementary Table 1 (available on the *Arthritis & Rheumatology* website at http://onlinelibrary.wiley.com/doi/10.1002/art.41605/abstract). Due to the limited volumes of samples available from pediatric individuals, we were unable to use all samples for each set of experiments, and thus the numbers of patients and controls analyzed differ for some experiments.

Cells and flow cytometry. An EasySep Direct Human Neutrophil Isolation Kit (Stemcell Technologies) was used for removal of erythrocytes from blood samples. Cells were treated with FcR block (Miltenyi Biotec) and Fixable Viability Stain 620 (BD Biosciences) or Zombie Aqua 516 (Biolegend), followed by extracellular staining. Antibodies used in this study were titrated in-house and are listed in Supplementary Table 2 (http://onlinelibrary.wiley.com/doi/10.1002/art.41605/abstract). For intracellular staining of Toll-like receptor 9 (TLR-9), cells were fixed and permeabilized using a Cytofix/Cytoperm kit (BD Biosciences), followed by staining with anti-human TLR-9. Results were analyzed using a BD LSRFortessa X-20 (BD Biosciences) equipped with 5 lasers. For downstream analysis with FlowJo software, neutrophils were gated as CD16+CD66b+ cells within the population of living cells that occurred as singlets only.

Cytokine measurements. Plasma and SF concentrations of interleukin-1β (IL-1β), IL-6, IL-10, IL-12/IL-23 p40 subunit, IL-17A, IL-1 receptor antagonist (IL-1Ra), tumor necrosis factor (TNF), interferon-γ (IFNγ), granulocyte colony-stimulating factor (G-CSF), granulocyte–macrophage colony-stimulating factor (GM-CSF), macrophage colony-stimulating factor (M-CSF), and chemokine CXCL8 were determined using customized Meso Scale Discovery multiplex technology. Detection limits of cytokine assays are shown in Supplementary Table 3 (http://onlinelibrary.wiley.com/doi/10.1002/art.41605/abstract).

Ex vivo stimulation of neutrophils. Freshly isolated peripheral blood neutrophils from adult healthy donors were exposed to cell-free plasma from the original donor or cell-free JIA SF, with or without 2 μg/ml anti-TNF (etanercept; Pfizer), 2 μg/ml anti–IL-1β (anakinra; Sobi), or 2 μg/ml anti–IL-6 (tocilizumab; Roche). Alternatively, cells were diluted in RPMI 1640 medium supplemented with 10% (volume/volume) fetal calf serum (both from Gibco) and 5 ng/ml GM-CSF, in the presence or absence of 10 ng/ml TNF, 10 ng/ml IL-1β, or 10 ng/ml IL-6 (all from PeproTech), with or without 2 μg/ml of the corresponding cytokine inhibitor. Cells were seeded in a 48-well plate at a final concentration of 2×10^6 cells/ml (total volume of 500 μl per well) and placed at 37°C with 5% CO_2 for 3–24 hours. Subsequently, cells were used for extensive phenotypic characterization by flow cytometry. Information on neutrophil survival under different culturing conditions is included in Supplementary Figures 1 and 2 (http://onlinelibrary.wiley.com/doi/10.1002/art.41605/abstract).

Statistical analysis. Kruskal-Wallis test with Dunn's multiple comparisons were performed to detect significant differences between the study groups. *P* values of 0.05 or less were considered significant.

Table 1. Cytokine levels in plasma and SF from patients with JIA compared to plasma from healthy controls*

Cytokine/chemokine	Control plasma (n = 10)	JIA plasma (n = 16)	JIA SF (n = 21)
IL-1β	<1	<1 (<1–46.5)	7.7 (<1–52.2)†
IL-6	0.7 (<0.5–4.1)	1.4 (<0.5–17.8)	1,602 (53.8–7,329)‡
IL-12/IL-23p40	262.8 (172.3–483.1)§	285.5 (134.1–570.2)¶	1,387 (97.3–2,156)#**
IFNγ	18.2 (<9–105.0)	10.8 (<9–74.5)	137.1 (<9–490.6)††
TNF	2.8 (<1–4.0)	2.1 (<1–4.1)	10.5 (1.5–22.8)††
IL-17A	<4 (<4–4.7)§	<4 (<4–14.1)¶	9.3 (<4–69.1)#
IL-10	<1 (<1–3.9)	<1 (<1–1.1)	6.9 (<1–22.3)‡‡
IL-1Ra	278.0 (107.9–941.5)	160.7 (79.5–273.5)	3,590.0 (398.5–11,683)†
CXCL8	3.2 (2.0–11.5)	3.3 (1.4–9.3)	747.2 (117.6–4,986)‡
GM-CSF	13.9 (9.3–17.2)§	12.2 (6.7–16.2)¶	36.4 (14.5–110.9)#**
M-CSF	<0.5§	<0.5¶	1.2 (<0.5–3.5)#§§
G-CSF	10.3 (7.3–75.8)§	8.4 (4.2–17.8)¶	8.8 (1.7–25.8)#

* Results are represented as the median (range) pg/ml. Multiplex technology was used to measure cytokine concentrations in plasma samples from healthy controls, plasma samples from juvenile idiopathic arthritis (JIA) patients, and synovial fluid (SF) from JIA patients. Comparisons were made using Kruskal-Wallis test with Dunn's test for multiple comparisons. IL-1β = interleukin-1β; IFNγ = interferon-γ; TNF = tumor necrosis factor; IL-1Ra = IL-1 receptor antagonist; GM-CSF = granulocyte–macrophage colony-stimulating factor; M-CSF = macrophage colony-stimulating factor; G-CSF = granulocyte colony-stimulating factor.
† $P \leq 0.001$ versus controls; $P \leq 0.0001$ versus JIA plasma.
‡ $P \leq 0.0001$ versus controls; $P \leq 0.0001$ versus JIA plasma.
§ Data were available for 5 healthy controls.
¶ Data were available for 8 patients.
# Data were available for 13 patients.
** $P \leq 0.05$ versus controls; $P \leq 0.01$ versus JIA plasma.
†† $P \leq 0.05$ versus controls; $P \leq 0.0001$ versus JIA plasma.
‡‡ $P \leq 0.01$ versus controls; $P \leq 0.0001$ versus JIA plasma.
§§ $P \leq 0.05$ versus controls; $P \leq 0.05$ versus JIA plasma.

RESULTS

Elevated cytokine levels in SF from JIA patients. To explore the inflammatory environment, cytokine measurements were assessed in SF samples from the affected joints and circulation of JIA patients. Circulating cytokine values from healthy children were used for comparative purposes. JIA SF contained significantly elevated concentrations of the proinflammatory cytokines IL-1β, IL-6, IL-12/IL-23p40, IFNγ, and TNF, compared to plasma samples from either JIA patients or controls (Table 1). In addition, some JIA patients displayed a tendency toward enhanced synovial levels of IL-17A, but no significant differences were detected. Concentrations of the antiinflammatory cytokines IL-10 and IL-1Ra were significantly increased in JIA SF compared to plasma concentrations from JIA patients or healthy children. Interestingly, the most powerful neutrophil-attracting chemokine in humans, CXCL8, was abundantly present in JIA SF but not in the plasma samples from patients and controls. Quantification of M-CSF and GM-CSF revealed that the concentration of these myelopoietic cytokines was significantly higher in SF compared to plasma samples from JIA patients or controls. No significant alterations in G-CSF concentrations were detected.

Hypersegmented phenotype displayed in JIA SF neutrophils. Neutrophil maturation can be assessed based on the intensity of CD16 (Fcγ receptor III) and CD62L (L-selectin) expression (21,22). The following 3 distinct neutrophil subsets were described: $CD16^{med}CD62L^{high}$ immature neutrophils with a banded nucleus; $CD16^{high}CD62L^{high}$ mature neutrophils containing 3 or accidentally 4 nuclear lobes; and $CD62L^{low}$ hypersegmented cells with a larger number, on average, of nuclear lobes. As expected, the majority of circulating neutrophils isolated from the peripheral blood of patients and healthy donors were $CD16^{high}$-$CD62L^{high}$ mature cells (Figure 1A and Supplementary Figure 3A, http://onlinelibrary.wiley.com/doi/10.1002/art.41605/abstract). In contrast, most neutrophils in JIA SF displayed a hypersegmented character, as evidenced by a significantly enhanced percentage of $CD62L^{low}$ cells (Figure 1B and Supplementary Figure 3A). Notably, patients with polyarticular disease tended to contain an increased percentage of $CD62L^{low}$ cells in the circulation as well. An increased percentage of $CD62L^{low}$ neutrophils was also detected in pleural fluids from patients with pleural effusion (Figure 1B). However, in contrast to synovial neutrophils, the vast majority of pleural neutrophils retained a $CD16^{high}CD62L^{high}$ phenotype (Figure 1A). $CD16^{med}CD62L^{high}$ immature neutrophils represented only a minor percentage of the total neutrophil population in blood, synovial, and pleural fluids (Figure 1C and Supplementary Figure 3A).

Analysis of cytospin preparations confirmed the presence of hypersegmented neutrophils and the absence of immature cells in SF (Supplementary Figure 3B, http://onlinelibrary.wiley.com/doi/10.1002/art.41605/abstract). JIA SF and, to a lesser extent, pleural fluids (but not blood samples from JIA patients or controls) contained a significant population of CXCR4-expressing

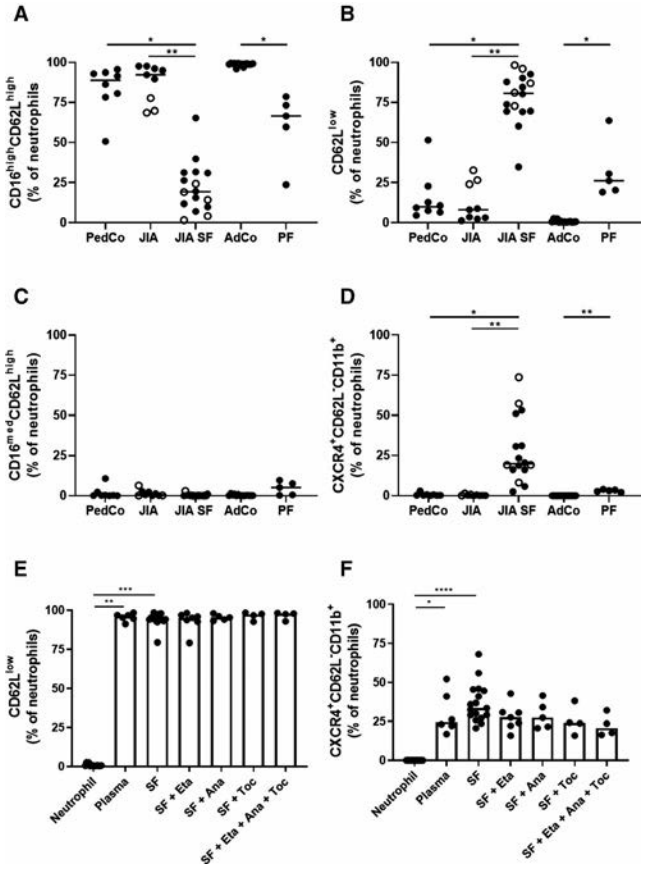

Figure 1. Analysis of neutrophil maturation and segmentation. **A–D**, Maturation characteristics of blood neutrophils from pediatric controls (PedCo), blood neutrophils from juvenile idiopathic arthritis (JIA) patients, and synovial fluid (SF) neutrophils from JIA patients were assessed based on CD16 and CD62L expression, using flow cytometry. Pleural fluid neutrophils (PF) from patients with pleural effusion and blood neutrophils from healthy adults (AdCo) were investigated for comparative purposes. Relative percentages of $CD16^{high}CD62L^{high}$ (**A**), $CD62L^{low}$ (**B**), and $CD16^{med}CD62L^{high}$ (**C**) neutrophils were determined, and relative percentages of CXCR4-positive aged neutrophils (**D**) are shown. Horizontal lines show the median. **E** and **F**, Blood neutrophils from healthy donors were exposed to cell-free plasma from the corresponding donor or patient SF, with or without 2 μg/ml anti–tumor necrosis factor (etanercept; Eta), anti–interleukin-1β (anakinra; Ana), or anti–interleukin-6 (tocilizumab; Toc) for 24 hours, and the presence of $CD62L^{low}$ (**E**) and CXCR4+ (**F**) neutrophils was determined. Bars show the median. Patients with oligoarticular or polyarticular JIA are represented by closed or open circles, respectively. * = $P \leq 0.05$; ** = $P \leq 0.01$; *** = $P \leq 0.001$; **** = $P \leq 0.0001$, by Kruskal-Wallis test with Dunn's test for multiple comparisons.

$CD11b^{high}CD62L^{low}$ neutrophils (Figure 1D). This phenotype has been associated with neutrophil aging (23). The observed shift toward the CXCR4+$CD62L^{low}$ phenotype could be mimicked by exposing healthy donor neutrophils to either plasma from the corresponding donor or JIA SF for 24 hours, and was not neutralized by inhibitors of TNF, IL-1β, or IL-6 (Figures 1E and F). Ex vivo stimulation of healthy neutrophils with SF for 3 or 6 hours did not induce a similar phenotypic shift (Supplementary Figures 2B and C, http://onlinelibrary.wiley.com/doi/10.1002/art.41605/abstract). Cultured neutrophils progressively reduced their CD16 expression to levels detected on immature cells, as previously described (22) (Supplementary Figure 3C).

Altered expression of adhesion and major histocompatibility complex (MHC) class II molecules on JIA SF neutrophils. CD66b (carcinoembryonic antigen–related cell adhesion molecule 8) was significantly up-regulated on JIA SF neutrophils (Figure 2A). CD62L shedding and up-regulation of CD66b are hallmark features of neutrophil activation. Pleural neutrophils from patients with pleural effusion also displayed a tendency toward increased expression of CD66b (Figure 2A). No up-regulation of CD66b was detected when healthy donor neutrophils were cultured in plasma from the same donor or in JIA SF for 24 hours (Supplementary Figures 2D and 4A, http://onlinelibrary.wiley.com/doi/10.1002/art.41605/abstract). The fact that CD66b was up-regulated on synovial and pleural neutrophils, but not on SF-treated healthy donor neutrophils, may indicate that the observed phenotypic alteration is related to extravasation (24). In addition to the activated phenotype, a notable percentage of JIA SF neutrophils expressed the MHC class II surface receptor HLA–DR, suggesting that these cells acquired the capacity to behave as professional antigen-presenting cells (Figure 2B). Pleural neutrophils also displayed up-regulation of HLA–DR but data did not reach statistical significance (Figure 2B). No significant up-regulation of HLA–DR expression was observed on healthy donor neutrophils 24 hours after subcultivation in plasma or JIA SF, suggesting that neither aging nor exposure to a cell-free inflamed environment alone is sufficient to induce up-regulation of HLA–DR expression (Supplementary Figures 2E and 4B, http://onlinelibrary.wiley.com/doi/10.1002/art.41605/abstract).

The presence of surface adhesion molecules on neutrophils is essential for their interaction with endothelial cells and subsequent extravasation into inflamed tissues. Quiescent neutrophils express CD11b (α_M integrin) and CD15 (sialyl-$Lewis^x$), which can be up-regulated upon activation by means of degranulation (25). As expected, CD11b and CD15 were abundantly present on neutrophils in blood samples from patients and controls (Figures 2C and D). Compared to circulating neutrophils from patients, the expression levels of these 2 major adhesion molecules were significantly increased on JIA SF neutrophils. In contrast, no significant alterations in CD11b and CD15 expression were detected on pleural neutrophils (Figures 2C and D). Healthy donor neutrophils stimulated with SF from JIA patients for 24 hours showed significantly lower surface levels of CD11b and CD15 (Supplementary Figures 4C and D, http://onlinelibrary.wiley.com/doi/10.1002/art.41605/abstract). However, a tendency toward enhanced CD11b and CD15 expression was detected when cells were treated with SF for 3 hours, but data did not reach statistical significance (Supplementary Figures 2F and G).

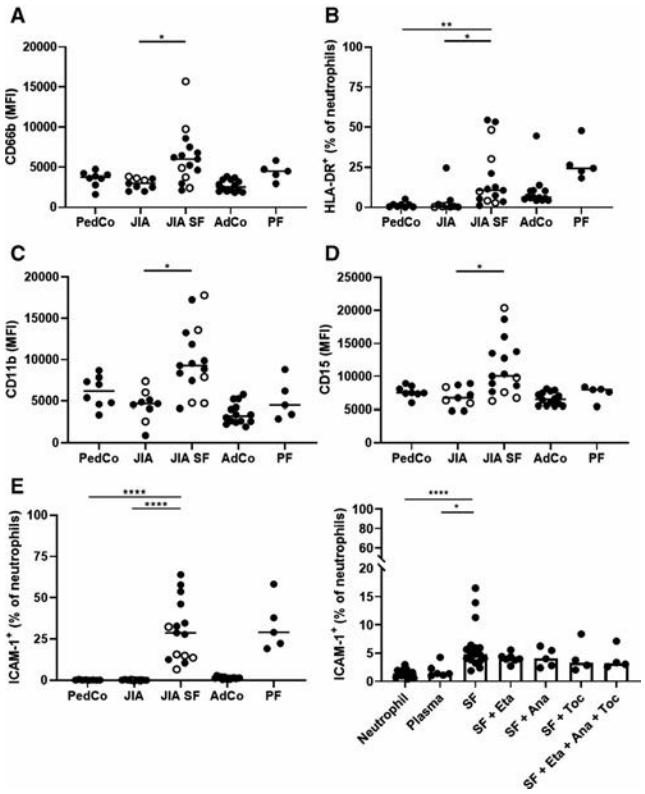

Figure 2. Analysis of adhesion molecule and HLA–DR expression. Expression of CD66b (**A**), HLA–DR (**B**), CD11b (**C**), CD15 (**D**), and intercellular adhesion molecule 1 (ICAM-1) (**E**; left) on neutrophils in blood from healthy pediatric controls, blood from JIA patients, and SF from JIA patients was determined by flow cytometry. Pleural neutrophils from patients with pleural effusion and blood neutrophils from healthy adults were investigated for comparative purposes. Fresh peripheral blood neutrophils from healthy donors were exposed to cell-free plasma from the corresponding donor or cell-free SF from JIA patients, with or without 2 μg/ml anti–tumor necrosis factor (etanercept), anti–interleukin-1β (anakinra), or anti–interleukin-6 (tocilizumab) for 24 hours, followed by analysis of ICAM-1 expression (**E**; right). Results show percentages of positive neutrophils or mean fluorescence intensity (MFI). Patients with oligoarticular or polyarticular disease are represented by closed or open circles, respectively. Horizontal lines and bars show the median. * = $P \leq 0.05$; ** = $P \leq 0.01$; **** = $P \leq 0.0001$, by Kruskal-Wallis test with Dunn's test for multiple comparisons. See Figure 1 for other definitions.

The α integrin subunit CD49d, which may play a role in neutrophil recruitment during inflammation (26), was absent from most circulating neutrophils, and a non-significantly enhanced percentage of CD49d-expressing neutrophils was present in synovial and pleural fluids (Supplementary Figure 4E, http://onlinelibrary.wiley.com/doi/10.1002/art.41605/abstract). Of note, incubation of healthy donor neutrophils with SF from JIA patients (but not with plasma from the original donor) for 24 hours provoked a significant up-regulation of CD49d, suggesting that up-regulation of CD49d occurs in response to inflammation (Supplementary Figures 2H and 4E). The increased CD49d expression was reduced with anti-TNF and disappeared upon treatment with anti-IL-1β or anti-IL-6 (Supplementary Figure 4E).

As expected, circulating neutrophils from patients and controls did not express intercellular adhesion molecule-1 (ICAM-1) (Figure 2E). However, a significant portion of JIA SF neutrophils were ICAM-1–positive. It has previously been demonstrated that up-regulation of ICAM-1 boosts neutrophil effector functions (27). A tendency for an increased percentage of ICAM-1–expressing neutrophils was found in pleural fluids. Strikingly, incubation of healthy donor neutrophils with JIA SF, but not with plasma, for 24 hours resulted in profound up-regulation of ICAM-1, independently of the presence of TNF, IL-1β, or IL-6 inhibitors (Figure 2E and Supplementary Figure 2I, http://onlinelibrary.wiley.com/doi/10.1002/art.41605/abstract).

Altered chemoattractant and TLR expression profile on JIA SF neutrophils. Analysis of CXCR1 and CXCR2 expression, both high-affinity receptors for CXCL8, revealed a significantly reduced expression level of CXCR1 and a trend toward down-regulation of CXCR2 on synovial neutrophils from JIA patients, but not on pleural neutrophils from patients with pleural effusion (Figures 3A and B). A trend toward decreased expression of both receptors was observed when comparing peripheral blood neutrophils from JIA patients to those from controls. Analysis of healthy donor neutrophils following ex vivo culturing in plasma from the same donor revealed spontaneous down-regulation of CXCR1 and CXCR2 after 24 hours, suggesting that the observed down-regulation of the 2 receptors on synovial neutrophils is related to aging (Figures 3A and B and Supplementary Figures 2J and K, http://onlinelibrary.wiley.com/doi/10.1002/art.41605/abstract). According to staining, a small but significant percentage of JIA SF neutrophils were positive for CXCR3 (Figure 3C). CXCR3 is not typically expressed by neutrophils but may be up-regulated during severe inflammation. A trend toward increased levels of CXCR3-positive neutrophils was observed in pleural fluids, but no significant differences were detected. Interestingly, up-regulation of CXCR3 on healthy donor neutrophils was found when cells were exposed to SF from JIA patients for 24 hours (Figure 3C and Supplementary Figure 2L).

Compared to blood neutrophils from healthy children, complement receptor C5aR was significantly less abundant on SF neutrophils from JIA patients (Figure 4A). Blood neutrophils from JIA patients displayed a trend toward down-regulation of C5aR. Since C5aR is internalized rapidly upon exposure to high ligand concentrations, down-regulation of the receptor at the protein level may indicate neutrophil activation. No alterations in C5aR expression were observed on pleural neutrophils. JIA SF neutrophils exhibited higher levels of formyl peptide receptor (FPR-1) compared to blood neutrophils from healthy children (Figure 4B). Moreover, FPR-1 expression on pleural neutrophils was significantly increased compared to blood neutrophils from healthy adults. Up-regulation of FPR-1, but not down-regulation of C5aR, was mimicked when

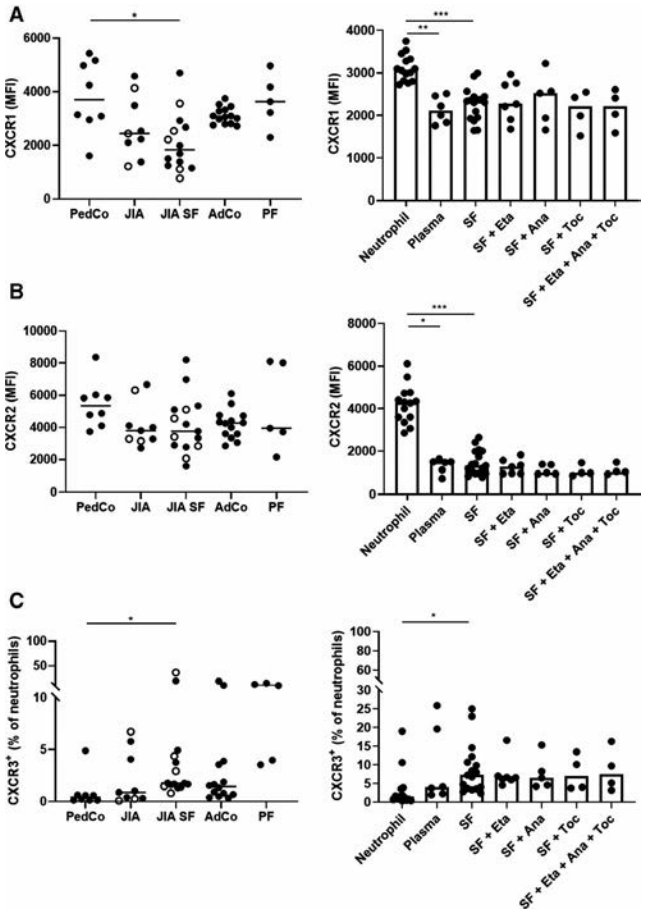

Figure 3. Analysis of CXCR1, CXCR2, and CXCR3 expression. Expression of CXCR1 (**A**; left), CXCR2 (**B**; left), and CXCR3 (**C**; left) on neutrophils in blood from healthy pediatric controls, blood from JIA patients, and SF from JIA patients was determined by flow cytometry. Pleural neutrophils from patients with pleural effusion and blood neutrophils from healthy adults were investigated for comparative purposes. Fresh peripheral blood neutrophils from healthy donors were exposed to cell-free plasma from the corresponding donor or cell-free SF from JIA patients, with or without 2 μg/ml anti–tumor necrosis factor (etanercept), anti–interleukin-1β (anakinra), or anti–interleukin-6 (tocilizumab) for 24 hours, followed by analysis of expression of CXCR1 (**A**; right), CXCR2 (**B**; right), and CXCR3 (**C**; right). Results show percentages of positive neutrophils or mean fluorescence intensity (MFI). Patients with oligoarticular or polyarticular disease are represented by closed or open circles, respectively. Horizontal lines and bars show the median. * = $P \leq 0.05$; ** = $P \leq 0.01$; *** = $P \leq 0.001$, by Kruskal-Wallis test with Dunn's test for multiple comparisons. See Figure 1 for other definitions.

healthy donor neutrophils were cultured in SF from JIA patients for 24 hours (Figures 4A and B and Supplementary Figures 2M and N, http://onlinelibrary.wiley.com/doi/10.1002/art.41605/abstract).

Leukotriene B_4 receptor (BLT-1) was significantly up-regulated on JIA SF neutrophils, but not on SF-treated healthy donor cells, compared to blood neutrophils from JIA patients (Figure 4C and Supplementary Figure 2O). Pleural neutrophils also displayed significantly elevated BLT-1 expression. JIA SF neutrophils showed a moderate but significant up-regulation of TLR-2 (Supplementary Figure 5A, http://onlinelibrary.wiley.com/doi/10.1002/art.41605/abstract). A trend toward increased TLR-4 and TLR-6 expression was observed on SF and blood neutrophils from JIA patients, but no significant differences were detected (Supplementary Figures 5B and C). The expression level of TLR-9 was similar across all study groups (Supplementary Figure 5D).

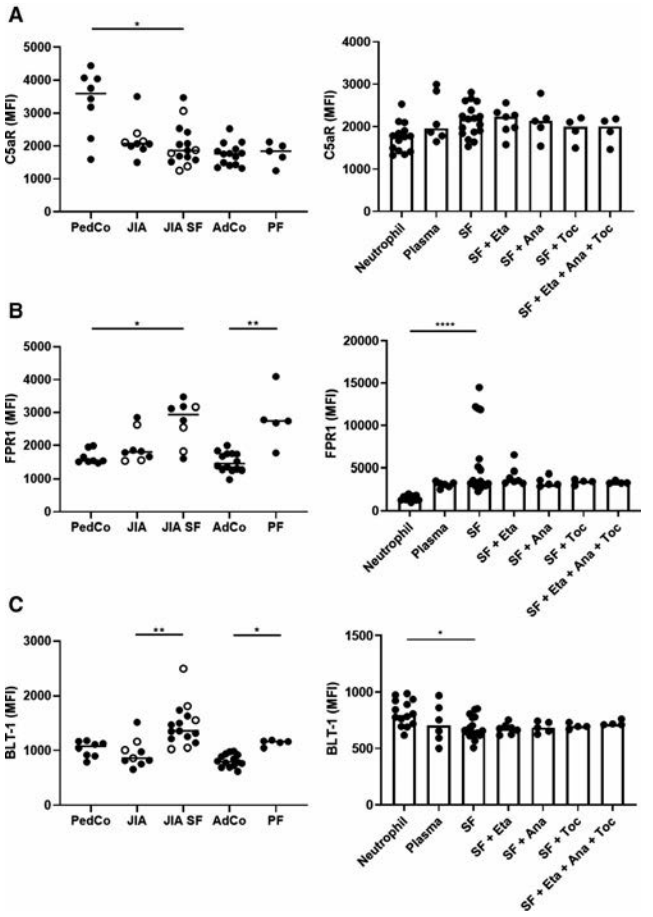

Figure 4. Analysis of C5aR, formyl peptide receptor (FPR-1), and leukotriene B_4 receptor (BLT-1) expression. Expression of C5aR (**A**; left), FPR-1 (**B**; left), and BLT-1 (**C**; left) on neutrophils in blood from healthy pediatric controls, blood from JIA patients, and SF from JIA patients was determined by flow cytometry. Pleural neutrophils from patients with pleural effusion and blood neutrophils from healthy adults were investigated for comparative purposes. Fresh peripheral blood neutrophils from healthy donors were exposed to cell-free plasma from the corresponding donor or cell-free SF from JIA patients, with or without 2 μg/ml anti–tumor necrosis factor (etanercept), anti–interleukin-1β (anakinra), or anti–interleukin-6 (tocilizumab) for 24 hours, followed by analysis of expression of C5aR (**A**; right), FPR-1 (**B**; right), and BLT-1 (**C**; right). Results show percentages of positive neutrophils or mean fluorescence intensity (MFI). Patients with oligoarticular or polyarticular disease are represented by closed or open circles, respectively. Horizontal lines and bars show the median. * = $P \leq 0.05$; ** = $P \leq 0.01$; **** = $P \leq 0.0001$, by Kruskal-Wallis test with Dunn's test for multiple comparisons. See Figure 1 for other definitions.

Correlations between phenotypic alterations in synovial neutrophils and local cytokine concentrations. Correlation studies were performed to evaluate potential associations between phenotypic characteristics of synovial neutrophils from JIA patients and the local cytokine concentrations. In addition, we exposed healthy donor neutrophils to 3 prototypical proinflammatory cytokines that are relevant therapeutic targets in the context of JIA and present at high concentrations in SF: IL-1β, IL-6, and TNF (Table 1). Synovial levels of IL-6 ($P = 0.0015$) and IL-1Ra ($P = 0.0014$) and, to a lesser extent, IL-1β ($P = 0.0031$) and CXCL8 ($P = 0.0040$), correlated positively with the abundance of $CD62L^{low}$ neutrophils in JIA SF and tended to correlate with the expression of CXCR4 (Figure 5). Nevertheless, CD62L shedding and up-regulation of CXCR4 also occurred spontaneously when healthy donor cells were cultured in plasma from the same donor for 24 hours (Figures 1E and F). Treatment with IL-1β or IL-6 had no additional effects on CD62L shedding and up-regulation of CXCR4 by healthy donor neutrophils, compared to medium alone (Supplementary Figures 6A and B, http://onlinelibrary.wiley.com/doi/10.1002/art.41605/abstract). Collectively, these results suggest that CD62L shedding and up-regulation of CXCR4 expression coincide with neutrophil aging in JIA SF.

A significant correlation between increased CD66b expression on JIA SF neutrophils and enhanced local concentrations of IL-6 ($P = 0.0001$), IL-10 ($P = 0.0001$), CXCL8 ($P = 0.0019$), and TNF ($P = 0.0003$) was revealed (Figure 5). Nevertheless, exposure of healthy donor neutrophils to JIA SF, which contained high concentrations of these cytokines, did not provoke up-regulation of CD66b on healthy donor neutrophils (Supplementary Figure 4A, http://onlinelibrary.wiley.com/doi/10.1002/art.41605/abstract). Likewise, stimulation of healthy donor cells with IL-1β or IL-6 had no significant effect on the intensity of CD66b expression (Supplementary Figure 6C). In contrast to cells treated with IL-1β or IL-6, TNF-treated cells tended to exhibit elevated levels of CD66b ($P = 0.0824$) (Supplementary Figure 6C). No effects of the 3 cytokines were observed in HLA–DR expression on neutrophils

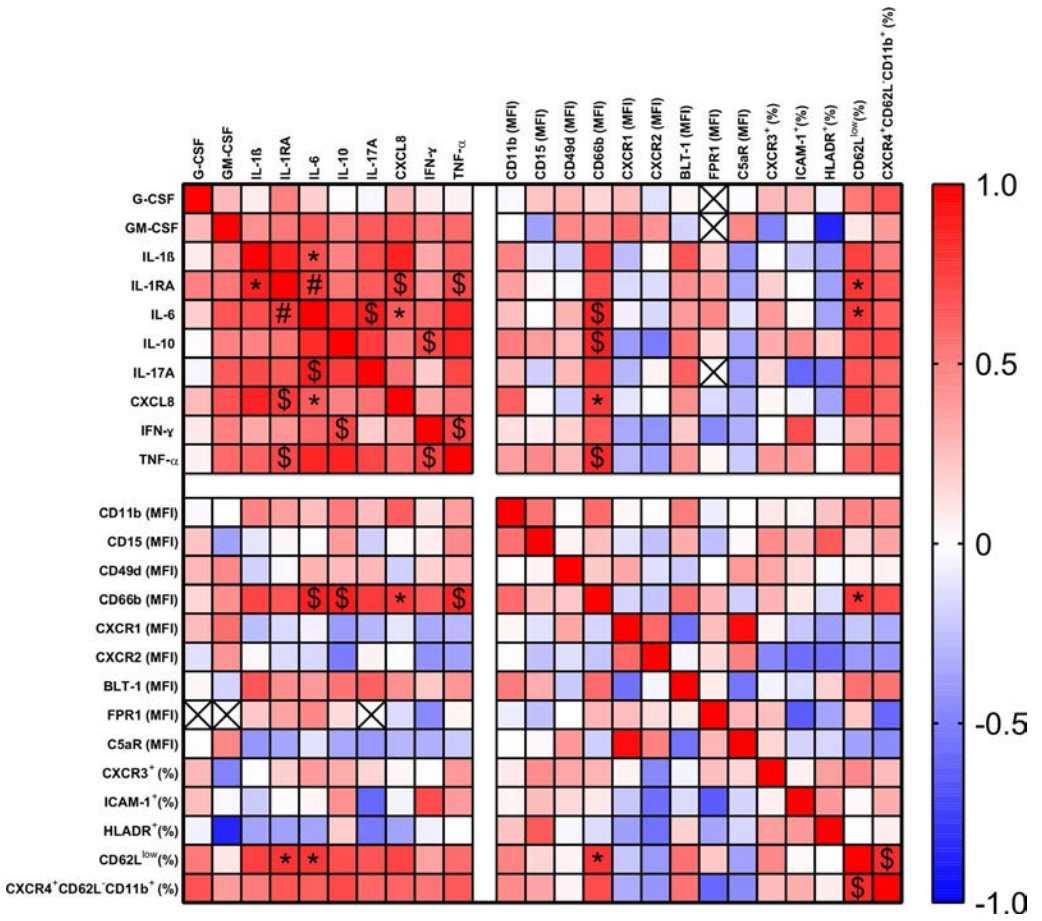

Figure 5. Correlation between phenotypic features of synovial neutrophils and local cytokine levels. Spearman's correlation coefficients were calculated to detect potential correlations between the abundance of synovial cytokines and phenotypic features of synovial neutrophils from juvenile idiopathic arthritis patients. *P* values lower than the Bonferroni-corrected alpha value (α/n) were considered significant. * = $P \leq 0.002$; $ = $P \leq 0.0004$; # = $P \leq 0.00004$; × = *P* was not determined. G-CSF = granulocyte colony-stimulating factor; GM-CSF = granulocyte–macrophage colony-stimulating factor; IL-1β = interleukin-1β; IL-1Ra = IL-1 receptor antagonist; IFNγ = interferon-γ; TNF = tumor necrosis factor; MFI = mean fluorescence intensity; BLT-1 = leukotriene B_4 receptor; FPR-1 = formyl peptide receptor; ICAM-1 = intercellular adhesion molecule 1.

(Supplementary Figure 6D). Moreover, no significant associations were found between the presence of a particular cytokine and expression levels of CD11b, CD15, CD49d, ICAM-1, CXCR1/2/3, BLT-1, FPR-1, C5aR, or HLA–DR on JIA SF neutrophils (Figure 5).

Evaluation of CD11b expression on healthy donor neutrophils 24 hours after stimulation with TNF, IL-1β, or IL-6 revealed that TNF, but not IL-1β or IL-6, induced a significant up-regulation of CD11b (Supplementary Figure 7A, http://onlinelibrary.wiley.com/doi/10.1002/art.41605/abstract). As expected, the TNF-induced up-regulation of CD11b was blocked upon administration of the TNF inhibitor etanercept. No significant changes in the expression level of CD15, CD49d, or ICAM-1–positive cells were detected upon incubation with TNF, IL-1β, or IL-6, although a trend toward increased ICAM-1–expressing neutrophils was found when cells were treated with TNF or IL-1β (Supplementary Figures 7B–D). All 3 cytokines failed to interfere with the expression of chemoattractant receptors CXCR1, CXCR2, and FPR-1 (Supplementary Figures 8A–C, http://onlinelibrary.wiley.com/doi/10.1002/art.41605/abstract). In addition, stimulation of healthy donor neutrophils with TNF, IL-1β, or IL-6 had no significant effects on the percentage of CXCR3-expressing cells, although a trend toward increased numbers of CXCR3-positive neutrophils was observed upon treatment with TNF (Supplementary Figure 8D). TNF-treated neutrophils showed a significant down-regulation of C5aR and a trend toward increased BLT-1 expression (Supplementary Figures 8E and F). Both TNF-mediated effects were blocked in the presence of etanercept.

DISCUSSION

Oligoarticular and polyarticular JIA are autoimmune diseases that have long been assumed to be caused by dysregulation of the adaptive immune system, with a central role for autoreactive T cells belonging to the Th1 and Th17 lineages and autoantigens that may include aggrecan, fibrillin, matrix metalloproteinase 3, and heat-shock proteins (28–33). Nevertheless, the original T cell–centered hypothesis has been challenged since it does not completely explain the full spectrum of immunopathologic phenomena observed in patients. Moreover, successful therapeutic strategies are either nonspecific (such as glucocorticoids or methotrexate) or target just 1 inflammatory cytokine downstream of the inflammatory cascade (TNF blockers, IL-6 blockade) or T cell interaction (CTLA-4 Ig).

Previous research efforts have revealed that peripheral blood neutrophils from polyarticular JIA patients are chronically activated cells characterized by transcriptional abnormalities, including disruption of gene regulatory networks in clusters of IFNγ- and CXCL8-modulated genes, even during remission (6,7). Moreover, a correlation was demonstrated between serum S100A12 levels and disease activity (9). Interestingly, associations between effective medical treatment and extensive modulation of the neutrophil transcriptional profile were unveiled (8). These observations suggest an important role for neutrophils in JIA pathogenesis, piquing our interest to investigate the phenotypic characteristics of neutrophils present in the circulation and in inflamed joints from JIA patients.

Evidence of neutrophil activation at the protein level has only been published for patients with systemic-onset JIA, which is believed to be an autoinflammatory disease driven mainly by aberrant innate immune responses (34). The present study is the first to characterize neutrophils, present in the blood and SF of oligoarticular and polyarticular JIA patients, at the protein level. Our findings suggest the existence of strongly activated neutrophils in SF from JIA patients, which are characterized by the following: CD62L shedding; up-regulation of CD66b, CD11b, and CD15; down-regulation of CXCR1; and up-regulation of alternative surface molecules including, but not limited to, HLA–DR and ICAM-1. In pleural fluids, neutrophil activation was less evident, since no significant alteration in the expression of CD66, CD11b, CD15, or CXCR1 was detected. Neutrophils were not activated or hardly activated in peripheral blood of JIA patients at the protein level. This corresponds to the absence of major signs of systemic inflammation at the moment of sampling, as evidenced by low C-reactive protein levels, erythrocyte sedimentation rates (Supplementary Table 1, http://onlinelibrary.wiley.com/doi/10.1002/art.41605/abstract), and plasma cytokine concentrations (Table 1).

Importantly, down-regulation of CD62L and CXCR1/2 occurred spontaneously when healthy donor neutrophils were cultured for 24 hours in plasma from the corresponding donor, indicating that these phenotypic changes presumably coincide with neutrophil aging. Moreover, up-regulation of CD49d, ICAM-1, FPR-1, and CXCR3 was mimicked when healthy donor neutrophils were exposed to JIA SF, suggesting that the local milieu with enhanced concentrations of proinflammatory mediators is at least partially responsible for the increased expression of these molecules on synovial neutrophils. SF neutrophils from JIA patients, but not plasma- or SF-treated healthy donor cells, are characterized by up-regulation of CD66b, HLA–DR, CD11b, CD15, and BLT-1 and down-regulation of C5aR. Pleural neutrophils from patients with pleural effusion also displayed a trend toward higher surface levels of HLA–DR expression and decreased expression of C5aR. Therefore, these phenotypic alterations may be related to neutrophil extravasation.

Analysis of nuclear segmentation properties revealed an increased percentage of hypersegmented neutrophils in JIA SF. The functional characteristics of this particular neutrophil subset are poorly defined. Neutrophils with increased numbers of nuclear lobes are believed to be capable of suppressing the proliferation of T cells via CD11b/CD18-dependent release of hydrogen peroxide and show a unique proteome profile (21,35). Hypersegmentation has been proposed to be associated with neutrophil aging. Nevertheless, there has been speculation that banded cells may mature directly into hypersegmented neutrophils under particular pathophysiologic circumstances (36). In addition, it has been suggested

that CD62L^{low} hypersegmented neutrophils, present in the bone marrow, enter the circulation only during acute inflammation (21). Thus, it remains an open question whether all CD62L^{low} hypersegmented neutrophils are aged cells.

Functionally, it has been demonstrated that CD62L^{low} aged neutrophils display an impairment in induction of shape change and chemotaxis, but also show an enhanced surface expression of CD18 and increased hydrogen peroxide production (37). Evidence of the presence of aged neutrophils in inflamed joints from JIA patients was provided when the expression of chemokine receptors was investigated. Our results show a significant portion of CXCR4-positive neutrophils present in JIA SF. Up-regulation of CXCR4 on SF neutrophils from patients with various forms of arthritis has previously been reported and is a hallmark feature of aged neutrophils, allowing them to home back to the bone marrow following senescence (38). Although aged neutrophils show diminished proinflammatory activity in vitro, they presumably represent a population of superior mediators of inflammation in vivo (23,37,39,40).

Neutrophils may up-regulate MHC class II molecules on their cellular surface, presumably in a CD11b-dependent manner and in response to T cell–derived cytokines, including GM-CSF, IFNγ, and IL-3 (19,20,41,42). MHC class II–expressing neutrophils may actively present antigens to T cells, suggesting that they are potentially critical players acting at the intersection between innate and adaptive immunity (43–45). The existence of MHC class II–positive neutrophils in vivo has been demonstrated in the context of rheumatoid arthritis (41). Here, we report the presence of HLA–DR-expressing neutrophils in inflamed joints from JIA patients. This subset of neutrophils may fulfill a key role in regulating the adaptive immune response, favoring the idea that JIA is driven by an intriguing interplay between innate and adaptive immune cells.

ICAM-1 is generally absent on neutrophils or expressed only at very low levels. Exposure to inflammatory signals including lipopolysaccharide and TNF evokes up-regulation of ICAM-1 on neutrophils (27). Functionally, ICAM-1–expressing neutrophils excel in terms of ROS production, phagocytic capacity, and the ability to release neutrophil extracellular traps (27,46). Our observation that a significant portion of SF neutrophils from JIA patients are ICAM-1–positive cells suggests the presence of a subpopulation with altered proinflammatory activity.

In conclusion, the present study is the first to provide a comprehensive phenotypic profile of neutrophils present in the circulation and inflamed joints of oligoarticular and polyarticular JIA patients. Our data indicate that synovial neutrophils have an activated phenotype, which allows us to speculate that neutrophils are important orchestrators of innate and adaptive immune events in JIA pathogenesis.

ACKNOWLEDGMENTS

The authors thank all patients, healthy volunteers, and their legal representatives.

AUTHOR CONTRIBUTIONS

All authors were involved in drafting the article or revising it critically for important intellectual content, and all authors approved the final version to be published. Dr. Proost had full access to all of the data in the study and takes responsibility for the integrity of the data and the accuracy of the data analysis.

Study conception and design. Metzemaekers, Malengier-Devlies, Matthys, De Somer, Wouters, Proost.

Acquisition of data. Metzemaekers, Malengier-Devlies, Yu, Vandendriessche, Yserbyt, De Somer.

Analysis and interpretation of data. Metzemaekers, Malengier-Devlies, Matthys, De Somer, Wouters, Proost.

REFERENCES

1. Leong JY, Guan YJ, Albani S, Arkachaisri T. Recent advances in our understanding of the pathogenesis of juvenile idiopathic arthritis and their potential clinical implications [review]. Expert Rev Clin Immunol 2018;14:933–44.
2. Lin YT, Wang CT, Gershwin ME, Chiang BL. The pathogenesis of oligoarticular/polyarticular vs systemic juvenile idiopathic arthritis [review]. Autoimmun Rev 2011;10:482–9.
3. Macaubas C, Nguyen K, Milojevic D, Park JL, Mellins ED. Oligoarticular and polyarticular JIA: epidemiology and pathogenesis [review]. Nat Rev Rheumatol 2009;5:616–26.
4. Wedderburn LR, Robinson N, Patel A, Varsani H, Woo P. Selective recruitment of polarized T cells expressing CCR5 and CXCR3 to the inflamed joints of children with juvenile idiopathic arthritis. Arthritis Rheum 2000;43:765–74.
5. Hinks A, Cobb J, Marion MC, Prahalad S, Sudman M, Bowes J, et al. Dense genotyping of immune-related disease regions identifies 14 new susceptibility loci for juvenile idiopathic arthritis. Nat Genet 2013;45:664–9.
6. Jarvis JN, Petty HR, Tang Y, Frank MB, Tessier PA, Dozmorov I, et al. Evidence for chronic, peripheral activation of neutrophils in polyarticular juvenile rheumatoid arthritis. Arthritis Res Ther 2006;8:R154.
7. Jarvis JN, Jiang K, Frank MB, Knowlton N, Aggarwal A, Wallace CA, et al. Gene expression profiling in neutrophils from children with polyarticular juvenile idiopathic arthritis. Arthritis Rheum 2009;60:1488–95.
8. Hu Z, Jiang K, Frank MB, Chen Y, Jarvis JN. Modeling transcriptional rewiring in neutrophils through the course of treated juvenile idiopathic arthritis. Sci Rep 2018;8:7805.
9. Foell D, Wittkowski H, Hammerschmidt I, Wulffraat N, Schmeling H, Frosch M, et al. Monitoring neutrophil activation in juvenile rheumatoid arthritis by S100A12 serum concentrations. Arthritis Rheum 2004;50:1286–95.
10. Liew PX, Kubes P. The neutrophil's role during health and disease [review]. Physiol Rev 2019;99:1223–48.
11. Lefkowitz DL, Gelderman MP, Fuhrmann SR, Graham S, Starnes JD III, Lefkowitz SS, et al. Neutrophilic myeloperoxidase-macrophage interactions perpetuate chronic inflammation associated with experimental arthritis. Clin Immunol 1999;91:145–55.
12. Pereira HA, Shafer WM, Pohl J, Martin LE, Spitznagel JK. CAP37, a human neutrophil-derived chemotactic factor with monocyte specific activity. J Clin Invest 1990;85:1468–76.
13. Bennouna S, Denkers EY. Microbial antigen triggers rapid mobilization of TNF-α to the surface of mouse neutrophils transforming them into inducers of high-level dendritic cell TNF-α production. J Immunol 2005;174:4845–51.
14. Scapini P, Carletto A, Nardelli B, Calzetti F, Roschke V, Merigo F, et al. Proinflammatory mediators elicit secretion of the intracellular B-lymphocyte stimulator pool (BLyS) that is stored in activated

neutrophils: implications for inflammatory diseases. Blood 2005; 105:830–7.

15. Ethuin F, Gerard B, Benna JE, Boutten A, Gougereot-Pocidalo MA, Jacob L, et al. Human neutrophils produce interferon γ upon stimulation by interleukin-12. Lab Invest 2004;84:1363–71.
16. Silvestre-Roig C, Hidalgo A, Soehnlein O. Neutrophil heterogeneity: implications for homeostasis and pathogenesis. Blood 2016;127:2173–81.
17. Headland SE, Norling LV. The resolution of inflammation: principles and challenges. Semin Immunol 2015;27:149–60.
18. Metzemaekers M, Gouwy M, Proost P. Neutrophil chemoattractant receptors in health and disease: double-edged swords. Cell Mol Immunol 2020;17:433–50.
19. Sandilands GP, Ahmed Z, Perry N, Davison M, Lupton A, Young B. Cross-linking of neutrophil CD11b results in rapid cell surface expression of molecules required for antigen presentation and T-cell activation. Immunology 2005;114:354–68.
20. Matsushima H, Geng S, Lu R, Okamoto T, Yao Y, Mayuzumi N, et al. Neutrophil differentiation into a unique hybrid population exhibiting dual phenotype and functionality of neutrophils and dendritic cells. Blood 2013;121:1677–89.
21. Tak T, Wijten P, Heeres M, Pickkers P, Scholten A, Heck AJ, et al. Human CD62L(dim) neutrophils identified as a separate subset by proteome profiling and in vivo pulse-chase labeling. Blood 2017;129:3476–85.
22. Arebro J, Ekstedt S, Hjalmarsson E, Winqvist O, Georén SK, Cardell LO. A possible role for neutrophils in allergic rhinitis revealed after cellular subclassification. Sci Rep 2017;7:43568.
23. Zhang D, Chen G, Manwani D, Mortha A, Xu C, Faith JJ, et al. Neutrophil ageing is regulated by the microbiome. Nature 2015;525:528–32.
24. Fortunati E, Kazemier KM, Grutters JC, Koenderman L, van den Bosch VJ. Human neutrophils switch to an activated phenotype after homing to the lung irrespective of inflammatory disease. Clin Exp Immunol 2009;155:559–66.
25. Sengelov H, Follin P, Kjeldsen L, Lollike K, Dahlgren C, Borregaard N. Mobilization of granules and secretory vesicles during in vivo exudation of human neutrophils. J Immunol 1995;154:4157–65.
26. Kadioglu A, de Filippo K, Bangert M, Fernandes VE, Richards L, Jones K, et al. The integrins Mac-1 and α4β1 perform crucial roles in neutrophil and T cell recruitment to lungs during Streptococcus pneumoniae infection. J Immunol 2011;186:5907–15.
27. Woodfin A, Beyrau M, Voisin M-B, Ma B, Whiteford JR, Hordijk PL, et al. ICAM-1-expressing neutrophils exhibit enhanced effector functions in murine models of endotoxemia. Blood 2016;127: 898–907.
28. Kamphuis S, Hrafnkelsdottir K, Klein MR, de Jager W, Haverkamp MH, van Bilsen JH, et al. Novel self-epitopes derived from aggrecan, fibrillin, and matrix metalloproteinase-3 drive distinct autoreactive T-cell responses in juvenile idiopathic arthritis and in health. Arthritis Res Ther 2006;8:R178.
29. Sedlackova L, Velek J, Vavrincova P, Hromadnikova I. Peripheral blood mononuclear cell responses to heat shock proteins and their derived synthetic peptides in juvenile idiopathic arthritis patients. Inflamm Res 2006;55:153–9.
30. De Graeff-Meeder ER, van der Zee R, Rijkers GT, Schuurman HJ, Kuis W, Bijlsma JW, et al. Recognition of human 60 kD heat shock protein by mononuclear cells from patients with juvenile chronic arthritis. Lancet 1991;337:1368–72.
31. Massa M, Passalia M, Manzoni SM, Campanelli R, Ciardelli L, Yung GP, et al. Differential recognition of heat-shock protein dnaJ–derived epitopes by effector and Treg cells leads to modulation of inflammation in juvenile idiopathic arthritis. Arthritis Rheum 2007;56:1648–57.
32. De Kleer IM, Kamphuis SM, Rijkers GT, Scholtens L, Gordon G, de Jager W, et al. The spontaneous remission of juvenile idiopathic arthritis is characterized by CD30+ T cells directed to human heat-shock protein 60 capable of producing the regulatory cytokine interleukin-10. Arthritis Rheum 2003;48:2001–10.
33. Nguyen TT, Gehrmann M, Zlacka D, Sosna A, Vavrincova P, Multhoff G, et al. Heat shock protein 70 membrane expression on fibroblast-like synovial cells derived from synovial tissue of patients with rheumatoid and juvenile idiopathic arthritis. Scand J Rheumatol 2006;35:447–53.
34. Ter Haar NM, Tak T, Mokry M, Scholman RC, Meerding JM, de Jager W, et al. Reversal of sepsis-like features of neutrophils by interleukin-1 blockade in patients with systemic-onset juvenile idiopathic arthritis. Arthritis Rheumatol 2018;70:943–56.
35. Pillay J, Kamp VM, van Hoffen E, Visser T, Tak T, Lammers JW, et al. A subset of neutrophils in human systemic inflammation inhibits T cell responses through Mac-1. J Clin Invest 2012;122:327–36.
36. Casanova-Acebes M, Pitaval C, Weiss LA, Nombela-Arrieta C, Chevre R, A-Gonzalez N, et al. Rhythmic modulation of the hematopoietic niche through neutrophil clearance. Cell 2013;153:1025–35.
37. Tanji-Matsuba K, van Eeden SF, Saito Y, Okazawa M, Klut ME, Hayashi S, et al. Functional changes in aging polymorphonuclear leukocytes. Circulation 1998;97:91–8.
38. Bruhl H, Wagner K, Kellner H, Schattenkirchner M, Schlondorff D, Mack M. Surface expression of CC- and CXC-chemokine receptors on leucocyte subsets in inflammatory joint diseases. Clin Exp Immunol 2001;126:551–9.
39. Rankin SM. The bone marrow: a site of neutrophil clearance. J Leukoc Biol 2010;88:241–51.
40. Uhl B, Vadlau Y, Zuchtriegel G, Nekolla K, Sharaf K, Gaertner F, et al. Aged neutrophils contribute to the first line of defense in the acute inflammatory response. Blood 2016;128:2327–37.
41. Sandilands GP, McCrae J, Hill K, Perry M, Baxter D. Major histocompatibility complex class II (DR) antigen and costimulatory molecules on in vitro and in vivo activated human polymorphonuclear neutrophils. Immunology 2006;119:562–71.
42. Samadi N, Polak D, Kitzmuller C, Steinberger P, Zlabinger GJ, Jahn-Schmid B, et al. T-cell-derived cytokines enhance the antigen-presenting capacity of human neutrophils [letter]. Eur J Immunol 2019;49:1441–3.
43. Fanger NA, Liu C, Guyre PM, Wardwell K, O'Neil J, Guo TL, et al. Activation of human T cells by major histocompatability complex class II expressing neutrophils: proliferation in the presence of superantigen, but not tetanus toxoid. Blood 1997;89:4128–35.
44. Ashtekar AR, Saha B. Poly's plea: membership to the club of APCs. Trends Immunol 2003;24:485–90.
45. Radsak M, Iking-Konert C, Stegmaier S, Andrassy K, Hansch GM. Polymorphonuclear neutrophils as accessory cells for T-cell activation: major histocompatibility complex class II restricted antigen-dependent induction of T-cell proliferation. Immunology 2000;101:521–30.
46. Ode Y, Aziz M, Wang P. CIRP increases ICAM-1(+) phenotype of neutrophils exhibiting elevated iNOS and NETs in sepsis. J Leukoc Biol 2018;103:693–707.

Arthritis & Rheumatology
Vol. 73, No. 5, May 2021, pp 885–895
DOI 10.1002/art.41591

American College of Rheumatology
Empowering Rheumatology Professionals

Amelioration of Murine Macrophage Activation Syndrome by Monomethyl Fumarate in Both a Heme Oxygenase 1–Dependent and Heme Oxygenase 1–Independent Manner

Chhanda Biswas, Niansheng Chu, Thomas N. Burn, Portia A. Kreiger, and Edward M. Behrens

Objective. Macrophage activation syndrome (MAS) is characterized by increased serum levels of ferritin and heme oxygenase 1 (HO-1), and yet no known function is ascribed to these molecules in MAS. Because HO-1 is antiinflammatory, we hypothesized that pharmacologic activation of HO-1 could ameliorate MAS disease activity. Dimethyl fumarate (DMF), a treatment approved by the US Food and Drug Administration for multiple sclerosis, activates HO-1. Monomethyl fumarate (MMF) is the active metabolite of DMF. We therefore evaluated whether MMF could elicit HO-1–dependent therapeutic improvements in a murine model of MAS.

Methods. We induced MAS by repeated activation of Toll-like receptor 9 (TLR-9) in wild-type and myeloid-specific HO-1–deficient mice. MMF was administered twice daily to test its efficacy. We assessed organ weights, serum cytokine levels, histologic features of the spleen and liver tissue, and complete blood cell counts to evaluate disease activity. Statistical testing was performed using Student's *t*-test or by 2-way analysis of variance as appropriate.

Results. The presence of HO-1 was required for the majority of TLR-9–induced interleukin-10 (IL-10). IL-10 production in TLR-9–induced MAS was found to correlate with the myeloid–HO-1 gene dose in myeloid cells ($P < 0.001$). MMF treatment increased the levels of HO-1 in splenic macrophages by ~2-fold ($P < 0.01$), increased serum levels of IL-10 in an HO-1–dependent manner in mice with TLR-9–induced MAS ($P < 0.005$), and improved multiple disease parameters in both an HO-1–dependent and HO-1–independent manner.

Conclusion. TLR-9–induced production of IL-10 is regulated by HO-1 activity both in vitro and in vivo. Therapeutic enhancement of the HO-1/IL-10 axis in a murine model was able to significantly ameliorate MAS disease activity. These results suggest that HO-1 may be viable as a MAS therapeutic target, and treatment with DMF and MMF should be considered in future investigations of MAS therapy.

INTRODUCTION

Macrophage activation syndrome (MAS) is a cytokine storm syndrome typically seen in association with inflammatory rheumatic conditions (1) that presents with fever, bicytopenia, organomegaly, coagulopathy, and multisystem organ failure. Thus, MAS is similar to the related syndrome of hemophagocytic lymphohistiocytosis (HLH) in its clinical presentation. Accordingly, hemophagocytes (macrophages observed to be consuming red blood cells [RBCs]) and elevated serum markers of iron metabolism such as ferritin are prominent in both conditions. In addition to elevated ferritin, MAS/HLH has also been associated with increased serum heme oxygenase 1 (HO-1) levels (2,3). It remains unclear why this constellation of hemophagocytosis, ferritin, and HO-1 are altered in MAS/HLH. In the case of bacterial sepsis as well as infectious cytokine storm syndrome, it has been reported that the hemophagocytes themselves are a major contributor to HO-1 levels (4). Furthermore, in murine models of HLH, the hemophagocytic compartment has been shown to produce copious amounts of protective antiinflammatory interleukin-10 (IL-10) (5). Taken together, the association of HO-1 and IL-10 being produced in the same cellular compartment led us to

Dr. Behrens' work was supported by the National Institute of Allergy and Infectious Diseases, NIH (grant R01-AI-121250).

Chhanda Biswas, PhD, Niansheng Chu, MD, Thomas N. Burn, PhD, Portia A. Kreiger, MD, Edward M. Behrens, MD: Children's Hospital of Philadelphia, Philadelphia, Pennsylvania.

No potential conflicts of interest relevant to this article were reported.

Address correspondence to Edward M. Behrens, MD, Children's Hospital of Philadelphia, 3615 Civic Center Boulevard, Room 1102, Philadelphia, PA 19104. Email: Behrens@email.chop.edu.

Submitted for publication August 19, 2020; accepted in revised form November 10, 2020.

consider whether there was a mechanistic connection between HO-1 and IL-10.

IL-10 is one of the best-known antiinflammatory cytokines and has both autocrine and paracrine effects on the inhibition of proinflammatory responses and thus in shaping innate and adaptive immune cells (6,7). We have previously published a study illuminating a critical role for IL-10 in limiting the pathology of a murine model of MAS, which relies on repeated stimulation of Toll-like receptor 9 (TLR-9) (8). This TLR-9–MAS model recapitulates many of the features of MAS and has been used to predict interferon-γ (IFNγ) blockade as an important therapeutic approach (8) and CXCL9 as a marker of disease activity (9). Both of these observations in the murine model have been successfully translated to clinical use in humans for MAS. Additionally, the TLR-9–MAS model has been shown to be influenced by IL-18, reminiscent of MAS in the context of systemic juvenile idiopathic arthritis (10). We therefore used this well-characterized murine model to explore HO-1 and its connection to IL-10 biologic processes in MAS and investigated whether therapeutic targeting of HO-1 and its upstream transcription factor Nrf2 might be a useful approach.

HO-1, encoded by the gene *HMOX1,* is evolutionarily conserved across the phylogeny (11,12) and is better understood for its canonical function in the degradation of heme into free iron (Fe^{2+}), carbon monoxide (CO), and a transient product, biliverdin, which is rapidly converted to bilirubin (13). Typically, HO-1 transcription is regulated by Nrf2, which upon activation, escapes proteasomal degradation and translocates to the nucleus (14). Simultaneously, heme replaces Bach1, a suppressor of HO-1, in the nucleus and allows Nrf2, in a complex with musculoaponeurotic fibrosarcoma (Maf) protein, to bind to the antioxidant response element (15) of HO-1, facilitating promoter activation and its transcription (16). Like Nrf2, HO-1 is also induced by many stressors, including inflammation (17).

One of the products of the HO-1 enzymatic reaction on heme is free Fe^{2+}. When in excess, Fe^{2+} is sequestered by the iron-binding molecule ferritin (18) to prevent toxicity from highly reactive Fe^{2+} and also as a store for the iron pool to be reused when required. However, HO-1 also has potential as an antiinflammatory molecule, particularly in context with other reaction products (carbon monoxide [CO] [19]) and bilirubin (20,21), although the underlying mechanisms are not well understood. Increasing HO-1 activity, through Nrf2 or other regulators, therefore has the potential to be a regulator of immune activity during systemic inflammatory processes.

Given its role in both regulating inflammation and oxidative stress, the Nrf2/HO-1 axis has been targeted pharmacologically with the compound dimethyl fumarate (DMF), a medication approved by the US Food and Drug Administration (FDA) for relapsing–remitting multiple sclerosis (22). DMF is rapidly converted into monomethyl fumarate (MMF), the biologically active compound (23). MMF in turn increases Nrf2 activity to potentiate its downstream targets including HO-1 (24).

Herein, we show that loss of HO-1 function through multiple means significantly suppresses TLR-9–induced IL-10 production in vitro, as well as in vivo, using myeloid-specific *HMOX1* gene–ablated mice. This loss of function does not make disease significantly worse, likely due to redundant sources of IL-10. However, induced gain-of-function of this axis using the Nrf2/HO-1–inducing drug MMF can ameliorate many of the features of TLR-9–induced MAS in both an HO-1–dependent and –independent manner. These results may have direct translatable potential in the use of clinically available drugs that target this same pathway, such as DMF and other methyl esters of fumarate.

MATERIALS AND METHODS

Mice. This study was carried out in the animal facility of Children's Hospital of Philadelphia (Philadelphia, Pennsylvania) and was approved by the Institutional Animal Care and Use Committee (protocol no. 921). C57BL/6 (wild-type [WT]) and LysMcre mice were purchased from The Jackson Laboratory and bred in our facility. The *HMOX1*$^{fl/fl}$ mice were a generous gift from Dr. Zoltan Arany (Perelman School of Medicine, University of Pennsylvania). *HMOX1*$^{fl/fl}$ mice were crossbred with LysMcre mice in our facility and genotyped regularly to obtain mice with deletion of the HO-1 gene in myeloid lineage and are designated as *HMOX1*^{WT} (intact HO-1), *HMOX1*$^{WT/fl}$ (x LysMcre; HO-1–haplodeficient), and *HMOX1*$^{fl/fl}$ (x LysMcre; complete HO-1 deficiency).

Macrophages and TLR-9 activation. We extracted bone marrow (BM) from the hind limbs of mice and filtered it over a 70-μm strainer to obtain a single-cell suspension, followed by RBC lysis. Bone marrow–derived macrophages (BMMs) were derived by culture in macrophage colony-stimulating factor–enriched media of L929 cells. We obtained RAW264.7 cells from ATCC. Class B CpG 1826 oligonucleotide was synthesized by Integrated DNA Technologies. Macrophages were treated with 1 μg/ml of CpG for 18–20 hours for cytokine analysis in cell supernatant, and treated for 0–2 hours for analysis of protein expression level by Western blotting as described below.

Stable knockdown of HO-1 with short hairpin RNA (shRNA). The lentiviral vectors used to knock down endogenous HO-1 expression in RAW cells were a gift from Dr. La Ping (Children's Hospital of Philadelphia, Philadelphia, Pennsylvania). knock down was carried out as previously described (25). Briefly, based on the highest knockdown efficiency, clone 6 (71758) was used to knock down HO-1, and clone 11, which has no effect on HO-1 expression, was used as a control (nonspecific or scrambled shRNA).

Induction and assessment of MAS in mice. MAS was induced by repeated activation of TLR-9 as described in our previous studies (8,26). Briefly, 8-week-old mice were injected with 5 doses of phosphate buffered saline (PBS) or

50 μg of CpG 1826 intraperitoneally every other day for 9 days whereas MMF (product no: 4511; Tocris) in DMSO was injected at a dosage of 45 mg/kg of body weight based on standard dosing used in other murine studies (23,27) every day (once in the morning and once in the evening). The control group received DMSO instead of MMF. On day 10, mice were euthanized 24 hours after the last injection of MMF, blood was collected from the mice for determination of the complete blood cell count and differential blood cell count, and serum was collected for cytokine analysis by enzyme-linked immunosorbent assay (ELISA). Thereafter, mice were euthanized, and the spleens and livers were harvested, with tissue samples formalin-fixed, and then embedded in paraffin for tissue sectioning and slide preparation for histology and immunohistochemical analyses. To obtain a single suspension of spleen leukocytes, spleens were disrupted and incubated in the presence of DNAse and collagenase at a temperature of 37°C, followed by filtering over 70-μm strainers and RBC lysis. The cells were counted and then adhered for 2 hours on petri dishes to obtain plastic-adherent macrophages.

Histology and Immunohistochemistry. Slides from paraffin-embedded tissue sections were stained with hematoxylin and eosin or were immunostained for HO-1 (product no. ADI-SPA-896; Enzo), followed by nuclear staining using ProLong Gold antifade reagent with DAPI (P36931; Invitrogen). Images were acquired on an Eclipse 90i microscope (Nikon) using NIS-elements software.

Cytokine analysis. TLR-9 activation of cell supernatants induced cytokine expression. Cytokine levels in the serum were measured using BD OptEIA ELISA kits (product nos. 555256 [for IL-12], 555252 [for IL-10], 555268 [for tumor necrosis factor (TNF)], and 555240 [for IL-6]).

Preparation of protein lysates. Cells were harvested in the presence of a Halt cocktail of protease and phosphatase inhibitors (product no. 1861281) and were either homogenized in M-PER mammalian protein extraction buffer (product no. 78501; Thermo Scientific) or fractionated into cytoplasmic and nuclear fractions using NE-PER nuclear and cytoplasmic extraction reagent

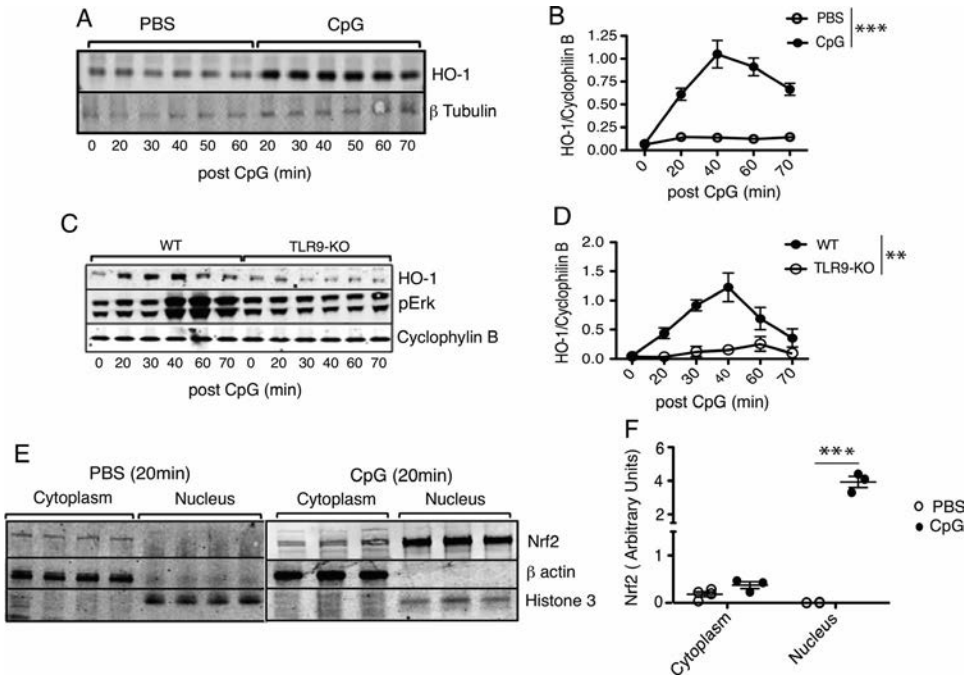

Figure 1. Induction of heme oxygenase 1 (HO-1) and Nrf2 protein expression by Toll-like receptor 9 (TLR-9) activation in mouse macrophages. **A** and **B**, Bone marrow–derived macrophages (BMMs) were stimulated with CpG or phosphate buffered saline (PBS) for the indicated periods of time. Whole BMM lysates were immunoblotted for HO-1, with β-tubulin used as the loading control (**A**). HO-1 band intensities in each stimulation group were normalized to the values for cyclophilin B, with results expressed as the mean ± SEM of 5 repeated experiments (**B**). **C** and **D**, Expression of HO-1 and phosphorylation of Erk (pErk) in CpG-stimulated BMMs from wild-type (WT) mice and CpG-stimulated, TLR-9–activated BMMs from HO-1–knockout (KO) mice was examined by immunoblotting (**C**), with results quantified as the mean ± SEM of 3 independent experiments (**D**). **E** and **F**, Cytoplasmic and nuclear Nrf2 expression from lysates of PBS- or CpG-activated BMMs was examined by immunoblotting (**E**), with results quantified as the mean ± SEM arbitrary units (**F**). Each lane in **E** represents a lysate from an individual experiment, with a total of 5 independent experiments. In **F**, β-tubulin or laminin B was used as normalization loading controls for PBS- or CpG-activated BMMs. ** = $P < 0.01$; *** = $P < 0.005$, by analysis of variance (ANOVA) for repeated measures in **B** and **D** and by ANOVA followed by pairwise multiple comparisons in **F**.

(product no. 78833; Thermo Scientific). Protein content in lysates was measured using a 96-well plate–based Bradford assay (product no. 5000006; Bio-Rad protein assay reagent concentrate).

Western blotting. Protein samples (10–12 μg) were resolved by sodium dodecyl sulfate–polyacrylamide gel electrophoresis on 4–12% Bis-Tris gels (Invitrogen), electrotransferred to nitrocellulose membranes (catalog no. 10484060; Bio-Rad), and assessed for the immunosignal of proteins using antibodies against HO-1 (catalog no. ADI-SPA-896; Enzo), Nrf2 (catalog no. 12721; Cell Signaling Technology), Erk (catalog no. 4695; Cell Signaling Technology), p-ERK (catalog no. 4379; Cell Signaling Technology), cyclophilin B (CYP-B) (catalog no. PA1-027A; Thermo Fisher Scientific), β-tubulin (catalog no. 2146; Cell Signaling Technology), β-actin (catalog no. 66009-1-Ig; ProteinTech), Calnexin (catalog no. ab22595; Abcam), and histone 3 (catalog no. 4499; Cell Signaling Technology). Fluorescence-tagged respective secondary antibodies included goat anti-rabbit (IRDye 800CW), donkey anti-mouse (IRDye 800CW), or donkey anti-mouse IgG (IRDye 680RD) (all from Li-Cor). Densitometric digital assessments were documented using an Odyssey system (make 9120; Li-Cor). Signals were plotted as bar graphs or scatterplots after the values were normalized against the values for the respective loading controls.

Statistical analysis. Values are shown as the mean ± SEM. Depending on the structure being compared, paired 1-tailed or 2-tailed *t*-tests or one-way or two-way analyses of variance were performed, using GraphPad Prism version 7 software.

RESULTS

Induction of HO-1 expression by TLR-9 activation in macrophages. To test our hypothesis that endogenous TLR-9–driven IL-10 production is regulated by HO-1, we first tested whether HO-1 expression is altered by TLR-9 activation via a class B CpG 1826 oligonucleotide. We observed an induction of HO-1 protein expression in CpG-treated BMMs within 20 minutes, with maximal levels shown within 40–60 minutes, followed by a gradual decline by 70 minutes (Figure 1A). This induction was robustly reproducible over an average of 5 experiments (Figure 1B), and the HO-1 induction was specific to TLR-9 activation as the signal was absent in CpG-treated TLR-9–knockout BMMs (Figures 1C and D).

Association of Nrf2 activation with TLR-9–driven HO-1 induction. Nrf2 is the major transcriptional regulator of HO-1, and therefore we also assessed TLR-9–induced nuclear localization of Nrf2. In CpG-activated BMMs, we observed nuclear localization of Nrf2 (Figures 1E and F) within 20 minutes of CpG activation, whereas Nrf2 remained cytoplasmic in PBS-treated BMMs (Figures 1E and F).

Regulation of TLR-9–driven IL-10 production by HO-1. To evaluate the possibility that HO-1 regulates IL-10, we used 3 μ*M* of zinc protoporphyrin (ZnPP), a known inhibitor of HO-1 enzyme function (28). This dose of ZnPP substantially reduced production of IL-10 by BMMs stimulated with CpG (Figure 2A). As might be expected with a loss of autocrine IL-10, ZnPP-treated BMMs produced increased levels of TNF and IL-6 in response to CpG.

We further validated HO-1–dependent IL-10 regulation by shRNA knockdown of HO-1 in the RAW 264.7 macrophage cell line. Knockdown of HO-1 expression by ~80% (Supplementary Figures 1A and B, available on the *Arthritis & Rheumatology* website at http://onlinelibrary.wiley.com/doi/10.1002/art.41591/abstract) significantly blocked TLR-9–induced IL-10 production (Supplementary Figure 1C). This effect was absent in BMMs that received nonspecific scrambled shRNA. As with ZnPP, we observed a 2.8-fold increase in TNF, though IL-6 was not affected (Supplementary Figure 1C) perhaps due to the differences between BMMs and the RAW cell line. Finally, we made BMMs genetically deficient in HO-1 by crossing mice expressing Cre recombinase under the control of the myeloid-specific *Lyz2* promoter to mice harboring loxP sites flanking coding elements of *Hmox1* (29). We observed a 50% decrease in IL-10 in HO-1–deleted (*HMOX1*$^{fl/fl}$) mouse BMMs (Figure 2B) as compared to BMMs from WT (*HMOX1*^{WT}) mice. ZnPP-mediated HO-1 inhibition blocked IL-10 in *HMOX1*^{WT} mouse BMMs without showing any effect on the residual IL-10 in *HMOX1*$^{fl/fl}$ *mouse* BMMs (Figure 2B), consistent with HO-1–specific regulation of IL-10. Thus, using 3 different approaches to eliminate HO-1 activity or expression, we demonstrated that TLR-9–induced IL-10 production in macrophages is regulated by HO-1.

Rescue of IL-10 production by exogenous CO in HO-1–deficient mouse BMMs. Carbon monoxide is one of the major products produced by the enzymatic action of HO-1 on heme. Although not one of the canonical signaling molecules thought to control immune function, CO has been reported to have an antiinflammatory role via IL-10 production in a mouse model of sepsis (19). We therefore tested whether exogenous CO (in the form of CO-releasing molecule 2 [CORM-2]) can rescue IL-10 production that is impaired due to HO-1 inhibition by ZnPP. Indeed, CORM-2 restored IL-10 to normal levels in ZnPP-treated BMMs (Figure 2C). This effect was further validated by demonstrating rescue of IL-10 by CORM-2 in *HMOX1*$^{fl/fl}$ mouse BMMs (Supplementary Figure 1D). Notably, CORM-2 had no additional effect in BMMs that were not inhibited by ZnPP or that were genetically sufficient for HO-1 (Supplementary Figure 2D, available on the *Arthritis & Rheumatology* website at http://onlinelibrary.wiley.com/doi/10.1002/art.41591/abstract), suggesting that endogenous HO-1 provides saturating amounts of CO that drive IL-10 production. Taken together, these findings provide evidence that TLR-9–driven IL-10 production in macrophages is regulated by HO-1 function, at least in part by the product of its enzymatic reaction, CO.

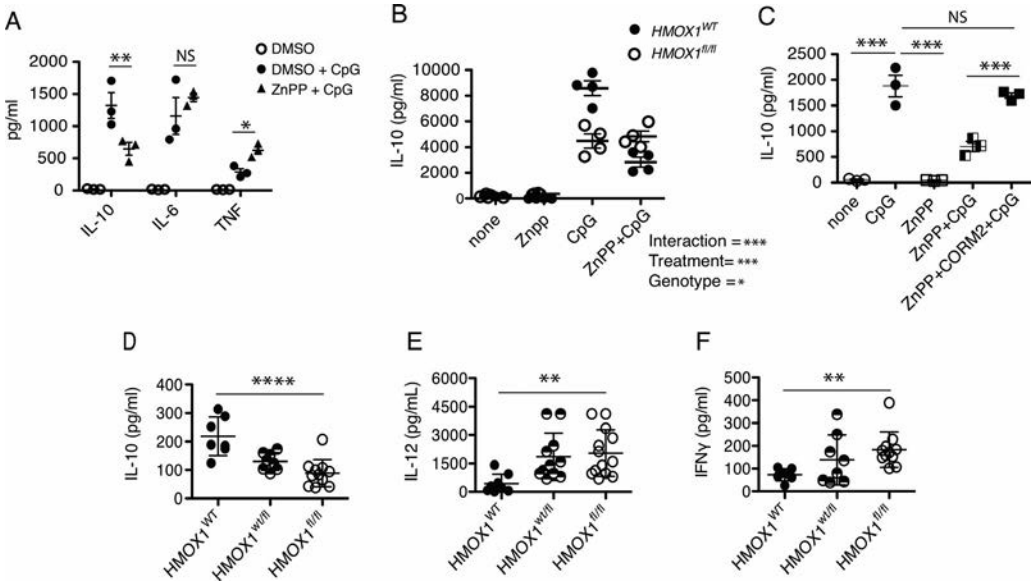

Figure 2. Regulation of TLR-9–driven interleukin-10 (IL-10) production in mouse macrophages by the HO-1 axis. **A**, Cytokine pattern in the supernatants of BMMs treated with zinc protoporphyrin (ZnPP) or DMSO followed by CpG is shown. **B**, IL-10 released by CpG-treated *HMOX1*^{WT} and *HMOX1*$^{fl/fl}$ mouse BMMs is shown. **C**, BMMs were treated with DMSO or ZnPP (as described in **A**). Carbon monoxide–releasing molecule 2 (CORM-2) was additionally added, followed by treatment with 1 μg/ml of CpG. Levels of released IL-10 were measured. Data in **A**–**C** are representative of 3 independent experiments. **D**–**F**, *HMOX1*^{WT}, *HMOX*$^{wt/fl}$, and *HMOX1*$^{fl/fl}$ mice received repeated injections (5 doses) of CpG intraperitoneally every other day, and serum levels of IL-10 (**D**), IL-12 (**E**), and interferon-γ (IFNγ) (**F**) were measured. Symbols represent individual samples; bars show the mean ± SEM. ** = $P < 0.01$; *** = $P < 0.005$; **** = $P < 0.0001$ by one-way ANOVA with pairwise tests for multiple comparisons. NS = not significant; TNF = tumor necrosis factor (see Figure 1 for other definitions).

Correlation of the gene dose of myeloid *HMOX1* with in vivo TLR-9–driven production of IL-10 in mouse serum. To validate whether myeloid HO-1 regulates systemic IL-10 production in vivo, we measured serum IL-10 levels after activation of TLR-9 in mice with different gene doses of the HO-1 gene (*HMOX1)* in myeloid lineage. Serum levels of IL-10 were found to be correlated with the myeloid gene dose using a series of 3 murine genotypes treated with repeated doses of CpG: *HMOX1*^{WT} (HO-1 intact), *HMOX1*$^{WT/fl}$ (HO-1 haplodeficient), and *HMOX1*$^{fl/fl}$ (HO-1-depleted) (Figure 2D). As expected, with increased copies of intact *HMOX1* genes, CpG treatment induced higher serum levels of IL-10 (Figure 2D). Reflecting the biologic relevance of these alterations in IL-10, we also observed a correlation of increased levels of IL-12 (Figure 2E) and IFNγ (Figure 2F) with the lower IL-10 levels seen in *HMOX1*-deficient mice.

Association of TLR-9–induced MAS with increased HO-1–positive cellularity in mouse spleens. Given our data that CpG increased protein levels of HO-1 in BMMs in a TLR-9–dependent manner, and clinical reports that serum HO-1 is increased in patients with hemophagocytic syndromes (2,3), we next assessed HO-1 levels in the TLR-9–MAS murine model (8). HO-1 is constitutively high in the mouse spleen (30,31); however, whether there are additional increases during TLR-9–mediated inflammation is unknown. Relative to PBS-treated control mice, spleens from mice receiving CpG treatment contained a large population of HO-1–positive cells as assessed by immunohistochemical analyses (Figure 3A) and also as determined according to the number of HO-1–positive cells (Figure 3B). We additionally demonstrated increased total splenic HO-1 content by Western blotting of spleen lysates from mice receiving CpG treatment (Figures 3C and D). Thus, HO-1 levels are increased in vivo by CpG treatment, which is consistent with our in vitro data.

The HO-1 response in vivo could be attributable to direct effects of TLR-9 signaling or to downstream mediators, in particular IFNγ, which is elevated in these mice and required for disease development and progression. IFNγ has been reported to act in concert with lipopolysaccharide to induce HO-1 in macrophages (32). We therefore investigated if IFNγ has any influence on TLR-9–driven HO-1 induction in vivo. We treated WT and IFNγ$^{-/-}$ mice with repeated CpG stimulation, additionally including add-back therapy of IFNγ intraperitoneally. We observed a significant increase in HO-1–positive cells in IFNγ$^{-/-}$ mice injected with CpG, irrespective of exogenous administration of IFNγ. Additionally, IFNγ alone did not induce HO-1 (Figure 3E and Supplementary Figure 2, available on the *Arthritis & Rheumatology* website at http://onlinelibrary.wiley.com/doi/10.1002/art.41591/abstract). These results suggest that in vivo TLR-9 stimulation increases splenic HO-1 expression independent of IFNγ.

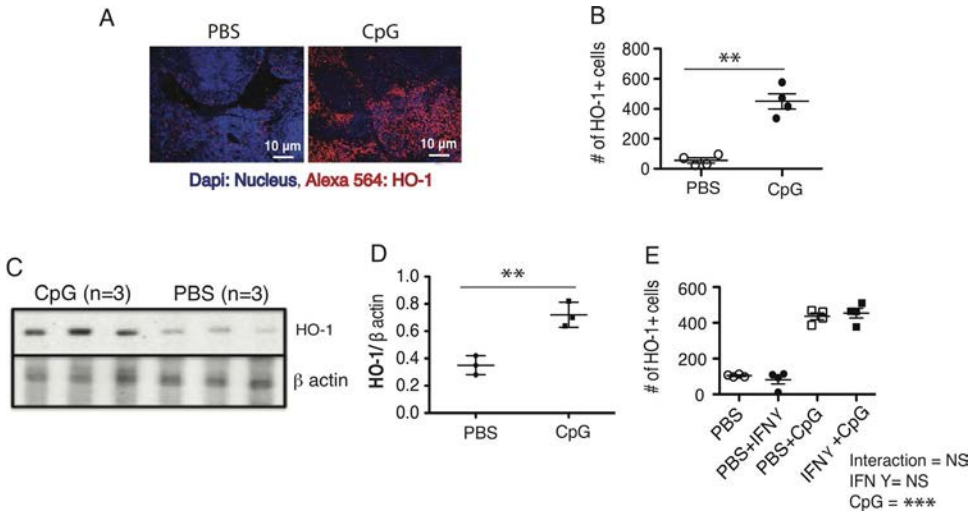

Figure 3. Effects of CpG treatments on mouse splenic HO-1 expression in vivo. **A**, Representative images from immunohistochemical analysis of spleen sections from CpG-treated wild-type mice show increased numbers of cells expressing HO-1. **B**, The results were quantified as the number of cells per high-power field (20× magnification) in 8 different fields. **C**, HO-1 levels were assessed by Western blotting of homogenates of lymphocyte suspensions from the spleens of *HMOX1*$^{fl/fl}$ mice. Results are representative of 4 experiments. **D**, Western blot findings were quantified as the number of cells per high-power field (60× magnification). Results in spleens from interferon-γ (IFNγ)–KO mice are described in Supplementary Figure 3 (available on the *Arthritis & Rheumatology* website at http://onlinelibrary.wiley.com/doi/10.1002/art.41591/abstract). **E**, The number of HO-1+ splenic cells per high-power field (60× magnification) was determined in each treatment group with or without IFNγ add-back therapy. In **B**, **D**, and **E**, symbols represent individual mice; bars show the mean ± SEM. ** = $P < 0.01$; *** = $P < 0.005$ by Student's unpaired 2-tailed *t*-test in **B**–**D** and by two-way ANOVA in **E**. NS = not significant (see Figure 1 for other definitions).

Increased Nrf2/HO-1 activity and reduction of MAS pathologic changes by MMF. After we established a role for myeloid HO-1 in IL-10 production via CO, we became interested in manipulation of this pathway to treat MAS. Of note, we have already established a protective role for IL-10 in the TLR-9–MAS murine model in previous studies (8,33). Taken together, these data raise the possibility that increasing levels of myeloid HO-1, and subsequently IL-10, might be able to counteract this inflammation and protect against disease. We postulated that pharmacologically enhancing Nrf2 activity using MMF could augment downstream HO-1 activity and IL-10 levels to suppress IFNγ and MAS pathology. To validate this approach, we first checked if MMF, a reported Nrf2/HO-1 inducer (23), could induce HO-1 in mouse spleen macrophages. Mice were injected with MMF intraperitoneally every 12 hours over 3 doses. Spleens were harvested 4 hours after the last dose, and plastic-adherent macrophages from splenic single-cell suspensions were assessed for Nrf2 and HO-1 expression level by Western blotting (Supplementary Figure 3A, available on the *Arthritis & Rheumatology* website at http://onlinelibrary.wiley.com/doi/10.1002/art.41591/abstract). The immunologic signal from Nrf2 and HO-1 was significantly increased in MMF-treated mice compared to the control group (Figure 4A).

Next, we investigated if MMF therapy could enhance systemic IL-10 production and resolve MAS pathology. Mice were injected with MMF or DMSO (control) twice a day, along with a simultaneous CpG injection every other day. On day 10, serum levels of IL-10 were significantly higher in MMF-treated mice compared to control mice (Figure 4B). This finding was also associated with a simultaneous decrease in the levels of proinflammatory cytokines such as IL-12 and IFNγ (Figure 4B). Additionally, MMF treatment corrected erythrocyte and platelet counts in the blood to control levels seen in mice treated with DMSO alone or MMF alone (Figures 4C and D). MMF treatment also reduced the organomegaly occurring in both the spleens and livers of mice (Figures 4E and F), a finding that was also confirmed based on the reduced cellularity observed in the mouse spleens (Supplementary Figure 3B, available on the *Arthritis & Rheumatology* website at http://onlinelibrary.wiley.com/doi/10.1002/art.41591/abstract). Taken together, these data establish that MMF therapy increases levels of Nrf2/HO-1 in macrophages, increases serum levels of IL-10 in TLR-9–induced MAS, and protects against multiple manifestations of TLR-9–induced MAS disease activity.

Mediation of the protective effects of MMF therapy on TLR-9–induced MAS primarily through HO-1 activity. In order to test whether MMF exerts its activity through HO-1, we repeated similar MMF treatments in CpG-treated *HMOX1*^{WT} and *HMOX1*$^{fl/fl}$ mice. As anticipated, serum IL-10 was elevated 3-fold by MMF in *HMOX1*^{WT} mice; however, this effect was completely lost in *HMOX1*$^{fl/fl}$ mice (Figure 5A). Consistent with our prior results, *HMOX1*$^{fl/fl}$ mice had a slightly higher amount of IL-12 (Figure 5B) and IFNγ (Supplementary Figure 4, available on the *Arthritis & Rheumatology* website at

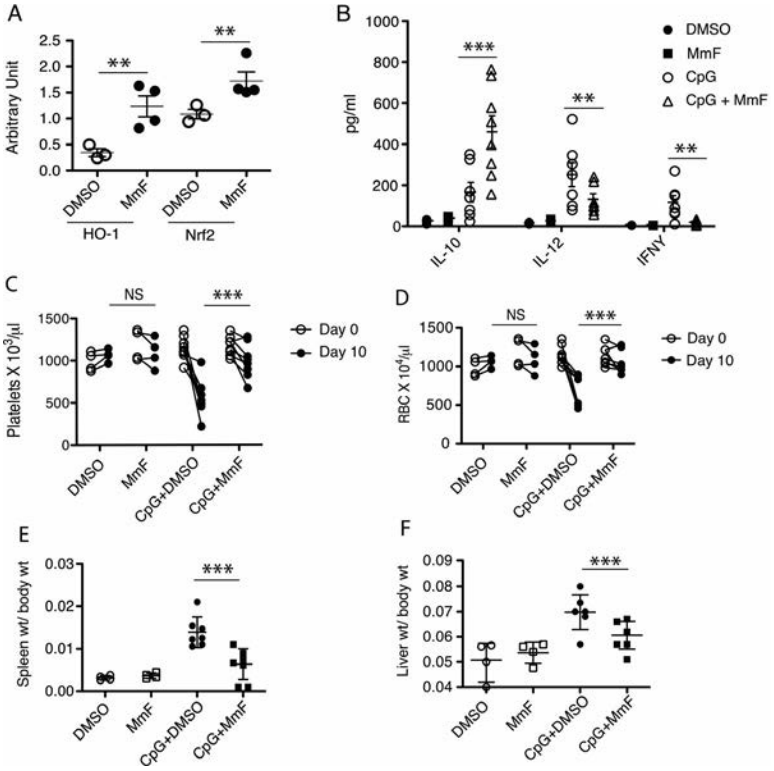

Figure 4. Activation of the Nrf2/HO-1 axis and amelioration of TLR-9–driven macrophage activation syndrome (MAS) by monomethyl fumarate (MMF). Mice were injected with MMF or DMSO twice a day, with the final dose injected ~4 hours prior to euthanasia. Single-cell suspensions were prepared from harvested spleen tissue and seeded on plastic tissue culture dishes. After 2 hours of incubation, the adherent macrophages were collected and lysed, and Nrf2 and HO-1 levels were assessed by Western blotting. Results are representative of 3 experiments (the effects of MMF therapy on interferon-γ [IFNγ] levels are shown in Supplementary Figure 4, available on the *Arthritis & Rheumatology* website at http://onlinelibrary.wiley.com/doi/10.1002/art.41591/abstract). **A**, Macrophage expression of HO-1 and Nrf2 was assessed in DMSO- and MMF-treated mice. Values were normalized to those of their respective loading controls. **B**, Mice were treated with DMSO, MMF, CpG, or CpG and MMF, and serum levels of interleukin-10 (IL-10), IL-12, and IFNγ were measured by enzyme-linked immunosorbent assay. **C** and **D**, Platelet counts (**C**) and red blood cell (RBC) counts (**D**) were determined in the treatment groups described in **B**, prior to the first dose of CpG (day 0) and 24 hours after the last dose of CpG (day 10). Values are the mean counts. **E** and **F**, Spleen weight (wt) to body weight ratios (**E**) and liver weight to body weight ratios (**F**) were determined in the treatment groups described in **B**. In **A**, **B**, **E**, and **F**, symbols represent individual samples; bars show the mean ± SEM. ** = $P < 0.01$; *** = $P < 0.005$ by Student's unpaired *t*-test in **A**, **B**, **E**, and **F** and by two-way ANOVA for day 10 versus day 0 in **C** and **D**. NS = not significant (see Figure 1 for other definitions).

http://onlinelibrary.wiley.com/doi/10.1002/art.41591/abstract) relative to *HMOX1*^{WT} mice. IL-12 was slightly reduced by MMF treatment, but in an HO-1–independent manner. IFNγ was unaffected by MMF therapy in these experiments, perhaps owing to the difference in the background of the HMOX1 mice compared to the inbred C57BL/6 mice used in previous experiments. Interestingly, despite this alteration in cytokine levels, the *HMOX1*$^{fl/fl}$ mice did not have significantly worsened disease (Figures 5C–F). We have observed in many different scenarios that small amounts of IL-10 remain protective in the TLR-9–MAS model, and so the residual IL-10 production seen in HO-1 deficiency both in vitro and in vivo may explain why the disease is not significantly more severe in HO-1–deficient mice. While loss of function of HO-1 did not affect disease, gain of function through MMF treatment clearly improved disease parameters. This was further confirmed by the observation that MMF-treated *HMOX1*^{WT} mice experienced almost complete recovery from anemia and thrombocytopenia, and *HMOX1*$^{fl/fl}$ mice experienced a partial recovery (Figures 5C and D), demonstrating that the full effect of MMF requires the presence of functional myeloid HO-1.

Improvement of organomegaly by MMF in an HO-1–independent manner. MMF partially protected *HMOX1*$^{fl/fl}$ mice from hepatosplenomegaly, suggesting an HO-1–independent effect of MMF (Figures 5E and F). In order to better investigate these effects, we carefully examined histologic features of the liver tissue in these animals. Livers from WT mice and *HMOX1*$^{fl/fl}$ mice were completely normal in appearance at baseline (Supplementary Figure 5, available on the *Arthritis & Rheumatology* website at http://onlinelibrary.wiley.com/doi/10.1002/art.41591/abstract). However, upon CpG treatment, livers from *HMOX1*$^{fl/fl}$ mice had an increased degree of lobular and portal inflammatory infiltration

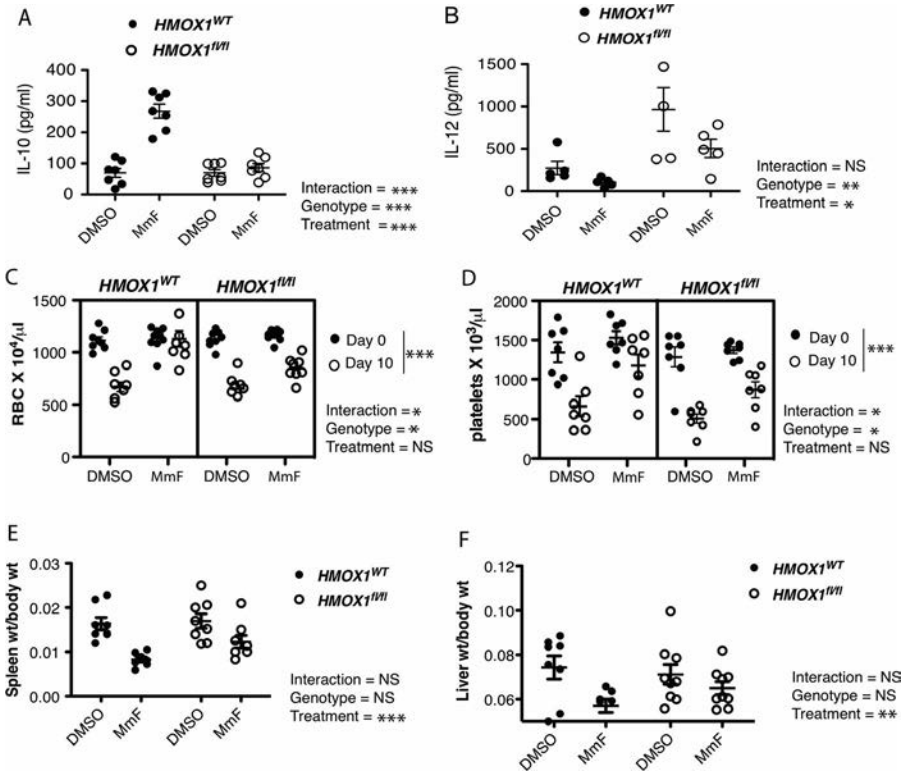

Figure 5. HO-1–dependent effects of monomethyl fumarate (MMF) therapy on the disease manifestations of TLR-9–induced macrophage activation syndrome (MAS) in mice. *HMOX1*^{wt} and *HMOX1*$^{fl/fl}$ mice were treated with 5 doses of CpG to induce MAS, and MMF or DMSO was then administered twice daily. Mice were euthanized on day 10 for assessment of MAS disease activity parameters. **A** and **B**, Serum measurements of interleukin-10 (IL-10) (**A**) and IL-12 (**B**) were determined by enzyme-linked immunosorbent assay. **C** and **D**, Red blood cell (RBC) counts (**C**) and platelet counts (**D**) were determined. **E** and **F**, Spleen weight (wt) to body weight ratios (**E**) and liver weight to body weight ratios (**F**) were also measured. Symbols represent individual mice; bars show the mean ± SEM. * = $P < 0.05$; ** = $P < 0.01$; *** = $P < 0.005$ by two-way ANOVA. NS = not significant (see Figure 1 for other definitions).

(Figures 6A and B), suggesting a role for endogenous HO-1 in limiting hepatic inflammation induced by TLR-9–driven MAS, even though no change in the disease parameters noted above were otherwise observed in mice. MMF was able to reduce previously mentioned indications of disease activity in both WT mice and *HMOX1*$^{fl/fl}$ mice, demonstrating a non–HO-1 mechanism for MMF in reducing hepatic inflammation induced by TLR-9–driven MAS. Additionally, MMF was able to reduce histologic evidence of endothelial activation independent of mouse genotype (Figure 6C), also suggesting HO-1–independent effects of the drug.

DISCUSSION

Increases in markers of iron metabolism, including hyperferritinemia and excessive serum HO-1, have been well described in hyperinflammation or cytokine storms. However, functional roles for these molecules in disease progression remain incompletely understood. Our present investigation utilizes the MAS mouse model of repeated TLR-9 activation, which exhibits many clinical features of MAS including hyperferritinemia, sustained amplification of tissue inflammatory monocytes and macrophages, cytopenia, organomegaly, and pathology driven by IFNγ. Studying both loss of function using the *HMOX1*$^{fl/fl}$ mouse model, and gain of function using MMF therapy, we delineate a role for HO-1 in controlling TLR-9–induced IL-10. However, this IL-10 source is redundant, as deleting *HMOX1* does not eliminate all IL-10, nor does it result in significant worsening of disease. Additionally, MMF therapy administered to *HMOX1*$^{fl/fl}$ mice resulted in significant protection against disease worsening as determined based on a number of disease activity parameters despite the fact that levels of IL-10 do not increase in response to MMF treatment in these mice. This suggests that MMF has at least some IL-10–independent functions. The extent to which the effects of MMF on the serum levels of IL-10 play a role in the reduction of inflammation needs further exploration. Nonetheless, these data help set the stage for considering MMF therapy, or its US Food and Drug Administration–approved parent compound, DMF, in the treatment of hyperinflammatory syndromes, even if levels of ferritin and HO-1 may already be elevated.

Multiple recent studies on Nrf2 regulation by TLR activation and immunomodulation have documented the intersection of these 2 pathways (15,34). Herein, we demonstrate that TLR-9 activation is also associated with Nrf2 induction (Figures 1 and 4). Nrf2 regulates genes, including HO-1, involved in the response to

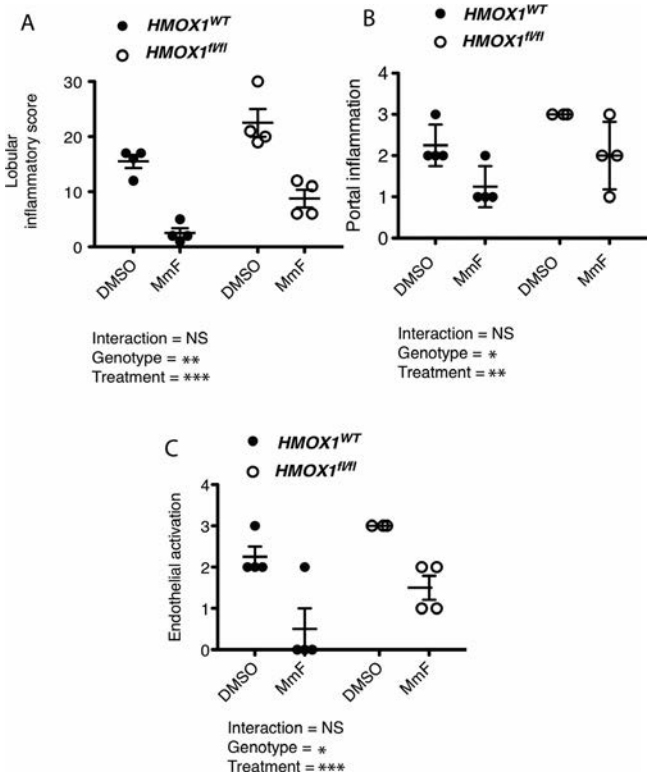

Figure 6. Improvement of hepatic inflammation by monomethyl fumarate (MMF) treatment in an HO-1–independent manner. Hematoxylin and eosin–stained tissue sections from the livers of mice with TLR-9–induced macrophage activation syndrome (MAS) were assessed according to genotype and treatment. Representative results are shown. A pathologist who was blinded with regard to the treatment groups scored the tissue for various histologic features, including lobular (**A**) and portal (**B**) inflammatory scores and endothelial activation (**C**). Results in **A** are the number of inflammatory foci per high-power field (100× magnification) in the most involved area. Scores in **B** are on a scale of 0–4, with 0 indicating absence of inflammation and 4 representing severe inflammation. Scores in **C** indicate the presence of morphologic changes in vascular endothelial cells on a scale of 0–4, with 0 being normal and 4 representing severe changes, including rounding of cells, plumpness of cytoplasm, and enlargement of nuclei. Symbols represent individual mice; bars show the mean ± SEM. * = $P < 0.05$; ** = $P < 0.01$; *** = $P < 0.005$ by two-way ANOVA. NS = not significant (see Figure 1 for other definitions).

oxidative stress. Though HO-1 is typically studied in the context of heme metabolism, we established a link between HO-1 activity and TLR-9–induced IL-10 production in the present study. This important link between TLR-9–induced Nrf2 and IL-10 production, which can be therapeutically manipulated by MMF, demonstrates the clinical importance of dissecting this biologic process. Further studies that uncover more specific or more potent regulators of this signaling cascade may provide even better therapeutic targets.

Like nitric oxide, CO is known to bind the gaseous receptor soluble guanylyl cyclase (sGC), which converts GTP to cGMP (35,36). This biochemical step is involved in increased protein phosphorylation by the activation of protein kinases (MAP kinases) and has been studied for its antithrombotic effects, among others (37,38). Herein, we demonstrate a role for CO in the regulation of IL-10, and future work will investigate whether sGC or other downstream signaling molecules mediate this effect. Treatment with low-dose CO (100–125 parts per million) was tolerated in early-phase clinical trials in patients with idiopathic pulmonary fibrosis or chronic obstructive pulmonary disease and was shown to reduce certain aspects of disease progression (39,40). We demonstrate in mouse BMMs that the CO-releasing molecule CORM-2 was able to bypass HO-1 deficiency and rescue TLR-9–induced IL-10 production in mice (Figure 2). This suggests a role for HO-1 enzyme activity in IL-10 production via CO. However, CO obviously has a small therapeutic window, and given that the effects of the MMF/Nrf2/HO-1 axis are clearly larger than IL-10 induction, targeting other molecules in this pathway is perhaps more desirable, which highlights the need for additional studies to understand these biologic processes.

Accordingly, we note that while a number of the effects of MMF therapy operated through HO-1 in the TLR-9–MAS model (Figure 4), organomegaly appeared to have MMF-responsive, HO-1–independent effects (Figure 5). In these cases, MMF effects could be Nrf2-dependent but HO-1–independent, or they could be mediated independent of both Nrf2 and HO-1. Nrf2 controls the transcription of dozens of genes beyond *Hmox1*, many of which have been shown to interact with inflammatory signaling (15). It is therefore of interest to consider how MMF therapy might have other antiinflammatory effects beyond HO-1–induced IL-10 production. Dissection of this biologic process may reveal additional therapeutic targets of importance in cytokine storms.

It is not likely that HO-1 and ferritin are elevated in hemophagocytic syndromes specifically to regulate IL-10 from an evolutionary perspective. Heme, an essential prosthetic moiety of hemoproteins, is typically involved in crucial biologic processes, related to primarily oxygen transport, metabolism, and storage as well as electron transfer. Heme and iron may be sequestered during inflammation as part of a response to prevent bacteria from utilizing these metabolites for their life cycle (41). Thus, it makes sense for this process to invoke heme metabolic pathways when systemic inflammation is present as part of an attempt to make the environment less hospitable for pathogens. However, excessive free iron produced by HO-1 activity is highly toxic and causes oxidative stress, which contributes to lipid peroxidation and lipid membrane injury, thereby leading to apoptosis. The protective antioxidant responses needed to manage such iron sequestration are well known to invoke antiinflammatory pathways as well. Thus, it is a potentially advantageous side effect of iron sequestration activity that these pathways can also act as a "brake" on inflammation. Pharmacologically targeting these antioxidant/anti-inflammatory pathways provides a novel approach to enhancing the organism's own mechanisms as a way to limit pathologic systemic inflammation.

Interestingly, MMF is the biologically active metabolite of the parent compound DMF, which is an FDA-approved drug used primarily for the treatment of relapsing–remitting multiple sclerosis. The promising results of MMF therapy in the TLR-9–MAS model suggest the value of continued exploration of both DMF and MMF treatment in systemic inflammation at the basic and translational levels. The present study supports the notion that these agents may be a novel approach in the treatment of MAS that needs to be further evaluated in human studies.

ACKNOWLEDGMENT

We would like to thank Scott M. Gordon for his review and proofreading of this manuscript.

AUTHOR CONTRIBUTIONS

All authors were involved in drafting the article or revising it critically for important intellectual content, and all authors approved the final version to be published. Dr. Behrens had full access to all of the data in the study and takes responsibility for the integrity of the data and the accuracy of the data analysis.

Study conception and design. Biswas, Behrens.
Acquisition of data. Biswas, Chu, Burn, Kreiger.
Analysis and/or interpretation of data. Biswas, Behrens.

REFERENCES

1. Weaver LK, Behrens EM. Hyperinflammation, rather than hemophagocytosis, is the common link between macrophage activation syndrome and hemophagocytic lymphohistiocytosis [review]. Curr Opin Rheumatol 2014;26:562–9.
2. Takahashi A, Mori M, Naruto T, Nakajima S, Miyamae T, Imagawa T, et al. The role of heme oxygenase-1 in systemic-onset juvenile idiopathic arthritis. Mod Rheumatol 2009;19:302–8.
3. Kirino Y, Takeno M, Iwasaki M, Ueda A, Ohno S, Shirai A, et al. Increased serum HO-1 in hemophagocytic syndrome and adult-onset Still's disease: use in the differential diagnosis of hyperferritinemia. Arthritis Res Ther 2005;7:R616–24.
4. Schaer DJ, Schaer CA, Schoedon G, Imhof A, Kurrer MO. Hemophagocytic macrophages constitute a major compartment of heme oxygenase expression in sepsis. Eur J Haematol 2006;77:432–6.
5. Ohyagi H, Onai N, Sato T, Yotsumoto S, Liu J, Akiba H, et al. Monocyte-derived dendritic cells perform hemophagocytosis to fine-tune excessive immune responses. Immunity 2013;39:584–98.
6. Bogdan C, Vodovotz Y, Nathan C. Macrophage deactivation by interleukin 10. J Exp Med 1991;174:1549–55.
7. Ng TH, Britton GJ, Hill EV, Verhagen J, Burton BR, Wraith DC. Regulation of adaptive immunity; the role of interleukin-10 [review]. Front Immunol 2013;4:129.
8. Behrens EM, Canna SW, Slade K, Rao S, Kreiger PA, Paessler M, et al. Repeated TLR9 stimulation results in macrophage activation syndrome-like disease in mice. J Clin Invest 2011;121:2264–77.
9. Bracaglia C, de Graaf K, Marafon DP, Guilhot F, Ferlin W, Prencipe G, et al. Elevated circulating levels of interferon-γ and interferon-γ-induced chemokines characterise patients with macrophage activation syndrome complicating systemic juvenile idiopathic arthritis. Ann Rheum Dis 2017;76:166–72.
10. Girard-Guyonvarc'h C, Palomo J, Martin P, Rodriguez E, Troccaz S, Palmer G, et al. Unopposed IL-18 signaling leads to severe TLR9-induced macrophage activation syndrome in mice. Blood 2018;131:1430–41.
11. Kikuchi G, Yoshida T, Noguchi M. Heme oxygenase and heme degradation. Biochem Biophys Res Commun 2005;338:558–67.
12. Loboda A, Damulewicz M, Pyza E, Jozkowicz A, Dulak J. Role of Nrf2/HO-1 system in development, oxidative stress response and diseases: an evolutionarily conserved mechanism. Cellular Mol Life Sci 2016;73:3221–47.
13. Tenhunen R, Marver HS, Schmid R. Microsomal heme oxygenase: characterization of the enzyme. J Biol Chem 1969;244:6388–94.
14. Sun J, Brand M, Zenke Y, Tashiro S, Groudine M, Igarashi K. Heme regulates the dynamic exchange of Bach1 and NF-E2-related factors in the Maf transcription factor network. Pro Natl Acad Sci U S A 2004;101:1461–6.
15. Cuadrado A, Manda G, Hassan A, Alcaraz MJ, Barbas C, Daiber A, et al. Transcription factor NRF2 as a therapeutic target for chronic diseases: a systems medicine approach [review]. Pharmacol Rev 2018;70:348–83.
16. Davudian S, Mansoori B, Shajari N, Mohammadi A, Baradaran B. BACH1, the master regulator gene: a novel candidate target for cancer therapy. Gene 2016;588:30–7.
17. Abraham NG, Kappas A. Pharmacological and clinical aspects of heme oxygenase [review]. Pharmacol Rev 2008;60:79–127.
18. Rohrer JS, Joo MS, Dartyge E, Sayers DE, Fontaine A, Theil EC. Stabilization of iron in a ferrous form by ferritin: a study using dispersive and conventional x-ray absorption spectroscopy. J Biol Chem 1987;262:13385–7.
19. Uddin MJ, Li CS, Joe Y, Chen Y, Zhang Q, Ryter SW, et al. Carbon monoxide inhibits tenascin-C mediated inflammation via IL-10 expression in a septic mouse model. Mediators Inflamm 2015;2015:613249.
20. Bock KW, Kohle C. Contributions of the Ah receptor to bilirubin homeostasis and its antioxidative and atheroprotective functions. Biol Chem 2010;391:645–53.
21. Sheikh SZ, Hegazi RA, Kobayashi T, Onyiah JC, Russo SM, Matsuoka K, et al. An anti-inflammatory role for carbon monoxide and heme oxygenase-1 in chronic Th2-mediated murine colitis. J Immunol 2011;186:5506–13.
22. Gold R, Arnold DL, Bar-Or A, Hutchinson M, Kappos L, Havrdova E, et al. Long-term effects of delayed-release dimethyl fumarate in multiple sclerosis: interim analysis of ENDORSE, a randomized extension study. Mult Scler 2017;23:253–65.
23. Cho H, Hartsock MJ, Xu Z, He M, Duh EJ. Monomethyl fumarate promotes Nrf2-dependent neuroprotection in retinal ischemia-reperfusion. J Neuroinflammation 2015;12:239.
24. Singh D, Reeta KH, Sharma U, Jagannathan NR, Dinda AK, Gupta YK. Neuro-protective effect of monomethyl fumarate on ischemia reperfusion injury in rats: role of Nrf2/HO1 pathway in peri-infarct region. Neurochem Int 2019;126:96–108.
25. Biswas C, Shah N, Muthu M, La P, Fernando AP, Sengupta S, et al. Nuclear heme oxygenase-1 (HO-1) modulates subcellular distribution and activation of Nrf2, impacting metabolic and anti-oxidant defenses. J Biol Chem 2014;289:26882–94.
26. Weaver LK, Chu N, Behrens EM. TLR9-mediated inflammation drives a Ccr2-independent peripheral monocytosis through enhanced extramedullary monocytopoiesis. Proc Natl Acad Sci U S A 2016;113:10944–9.
27. Yao Y, Miao W, Liu Z, Han W, Shi K, Shen Y, et al. Dimethyl fumarate and monomethyl fumarate promote post-ischemic recovery in mice. Transl Stroke Res 2016;7:535–47.
28. Nowis D, Bugajski M, Winiarska M, Bil J, Szokalska A, Salwa P, et al. Zinc protoporphyrin IX, a heme oxygenase-1 inhibitor, demonstrates potent antitumor effects but is unable to potentiate antitumor effects of chemotherapeutics in mice. BMC Cancer 2008;8:197.
29. Schallner N, Pandit R, LeBlanc R III, Thomas AJ, Ogilvy CS, Zuckerbraun BS, et al. Microglia regulate blood clearance in

subarachnoid hemorrhage by heme oxygenase-1. J Clin Invest 2015; 125:2609–25.

30. Braggins PE, Trakshel GM, Kutty RK, Maines MD. Characterization of two heme oxygenase isoforms in rat spleen: comparison with the hematin-induced and constitutive isoforms of the liver. Biochem Biophys Res Commun 1986;141:528–33.
31. Maines MD, Trakshel GM, Kutty RK. Characterization of two constitutive forms of rat liver microsomal heme oxygenase: only one molecular species of the enzyme is inducible. J Biol Chem 1986;261:411–9.
32. Koike A, Minamiguchi I, Fujimori K, Amano F. Nitric oxide is an important regulator of heme oxygenase-1 expression in the lipopolysaccharide and interferon-γ-treated murine macrophage-like cell line J774.1/JA-4. Biol Pharm Bull 2015;38:7–16.
33. Weaver LK, Chu N, Behrens EM. Interferon-γ–mediated immunopathology potentiated by Toll-like receptor 9 activation in a murine model of macrophage activation syndrome. Arthritis Rheumatol 2019;71:161–8.
34. Mohan S, Gupta D. Crosstalk of Toll-like receptors signaling and Nrf2 pathway for regulation of inflammation. Biomed Pharmacother 2018;108:1866–78.
35. Pan J, Yuan H, Zhang X, Zhang H, Xu Q, Zhou Y, et al. Probing the molecular mechanism of human soluble guanylate cyclase activation by NO in vitro and in vivo. Sci Rep 2017;7:43112.
36. Makino R, Obata Y, Tsubaki M, Iizuka T, Hamajima Y, Kato-Yamada Y, et al. Mechanistic insights into the activation of soluble guanylate cyclase by carbon monoxide: a multistep mechanism proposed for the BAY 41–2272 induced formation of 5-coordinate CO-heme. Biochemistry 2018;57:1620–31.
37. Soni H, Jain M, Mehta AA. Investigation into the mechanism(s) of antithrombotic effects of carbon monoxide releasing molecule-3 (CORM-3). Thromb Res 2011;127:551–9.
38. Brune B, Ullrich V. Inhibition of platelet aggregation by carbon monoxide is mediated by activation of guanylate cyclase. Mol Pharmacol 1987;32:497–504.
39. Casanova N, Zhou T, Gonzalez-Garay ML, Rosas IO, Goldberg HJ, Ryter SW, et al. Low dose carbon monoxide exposure in idiopathic pulmonary fibrosis produces a CO signature comprised of oxidative phosphorylation genes. Sci Rep 2019;9:14802.
40. Gomperts E, Belcher JD, Otterbein LE, Coates TD, Wood J, Skolnick BE, et al. The role of carbon monoxide and heme oxygenase in the prevention of sickle cell disease vaso-occlusive crises. Am J Hematol 2017;92:569–82.
41. Wang L, Cherayil BJ. Ironing out the wrinkles in host defense: interactions between iron homeostasis and innate immunity. J Innate Immun 2009;1:455–64.

American College of Rheumatology
Empowering Rheumatology Professionals

Arthritis & Rheumatology
Vol. 73, No. 5, May 2021, pp 896–902

LETTERS

DOI: 10.1002/art.41643

Regulatory action to protect access to hydroxychloroquine for approved rheumatic indications during COVID-19 in New Zealand

To the Editor:

The rapid spread of coronavirus disease 2019 (COVID-19) brought into sharp focus the conundrum of how to balance evidence-based prescribing versus empirical treatment with repurposed drugs for a pandemic with a high mortality risk. Initial attention focused on hydroxychloroquine (HCQ)/chloroquine (CQ) due to evidence of in vitro activity against the novel severe acute respiratory syndrome coronavirus 2 (1), yet the external validity of these data was limited by knowledge that in vitro antiviral activity did not equate to efficacy in randomized controlled trials (RCTs) of HCQ/CQ treatment for influenza, dengue fever, chikungunya virus, and HIV infection (1). Nonetheless, there was unprecedented interest in HCQ/CQ for use in clinical practice before the results of RCTs were available, potentially affecting medication supply for rheumatology patients.

On March 28, 2020, the US Food and Drug Administration (FDA) issued an emergency use authorization for HCQ/CQ in hospitalized COVID-19 patients in the US (2). Following reports of HCQ toxicity in COVID-19, the FDA issued a statement of caution on April 24, 2020, and the emergency use authorization was revoked on June 15, 2020 after findings from RCTs demonstrated that HCQ was not effective for treating COVID-19 and exposed patients to risk of serious adverse events (2). These actions were associated with a 7-fold increase in new community HCQ/CQ prescriptions during the month of March 2020, compared with March 2019, attributable to clinicians who did not routinely prescribe HCQ/CQ (3) and a marked increase in off-label prescriptions for COVID-19 (4). New prescriptions for HCQ in the US in June 2020 remained slightly higher (1.3-fold) than in June 2019 (3).

New Zealand charted a different regulatory path, limiting funded use of HCQ to approved indications, such as rheumatic conditions, on March 24, 2020 (5). CQ is not approved for use in New Zealand. The weeks beginning March 15 and March 22, 2020 saw 4.8-fold and 3.7-fold increases in new HCQ users, respectively. However, prescribing then immediately returned to levels comparable to previous years. Mean rates of new HCQ use in New Zealand (2017–2020) and new HCQ/CQ use in the US (2019–2020) are shown in Figure 1.

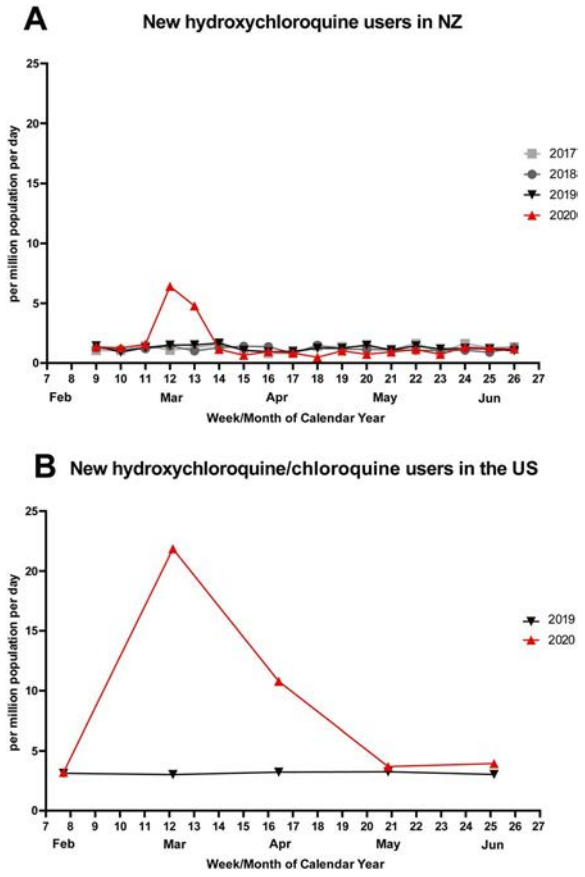

Figure 1. Mean rates of new hydroxychloroquine (HCQ) use (defined as a filled prescription for HCQ for a patient with no previous dispensing records for HCQ) for 2017–2020 in New Zealand (NZ) (**A**), and of new HCQ/CQ use for 2019 and 2020 in the US (**B**). In New Zealand, the majority of outpatient medications, including HCQ, are publicly funded, and centralized data on funded community use of medications are maintained by the Ministry of Health. New HCQ use in New Zealand increased significantly during 2 weeks in March 2020 (4.8-fold and 3.7-fold) but then returned to rates comparable to previous years. In the US, published monthly data on new prescriptions for HCQ/chloroquine (CQ) are available for comparison (3). New HCQ/CQ use in the US increased 7.2-fold in March 2020 compared to March 2019. Subsequent months were notable for increases in HCQ/CQ prescriptions of 3.3-fold (April), 1.1-fold (May), and 1.3-fold (June) compared to the same months in 2019.

While the contrasting patterns of use between New Zealand and the US likely reflect numerous differences between the 2 countries, including cultural factors, nonpharmaceutical public health interventions, and contrasting health care and political

situations (6), these data suggest that regulatory policy in each country influenced the use of HCQ/CQ for COVID-19.

What can we learn from the differing experiences in New Zealand and the US? When potential medications for COVID-19 are proposed for clinical use without RCT evidence of efficacy and safety, strong regulatory action to restrict access circumvents excessive medication dispensing that may cause shortages.

Eamon Duffy, BPharm
Nicola Arroll, MPH
Auckland District Health Board
Auckland, New Zealand
Richard Beasley, MBChB, MD, DSc
Medical Research Institute of New Zealand and Capital and Coast District Health Board
Wellington, New Zealand
Thomas Hills, MBChB, MSc, DPhil
Auckland District Health Board
Auckland, New Zealand
and Medical Research Institute of New Zealand
Wellington, New Zealand

1. Roustit M, Guilhaumou R, Molimard M, Drici MD, Laporte S, Montastruc JL, et al. Chloroquine and hydroxychloroquine in the management of COVID-19: much kerfuffle but little evidence [review]. Therapie 2020;75:363–70.
2. US Food and Drug Administration. Coronavirus (COVID-19) update: FDA revokes emergency use authorization for chloroquine and hydroxychloroquine. June 2020. URL: https://www.fda.gov/news-events/press-announcements/coronavirus-covid-19-update-fda-revokes-emergency-use-authorization-chloroquine-and.
3. Bull-Otterson L, Gray EB, Budnitz DS, Strosnider HM, Schieber LZ, Courtney J, et al. Hydroxychloroquine and chloroquine prescribing patterns by provider specialty following initial reports of potential benefit for COVID-19 treatment—United States, January–June 2020. MMWR Morb Moral Wkly Rep 2020;69:1210–5.
4. Vaduganathan M, van Meijgaard J, Mehra MR, Joseph J, O'Donnell CJ, Warraich HJ. Prescription fill patterns for commonly used drugs during the COVID-19 pandemic in the United States. JAMA 2020;323:2524–56.
5. PHARMAC. COVID-19: Hydroxychloroquine. URL: https://pharmac.govt.nz/news-and-resources/covid19/covid-19-hydroxychloroquine/.
6. Baker MG, Wilson N, Anglemyer A. Successful elimination of Covid-19 transmission in New Zealand [letter]. N Engl J Med 2020;383:e56.

DOI 10.1002/art.41634

Antiphospholipid autoantibodies and thrombosis in patients with COVID-19: comment on the article by Bertin et al

To the Editor:

We read with great interest the letter by Bertin et al (1) on their study exploring the involvement of antiphospholipid antibodies (aPLs) in a cohort of patients with severe acute respiratory syndrome coronavirus 2 (SARS–COV-2). Bertin and colleagues observed that levels of IgG anticardiolipin antibodies (aCLs) were significantly associated with severe coronavirus disease 2019 (COVID-19) manifestations (odds ratio [OR] 6.50; $P = 0.009$).

Helms et al reported that a significant number of patients with COVID-19–related acute respiratory distress syndrome (ARDS) developed life-threatening thrombotic complications, with 25% of computed tomography pulmonary angiography findings showing pulmonary embolism (2). They also reported that 88% of patients tested were positive for lupus anticoagulant (LAC) during their intensive care unit (ICU) stay. Bowles et al also described abnormal coagulation test results, in particular the presence of LAC in 31 of 34 COVID-19 patients tested (91%) (3). Moreover, Zhang et al described 3 COVID-19 patients with thrombosis and an atypical pattern of aPLs, including IgA aCL and IgA anti–β_2-glycoprotein I (anti-β_2GPI) without LAC (4). The significance of IgA antibodies is not fully understood.

Positivity of aPLs may favor thrombotic events in patients with COVID-19–related ARDS via endothelial injury (5). We assessed the association between thrombotic complications during COVID-19–related ARDS and the presence of aPLs, including IgA aCL and IgA anti-β_2GPI. Levels of aPLs were measured using enzyme-linked immunosorbent assay (Inova Diagnostics), according to the manufacturer's instructions.

We conducted an observational single-center study, which included all patients with COVID-19–related ARDS confirmed by reverse transcriptase–polymerase chain reaction (n = 37), consecutively admitted to our ICU between March 8, 2020, and March 30, 2020. Patients with pneumonia-associated ARDS who were previously included in a single-center prospective cohort between January 2014 and December 2018 were used as controls (non–COVID-19–related ARDS group, n = 31). Levels of aPLs and biomarkers were measured within 48 hours of ICU admission. The thromboembolic events were retrospectively recorded.

Data on patient characteristics, aPL levels, and outcomes are shown in Table 1. Compared with patients with non–COVID-19–related ARDS, patients with COVID-19–related ARDS did not show significant differences regarding age, sex, associated comorbidities (except for more frequent obesity), severity scores (i.e., Sequential Organ Failure Assessment score and Simplified Acute Physiology Score II), and invasive mechanical ventilation support upon admission to the ICU. More thrombotic complications (including pulmonary embolism) were diagnosed in patients with COVID-19–related ARDS than in patients with non–COVID-19–related ARDS. Overall, the prevalence of aPLs did not differ significantly between patients with COVID-19–related ARDS and patients with non–COVID-19–related ARDS (11 [30%] versus 9 [29%], $P = 0.950$), no matter the type of antibody considered. The rate of thromboembolic events was similar in patients with versus those without aPLs (9 [45%] versus 23 [48%], $P = 0.83$), and these findings were similar when the type of aPL (IgA versus IgG/IgM) or the type of thrombotic event was separately considered (data not shown).

Table 1. Characteristics and outcomes of patients with COVID-19–related ARDS and those with non–COVID-19–related ARDS*

	COVID-19–related ARDS (n = 37)	Non–COVID-19–related ARDS (n = 31)	*P*†
Demographic characteristics and comorbidities			
Age, median (IQR) years‡	63 (50–73)	57 (42–70)	0.378
Male sex	31 (84)	24 (77)	0.506
Obesity§	13 (37)	4 (13)	0.025
Characteristics upon ICU admission			
SOFA score, median (IQR)	9 (6–10)	9 (6–11)	0.483
SAPS II score, median (IQR)	38 (32–45)	39 (31–54)	0.808
Invasive mechanical ventilation	19 (51)	18 (58)	0.476
Pao_2/Fio_2 ratio, median (IQR) mm Hg	126 (97–175)	91 (70–130)	0.017
$PaCo_2$, median (IQR) mm Hg§	40 (37–48)	46 (40–51)	0.110
Thrombotic events			
Any thromboembolic event	24 (65)	8 (26)	0.001
Pulmonary embolism	9 (24)	2 (7)	0.046
Thromboembolic disease¶	12 (32)	3 (10)	0.024
Renal replacement therapy circuit thrombosis#	11 (55)	0 (0)	0.001
aPL			
IgA aCL or IgA anti-β_2GPI	7 (19)	6 (19)	0.964
IgM or IgG aCL or IgM or IgG anti-β_2GPI	6 (16)	4 (13)	0.745
Any aPL	11 (30)	9 (29)	0.950
Outcomes			
Invasive mechanical ventilation	36 (97)	31 (100)	>0.99
Ventilator-associated pneumonia‡	27 (75)	13 (42)	0.006
Shock	28 (76)	21 (68)	0.468
Renal replacement therapy	20 (54)	15 (48)	0.641
Extracorporeal membrane oxygenation	9 (24)	8 (26)	0.888
No. organ failure–free days at day 28, median (IQR)**	0 (0–15)	14 (0–20)	0.004
Day-28 mortality††	12 (32)	3 (11)	0.040
ICU mortality‡‡	13 (50)	5 (16)	0.006

* Except where indicated otherwise, values are the number (%) of patients. COVID-19 = coronavirus disease 2019; ARDS = acute respiratory distress syndrome; IQR = interquartile range; ICU = intensive care unit; SOFA = Sequential Organ Failure Assessment; SAPS II = Simplified Acute Physiology Score II; Fio_2 = fraction of inspired oxygen; aPL = antiphospholipid antibody; aCL = anticardiolipin antibody; anti-β_2GPI = anti–β_2-glycoprotein I.
† Determined by Mann-Whitney test for continuous variables; by chi-square test or Fisher's exact test for categorical variables.
‡ Data were available for a total of 67 patients.
§ Data were available for a total of 66 patients.
¶ Thromboembolic disease denotes pulmonary embolism or deep venous thrombosis.
# Data were available for a total of 35 patients.
** Data were available for a total of 63 patients.
†† Data were available for a total of 65 patients.
‡‡ Data were available for a total of 57 patients.

In conclusion, we also observed that patients with COVID-19–related ARDS experienced more thrombotic events than patients with non–COVID-19–related ARDS. However, the occurrence of aPLs was of similar magnitude in patients with COVID-19–related ARDS and patients with non–COVID-19–related ARDS, with no significant association with thrombosis. The findings of Bertin et al could be related to the severity of the pulmonary condition regardless of the SARS–COV-2 infection (6). The pathophysiology of thrombosis in patients with COVID-19–related ARDS warrants further research.

T. Frapard, MD
Hôpitaux Universitaires Henri Mondor AP-HP and Université Paris-Est Créteil Val de Marne
S. Hue, MD, PhD
Hôpitaux Universitaires Henri Mondor AP-HP INSERM U955 and Université Paris Est Créteil
C. Rial, MD
Hôpitaux Universitaires Henri Mondor AP-HP
N. de Prost, MD, PhD
A. Mekontso Dessap, MD, PhD
Hôpitaux Universitaires Henri Mondor AP-HP and Université Paris-Est Créteil Val de Marne Créteil, France

1. Bertin D, Brodovitch A, Beziane A, Hug S, Bouamri A, Mege JL, et al. Anticardiolipin IgG autoantibody level is an independent risk factor for COVID-19 severity [letter]. Arthritis Rheumatol 72:1953–5.
2. Helms J, Tacquard C, Severac F, Leonard-Lorant I, Ohana M, Delabranche X, et al, and the Clinical Research in Intensive Care and Sepsis Trial Group for Global Evaluation and Research in Sepsis. High risk of thrombosis in patients with severe SARS-CoV-2 infection: a multicenter prospective cohort study. Intensive Care Med 2020;46:1089–98.
3. Bowles L, Platton S, Yartey N, Dave M, Lee K, Hart DP, et al. Lupus anticoagulant and abnormal coagulation tests in patients with COVID-19. N Engl J Med 2020;383:288–90.

4. Zhang Y, Xiao M, Zhang S, Xia P, Cao W, Jiang W, et al. Coagulopathy and antiphospholipid antibodies in patients with COVID-19. N Engl J Med 2020;382:e38.
5. Varga Z, Flammer AJ, Steiger P, Haberecker M, Andermatt R, Zinkernagel AS, et al. Endothelial cell infection and endotheliitis in COVID-19. Lancet 2020;395:1417–8.
6. Wiedermann FJ, Lederer W, Mayr AJ, Sepp N, Herold M, Schobersberger W. Prospective observational study of antiphospholipid antibodies in acute lung injury and acute respiratory distress syndrome: comparison with catastrophic antiphospholipid syndrome. Lupus 2003;12:462–7.

DOI 10.1002/art.41633

Reply

To the Editor:

We recently showed that IgG aCLs are highly and independently associated with COVID-19 severity. This result is essential for the management of the risk of thrombosis, which is well established today in COVID-19 (1). In their study, Dr. Frapard et al also described the prothrombotic state of COVID-19 patients, especially those with ARDS. Since they found no significant difference in aPL positivity between COVID-19–related and non–COVID-19–related ARDS patients, they suggest that the association between aCLs and disease severity could be related to pulmonary injury regardless of the SARS–CoV-2 infection. However, the lack of a difference between the 2 groups does not mean that they are identical.

A major difference between the 2 studies is the positivity rate of aPLs and their profile. We detected aPLs in >50% of patients with severe COVID-19, and among them, 87% were IgG aCL positive. In contrast, Frapard and colleagues reported a low prevalence of aCLs in 37 COVID-19 patients with ARDS (16%) without any specific aPL profile. Thus, it is difficult to draw conclusions based on so few aPL-positive patients. Because of the lack of a standardized assay and aPL heterogeneity, their detection is dependent on enzyme-linked immunosorbent assays (2), which were provided by different manufacturers in the 2 studies. In particular, coating or buffer composition can influence the interaction between cardiolipin and cofactor proteins (3), and can influence whether antibodies are detected or not. Moreover, knowing the difficulties of interpreting aPL positivity, we pay close attention to their routine detection. All positive samples are controlled in duplicate, and, to address the specificity, the absorbance of uncoated wells treated in the same conditions is subtracted in order to avoid nonspecific binding (4). In contrast to Frapard and colleagues who focused on patients in the ICU, we also included patients with severe COVID-19 who were not admitted to the ICU and observed that 29% were positive for IgG aCL (Figure 1A). There was no difference in IgG aCL levels between aCL-positive patients admitted versus those not admitted to the ICU (Figure 1B), suggesting that IgG aCL positivity in severe COVID-19 is not attributable to the pulmonary complications alone.

If the link between viral infection and aPL detection is well described in the literature (5), the relationship between aPL positivity and lung injury is not obvious. To support their hypothesis, Frapard et al referenced a study by Wiedermann et al (6), in which an association between aPL positivity and lung injury was not shown except in 1 patient with catastrophic antiphospholipid syndrome (CAPS). In the literature, the association between aPL positivity and ARDS is rarely described and only reported in the context of APS or CAPS (7). Consistent with our results, Zuo et al (8) recently reported that half of patients hospitalized for

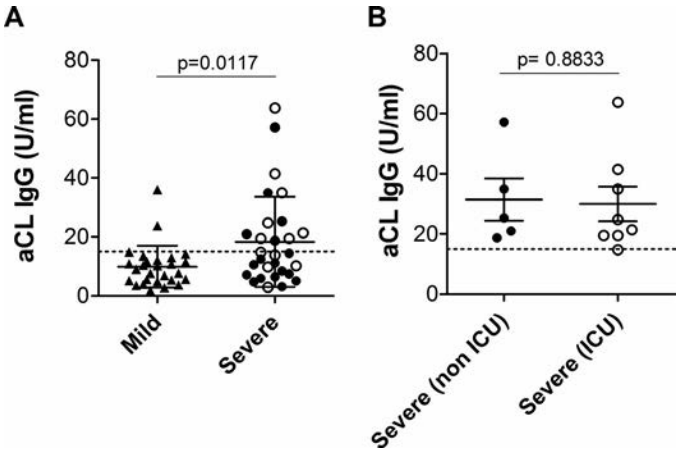

Figure 1. **A**, Levels of IgG anticardiolipin antibodies (aCL) in patients with mild coronavirus disease 2019 (COVID-19) and patients with severe COVID-19. **B**, Levels of IgG aCL in patients with severe COVID-19 who were not admitted to the intensive care unit (ICU) and patients with severe COVID-19 who were admitted to the ICU. Solid symbols represent patients not admitted to the ICU, and open symbols represent patients admitted to the ICU; horizontal lines and error bars show the mean ± SEM. Broken lines represent the manufacturer's cutoff for positivity (15 units/ml). *P* values were determined by Mann-Whitney U test.

COVID-19 were positive for aPLs, and they demonstrated that IgG aPL could be pathogenic by promoting neutrophil extracellular trap release.

In conclusion, we thank Frapard and colleagues for expressing their interest in our study, which prompted a constructive debate about the importance of aCLs in thrombosis in COVID-19 patients.

Daniel Bertin, PharmD, MSc
Hôpital de la Conception, AP-HM
Aix-Marseille Université
CNRS
Institute of NeuroPhysiopathology
UMR 7051
and UMR 13916
Alexandre Brodovitch, PhD
Abdelouahab Beziane, PhD
Hôpital de la Conception, AP-HM
Jean Louis Mege, MD, PhD
Hôpital de la Conception, AP-HM
Aix-Marseille Université
Institut Hospitalo-Universitaire Méditerranée Infection, IRD
and Microbe, Evolution, Phylogénie et Infection
Xavier Heim, PharmD, MSc
Nathalie Bardin, PharmD, PhD
Hôpital de la Conception, AP-HM
Aix-Marseille Université
Centre de recherche en CardioVasculaire et Nutrition
and INSERM UMRS 1263
Marseille, France

1. Piazza G, Morrow DA. Diagnosis, management, and pathophysiology of arterial and venous thrombosis in COVID-19. JAMA 2020; 324:2548–9.
2. Chayoua W, Kelchtermans H, Moore GW, Gris JC, Musial J, Wahl D, et al. Detection of anti-cardiolipin and anti-β2glycoprotein I antibodies differs between platforms without influence on association with clinical symptoms. Thromb Haemost 2019;119:797–806.
3. Chamley LW, McKay EJ, Pattison NS. Cofactor dependent and cofactor independent anticardiolipin antibodies. Thromb Res 1991; 61:291–9.
4. Pellegrino NM, Caccavo D. Variability in anticardiolipin antibody detection: role of nonspecific IgG binding and different microtiter plates. Clin Appl Thromb Hemost 2007;13:404–9.
5. Martirosyan A, Aminov R, Manukyan G. Environmental triggers of autoreactive responses: induction of antiphospholipid antibody formation [review]. Front Immunol 2019;10:1609.
6. Wiedermann FJ, Lederer W, Mayr AJ, Sepp N, Herold M, Schobersberger W. Prospective observational study of antiphospholipid antibodies in acute lung injury and acute respiratory distress syndrome: comparison with catastrophic antiphospholipid syndrome. Lupus 2003;12:462–7.
7. Maioli G, Calabrese G, Capsoni F, Gerosa M, Meroni PL, Chighizola CB. Lung disease in antiphospholipid syndrome [review]. Semin Respir Crit Care Med 2019;40:278–94.
8. Zuo Y, Estes SK, Ali RA, Gandhi AA, Yalavarthi S, Shi H, et al. Prothrombotic autoantibodies in serum from patients hospitalized with COVID-19. Sci Transl Med 2020;12:eabd3876.

DOI 10.1002/art.41646

The importance of establishing a suitable study population in osteoarthritis studies: comment on the article by MacFarlane et al

To the Editor:

We read with interest the article by MacFarlane et al (1), in which they investigated the long-term effects of vitamin D and omega-3 fatty acid (n-3 FA) supplementation on chronic knee pain and reported that neither treatment was superior to placebo for reducing pain or improving function or stiffness.

The study population consisted of Vitamin D and Omega-3 Trial (VITAL) participants who were considered likely to have knee osteoarthritis (OA). Medical records were requested from only 29% of participants to validate OA, and of those patients, medical records were obtained for only 57%. Physical examination was not performed. In addition to OA, other local knee diseases, such as bursitis, meniscopathy, tendinitis, and systemic inflammatory diseases, may cause knee pain. Additionally, hip diseases may cause referred pain in the knee.

Another important issue is that pain in OA may consist of nociceptive, inflammatory, and neuropathic pain to varying degrees, making targeted therapy problematic (2). In their study, MacFarlane and colleagues queried the use of opioids and/or neuropathic pain medications with a single question. This is not enough to evaluate the presence of neuropathic pain. Screening questionnaires such as PainDETECT and DN4 can be used to indicate how likely it is that pain is neuropathic.

A study by Yazici et al, which assessed the safety and efficacy of lorecivivint for the treatment of symptomatic knee OA, demonstrated that there were no statistically significant differences in Western Ontario and McMaster Universities Osteoarthritis Index (WOMAC) pain scores between the placebo and lorecivivint groups in the analysis of all subjects (3). However, a subgroup analysis of the patients with unilateral symptomatic knee OA and those with unilateral symptomatic knee OA but without widespread pain showed that patients receiving the 0.07-mg dose of lorecivivint had significantly lower WOMAC pain and function subscale scores compared with those receiving placebo (3). This study highlights the importance of establishing a suitable study population.

Finally, the presence of fibromyalgia, anxiety, and mood disorders were not evaluated by MacFarlane et al. The frequency of these diseases is higher in patients with chronic pain and associated with more severe pain and worse treatment response.

In conclusion, the negative results in this study by MacFarlane and colleagues could have been caused by the heterogeneity of the patients rather than the ineffectiveness of the interventions. We believe that there is a need for well-designed prospective studies

that include valid clinical and/or radiologic outcome measures to determine the effectiveness of these drugs in patients with knee OA without neuropathic pain.

Duygu Tecer, MD
Muhammet Cinar, MD
Sedat Yilmaz, MD
University of Health Sciences and Gulhane Education and Research Hospital Ankara, Turkey

1. MacFarlane LA, Cook NR, Kim E, Lee IM, Iversen MD, Gordon D, et al. The effects of vitamin D and marine omega-3 fatty acid supplementation on chronic knee pain in older US adults: results from a randomized trial. Arthritis Rheumatol 2020;72:1836–44.
2. Fu K, Robbins SR, McDougall JJ. Osteoarthritis: the genesis of pain [review]. Rheumatology (Oxford) 2018;57 Suppl 4:iv43–50.
3. Yazici Y, McAlindon TE, Gibofsky A, Lane NE, Clauw D, Jones M, et al. Lorecivivint, a novel intraarticular CDC-like kinase 2 and dual-specificity tyrosine phosphorylation-regulated kinase 1A inhibitor and Wnt pathway modulator for the treatment of knee osteoarthritis: a phase II randomized trial. Arthritis Rheumatol 2020;72:1694–706.

DOI 10.1002/art.41642

Reply

To the Editor:

We appreciate the comments from Dr. Tecer et al. Our intent in reporting the results of a randomized trial of the efficacy of n-3 FA and/or vitamin D supplementation on knee pain in a large community-based population of older adults (VITAL) was that our findings would be generalizable to the broader knee OA population and relevant to the practicing clinician. We recruited participants nationwide, reducing biases from focusing only on a local population, but precluding the ability to perform physical examinations. We did not include fibromyalgia or mood disorders in the analysis. However, a strength of this trial is the large cohort and randomization, such that these potential confounders would be equally distributed among the treatment groups and thus the results would still be valid.

We agree that pain in knee OA is complex, with intraarticular and periarticular structures as well as neural processes likely contributing. However, in clinical practice, clinicians very rarely attempt to parse out the specific pain generators for each patient. Measures such as PainDETECT are certainly of interest in OA research, but are not used in the clinical setting (1). Our goal was to inform practicing clinicians on the use of vitamin D and n-3 FA for pain in the knee OA population as a whole, where subtyping is not feasible.

The OA research community has grappled with how best to subset what is likely a heterogeneous disease; however, to date there are no widely accepted phenotype classifications (2–4). For potential disease-modifying OA drugs, it is critical that the drug be targeted to the appropriate population, as approval from institutions such as the Food and Drug Administration is based on evidence of patient-reported outcome measures such as pain and change in structural end points (5). We thus studied the supplements as they are currently being used in practice, for the general knee pain population. Our subgroup analyses were predicated on information a clinician would likely have on hand.

Thus, we agree that understanding medication efficacy in knee OA is nuanced in part due to the heterogeneity of the disease and the complexity of pain perception itself. Certainly, future investigations could be specifically designed to investigate specific subtypes of knee OA participants; however, that was not the aim of this trial.

Supported by the NIH (grants R01-AR-059086, K24-AR-066109, U01-CA-13892, R01-CA-13892, and P30-AR-072577) and a Rheumatology Research Foundation Scientist Development Award. Dr. MacFarlane has received consulting fees from Flexion Therapeutics (less than $10,000) and research support from Flexion Therapeutics, Samumed, and Amgen. Dr. Katz has received research support from Flexion Therapeutics and Samumed. No other disclosures relevant to this letter were reported.

Lindsey A. MacFarlane, MD, MPH
Brigham and Women's Hospital Harvard Medical School
I-Min Lee, MBBS, ScD
Jeffrey N. Katz, MD, MSc
JoAnn E. Manson, MD, DrPH
Brigham and Women's Hospital Harvard Medical School Harvard T. H. Chan School of Public Health
Karen H. Costenbader, MD, MPH
Brigham and Women's Hospital Harvard Medical School Boston, MA

1. Freynhagen R, Baron R, Gockel U, Tölle TR. PainDETECT: a new screening questionnaire to identify neuropathic components in patients with back pain. Curr Med Res Opin 2006;22:1911–20.
2. Driban JB, Sitler MR, Barbe MF, Balasubramanian E. Is osteoarthritis a heterogeneous disease that can be stratified into subsets? [review]. Clin Rheumatol 2010;29:123–31.
3. Kraus VB, Blanco FJ, Englund M, Karsdal MA, Lohmander LS. Call for standardized definitions of osteoarthritis and risk stratification for clinical trials and clinical use [review]. Osteoarthritis Cartilage 2015;23:1233–41.

4. Karsdal MA, Michaelis M, Ladel C, Siebuhr AS, Bihlet AR, Andersen JR, et al. Disease-modifying treatments for osteoarthritis (DMOADs) of the knee and hip: lessons learned from failures and opportunities for the future [review]. Osteoarthritis Cartilage 2016;24:2013–21.
5. Conaghan PG, Hunter DJ, Maillefert JF, Reichmann WM, Losina E. Summary and recommendations of the OARSI FDA osteoarthritis Assessment of Structural Change Working Group. Osteoarthritis Cartilage 2011;19:606–10.

DOI 10.1002/art.41641

Clinical Images: An unusual presentation of erosive gout

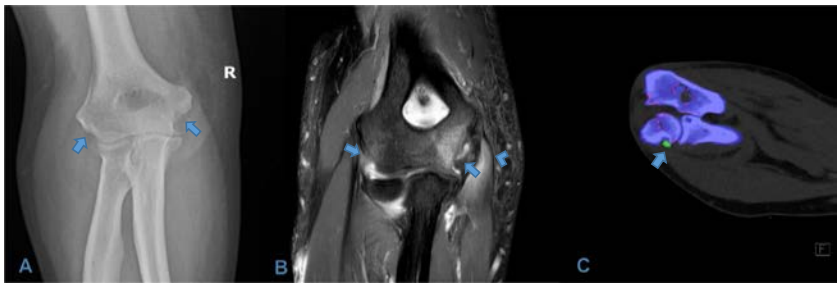

The patient, a 44-year-old man, presented with a 4-week history of painful contractures of the elbows and left knee. His medical record was notable for metabolic syndrome and antiphospholipid syndrome, with a previous extensive thrombotic event in the right leg, necessitating an above-knee amputation. Physical examination demonstrated flexion contractures of the elbows and left knee. There were no signs of uveitis or dactylitis and no personal or family history of relevant autoimmune diseases. No recent infection was documented. Markers of inflammation and blood urate concentration were elevated, yet there was no known history of gout. The patient was negative for rheumatoid factor, anti–citrullinated protein antibodies, and HLA–B27. While radiography of the right elbow revealed marginal epicondylar erosions (**arrows** in **A**), magnetic resonance imaging showed mild synovitis, erosions (**arrows** in **B**), and common flexor tendonitis (**arrowhead** in **B**). Arthrocentesis of the right elbow failed due to technical limitations. Crystal-associated disease was suspected. However, the prolonged oligoarticular presentation and the absence of external signs of inflammation did not support a diagnosis of gout/calcium pyrophosphate deposition disease. As such, peripheral spondyloarthritis was considered, and intraarticular glucocorticoids were administered, resulting in prompt improvement. A few months later, dual-energy computed tomography (DECT) was performed, showing prominent intraerosional monosodium urate monohydrate (MSU) crystals (**arrow** in **C**). Gout was eventually diagnosed. This case is noteworthy due to the occurrence of erosions and MSU crystals in the absence of previous clinical events, as well as the prolonged oligoarticular presentation and the lack of external signs of inflammation. Atypical manifestations of gout, including axial arthropathies, entrapment neuropathies, tophaceous presentations, and panniculitis (1), may make diagnosis difficult. While the gold standard for diagnosis relies on the demonstration of MSU crystals in synovial fluid or tophi aspirates (2), arthrocentesis is not always feasible. In such instances, DECT can provide important diagnostic information through the detection of MSU deposits (3).

1. Ning TC, Keenan RT. Unusual clinical presentations of gout [review]. Curr Opin Rheumatol 2010;22:181–7.
2. Richette P, Doherty M, Pascual E, Barskova V, Becce F, Castaneda J, et al. 2018 updated European League Against Rheumatism evidence-based recommendations for the diagnosis of gout. Ann Rheum Dis 2020;79:31–8.
3. Bongartz T, Glazebrook KN, Kavros SJ, Murthy NS, Merry SP, Franz WB III, et al. Dual-energy CT for the diagnosis of gout: an accuracy and diagnostic yield study. Ann Rheum Dis 2015;74:1072–7.

Fadi Kharouf, MD
Yusef Azraq, MD
Hebrew University Hadassah Medical Center
Yaakov Applbaum, MD
Hebrew University and Shaare Zedek Medical Center
Hagit Peleg, MD
Hebrew University Hadassah Medical Center
Jerusalem, Israel